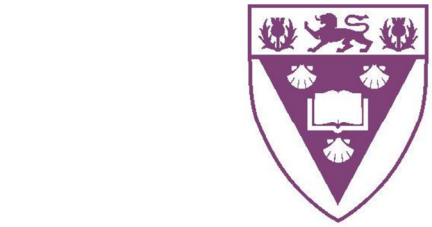

RHODES UNIVERSITY

Grahamstown • 6140 • South Africa

A GEOCHEMICAL AND MORPHOLOGICAL INVESTIGATION OF PLACER GOLD GRAINS FROM THE SOUTHERN SEWARD PENINSULA, ALASKA: IMPLICATIONS FOR SOURCE AND TRANSPORT MECHANISMS

By

Ernest J.H. Gauntlett

A thesis submitted in partial fulfilment of the requirements for the degree of

MASTER OF SCIENCE

(Economic Geology)

M.Sc. Economic Geology Programme

Geology Department

Rhodes University

P.O. Box 94

Grahamstown, 6140

South Africa

February 2015

Declaration

I, Ernest J.H. Gauntlett, declare this thesis to be my own work. It is submitted in partial fulfilment of the Degree of Master of Science at Rhodes University. It has not been submitted before for any degree or examination in any other university or tertiary institution.

Signature of the candidate: 

Date: 16/02/2015.

Abstract

This study presents the first detailed geochemical and morphological characterisation of gold grains from the southern Seward Peninsula, Alaska, a region with significant historical and on-going placer gold mining. Quantitative Au, Ag, Hg, and Cu data are presented for gold grains from eleven sites. Additionally, quantitative Te, W, As, and Sb trace element data are presented for gold grains from ten of the eleven sites. Although it is acknowledged that quantitative trace element analysis of gold grains is a relatively new endeavour, the limited trace element data obtained in this study suggest that trace element analysis could be useful for characterising gold sources on the southern Seward Peninsula. Major and minor element geochemical profiling is sufficient at differentiating between sites from regional provenance systems but insufficient at differentiating between sites within a single system. Differentiating among sites within a single system will likely require microchemical analysis of mineral inclusions and analysis of trace element signatures.

Analysis of gold alloy chemistry identifies four gold “types” across the southern Seward Peninsula and suggests that these types are associated with particular stratigraphic units. Type 1 gold is Au-Ag alloy containing 4 to 20% Ag and is associated with Devonian to Ordovician schists and marbles. Type 2 gold, present at a single site (AK021), has uniquely elevated Ag content relative to Type 1 sites (16% vs. 8% modal Ag content) but similar Cu and Hg abundances. Field evidence suggests a local palaeo (possibly Cretaceous) fluvial conglomerate source for these grains. Given that Ag content has been shown to increase with vertical or lateral zonation from a hydrothermal source as the fluid migrates and evolves, it is proposed that these grains may represent a previous placer development cycle sourced from higher up in the mineralised lithographic sequence. Type 3 gold is Au-Ag-Hg alloy with Ag contents of 5 to 20% and Hg contents always in excess of 0.1% and often above 0.5%. Type 3 gold is always associated with Ordovician mafic schists. Type 4 gold is exsolved gold from arsenopyrite, containing high Ag (21 – 25%) and no Hg. The presence of Type 3 primary Au-Ag-Hg alloy with very low average Cu contents (0.00 – 0.05%) provides evidence for an orogenic gold mineralisation event related to hydrothermal fluid derived from metasediments during regional metamorphism.

Morphological analysis reveals that placer gold grain populations on the southern Seward Peninsula are typically immature with limited flattening and folding.

Along with the absence of Ag depletion in grain rims, the morphological analysis precludes significant fluvial or marine transport and suggests glacial transport mechanisms have been prevalent across the southern Seward Peninsula with recent fluvial and marine overprinting present in some locations. Morphological and geochemical assessments reveal the presence of secondary Au-Ag-Hg alloy supergene development in marine and beach environments.

Relevant to the continued exploration of the Nome offshore gold placer, this study indicates that areas offshore known glacial pathways, particularly those draining Nome Group Devonian to Ordovician micaceous and graphitic schists as well as Ordovician mafic schists, should be prioritised as exploration targets. Areas not directly offshore glacial pathways, as well as areas offshore glacial pathways draining the non- to poorly-mineralised Kigluaik Group lithologies, should be deprioritized. Clast lithologies thus have the potential to act as important indicators for mineralised glacial and re-worked sediments when exploring offshore of Nome.

Gold fineness on the southern Seward Peninsula is relatively high, and an average of 910 is recommended for resource and financial modelling during pre-feasibility and feasibility studies.

Keywords: *Nome, Seward Peninsula, Gold, Placer, Morphology, Geochemical Fingerprinting, Geochemical Profiling, Au-Ag-Hg alloy, Major Elements, Trace Elements, EMPA, Gold Fineness, Exploration*

Acknowledgements

From Rhodes University I would like to thank Prof. Yong Yao for his advice and support during the compilation of this thesis, Dr. Gelu Costin for his assistance in collecting the major and trace element data, John Hepple and his workshop team for grain polishing and thin sections, and Ashley Goddard for her extensive help regarding all things administrative during the course of my M.Sc.

I would like to thank Dr. Rob Chapman of Leeds University (U.K.) for his thoughts and insights into this thesis, leading to a better piece of work.

I would like to thank AuruMar (Pty) Ltd. for funding this research and allowing me to develop this project into one of my own. I specifically thank AuruMar for the permission to use their gold grains and to publish this work. I further acknowledge former AuruMar geologists Urban Burger and Dr. Evelyn Mervine for their assistance in the field and discussions regarding Nome mineralisation and geology.

I am grateful to my wife, Dr. Evelyn Mervine, for her support whilst I attended to my M.Sc. studies in Grahamstown, as well as during all the weekends and holidays I was indisposed whilst compiling this thesis. Furthermore, I thank her for sharing her academic acumen and insights into the project as well as for her assistance during sample collection, including hours of kneeling in freezing Nome streams.

I am indebted to the following persons and corporations for samples and permission to sample their leases:

- Adem Boechman for collecting and allowing the use of sample ADEM,
- Bill Richards for acquiring sample AK123 and the relevant permissions,
- The Crutch family for allowing sampling on their land to acquire AK111,
- AuruMar for the use of 2011 field sample datasets (samples AK015, AK021, AK028, and AK032),
- AuruMar for the use of 2012 Nome sonic coring sample AUR-12-854,
- AuruMar for allowing me time to conduct field visits and sample sites AK100, AK111, AK117, and AK121,
- The Bering Straits Native Corporation (BSNC) for hand samples from Rock Creek Mine (sample RC4).

The use of the Rhodes University Jeol JXA 8230 Superprobe instrument, sponsored by NRF/NEP grant 40113 (UID 74464), is kindly acknowledged.

Contents

List of Abbreviations

Abbreviation	Definition
µm	Micron (1000th of a millimetre)
AGA	AngloGold Ashanti
ATV	All-Terrain Vehicle
BE	Backscatter Electron
BSNC	Bering Straits Native Corporation
DB	De Beers
EMP	Electron Microprobe
EMPA	Electron Microprobe Analyser
EP	Exploration Panel
Km	Kilometre
kV	Kilovolts
kya	Thousand Years Before Present
LA-ICP-MS	Laser Ablation Inductively Coupled Mass Spectrometer
LLD	Lower Limit of Detection
Ma	Million Years Before Present
mm	Millimetre
nA	Nanoamps
ppb	Parts Per Billion
ppm	Parts Per Million
PSD	Particle Size Distribution
RC	Rock Creek
SE	Secondary Electron
SEI	Secondary Electron Image
WD	Working Distance
WDS	Wavelength Dispersive Spectrometry

List of Figures

List of Tables

1 Introduction

Placer gold has been extracted from Nome and the surrounding areas since the late nineteenth century, with a total of ~5 million ounces of gold extracted in total between 1898 and 1993 (Bundtzen et al., 1992; Bundtzen et al., 1994). Although onshore occurrences of placer gold are widespread, the negative economic viability of the dwindling onshore reserves has resulted in many exploration companies looking towards the offshore for new placer gold resources (Schaffer, 2013). AuruMar was one such exploration company and was a joint venture between AngloGold Ashanti (AGA) and De Beers (DB), with AGA's interest primarily in extracting saleable gold and DB's interest primarily in continuing their propriety development of offshore mining technologies, such as those implemented in diamond mining offshore the Southern African West Coast (Scott, 2011).

AuruMar successfully bid on 26 offshore exploration and mining leases at Nome in September 2011, after conducting onshore field campaigns in July 2011. The company conducted an extensive offshore drilling campaign from July to September 2012. Further offshore sampling exercises, as well as onshore field visits to assess the potential for further extents of the offshore deposit were conducted during July and August of 2013. Unfortunately, AuruMar closed down in December 2013 due to external factors.

The author of this study was intimately involved in the Nome exploration venture as a responsible geologist on site during both the 2012 and 2013 offshore campaigns and during the 2013 onshore field visits. This study was developed by the author to aid AuruMar in its further offshore exploration targeting by providing a geochemical benchmark of gold grain profiles from across the southern Seward Peninsula. This would have supported the development of a geological framework for gold grain transport mechanisms across the peninsula, constrained by morphological and textural features of gold grains and the clast lithologies present in their host streams.

1.1 Location and General Background

Nome is located on the south-western coastline of the Seward Peninsula in western Alaska. The town is relatively small with a permanent population of ~3,800 people (2012 census estimate) and relatively isolated with access only by plane or sea (during the ice-free summer months). The town is built on the coastal plain of the Snake and Nome rivers, which drain from the foothills north of the town into Norton Sound, a shallow inlet of the northern Bering Sea (Figure 1).

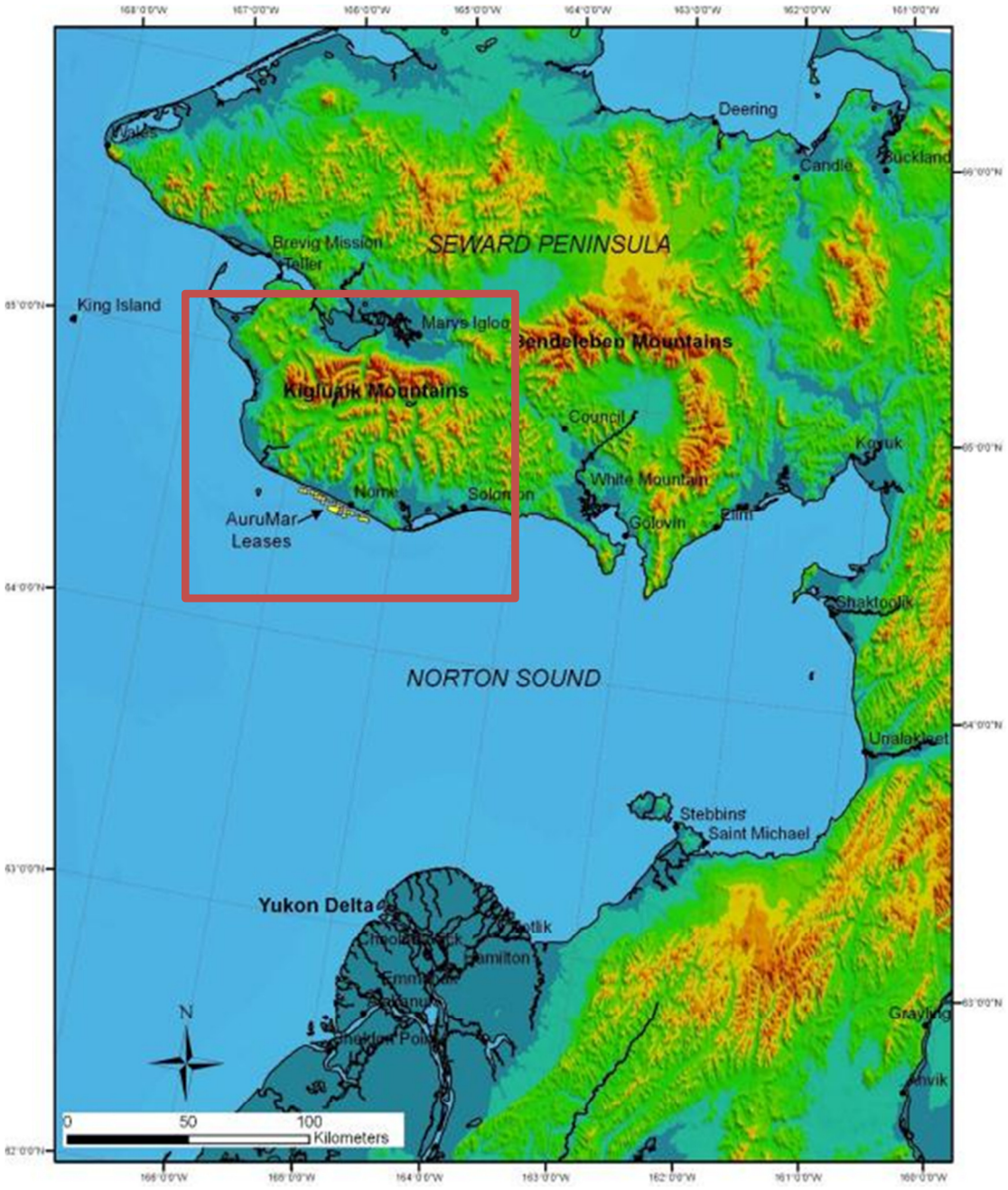

Figure 1: Digital elevation map showing Norton Sound, Seward Peninsula, and Yukon Delta areas. Nome is located on the southwest coast of the Seward Peninsula. Digital Terrain Model from Jarvis et al. (2006).

The town owes its founding to the Nome gold rush in the late 19th century. Gold was first discovered near Nome in what is now Anvil Creek in the summer of 1898. In 1899 gold was found on the beaches along the fledgling town. The twin discoveries resulted in a rush of prospectors, and the town's population reached 10,000 by mid-summer of 1899. The town continued to grow to almost 20,000 in the early 20th century but dropped quickly to only 2,600 by 1909. It is estimated that over 5 million ounces of gold have been produced at Nome and the surrounding areas from the onshore placers (Bundtzen et al., 1994).

1.2 Research Objectives

There is currently a poor understanding of the source for much of the placer gold present on the Seward Peninsula, including the extensively mined deposits mined in the vicinity of Nome (Garnett, 2000). Although various hard rock sources have been located and exploited, none are large enough, individually or together, to produce the amount of gold present in streams and the onshore and offshore placers (Bundtzen et al., 1992). Although not integral to the exploration framework, an understanding of gold geochemistry is potentially able to constrain gold ore mineralisation style to orogenic, magmatic (porphyry), oxidized/reduction intrusion hydrothermal, or other as described in Robert et al. (2007), Chapman et al. (2009), and further in Section 3.1. If the gold source rocks could be identified, through geochemical profiling and other analysis, then regional exploration targets can be prioritized.

It is currently unknown whether a single or multiple source(s) of primary gold contributed to the gold currently found in the Nome placer. Gold chemistry has the potential to identify different populations of gold (e.g. Dumula and Mortensen, 2002, Chapman et al., 2010). If gold populations can be related to specific drainage systems (spatial) or erosion pulses during glacial events (temporal), the understanding of the development of the Nome placer can be greatly enhanced. In order to investigate this spatial distribution of placer gold, the southern Seward Peninsula region has been separated by drainage basins which are referred to as various "systems". Four main systems have been defined: the Teller, Sinuk, Nome, and Solomon systems.

There is uncertainty as to the significance of various transport mechanisms operating across the Seward Peninsula relating to gold mobility. Gold morphology

studies (analysis of flattening/rolling, presence of inclusions, and especially the presence of folding) can help ascertain the degree to which gold has been subjected to fluvial processes whereas glacial processes are more likely to retain primary gold morphology and suffer no folding (Youngson and Craw, 1999; Craw et al., 2006; Rasmussen et al., 2007). Morphology studies can also identify marine and wind processes, should these have played a noteworthy role in placer development.

Of particular interest in placer gold resource development is the gold fineness (percentage pure gold in a gold grain after other major elements, typically Ag, Hg, and Cu, are removed) within a deposit. This factor is of economic importance as fineness effects the financial modelling of mine feasibility. Differences in fineness between onshore grains from different systems as well as between onshore versus offshore grains may also provide information on aspects of the placer development.

2 Geological Setting

2.1 Tectonic Setting and Regional Geology of the Seward Peninsula

The Seward Peninsula (Figure 1) protrudes approximately 85 km into the Bering Strait, from western Alaska towards Siberia, and forms the westernmost extension of the North American mainland. The peninsula is bordered to the north by the Chukchi Sea and Kotzebue Sound and to the south by the Bering Sea and Norton Sound. The peninsula is approximately 330 km long and 145 km wide. Three physiographic regions constitute the Seward Peninsula: the low coastal plains, an irregular interior upland with elevations up to 600 m, and a mountain belt with its highest peak at 1,400 m. The mountain belt, consisting of the Kigluaik and Bendeleben ranges, divides the peninsula into a southern and northern part. The mountains are characterised by the presence of glaciated U-shaped valleys and glacial cirques.

Most of the Seward Peninsula is underlain by rock sequences that were part of a Late Proterozoic to early Palaeozoic continental margin known as the Arctic Alaska-Chukotka terrane (Amato et al., 2009; Till et al., 2011), see Figure 2. The Arctic Alaska-Chukotka terrane consists primarily of low to high grade metamorphic suites of blueschist, greenschist, and amphibolite facies schists and marbles. These high pressure metamorphic rocks record the subduction of the continental margin during the Jurassic (Till et al., 2011).

The metamorphic rocks were then modified in the Early Cretaceous during the Brooks Range Orogeny, which likely exhumed some of the high pressure metamorphic rocks (Till et al., 2011). In the mid-Cretaceous, amphibolite to granulite facies metamorphism overprinted many of the rocks of the Seward Peninsula and, around the same time, a period of magmatism began that lasted until the Late Cretaceous which introduced three suites of granitic rocks. During the Cenozoic, some mafic volcanic rocks were erupted in the central and northern parts of the Seward Peninsula (Till et al., 2011).

The Seward Peninsula has been subject to multiple metamorphic events with the bulk of the Nome Complex having been metamorphosed to at least greenschist facies and, in some places, amphibolite facies (Till et al., 2011). Recently, it has been shown that metamorphism to this grade is a key driver for the formation of orogenic

gold, with resultant rocks being depleted in a suite of ore-forming elements relative to unmetamorphosed protoliths (Pitcairn et al., 2006). Across the southern Seward Peninsula, the presence of this level of metamorphism coupled with an abundance of regional faulting, the absence of identified primary gold sources, and significant igneous activity strongly suggests that regional metamorphism of the Nome Complex mobilised ore-forming minerals in hydrothermal fluids, which resulted in widespread low level mineralisation throughout the peninsula. In addition to general hypotheses based on regional geology, geochemical evidence can be a powerful tool for confirming mineralisation style.

The area of focus for this study is the south western quadrant of the Seward Peninsula (red box in Figure 1, also see Figure 2), which is underlain primarily by two geological groups, the Nome Group and the Kigluaik Group (Figure 3).

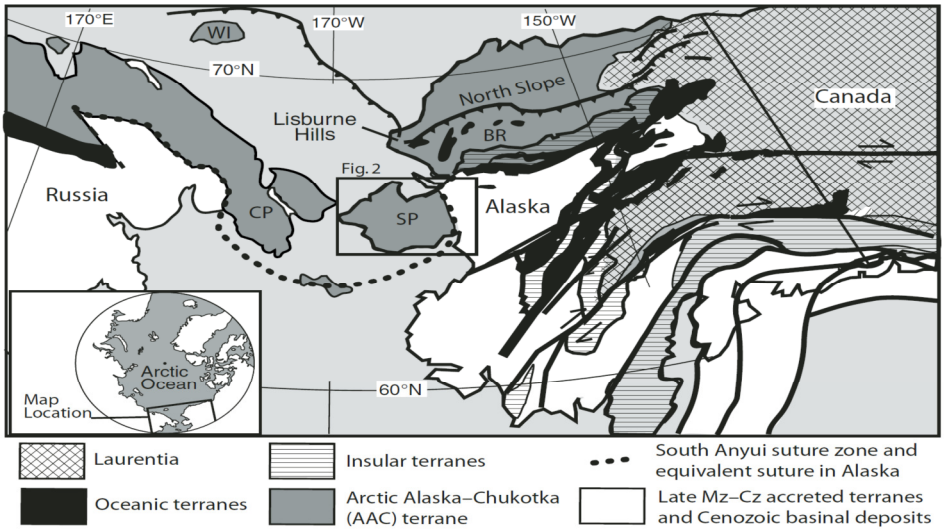

Figure 1. Index map of the Bering Strait region, with inset showing the circum-Arctic position of the Arctic Alaska–Chukotka terrane (modified from Amato et al., 2004; Colpron et al., 2007) and box showing location of Figure 2. All of the samples in this study come from Seward Peninsula. SP—Seward Peninsula; CP—Chukotka Peninsula; WI—Wrangel Island; BR—Brooks Range.

Figure 2: Map of the Bering Strait region showing the location of the Arctic Alaska-Chukotka terrane. SP = Seward Peninsula, CP = Chukotka Peninsula, WI = Wrangel Island, and BR = Brooks Range. Quadrangle shows the area enlarged in. Figure from Amato et al., 2009.

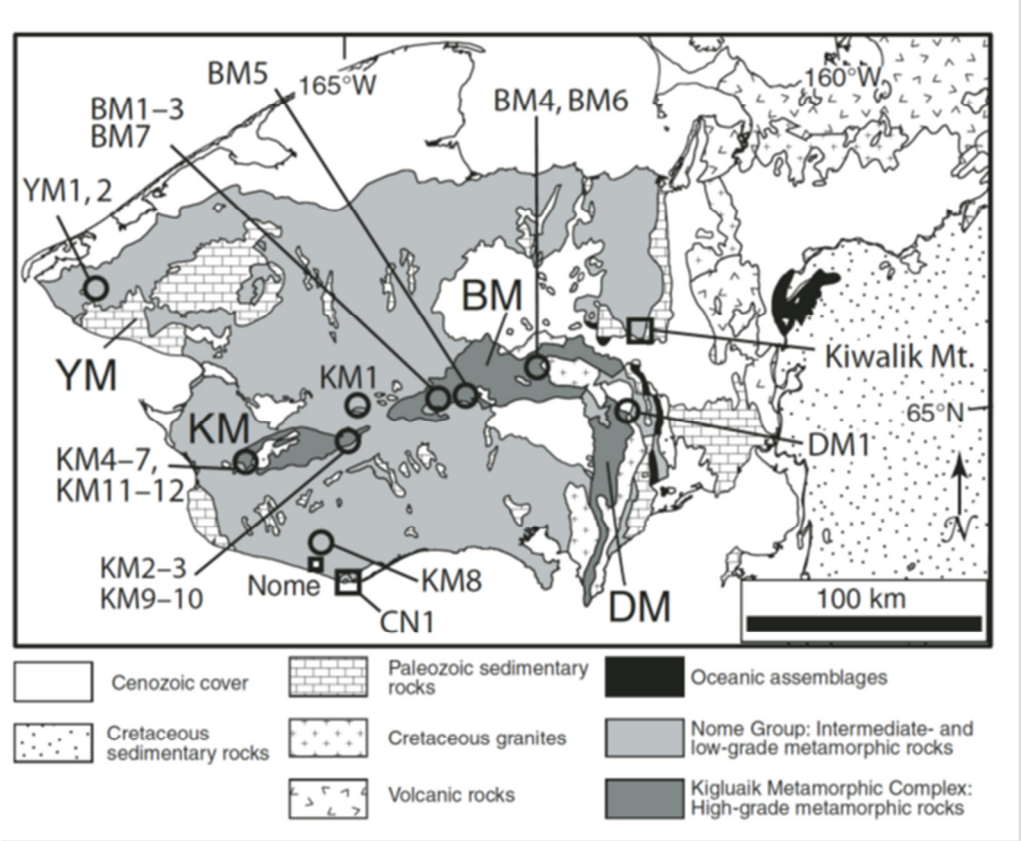

Figure 3: Simplified geologic map of the Seward Peninsula showing the Nome Group and Kigluaik Group and the various mountain ranges. YM = York Mountains, KM = Kigluaik Mountains, BM = Bendeleben Mountains, DM = Darby Mountains, and CM = Cape Nome. Other abbreviations (e.g. BM5) refer to samples described in Amato et al., 2009, from where this figure has been extracted.

2.2 Local Geology of the Southern Seward Peninsula

The onshore geology of the southern Seward Peninsula, as mapped by the U.S. Geological Survey (Till et al., 2011), is presented in Figure 4. The map lithology codes are explained in Table 1. Note that the tan coloured portions of the map represent recent, largely unconsolidated sediments.

Utilising the nomenclature of Till et al., 2011, the Nome Group is divided into three general sequences:

a) A layered sequence of mappable lithologic units that occur in a consistent, layer-cake structural relation to each other and which cover most of the central Seward Peninsula. The primary units are a Devonian to Ordovician basal pelitic schist unit (DOx), a Devonian mixed interlayered marble and graphitic schist unit (Dcs), an Ordovician mafic schist unit (Ocs), and an Ordovician impure chlorite marble (Oim).

b) Scattered Palaeozoic metacarbonate units of minor dolostones and marbles that are widely distributed. The most important unit near Nome

is the “Marble of the Moon Mountains” (Pzmm) unit of calcite-rich marble, which is exposed west of the Sinuk River.

c) Metaturbidites, which are exposed primarily on the north and southeast coasts of the Seward Peninsula. These are not significantly exposed on the Nome coastal plain.

The contact between the Kigluaik and Nome Groups is commonly faulted but may be transitional metamorphic towards the southeast. The upper half of the Sinuk River has entrenched itself along this fault line (Figure 4).

The Kigluaik Group is dominated by a massive pelitic and semi-pelitic biotite gneiss (PzZh), which has undergone upper amphibolite to granulite facies metamorphism. Lithologically, this unit is a higher grade version of portions of the Nome Group (Dcs and DOx). The high grade equivalent of the Nome Group Ocs unit is the geochemically similar Pznp unit found to the west of the Kigluaik mountains (Ayuso and Till, 2007). Another common unit within the Kigluaik Group is a high grade orthogneiss (Zo) representing a Proterozoic magmatic component. Cretaceous magmatic units are also present as diorites (Kdi) and granites (Kg) (Till et al., 2011).

Table 1: List of Primary Geologic Units of the Southern Seward Peninsula after Till et al., 2011.

Nome Area	
Zn	Late Proterozoic Metagranites
Ocs	Ordovician Casadepaga Schist
Oim	Ordovician Chlorite Marble
Dox	Devonioan mixed marble, graphitic schist and mica-schist
Dcs	Devonian mica-schist, calcaeous and graphitic schists
Kigluaik Area	
Zo	Proterozoic Orthogneiss
PzZh	Palaeo/Protero-zoic high grade metasedimentary and metaigneous
Kg	Cretaceous granites
Kdi	Cretaceous diorites
Sinuk Area	
Pzmm	Palaeozoic Marble of the Moon Mountains
Kgu	Cretaceous granites

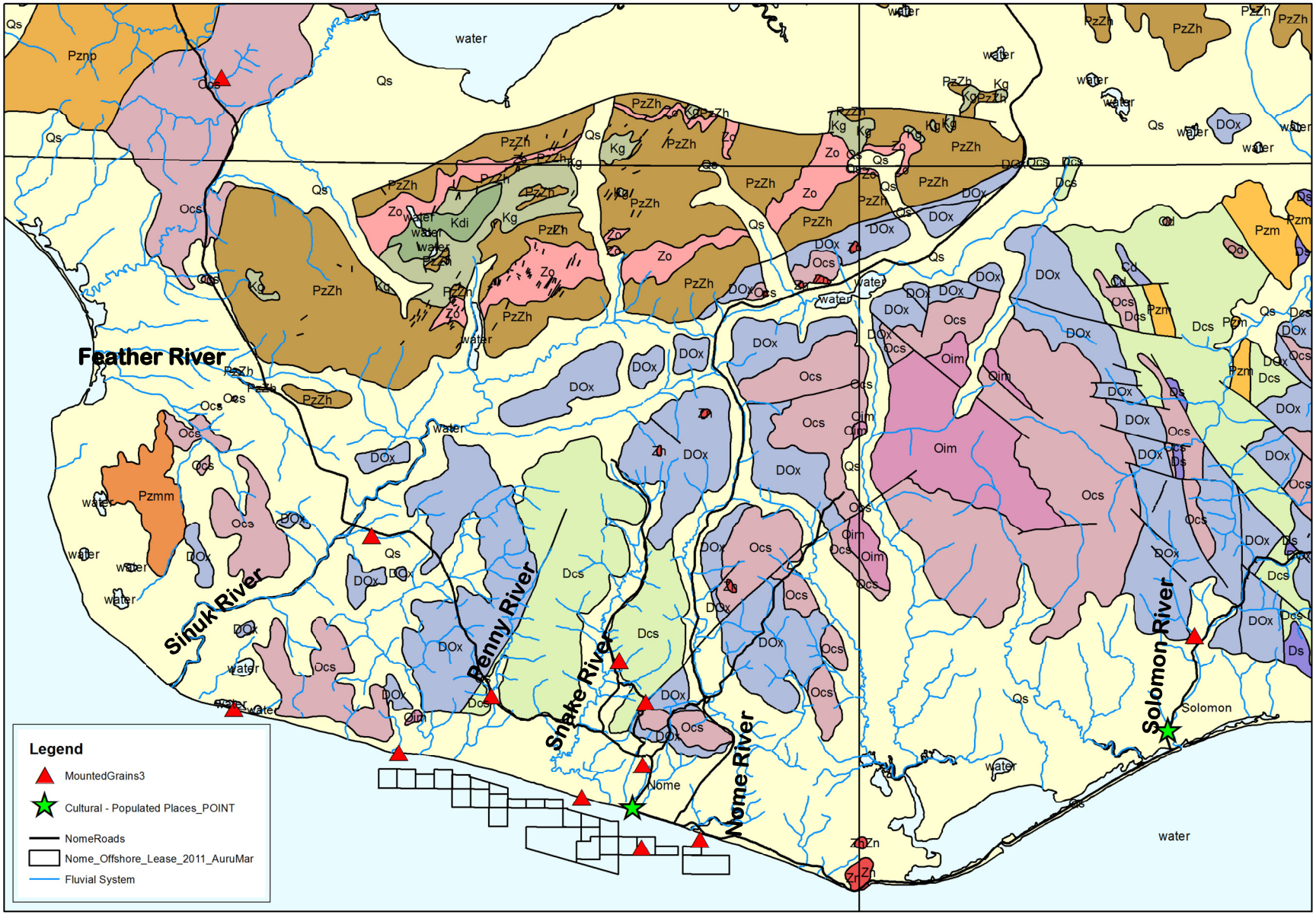

Figure 4: Onshore geology of the southern Seward Peninsula as mapped by the U.S. Geological Survey. Red triangles indicate the 12 sample sites used in this study. After Till et al., 2011.

2.3 Geomorphology and Cenozoic Geology of the Southern Seward Peninsula

The bedrock of the Nome region is covered in many places by glacial, marine, alluvial, and colluvial sediments of Pliocene, Pleistocene, and Holocene age. Many of these sediments are extremely gold rich and thus they have been extensively mined since 1898 (Bundtzen et al., 1994).

The sediment record at Nome can be explained through the action of at least two glaciations and of multiple marine transgressions and regressions. These glaciations have carved glacial valleys into the Nome Complex foothills, some of which display typical U-shaped profiles (e.g. Snake River Valley, Figure 5). Two large piedmont glaciations are recorded at Nome (Kaufman and Manley, 2004), namely the Sinuk Glaciation (Figure 6), a Pliocene-Pleistocene glaciation with a poorly constrained age, and the Nome River Glaciation, which has been dated to Middle Pleistocene age (constrained to between 400,000 kya and 280,000 kya) by Kaufman et al. (1991). Subsequent glacier advances, such as the Stewart River, Salmon Lake, and Mount Osborn/Wisconsin Glaciations, were restricted to the highest mountain valleys only (Kaufman and Manley, 2004).

Figure 5: View looking north up the Snake River valley. Note the classic U-shape typical of a glacially carved valley.

The Cenozoic sediments located at Nome have been modified by at least three transgressions related to the rise and fall of sea level (Kaufman and Brigham-Grette, 1993; Brigham-Grette and Hopkins, 1995). From oldest to youngest, these transgressions are:

a. **Beringian Transgression:** Probably a set of three transgressions that occurred at approximately 2.7 to 2.1 Ma creating and upgrading the Submarine Beach auriferous deposits.
b. **Anvilian Transgression:** A transgression, pre-dating the Nome Glaciation, which occurred at approximately 0.5 to 0.4 Ma. This transgression created Third Beach and related auriferous sediments (i.e. Monroeville and Intermediate "Beaches" – likely a misnomer. These deposits consist of auriferous sediments that were deposited, or at least redistributed, in a shallow nearshore environment at a time when the strand line lay at Third Beach).
c. **Pelukian Transgression:** A transgression that occurred at approximately 125,000 kya which created and upgraded the Second Beach auriferous sediments.

The spatial distribution and ages of the glacial and beach sediments that were deposited and re-worked as a result of the two major glaciations and three transgressions are shown in Figure 7. In summary, the Cenozoic development of the Nome coastal plain is as follows:

a. Multiple Beringian transgressions and the development of Submarine beach and Fourth Beach.
b. The Sinuk Glaciation.
c. The Anvillian transgression and development of Monroeville Beach and Third Beach.
d. The Nome River Glaciation.
e. The Pelukian Transgression and development of Second Beach.
f. The Salmon Lake Glaciation (constrained to highest mountain valleys).
g. The Pleistocene/Holocene Transgression forming the current day beach.

In addition to the palaeo-processes of glacial valley and beach development, the landscape is also impacted by on-going geomorphological processes important to

the development a gold placer. Of particular importance are the processes associated with the periglacial environment. Periglacial lowering of valley slopes through solifluction and subsequent fluvial incision during warmer months is an effective process for mass sediment movement down slopes (Matsuoka, 2001). Figure 8 shows an excellent example of “stone polygon” ground, which develops through the shattering of basement rocks as a result of freeze/thaw action, – as well as solifluction terraces and lobes on a hill slope. Although the general rate of movement of terrace and lobe fronts is thought to be low (~10 mm/year according to Alexander and Price, 1980), the abundance and consecutive succession of these terraces migrating over seasons towards the valley base can result in substantial amounts of basement detritus being deposited where fluvial creeks and rivers can further distribute the material. This effective process of mass sediment erosion undoubtedly has an impact on gold liberation and transport into fluvial placers.

The Seward Peninsula is drained by a variety of river systems, which are primarily entrenched in glacial valleys (Figure 4). The largest river is the Sinuk River to the west of Nome, whilst the immediate Nome area is drained by (from west to east) the Penny River, the Snake River, and the Nome River. The Solomon River drains the land to the east of the study area.

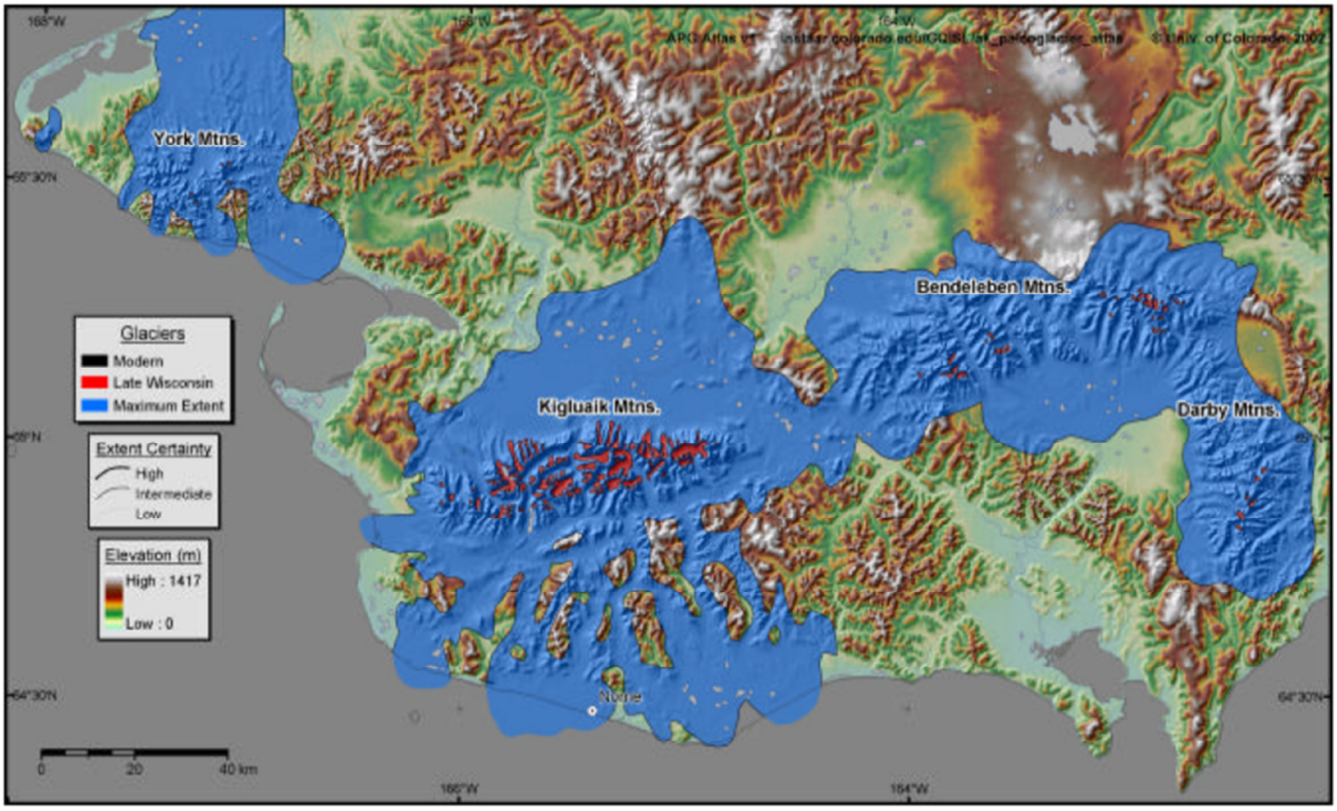

Figure 6: Maximum glacial extent in the Nome region for Pliocene-Pleistocene and Holocene glaciations (blue). Note that the maximum glacial extents into offshore regions are poorly constrained and could extend farther than indicated on this map (Kaufman and Manley, 2004).

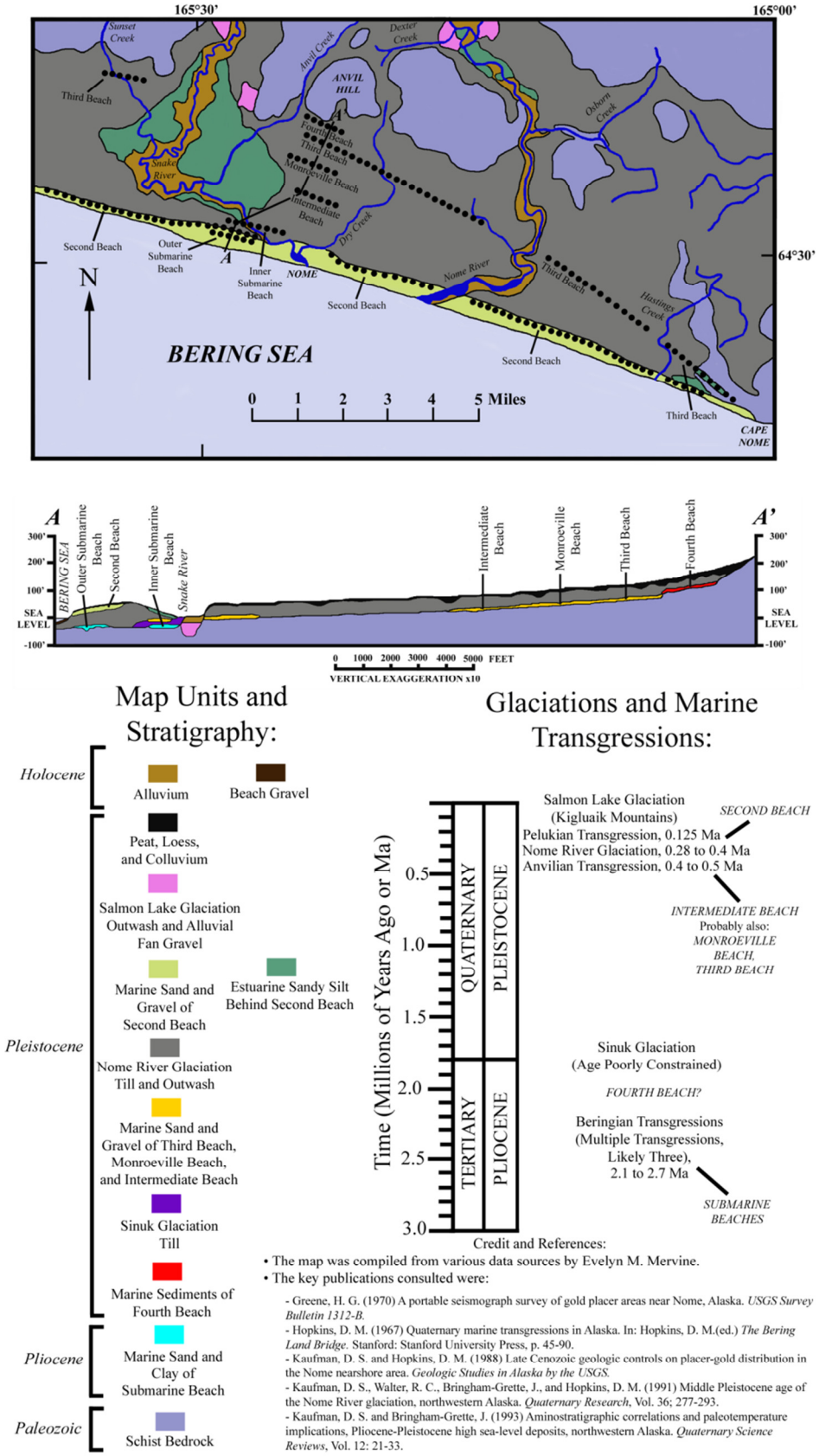

Figure 7: Generalized map of Cenozoic sediments on the Nome coastal plain (from Mervine, 2013). The locations of important mineralised "beaches" are indicated by the dotted lines. The map and cross-section are modified from Greene (1970).

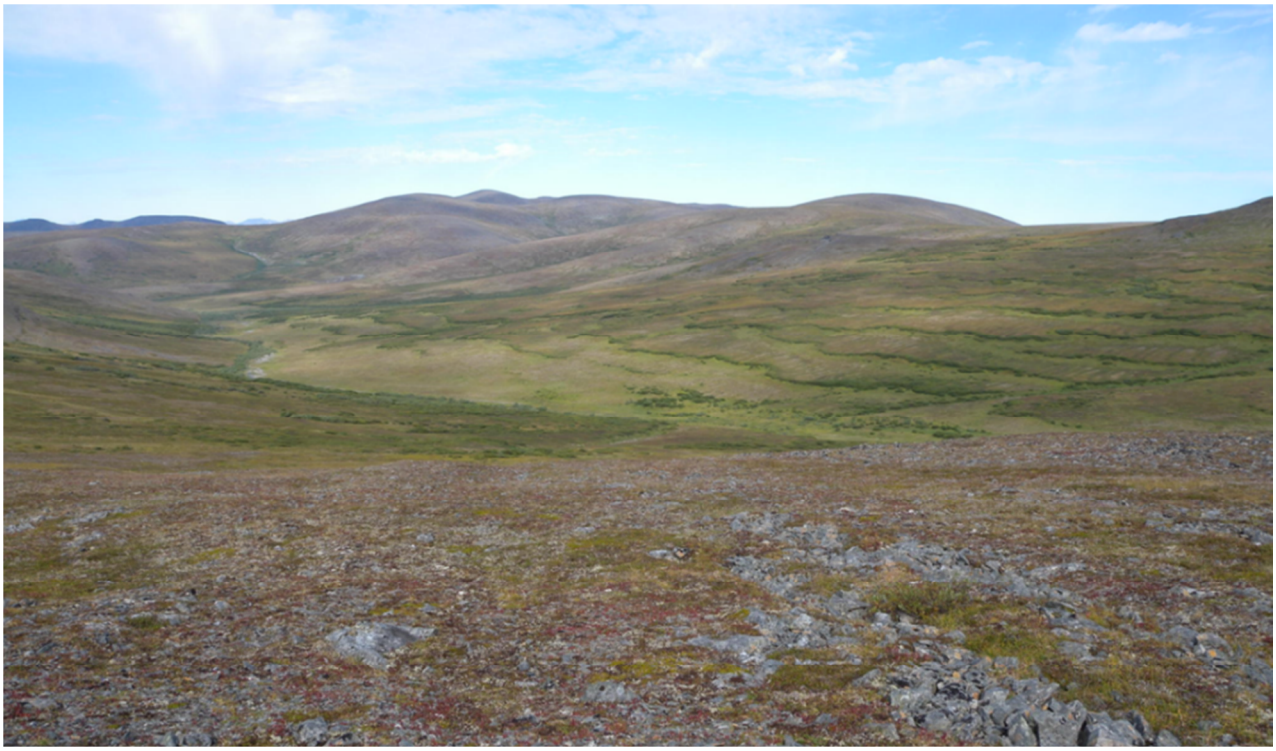

Figure 8: The periglacial landscape showing shattered Nome Complex rocks in the foreground as a result of freeze/thaw action and solifluction terraces and lobes in the background. Photo: U. Burger on Solomon-Council Highway.

3 Review on Gold Chemistry, Genesis, and Profiling

3.1 Gold Chemistry

Natural gold occurs predominantly as a native metal, which is commonly alloyed with variable amounts of other metals, particularly silver (Ag) and also sometimes mercury (Hg), copper (Cu), palladium (Pd), antimony (Sb), platinum (Pt), and bismuth (Bi) (Chapman et al., 2002; Chapman et al., 2009). Other elements that may be associated with gold include nickel (Ni), thallium (Tl), barium (Ba), lead (Pb), zinc (Zn), tellurium (Te), bismuth (Bi), tungsten (W), uranium (U), tin (Sn), fluorine (F), boron (B), molybdenum (Mo), and tellurium (Te) (Robert et al., 1997; Oberthür and Weiser, 2008). These metals may alloy with gold as major elements (concentrations >1%) or as minor elements (concentrations between 0.1% and 1%), as often seen with Ag and sometimes with Hg, Cu, and Pd. More commonly, these metals (and other elements) may only be present in trace element concentrations (<1000 ppm). In addition, gold grains may also contain inclusions, which when analysed provide an opportunity for microchemical signature classification. For example, significant concentrations of sulphur (S), iron (Fe), and arsenic (As) may be detected when there are inclusions of minerals such as pyrite (FeS_2) and arsenopyrite (FeAsS) present (Chapman and Leake, 2000).

Because there is a wide variety in styles of gold mineralization there is also a wide variety in the chemical composition of gold. The chemical composition of gold can thus potentially be used to identify and profile distinct gold deposits and the genetic processes that led to the gold mineralisation (Robert et al., 2007). For example, variation in the proportions of major and minor elements have been used to distinguish gold deposits in a region (Watling et al., 1994; Leake et al., 1998; Outridge et al., 1998; Dixon, 2012). Alloy compositions and microchemical signatures associated with different styles of gold mineralisation are well summarised in Chapman et al. (2009), from which Table 2 has been extracted.

Table 2: Alloys and microchemical signatures associated with different styles of gold mineralisation (from Table 6 in Chapman et al., 2009, and references therein).

		Mineralization/microchemical signature			
Style of mineralization	Locations	Ag range (%)	Other metals	Inclusion suite, (I)/mineralogy (M)	Comments
Orogenic: Phanerozoic	Caledonides in the UK,[1] Malaysia,[2] New South Wales,[3] Klondike district, Yukon[4]	4–20	Occasional Hg to 10%	(I): S,As,±Sb	Ag shows little variation in individual occurrences
Orogenic: Archean	Mazoe, Cheguti, Kadoma, Kwekwe, Silobela, Zvishavane, Zimbabwe[5]	5–50	Occasional Hg to 3%	(I): S, As, ± Te,Bi	Ag shows little variation in individual occurrences
Epithermal: low sulfidation	Eureka Dome, Yukon,[4] Ochil Hills, Scotland[4]	1–50	Hg common to 10%	(I):S, ±As, ±Te,Bi	Ag highly variable in the same occurrence
Epithermal: high sulfidation	Mount Kasi, Vanua Levu, Fiji[6]	Reported as variable		(M): Cu-Sb-As-S-Te	Limited information available, enargite inclusions would be expected
Porphyry	Glasdir, N. Wales,[1] Glen Lednock, Scotland[1]	Variable: 5– 50		(I) S, AsS, Bi, Te	Limited information available worldwide; in the UK, MoS_2 inclusions observed
Intrusion related	Curraghinalt,Co. Tyrone and Balwoges, Donegal, N. Ireland,[1] Scroggie Creek, Yukon[7]	8–20	May show elevated Cu (to 2%)	(I) S, ±As, ±Te ±Bi	Limited information available worldwide
Skarn	Veletanga, Equador[8]	>11		(I) Pb-Ag-Te-S	Limited information available
Oxidizing hydrothermal: low temperature (T <120°C)	Devon, UK,[9] Svoboda nod Úpou, Czech R.,[10] Serra Pelada, Brazil[11]	0–6	Pd or Hg to 12%, Rare Cu to 4%	(I) Selenides	Ag often extremely low; Au-Pd alloys common; sulfides absent from high Au and Au-Pd alloys
Oxidizing hydrothermal: high temperature (T >600°C)	Cauê, iron mine,[12] Conceição iron mine,[13] Itabira, Brazil		Pd to 19.2%, Cu to 2%,	(M): mertierite II, palladseite, minor sulfides	The complex polymetallic selenides reported in low-temperature oxidizing hydrothermal mineralization are absent here
Authigenic	Kalgoorlie, Western Australia,[14] New Zealand, [15] Argentina[16]	0	None	None	

References:[1] = Chapman (2007),[2] = Henney et al. (1994),[3] = Chapman et al. (2002),[4] = Chapman and Mortensen (2007),[5] = Styles et al. (1995),[6] = Naden and Henney (1995),[7] = Mortensen et al. (2005),[8] = Potter and Styles (2003),[9] = Leake et al. (1991),[10] = Tásler et al. (2003),[11] = Cabral et al. (2002b),[12] = Olivo et al. (1995),[13] = Olivo et al. (2001),[14] = Lawrance and Griffin (1994),[15] = Youngson and Craw (1995),[16] = McCready et al. (2003)

3.2 Gold Ore Genesis

Classification of the style of gold mineralisation has evolved considerably over the past few decades. Early classification schemes were based on the "Lindgren Model" (Lindgren, 1907; Lindgren, 1933), which classified gold mineralisation style based on temperature and depth (epithermal, mesothermal, hypothermal). Later definitions broadened the classification based on the characteristics of the deposit, such as the presence of veins and stockworks or the host rock minerals present (Boyle, 1979). Recently, gold deposits have been classified based on geological processes, specifically distinguishing between gold related to igneous activity (e.g. epithermal, porphyry, skarns, volcanogenic massive sulphide) or to metamorphism resulting in "orogenic" gold (Groves et al., 2003; Groves et al., 2005; Robert et al., 2007; Hronsky et al., 2012). In addition to gold deposits associated with igneous activity and metamorphism, a third type of gold deposit is placers formed by the

erosion and redistribution of gold from one or more primary deposit in a concentrated area (Garnett and Bassett, 2005). Due to widespread mineralisation across a large area or metamorphic terrane orogenic gold deposits are increasingly being seen as an important mineralisation style contributing to the development of placers (Groves et al., 1998; Pitcairn et al., 2006).

3.3 Geochemical Gold Profiling Techniques and Examples

For placer deposits, geochemical profiling is a powerful tool for linking placer gold grains to their sources. Commonly, the original sources of gold mineralisation which eroded to produce a placer deposit are enigmatic. In combination with analysis of gold morphology and mineral inclusions, geochemical profiling of gold has successfully been used to link placer gold grains with likely sources in a number of instances (Leake et al., 1998; Chapman and Leake, 2000; Dumula and Mortensen, 2001; Chapman et al., 2002; Chapman and Mortensen, 2006; Rasmussen et al., 2007; Chapman et al., 2010). Even when a physical source cannot be identified, information can still be obtained about the type of gold source (e.g. epithermal, orogenic, volcanogenic massive sulphide, porphyry, greenstone belt) from which placer grains originated. Where multiple sources have contributed to a placer deposit, gold profiling can help distinguish the temporal and spatial distribution of grains from various sources.

To date, the most common way to analyse elements in gold has been with the electron microprobe (EMP), which can analyse major and minor elements but generally not trace elements (detection limits are ~0.3 to 0.5 weight percent for most elements, e.g. Leake et al., 1998). However, recent advances in EMP technology and equipment have lowered detection limits for trace elements significantly (down to ~10 to 50 ppm), paving the way for the future use of this technology across a broader spectrum of elements.

Since the mid-1990s Laser Ablation Inductively Coupled Mass Spectrometry (LA-ICP-MS) has been employed for geochemical gold profiling (Watling et al., 1994; Outridge et al., 1998). LA-ICP-MS can analyse a large suite of trace elements down to very low concentrations (a few parts per billion). Unfortunately, there are only a handful of papers reporting LA-ICP-MS trace element data for gold grains, resulting in a small database for comparison (e.g. Watling et al., 1994; Outridge et al., 1998; Žitňan et al., 2010; Gauert et al., 2011).

3.3.1 Gold Profiling Using Electron Microprobe Analysis (EMPA)

To give an example of the power of gold profiling for placer deposits, Leake et al. (1998) carried out a chemical study of 1794 placer gold grains from 55 sites in a 7 km by 18 km area in Leadhills, Scotland. An EMP was used to analyse major and minor elements (Au, Ag, Cu, Hg, and Pd) of the gold grains as well as mineral inclusions. Based on gold chemistry and inclusions, four distinct populations and one sub-population of placer gold grains (Table 3) were identified. For three of these gold populations, Leake et al., 1998 identified a likely source. For Type 1 and 1a, the likely source is a mesothermal (orogenic) shear zone deposit. For Type 2, the likely source is Tertiary mafic dykes. For Type 3, the source is uncertain but could possibly be glacially moved ultramafic material. For Type 4, the likely source is Permian redbeds. Futhermore, Leake et al. (1998) were able to map out abundances of particular types of gold, which improved the geological understanding of the placer deposit. The example of Leake et al. (1998) illustrates that unravelling the source(s) of placer gold grains can be complex but that geochemical profiling is a powerful tool for helping to do so.

Another example is a study of placer gold grains from the Steward River area, Yukon, Canada (Dumula and Mortensen, 2001). This study employed EMP analysis and was thus limited to analysis of the elements Ag, Au, Cu, and Hg. Nevertheless, Dumula and Mortensen, (2002) were able to identify likely style(s) of lode mineralisation for placer gold grains in several streams. In the Eureka and Black Hills Creeks, the high levels of Ag and Hg and low Cu indicated an epithermal gold source in the Eureka Dome or Henderson Dome area. In the Moosehorn Range Creeks, the high fineness, high Cu, and low Hg indicated that the placer grains were likely derived from intrusion-related, gold-bearing quartz veins. Placer grains in the Thistle, Kirkman, and Blueberry Creeks were similar to those in Moosehorn, suggesting that perhaps there is an undiscovered intrusion in the vicinity. Again, geochemical

Table 3: Types of placer gold grains identified by geochemical profiling and inclusion assemblages in the Leadhills area, Scotland. From Table 3, Leake et al., 1998.

Type	Gold composition	Inclusion assemblage
1	8–13% Ag	arsenopyrite, pyrrhotite, pyrite, chalcopyrite, galena, sphalerite, cobaltite, aurostibite
1a	3–8% Ag	arsenopyrite, pyrrhotite, pyrite, chalcopyrite, galena, cobaltite, gersdorffite, pentlandite?
2	16–31% Ag	gersdorffite/ullmanite, pyrite, Ni arsenide, ullmanite, breithauptite, pentlandite
3	<1% Ag, 0–5.3% Cu	isoferroplatinum, tulameenite, Cu–Pt, Cu oxide
4	<3% Ag, 0–6.3% Pd	clausthalite, tiemannite, Cu selenide

profiling of gold proved a valuable tool for identifying potential sources for placer gold grains.

3.3.2 Gold Profiling Using Laser Ablation Inductively Coupled Mass Spectrometry (LA-ICP-MS)

A good example of the powerful nature of LA-ICP-MS analysis of a wide set of trace elements is a study by Brown et al. (2003) in the Cleo gold deposit in Western Australia. In this study, trace elements were used to distinguish between two lodes: a banded iron formation hosted ore zone in the Sunrise Shear Zone and a high grade, vein-hosted ore in the Western Lodes. The two ore zones are very similar in major element chemistry, isotopes, and fluid inclusions. However, the Sunrise Shear Zone gold is enriched in Ni, Pb, Sn, Te, and Zn and depleted in As, Bi, Cd, Cu, and Sb relative to the Western Lodes gold. Trace elements thus indicate two separate mineralization events for these deposits. In this study, analysis of trace elements provided insight, which major element data could not, into mineralisation mechanisms that helped the researchers understand why higher grade ore was encountered in the Western Lodes.

4 Methodology

4.1 Sampling Challenges

The lack of local infrastructure limits the range of sample sites accessible across the southern Seward Peninsula. There are four gravel roads originating at Nome: a coastal road heading east past Safety Sound towards the village of Council (Nome-Council Highway), a north-western route towards the village of Teller (Nome-Teller Highway), a well maintained northern route up the Nome River valley towards Salmon Lake and Mary's Igloo (Nome-Salmon Lake Highway), and a jeep track northern route up the Snake River Valley.

The Nome-Teller Highway is the best maintained route and provides access to the geology of the Sinuk and Teller systems. The Nome-Council Highway is a major road and is generally well maintained, granting access to the Solomon system. The Nome-Salmon Lake Highway is well maintained but does not grant easy access to streams for sampling; however, it is a route key to enabling an overall understanding of the local geology. The northern road along the Snake River valley is somewhat maintained and grants access to multiple streams draining the Nome Complex, but after heavy rains it is often washed away at stream crossings. During the 2013 field season, this route had suffered substantial damage and was not navigable past Rock Creek Mine, limiting access to the inland portions of the Nome system up this valley.

When sampling, care must be taken not to trespass on private land. Much of the land around Nome is privately owned and leased for artisanal gold mining. Trespassing is not condoned and permission must be granted to access private land for sampling. This was a particular challenge up the Nome River valley and restricted sampling of this area. The danger of conducting field sampling in the remoteness of the Alaskan tundra is further enhanced by the presence of brown and black bears in the region. Great care must be taken in order to not startle any bears or cause any confrontation with one. Bear mace (pepper-spray) is available at local stores in Nome should field visits without a gun-wielding guide be required.

4.2 Field Sample Collection

Sample collection was completed during three field seasons in the vicinity of Nome, Alaska, from 2011 to 2013. The author was primarily responsible for the collection of six of the twelve samples used in this study (AK100, AK111, AK117, AK121, AK123, AUR-12-854, and RC4), whilst the remaining six samples were donated to the study by Nome locals (AK123 and ADEM) or were collected by an AuruMar colleague (AK015, AK021, AK028, and AK032).

Samples were collected in the field using a standard riffled gold pan. Stream or beach sediment was loaded into a pan, large lithic clasts were removed and the remainder roughly panned until a majority heavy mineral concentrate remained (Figure 9). A quick visual scan was conducted to ascertain the rough number of grains present. If less than ~20 gold grains were immediately visible, further sediment was added to the pan and the process repeated until sufficient gold grains were visible. The heavy mineral sample was then carefully decanted into a labelled sealable bag, along with a tin label.

Post field collection the sample was further concentrated by careful panning in a laboratory. The sample was panned down until only ~20 g of heavy mineral concentrate (primarily magnetite, rutile, garnet, ilmenite, and gold) remained. The sample was then allowed to air dry.

Figure 9: Photographs of the author panning various stream sediments on the Seward Peninsula. Photographs courtesy of Dr. Mervine and Dr. Saravanakumar.

4.3 General Sample Preparation

Gold grains from the panned concentrate were picked under a binocular microscope using a single bristle from an artist's paintbrush. This minimised morphological damage to the soft grains, which can be easily damaged when picking is done using a harder tool such as a pair of tweezers. As a general rule, twenty grains from each site were required to produce a statistically robust dataset. This was achieved for all samples except sample AK032 and RC4 (see Table 4).

After picking, gold grains from each sample site were mounted on double sided carbon tape on a glass slide. The slide was appropriately labelled with the Sample ID and markings to indicate top and bottom so as to be able to assign a unique grain ID to each gold grain. Once mounted, gold grains again are very difficult to remove again, and therefore care was taken to mount gold grains of similar thickness together to better facilitate grain polishing at a later stage. Thus, multiple slides were prepared for sample sites where gold grain thickness varied substantially.

Table 4: List of samples used in this study.

Sample ID	Location	# Slides	# Grains Imaged	# Grains Analysed	Eastings	Northings
AK021	Washington Creek	1	40	35	457704	7176425
AK028	Gold Run Creek	3	23	21	444688	7216175
AK032	Sinuk Coastal Plain	1	9	5	445774	7161335
AK100	Penny River	1	20	12	468109	7162485
AK111	Anvil Creek	2	20	20	481462	7161934
AK117	West of Cripple River	1	20	0	460075	7157502
AK121	West Beach	1	25	25	475929	7153674
AK123	Monroeville Beach	2	20	20	481195	7156505
AK015	Shovel Creek	1	20	6	529070	7167694
AUR-12-854	Exploration Panel (EP1)	2	24	4	481107	7149309
ADEM	Offshore Nome River	1	20	13	486200	7150000
RC4	Rock Creek Mine	4	2	2	479152	7165558

The "# Grains Imaged" refers to the number of grains from each site isolated and mounted and imaged by secondary electron imaging. The "# Grains Analysed" refers to the number of grains from each site which survived the polishing process and could be analysed by the EMP. Eastings and Northings are reported in the UTM 3N projection and WGS84 geodetic reference system.

4.4 Rhodes University EMPA

Rhodes University Geology Department acquired a new generation JEOL JXA 8230 Superprobe in 2012 which is currently under the management of Dr. Gelu Costin. The system has the following technical configuration (extracted from https://www.ru.ac.za/geology/epma/):

- W and LaB_6 electron gun.
- Computer automation operating through PC compatible JEOL software on Windows XP platform.
- Four wavelength-dispersive spectrometers (WDS), namely
    - One FCS type spectrometer with 4 crystals: LDE1, LDE2, TAP, and PETJ.
    - Two L type spectrometers with 2 crystals each: TAP, LiF (gas-flow counter), and LiFL, PETL (xenon counter), respectively.
    - One XCE type spectrometer with 2 crystals: PETL, TAPL.
- Secondary-electron (SE) and backscattered-electron (BSE) detectors
- "MiniCL" Gatan CL imaging system (visible range: 185 nm - 850 nm)
- Accelerating voltage: 0.2 to 30 kV
- Auto-focus system for optimal sample positioning
- Carbon coating: Q150T E High Vacuum Evaporator with film thickness monitor module

In this study, the Rhodes University EMP was employed to

- Conduct high resolution (1-10 microns scale) BSE/SE imaging
- Conduct qualitative element analysis (WDS scans) to determine major elements present in gold grains of interest
- Conduct standard quantitative analysis of major, minor and trace elements in gold grains as point analysis
- Conduct qualitative element mapping of selected elements for gold grains of interest

4.5 Secondary Electron Imaging (SEI)

High resolution secondary electron images of gold grains were obtained in order to conduct particle size measurements as well as to conduct textural analysis of the grain surface and grain morphological analysis. Because gold is a good conductor of electrons and the grains were mounted on carbon tape, it was not necessary to carbon coat the slides prior to imaging. Slides were loaded into the JEOL JXA-8230 EMP. The EMP was set to Secondary Electron (SE) mode and secondary electron image (SEI) photographs were acquired for each grain using a 15.0 kV excitation voltage and a working distance (WD) of 11.1 mm. Magnification for each grain was individually set such that the grain filled the image (i.e. highest resolution in a single image). Contrast and brightness settings were calibrated such that surface textures and features were highlighted. For certain grains a duplicate image in Backscattered Electron (BE) imaging mode was taken to provide compositional contrast within the selected grain. All images have an associated scale bar, timestamp, and probe settings imprint on them.

Qualitative wavelength dispersive spectrometer (WDS) scans were conducted on selected grains (approximately 10% of the dataset) to identify the major elements present and thus allow an informed recipe to be designed prior to quantitative EMP analysis. Grains from all sites showed significant presence of silver (Ag) in addition to gold (Au). Copper (Cu) was rarely observed. Although not quantitative, this exercise revealed that significant variation in Ag and Cu may exist across different sites (Figure 10) and potentially even within sites.

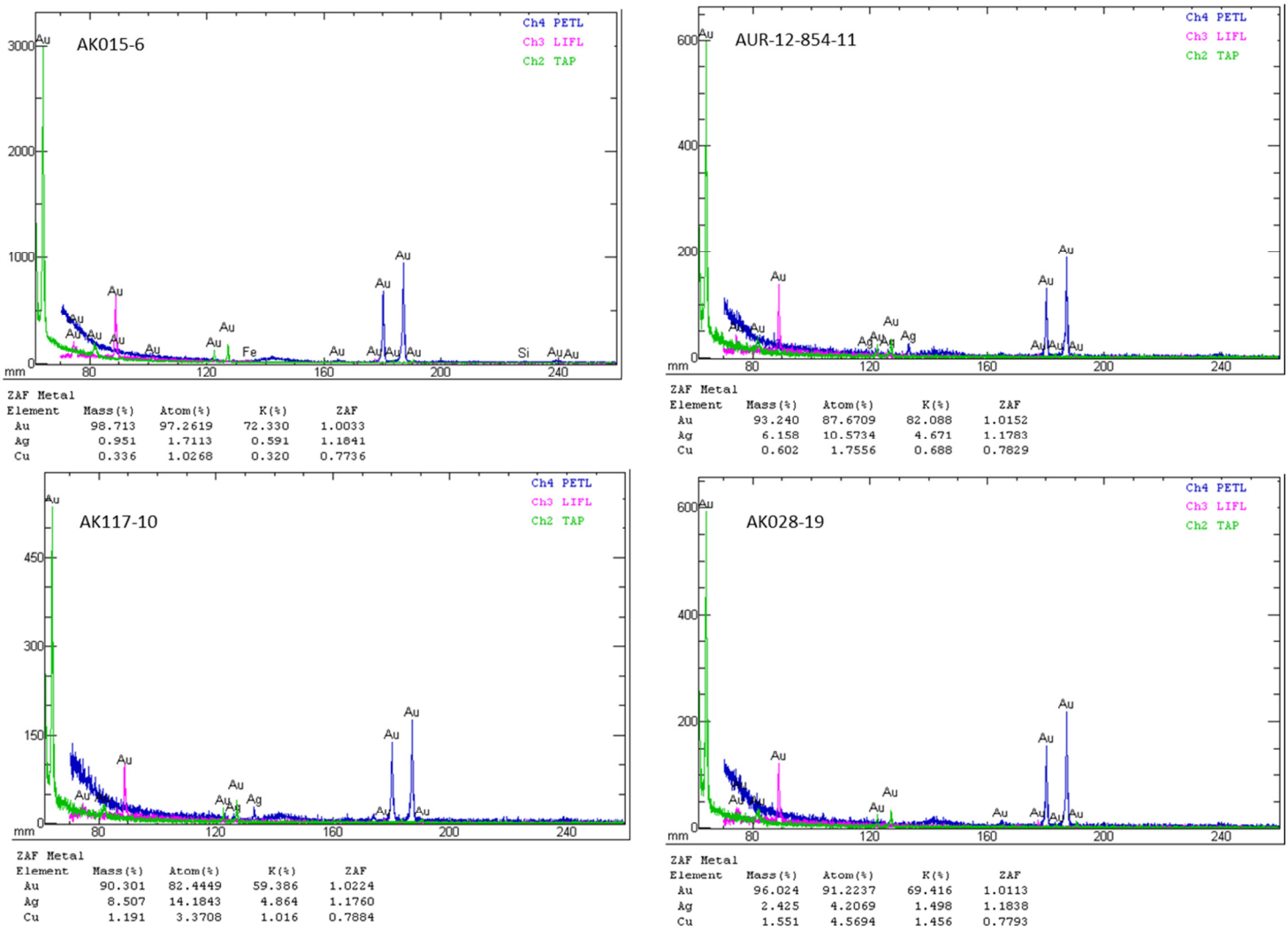

Figure 10: Examples of WDS scans performed to identify the major elements present.

4.6 Sample Preparation for Electron Micro Probe (EMP) analysis

In order to conduct quantitative EMP analysis, a well-polished grain surface needs to be presented to the electron beam. Grinding and polishing also allows the core of the grain to be exposed for analysis. Analysis of grain cores is advantageous because the cores do not contain embedded gangue material picked up during grain transport and are also unlikely to have been significantly affected by chemical processes, such as silver leaching.

Once all grains on a slide had been imaged, the slide was sent to the Rhodes University Geological Workshop for polishing. Resin was applied to each slide until all grains were covered. This ensured immobility of grains during the polishing process. The slide was subject to grinding at 10 µm intervals until all grains were exposed. The grains were then polished using a series of 9 µm, 3 µm, and 1 µm

polishing mats to present a well-polished surface. Due to the polishing method used, thicker grains were ground more in order to expose adjacent thinner grains. On some occasions, grains were plucked out of the resin during the grinding process resulting in the loss of the grain. Thus, the number of grains which were analysed by EMP is less than the number of grains imaged, with the difference between these numbers reflective of the number of grains lost for each sample (Table 4). In particular, three samples suffered severe grain loss: Sample AK117 suffered complete loss of all grains during polishing, Sample AUR-12-854 suffered loss of twenty of twenty-four grains, and Sample AK015 suffered loss of fourteen of twenty grains. The remainder of the samples fared better with none to minimal loss (<10% of total grains) up to a maximum of 40% grain loss. After polishing, the slides were carbon coated using a Q150T E High Vacuum Evaporator. Carbon coating was required to ensure conductivity of electrons across the non-conductive resin covered surface of each slide.

4.7 EMP calibration

EMP calibration was undertaken to ensure quantitative major, minor, and trace element analysis following a similar process to that described in Youngson et al. (2002). For Au, Ag, and Cu, pure metal standards were used, whilst a crystalline cinnabar standard was used for Hg. Given that Au and Hg lie adjacent to each other on the Periodic Table, the wavelengths of generated K, L, and M line X-rays for each element are similar. In order to avoid resultant interference between Au and Hg, both background positions for Hg were set on the side of the Hg peak farthermost away from the Au peak, in contrast to the norm of measuring on either side of the Hg peak. Similarly, both background positions for Au were set on the side of the Au peak farthermost away from the Hg peak. Pure metal standards were also used to calibrate trace elements (Te, Sb, Bi, Sn, W, Pb, and Zn) whilst arsenopyrite (FeAsS) was used to calibrate for As. Conventional ZAF correction procedures, incorporating the mass absorption coefficients of Henke et al. (1982), were used.

4.8 EMP Analysis

4.8.1 Major and Minor Element Analysis

The Rhodes University JEOL JXA 8230 Superprobe was used to analyse Au, Ag, Hg, and Cu using a spot size of 1 µm, a current of 20 nA, and an accelerating voltage of 15.0 kV. Counting times were 10 seconds (and 5 seconds each for positive and negative background) for Au and 30 seconds (and 10 seconds each for positive and negative background) for Ag, Hg, and Cu. The detection limits achieved were as follows: Au = 650 ppm, Ag = 350 ppm, Hg = 300 ppm, and Cu = 170 ppm. Appendix C presents a dataset of the major and minor elements (Au, Ag, Hg, and Cu) available for grains from eleven sites across the southern Seward Peninsula, excluding Site AK117 (grains lost during polishing).

4.8.2 Trace Element Analysis

After major and minor element analysis had been completed, the probe was calibrated for trace element analysis. A large suite of ten trace elements were initially identified for analysis (Cu, Hg, Te, As, Sb, Bi, Sn, W, Pb, and Zn). For trace element analysis, a spot size of 1 µm was used with a current of 150 nA and an accelerating voltage of 15.0 kV. Counting times were 100 seconds (and 50 seconds each for positive and negative background). The detection limits achieved were as follows: Cu = 30 ppm, Hg = 70 ppm, Te = 30 ppm, As = 40 ppm, Sb = 10 ppm, Bi = 30 ppm, Sn = 20 ppm, W = 40 ppm, Pb = 50 ppm, and Zn = 20 ppm.

Unfortunately, after analysis of selected grains from Sites AK028, AK032, AK121 and ADEM, none showed any result for Bi, Zn, Pb, and Sn. As trace element analysis is time consuming, it was decided to not analyse Zn, Pb, and Sn further. Thus, Appendix F presents a dataset of the remaining seven trace elements (Cu, Hg, Te, Bi, As, Sb, and W) available for grains from ten sites across the southern Seward Peninsula, excluding Site AK117 (grains lost during polishing) and Site RC4 (trace elements not analysed).

5 Sampling and Sample Descriptions

5.1 Introduction to Sample Sites

A total of 241 gold grains were sourced from eleven placer gold sample sites across the Seward Peninsula. In addition, ore specimens from a local hard rock gold mine (Rock Creek) were collected and polished thin sections were produced. Two occurrences of primary gold were identified in the polished sections for analysis. Of the eleven placer sites, one site is in the Teller system, one site is in the Solomon system, two are in the Sinuk system, and seven are in the Nome system (Figure 11). Sites were selected on the basis of being accessible for sampling, having sufficient grains in a sample to be statistically robust (usually > 20 grains), and displaying variation in deposit style (i.e. beach, marine, glacial, or fluvial). Ideally, sample sizes of >50 grains should have been used. However, funding and time constraints limited total grains for morphological and geochemical analysis to ~250. Larger sample sizes would have thus resulted in fewer sites for investigation, which in turn would have impacted on the feasibility of the research objectives.

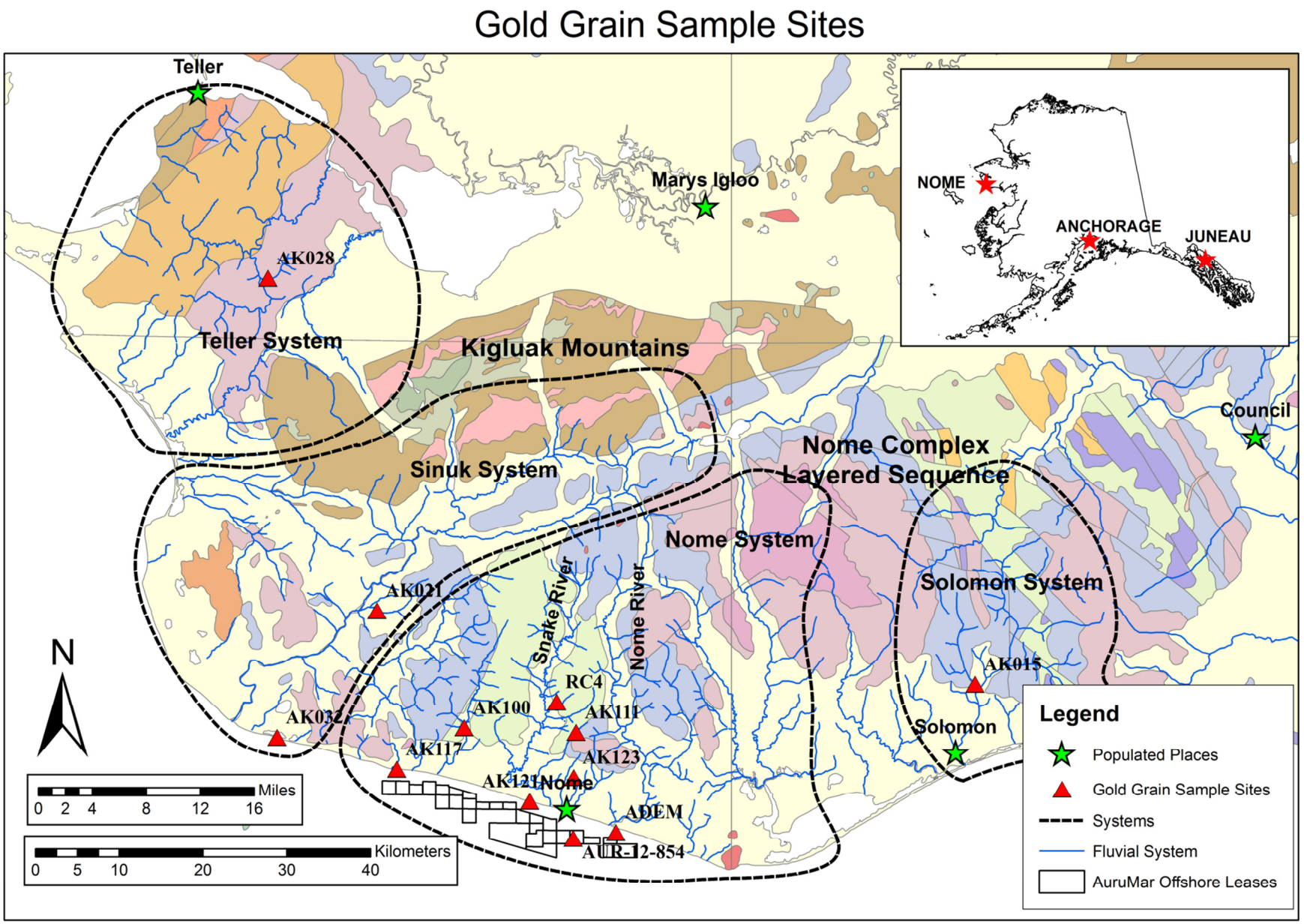

Figure 11: Map of the southern Seward Peninsula showing sample sites relevant to this study overlain on the geology of the region (Till et al., 2011).

5.2 Solomon System Sites

5.2.1 AK015 – Shovel Creek

Shovel Creek is a tributary of the Solomon River and is located approximately 50 km ENE of the City of Nome alongside the Nome-Council Highway. This sample represents the only placer gold grains from the Solomon system analysed in this study. The Solomon system is fed by a separate drainage basin to that of the Nome system; the two systems are separated by a watershed which runs through Safety Sound. There is limited field evidence of glacial activity in the Shovel Creek valley, and it is preliminary believed that gold in Shovel Creek has been restricted to fluvial transport. The latest geological map of the Seward Peninsula (Till et al., 2011) shows that Shovel Creek primarily drains mixed marble, graphitic metasiliceous rock, and schist of Devonian to Ordovician age (DOx). These rocks are all of the Nome Complex Layered Sequence. Field observations of the site reveal a predominantly marble dominated stream clast assemblage (~40%), with appreciable amounts of graphitic schist (~20%), pelitic schist (~20%), Casadepaga Schist (Ocs, ~10%), and quartz (~10%), as shown on Figure 12.

Although intense panning was conducted at this site, only 12 gold grains were recovered from stream panning. The heavy mineral concentrate recovered is dominated by garnet and minor magnetite. Although insufficient gold grains were recovered by the author during the 2013 field campaign, a previous field sampling exercise by AuruMar recovered hundreds of Shovel Creek gold grains from scraping the channels of an abandoned historic sluice box located alongside the creek. Twenty grains of similar size (a-axis ~1 mm) were selected from the two sampling efforts to comprise the sample. The sample was taken on land owned by the State of Alaska.

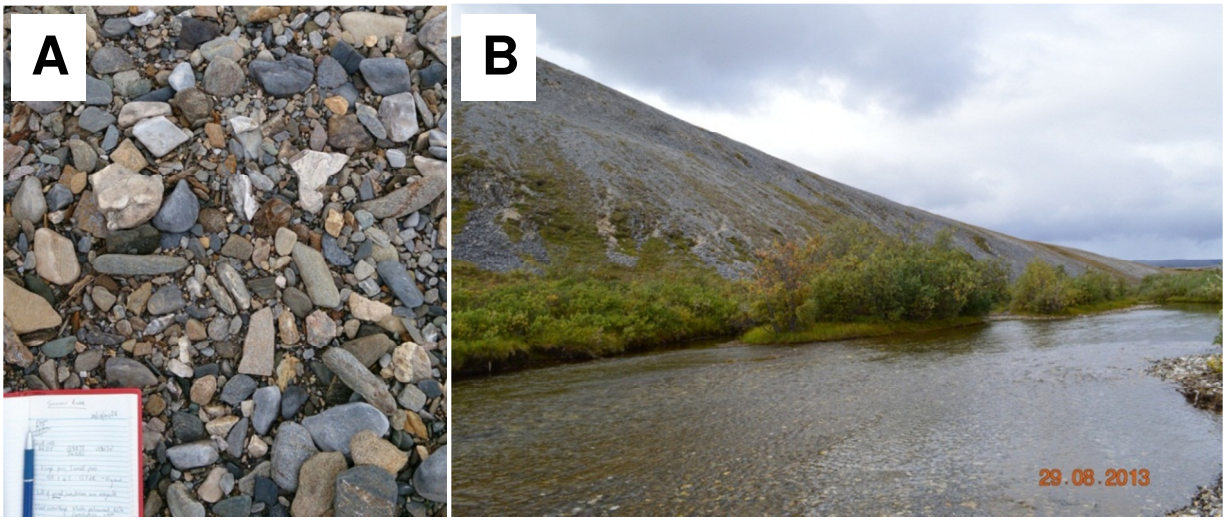

Figure 12: A: Clast assemblage from Shovel Creek. Note abundance of marble, graphitic schist, and pelitic schist. B: Shovel creek with actively eroding hillside (DOx) in the immediate background.

5.3 Teller System Sites

5.3.1 AK028 – Gold Run Creek

Gold Run Creek is located ~72 km NNW of the City of Nome and ~22 km SSE of the village of Teller, along the Nome-Teller Highway. Gold Run Creek drains Ordovician aged Casadepaga Schist (Ocs) exclusively. However, it should be noted that this site is in close proximity to what has previously been interpreted as the terminal moraine produced by a sizeable valley glacier (as evidenced by digital terrain model maps), which would have filled Canyon Creek to the SE (Figure 13). The Canyon Creek valley glacier would have drained the Proterozoic high grade metamorphic rocks and Cretaceous aged intrusions of the Kigluaik Mountains.

Stream clasts in Gold Run Creek are predominantly well-rounded discoidal Casadepaga Schist. Angular quartz and minor volcanics and granitoid/gneissic rocks are also present. Larger, sub-angular boulders of Casadepaga Schist often display evenly spaced relief features, which are possibly evidence of glacial striation (Figure 14).

Insufficient gold grains for this study were recovered from this site during the 2013 field campaign and use was made of the AuruMar grain dataset from a similar 2011 field campaign to provide 23 gold grains. Of note is that gold grains from Gold Run Creek are significantly coarser than other sites sampled with the average a-axis measuring in excess of 1 mm and grains of up to 5 mm being present. The sample was taken on land owned by the State of Alaska.

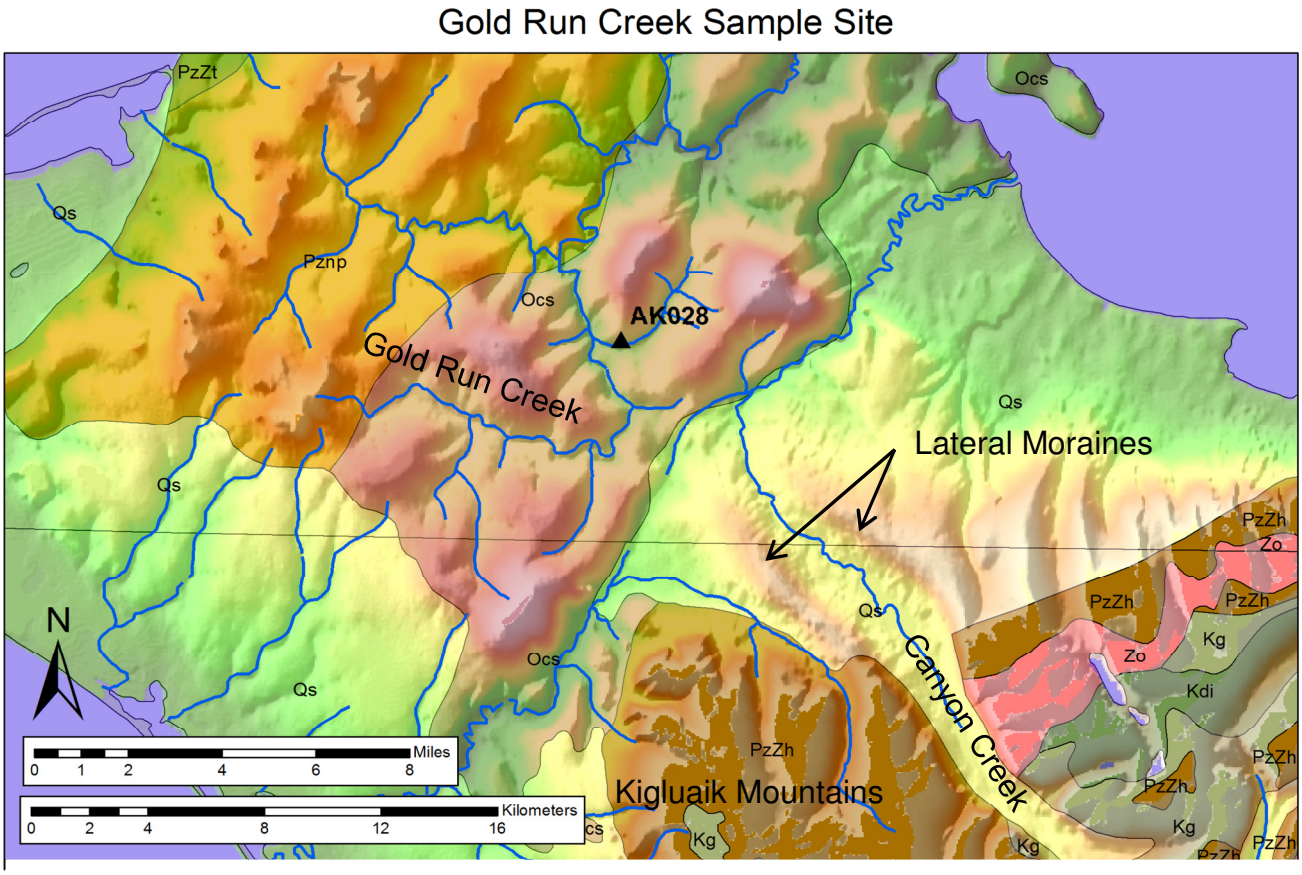

Figure 13: Map of the region in the vicinity of Gold Run Creek. Black triangles indicate sample sites used in this study. Background regional geology after Till et al., 2011.

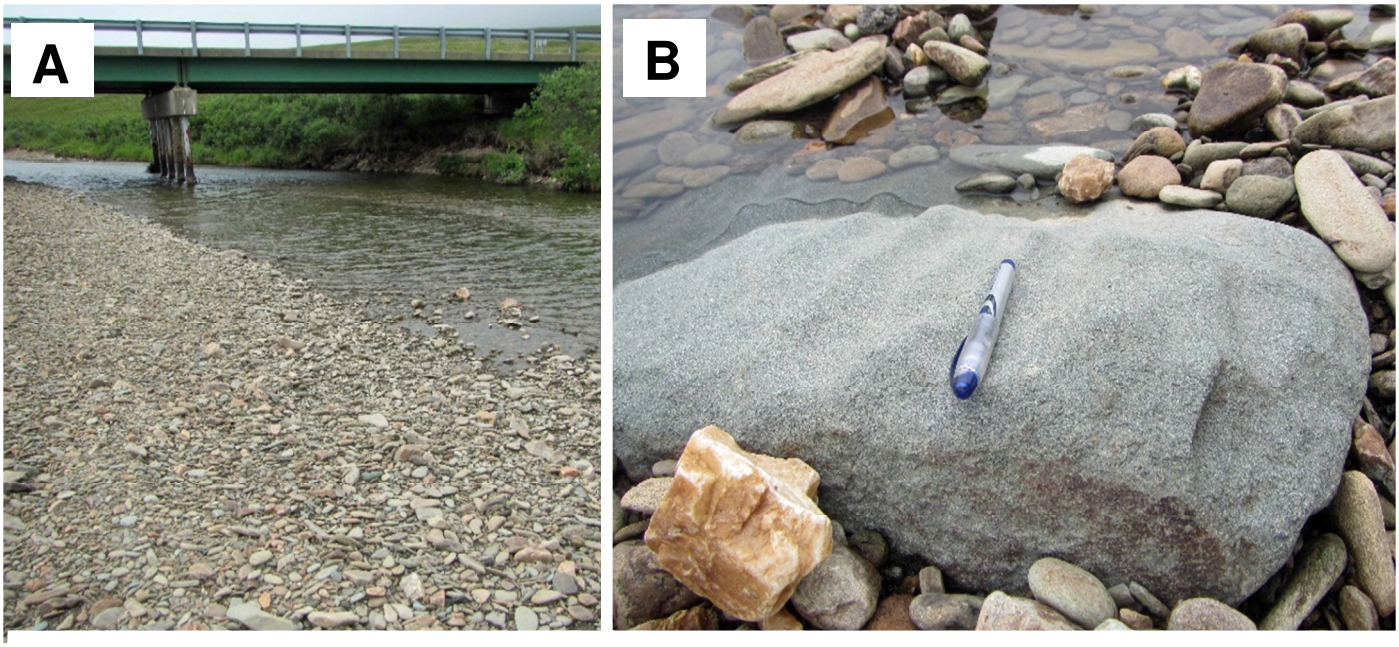

Figure 14: A: A view of Gold Run Creek looking west towards the Nome-Teller Highway. The stream is dominated by lighter coloured schist and leucocratic granitoids. B: Large boulders of Casadepaga Schist with evenly spaced "striation" marks.

5.4 Sinuk System Sites

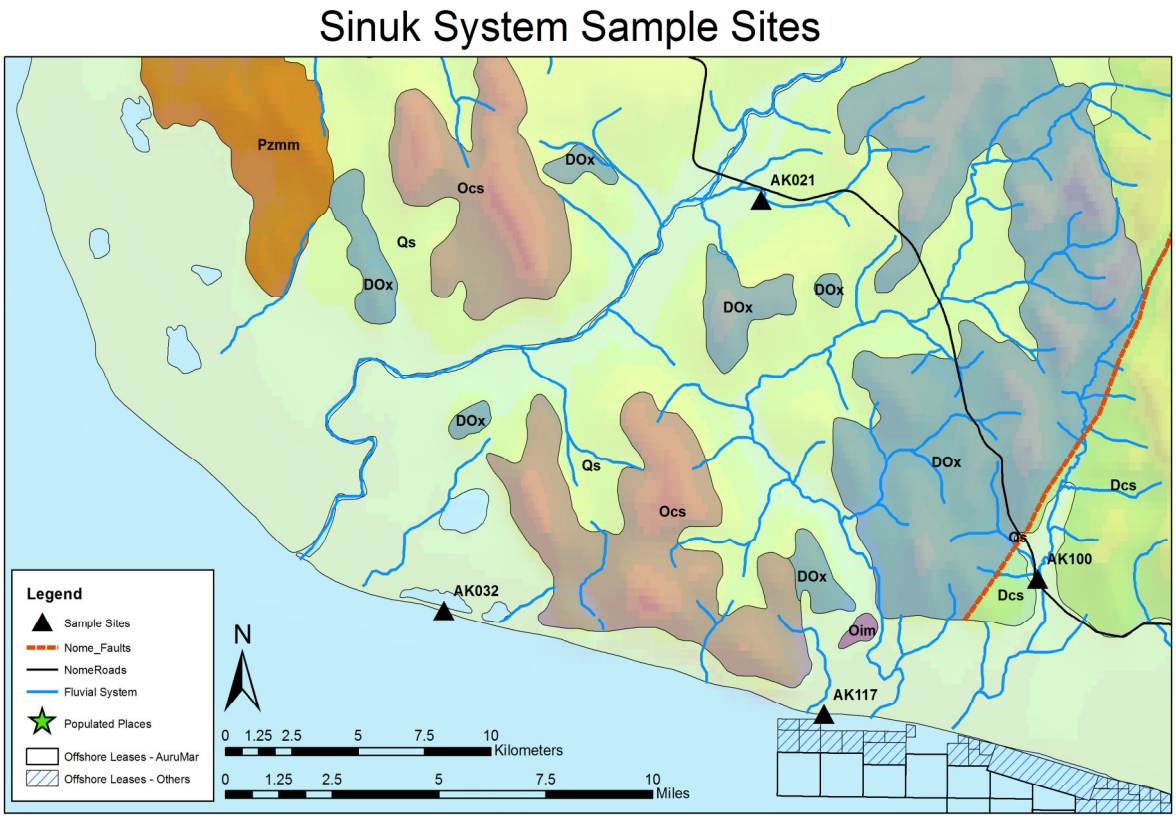

Figure 15: Sinuk sample sites west of Nome. AK032 is on the beach ~5 km east of the Sinuk River mouth and AK021 is from a tributary to the Sinuk River (Washington Creek) alongside the Nome-Teller Highway. Black triangles indicate sample sites used in this study. Background regional geology after Till et al., 2011.

5.4.1 AK021 – Washington Creek

Washington Creek is a tributary to the Sinuk River, about 1 km from the confluence to the Sinuk River, is relatively small at <10 km long, and drains DOx (Devonian to Ordovician marbles and schists) exclusively. The site is directly alongside the Nome-Teller Highway thereby making it an accessible site.

At the sampled site, Washington Creek directly cuts into a conglomerate (Figure 16). The conglomerate primarily contains rounded schist clasts and minor quartz, which are hosted in a silty to sandy matrix. The grey conglomerate is very soft and contains substantial organic material (lignite is seen preserved, e.g. Figure 17). A veneer of leucocratic granitoids lies above the conglomerate (Figure 16).

The conglomerate was interpreted as mid- to late-Cretaceous based on the absence of Cretaceous intrusive clasts (Collier et al., 1908; Sainsbury et al., 1972) and represents lithified fluvial outwash material deposited during flood events. The

veneer of granitoids is recent and may represent gravels deposited from the nearby Sinuk River (which drains the granitoid-bearing Kigluaik mountains) when in flood.

Although the site was visited by the author in 2013, the 40 gold grains analysed during this study were collected during an AuruMar field excursion in 2011. The sample was taken on land owned by the State of Alaska.

Figure 16: Two images of Washington Creek. The left image shows a basal conglomerate over which the creek flows. The right image shows the granitoid veneer which overlies much of the conglomerate.

Figure 17: Two close-ups of the Washington Creek conglomerate. The left image shows the conglomerate containing large pebble to cobble rounded schist clasts. The right image shows organic matter (lignite) hosted within the conglomerate indicating rapid burial of the material, likely during a flood event.

5.4.2 AK032 – Sinuk Coastal Plain

Access to the Sinuk system is limited with the only means of reaching the lower coastal plain being by four wheeler ATV (all-terrain vehicle). Furthermore, two major rivers must be forded and thus the area can only be accessed during low river water levels. During 2013, the author landed on the Sinuk beach by boat to conduct a field clast assembly analysis and site description. However, a sample (AK032) from the 2011 AuruMar dataset was utilised.

The site sampled is located 35 km due WNW of Nome and 5 km east of the Sinuk River mouth. The beach is dominated by rounded granitoids (30%) and angular marble clasts (20%). Angular graphitic schist (20%), Casadepaga Schist (15%), quartz (10%), and pelitic schists (5%) make up the remainder. Garnet rich zones are often present along the base of the high water berm and the storm berm (Figure 18). The garnet sand below the high water berm was sampled, and nine grains were recovered. Grains were relatively coarse for beach grains and had an average a-axis size of 850 µm. The sample was taken on land owned by the State of Alaska.

Figure 18: Photographs of the sampled site for AK032 on the Sinuk coastal plain. Note the angularity of the various schists and the rounding of the granitoids and marbles. The bladed and discoidal shapes of the schists may be attributed to the nearby presence of their parent formation and the beach depositional environment.

5.5 Nome System Sites

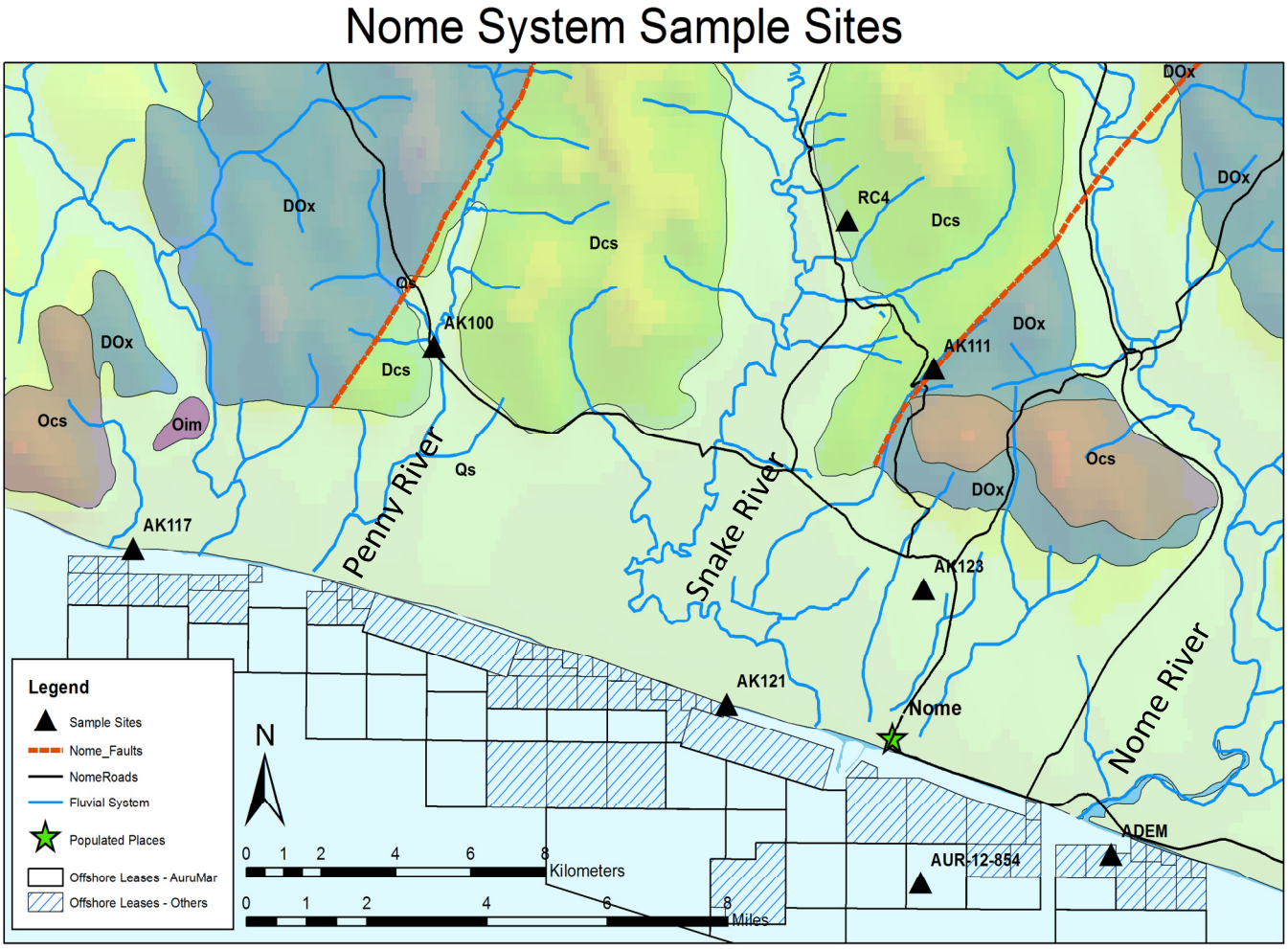

Figure 19: Nome System sample sites shown as black triangles. Background regional geology after Till et al., 2011.

5.5.1 AK100 – Penny River

The Penny River is one of three major rivers of the Nome system (the others being the Nome River and the Snake River). The Penny River is remarkably straight unlike the adjacent Snake River, which is known for its sinuosity. This feature of the Penny River may be attributed to the fact that it is entrenched along a substantial regional fault (Till, et al., 2011), which bounds the older Devonian-Ordovician marbles and schists (DOx) and the Devonian pelitic and graphitic schists (Dcs). The Penny River thus drains these two formations almost exclusively and is a key sample site (Figure 19).

Sample AK100 was taken from inner stream bank gravels (Figure 20) just inland of the Nome-Teller Highway Bridge, ~15 km NW of Nome. Stream gravels were comprised of a variety of marbles, schists, and quartz along with minor granites and gneisses. Panned concentrate was particularly rich in magnetite and garnet

Figure 20: The author and geologist Dr. Evelyn Mervine sampling Penny River inner stream gravels.

along with accessory rutile, goethite, and zircon. Gold grains recovered from this sample numbered 65 of which the 20 largest were selected for analysis (average a-axis of the selected grains equalled 460 µm). The sample was taken on land owned by the State of Alaska.

5.5.2 AK111 – Anvil Creek

Anvil Creek is the site which precipitated the Nome gold rush in 1898 (Chandonnet, 2005). The area is 8 km directly north of Nome and has been extensively worked over the last 100 years. The area is characterised by a large number of diggings and workings throughout the hillsides between Anvil Creek and Dexter Creek. Geologically, the area lies on a NE-SW trending regional fault (Till et al., 2011), which bounds the older Devonian-Ordovician marbles and schists (DOx) and the Devonian pelitic and graphitic schists (Dcs). Thick gravel sequences of up to 50 m thickness are present in places and have been interpreted as glacial outwash related (Nelson and Hopkins, 1972).

The sampled site is a contact exposure between dark grey graphitic schist (Dcs) and overlying outwash gravels (Figure 21). The contact was exposed by recent workings with earth moving equipment owned and operated by the lease owner. This site represents an excellent example of gold grains recovered from basal contact outwash gravels on bedrock. A few pans worth of basal gravel was recovered from the contact zone and panned. A total of 82 gold grains were recovered from a concentrate rich in garnet, magnetite, goethite, and pyrite. Twenty of the largest grains were selected for further analysis with an average a-axis of 1100 µm. The area is entirely owned and leased by private small scale and recreational miners and as such permission had to be attained in order to sample the site (owned by the Crutch family).

Figure 21: Anvil Creek (AK111) sample site. Dark grey graphitic schist (arrow) overlain by ~3 m package of outwash gravels.

5.5.3 AK117 – West of Cripple River

AK117 is a heavy mineral sand sample from the base of the storm berm on West beach, ~500 m east of Rodney Creek and 1.5 km west of Cripple Creek (Figure 19). The sample was taken from a heavy mineral sand (primarily garnet and magnetite) veneer of approximately 4 cm thickness that developed at the base of the storm berm (Figure 22) and was reworked by marine processes. A single large sample pan produced over 175 gold grains, mostly of the ~100 µm to ~200 µm size range. The coarsest 20 grains were selected for EMP analysis. The sample was taken on land owned by the State of Alaska.

Figure 22: The storm berm east of Rodney Creek on West Beach with a well-developed, approximately 4 cm thick heavy mineral sand veneer at its base.

5.5.4 AK121 – West Beach

Extending from the Snake River mouth to approximately 4 km west of Nome is the recreational beach mining area known as West Beach. This area is open to all small scale recreational mining activities with restrictions (no earth moving equipment and maximum 4-inch hose water supply) and caters primarily for “shovel-and-sluice box” workers.

West Beach is characterised by a relatively constant width of ~40 m (low-tide mark to beach cliff), a beach cliff of ~3 m to 5 m height and moderate incline (high tide mark ~9 m from low-tide mark and spring tide ~20 m from low-tide mark). It is noted that in general the beach cliff is seen to reduce in height towards the west until it is only 1 m high near Penny River. During severe storms, it has been observed that the beach cliff can retreat substantially due to collapse. A retreat of between 2 m and 3 m was observed by the author between 2012 and 2013 following severe storm weather during autumn of 2012.

The beach cliff is primarily gravel material, possibly glacial outwash in places but also likely mine tailings from extensive dredge mining in the area during the early to mid-20th century. The gravels overlie dark grey clast-bearing glacial diamict, which can become exposed in the beach cliff during retreat or when digging to some depth (usually less than 0.5 m). The contact between the beach material (or outwash material in the case of the beach cliff) and the underlying diamict is usually particularly rich in coarse gold.

AK121 was collected from a contact between overlying outwash gravels and basal diamict on West Beach (Figure 23 A). The sample produced 126 gold grains, of which 25 of the coarsest grains were selected for further analysis (average a-axis of 700 µm). The sample was taken on land owned by the State of Alaska. The clast assemblage present remains approximately constant for the extent of West Beach at 60% quartz, 15% graphitic schist (Dcs), 15% pelitic schist (DOx), and 10% marble (DOx) and granitoids. Trace Casadepaga Schist (Ocs) is sometimes observed. Garnet sands are common along the beach (along with accessory fine gold) and highlight the marine upgrading process (Figure 23 B).

The clast distribution on the beach shows an interesting sorting pattern with rounded granitoids and quartz collecting on the lower beach and discoidal schists and blocky marbles collecting preferentially along the base of the beach cliff (Figure 24). This highlights the distributive force of the sea during storm events.

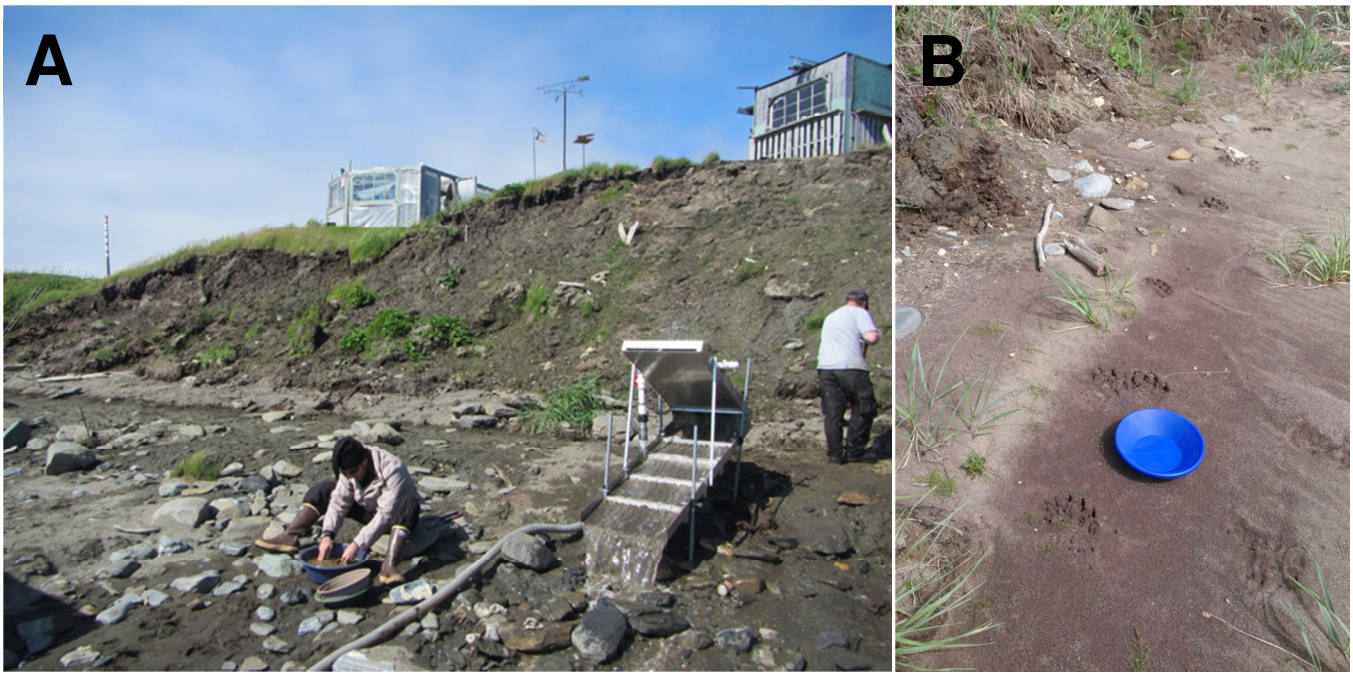

Figure 23: A: Sample AK121 was taken from the contact between overlying gravels and diamict at the base of the beach cliff on West Beach. B: Runs of garnet sand are common all along West Beach. Brown bear tracks can also sometimes be identified.

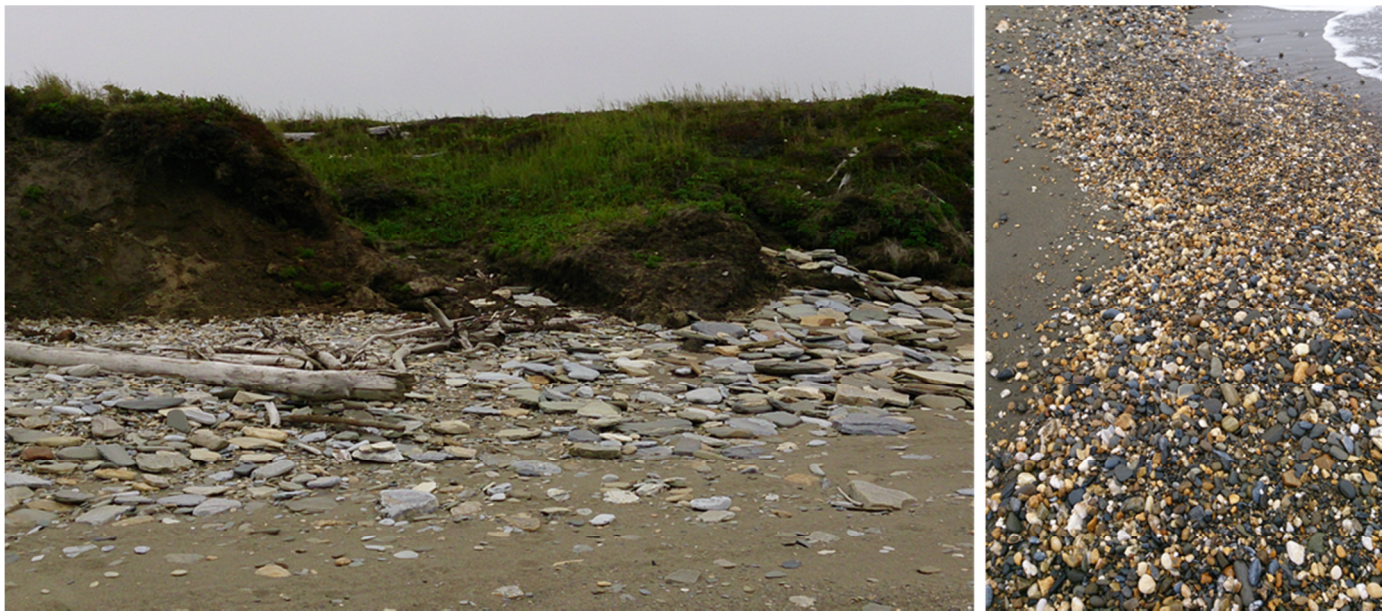

Figure 24: Sorting of clasts on West Beach. On the lower beach rounded quartz and granitoids are common, whilst blocky marble and discoidal schists collect at the base of the beach cliff.

5.5.5 AK123 – Monroeville Beach

Monroeville Beach is a buried auriferous deposit of Quaternary age located near Nome, approximately 4 km inshore of the present day coastline. Although commonly referred to as a "beach", Monroeville actually represents a shallow marine deposit formed offshore of Third Beach, which represents the proper paleoshoreline (Hopkins et al., 1960). The deposit lies on basal schist bedrock (DOx) and is covered by surficial sediments of the Nome coastal plain. The deposit is semi-parallel to the current strand-line and is relatively extensive with a known linear extent of ~4 km.

The deposit is currently being mined by the Nome Gold Alaska Corporation, and grains for Monroeville Beach were kindly supplied under permission by Bill Richards, a contract geologist working for Nome Gold. The grains (Figure 25) were collected from a mining pit, ~20 m below the surface and ~2 m above bedrock, well within the shallow marine sediment package of coarse sand and pebble to cobble gravel. It was observed that cobbles recovered along with the gold had abundant surface glacial striations, indicating that the Monroeville sediments include reworked glacial sediments. Twenty of the coarsest grains (average b-axis of 1600 µm) were selected for further analysis.

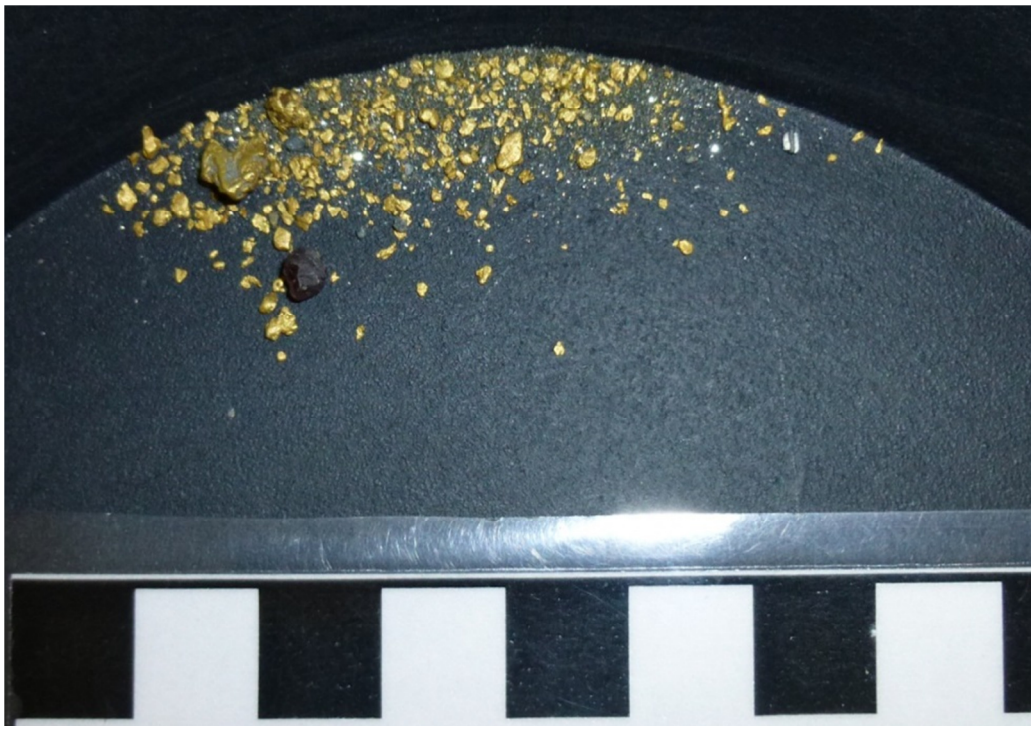

Figure 25: Gold from Monroeville Beach. Sample donated by Bill Richards with permission from Nome Gold Alaska Corporation.

5.5.6 AUR-12-854 – Deep Offshore Exploration Panel

The author was a responsible geologist during an extensive sampling campaign undertaken by AuruMar offshore of Nome in 2012. Sampling was conducted using a sonic corer, which is capable of delivering high quality un-disturbed sediment cores of up to 3 m length. Although most samples were assayed for gold grade, some cores were kept aside for further geological investigation.

In general, the geology offshore Nome consists of surficial sands and gravels, in the form of a transgressive lag or one formed during storm events and associated re-working. The lag overlies various glacial packages including glacial diamict and muds. The degree of gold mobility in the offshore is also unknown, and thus movement of gold across the shelf may have a large impact on mixing of gold populations. Thus, this site was selected in order to investigate whether populations identified onshore can be seen offshore.

Sample AUR-12-854 comes from the top 0.5 m of Core 138 taken at 18 m water depth. Sample AUR-12-854 primarily sampled sandy gravel transgressive lag material thought to be upgraded from the underlying and nearby glacial sediments (Figure 26). Importantly, the sample includes the contact between the transgressive gravelly sand (lag) and the underlying glacial muds. It is believed that this contact is the highly mineralised zone. Twenty-four grains with an average a-axis of 660 µm were recovered and selected for analysis. The core was taken approximately 4.5 km SW of the Nome River mouth in 18 m of water (Figure 19). This site, being

Figure 26: The top metre of Core 138. The top ~40 cm is dominated by a gravelly sand unit which overlies laminated glacial muds.

approximately half-way between the Snake River mouth and the Nome River mouth may, represent a mixed population of gold entering the system from both a Snake River and Nome River glacial lobe (which along with the Penny River lobe make up the Nome System).

5.5.7 ADEM – Shallow Offshore Nome River

The sample ADEM was recovered by Mr. Adem Boechman during the 2012 Nome winter. Mr. Boechman was contracted to mine one of the small, shallow water mining leases through the near-shore ice by shallow water diving through a pre-cut ice-hole using a vacuum hose. Gold grains were collected by the author from the dive tailings from this site with the permission of Mr. Boechman. The sample was recovered in ~6 m water depth from a site ~1 km ESE of the current day Nome River mouth (Figure 19). Although no image of the site exists, a nearby dive site with a similar geology was photographed and is shown in Figure 27.

This sample comes from a key site that is believed to be representative of gold distributed by the Nome River glacial lobe. Additionally, due to difficultly in acquiring samples from the Nome River valley as a result of poor access, this site is the only one from this perceived glacial lobe.

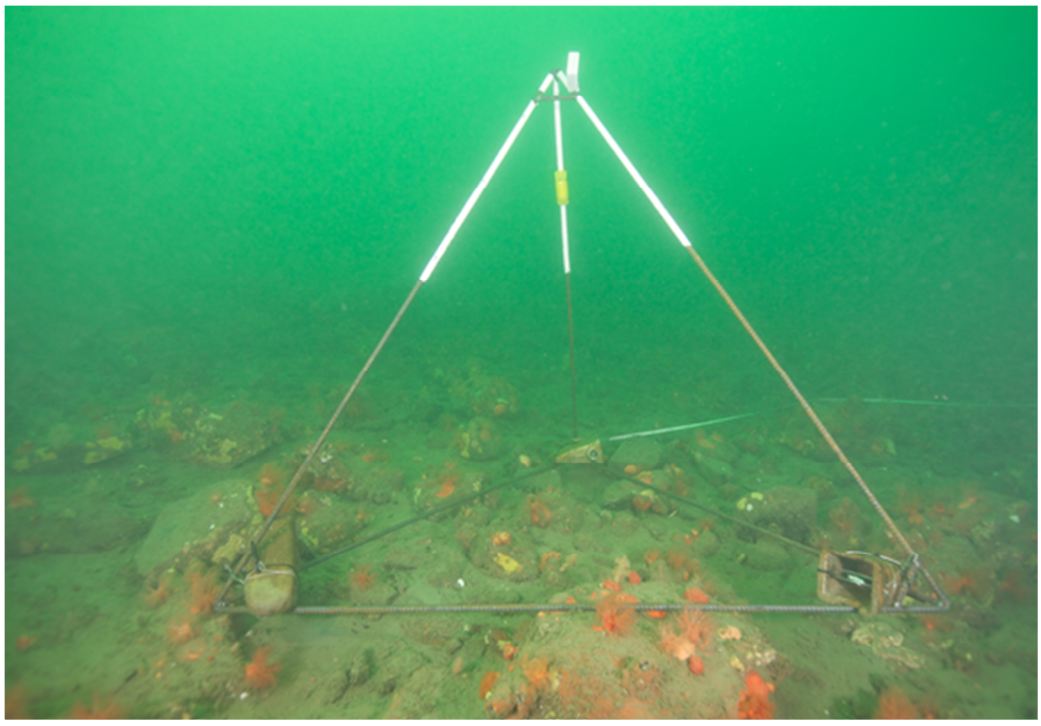

Figure 27: A typical near-shore site offshore Nome, Alaska. The seabed is typically characterised by a transgressive lag, which can be comprised of sandy to pebble lag gravels, with scattered cobbles and boulders common. Each edge of the frame shown is 1 m in length.

5.5.8 RC4 – Rock Creek Mine Ore Sample

Rock Creek mine (Figure 28) is located ~10 km north of Nome up the Snake River valley. The mine was developed by Canadian mining company NovaGold Resources Inc., with first gold production achieved in September of 2008. By November 2008 mining was suspended due to technical and start up issues, environmental concerns, and the global recession. In 2012 the mine was sold to the Bering Straits Native Corporation (BSNC). Although 75% of the gold is recoverable by gravitational means, an 88% recovery can be achieved when coupled with flotation and cyanidation (BSNC, pers. comm., 2013), indicating the presence of both coarse and fine gold. The deposit had been independently assessed by AMEC to contain ~404,000 oz. gold at an average grade of ~1.31 g/t (Otto et al., 2009)

The ore body is hosted within the Nome Complex (Dcs), a mixture of complexly deformed pelitic schist, calc-schists and marbles. Gold is hosted in two generations of tension and Albion-style quartz veins (Otto et al., 2009), which commonly contain sulphides and sulphosalts.

A hand sample was recovered by the author from the ore stockpile during a visit in 2013 (Figure 29). The sample contained a ~2 cm thick quartz vein with sulphide mineralisation (arsenopyrite and pyrite) developed along the contact with the surrounding pelitic schist. Four thin sections were made from the sample, one of which revealed visible gold under the microscope (RC4). The gold-bearing section was subject to further analysis with the EMP.

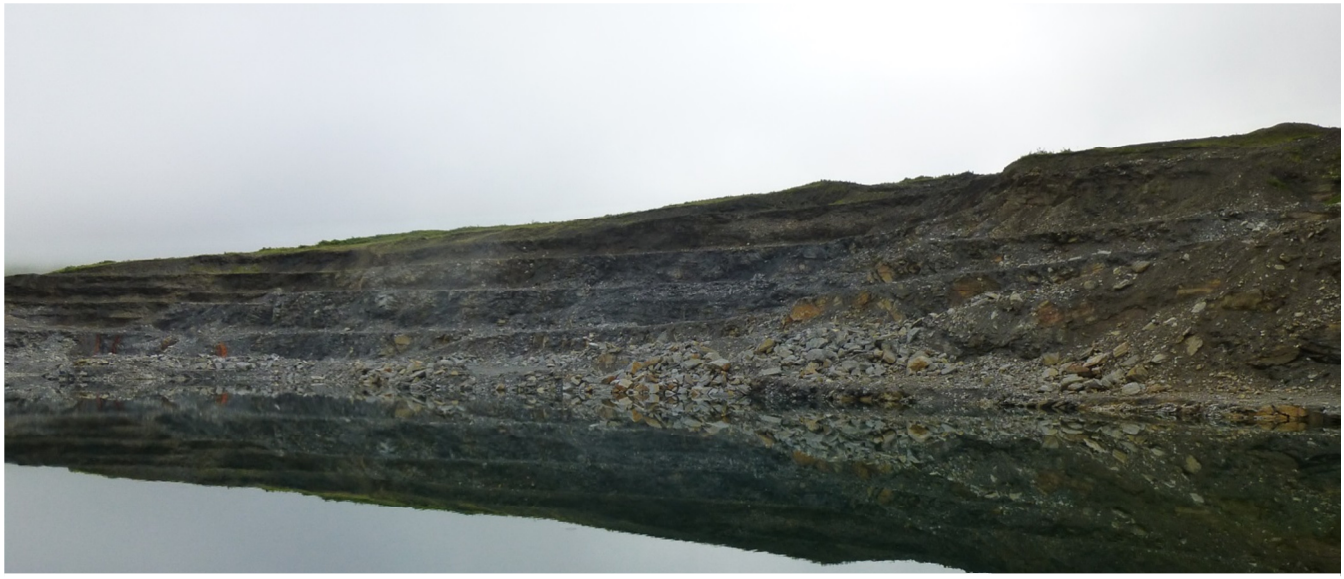

Figure 28: The Rock Creek Mine pit, now filled with water, has been developed in graphitic schists of the Devonian Dcs formation. Benches are ~3 m high.

Figure 29: The Rock Creek ore body is quartz veined foliated graphitic schists (Dcs). Here large pyrite and arsenopyrite can be seen on the contact zone between the quartz vein and the surrounding ore. This sample was cut into four polished thin sections (RC4).

6 Results

Table 4 (Section 4.3) shows the twelve sample sites, eleven of which are placer sample sites, from which gold grains were collected for this study. A total of 241 placer gold grains and 2 primary gold occurrences (RC4) were imaged by Secondary Electron Imaging (see Appendix A) for particle size and morphological assessment, of which 163 were analysed for major, minor, and trace elements. This section reports the lithological clast assemblage of the 12 sites, the morphological characteristics of gold grain populations from each of the sites, and their major and trace geochemistry.

6.1 Qualitative Clast Assemblage

During 2013, the author and other AuruMar geologists conducted an extensive field sampling exercise to collect the gold grains to be used in this study, whilst simultaneously conducting qualitative lithological clast assemblage assessments of all sites visited (Table 5). Twenty-nine sites were visited in addition to the "Deep Offshore" site (AUR-12-854), which was sampled by the author in 2012.

Figure 30 shows the lithological clast assemblage distribution across the Seward Peninsula in relation to the bedrock geology (after Till et al., 2011). The following observations have been made:

- Correlation between abundance of graphitic schists and proximity to DOx unit;
- Correlation between abundance of marbles and proximity to DOx unit;
- Correlation between abundance of micaceous schists and proximity to Dcs unit;
- Correlation between abundance of meta-volcanics and proximity to Ocs unit;
- Higher abundance of quartz along the beaches, offshore, and in the Snake River drainage than elsewhere;
- Higher abundance of granitoids in the Sinuk system than in the Nome and Solomon systems (AK021, AK032);
- Higher abundance of granitoids in the Penny River (AK100) and Cripple Creek beach (AK117) within the Nome system.

Table 5: Lithological Clast Assemblage data collected for sites across the Southern Seward Peninsula.

Sample	Location	Eastings	Northings	Graphitic Schists (DOx)	Mica Schists (Dcs)	Quartz	Marble (Oim, DOx)	Granitoids (Zo, PzZh, Kg, Kgu, Zn)	Meta-volcanics (Ocs)
AK015	Shovel Creek	529070	7167694	20	30	5	40	0	5
AK021	Washington Creek	457704	7176425	40	10	0	5	40	5
AK028	Gold Run Creek	444688	7216175	5	70	5	0	10	10
AK032	Sinuk Coastal Plain	445774	7161335	20	10	10	40	20	0
AK100	Penny River	468109	7162485	30	30	15	10	10	5
AK111	Anvil Creek	481462	7161934	60	20	20	0	0	0
AK117	West of Cripple River	460075	7157502	20	45	5	0	25	5
AK121	West Beach	475929	7153674	20	15	60	2	3	0
AK123	Monroeville Beach	481195	7156505	10	60	10	20	0	0
AUR-12-854	Exploration Panel (Offshore)	481107	7149309	13	51	27	1	1	7
ADEM	Offshore East Beach	486200	7150000	5	60	10	15	0	10
RC4	Rock Creek Mine	479152	7165558	20	60	20	0	0	0
* **N/A**	Sunset Creek	472132	7160889	0	90	10	0	0	0
* **AK101**	Arctic Creek	465985	7168055	0	50	0	30	20	0
* **AK102**	Cripple River	464406	7172879	20	40	5	30	5	0
* **N/A**	Feather River	448294	7189838	0	5	5	0	85	5
* **N/A**	Sinuk River	456153	7177479	5	20	5	0	60	10
* **AK105**	2nd Beach	489355	7150362	30	50	10	10	0	0
* **AK106**	Prospect Creek	478211	7167318	10	80	10	0	0	0
* **AK107**	Divining Creek	479438	7170243	10	80	10	0	0	0
* **N/A**	Dexter Creek	486076	7162014	10	75	10	5	0	0
* **AK108**	Extra Dry Creek	486968	7160595	0	80	20	0	0	0
* **N/A**	Nome River	487152	7162428	20	60	15	0	5	0
* **AK113**	Sampson Creek	486872	7177148	0	15	5	0	0	80
* **N/A**	Nome River	488915	7179668	20	40	20	0	5	15
* **AK114**	Rocky Mountain Creek	489866	7182806	0	75	25	0	0	0
* **AK115**	Sulphur Creek	489823	7187702	5	40	10	5	0	40
* **N/A**	West Beach	472277	7154797	20	15	60	2	3	0
* **AK122**	Glacier Creek	479942	7163601	20	60	20	0	0	0
* **N/A**	Big Hurrah Creek	532808	7170038	65	30	3	0	2	0

Explanation:

Values are in percentage based on a qualitative assessment of the lithologies present at each site. The assessment was conducted by three workers collaboratively (E. Gauntlett, U. Burger, and Dr. E. Mervine) to ensure consistency. Sites demarcated with an "*" did not form any further part of this study.

Eastings and Northings are reported in the UTM 3N projection and WGS84 geodetic reference system.

Geological units mentioned are presented only as a potential source for the clast lithology and are not necessarily correct. They are meant only as a guide when read in collaboration with the geological map (e.g. Figure 30) and are after the nomenclature of Till et al. (2011).

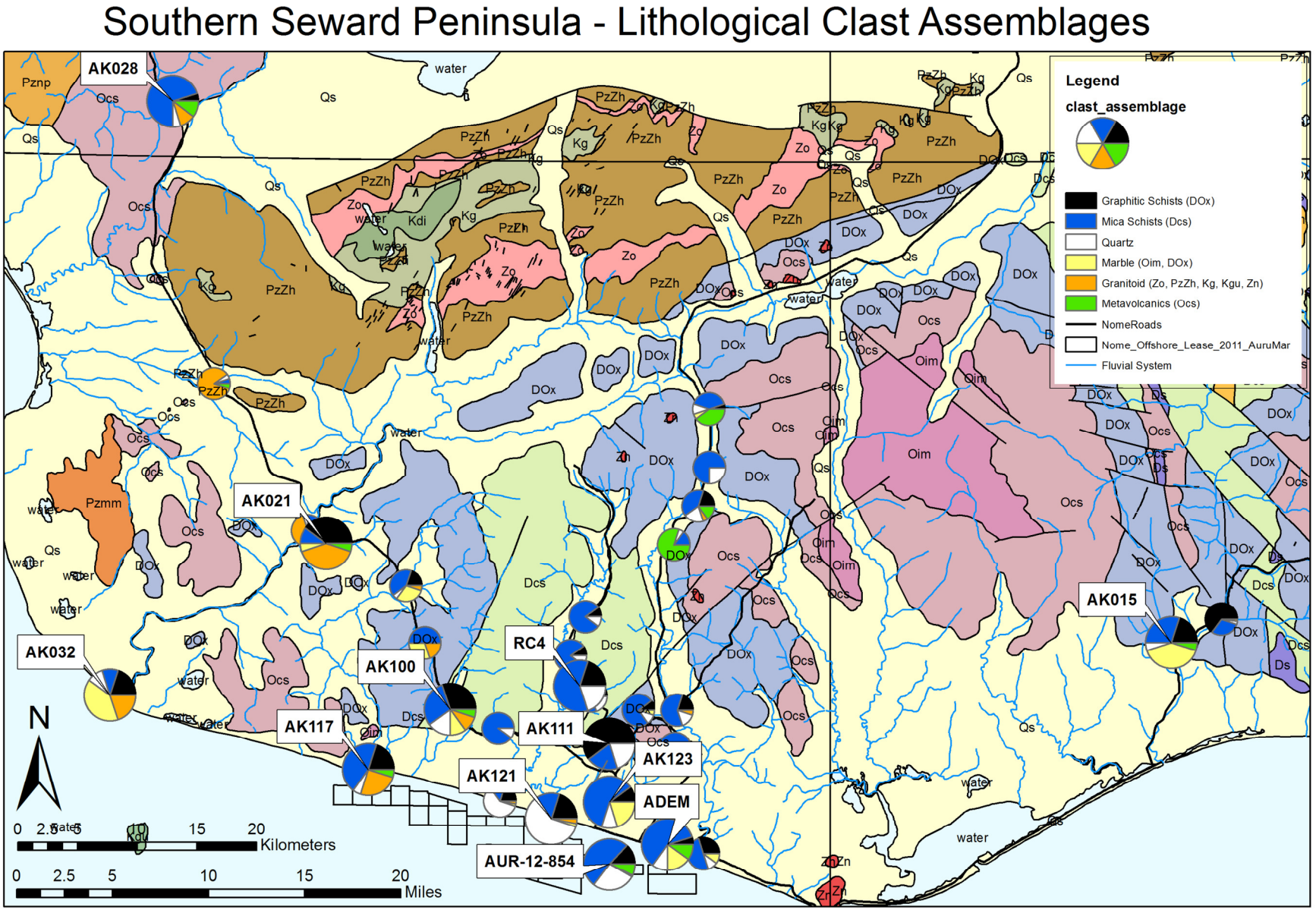

Figure 30: The lithological clast assemblage distribution across the southern Seward Peninsula is shown as pie-charts (larger pie charts are sampled sites for this study whilst smaller pie charts are additional data supplementing this study). The geology of the Seward Peninsula as mapped by the U.S. Geological Survey is shown in the background (after Till et al., 2011).

6.2 Gold Grain Particle Statistics

6.2.1 Gold Grain Particle Statistics Results

A possible parameter distinguishing gold grain transport mechanisms and population mixing is the particle size distribution (PSD) of a population. The PSD of a gold grain population may help define a particular population or part thereof (e.g. Rasmussen et al., 2007). For all the gold grains (Appendix A) each gold grain secondary electron image (SEI) was subject to a-axis (maximum length) and b-axis (maximum width at 90° to a-axis) measurement using freely available image analysis software JMicroVision (available from http://www.jmicrovision.com). No c-axis measurement was possible given that gold grains were mounted to carbon paper in preparation for EMP analysis. Additionally, each gold grain's area was calculated by the software. The axes length and grain area results are shown in Appendix B whilst Figure 31 illustrates the a-axis versus b-axis distribution for all placer grains (i.e. excluding Rock Creek grains). Figure 32 illustrates the PSD based on grain area for each placer site.

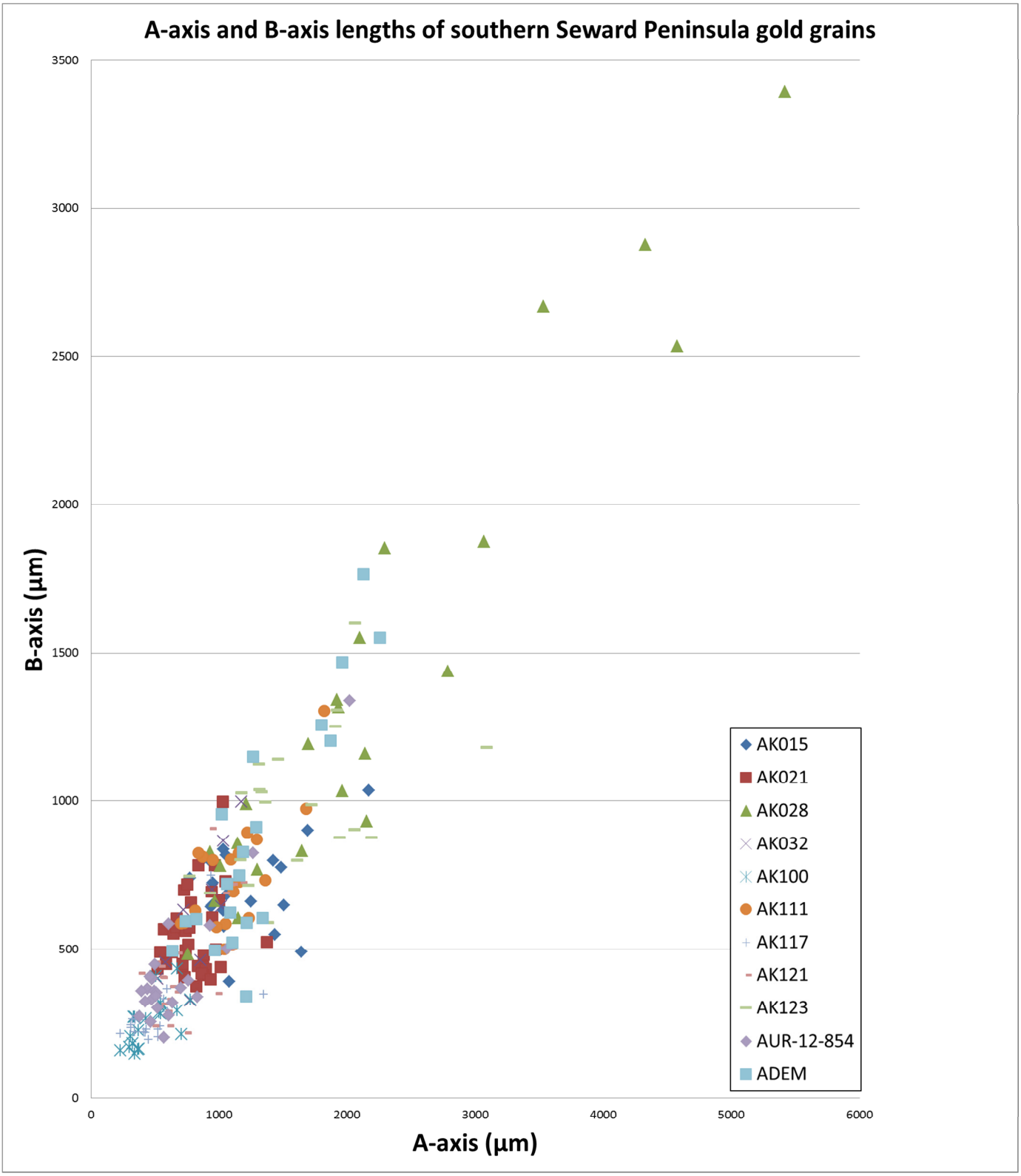

Figure 31: A-axis vs. B-axis scatterplot for all eleven placer gold grain sites. Note the tight distribution for some sites (e.g. AK021, AK100, AK117, AK121, and AUR-12-854) versus the broad distribution of others (e.g. AK028, AK123, and ADEM).

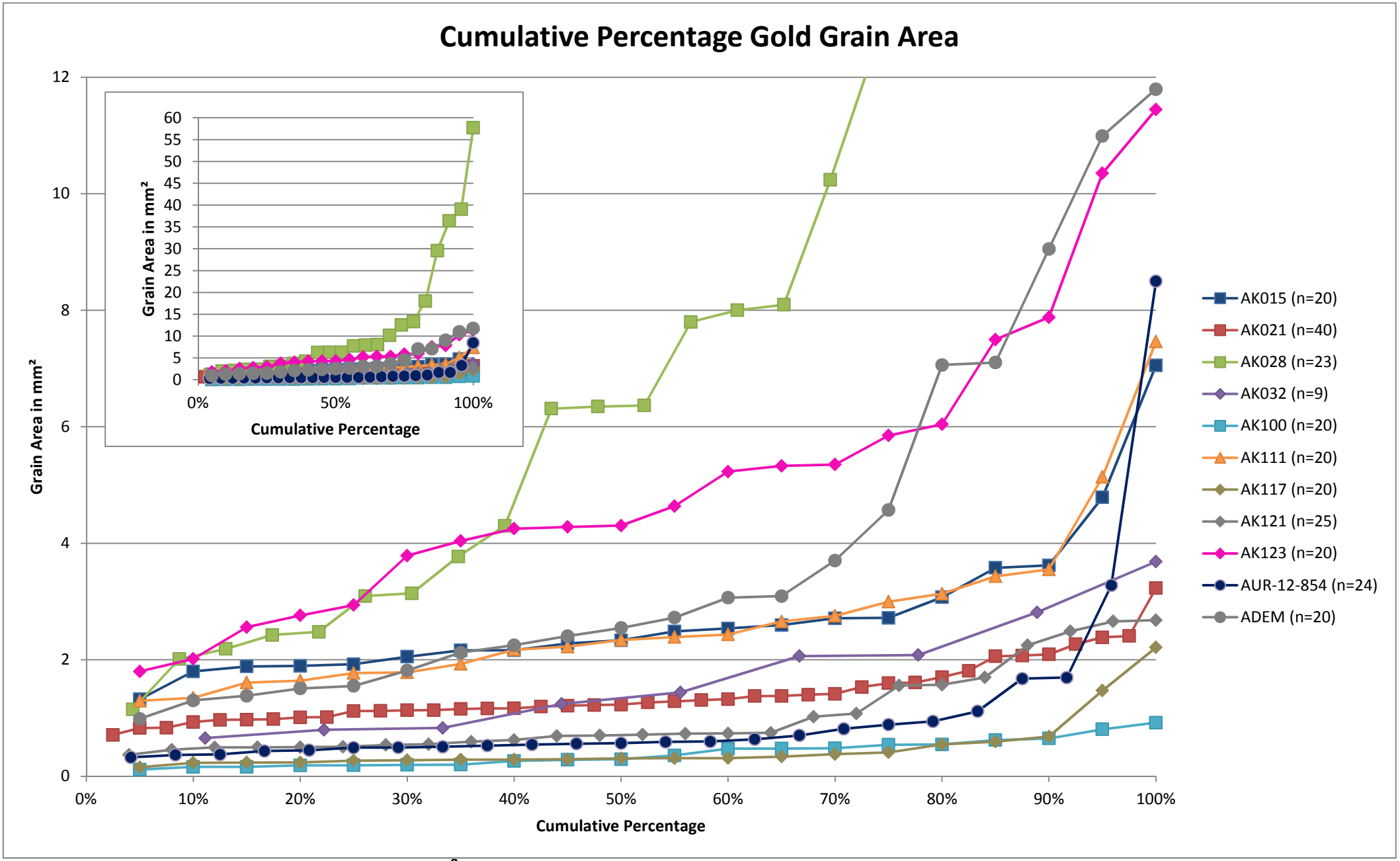

Figure 32: Particle Size Distribution (in mm^2) for grain particles from southern Seward Peninsula sites. Note the extreme variation in sample AK028 to 58 mm^2 (inset).

Table 6: Summary of particle statistics of grains from each placer site. Data extracted from Appendix B.

AK015 (n=20)	a-axis (µm)	b-axis (µm)	Elongation	Area (mm2)	AK117 (n=20)	a-axis (µm)	b-axis (µm)	Elongation	Area (mm2)
Maximum	2169	1035	3.34	7.05	Maximum	1346	750	3.87	2.21
Minimim	772	391	1.04	1.32	Minimim	228	196	1.06	0.15
Average	1215	708	1.78	2.75	Average	498	281	1.80	0.49
Standard Deviation	352	148	0.60	1.28	Standard Deviation	253	120	0.65	0.49
Coeffecient of Variation	0.29	0.21	0.34	0.46	Coeffecient of Variation	0.51	0.43	0.36	1.00
AK021 (n=40)					**AK121 (n=25)**				
Maximum	1374	998	2.62	3.23	Maximum	1175	908	3.39	2.68
Minimim	519	376	1.00	0.71	Minimim	380	218	0.91	0.37
Average	807	552	1.52	1.42	Average	710	438	1.72	1.06
Standard Deviation	166	132	0.43	0.52	Standard Deviation	244	168	0.58	0.74
Coeffecient of Variation	0.21	0.24	0.28	0.37	Coeffecient of Variation	0.34	0.38	0.34	0.70
AK028 (n=23)					**AK123 (n=20)**				
Maximum	5417	3395	2.31	57.78	Maximum	3090	1600	2.62	11.45
Minimim	754	485	1.12	1.15	Minimim	767	590	1.03	1.80
Average	2174	1391	1.58	12.38	Average	1596	984	1.65	5.12
Standard Deviation	1258	794	0.30	14.62	Standard Deviation	530	242	0.50	2.56
Coeffecient of Variation	0.58	0.57	0.19	1.18	Coeffecient of Variation	0.33	0.25	0.30	0.50
AK032 (n=9)					**AUR-12-854 (n=24)**				
Maximum	1175	998	2.37	3.68	Maximum	2020	1339	2.80	8.50
Minimim	521	327	1.14	0.66	Minimim	378	204	1.03	0.32
Average	847	610	1.47	1.73	Average	668	428	1.61	1.13
Standard Deviation	218	223	0.41	1.02	Standard Deviation	362	234	0.46	1.69
Coeffecient of Variation	0.26	0.36	0.28	0.59	Coeffecient of Variation	0.54	0.55	0.28	1.50
AK100 (n=20)					**ADEM (n=20)**				
Maximum	777	435	3.30	0.92	Maximum	2254	1766	3.54	11.80
Minimim	228	150	1.22	0.11	Minimim	634	342	1.07	0.99
Average	462	256	1.85	0.40	Average	1305	872	1.62	4.05
Standard Deviation	158	81	0.50	0.23	Standard Deviation	457	401	0.56	3.32
Coeffecient of Variation	0.34	0.32	0.27	0.59	Coeffecient of Variation	0.35	0.46	0.34	0.82
AK111 (n=20)									
Maximum	1820	1305	2.14	7.46					
Minimim	701	501	1.02	1.29					
Average	1110	744	1.52	2.70					
Standard Deviation	285	189	0.33	1.44					
Coeffecient of Variation	0.26	0.25	0.22	0.53					

6.2.2 Gold Grain Particle Statistics Observations

Some sites display excellent clustering of particle size within a relatively small range reflecting a well sorted population (e.g. AK021, AK100, AK117, AK121, and AUR-12-854) whereas others show a wide distribution of particle size reflecting an immature or poorly sorted population (e.g. AK028, AK123, and ADEM). Sites AK111 and AK015 are examples of moderately sorted gold particle populations whereas Site AK032 has an indeterminate population as a result of too few particles (see Figure 31).

In addition to particle size sorting, the average grain size for each site also varies significantly. In particular, Sites AK021, AK100, AK117, AK121, and AUR-12-

854 have small average grain sizes (<1.50 mm^2), whereas Sites AK015, AK032, and AK111 have moderate average grain sizes (between 1.50 mm^2 and 3.00 mm^2), and Sites AK028, AK123, and ADEM have large average grain sizes >3.00 mm^2 (see Figure 32 and Table 6).

Grain elongation (defined as the ratio of the a-axis to the b-axis) for Sites AK021, AK032, and AK111 average around 1.50, whilst Sites AK028, AUR-12-854, and ADEM average around 1.60 and Sites AK015, AK100, AK117, and AK121 average around 1.80 (Table 6).

6.3 Gold Grain Textures and Morphology

All SEI of gold grains (Appendix A) were subject to qualitative analysis using a descriptive process developed by other placer gold workers (e.g. Youngson et al., 2002 and described in Youngson and Craw, 1999). Each grain was assessed for the presence of primary features, degree of abrasion, degree of rounding, degree of flattening, presence of folding, presence of aeolian textures, degree of secondary gold accretion, and degree of gold dissolution and/or surface pitting (Appendix B). These parameters and their relevance are described below:

- Presence of primary features: given the extremely high malleability and ductility of gold, grains released from a primary source rarely retain their primary features of crude to rounded octahedra faces or elongated dendritic forms for any significant transport distance (perhaps only tens of metres). The abundance of primary features still visible is a strong proxy for the distance a grain has travelled (Townley et al., 2003).
- Degree of abrasion: given the softness of gold, the abundance of abrasion marks on gold grains can be used as a proxy for distance travelled and can also indicate the transport mechanism (fluvial transport along a gravel bedload or suspended transport within a glacier (Youngson and Craw, 1999). Care must be taken when assessing this feature because, in some cases, abrasion history can be masked by later stage gold accretion, thus under-reporting the true degree of abrasion experienced.
- Degree of rounding: Gold particle rounding is generally a result of edge abrasion. This type of all-round abrasion is typical of fluvial transport (Youngson and Craw, 1999). For a fluvially transported gold particle within

1 km of its source, the degree of rounding remains minor and usually does not progress beyond sub-angular (Townley et al., 2003).

- Degree of flattening: This parameter is arguably the best to describe transport distance of a gold particle within a fluvial system. Many workers (e.g. Youngson and Craw, 1999; Townley et al., 2003) have been able to quantify flattening using the Cailleux flatness index, which is defined as [(a + b)/2c]. However, this study was unable to quantify the c-axis and as such this parameter remains qualitative.
- Presence of folding: In the early phases of transport, particle edges are folded inwards during abrasion, resulting in greater overall particle rounding. Major shape transformation begins to occur once the grain has flattened sufficiently to allow for high degrees of overlap folding. In gravel bedload systems, intense folding results in grains attaining elongate, rod shapes.
- Presence of aeolian textures: Aeolian transport of gold grains produces morphological features unique to wind transport. The typical evolution pathway of the change in morphology with aeolian transport distance is as follows: Initially flattened grain edges are progressively peened inward during saltation. These peened edges thicken until the platy grain evolves into one with a thickened rim, then further evolves into a bowl or toroidal shape. Finally, the grain edges are thickened and peened to such an extent that the grain is sub-spherical to spherical in shape (Youngson, 2005; Craw et al., 2006).
- Degree of secondary gold accretion: This parameter typically refers to the observation of gold accretion in the form of coatings of crystalline or amorphous gold by chemical accretion onto pre-existing grains, which occurs prior to erosion, during transport, or post-deposition. Additionally, the formation of secondary (post-deposition) α-phase Au-Ag-Hg alloys may also be observed (Youngson et al., 2002).
- Degree of gold dissolution and/or surface pitting: This parameter refers to the dissolution of small pits of silver and gold from the particle as a result of reactant water composition. This process drives secondary gold accretion (Falconer et al., 2006).

Table 7: Summary of grain morphological parameters from each placer site. Values are normalised to 100 percent. The parameter fields are the same as those described in the explanation to Appendix B.

Parameter		Shovel Creek	Washington Creek	Gold Run Creek	Sinuk Coastal Plain	Penny River	Anvil Creek	Cripple Creek Beach	West Beach	Monroeville Beach	Deep Offshore	Shallow Offshore
		AK015 n=20	AK021 n=40	AK028 n=23	AK032 n=9	AK100 n=20	AK111 n=20	AK117 n=20	AK121 n=25	AK123 n=20	AUR-12-854 n=24	ADEM n=20
Presence of Primary Features	x	0	0	0	0	5	0	15	0	0	0	0
	r	55	58	70	67	40	60	75	84	80	88	95
	c	40	35	26	22	30	20	10	12	10	13	5
	a	5	8	4	11	25	20	0	4	10	0	0
Degree of Abrasion	x	0	0	0	0	0	0	5	0	0	0	0
	r	45	13	39	67	25	15	65	60	20	50	50
	c	35	48	52	33	30	30	30	40	55	33	45
	a	20	40	9	0	45	55	0	0	25	17	5
Degree of Rounding	a	0	0	0	0	0	0	0	0	0	0	0
	sa	0	5	4	11	20	5	0	0	0	8	0
	sr	20	20	26	33	35	50	25	16	20	29	5
	r	45	20	26	56	35	15	30	16	20	13	5
	wr	35	55	43	0	10	30	45	68	60	50	90
Degree of Flattening	uf	20	8	39	11	50	75	10	44	35	21	15
	mf	60	38	61	33	35	20	40	40	45	54	80
	wf	20	55	0	56	15	5	50	16	20	25	5
Presence of Folding	x	80	45	87	56	95	100	60	92	100	92	100
	✓	20	55	13	44	5	0	40	8	0	8	0
Presence of Aeolian Features	x	85	95	96	89	100	90	90	96	100	96	100
	✓	5	0	0	11	0	0	0	0	0	0	0
	?	10	5	4	0	0	10	10	4	0	4	0
Abundance of Accretion Features	x	20	0	22	0	0	0	0	0	0	8	0
	r	60	50	57	11	25	25	30	32	85	50	5
	c	20	33	17	0	25	60	20	32	15	42	95
	a	0	18	4	89	50	15	50	36	0	0	0
Abundance of Dissolution Features / Pitting	x	0	0	9	0	0	0	0	0	0	0	0
	r	55	30	17	44	25	15	10	20	70	63	20
	c	30	58	52	33	30	60	40	68	20	29	80
	a	15	13	22	22	45	25	50	12	10	8	0

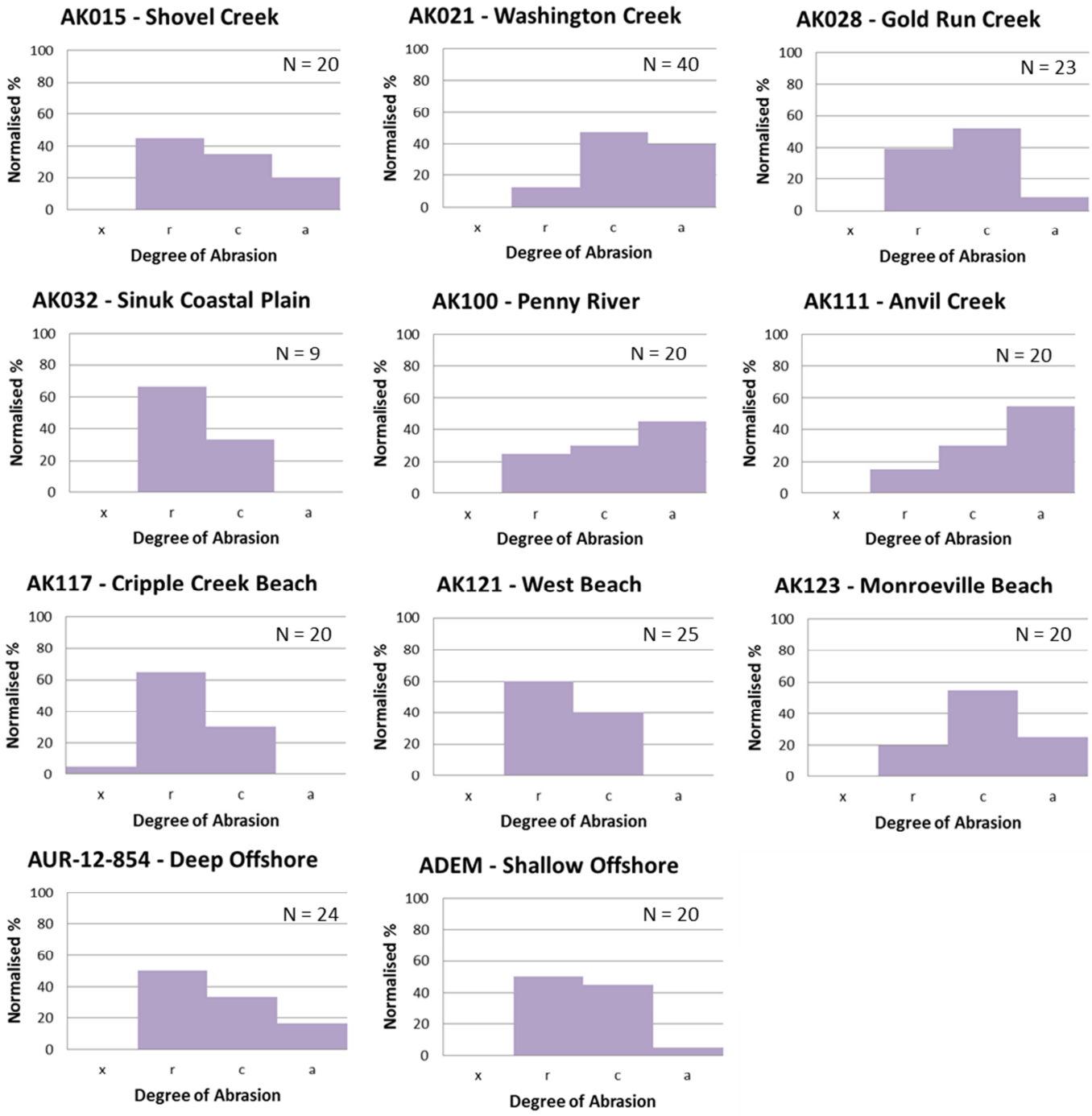

Figure 33: Normalised histograms of abrasion data for gold grains from the eleven placer sites sampled for this study (data from Appendix B). The degree of abrasion abbreviations on the x-axis are: absent (x), rare (r), common (c), and abundant (a).

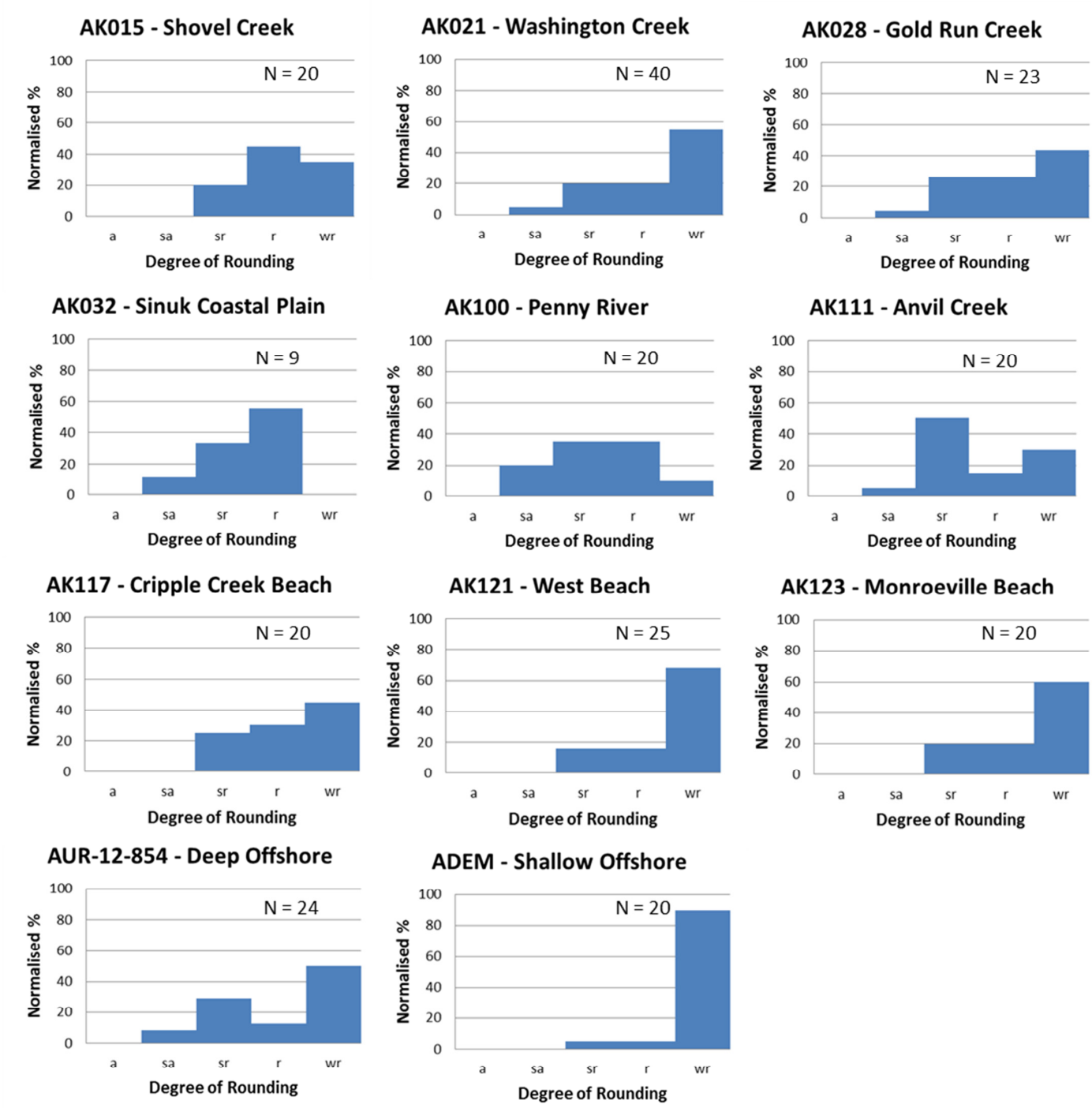

Figure 34: Normalised histograms of roundness data for gold grains from the eleven placer sites sampled for this study (data from Appendix B). The degrees of rounding abbreviations on the x-axis are: very angular (va), angular (a), sub-angular (sa), sub-rounded (sr), rounded (r), and well rounded (wr).

6.3.1 Placer Gold Grain Textures and Morphology Observations

Table 7 presents a summary of textural and morphological data from all grains from the eleven placer sites studied. In general, the presence of primary features is uncommon at all sites (i.e. “not observed” or “rare” observations recorded for >50% grains from a particular site), but is slightly more common in samples AK100 (55% common to abundant).

Almost all grains from all samples display some degree of abrasion. Samples AK021, AK100, AK111, and AK123 display high degrees of abrasion where abrasion is common to abundant in greater than 75% of the grains (e.g. AK100-10, Figure 35). Samples AK015, AK028, AUR-12-854, and ADEM display moderate degrees of abrasion (50% to 75% of grains displaying common to abundant abrasion) and the beach samples of AK032, AK117, and AK121 display low degrees of abrasion, where less than 50% of the grains are abraded (see Figure 33), although this is likely as a result of masking by late-stage gold accretion on the surface.

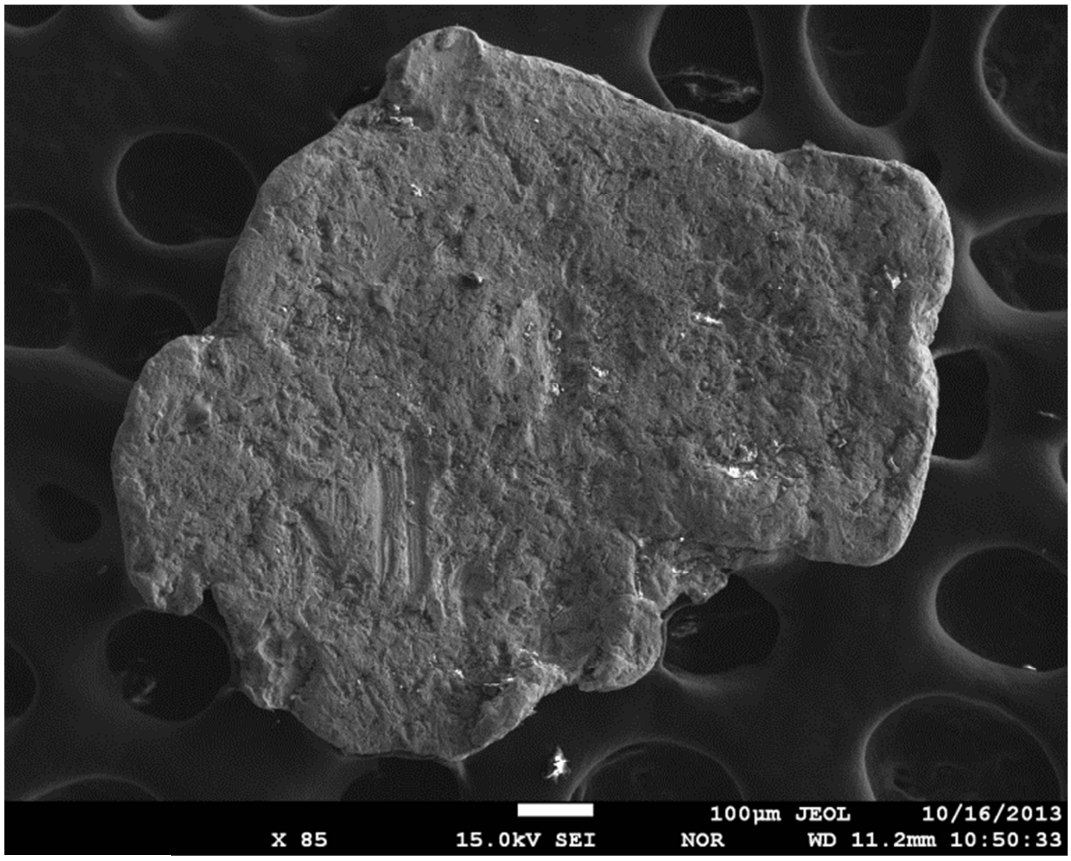

Figure 35: Secondary electron image of grain AK100-10 showing abrasion marks (lower left quadrant).

No samples displayed a complete absence of rounding, which indicates that all samples contain a gold particle population which has been transported. However, variation in the degree of placer gold grain rounding can be a meaningful indicator of transport distance and mechanism and thus has been investigated further for the grains in this study (Figure 34). The beach and shallow offshore samples of AK117, AK121, AK123, and ADEM display a skewness towards the well-rounded end of the roundness spectrum, whereas the fluvial samples of AK015, AK021, AK028, and AK100 display a flatter distribution from sub-angular to well-rounded, with some of the samples displaying more rounding than others (e.g. AK021). The Sinuk Coastal Plain samples (AK032) show a skewed distribution towards rounded but lack the well-rounded grains, possibly because this sample only has 9 grains. Interestingly, samples AK111 and AUR-12-854 show a clear bi-modal distribution of particle roundness, with peaks at sub-rounded and well-rounded.

The qualitative assessment of flattening into three categories (well-flattened, moderately flattened, and un-flattened) reveals that most samples contain well flattened (AK021, AK032, and AK117) to moderately flattened (AK015, AK028, AK121, AK123, AUR-12-854, and ADEM) grains. However, samples AK100 and AK111 show a high percentage of un-flattened grains.

Samples AK021, AK032, and AK117 contain a substantial number of grains with observable folding whereas samples AK100, AK111, AK121, AK123, AUR-12-854, and ADEM show very low degrees of visible folding. Sample AK015 contains three unusual grains that are reminiscent of multiple grains folding into each other (e.g. Figure 36) although it is worth noting that grains from this sample do not display a high degree of folding.

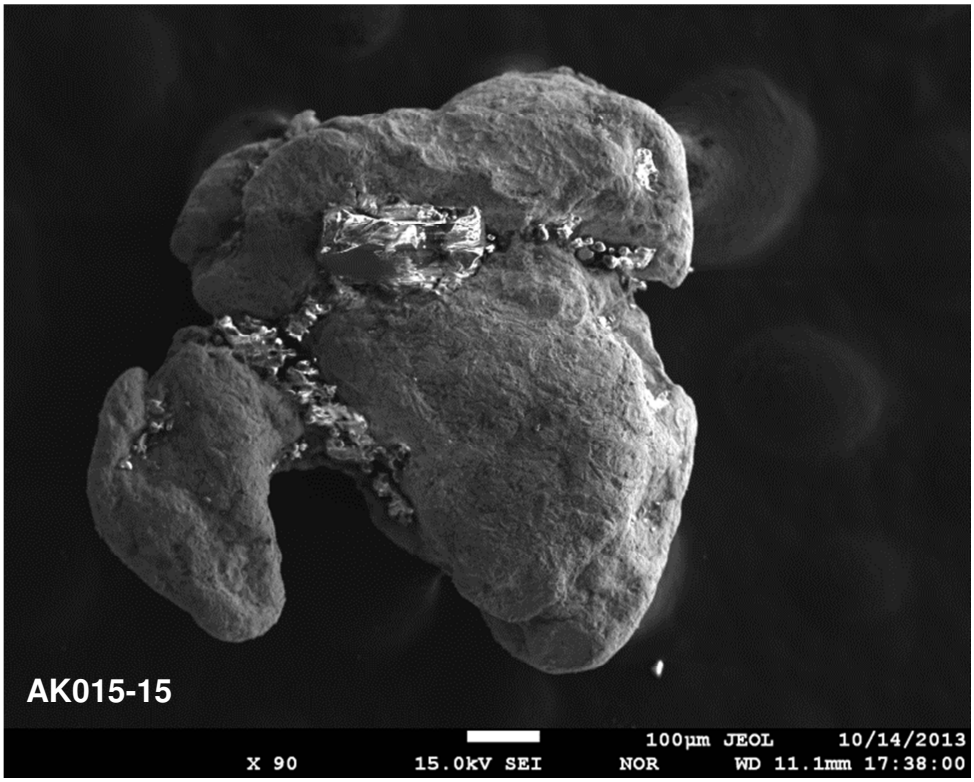

Figure 36: Secondary electron image of grain AK015-15 showing possible merging and folding together of multiple grains (likely 3, centre, top, and left) with gangue minerals in the folds.

No gold grains from any samples displayed noteworthy morphological evidence for aeolian transport, with the possible exception of a single grain from the Sinuk Coastal Plain sample (AK032-5), which displays potential evidence for minor aeolian transport (Figure 37).

Chemical accretion of anhedral, rounded, amalgamated gold aggregates onto existing gold grains was observed, specifically in the beach or marine samples of AK032, AK117, AK121, AK123, AUR-12-854, and ADEM (Figure 38 and Figure 39).

Samples AK117 and AK121 display excellent examples of hexagonal secondary growth Au-Ag-Hg alloy (Figure 40 and Figure 41).

Dissolution pitting is commonly observed in all samples with the following samples perhaps showing a higher average degree of common to abundant pitting: AK021, AK028, AK032, AK100, AK111, AK117, AK121, and ADEM.

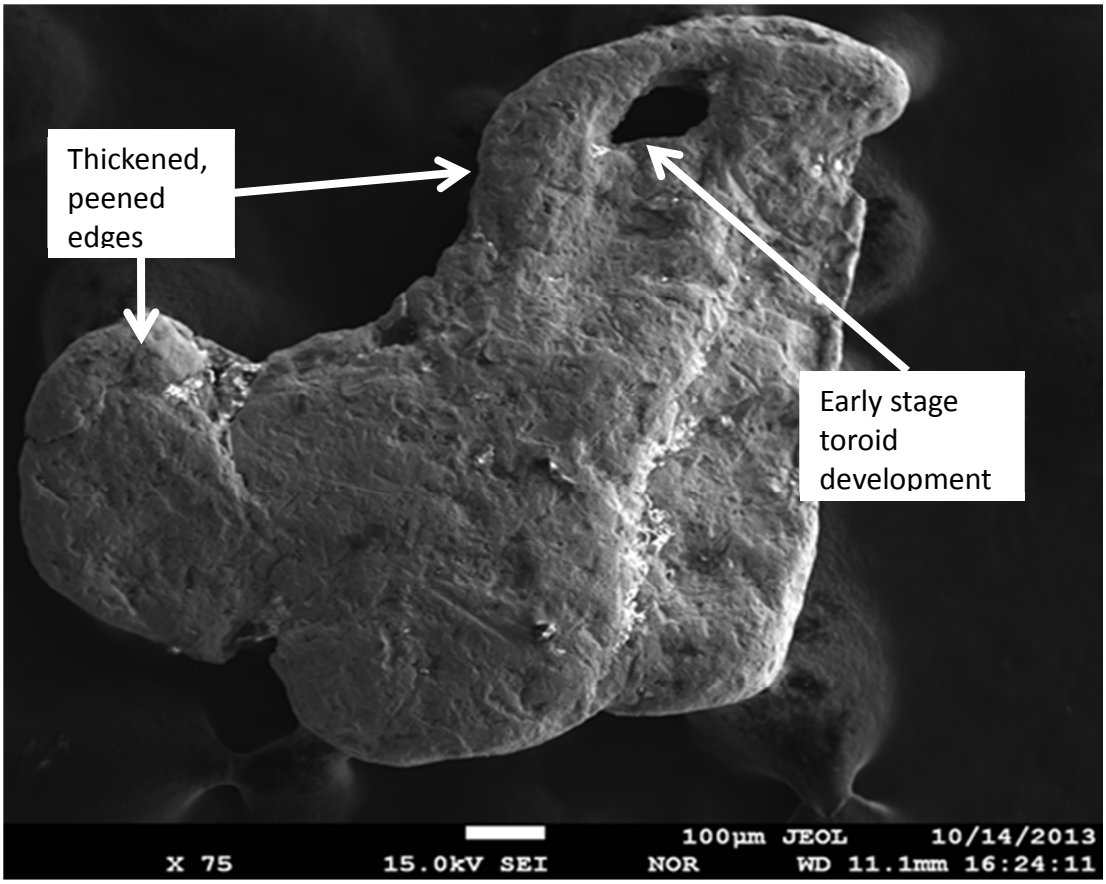

Figure 37: Secondary electron image of grain AK032-5 showing possible evidence of aeolian transport with thickened and peened edges and early stage toroid development.

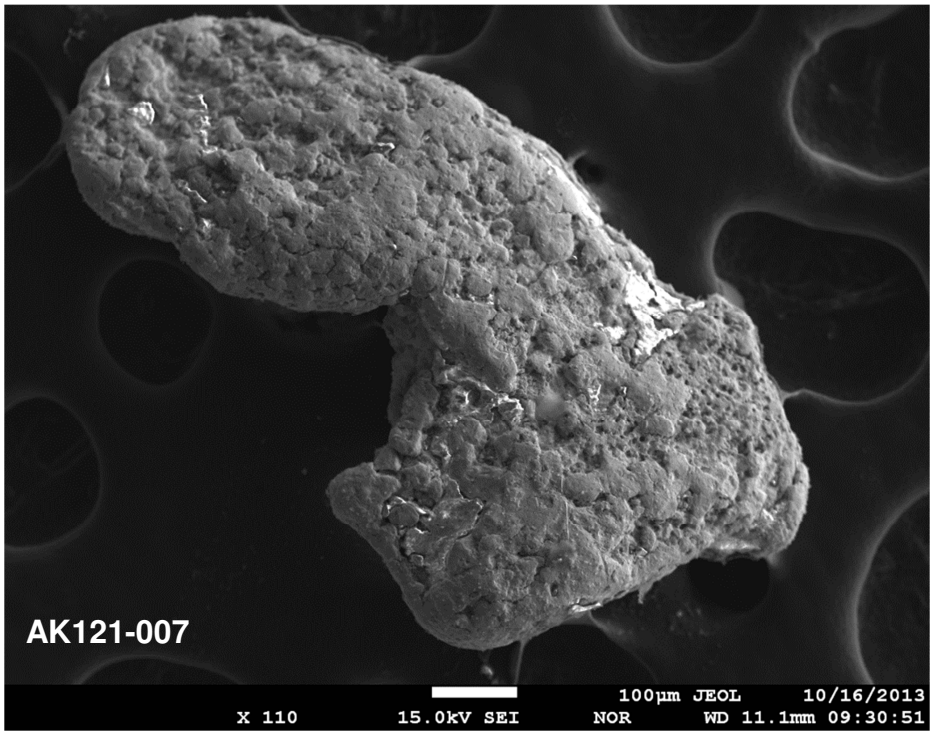

Figure 38: Secondary electron image of grain AK121-7 displaying anhedral, rounded, amalgamated gold aggregates across the grain.

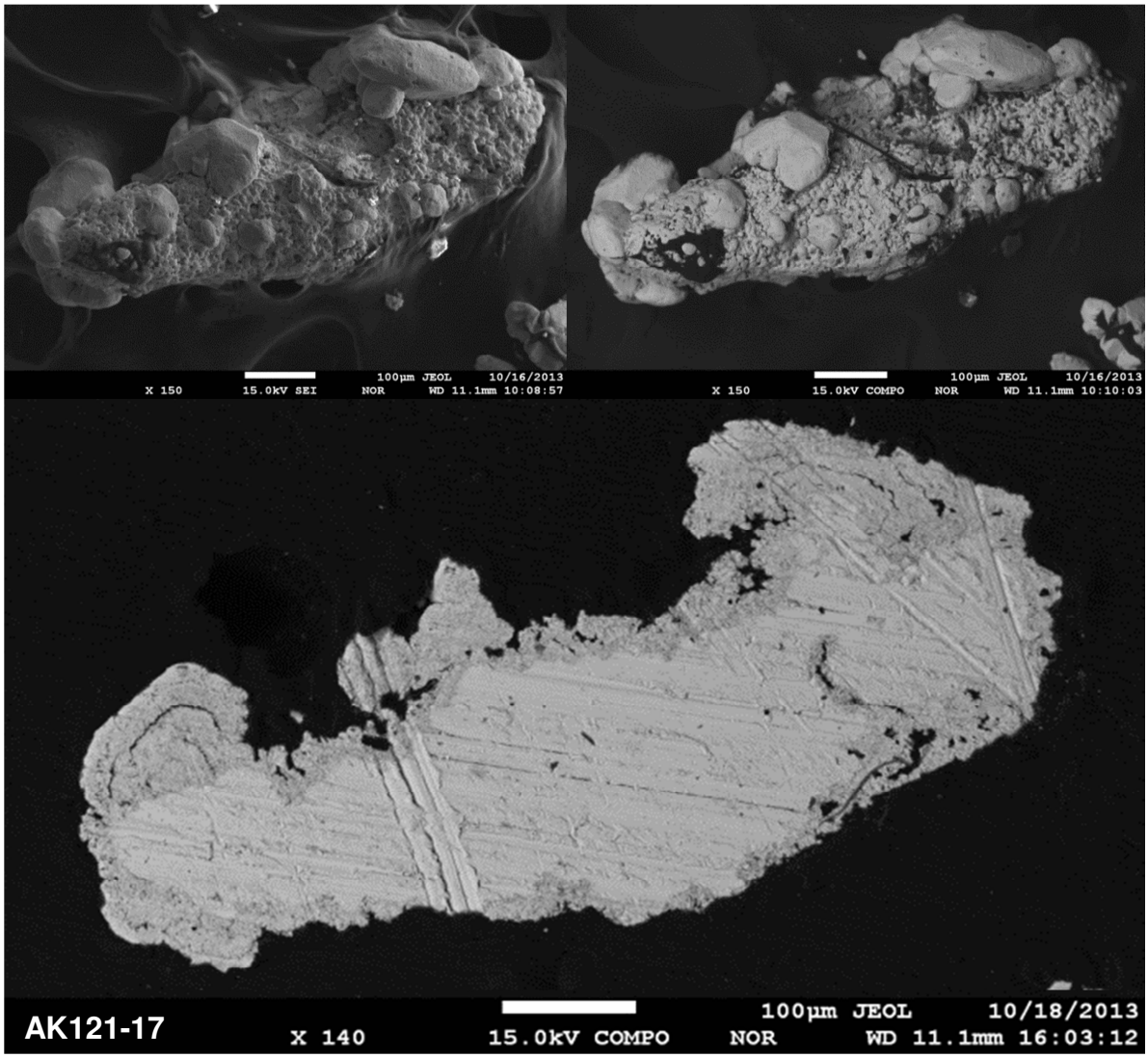

Figure 40: Grain AK121-17 showing secondary hexagonal Au-Ag-Hg growth. Top left is a Secondary Electron Image (SEI), top right is a Backscatter Electron (BE) image, and bottom is a BE image of a polished cross section of the grain, highlighting the compositional variation between grain rim (growths) and grain core.

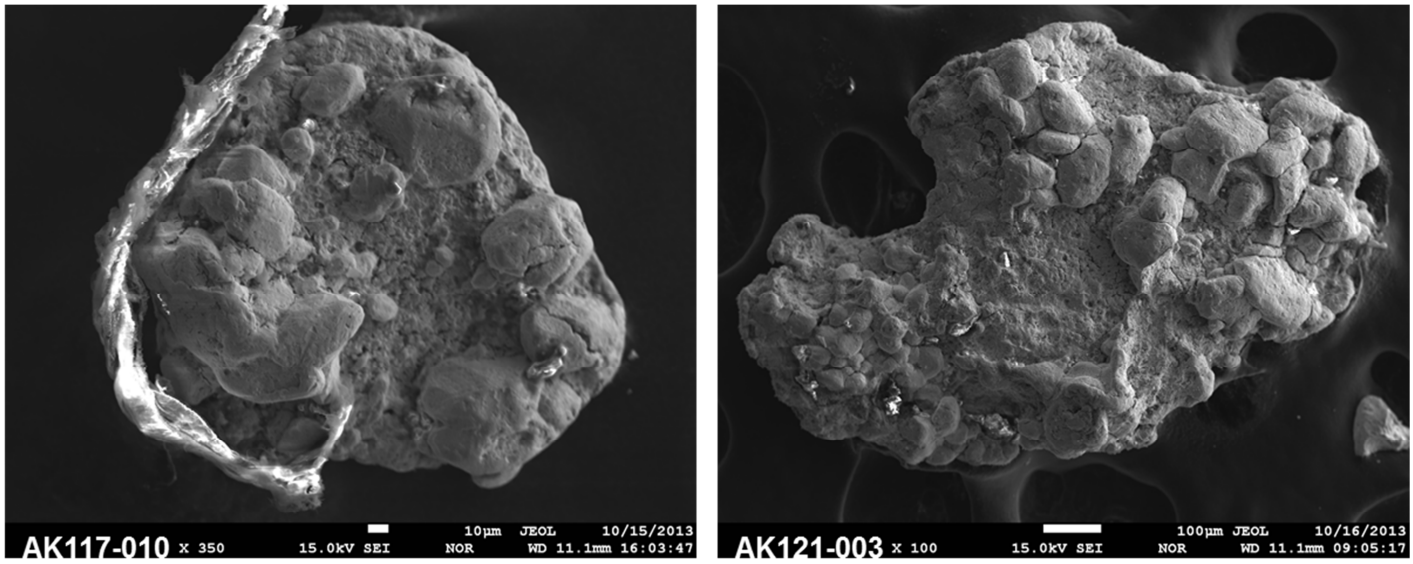

Figure 41: Secondary electron image of grains AK117-10 (left) and AK121-3 (right) displaying excellent examples of secondary growth hexagonal Au-Ag-Hg alloy.

6.3.2 Rock Creek (RC4) Gold

Rock Creek thin section RC4 provided two instances of gold hosted within arsenopyrite (FeAsS). These grains are not crystalline and appear to have formed along arsenopyrite grain cleavage and intergranular spaces (e.g. cracks). It would appear that the gold is exsolving out of the arsenopyrite and crystallising in void spaces. These grains were analysed and are reported as RC4.

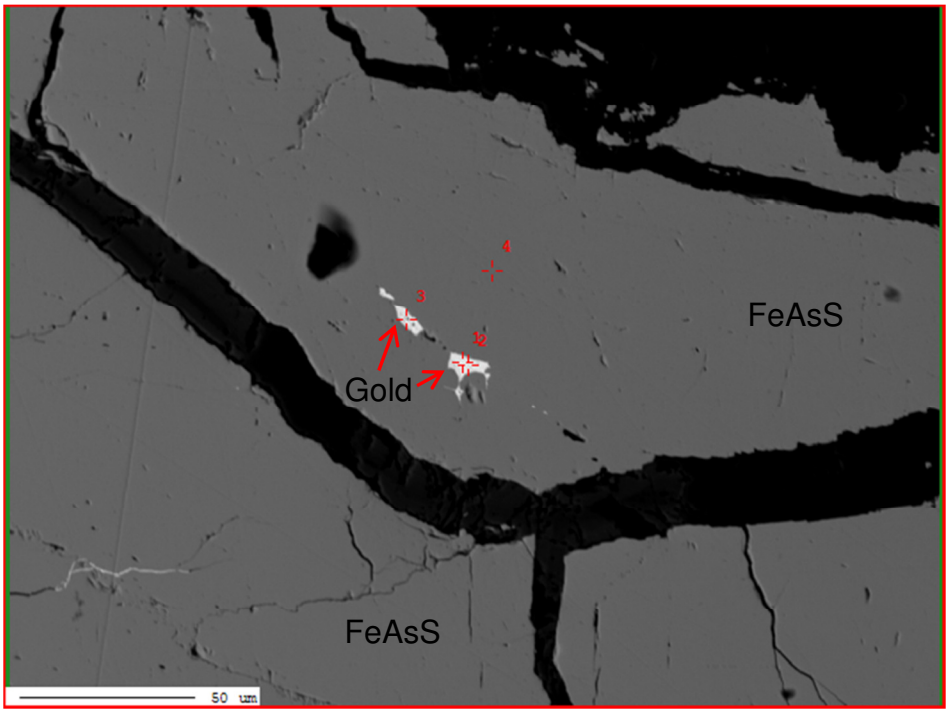

Figure 42: Gold present along cracks in arsenopyrite within thin section RC4. This image shows analyses RC4-1 to RC4-4.

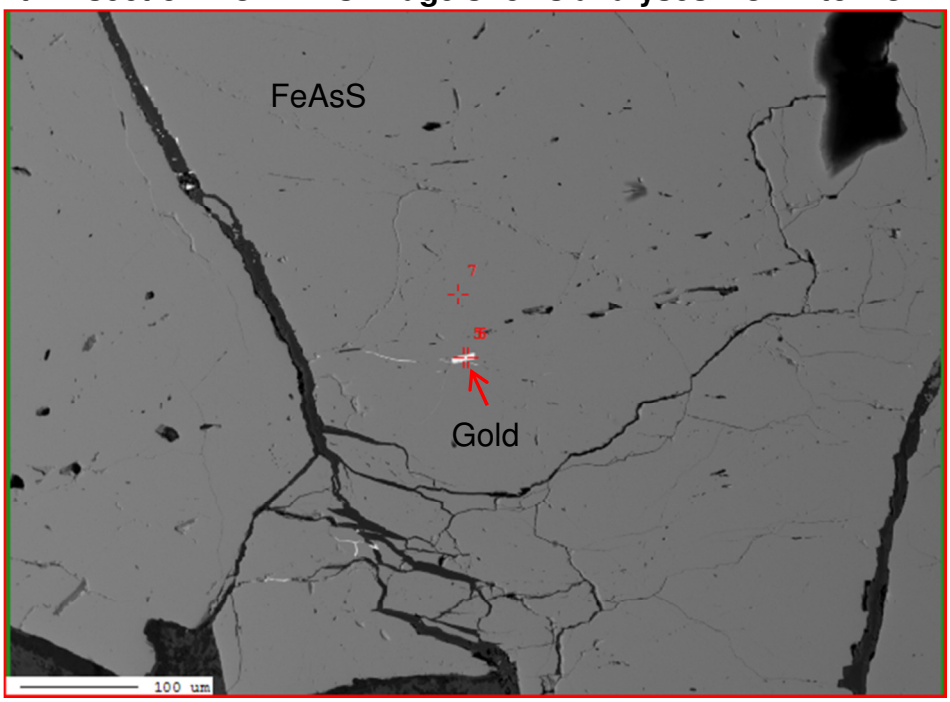

Figure 43: Gold present along cracks in arsenopyrite within thin section RC4. This image shows analysis RC4-5 to RC4-7.

6.4 Major and Minor Element Geochemistry

Four major and minor elements (Au, Ag, Hg, and Cu) were analysed from 163 grains from 11 sites (no grains from AK117 were available after polishing) across the southern Seward Peninsula, including RC4 (Table 4). Most grains were analysed twice in the core and once on the rim (average analyses per grain is 3.08), generating 502 individual analyses. Multiple analyses of each grain are denoted by a letter following the grain ID (e.g. AK015-1b denotes the second analysis of grain AK015-1).

Each analysis was assessed for quality via the following process:

1. All analyses where Total Mass percent of major and minor elements (Au + Ag + Hg + Cu) reported < 95% or >105% were removed. This reduced the dataset to 456 analyses (i.e. 46 were removed).
2. Seven (7) erroneous analyses were removed (e.g. analysis of silicates), reducing the dataset to 449 analyses.

This filtered major and minor element dataset is presented in Appendix D.

6.4.1 Individual Grain Analyses

For the purposes of geochemical characterisation and population assessment only a single representative core analysis from each grain was required. Thus, the dataset was further reduced in the following manner:

1. All rim analyses were removed reducing the dataset to 347 analyses (i.e. 102 rim analyses were removed).
2. Where present, replicate analyses from a single grain were assessed, and a single analysis was selected to represent the grain. Assessment criteria included:
    - Removing analyses which didn't agree with replicate analyses from the same grain
    - Preferring analyses which had a Total Mass percent of major and minor elements (Au + Ag + Hg + Cu) of between 98.5% and 101.5% over those that did not
    - Preferring analyses with lower Error % in the minor elements

In this way, 187 replicate analyses were removed, and the dataset was reduced to 160 analyses from 160 individual grains (Appendix D), although the entire dataset is available in Appendix C.

6.4.2 Observations from Individual Grain Analyses

Ternary plots are have been made to investigate whether grains from individual sites have similar properties and whether their chemistry is homogenous or heterogeneous. Commonly used plots for defining gold populations are the Au-Ag-Hg and Au-Ag-Cu ternary plots (e.g. Townley et al., 2003; Chapman et al., 2009). The Au-Ag-Hg ternary plot presented in Figure 44 reveals that Sites AK028 (maximum Hg = 9.2% and average Hg = 1.8%) and AK015 (maximum Hg = 1.9% and average Hg = 0.4%) have significantly more Hg than the other sites, which tend to plot on the Au-Ag solid solution line. Other sites with notable Hg heterogeneity are AK021 (single grain with Hg = 0.4%), AK032 (single grain with Hg = 0.6%), AK100 (single grain with Hg = 0.2%), AK121 (three grains with Hg > 0.2%), and ADEM (single grain with Hg = 0.4%).

Other than the high concentrations of Hg seen in Sites AK015 and AK028 (Figure 44 and Figure 45), which are likely characteristic of their source chemistry, exceptionally high values of Hg were recorded in two grains from Site AK121. The results were of Hg = 24.9% (AK121-13c_growth) and Hg = 18.3% (AK121-17c_growth). These anomalously high Hg contents relate directly to Hg-rich gold growths observed on multiple grains from Sites AK121 and AK117 (see Figure 40 and Figure 41 and Section 6.3.1).

As expected, given that most grains (other than site AK028 with up to 9.2% Hg and Cu = 1.8%) are composed of only Au and Ag (Figure 44), there is an inverse relationship between Au and Ag (i.e. the more silver present, the lower the percentage Au). Given the range of Ag (2% to 25%), it appears that there is some clustering of grains within a site along the Au-Ag line within a constrained range (Figure 45). However, Figure 45 is not the ideal figure to highlight this phenomenon and some workers (e.g. Chapman and Mortensen, 2006) have better illustrated Ag contents in gold grains using a cumulative percentile plot (Figure 46). Figure 46 contrasts the difference in Ag% percentage across the sites and within sites. Of particular note is the high average Ag% (and non-existent Hg or Cu) recorded for the hard-rock gold sample of RC4 (Ag range is 21.5% to 25.3%). AK021 is unique in that it has an elevated Ag% relative to the other sites (modal Ag% = 16.0%). Site AK032 and AK100 have the broadest ranges in Ag-content (4.4% to 22% with an average of 12.2% for AK032 and 2.2% to 22.6% with an average of 10.1% for AK100). AK032 is made unique by a steep slope, indicating a sample containing highly mixed gold

grain populations. The prominent break in slope shown in AK100 may indicate a mixing of two populations (one with Ag < 10% and the other with Ag > 10%). Site AK015 is also notable amongst the sites in that is has the tightest range in Ag% and the lowest average Ag-content (4.9% to 7.9% and an average Ag% of 6.1%). These data suggest that there is a single population and gold grain provenance for this site.

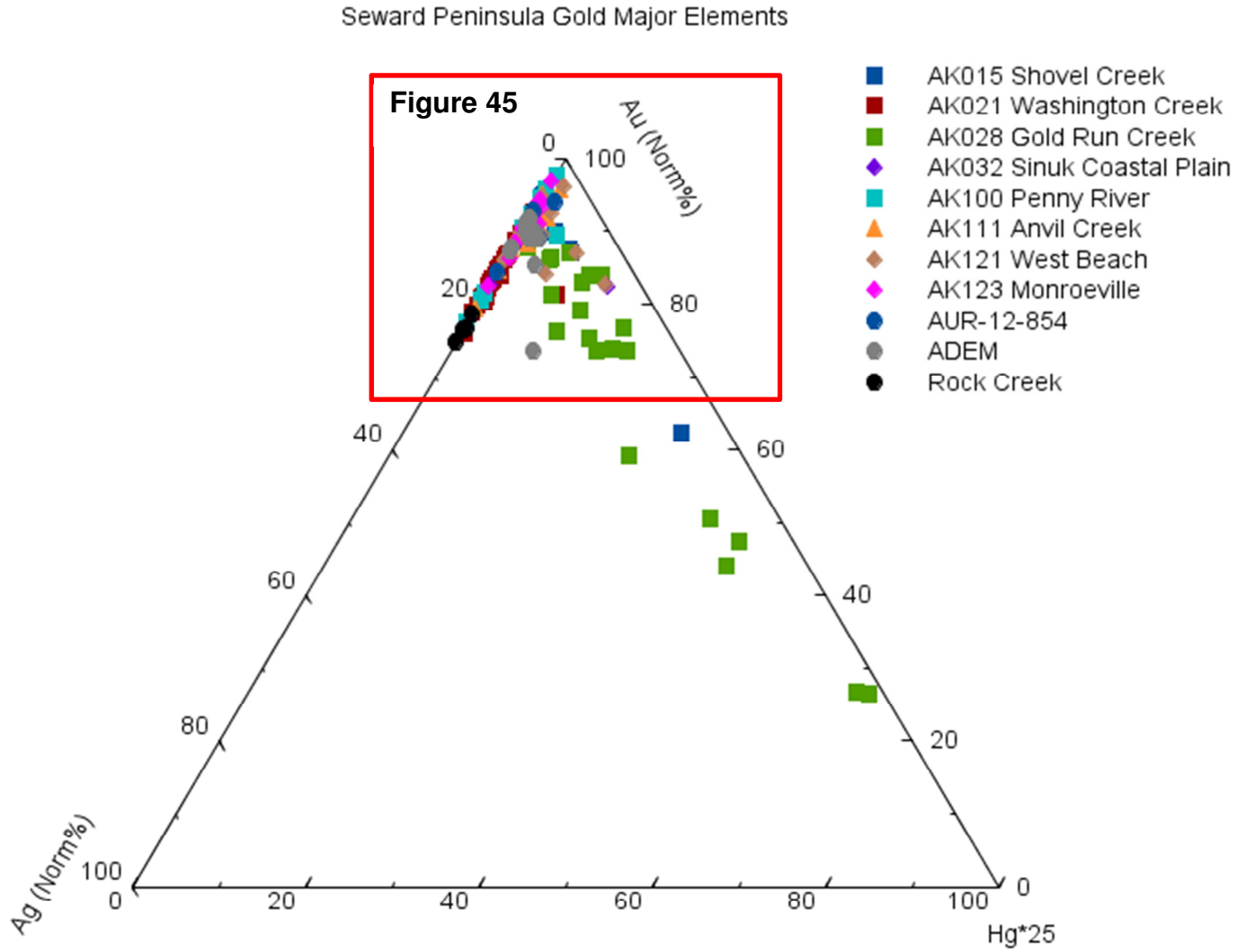

Figure 44: Au-Ag-(Hg X 25) ternary plot of southern Seward Peninsula gold grains. Note that due to generally low concentrations, Hg is shown as percentage Hg X 25. The red box denotes zoomed in area shown in Figure 45.

Site ADEM displays an elevated Ag-content profile with an apparent absence of low Ag-content grains. The remaining sites of AK028, AK111, AK121, AK123, and AUR-12-854 track a relatively tight field of Ag% vs. cumulative percentile with two breaks in slope at approximately 10% and 80% cumulative percentile.

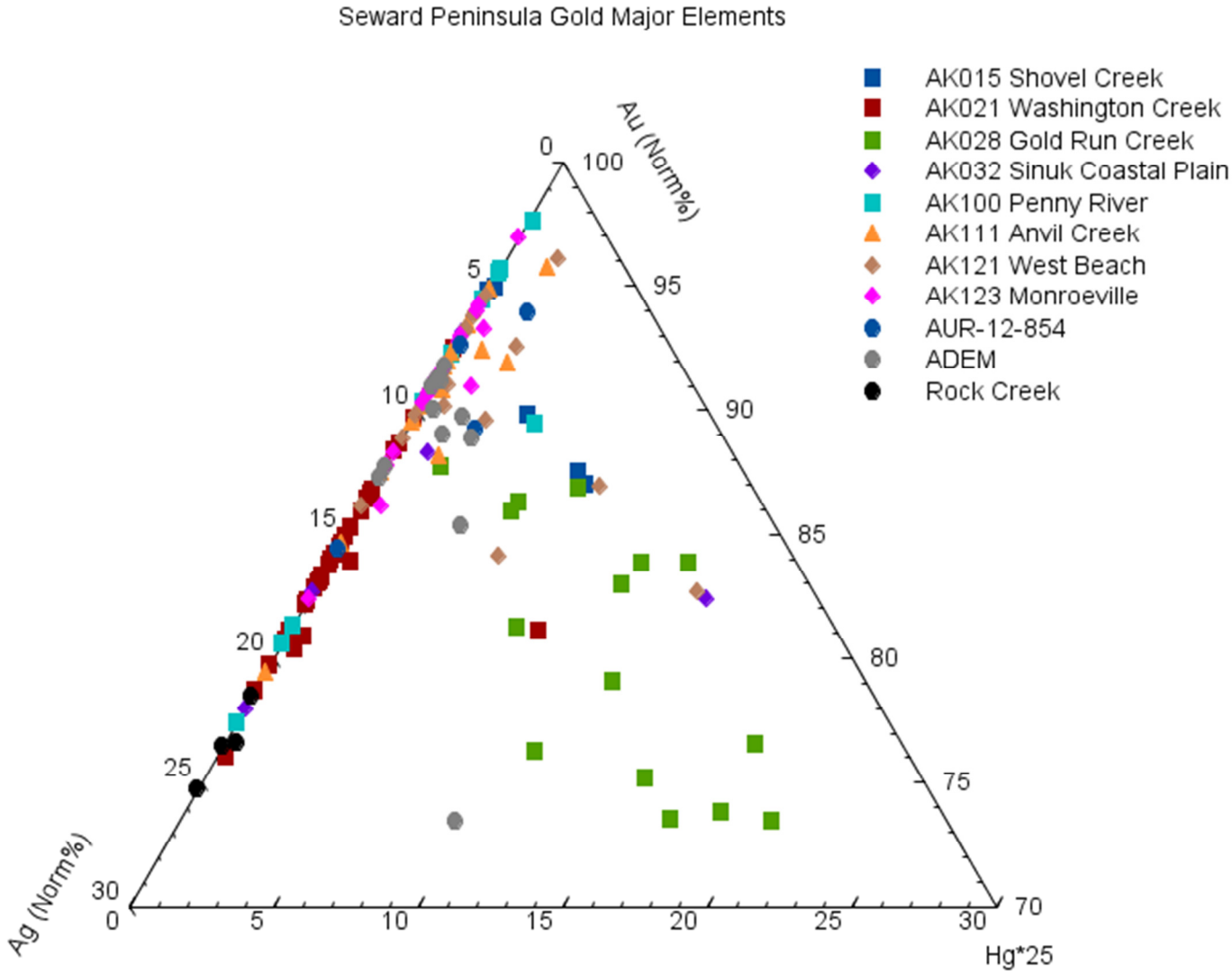

Figure 45: Au-Ag-(Hg X 25) ternary plot of southern Seward Peninsula gold grains. Note that due to generally low concentrations, Hg is shown as percentage Hg X 25.

A useful parameter when analysing gold grain major element chemistry is the fineness. Fineness is defined as the ratio of gold content as a proportion of gold plus silver content, normalised to 100% (Equation 1). The value is factorless and is reported to 1000. Morrison et al. (1991) studied the relationship between Ag content (fineness) and different types of gold deposit and found it to be partially characteristic of style of mineralisation. This parameter is useful to compare against other major or minor elements (such as Hg and Cu) as it is representative of both Au and Ag content and removes the influence of other major elements (as it is normalised to [Au+Ag] = 100%).

Equation 1: $$\boldsymbol{Fineness} = \frac{[\boldsymbol{Au}\%]}{[\boldsymbol{Au}\%+\boldsymbol{Ag}\%]}\ \boldsymbol{X\ 1000}$$

Gold grains from sites across the southern Seward Peninsula typically have a high fineness of >800 (Figure 47). An exception is RC4 with all four grains analysed reporting a fineness of between 750 and 785. Site AK015 has the highest average fineness and smallest fineness range of all sites whereas Site AK021 has the lowest average fineness and the broadest fineness range. Contrary to information supplied by a local gold buyer in Nome, who commented that gold coming from onshore leases routinely has higher fineness than that coming from offshore leases (and thus draws a higher premium), this study does not find there to be a significant difference in fineness between the onshore and offshore. However, it can perhaps be said that the beach and marine sites (AK121, AK123, AUR-12-854 and ADEM) have tighter fineness ranges than the ranges of fluvial sites (with the exception of AK015).

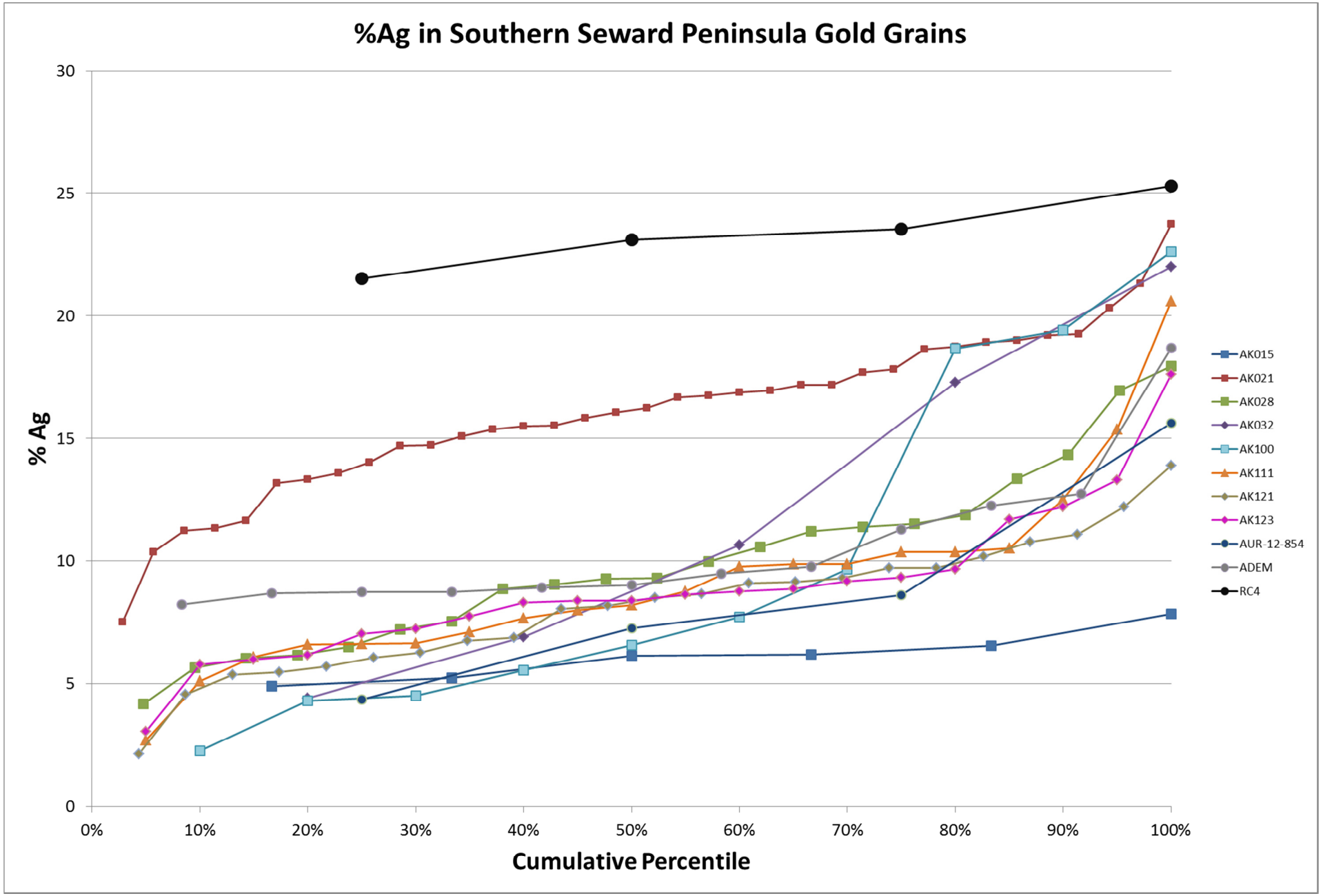

Figure 46: Cumulative percentile vs. percentage Ag plot for gold grains from eleven sites across the southern Seward Peninsula.

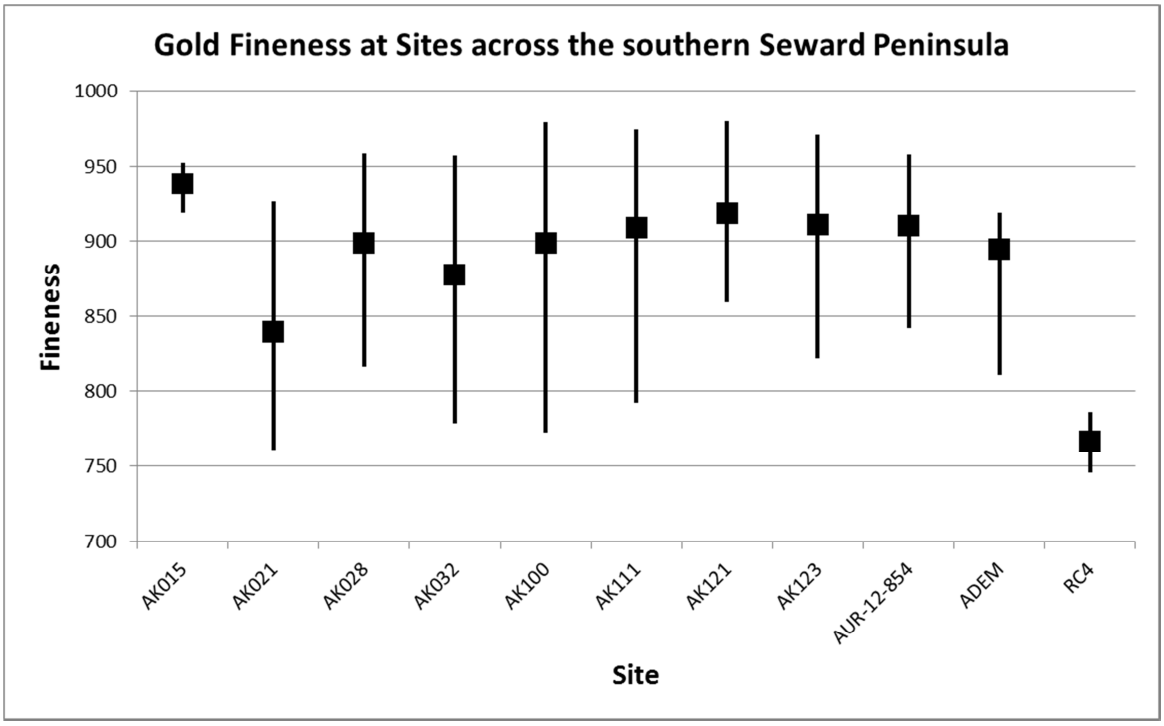

Figure 47: Gold fineness range of sites across the southern Seward Peninsula with the average shown as a block.

The Cu content of gold is sometimes high enough that it can be considered a major element, particularly in gold from intrusion related or oxidising hydrothermal mineralisation events (Chapman et al., 2009). Therefore, high Cu content has sometimes been considered to be characteristic of these types of gold deposits. However, a recent study showed that orogenic gold, which typically reports copper contents below detection limits, can on rare occasions contain Cu in excess of 0.5% (Moles et al., 2013). Knight and McTaggart (1990) have also used observations of increasing Cu content with increasing fineness to explain gold mineralisation in Cu-poor systems.

However, increasing fineness associated with an increasing in Cu content was not seen in this dataset (Figure 48). In gold grains from the southern Seward Peninsula, Cu remains a minor element reporting below 0.2% in all grains (site averages are 0.00% to 0.05%), except for an outlier (a single grain: AK028-17 reported Cu of 1.8%). Only two other grains reported a Cu-content above 0.1% (AUR-12-854-22, and AK032-2). Such Cu content anomalies are not entirely unexpected, nor irregular (Moles et al., 2013). No discernable trends in Cu content are observed in this dataset, even when grain populations are split between “fluvial” and “beach/marine” as in Figure 48.

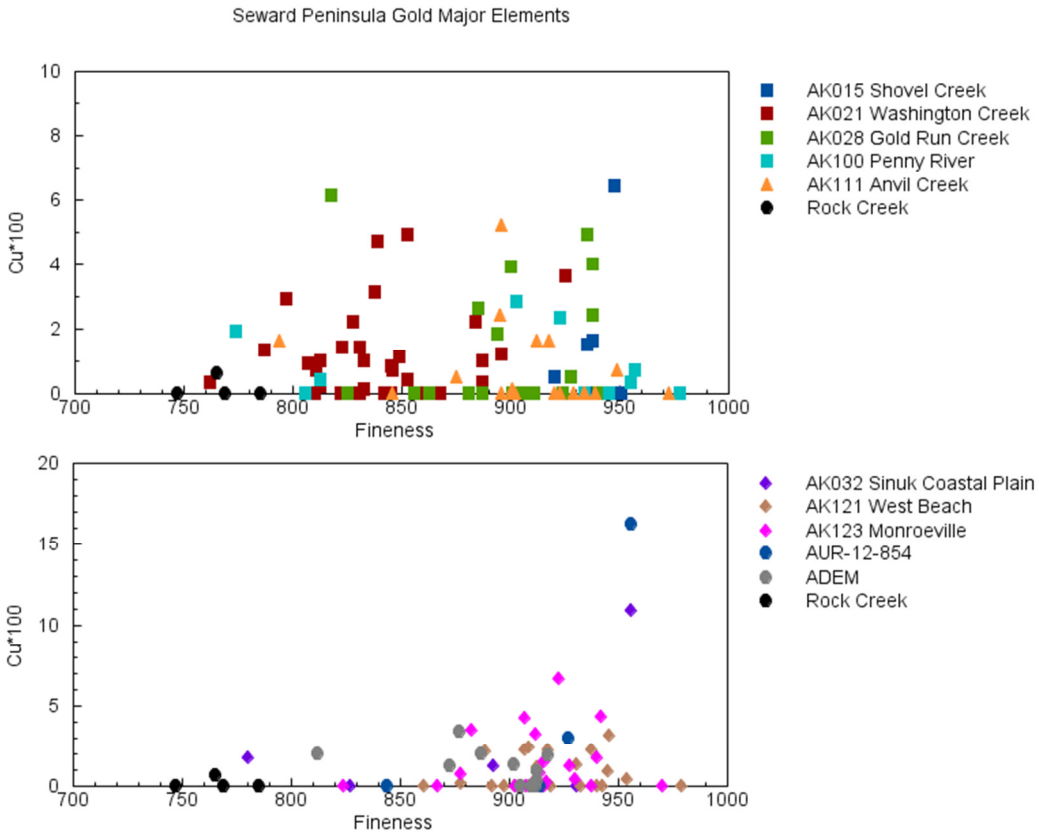

Figure 48: Fineness plots vs. percentage Cu X 100 for gold grains from eleven sites across the southern Seward Peninsula.

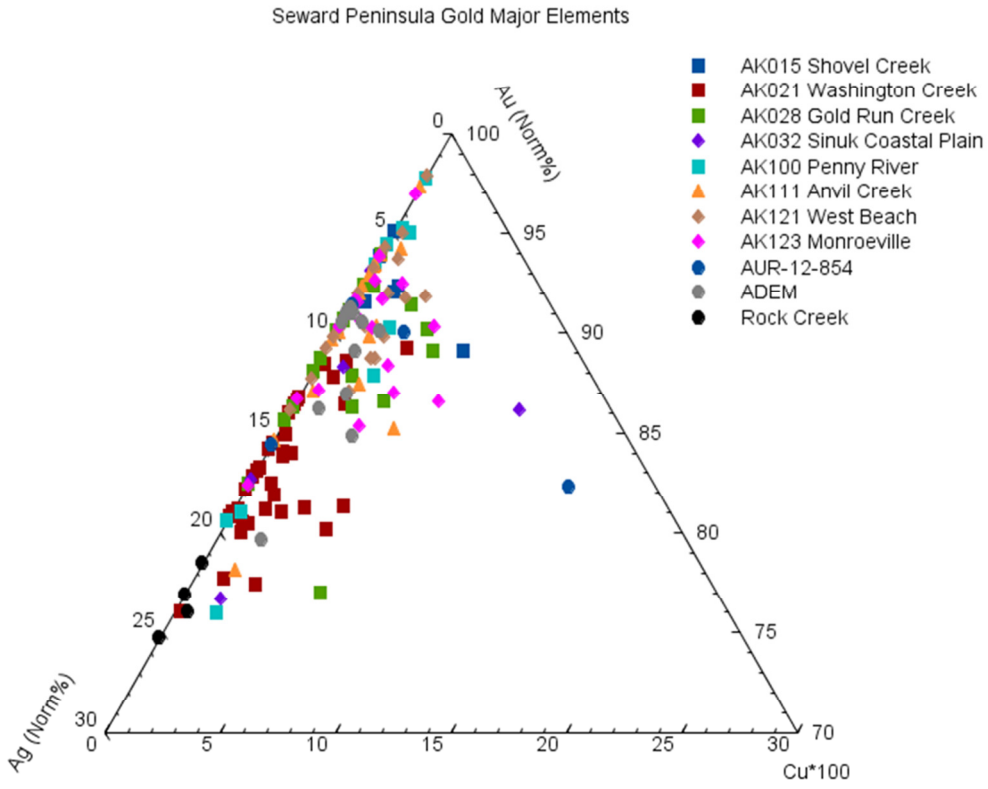

Figure 49: Au-Ag-(Cu X 100) ternary plot of southern Seward Peninsula gold grains. Note that due to very low Cu concentrations, Cu is shown as percentage Cu X 100.

6.4.3 Rim versus Core Analysis

The primary focus of EMP analysis in this study was to understand the major, minor, and trace element chemistry of unaltered southern Seward Peninsula gold grains. However, it is acknowledged that major and minor element gold chemistry can be significantly altered during weathering and transportation (e.g. Knight et al., 1999). Although no clearly definable rims other than those associated with gold growth (AK121-17 in Figure 40, and AK117-10 and AK121-3 in Figure 41) were noted during gold grain imaging (and particularly using backscatter electron viewing), it became routine during EMP analysis of gold grains to analyse a rim point (defined as a point within 10 µm of the polished grain edge) for comparison purposes to core data. The dataset, which is presented in Appendix E, was prepared in the same way as that described in Section 6.4. Furthermore, only core analyses which have a quality rim analysis (Au + Ag + Hg + Cu reported < 95% or >105%) are shown in Appendix E.

Regarding Ag and Hg contents, site ADEM reported notable depletion in Ag and Hg content in the grain rim related to its core in more than half the comparisons available. The most noteworthy are Ag_{core}/Ag_{rim} depletion values of 64, 24, and 19 for grains ADEM-4, ADEM-6, and ADEM-14. A similar observation, though to a lower degree, is made for a two grains from Site AK111 (AK111-20 has an Ag_{core}/Ag_{rim} ratio of 3 and AK111-7 a ratio of 2).

The largest variation in Hg_{core}/Hg_{rim} ratios was seen in grains from Site AK028, where approximately half the grains assessed showed an increase in Hg_{core}/Hg_{rim} ratio. As supergene processes have shown to typically develop Hg-rich rims (see Section 7.1.1) this is likely not as a result of any supergene process but rather highlights the heterogeneity of Hg content in grains from this site. Already discussed is the enrichment of Hg in the rims (gold growths) of grains from sites AK121 and AK117 (not analysed due to sample loss although morphology assessment revealed secondary gold growths). Correlated with this is an expected decrease in rim gold content for these sites. This is clearly seen with AK121-13 and AK121-17 having Au_{core}/Au_{rim} ratios of 1.31 and 1.24, respectively. Grain AK032-9 shows a 5X enrichment in Hg in its rim relative to its core but no effect is seen in Au or Ag core/rim ratios. This may indicate early stage Hg-rich gold growth. Grain rims of ADEM-2 and ADEM-3 show Hg enrichment, likely related to secondary Au-Ag-Hg alloy development.

Cu contents are generally very low for all grains (<0.2%), and variations at these levels might not be diagnostic. However, it is noted that in most Cu_{core}/Cu_{rim} assessments from all sites there appears to be depletion in Cu content of the grain rims relative to its core. One good example is grain AUR-12-854-22, which has a core Cu content of 0.16% and a rim Cu content of 0.02%, a depletion ratio of about 8X. For this grain, similar depletion is also seen for Ag and Hg.

6.5 Trace Element Geochemistry

Trace element abundances in gold grains can aid in constraining population groups where major elements are not able to do so sufficiently and can also provide insights into mineralisation styles and ore-forming processes (e.g. Žitňan et al., 2010). An example of this is described in Section 3.3.2 where Brown et al. (2003) successfully used trace elements to distinguish between highly and poorly mineralised lodes, thus indicating two separate mineralization events for these deposits.

The trace element analysis of southern Seward Peninsula grains focuses on the elements Cu, Te, Hg, W, As, and Sb, after it was found additional trace elements were not detectable in grains analysed at the beginning of the study (see Section 4.8.2). Although trace element ratios and relationships are sometimes used to identify populations and trends (Watling et al., 1994; Outridge et al., 1998; Žitňan et al., 2010), this study did not attempt such an exercise given the relatively high errors achieved and the paucity of trace element data across the range of five trace elements analysed. However, general trace element observations were made, particularly regarding presence or absence of trace element abundances and averages (Table 8).

The presence of Cu in gold grains from most sites was identified during major and minor element analysis (Section 6.3.2). Cu was also re-analysed as a trace element to provide greater resolution (30 ppm vs. 170 ppm detection limit). As was previously noted in Section 6.4.2, Cu trace element data support the observation that sites AK028 and AUR-12-854 have high averages as a result of anomalously high individual grains (Figure 50). These elevated Cu anomalies are not unexpected and are routinely observed in placer gold deposits (Moles et al., 2013). Grains from Site AK032 also have anomalously high Cu content with a trace element average

abundance of 400 ppm. Of interest is the very low Cu content observed in grains from Site AK021.

Tellurium (Te) is present in almost all gold grains in some amount with most sites averaging between 35 ppm and 93 ppm. It is noted that grains from AK021 are consistently slightly richer in Te than other sites (Figure 51).

Mercury (Hg) contents, as previously discussed in section 6.4.1, are anomalously high in grains from Sites AK015 (average ~1500 ppm) and AK028 (average ~11,500 ppm), reflective of primary Au-Ag-Hg alloy. Grains from Site AK032 have an average Hg content of ~900 ppm whereas the remainder of the sites have average Hg ranges of 20 ppm to 150 ppm.

Tungsten (W) is observed to be present in small amounts with grains from sites AK100 and AK121 having perhaps slightly higher W than elsewhere (Figure 53).

Arsenic (As), like Te, is present in most grains. Of note are the very low concentrations in grains from site AK015 and AK028, both Au-Ag-Hg alloy sites. Site AK100 has consistently higher As content (Figure 52), apart from anomalously high As contents in individual grains from AUR-12-854 and AK021 (with the highest reported As content of ~10,000 ppm).

Antimony (Sb) is relatively low in grains from all sites (reporting 0 ppm to 40 ppm), except for site AK021 which reported a single analysis of 400 ppm.

A summary of the observations discussed in sections 6.4 and 6.5 is presented in Table 11.

Table 8: Trace element average abundances in gold grains from ten sites across the southern Seward Peninsula.

Site	Cu	Te	Hg	W	As	Sb
	Avg ppm	Avg ppm	Avg ppm	Avg ppm	Avg ppm	Avg ppm
AK015	113	46	1424	20	24	10
AK021	22	93	93	20	328	21
AK028	1721	68	11451	23	22	11
AK032	400	47	886	21	131	11
AK100	137	62	20	38	193	12
AK111	80	71	22	23	28	11
AK121	50	35	36	29	32	10
AK123	84	63	20	20	30	11
AUR-12-854	696	38	20	21	160	10
ADEM	75	75	151	23	103	14

Explanation:

Table 8 reports the average abundances of trace elements from each site. Average abundance was calculated using all quality quantitative analyses where Au + Ag + Hg + Cu reported < 95% or >105% (see Appendix G). Should “no result” have been reported, a value equal to half the detection limit was used (i.e. 15 ppm for Cu and Te; 20 ppm for Hg, W, and As; and 10 ppm for Sb).

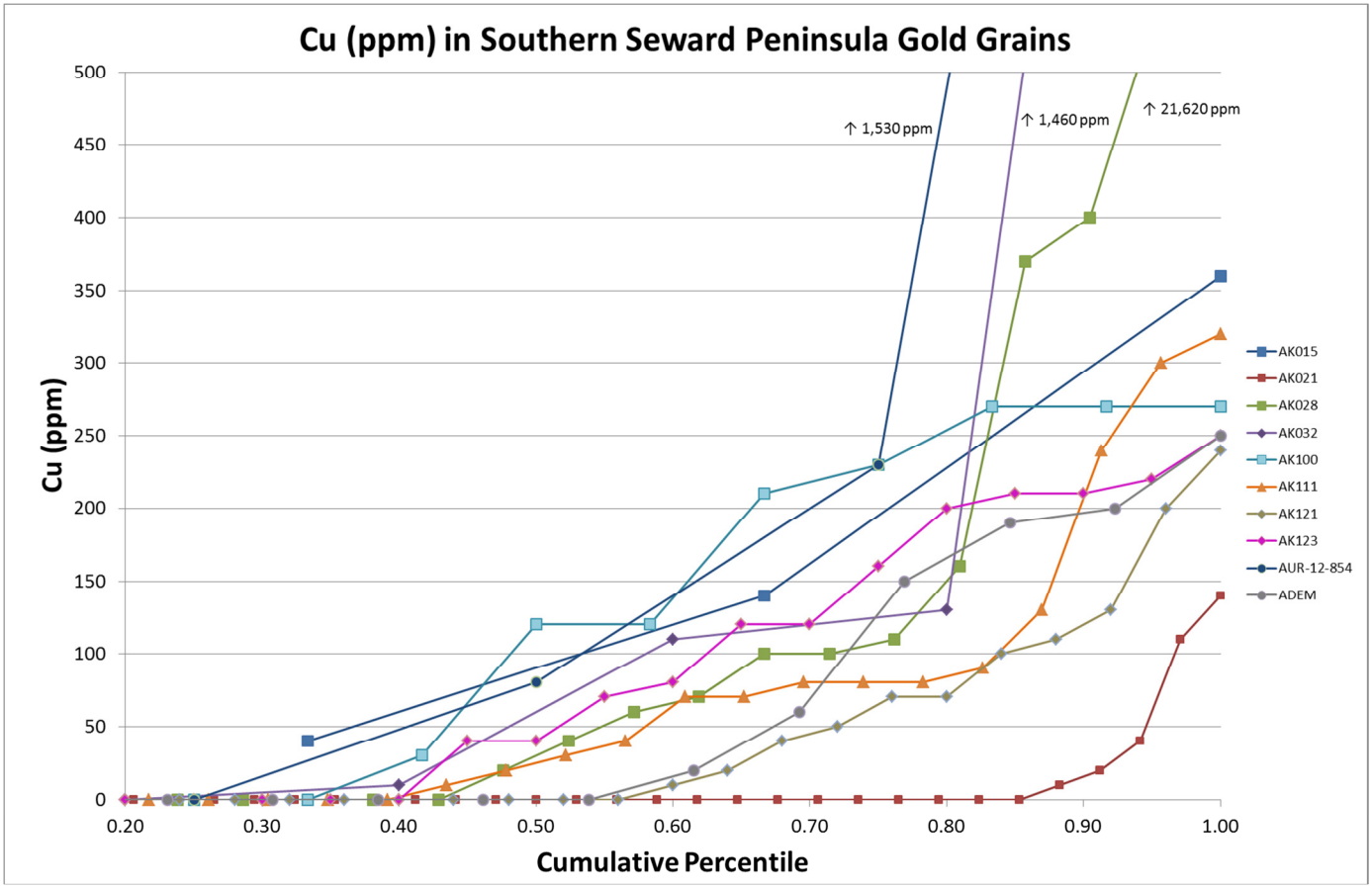

Figure 50: Cumulative percentile vs. Cu (ppm) plot for gold grains from ten sites across the southern Seward Peninsula. Detection limit for Cu is 30 ppm.

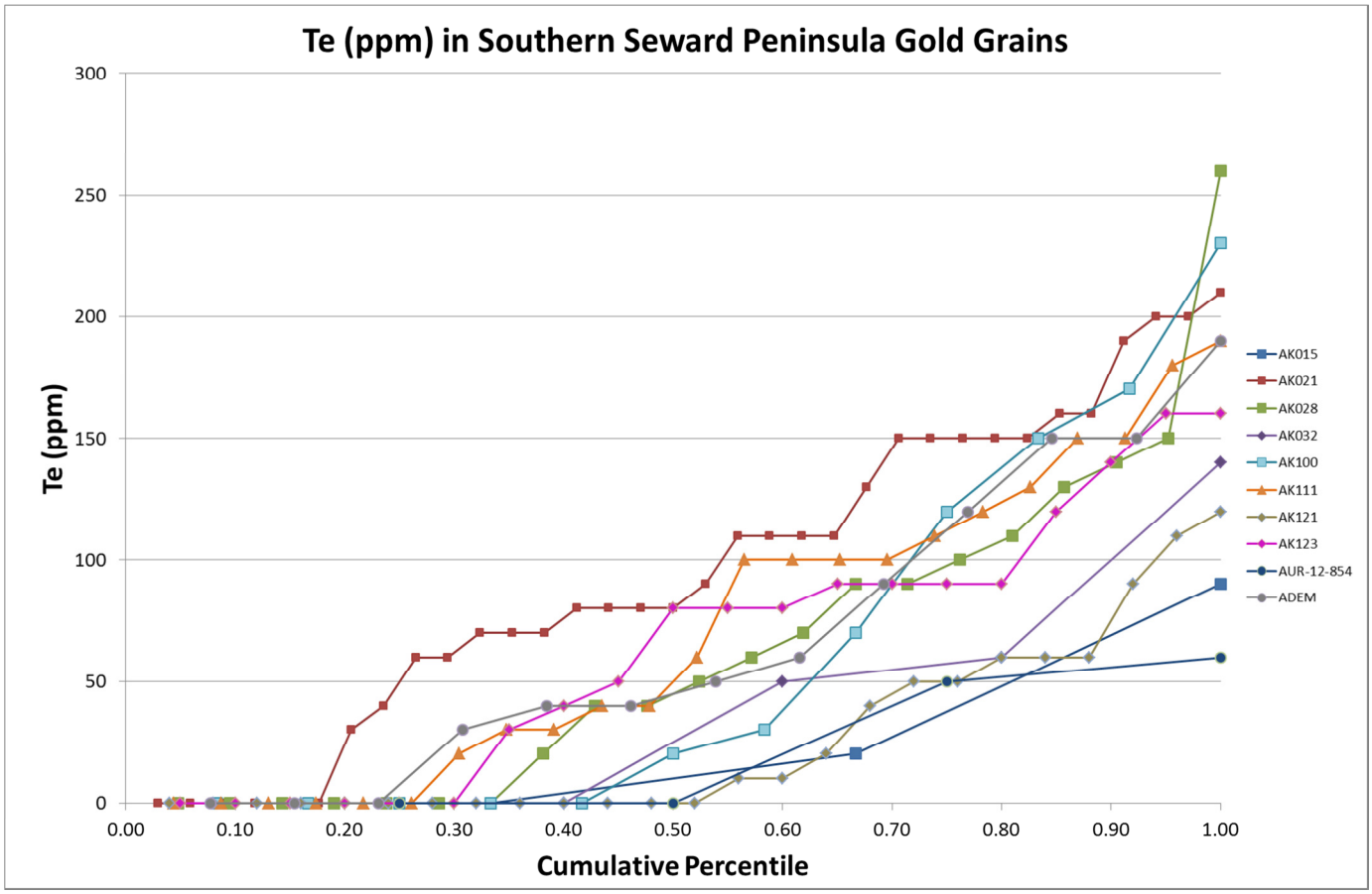

Figure 51: Cumulative percentile vs. Te (ppm) plot for gold grains from ten sites across the southern Seward Peninsula. Detection limit for Te is 30 ppm.

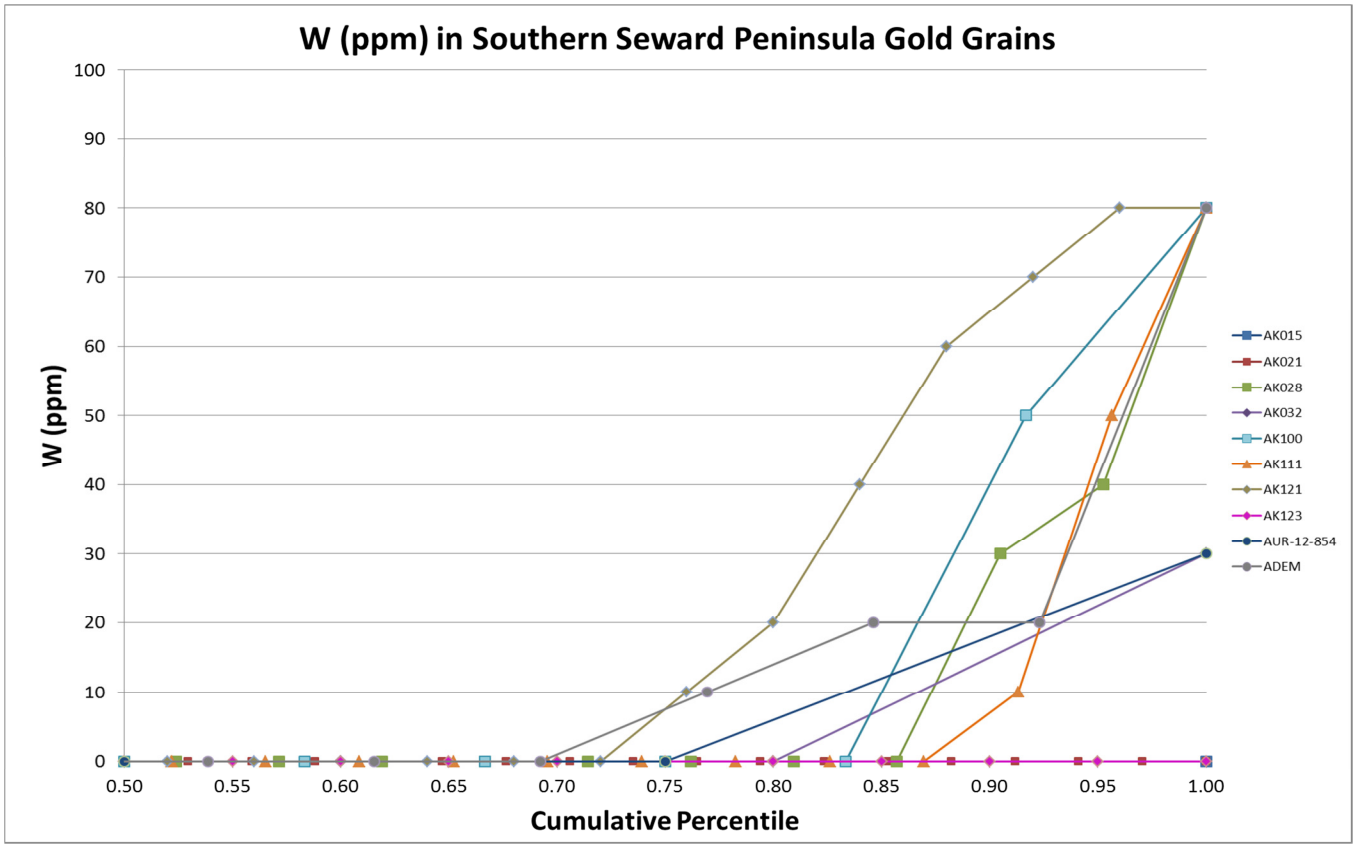

Figure 53: Cumulative percentile vs. W (ppm) plot for gold grains from ten sites across the southern Seward Peninsula. Detection limit for W is 40 ppm.

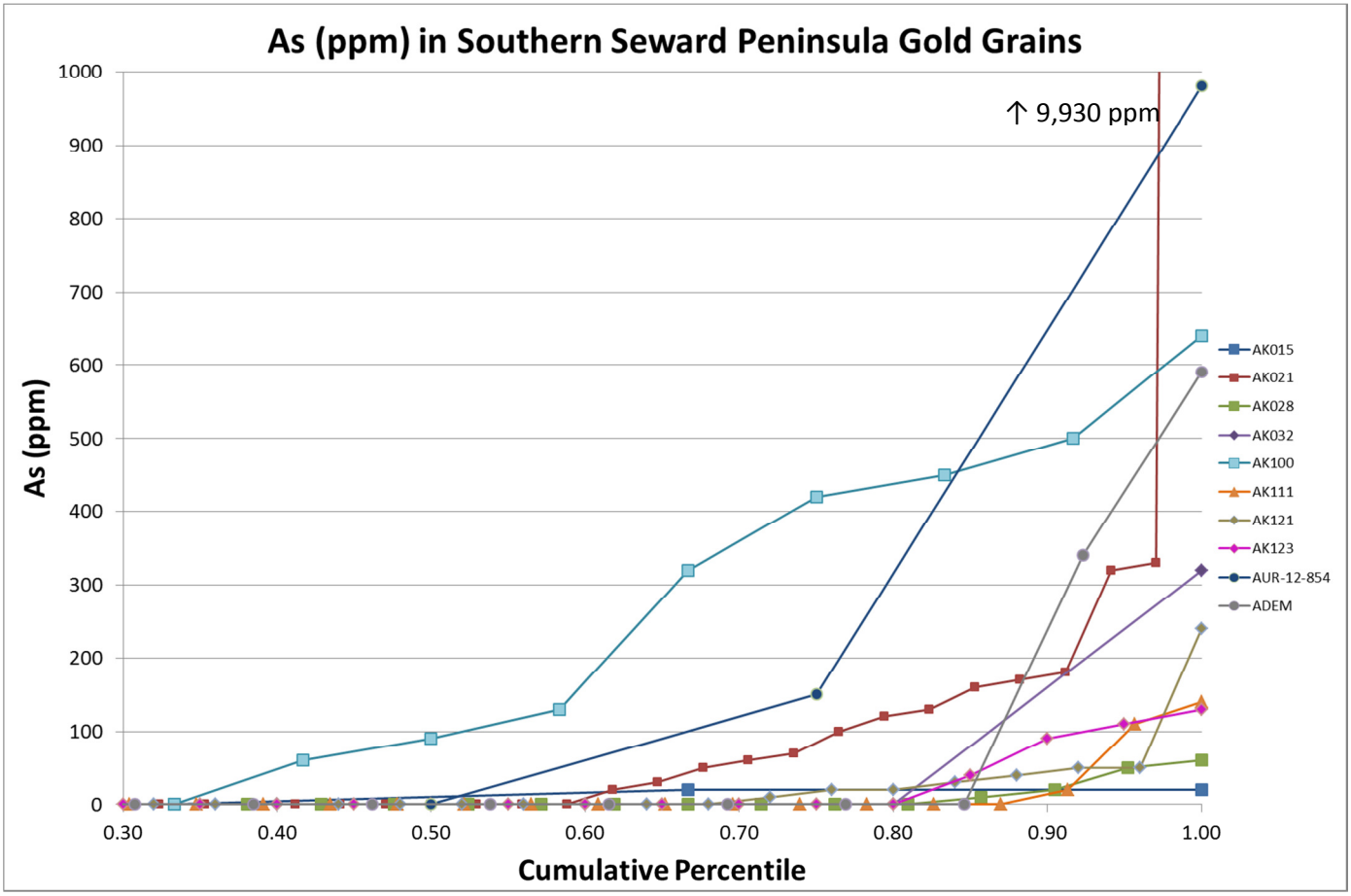

Figure 52: Cumulative percentile vs. As (ppm) plot for gold grains from ten sites across the southern Seward Peninsula. Detection limit for As is 40 ppm.

6.6 Elemental Map Results and Observations

Since gold grains are commonly heterogeneous, using a probe to collect gold grain chemistry data may erroneously result in a single analysis or set of analyses being reported as representative for the entire gold grain. Therefore, to investigate the geochemical heterogeneity of gold grains, BSE images are often consulted. Although BSE imaging is typically sufficient to assess the alloy heterogeneity or homogeneity of gold grains, there have been occasions where BSE has not been sufficient, such as described in Chapman et al. (2010), where Ag and Hg contents varied substantially with a negative correlation across a grain of Au-Ag-Hg alloy. Therefore, to investigate alloy heterogeneity from sites across the southern Seward Peninsula, qualitative elemental maps were taken for at least one grain per site (Table 9 and Appendix H). Four elements could be mapped per run, and therefore two map runs were conducted, resulting in element mapping of a suite of eight elements (Au, Ag, Cu, W and Hg, Bi, As, Fe) for all sites excluding AK117 (no polished grains) and RC4. RC4 was gold hosted within arsenopyrite, so the elements mapped were Au, Ag, Bi, Fe and S, Cu, Te, and As. The full dataset of all maps can be found in Appendix H. Maps were taken using an accelerating voltage of 15.0 kV, probe current of either 20 nA or 150 nA, and a dwell time of 10 seconds per site. Grid spacing varied between 0.76 µm and 1 µm for all maps other than RC4 grains, which had a grid spacing of 0.20 µm.

Table 9: Selected gold grains for which elemental maps were obtained.

Map 1 Au, Ag, Cu, W	Map 2 Hg, Bi, As, Fe
AK015-1	AK015-1
AK021-6	AK021-6
AK028-3	AK028-3
AK032-7	AK032-7
AUR-12-854-21	AUR-12-854-21
AK100-4	AK100-4
AK100-18	AK100-18
AK111-5	AK111-5
AK121-17	AK121-17
AK123-8	AK123-8
ADEM-4	
ADEM-7	ADEM-7
Au, Ag, Bi, Fe	**S, Cu, Te, As**
RC4-1	RC4-1
RC4-2	RC4-2

Almost all of the elemental maps showed very little variation throughout an individual grain (e.g. AUR-12-854-21 in Figure 54). AUR-12-854-21 is entirely homogenous and shows no evidence of rim development or any other heterogeneous phenomena. This also appears to be true for grains AK028-3, AK032-7, AK100-4, AK100-18, AK111-5, and ADEM-7.

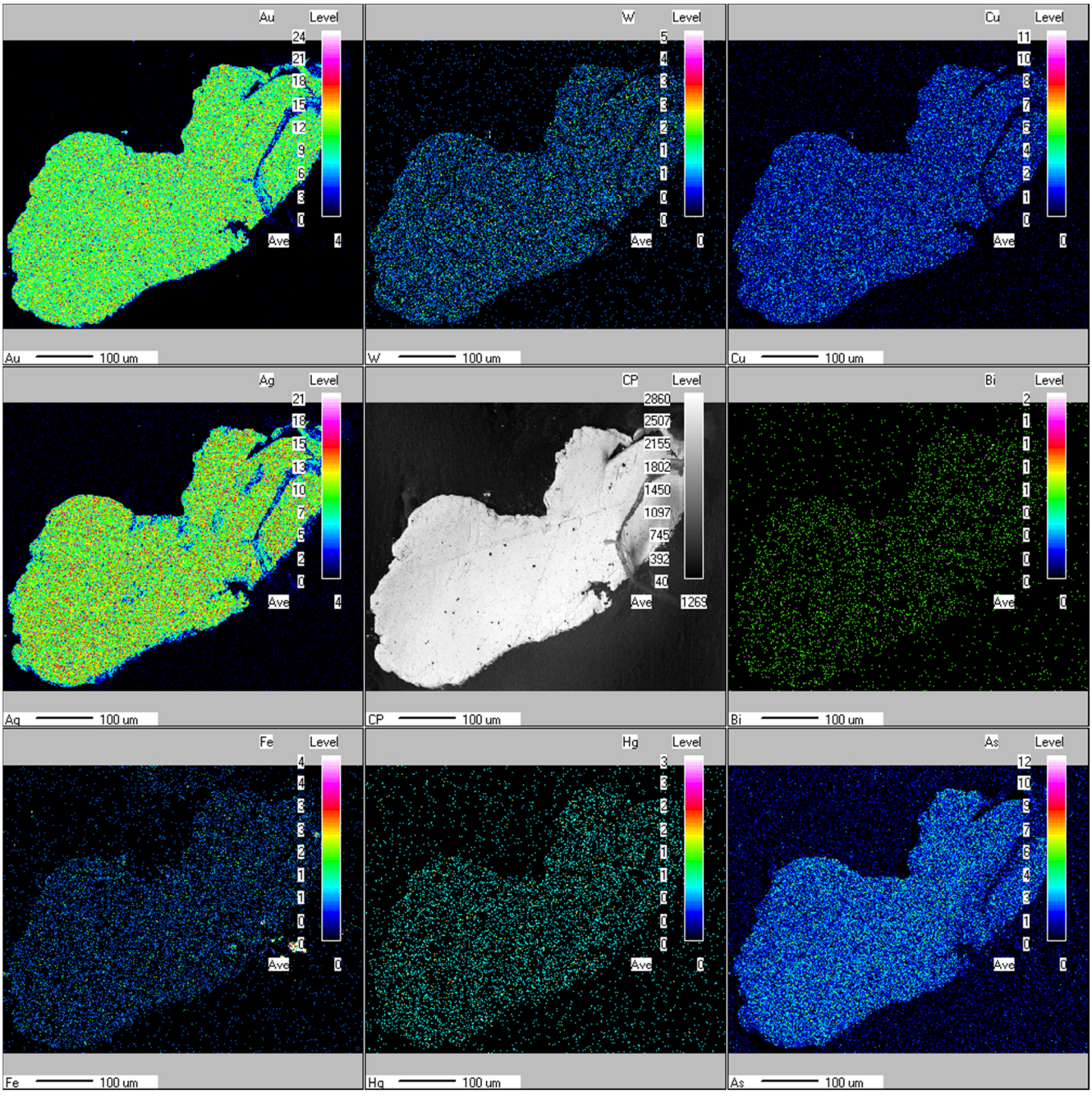

Figure 54: Elemental map of gold grain AUR-12-854-21 of elements (from right to left, top to bottom) Au, W, Cu, Ag, Bi, Fe, Hg, and As. The centre image is a Composition Image (i.e. backscatter electron image). Probe conditions were an accelerating voltage of 15 kV, current of 20 nA, and sampling grid of 0.86 µm X 0.86 µm.

Some grains display minor heterogeneity in Au, Ag, and Hg contents (grain AK015-1 shows Ag-depletion in its rim coupled with Hg enrichment), Au, Ag and As contents (grain AK021-6 shows Ag and As enrichment in coupled with gold depletion in one area), and Au-Ag exsolution patterns (both grain AK123-8 and ADEM-4 display Ag-enriched lines crossing the grain, see Figure 55).

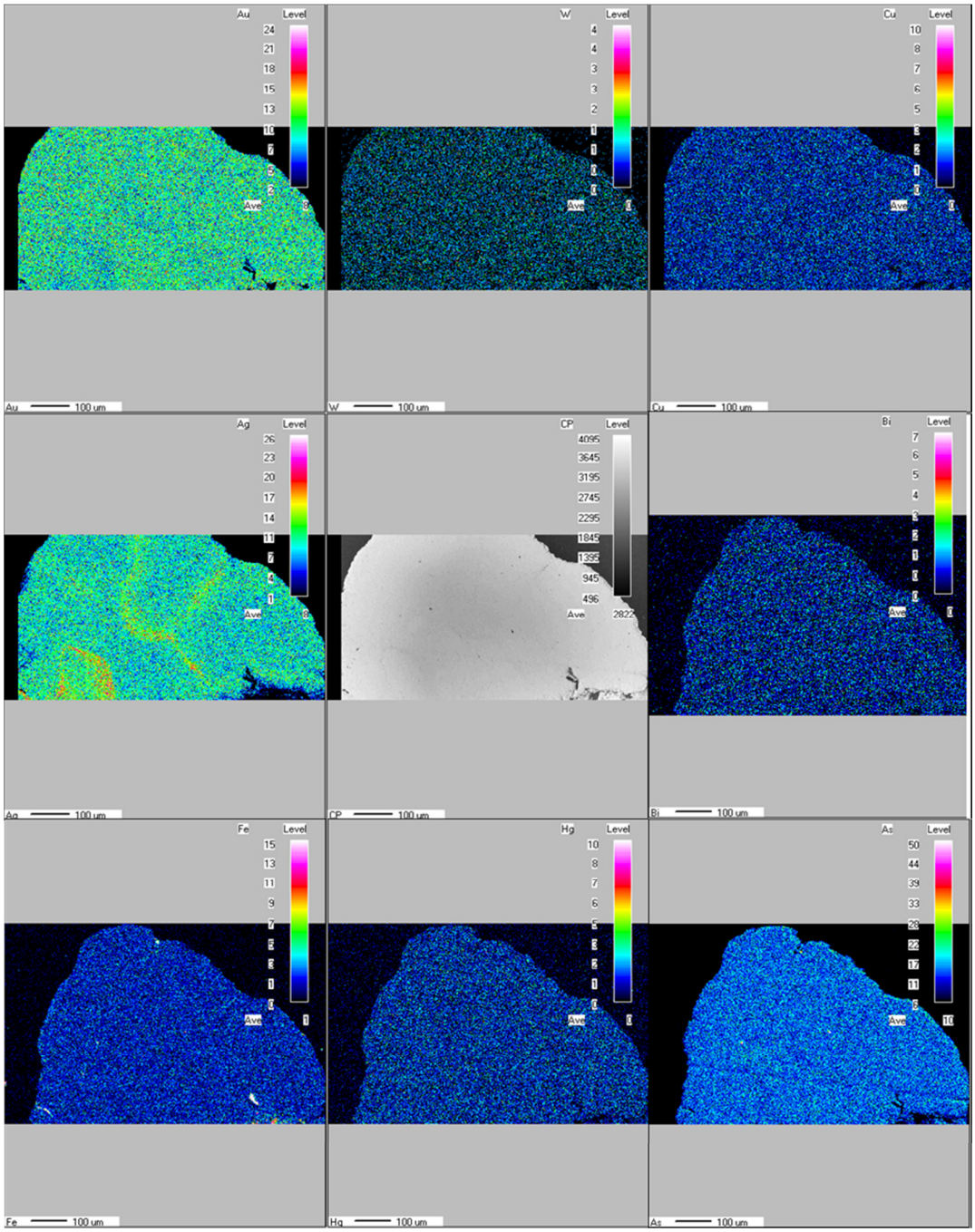

Figure 55: Elemental map of gold grain AK123-8 of elements (from right to left, top to bottom) Au, W, Cu, Ag, Bi, Fe, Hg, and As. The centre image is a Composition Image (i.e. backscatter electron image). Probe conditions were an accelerating voltage of 15 kV, current of 20 nA, and sampling grid of 0.76 µm X 0.76 µm.

An elemental map was also taken of grain AK121-17 (Figure 56), which was observed to have hexagonal gold growths present all around the core grain (refer to Figure 40). Point analyses taken of the core and rim showed an increase in Ag and Hg content in the growths, coupled with a decrease in Au content. The elemental map confirmed these point analyses unequivocally, in addition to identifying the existence of a slight depletion of As and possibly Cu in the growths relative to the core.

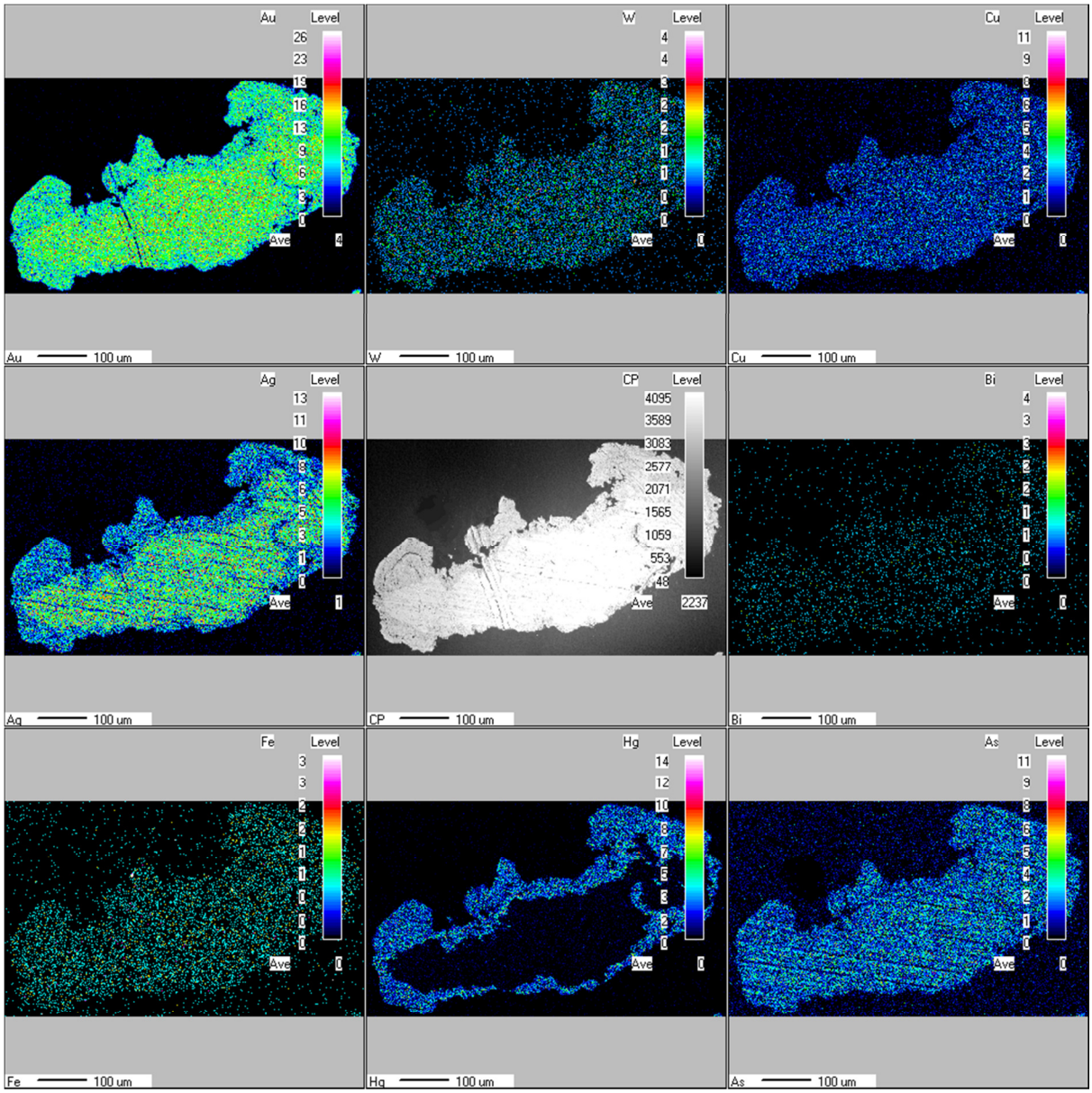

Figure 56: Elemental map of gold grain AK121-17 of elements (from right to left, top to bottom) Au, W, Cu, Ag, Bi, Fe, Hg, and As. The centre image is a Composition Image (i.e. backscatter electron image). Probe conditions were an accelerating voltage of 15 kV, current of 20 nA, and sampling grid of 1.00 µm X 1.00 µm.

7 Discussion

7.1 Supergene Gold Grain Alteration

Prior to the discussion of primary gold grain morphology and chemistry and their relation to populations and source, it is important to understand the supergene (post depositional) processes which can alter a grains morphology and chemistry so as to be able to identify and preclude such evidence from the interpretation. This section discusses two such processes identified in the southern Seward Peninsula: (1.) the secondary growth of Au-Ag-Hg alloy and (2.) silver enrichment and depletion.

7.1.1 Secondary Gold Growth

Three types of secondary Au-Ag-Hg alloys have been identified: hydrothermal, secondary, and synthetic (Youngson et al., 2002). Hydrothermal Au-Ag-Hg alloys are naturally occurring and represent precipitates from hydrothermal fluids or material re-crystallized during metamorphism. Secondary Au-Ag-Hg alloys form naturally at low temperatures in near surface environments as a result of interaction with anthropogenically introduced mercury. Synthetic Au-Ag-Hg alloys are formed artificially during gold-winning practices, such as amalgamation.

Secondary growth of Au-Ag-Hg alloys can occur as a result of the amalgamation of detrital gold with naturally occurring Hg (Nelson et al., 1975), but more typically represents the amalgamation of detrital gold with anthropogenic Hg introduced during mining activities (e.g. Knight and McTaggart, 1990; Bowell, 1992; Youngson et al., 2000; Youngson et al., 2002). Typically, secondary Au-Ag-Hg alloys display a hexagonal crystal structure (e.g. Figure 57A) (as opposed to cubic for hydrothermal Au-Ag-Hg alloy) or occur as anhedral, rounded, amalgamated aggregates (Figure 57 B and C) (Youngson et al., 2002).

A ternary plot of Au-Ag-Hg compositional variation in hydrothermal and secondary Au-Ag-Hg alloy is shown in Figure 58. All grain core data plot within the hydrothermal Au-Ag-Hg compositional space (with Sites AK028 and AK015 having the broadest distribution), whilst the hexagonal gold growths from AK121-17 and the amalgamated anhedral growths on the rim of AK121-13 plot in the secondary Au-Ag-Hg alloy field. Therefore, there is strong evidence from both morphology and major element analysis that secondary Au-Ag-Hg alloy formation occurs in the southern Seward Peninsula. Morphology observations (Table 7) identifies that Sites AK032,

AK117, AK121, AK123, AUR-12-854, and ADEM show morphological evidence for Au-Ag-Hg alloy accretion whilst Site AK100 shows some evidence and Sites AK015, AK021, AK028, and AK111 show minor to no evidence of secondary Au-Ag-Hg alloy accretion. The sites most affected are those of beaches (AK032, AK117, AK121, and AK123) and marine sites (AUR-12-854 and ADEM) while fluvial (AK015, AK021, and AK028) or buried glacial outwash (AK111) sites are least affected. Although it is noted that the sediments of the Seward Peninsula contain naturally high Hg content (Nelson et al., 1975), presumably from primary Au-Ag-Hg alloys or related source rocks, the association of secondary Au-Ag-Hg accretion with locations of historic and modern mining suggests that natural Hg does not have a major influence in the formation of the secondary Au-Ag-Hg alloys. Rather, these secondary alloys most likely formed a result of anthropogenic Hg introduced during extensive beach mining, which has also influenced the offshore sites.

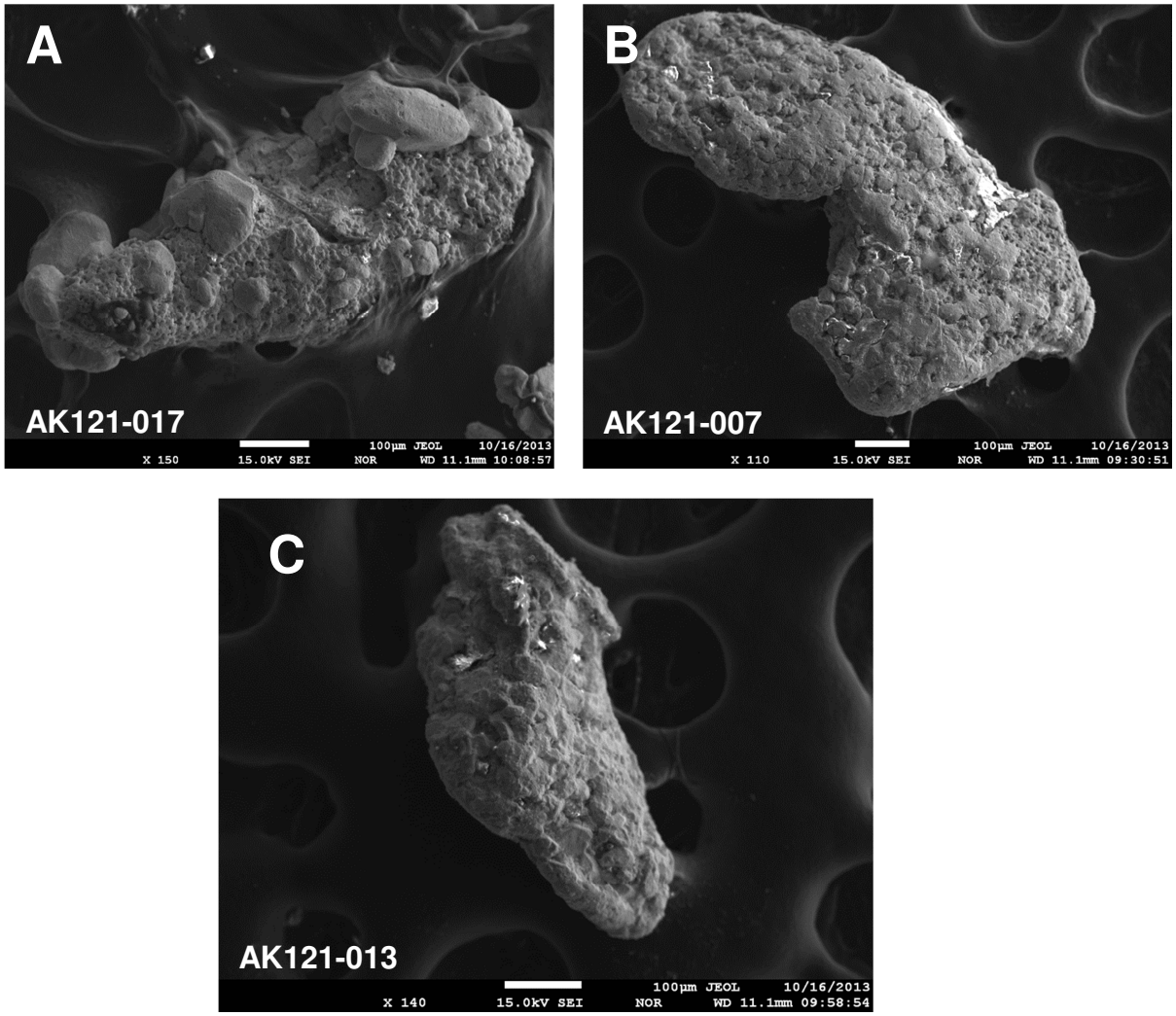

Figure 57: Secondary Au-Ag-Hg alloy coating gold grains from site AK121. A: Hexagonal Au-Ag-Hg alloy crystal growth, B and C: Amalgamated, rounded Au-Ag-Hg alloy aggregate.

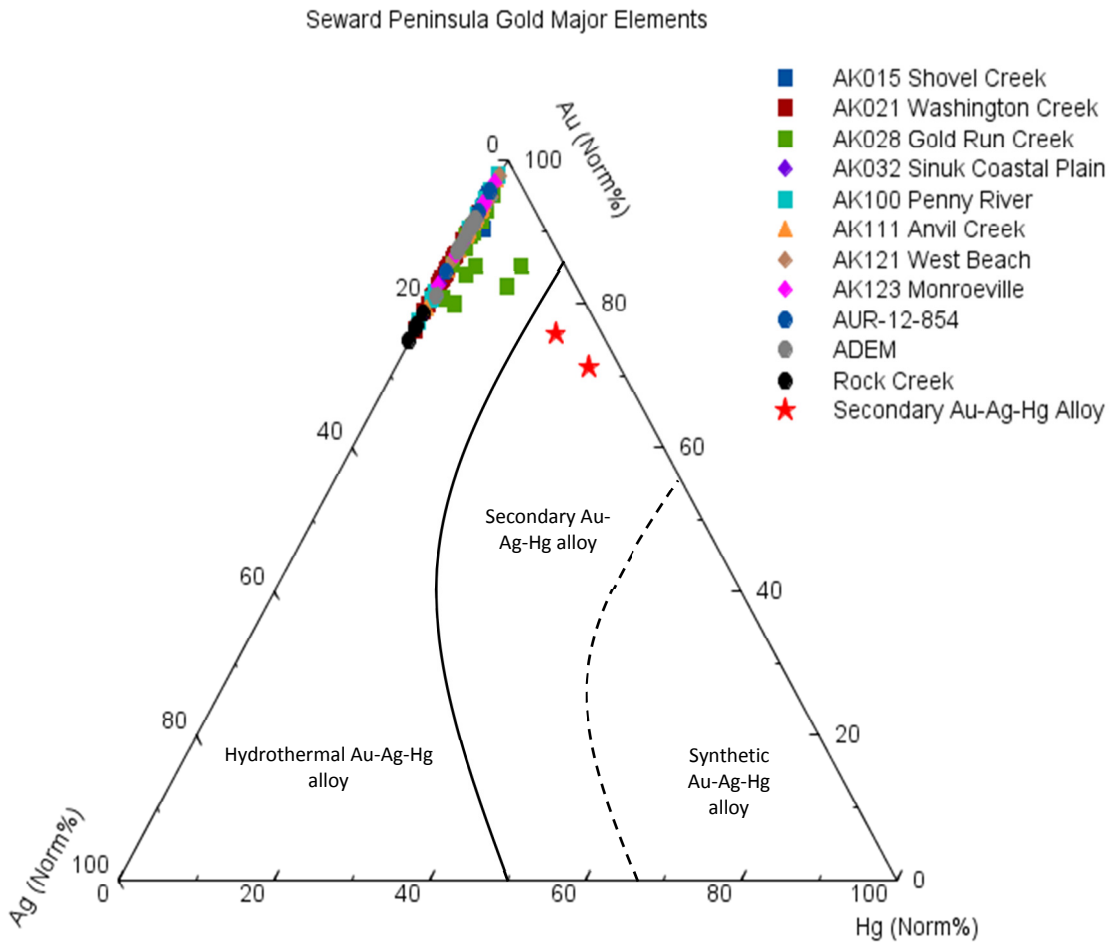

Figure 58: Au-Ag-Hg ternary plot showing compositional variation of southern Seward Peninsula gold grains. Of particular interest are the two analyses of secondary Au-Ag-Hg alloy taken from the rims of AK121-17 and AK121-13 (stars). Alloy composition fields from Youngson et al., 2002.

7.1.2.1 Silver Enrichment

Of interest are the Ag-enrichment zones seen in ADEM-4 (see elemental map in Appendix H) and AK123-8 (Figure 55). Although in both these grains, Ag-enrichment does not appear to be along fractures, other workers to have noted such occurrences (e.g. Dumula and Mortensen, 2001; Larizzatti et al., 2008). These workers relate Ag-enrichment to fractures or internal grain boundaries. Dumula and Mortensen (2002) interpreted such enrichment to be a primary feature of the grain related to late- or post-mineralisation and not to alteration. This process is, however, poorly understood.

7.1.2.2 Silver-Depleted or Gold-Enriched Rim Formation

Silver depletion (or gold enrichment) of gold grain rims is often noted in alluvial gold grains with three mechanisms for this process having been proposed (Groen et al. (1990) and McClenaghan and Cabri (2011)):

a) Preferential dissolution of Ag where Ag is leached out of Au-Ag electrum in the supergene environment, typically in fluvial systems or in certain organic-rich marine settings. Leaching typically occurs along the edges of grains and produces an Ag-depleted rim.
b) Cementation of secondary gold with low Ag-content where Au-rich amalgam precipitates out of solution onto the exterior of detrital gold grains.
c) A self-electrorefining process to dissolve electrum and immediately precipitate gold, thereby depleting the gold grain rim in Ag.

As discussed in Section 6.4.3, variation in Ag content between the core and rim was noted for site ADEM and, to a lesser degree, for Sites AK111 and AK015 (see Section 6.6). The depletion of silver (along with Hg-enrichment) from the grain rim in ADEM-2 and ADEM-3 is interpreted to be related to secondary Au-Ag-Hg alloy precipitation, which contains lower Ag-content than a typical grain core (as seen in AK121-17, Figure 56). In contrast, the absence of morphological evidence or Hg-enrichment in grains from AK015 and AK111 suggests that preferential dissolution is the cause for Ag-depletion.

7.2 Gold Grain Populations and Implications for Transport Mechanisms

The identification of individual populations of gold grains across the southern Seward Peninsula may provide insight into the movement and mixing of gold populations, their individual transport mechanisms, the potential for contribution from various sources, and the influence of supergene processes. Population identification for the grains in this study has been carried out by assessing variation in particle statistics, particle morphology, gold grain chemistry, and site clast lithology. A summary table of likely transport mechanisms for gold grain populations present at each site is presented in Table 10.

7.2.1 PSD, Morphology, and Textural Assessment

7.2.1.1 Site AK015 – Shovel Creek, Solomon System

This stream sample contains a moderately sorted gold grain population with morphology suggestive of a semi-mature fluvial population (degree of abrasion is rare to common, whilst rounding and flattening is moderate with minor folding). This sample likely represents a single population sourced locally, likely initially transported by periglacial processes (solifluction) and subsequently fluvially transported.

7.2.1.2 Site AK021 – Washington Creek, Sinuk System

Field observations (see Section 5.4) revealed that site AK021 (Washington Creek) is dominated by reworked fluvial gravels released from a local conglomerate. PSD analysis of gold grains from Site AK021 reveals an extremely mature and well sorted population, which is unusual for a proximal fluvial sample. Morphology assessments shows little variation in degree of abrasion (common to abundant), rounding (well-rounded) and flattening (well flattened). In addition, over half the grains from this site show evidence of folding, strongly suggesting that the gold grains from Site AK021 represent a single population that was fluvially transported and deposited into the local palaeo-placer conglomerate. The conglomerate containing such a well-sorted, mature gold population further suggests the palaeo provenance is somewhat distal from the current site.

7.2.1.3 Site AK028 – Gold Run Creek, Teller System

This site has a massive variation in particle size (1.15 to 57.78 mm^2) with the largest grains in this study recovered from this site; however, the relatively smooth cumulative curve suggests a single population. The large variation in PSD as well as the morphology assessments suggests an immature fluvial population with degree of abrasion, rounding, and flattening similar to that of AK015 - although less mature and with a greater presence of primary features observed (e.g. AK028-11). The morphology evidence does not unequivocally suggest glacial transport, although this cannot be precluded for at least a portion of its transport history. The retention of primary features and presence of large gold grains suggest this sample is close to source. This site is interpreted to have a gold grain population from a single source that was partially glacially and partially fluvially transported.

7.2.1.4 Site AK032 – Sinuk Coastal Plain, Sinuk System

This beach site generated a gold grain sample with a relatively well-sorted PSD typical of beach or marine deposits. The presence of secondary Au-Ag-Hg alloy growth over ~90% of the grains conceals abrasion history and highlights the operation of extensive supergene processes. Rounding and flattening suggest a relatively mature sample that has been well influenced by beach/marine processes. The presence of folding suggests that a portion of the sample transport history was fluvial. Sparse evidence for minor aeolian transport exists.

7.2.1.5 Site AK100 – Penny River, Nome System

Site AK100 (Penny River) generated a very well sorted sample with little variation in PSD. Such a mature river sample suggests input from a local palaeo-placer (such as with AK021) or fluvial transport from a relatively distal source. The considerable presence of primary features coupled with the relatively low degree of rounding (sub-angular to rounded), low degree of flattening, and absence of folding suggests that the grains have not been subject to fluvial transport over a long distance (Youngson and Craw, 1999). The high degree of sorting probably precludes a primary glacial transport mechanism. Morphology observations thus suggest that gold grains from this site were fluvially transported from a nearby source.

7.2.1.6 Site AK111 – Anvil River, Nome System

Grains from site AK111 were recovered from a basal contact between overlying glacial outwash gravels and diamict. The sample is moderately sorted, with morphology assessments revealing a moderate presence of primary features, high degree of abrasion, a bimodal distribution of rounding (sub-rounded and well-rounded), absence of folding, and low degree of flattening. Based on field observation and morphology, this sample consists of a single population which has been glacially transported with a minor fluvial overprint.

7.2.1.7 Site AK117 – West of Cripple River, Nome System

Site AK117 generated a beach sample which is extremely well sorted and fine grained (18 of 20 grains) with a second coarser population (2 of 20 grains). The sample has extensive secondary Au-Ag-Hg alloy growth over most grains, which conceals the abrasion history. However, the sample shows a high degree of rounding and flattening and substantial folding. The transport history of this sample is

concealed by beach/marine process overprinting and secondary Au-Ag-Hg alloy growth. However, since folding is evidence for transport in the bed-load of rivers (Youngson and Craw, 1999), it is interpreted that at least a portion of the transport history was fluvial.

7.2.1.8 Site AK121 – West Beach, Nome System

Like AK117, sample AK121 is mostly extremely well sorted (67% of grains are fine grained) with a break in slope in the cumulative percentile PSD plot showing a possible second population of moderately sorted, slightly coarser grains (33%). The abrasion history for this sample is obscured by secondary Au-Ag-Hg alloy growth. However, the degree of rounding and flattening is high, although little folding is observed. The relative absence of folding suggests that the sample was not fluvially transported but rather transported glacially to the current day beach, where marine processes have exposed the grains from the local beach impinging glacial sediments.

7.2.1.9 Site AK123 – Monroeville Beach, Nome System

Field observations and historic interpretations have identified Monroeville Beach as a Quaternary age buried shallow marine deposit associated with glacial gravels (Hopkins et al., 1960; Kaufman and Brigham-Grette, 1993; Brigham-Grette and Hopkins, 1995). This sample has a large variation in PSD, indicating either an immature sample population or a large mix of populations. The low degree of primary feature preservation and high degree of abrasion suggest a primary glacial transport mechanism whereas the moderate flattening, high degree of rounding, and absence of folding suggest beach processes. Morphology observations are very similar to that of AK121. The relative absence of secondary Au-Ag-Hg alloy is noted versus present day beach samples (suggesting that secondary Au-Ag-Hg alloy is anthropogenically introduced, see Section 7.1.1).

7.2.1.10 Site AUR-12-854 – Deep offshore (Exploration Panel 1), Nome System

This sample was collected offshore (~18 m water depth) from a coarse gravel lag overlying glacial diamict and represents a generally well sorted sample with 2 of 20 grains significantly coarser than the rest. Morphology observations reveal a low degree of abrasion (obscured by extensive Au-Ag-Hg secondary alloy growth), a

bimodal degree of rounding (sub-rounded and well rounded), a moderate degree of flattening, and an absence of folding. Morphologically, this sample is similar to AK111, suggesting that, like AK111, the sample was eroded from a glacial diamict or proximal glacial outwash. Moderate flattening suggests a moderate degree of marine/beach influence. This sample is interpreted to have been glacially transported offshore during the Nome glaciation event (the most recent glaciation to have crossed the current day shoreline) and to have been exposed to marine processes at a later stage.

7.2.1.11 Site ADEM – Shallow Offshore, Nome System

This sample was collected in shallow water (~6 m water depth) approximately 1 km ENE of the Nome River. The sample has a large variation in PSD (i.e. poorly sorted) which may indicate population mixing, or an immature population. Morphology assessments reveal a moderate degree of abrasion, though this has mostly been concealed by secondary Au-Ag-Hg alloy growth. An exceptionally high degree of rounding, coupled with moderate flattening and low folding, precludes extensive fluvial transport in favour of glacial transport past the present day shoreline and resultant marine re-working (more so than seen in AUR-12-854). This is understandable as in the shallower water wave and storm action presents a high energy marine reworking environment.

Table 10: Transport mechanisms for gold grains from sites across the southern Seward Peninsula. Interpretation from morphological evidence.

Transport Mechanism Evidenced	Shovel Creek	Washington Creek	Gold Run Creek	Sinuk Coastal Plain	Penny River	Anvil Creek	Cripple Creek Beach	West Beach	Monroeville Beach	Deep Offshore	Shallow Offshore
	AK015	AK021	AK028	AK032	AK100	AK111	AK117	AK121	AK123	AUR-12-854	ADEM
Glacial		?	?		?	✓	?	✓	✓	✓	✓
Fluvial	minor	✓	✓	✓	minor	minor	✓				
Marine/Beach				✓			✓	✓	✓	✓	✓
Aeolian				?							

7.2.2 Gold Grain Geochemical Assessment

A summary of the observed geochemical profiles for each site is presented in Table 11. Despite the acknowledged mixing of gold from various populations during transport, gold alloy compositions have been used to identify and define four unique populations associated with various fluvial systems and lithologies (Table 12). These four types are:

- Type 1 gold is Au-Ag alloy gold with typical Ag-contents of 4 to 20%. Most sites near the town of Nome located in Devonian to Ordovician schists and marbles (DOx) or Devonian mafic schists (Dcs) are identified as consisting of Type 1 gold.
- Type 2 gold, like Type 1, is Au-Ag alloy but with elevated Ag-contents, typically between 10% and 25% and associated with Cretaceous(?) conglomerate. Site AK021 grains are of Type 2 gold.
- Type 3 gold is Au-Ag-Hg alloy with Hg contents always in excess of 0.1%, often above 0.5%. Type 3 gold is always associated with Ordovician mafic schists (Ocs). This type is divided into two sub-types with Type 3a defined by AK028 with typical Ag-content and high Hg-content, and Type 3b defined by AK015 with low Ag-content and high Hg-content.
- Type 4 gold is the Rock Creek sample of exsolved gold from arsenopyrite, containing high Ag (21 – 25%) and no Hg.

Recognition of these four types of gold can be used to help identify transport paths and mixing of various gold populations which in turn can be useful for developing exploration geological models. The geochemical types of gold observed in each major river system are described in detail below.

Table 11: Summary table of major, minor, and trace element data for gold grains from individual sites across the southern Seward Peninsula.

Site ID	Site Name	Fineness range (average)	Cumulative Ag% Patterns	Hg-content (max, avg)	Cu-content (max, avg)	Rim vs. Core	Trace Element Abundances
AK015	Shovel Creek	920 - 951 (938)	Very tight range. Low average Ag-content (6.1%)	1.88%, 0.44%	0.06%, 0.02%	Not assessed	v. low As
AK021	Washington Creek	762 - 925 (840)	Elevated pattern with some distribution. Average Ag-content is 16.0%	0.37% ; 0.01%	0.05%, 0.01%	Significant Hg rim enrichment noted in single grain rim	high As, Sb. Elevated Te
AK028	Gold Run Creek	818 - 957 (899)	No distinguishing pattern with typical S-Curve	9.23%, 1.76%	1.81%, 0.01%	Core/Rim ratios inconsistent	some high Cu; v. low As
AK032	Sinuk Coastal Plain	780 - 956 (877)	Broad Ag% range, no slope break (mixed populations likely)	0.64%, 0.14%	0.11%, 0.03%	Minor Hg rim enrichment noted in single grain rim	some high Cu, As
AK100	Penny River	774 - 978 (899)	Broad Ag% range, one slope break (two populations likely)	0.18%, 0.02%	0.03%, 0.01%	Not assessed	mod W, high As
AK111	Anvil Creek	794 - 973 (909)	No distinguishing pattern with typical S-Curve	0.09%, 0.01%	0.05%, 0.01%	Rims rarely depleted in Ag and Hg	
AK121	West Beach	861 - 979 (918)	No distinguishing pattern with typical S-Curve	0.61%, 0.07%	0.03%, 0.01%	Hg-rich gold growths common	mod W
AK123	Monroeville Beach	824 - 970 (911)	No distinguishing pattern with typical S-Curve	0.06%, 0.01%	0.07%, 0.01%	No significant variation	
AUR-12-854	Exploration Panel (EP1)	844 - 956 (910)	No distinguishing pattern with typical S-Curve	0.10%, 0.04%	0.16%, 0.05%	Rims commonly depleted in Ag and Hg	some high Cu, As
ADEM	Offshore Nome River	812 - 918 (894)	One significant break in slope (two populations likely). Elevated low Ag-content values	0.42%, 0.07%	0.03%, 0.01%	Rims commonly depleted in Ag, Hg and Cu	some high As
RC4	Rock Creek Mine	747 - 785 (766)	Elevated pattern with consistent high Ag-content (23.4%)	0.02%, 0.00%	0.01%, 0.00%	Not assessed	Not assessed

Table 12: Gold "types" defined by alloy composition (Au, Ag, and Hg) across the southern Seward Peninsula. Stratigraphic units after Till et al. (2011), except the Cretaceous Conglomerate, which is described in Collier (1908) and Sainsbury (1972).

Gold Type	Sites Observed	Gold Overview	Ag-content range	Hg-content range	Stratigraphic unit associated with
Type 1	AK100, AK111, AK121, AK123, AUR-12-854, ADEM, (AK032)	Au-Ag alloy with moderate Ag	4 - 20%	<0.1%	DOx, (Dcs)
Type 2	AK021, (AK100, AK032)	Au-Ag alloy with high Ag	10 - 25 %	0%	Cretaceous(?) Conglomerate
Type 3a	AK028, (AK032)	Au-Ag-Hg alloy	4 - 18%	0.2 - >3%	Ocs
Type 3b	AK015	Au-Ag-Hg alloy with low Ag	4 - 8%	0.1 - 2%	Ocs
Type 4	RC4	Au-Ag alloy with very high Ag	21 - 25%	0%	DOx (exsolved gold)

7.2.2.1 Teller System (AK028)

Site AK028, representing the Teller system, contains Type 3a gold exclusively. It is geochemically defined as a hydrothermal Au-Ag-Hg alloy system (average Hg = 1.76%) with a high average fineness (~900) and very low Cu-content (apart from a single anomaly containing 1.8% Cu). Trace element data revealed that, like other Au-Ag-Hg sites (AK015), this site is depleted in arsenic (As). In general, the geochemical profile from this site is internally consistent, suggesting that there has been no significant mixing of gold sources (Figure 59).

7.2.2.2 Solomon System (AK015)

Site AK015, representing the Solomon system, appears to consist of a mix of Au-Ag-Hg alloy grains (Type 3b, average Hg = 0.66%) and Au-Ag alloy grains (Type 1, average Hg = 0.004%), with an exceptionally tight fineness range with low Ag-content constrained between 5% and 8% and moderate Cu-content (~180 ppm). Of significance is the total absence of W and Sb and very low As at this site. The mixing of the two gold types is believed to have occurred as a result of the proximal nature of both an Ocs unit (Type 3b) and DOx units (Type 1), see Figure 59.

7.2.2.3 Sinuk System (AK021, AK032)

The Sinuk system is represented by sites AK021 and AK032. Site AK021 contains Type 2 gold (Figure 59) and is defined as an Au-Ag alloy site unique amongst all sites in having an elevated Ag content (modal Ag content is approximately double that of other sites at 16.0%), very low Cu, and low Hg. Site AK021 has an elevated As content profile and the highest average As content of all sites (~900 ppm) as a result of a single As anomaly of 10,000 ppm. Site AK021 also has an elevated Te profile relative to other sites. Site AK021 has internally consistent geochemistry, especially identified by high Ag content, which suggests a single source (apart from a single grain with Type 3 grain with Hg content of 0.37%). Field observations and morphology analysis suggest that although the grains have been released from a local fluvial conglomerate, their original provenance may be somewhat distal and possibly outside of the current Sinuk System.

Site AK032 is a beach site and is thus expected to have a degree of geochemical variation or population mixing. Mixing of three gold types is observed in the sample from this site. Two grains are Au-Ag alloy with Ag content of 7% to 11% (Type 1), two grains are Au-Ag alloy with Ag content of 17% - 22% (Type 2), and one grain is Au-Ag-Hg alloy with Hg content of 0.64% (Type 3). Type 1 gold is likely sourced from nearby DOx units while the presence of Type 2 gold strongly suggests mixing of the high Ag-content AK021 population into AK032 and the presence of Au-Ag-Hg alloy suggests input from a local Ocs unit (Figure 59).

7.2.2.4 Nome System (AK100, AK111, AK121, AK123, AUR-12-854, ADEM)

The Nome system, represented by sites AK100, AK111, AK121, AK123, AUR-12-854, and ADEM consists of Type 1 gold, defined as having a modal Ag-content of between 6% and 9% (fineness ~ 910), very low Cu content, and low Hg content (Au-Ag alloys). All Nome system sites form a tight envelope in cumulative percent vs. Ag% space (Figure 46), with breaks in slope at 10% and 80% cumulative percent suggesting complex mixing of populations with similar chemistry. An important observation from site AK100 is that 30% of the grains have elevated Ag content (Type 2 gold), thereby showing that the AK100 population is a mix of the AK021 population (Sinuk system) and Nome system population (Figure 59). Sites AK121 and ADEM display an 87:13 mix of Type 1 gold and Type 3 gold, which is explained by the combined local presence of DOx and Ocs units (Figure 59).

The site RC4 is unique, being a hard rock site, and is characterised by high Ag contents of between 21% and 25%, no Cu, and no Hg.

Measured trace element abundances appear to be more varied between the sites and further work may reveal these variations to be diagnostic.

7.2.3 Clast Assemblages

The lithological clast assemblage data for each site (reported in Section 6.1) suggest that clast assemblage can be used to determine presence and extent of mixing of various source rocks and their possible gold contents. Figure 30 and Table 13, which employ the lithology nomenclature of Till et al. (2011), illustrate the predominant clast assemblages present at each site.

Table 13: Primary lithologies present at each sample site across the southern Seward Peninsula.

Major Clast Type Observed	Shovel Creek AK015	Washington Creek AK021	Gold Run Creek AK028	Sinuk Coastal Plain AK032	Penny River AK100	Anvil Creek AK111	Cripple Creek Beach AK117	West Beach AK121	Monroeville Beach AK123	Deep Offshore AUR-12-854	Shallow Offshore ADEM	Rock Creek RC4
DOx Devonian to Ordovician Marble, Schist, Graphitic Schist	✓	✓	X	✓	✓	✓	✓	✓	✓	✓	✓	X
Dcs Devonian Schist and Graphitic Schist	?	?	X	X	✓	✓	✓	✓	✓	✓	✓	✓
Ocs Ordivician Casadepaga Schist	?	?	✓	?	X	X	X	X	X	✓	✓	X
Kigulak Group Palaeo/Protero-zoic metamorphics and Cretaceous intrusions	X	✓	✓	✓	?	X	✓	X	X	X	X	X

It is tempting to search for trends in the gold major, minor, and trace element data substantiating a difference in gold grain chemistry with relation to local bedrock geology. Should such trends be present, gold grains from sample sites on or near Devonian to Ordovician schists and marbles (DOx sites AK021, AK100 and AK015) will be expected to share similar chemistry whilst gold grains from Ordovician Casadepaga Schists (Ocs site AK028) and Devonian Casadepaga Schists (Dcs sites AK111, AK123) will also be uniquely identifiable. However, within the limitations of the samples analysed, this seems to not be true and may reflect the complex Nome bedrock geology and mixed units.

However, even if clast lithology has little correlation to recovered gold grain chemistry, it may still reveal implications for transport paths and mechanisms across the peninsula. In general, clast lithologies will reflect the lithology of its provenance, albeit with more resistant lithologies becoming more dominant with distance (e.g. it is commonly observed that beach samples contain more marble and quartz than expected, as a result of the softer schist component weathering away (e.g. AK032, AK121)).

The presence of Kigluaik granitoids in the Sinuk System (Washington Creek (AK021) and Sinuk Coastal Plain (AK032)) substantiates significant Kigluaik input. The presence of Kigluaik granitoids at the Penny River (AK100) and Cripple Creek Beach (AK117) sites, which are across a watershed divide from AK021 and AK032, suggests that present day fluvial systems could not have delivered Kigluaik granitoids to these sites, however, glaciers may have been able to cross this relatively minor watershed divide.

The general absence of Kigluaik granitoids throughout the Nome System suggests that the Snake and Nome River valleys (and palaeo-glaciers) never cut significantly into the Kigluaik Mountains and thus the gold found in this system is locally sourced.

The presence of marble is related to the DOx unit in particular and not Dcs or Ocs (e.g. compare the marble-absent sites of AK028, AK111, and AK121 with the marble-rich sites of AK100, AK015) and thus an interesting observation is the abundance of marble at Monroeville Beach (AK123) and shallow offshore (ADEM). This observation suggests a strong influence of DOx as a provenance for these sites which is not seen in other Nome System sites (AK111, AK121, and AUR-12-854 in particular).

7.2.4 Combined Interpretation of Transport Pathways and Mechanisms

Figure 59 shows the transport pathways and mechanisms for placer gold grains across the southern Seward Peninsula, as interpreted by this study from field observations, clast assemblage abundance and distribution, gold grain morphology, and gold grain major and minor element chemistry.

Site AK015 contains a mixture of grains from Type 1 and Type 3b, both of which are fluvially immature, suggesting a local source. It is proposed, based on geochemical evidence from AK028, AK032, and ADEM (see below), that Type 3 Au-Ag-Hg alloy grains are sourced from local Ordovician Casadepaga Schist (Ocs) whilst Type 1 Au-Ag alloy grains are sourced from local Devonian-Ordovician schists and marbles (DOx).

Site AK021 is geochemically unique (Type 2 gold), and field observations strongly suggest that this sample reflects fluvially mature gold grains trapped in a local fluvial conglomerate, and has recently been released by present day streams. This palaeo-placer (conglomerate) contains distal gold grains which have been fluvially sourced, possibly from a now eroded higher sequence of Devonian Casadepaga Schist (Dcs) which may have overlain the exposed Devonian-Ordovician schists and marbles (DOx).

Site AK028 contains a fluvially immature population of Type 3a gold and is interpreted to have been locally sourced from local Ordovician Casadepaga Schist (Ocs) by combined periglacial and fluvial mechanisms. The possibility remains that glacial processes have sourced gold from the Kigluaik Mountains (along with granitoids seen in the clast assemblage). However, this interpretation is not preferred due to the absence of identified gold mineralisation associated with the Kigluaik Mountains.

The moderate degree of folding seen on grains of AK032 suggests a fluvial history, although not one representing tens of kilometres of transport. Most likely, these grains were introduced to the coastline or nearby by glacial processes, with a minor fluvial overprinting and significant beach/marine overprinting (flattening and accretion). Five of the nine grains collected were analysed for major and trace elements, of which two clearly show evidence of sourcing from the Type 2 (AK021) population (AK032-7 and AK032-8 with Ag contents of 17.3% and 22.0% respectively), and one (AK032-2) of Au-Ag-Hg alloy (Type 3).

Site AK100 contains gold of Types 1, 2, and 3. The presence of Type 2 grains suggests that the palaeo placer conglomerate extends onto the east side of a watershed divide, that a glacier has transported palaeo-placer grains across the divide or that Type 2 grains may be representative of gold from Dcs. The sample is well sorted, but fluvially immature, suggesting a local source.

Morphological and geochemical evidence suggests a similar source for sites AK111, AK123, and AUR-12-854. Grains from the same or similar source were transported glacially into offshore diamict (AUR-12-854), onshore diamict (AK111) or to the palaeo-marine site of AK123. All sites then have minor overprinting of later transport stages.

Site AK121 and ADEM, for the most part, seems to share similar chemistry and transport history to that of AK111, AK123, and AUR-12-854, other than a few grains of Type 3 primary Au-Ag-Hg alloy (AK121-7, AK121-8, AK121-12, AK121-17, ADEM-6, ADEM-9, and ADEM-11). These grains likely represent input from the nearby Ocs lithology or otherwise significant transport by marine processes.

Southern Seward Peninsula - Interpreted Transport Pathways and Mechanisms

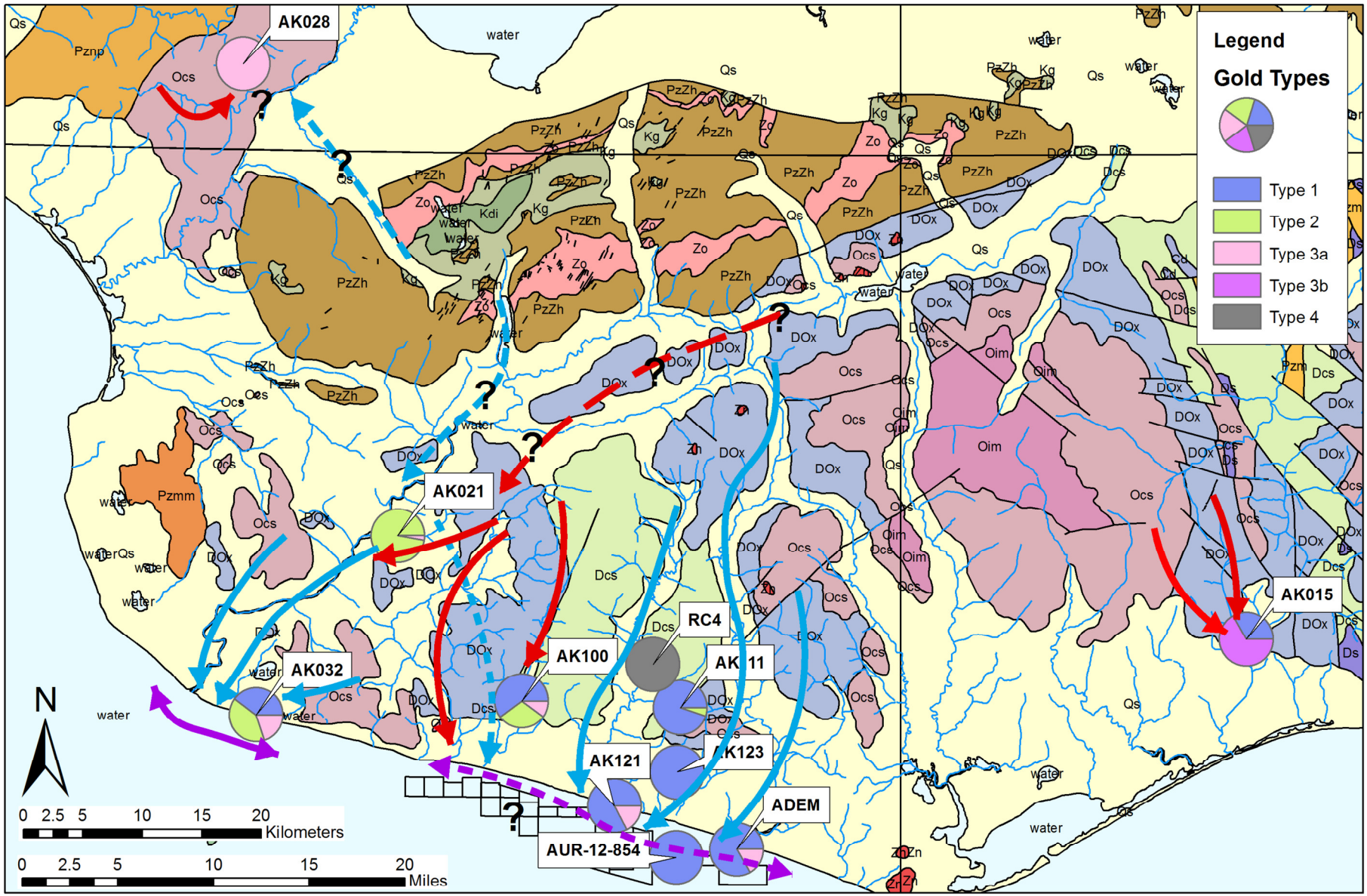

Figure 59: Gold type distribution from each sample site in this study is shown as a pie-chart. Gold grain transport paths and mechanisms across the southern Seward Peninsula are shown. Red Arrows = primarily fluvial transport, Blue Arrows = primarily glacial transport, Purple Arrows = marine transport. Background geology after Till et al., 2011.

7.3 Gold Ore Genesis

7.3.1 Gold Ore Genesis and Relationship to Alloy Composition

Gold grain fineness has been used by a variety of authors to determine whether a number of compositionally distinct populations are present and also to constrain bedrock source and possible mineralisation events (e.g. Youngson et al., 2002; Mortensen et al., 2006). Fineness is limited as an ore genesis diagnostic tool with Morrison et al. (1991) reporting a range of 780-1000 for Archean greenstone hosted gold and a range of 440-1000 for epithermal gold deposits. Pluton hosted lode type deposits typically have very high fineness gold with values greater than 900 and are associated with anomalously high amounts of one or more of the following elements: Bi, W, Te, Mo, As, and Sn (Lange and Gignoux, 1999).

Primary hydrothermal gold commonly forms as a result of precipitation from high temperature hydrothermal fluids and typically contains between 5% and 20% Ag (Hough et al., 2009). In addition to constraining mineralisation type, Au-Ag ratios have been used to indicate evolving fluid chemistry and temperature of emplacement (Gammons and Williams-Jones, 1995). An example of this is the identification of the more volatile and mobile Ag becoming enriched in the gold-silver alloy emplaced higher in the ore body or more distal from its centre (Chapman and Mortensen, 2006), which further implies that a small variation in Ag content is likely indicative of a relatively consistent emplacement environment. Additionally, excessively low Au/Ag ratios can be used to indicate metamorphic events, where high temperatures can decouple Ag from the Au-Ag solid solution, resulting in a gold ore with very low (<2%) Ag-content (Tomkins and Mavrogenes, 2002).

In addition to Au-Ag ratios, Cu content has also been used to construe potential ore-genesis. In a study to quantify Ag and Cu content with ore genesis, Townley et al. (2003) showed that moderate Ag content (~5%) grains coupled with low Cu (~0.1%) were found to come from epithermal systems, while grains with high Ag (~8%) and low Cu were indicative of Au-rich porphyries. Grains with variable Ag content and very high Cu content (>0.75%) were indicative of Cu-rich porphyries. However, a recent study (Moles et al., 2013) has shown a complete overlap with gold containing Cu up to 0.8% are also permissible for orogenic and plutonic gold formation processes.

A strong association exists between Au-Ag-Hg alloys and hydrothermal orogenic ore deposits (Boyle, 1979; Rytuba and Heropoulos, 1992). Furthermore, as hydrothermal Au-Ag-Hg alloys have been shown to be chemically stable, they can be used in the identification of different gold populations from different sources and their dispersion in a placer (Youngson et al., 2002).

7.3.2 Gold Alloy Compositions of Grains from the Southern Seward Peninsula and Implications for Source

Gold grain alloy compositions from all sites across the southern Seward Peninsula typically range between 5% and 20% Ag content (Figure 46), indicative of an orogenic source signature associated with hydrothermal fluid derivation from metasediments (Table 2 and Chapman et al. (2009)). This hypothesis is further confirmed by the very low Cu contents observed at all sites (site averages are between 0.00% and 0.05%). In addition, undetectable Bi and Sn and low W and Te contents preclude Cu-rich or Au-rich porphyry sources. The strong association between Au-Ag-Hg alloys and hydrothermal orogenic ore deposits and the observation of this occurrence, in particular at sites AK015 and AK028, provide support for such a genesis. These sites are excellent examples of hydrothermal Au-Ag-Hg alloys similar to those identified by Youngson et al. (2002) in New Zealand.

The elevated Ag content of site AK021 clearly makes it unique; however, it may be related to the same ore-genesis event. The homogeneity of Cu and Hg in most grain cores from the Nome system and AK021 suggests that a single episode of mineralisation is responsible for emplacement with the enrichment in Ag suggestive of vertical or lateral zonation (i.e. the centre of the hydrothermal system was in the Nome system, and the evolving fluid chemistry resulted in Au-Ag alloys towards the edges and into the Sinuk system to be enriched in the more mobile Ag).

7.4 Implications for Offshore Exploration

Morphological and textural observations have revealed that glacial transport is the primary mechanism responsible for gold transport across the peninsula, with secondary marine and fluvial reworking of glacially deposited sediments. This observation would support continued offshore exploration associated within primary and reworked glacial sediments.

Gold mineralisation across the peninsula appears to be restricted to the Nome Group and to be orogenic in origin. The presence of Kigluaik Group lithologies in a target area are believed to be indicative of a dilutive environment and thus these areas should be de-prioritized. Multiple gold populations (“types”) have been identified related to the Nome Group lithologic unit in which it was mineralised. The ubiquitous presence of Type 1 gold suggests that offshore exploration should target localities showing evidence of glacially transported DOx and Dcs clast assemblages. Type 4 gold, identified as exsolved gold in the hard rock sample from Rock Creek mine, is not recognised elsewhere on the Seward Peninsula suggesting this to be a negligible source.

Type 1 gold fineness ranges from 794 – 979, and it is recommended that an average gold fineness of 910 be used in financial and resource modelling. The unique signature of Type 3 gold and its relation to Ocs units should also be investigated, as this gold type offers an average fineness of 940 in the Solomon system and 900 in the Teller system.

8 Conclusions and Summary

A baseline dataset of combined gold grain sizes, morphology, texture, and major and minor element data (Au, Ag, Cu and Hg) for eleven placer sites and one hard-rock site across the southern Seward Peninsula has been presented. Trace element data (W, Sb, As, and Te) were also collected but were largely inconclusive. However, further acquisition of trace element data, using the correct EMPA parameters, may lead to greater resolution of gold profiling and could possibly further constrain ore genesis styles across the southern Seward Peninsula.

Gold grain sizes are varied and range from 150 µm to 3400 µm (b-axis) and 0.11 mm^2 to 57.78 mm^2 in area. Some sites display excellent sorting indicative of late fluvial or marine sorting (AK021, AK100, AK117, AK121, and AUR-12-854) whereas other sites display immature sorting indicative of primary glacial transport (especially AK028, AK123, and ADEM).

Morphological observations of moderate flattening and low degrees of folding suggest that glacial transport processes are overwhelmingly prevalent in the Nome system, with minor evidence of fluvial overprinting. A significant exception is Washington Creek (AK021), which contains gold grains that are extremely well sorted and rounded and which are moderately folded. Gold grains from beach and offshore sites (AK032, AK117, AK123, AUR-12-854 and ADEM) are typically more flattened than those from river systems or glacial contacts (AK015, AK028, AK100, AK111 and AK121[1]).

Clast assemblage distribution and abundances reveal that the Sinuk system (AK032 and AK021) is strongly influenced by clast input from the Kigluaik mountains and that this influence extends into the western Nome system (sites AK100 and AK117). However, it is noted that neither the Snake nor Nome Rivers cut back far enough north to sample the granulite facies Kigluaik mountain lithologies.

[1] Note site AK121 (West Beach) is categorised here as a “glacial contact” site and not a beach site as it was collected on the beach from the contact between freshly exposed diamict and overlying tundra.

Gold grain major element chemistry was sufficient to define four gold geochemical types based on alloy composition. These types differentiate among gold grains from:

1. The Nome System (Anvil Creek (AK111), West Beach (AK121), Monroeville Beach (AK123), Deep Offshore (AUR-12-854), and Shallow Offshore (ADEM)),
2. Washington Creek (AK021),
3. Shovel Creek (AK015) and Gold Run Creek (AK028), and
4. Rock Creek (RC4).

The gold type classification was able to identify substantial mixing of populations at the Sinuk Coastal Plain site (AK032) and Penny River site (AK100).

Major and minor element chemistry data reveal that gold grains from all sites have modal Ag contents of between 5 – 20% and very low average Cu content (<0.05%). Fineness values are also reported to be high (generally >800) except for exsolved gold in the Rock Creek (RC4) sample. The relationship between Ag and Cu contents is strongly suggestive of an orogenic hydrothermal mineralisation style and is likely related to repeated metamorphic events which have affected the rocks of the peninsula.

Major element chemistry data further reveal that gold from the Teller system (represented by the Gold Run Creek sample AK028) is primary Au-Ag-Hg alloy sourced from Ordovician Casadepaga Schist (Ocs). The Solomon System (represented by Shovel Creek sample AK015) is mixed between primary Au-Ag-Hg alloy and Au-Ag alloy originating from Ocs and Devonian-Ordovician schists and marble (DOx) sources. The remaining sample sites contain primarily Au-Ag alloy, other than where potential exists for sampling of local Ocs to present additional primary Au-Ag-Hg alloy grains (such as at sites AK032 and ADEM). The presence of Au-Ag-Hg alloy provides further evidence for an orogenic hydrothermal mineralisation style.

Elemental maps and rim/core analyses show little evidence for Ag-depletion (leaching) or gold-enrichment and as such this is not seen as a noteworthy supergene process in grains from the southern Seward Peninsula. However, some grains, specifically those from sites AK032, AK117, AK121, AK123, AUR-12-854, and ADEM, show morphological and geochemical evidence for secondary Au-Ag-Hg alloy development. These supergene secondary Au-Ag-Hg growths are interpreted to be

as a result of anthropogenically introduced mercury due to their presence only in beach and marine sites.

Regarding the Washington Creek sample (AK021), the combined observations of field evidence (local secondary source of palaeo- (Cretaceous(?)) fluvial outwash conglomerate), morphological evidence (rounded, flattened, folded), and major and minor element data (elevated Ag-content, but similar Hg- and Cu-content to other Nome system sites) suggests that these gold grains represent a previous cycle of placer development. This previous cycle may have sourced gold from the same host rocks and mineralising event, but higher up in the sequence (eroded Nome Complex rocks) where hydrothermal fluids had evolved to enriched Ag content levels.

9 Future Work and Recommendations

A key driver of this study was the desire to develop a baseline gold grain geochemical database for onshore sites across the southern Seward Peninsula for comparison with the geochemical composition of offshore gold grains to aid the development of a geological model for offshore gold exploration. Once additional gold grains from across the offshore AuruMar license area are analysed, comparison of the datasets may be able to inform offshore gold populations (in relation to onshore populations), gold movement and mixing, and possibly the potential for mineralisation extension. It is thus suggested that gold grains from the western and offshore most parts of the AuruMar leases be analysed to assess the offshore variation and the potential for correlation to onshore datasets.

Gold grain analyses conducted in this study indicate that major and minor element chemistry are sufficient to differentiate between “systems” (i.e. Teller System vs. Solomon System vs. Nome System) but are insufficient to differentiate between sites within a system. Trace element chemistry, however, may be able to do so and thus could be a powerful tool for understanding gold grain movement and population mixing both within the Nome System as well as offshore. Trace element analysis conducted during this study was largely unsuccessful due to the incorrect analysis parameters being utilised (15.0 kV instead of the higher 25.0 kV accelerating voltage which is now recommended).

This study concluded, based on presence of primary Au-Ag-Hg alloys, moderate Ag-content and low Cu-content, that the mineralisation style is orogenic. However, a complete microchemical assessment should be conducted to further define the various gold types present and supplement trace element interpretations.

The interpretation of the age of the Washington Creek conglomerate is uncertain and provides scope for considerable controversy. It is suggested that the conglomerate be dated robustly and a sample taken and disagglomerated to ascertain whether or not it truly hosts entrapped gold grains.

In summary, suggested future work is:

a) Offshore gold grains should be collected and analysed for comparison to the onshore geochemical baseline developed by this study.

b) Future trace element analysis should be undertaken at the higher accelerating voltage of 25kV. Grains from this study should be re-analysed under these conditions.
c) A microchemical study of gold grains from this study should be undertaken to further constrain ore-genesis and populations.
d) The age of the Washington Creek conglomerates should be determined through quantitative dating techniques.

10 References

Alexander, C.S., and Price, L.W., 1980, Radiocarbon dating of the rate of movement of two solifluction lobes in the Ruby Range, Yukon Territory: Quaternary Research, v. 13, no. 3, p. 365–379, doi: 10.1016/0033-5894(80)90063-0.

Amato, J.M., Toro, J., Miller, E.L., Gehrels, G.E., Farmer, G.L., Gottlieb, E.S., and Till, A.B., 2009, Late Proterozoic–Paleozoic evolution of the Arctic Alaska–Chukotka terrane based on U-Pb igneous and detrital zircon ages: Implications for Neoproterozoic paleogeographic reconstructions: Geological Society of America Bulletin, v. 121, p. 1219–1235.

Ayuso, R.A., and Till, A.B., 2007, Geochemical and Nd-Pb isotopic evolution of metabasites from attenuated continental lithosphere, Nome Group, Seward Peninsula, Alaska [abs.]: Geological Society of America Abstracts with Programs, v. 39, no. 6, p. 489.

Bowell, R.J., 1992, Supergene gold mineralogy at Ashanti, Ghana: Implications for the supergene behaviour of gold: Mineralogical Magazine, v. 56, p. 545–560.

Boyle, R.W., 1979, The geochemistry of gold and its deposits: Geological Survey of Canada Bulletin, v. 280, p. 584.

Brigham-Grette, J., and Hopkins, D.M., 1995, Emergent Marine Record and Paleoclimate of the Last Interglaciation Along the Northwest Alaskan Coast: Quaternary Research, v. 43, p. 159–173.

Brown, S.M., Johnson, C.A., Watling, R.J., and Premo, W.R., 2003, Constraints on the composition of ore fluids and implications for mineralising events at the Cleo gold deposit, Eastern Goldfields Province, Western Australia: Australian Journal of Earth Sciences, v. 50, no. 1, p. 19–38.

Bundtzen, T.K., Reger, R.D., Laird, G.M., Pinney, D.S., Clautice, K.H., Liss, S.A., and Cruse, G.R., 1994, Progress Report On The Geology And Mineral Resources Of The Nome Mining District: Public-Data File 94-39.

Bundtzen, T.K., Swainbank, R.C., Wood, J.E., and Clough, A., 1992, Alaska's Mineral Industry - 1991 Summary: Alaska Division of Geological & Geophysical Surveys Special Report, v. 46, p. 89.

Chandonnet, A., 2005, Gold Rush Grub: From Turpentine Stew to Hoochinoo: University of Alaska Press.

Chapman, R.J., and Leake, R.C., 2000, The Application of Microchemical Analysis of Alluvial Gold Grains to the Understanding of Complex Local and Regional Gold Mineralization : A Case Study in the Irish and Scottish Caledonides: Economic Geology, v. 95, p. 1753–1773.

Chapman, R.J., Leake, R.C., Bond, D.P.G., Stedra, V., and Fairgrieve, B., 2009, Chemical and Mineralogical Signatures of Gold Formed in Oxidizing Chloride Hydrothermal Systems and their Significance within Populations of Placer Gold Grains Collected during Reconnaissance: Economic Geology, v. 104, p. 563–585.

Chapman, R., Leake, B., and Styles, M., 2002, Microchemical Characterization of Alluvial Gold Grains as an Exploration Tool: Gold Bulletin, v. 35, no. 2, p. 53–65, doi: 10.1007/BF03214838.

Chapman, R.J., and Mortensen, J.K., 2006, Application of microchemical characterization of placer gold grains to exploration for epithermal gold mineralization in regions of poor exposure: Journal of Geochemical Exploration, v. 91, no. 1-3, p. 1–26, doi: 10.1016/j.gexplo.2005.12.004.

Chapman, R.J., Mortensen, J.K., Crawford, E.C., and Lebarge, W., 2010, Microchemical Studies of Placer and Lode Gold in the Klondike District , Yukon , Canada : 1 . Evidence for a Small , Gold-Rich , Orogenic Hydrothermal System in the Bonanza and Eldorado Creek Area: Economic Geology, v. 105, p. 1369–1392.

Collier, A.J., Hess, F.L., Smith, P.S., and Brooks, A.H., 1908, The gold placers of parts of the Seward Peninsula, Alaska: Geological Survey Bulletin, , no. 328, p. 341.

Craw, D., Youngson, J.H., and Leckie, D., 2006, Transport and concentration of detrital gold in foreland basins: Ore Geology Reviews, v. 28, no. 4, p. 417–430, doi: 10.1016/j.oregeorev.2005.03.006.

Dixon, R., 2012, Provenance of Illicit Gold with Emphasis on the Witwatersrand Basin Deposits: University of Pretoria, p 9-24.

Dumula, M.R., and Mortensen, J.K., 2001, Composition of placer and lode gold as an exploration tool in the Stewart River map area, western Yukon: Yukon Exploration and Geology, p. 87–102.

Falconer, D., Craw, D., Youngson, J.H., and Faure, K., 2006, Gold and sulphide minerals in Tertiary quartz pebble conglomerate gold placers, Southland, New Zealand: Ore Geology Reviews, v. 28, p. 525–545.

Gammons, C.H., and Williams-Jones, A.E., 1995, Hydrothermal Geochemistry of Electrum: Thermodynamic Constraints: Economic Geology, v. 90, p. 420–432.

Garnett, R.H.T., 2000, Marine Placer Gold, with Particular Reference to Nome, Alaska, *in* Moore, G.W. ed., Handbook of Marine Mineral Deposits, p. 67–101.

Garnett, R.H.T., and Bassett, N.C., 2005, Placer Deposits: Economic Geology, v. 100th Anni, p. 813–843.

Gauert, C.D.K., Brauns, M., Batchelor, D., and Simon, R., 2011, Gold provenance of the Black Reef conglomerate, West and East Rand, South Africa, *in* Society for Geology Applied to Mineral Deposits, Antagagasta, Chile, p. 1–3.

Greene, H.G., 1970, A Portable Refraction Seismograph Survey of Gold Placer Areas Near Nome, Alaska: Contributions to Economic Geology, Geological Survey Bulletin 1312-B, p. 1-33.

Groen, J.C., Craig, J.R., and Rimstidt, J.D., 1990, Gold-Rich Rim Formation on Electrum Grains in Placers: Canadian Mineralogist, v. 28, p. 207–228.

Groves, D.I., Condie, K.C., Goldfarb, R.J., Hronsky, J.M.A., and Vielreicher, R.M., 2005, 100th Anniversary Special Paper: Secular Changes in Global Tectonic Processes and Their Influence on the Temporal Distribution of Gold-Bearing Mineral Deposits: Economic Geology, v. 100, p. 203–224.

Groves, D.I., Goldfarb, R.J., Gebre-Mariam, M., and Robert, F., 1998, Orogenic gold deposits: A proposed classification in the context of their crustal distribution and relationship to other gold deposit types: Ore Geology Reviews, v. 13, p. 7–27.

Groves, D.I., Goldfarb, R.J., Robert, F., and Hart, C.J.R., 2003, Gold Deposits in Metamorphic Belts: Overview of Current Understanding, Outstanding Problems, Future Research, and Exploration Significance: Economic Geology, v. 98, p. 1–29.

Henke, B.L., Lee, P., Tanake, T.J., Shimabukuro, R.L., and Fujikawa, B.K., 1982, Low-energy x-ray interaction coefficients: Photoabsorption, scattering, and reflection: Atomic Data and Nuclear Data Tables, v. 27, no. 1, p. 1–144.

Hopkins, D.M., MacNeil, F.S., and Leopold, C.B., 1960, The coastal plain at Nome, Alaska: A Late Cenozoic type section for the Bering Strait region: International Geological Congress, v. 21, no. 4, p. 46–57.

Hough, R.M., Butt, C.R.M., and Fischer-Buhner, J., 2009, The Crystallography, Metallography and Composition of Gold: Elements, v. 5, no. 5, p. 297–302, doi: 10.2113/gselements.5.5.297.

Hronsky, J.M.A., Groves, D.I., Loucks, R.R., and Begg, G.C., 2012, A unified model for gold mineralisation in accretionary orogens and implications for regional-scale exploration targeting methods: Mineralium Deposita, v. 47, p. 339–358.

https://www.ru.ac.za/geology/epma/, 2014, EPMA Laboratory: Rhodes Univeristy Website.

Jarvis, A., Reuter, H.I., Nelson, A., and Guevara, E., 2006, Hole-filled seamless SRTM data V3: International Centre for Tropical Agriculture (CIAT): http://srtm.csi.cgiar.org, p. 1.

Kaufman, D.S., and Brigham-Grette, J., 1993, Aminostratigraphic corrections and paleotemperature implications, Pliocene-Pleistocene high sea-level deposits, Northwestern Alaska: Quaternary Science Reviews, v. 12, p. 21–33.

Kaufman, D.S., and Manley, W.F., 2004, Pleistocene Maximum and Late Wisconsinan glacier extents across Alaska, USA, *in* Ehlers, J. and Gibbard, P.L. eds., Quaternary Glaciations — Extent and Chronology. Part II: North America. Developments in Quaternary Science 2, p. 1–17.

Kaufman, D.S., Walter, R.C., Brigham-Grette, J., and Hopkins, D.M., 1991, Middle Pleistocene age of the Nome River glaciation, northwestern Alaska: Quaternary Research, v. 36, no. 3, p. 277–293, doi: 10.1016/0033-5894(91)90003-N.

Knight, J.B., and McTaggart, K.C., 1990, Lode and Placer Gold of the Coquihalla and Wells Areas, British Columbia, (92H, 93H): British Columbia Ministry of Energy, Mines and Petroleum Resources,, p. 105–118.

Knight, J.B., Morison, S.R., and Mortensen, J.K., 1999, The Relationship between Placer Gold Particle Shape , Rimming , and Distance of Fluvial Transport as Exemplified by Gold from the Klondike District, Yukon Territory, Canada: Economic Geology, v. 94, p. 635–648.

Lange, I.M., and Gignoux, T., 1999, Distribution, Characteristics, and Genesis of High Fineness Gold Placers, Ninemile Valley, Central-Western Montana: Economic Geology, v. 94, p. 375–386.

Larizzatti, J.H., Oliveira, S.M.B., and Butt, C.R.M., 2008, Morphology and composition of gold in a lateritic profile, Fazenda Pison “Garimpo”, Amazon, Brazil: Journal of South American Earth Sciences, v. 25, no. 3, p. 359–376, doi: 10.1016/j.jsames.2007.06.002.

Leake, R.C., Chapman, R.J., Bland, D.J., Stone, P., Cameron, D.G., and Styles, M.T., 1998, The origin of alluvial gold in the Leadhills area of Scotland: evidence from interpretation of internal chemical characteristics: Journal of Geochemical Exploration, v. 63, no. 1, p. 7–36, doi: 10.1016/S0375-6742(98)00012-0.

Lindgren, W., 1933, Mineral Deposits: McGraw Hill, New York and London, p. 930.

Lindgren, W., 1907, The relation of ore deposition to physical conditions: Economic Geology, v. 2, no. 2, p. 105–127.

Matsuoka, N., 2001, Solifluction rates , processes and landforms: a global review: Earth-Science Reviews, v. 55, no. 1-2, p. 107–134.

McClenaghan, M.B., and Cabri, L.J., 2011, Review of gold and platinum group element (PGE) indicator minerals methods for surficial sediment sampling: Geochemistry: Exploration, Environment, Analysis, v. 11, p. 251–263.

Mervine, E.M., 2013, Generalized map of Cenozoic sediments on the Nome coastal plain: AuruMar Internal Research Map.

Moles, N.R., Chapman, R.J., and Warner, R.B., 2013, The significance of copper concentrations in natural gold alloy for reconnaissance exploration and understanding gold-depositing hydrothermal systems: Geochemistry: Exploration, Environment, Analysis, v. 13, no. 2, p. 115–130, doi: 10.1144/geochem2011-114.

Morrison, G.W., Rose, W.J., and Jaireth, S., 1991, Geological and geochemical controls on the silver content (fineness) of gold in gold-silver deposits: Ore Geology Reviews, v. 6, p. 333–364.

Mortensen, J.K., Chapman, R., Lebarge, W., and Crawford, E., 2005, Compositional studies of placer and lode gold from western Yukon: Implications for lode sources: Yukon Exploration and Geology, v. 1, p. 247–256.

Nelson, C.H., and Hopkins, D.M., 1972, Sedimentary Processes and Distribution of Particulate Gold in the Northern Bering Sea: Geological Survey Special Paper, v. 689, p. 33.

Nelson, C.H., Pierce, D.E., Leong, K.A.M.W., Wang, F.F.H., Survey, U.S.G., Park, M., and Calif, U.S.A., 1975, Mercury Distribution in Ancient and Modern Sediment of Northeastern Bering Sea: Marine Geology, v. 18, p. 91–104.

Oberthür, T., and Weiser, T.W., 2008, Gold-bismuth-telluride-sulphide assemblages at the Viceroy Mine, Harare-Bindura-Shamva greenstone belt, Zimbabwe: Mineralogical Magazine, v. 72, no. 4, p. 953–970, doi: 10.1180/minmag.2008.072.4.953.

Otto, B.R., Piekenbrock, J., and Odden, J., 2009, Structural Evolution of the Rock Creek Gold Deposit , Seward Peninsula , Alaska: Economic Geology, v. 104, p. 945–960.

Outridge, P.M., Doherty, W., and Gregoire, D.C., 1998, Determination of trace elemental signatures in placer gold by laser ablation–inductively coupled plasma–mass spectrometry as a potential aid for gold exploration: Journal of Geochemical Exploration, v. 60, no. 3, p. 229–240, doi: 10.1016/S0375-6742(97)00049-6.

Pitcairn, I.K., Teagle, D.A.H., Craw, D., Olivo, G.R., Kerrich, R., and Brewer, T.S., 2006, Sources of Metals and Fluids in Orogenic Gold Deposits : Insights from the Otago and Alpine Schists , New Zealand: Economic Geology, v. 101, p. 1525–1546.

Rasmussen, K.L., Mortensen, J.K., and Falck, H., 2007, Morphological and compositional analysis of placer gold in the South Nahanni River drainage , Northwest Territories, *in* Emond, D.S., Lewis, L.L., and Weston, L.. eds., Yukon Exploration and Geology 2006, p. 237–250.

Robert, F., Brommecker, R., Bourne, B.T., Dobak, P.J., McEwan, C.J., Rowe, R.R., and Zhou, X., 2007, Models and Exploration Methods for Major Gold Deposit

Types, *in* Milkereit, B. ed., Proceedings of Exploration 07: Fifth Decennial International Conference on Mineral Exploration, p. 691–711.

Robert, F., Poulsen, K.H., and Dube, B., 1997, Gold Deposits and Their Geological Classification, *in* Gubins, A.G. ed., Proceedings of Exploration 97: Fourth Decennial International Conference on Mineral Exploration, p. 209–220.

Rytuba, J.J., and Heropoulos, C., 1992, Mercury in Epithermal gold systems—an important by-product.: US Geological Survey Bulletin, v. 1877, p. D1–D8.

Sainsbury, C.L., Hummel, C.L., and Hudson, T., 1972, Reconnaissance Geologic Map of the Nome Quadrangle, Seward Peninsula, Alaska:, 1–28 p.

Schaffer, M.B., 2013, Mining the Oceans: Development of Global Resources: International Affairs Forum, v. 4, no. 2, p. 117–126.

Scott, S.D., 2011, Marine Minerals : Their Occurrences, Exploration and Exploitation, *in* Oceans 2011, Dept. of Geol., Univ. Of Toronto, p. 1–8.

Till, A.B., Dumoulin, J.A., Werdon, M.B., and Bleick, H.A., 2011, Bedrock Geologic Map of the Seward Peninsula, Alaska, and Accompanying Conodont Data: Scientific Investigations Map 3131: U.S. Geological Survey.

Tomkins, A.G., and Mavrogenes, J.A., 2002, Mobilization of Gold as a Polymetallic Melt during Pelite Anatexis at the Challenger Deposit, South Australia: A Metamorphosed Archean Gold Deposit: Economic Geology, v. 97, p. 1249–1271.

Townley, B.K., Herail, G., Maksaev, V., Palacios, C., de Parseval, P., Sepulveda, F., Orellana, R., Rivas, P., and Ulloa, C., 2003, Gold grain morphology and composition as an exploration tool: application to gold exploration in covered areas: Geochemistry: Exploration, Environment, Analysis, v. 3, p. 29–38.

Watling, R.J., Herbert, H.K., Delev, D., and Abell, I.A., 1994, Gold fingerprinting by laser ablation inductively coupled plasma mass spectrometry: Spectrochimica Acta, v. 49B, no. 2, p. 205–219.

Youngson, J.H., 2005, Diagenetic silcrete and formation of silcrete ventifacts and aeolian gold placers in Central Otago, New Zealand: New Zealand Journal of Geology and Geophysics, v. 48, no. 2, p. 247–263, doi: 10.1080/00288306.2005.9515113.

Youngson, J.H., and Craw, D., 1999, Variation in Placer Style, Gold Morphology, and Gold Particle Behavior Down Gravel Bed-Load Rivers: An Example from the shotover/Arrow-Kawarau-Clutha River System, Otago, New Zealand: Economic Geology, v. 94, no. 134, p. 615.

Youngson, J., Wopereis, P., Kerr, L., and Craw, D., 2002, Au-Ag-Hg and Au-Ag alloys in Nokomai and Nevis valley placers, northern Southland and Central Otago, New Zealand, and their implications for placer-source relationships: New

Zealand Journal of Geology and Geophysics, v. 45, no. 1, p. 53–69, doi: 10.1080/00288306.2002.9514959.

Youngson, J.H., Wopereis, P., Kerr, L.C., and Craw, D., 2000, Compositional variation and distribution of Au-Ag-Hg and Au-Ag alloy in Nokomai and Nevis valley placers , New Zealand , and their implications for primary gold sources, *in* New Zealand Minerals & Mining Conference Proceedings, p. 1–13.

Žitňan, P., Bakos, F., and Schmiderer, A., 2010, Importance of alluvial gold geochemistry for exploration : Examples from placers in the Western Carpathians: Mineralia Slovaca, v. 42, p. 57–68.

11 Appendices

Appendix A: Secondary Electron Images (SEI) of gold grains from the southern Seward Peninsula

Appendix B: Gold grain particle statistics, morphology and textures for all grains from placer sites across the southern Seward Peninsula, Nome, Alaska

Appendix C: Major and Minor Element data of gold grains from the southern Seward Peninsula, Nome, Alaska

Appendix D: Filtered Major and Minor Element data for gold grains from the southern Seward Peninsula, Nome, Alaska

Appendix E: Comparison between major and minor element core and rim chemistry of gold grains from the southern Seward Peninsula, Nome, Alaska

Appendix F: Trace Element data of gold grains from the southern Seward Peninsula, Nome, Alaska

Appendix G: Filtered Trace Element data of gold grains from the southern Seward Peninsula, Nome, Alaska

Appendix H: Elemental maps of gold grains from the southern Seward Peninsula, Nome, Alaska

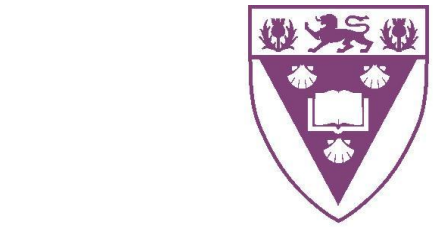

RHODES UNIVERSITY

Grahamstown • 6140 • South Africa

A GEOCHEMICAL AND MORPHOLOGICAL INVESTIGATION OF PLACER GOLD GRAINS FROM THE SOUHERN SEWARD PENINSULA, ALASKA: IMPLICATIONS FOR SOURCE AND TRANSPORT MECHANISMS

By

Ernest J.H. Gauntlett

MASTER OF SCIENCE

(Economic Geology)

APPENDICES

APPENDIX A

Secondary Electron Images (SEI) of gold grains from the southern Seward Peninsula


AK015-001
X 95
15.0kV SEI
100µm JEOL
NOR
10/14/2013
WD 11.1mm 16:44:32

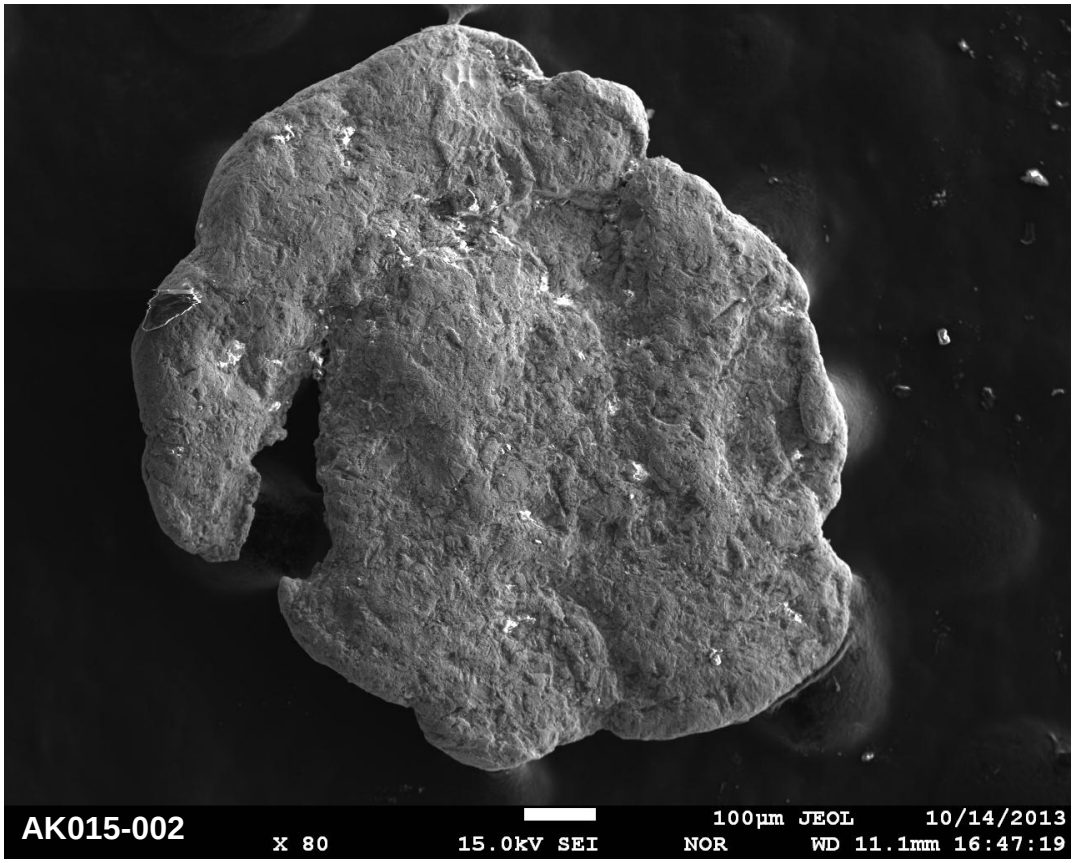
AK015-002
X 80
15.0kV SEI
100µm JEOL
NOR
10/14/2013
WD 11.1mm 16:47:19

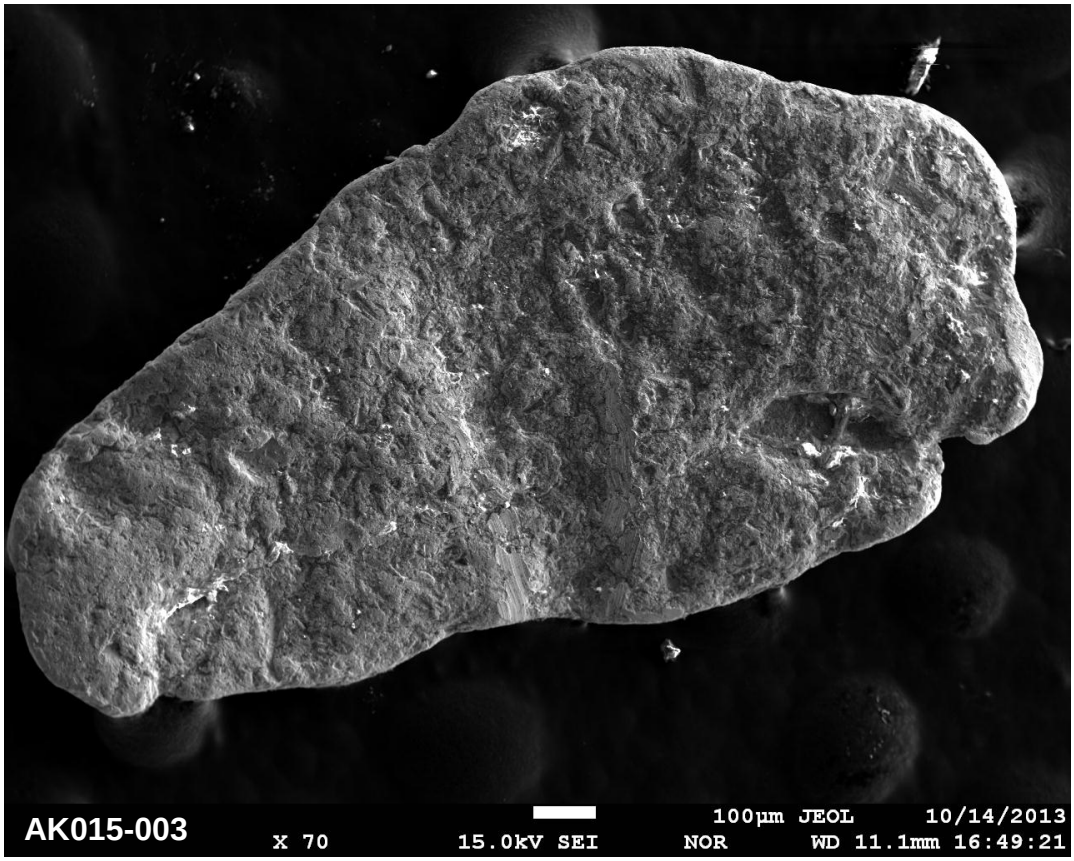
AK015-003
X 70
15.0kV SEI
100µm JEOL
NOR
10/14/2013
WD 11.1mm 16:49:21

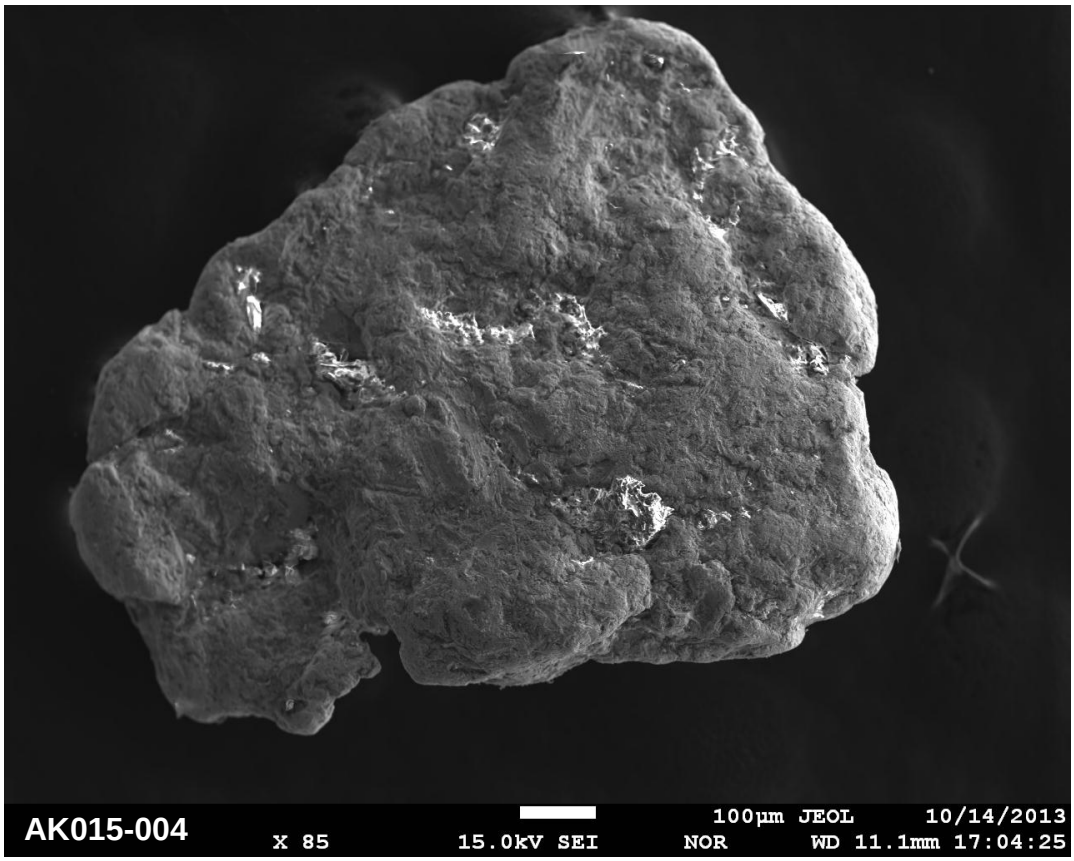
AK015-004
X 85
15.0kV SEI
100µm JEOL
NOR
10/14/2013
WD 11.1mm 17:04:25

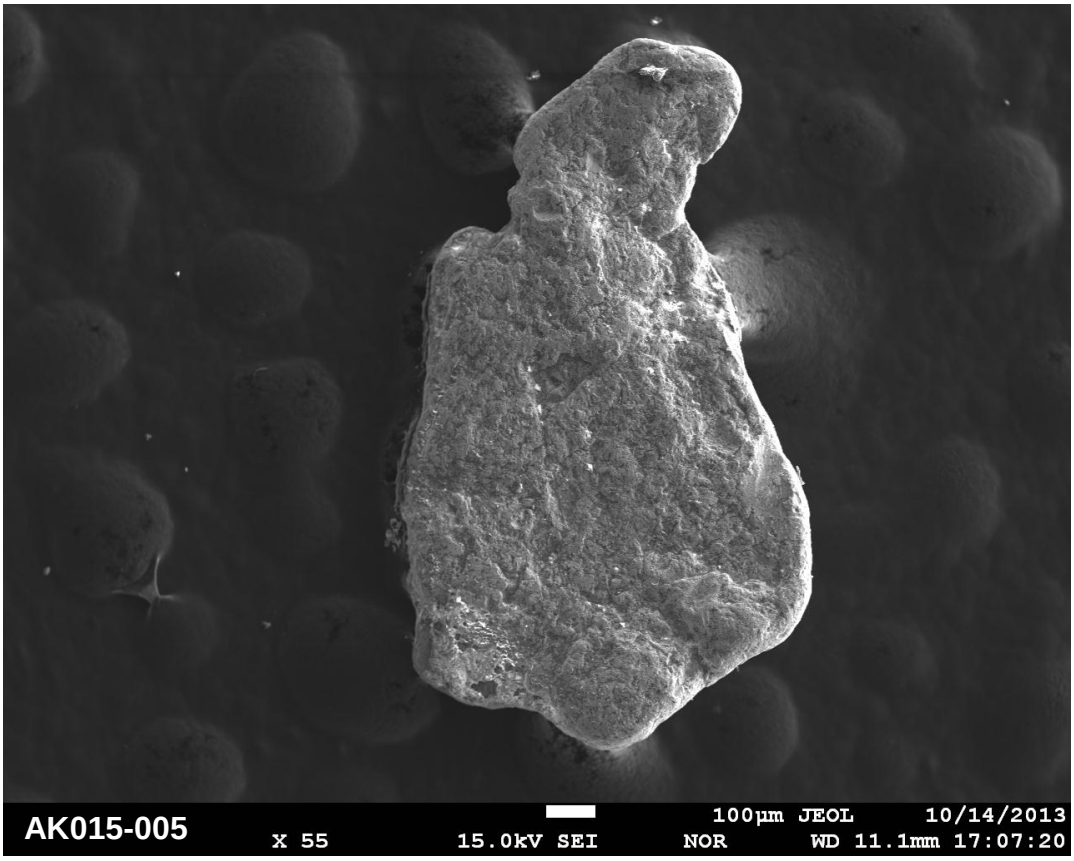
AK015-005
X 55
15.0kV SEI
100µm JEOL
NOR
10/14/2013
WD 11.1mm 17:07:20

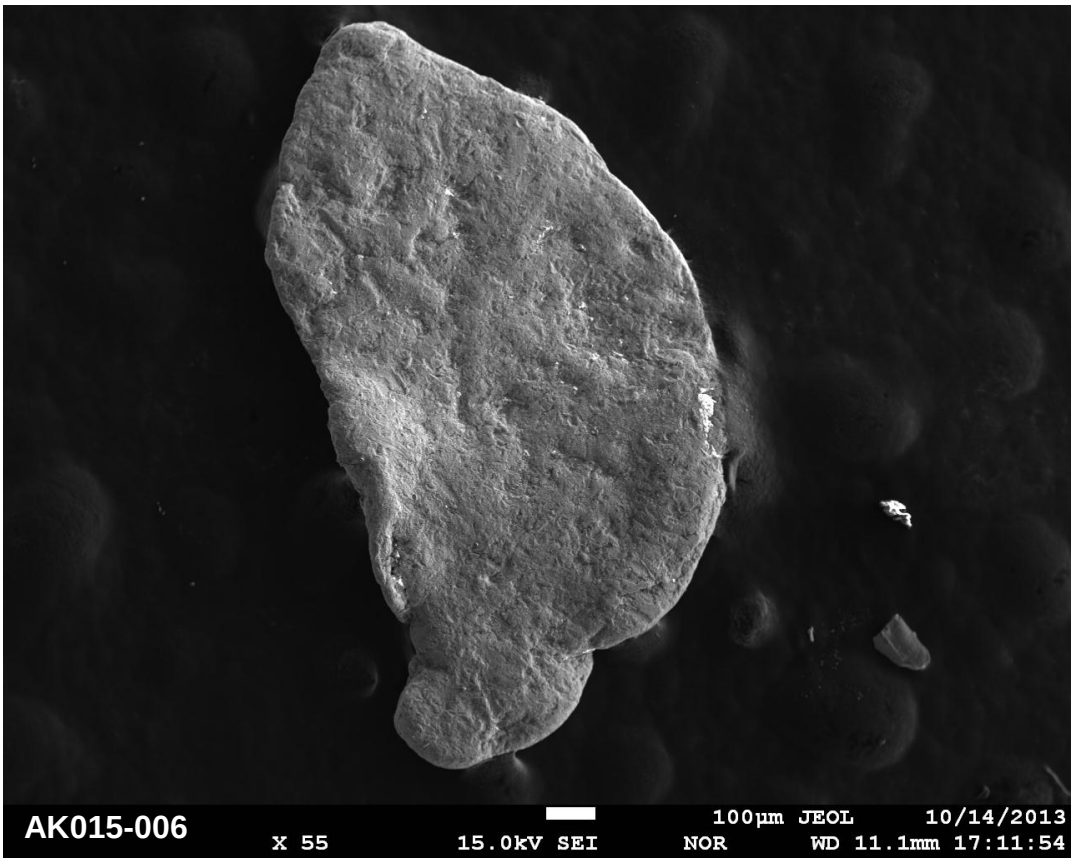
AK015-006
X 55
15.0kV SEI
100µm JEOL
NOR
10/14/2013
WD 11.1mm 17:11:54

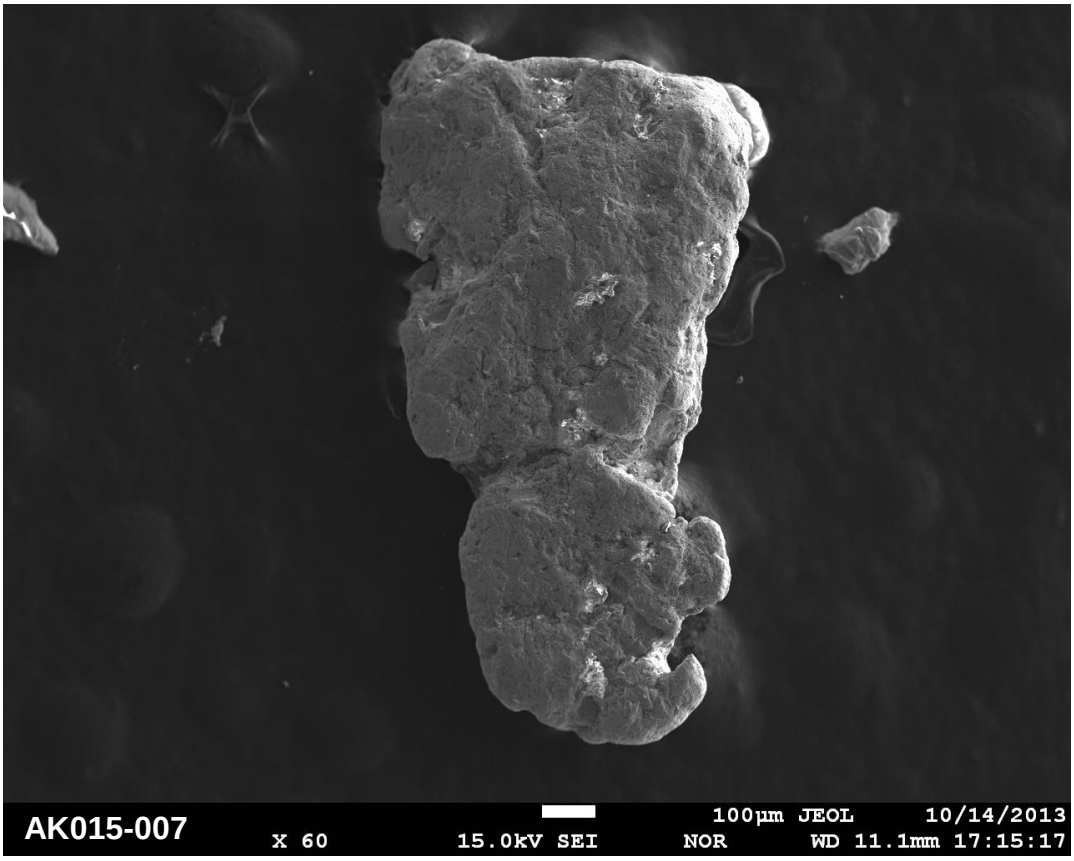
AK015-007
X 60
15.0kV SEI
100µm JEOL
NOR
10/14/2013
WD 11.1mm 17:15:17


AK015-008
X 55
15.0kV SEI
100µm JEOL
NOR
10/14/2013
WD 11.1mm 17:17:44

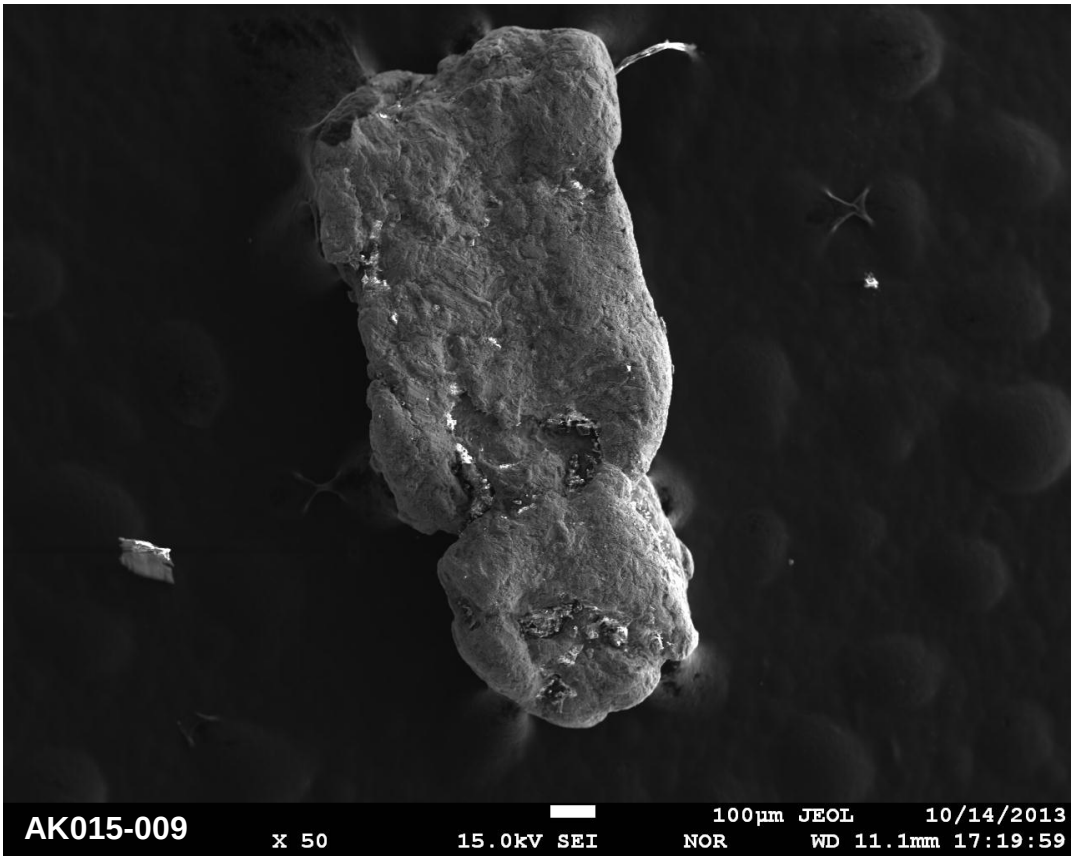
AK015-009
X 50
15.0kV SEI
100µm JEOL
NOR
10/14/2013
WD 11.1mm 17:19:59

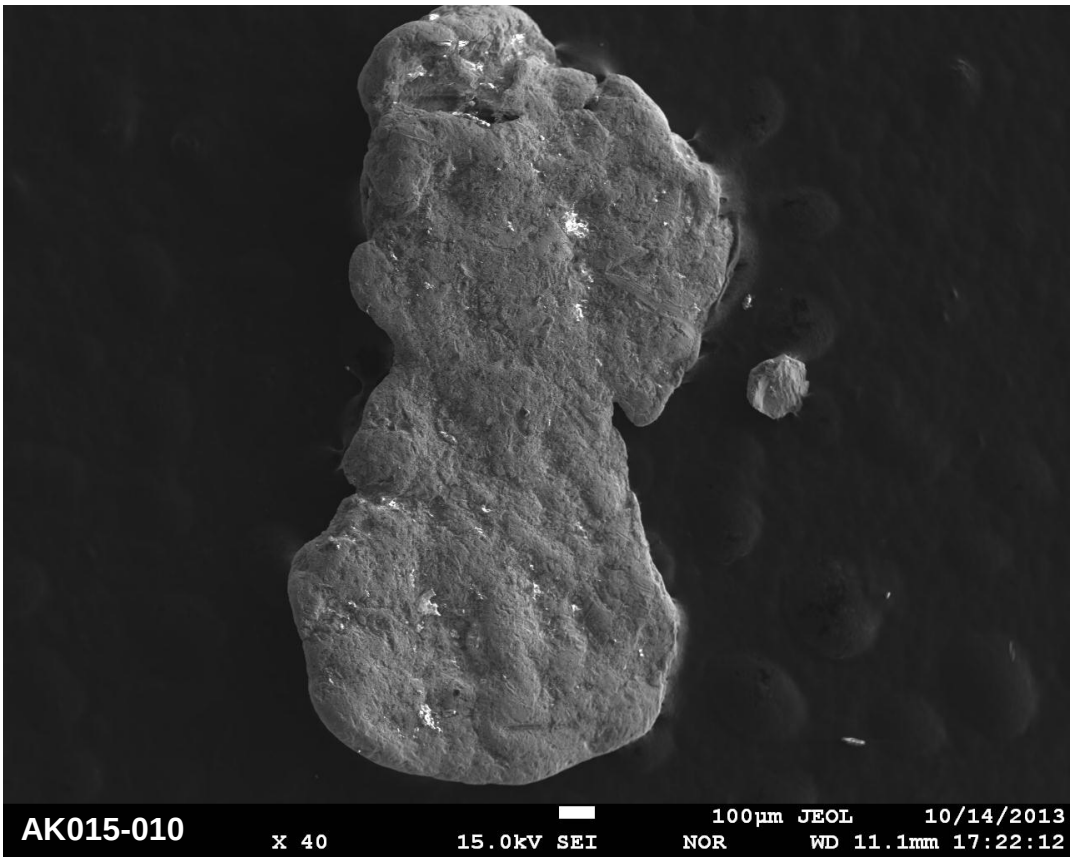
AK015-010
X 40
15.0kV SEI
100µm JEOL
NOR
10/14/2013
WD 11.1mm 17:22:12

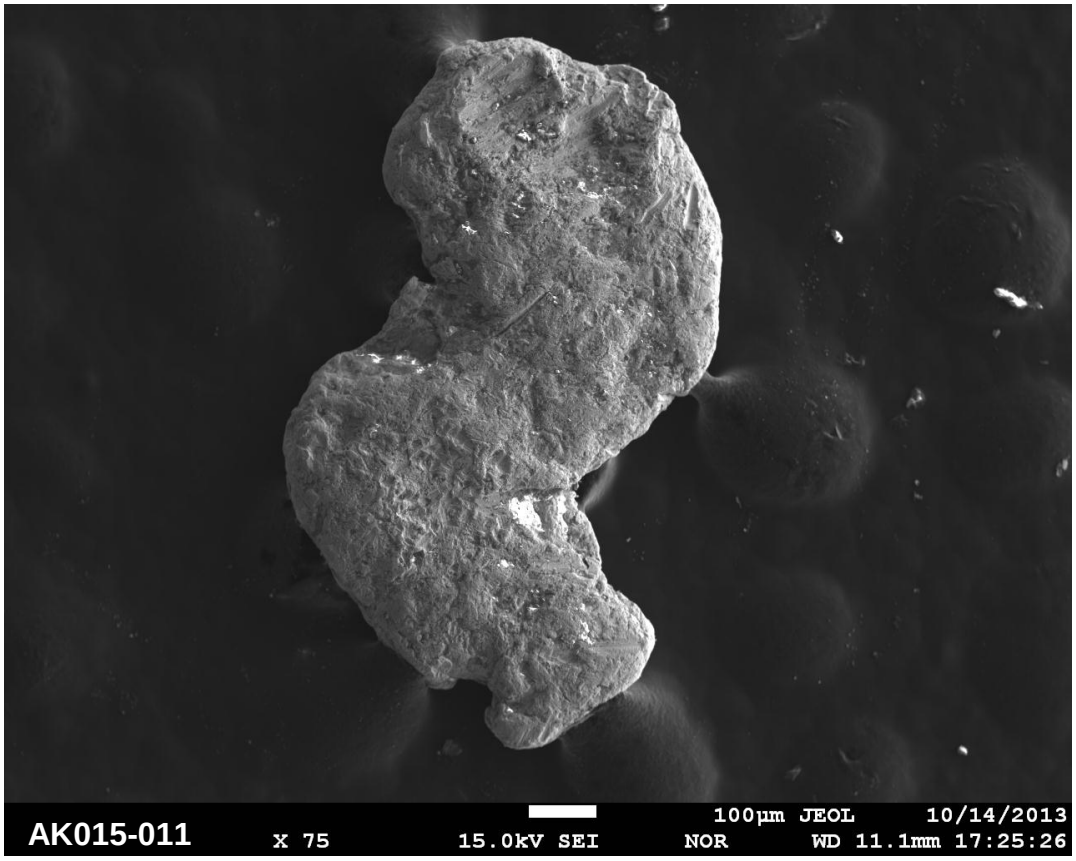
AK015-011
X 75
15.0kV SEI
100µm JEOL
NOR
10/14/2013
WD 11.1mm 17:25:26

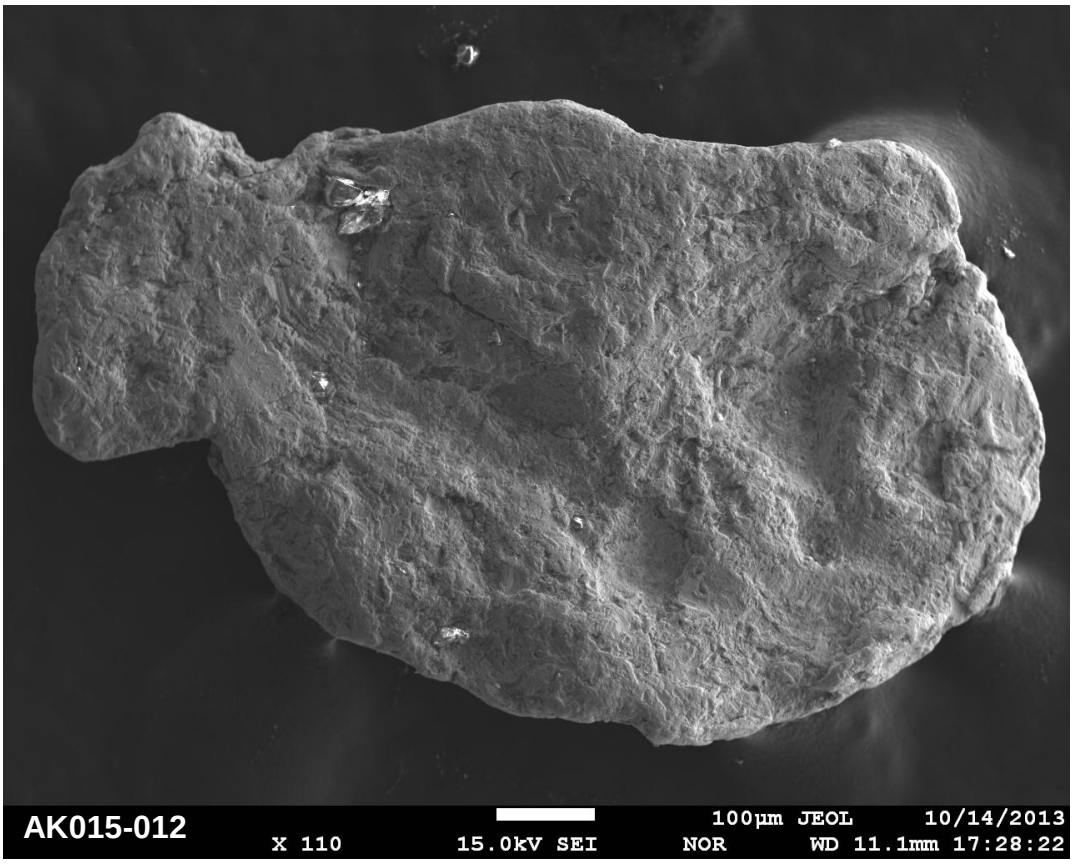
AK015-012
X 110
15.0kV SEI
100µm JEOL
NOR
10/14/2013
WD 11.1mm 17:28:22

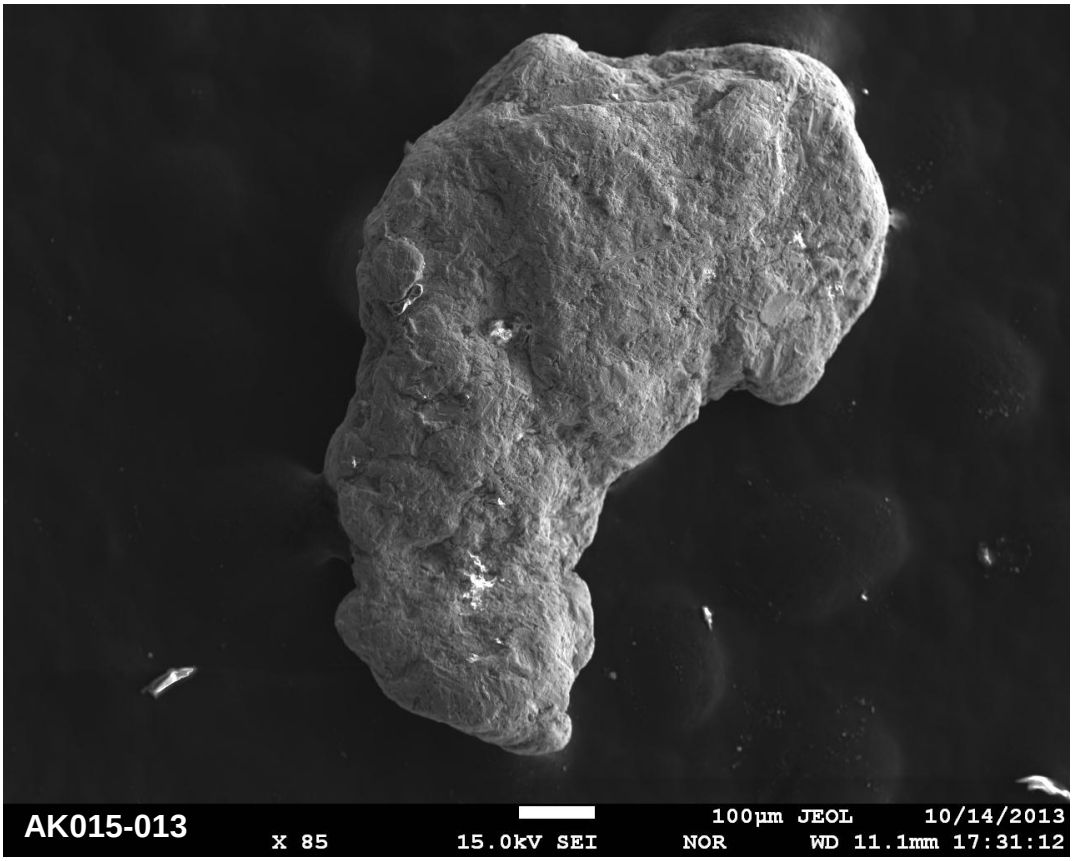
AK015-013
X 85
15.0kV SEI
100µm JEOL
NOR
10/14/2013
WD 11.1mm 17:31:12

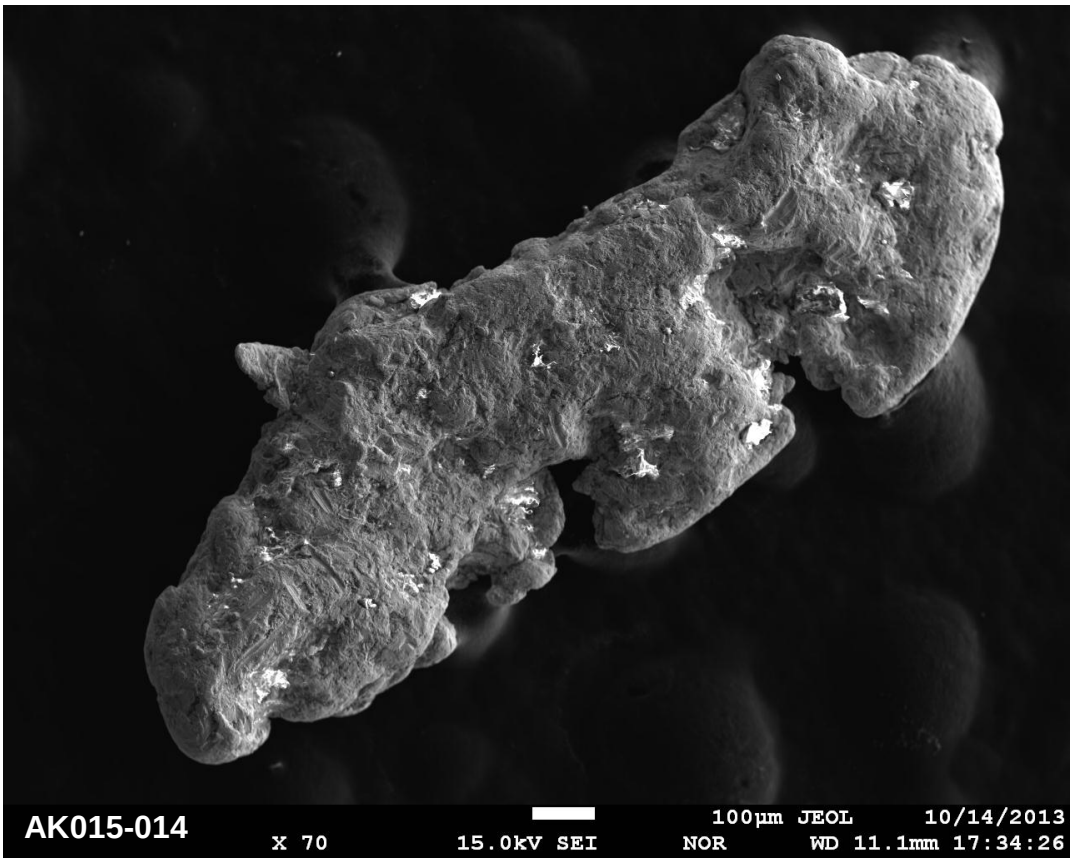
AK015-014
X 70
15.0kV SEI
100µm JEOL
NOR
10/14/2013
WD 11.1mm 17:34:26

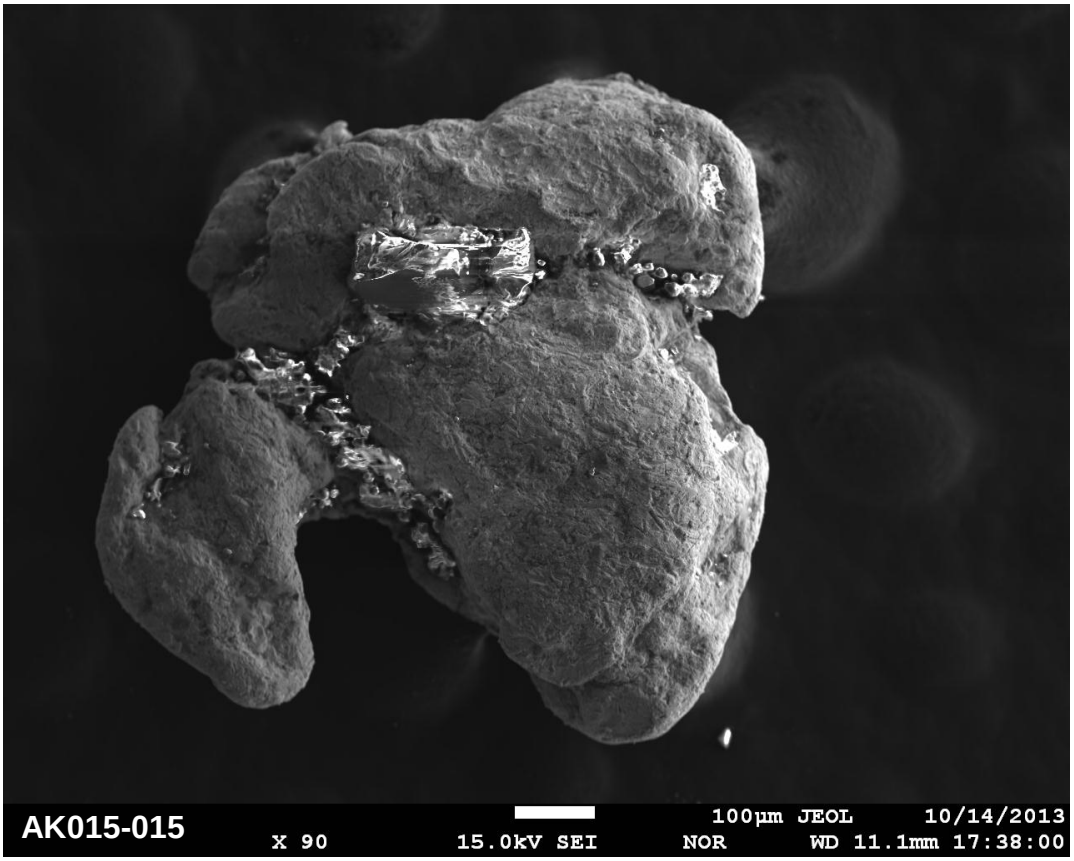
AK015-015
X 90
15.0kV SEI
100µm JEOL
NOR
10/14/2013
WD 11.1mm 17:38:00

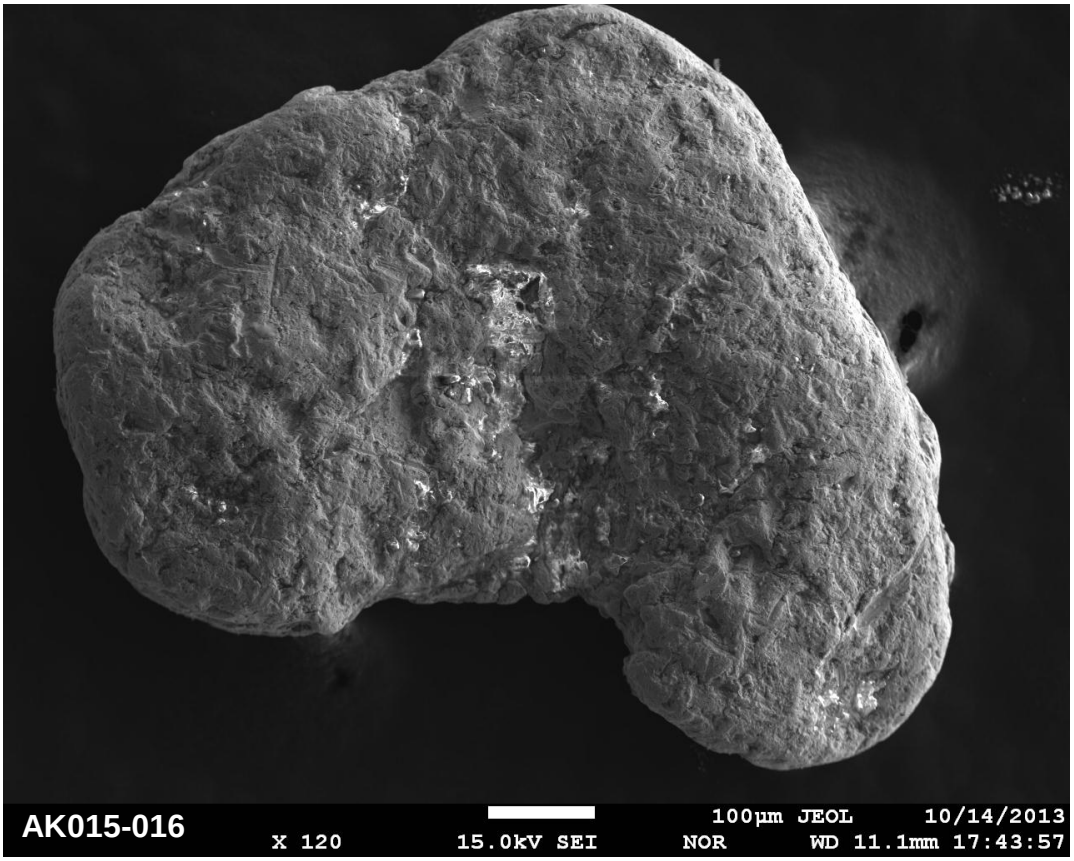
AK015-016
X 120
15.0kV SEI
100µm JEOL
NOR
10/14/2013
WD 11.1mm 17:43:57

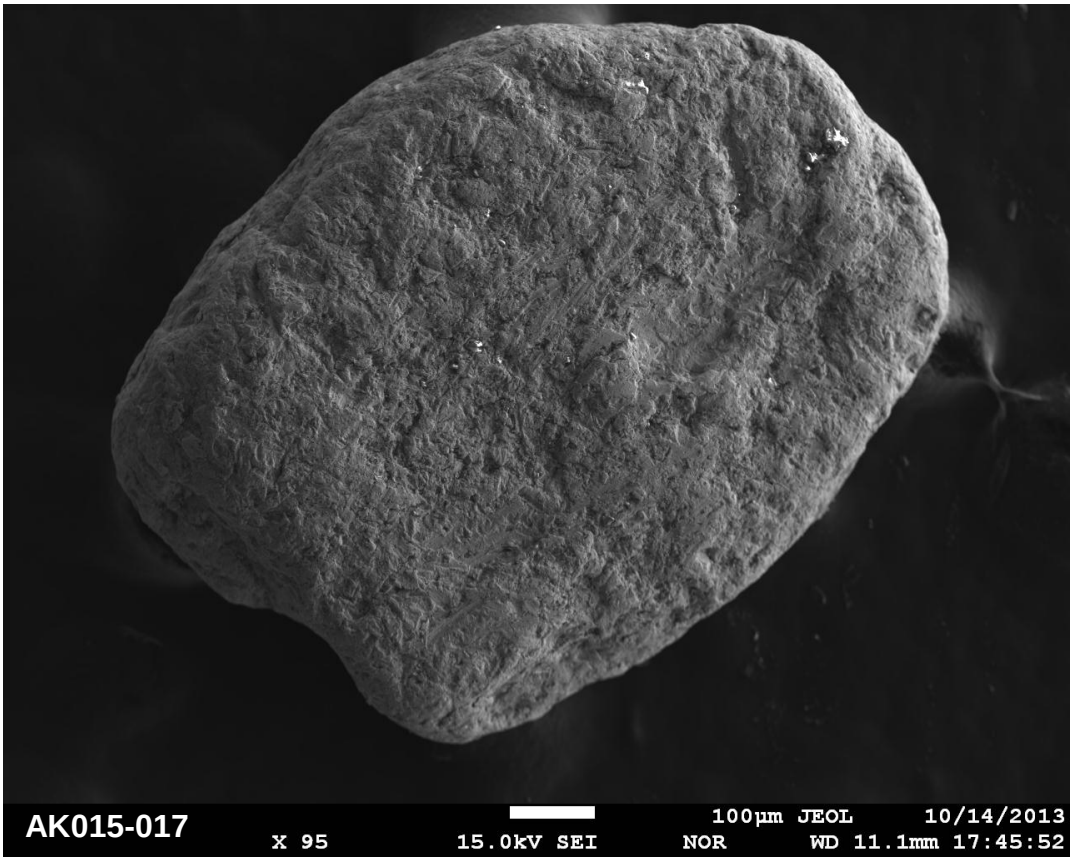
AK015-017
X 95
15.0kV SEI
100µm JEOL
NOR
10/14/2013
WD 11.1mm 17:45:52

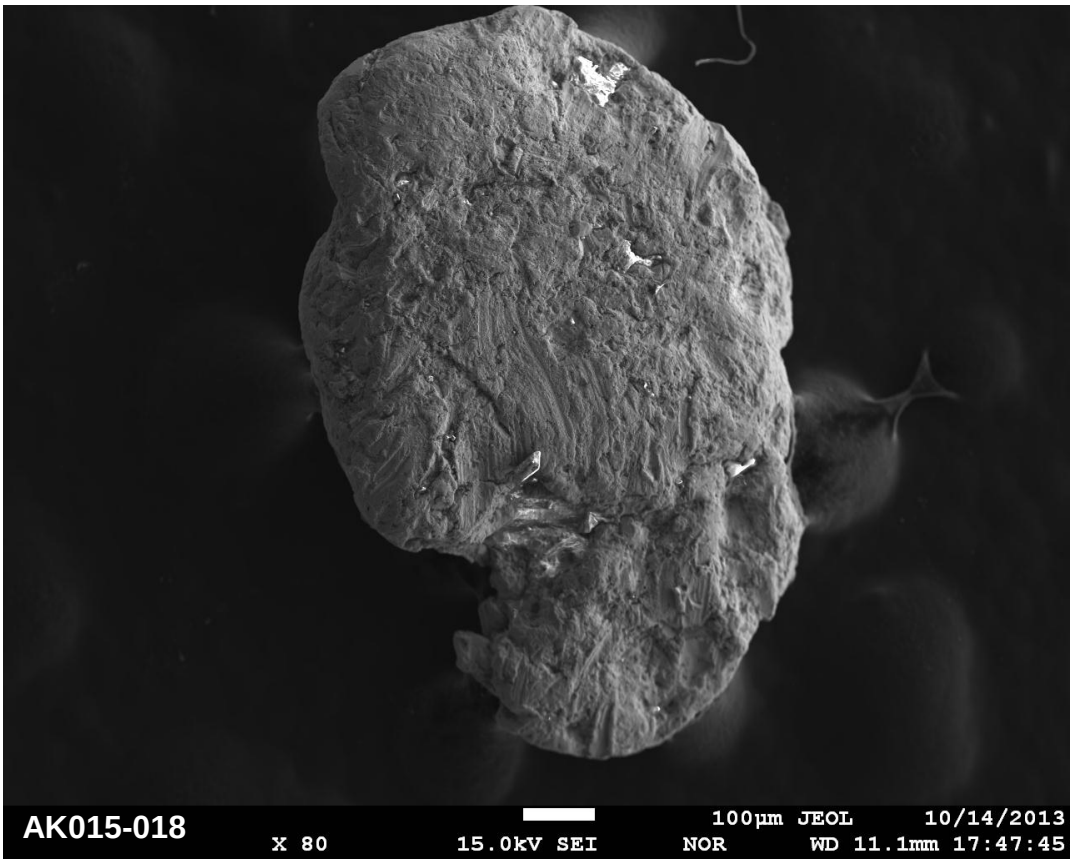
AK015-018
X 80
15.0kV SEI
100µm JEOL
NOR
10/14/2013
WD 11.1mm 17:47:45

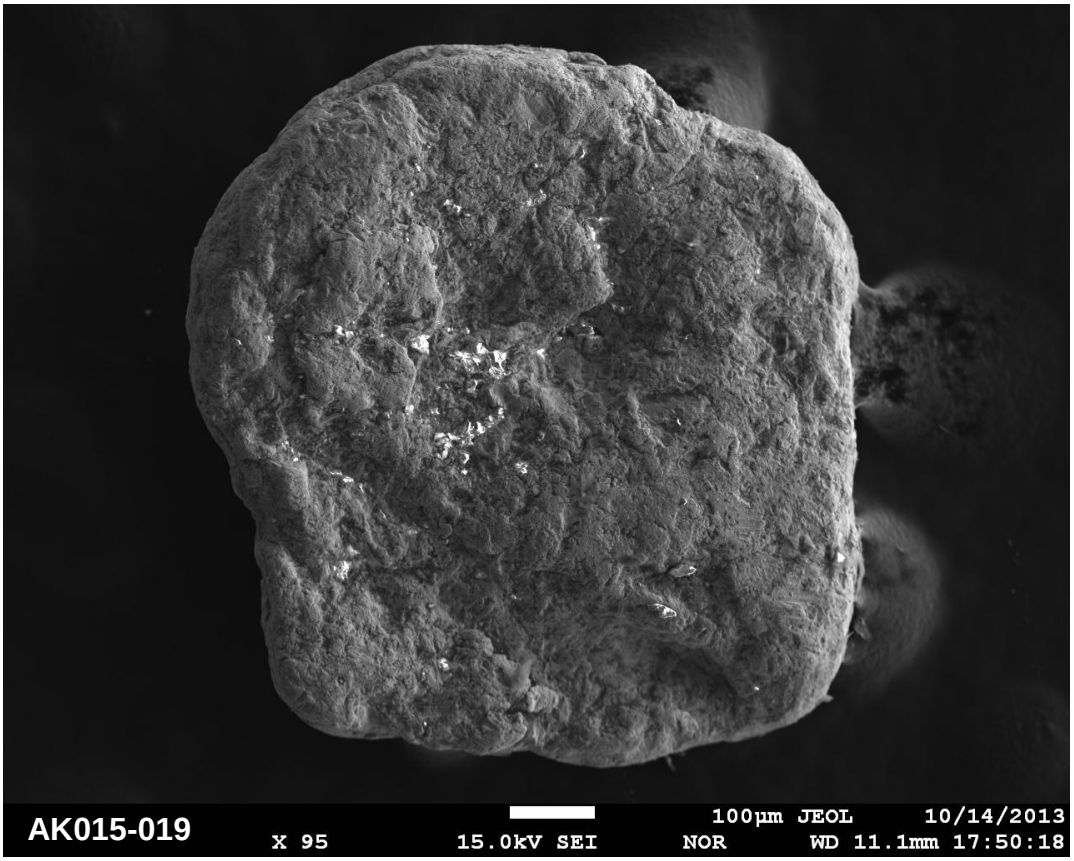
AK015-019
X 95
15.0kV SEI
100µm JEOL
NOR
10/14/2013
WD 11.1mm 17:50:18

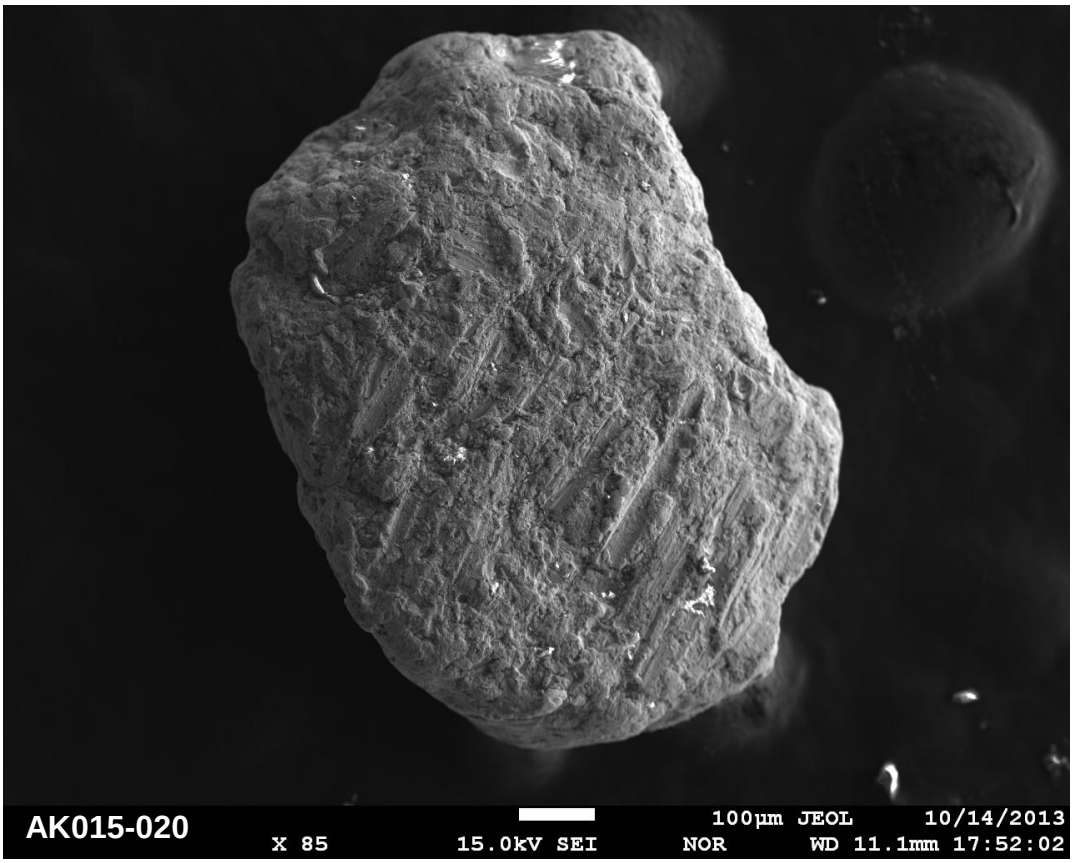
AK015-020
X 85
15.0kV SEI
100µm JEOL
NOR
10/14/2013
WD 11.1mm 17:52:02

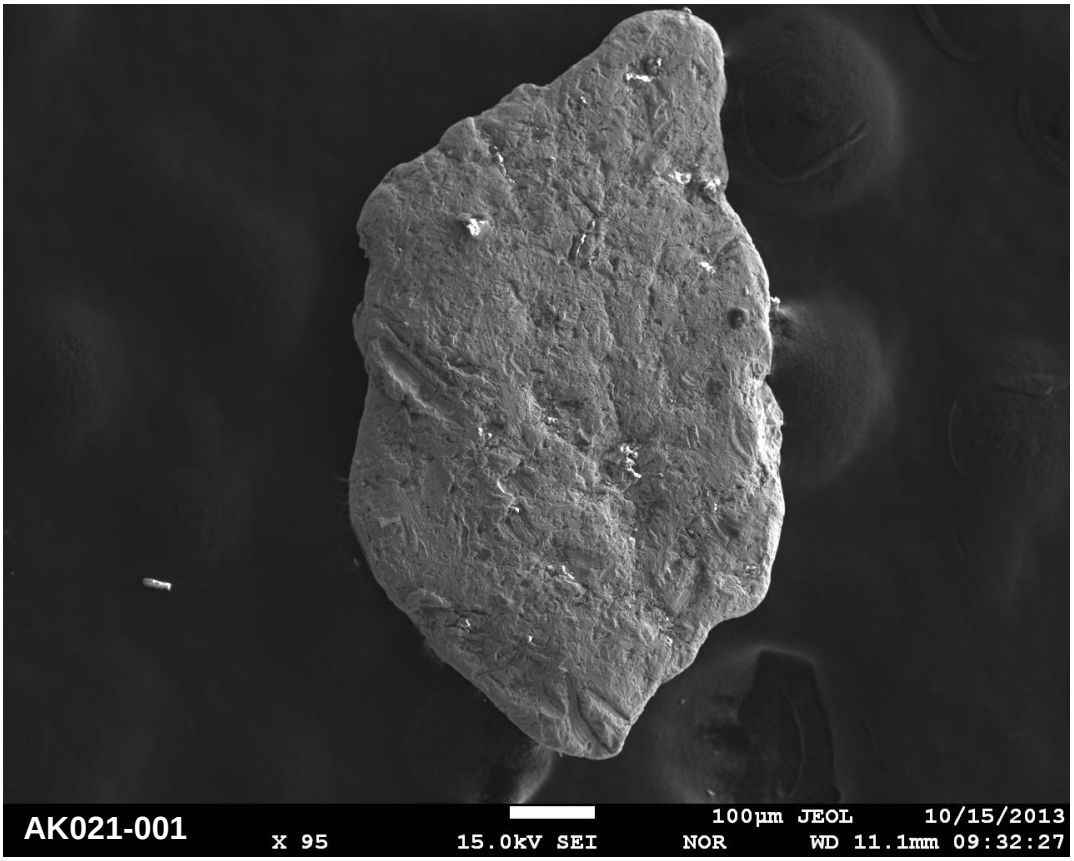
AK021-001
X 95
15.0kV SEI
100µm JEOL
NOR
10/15/2013
WD 11.1mm 09:32:27

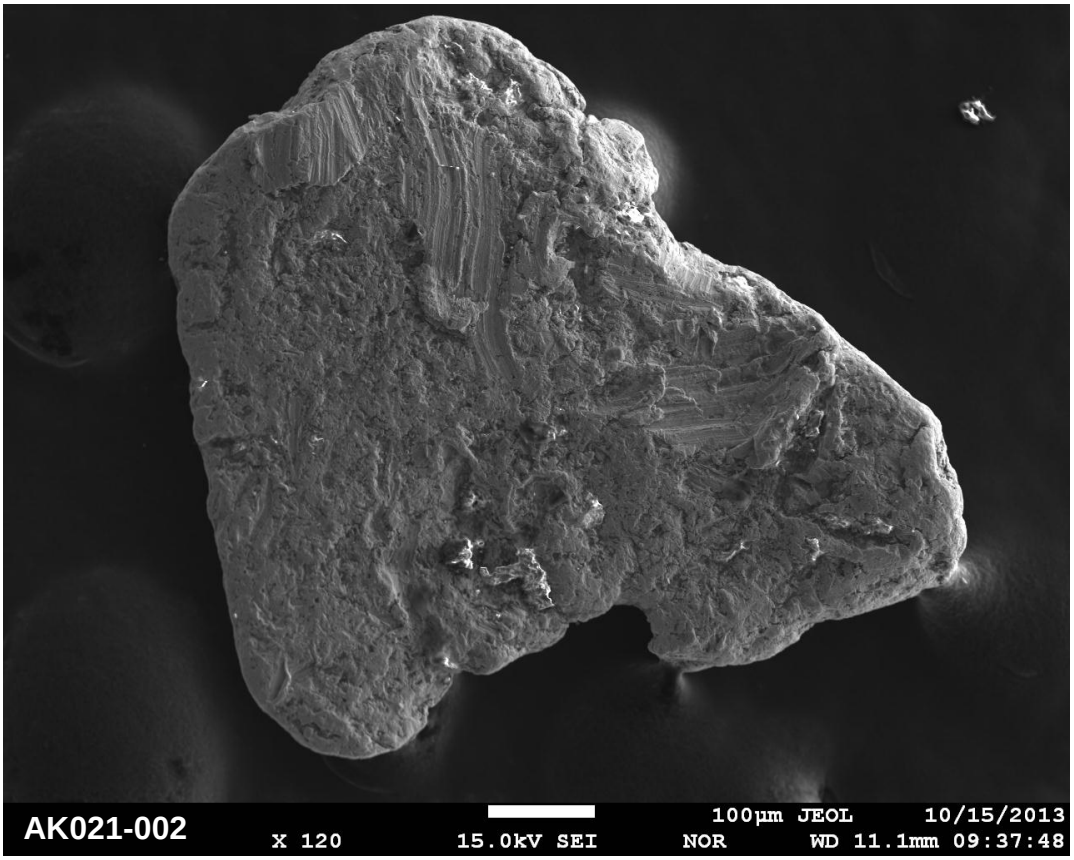
AK021-002
X 120
15.0kV SEI
100µm JEOL
NOR
10/15/2013
WD 11.1mm 09:37:48

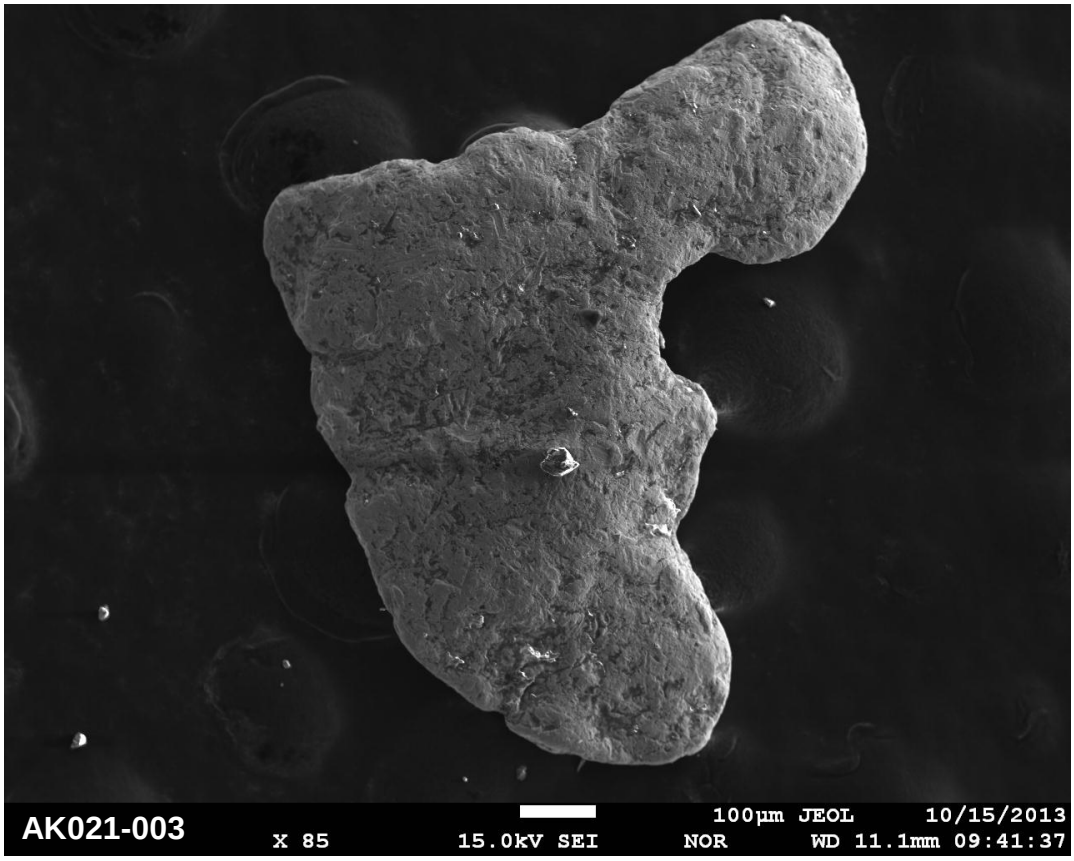
AK021-003
X 85
15.0kV SEI
100µm JEOL
NOR
10/15/2013
WD 11.1mm 09:41:37

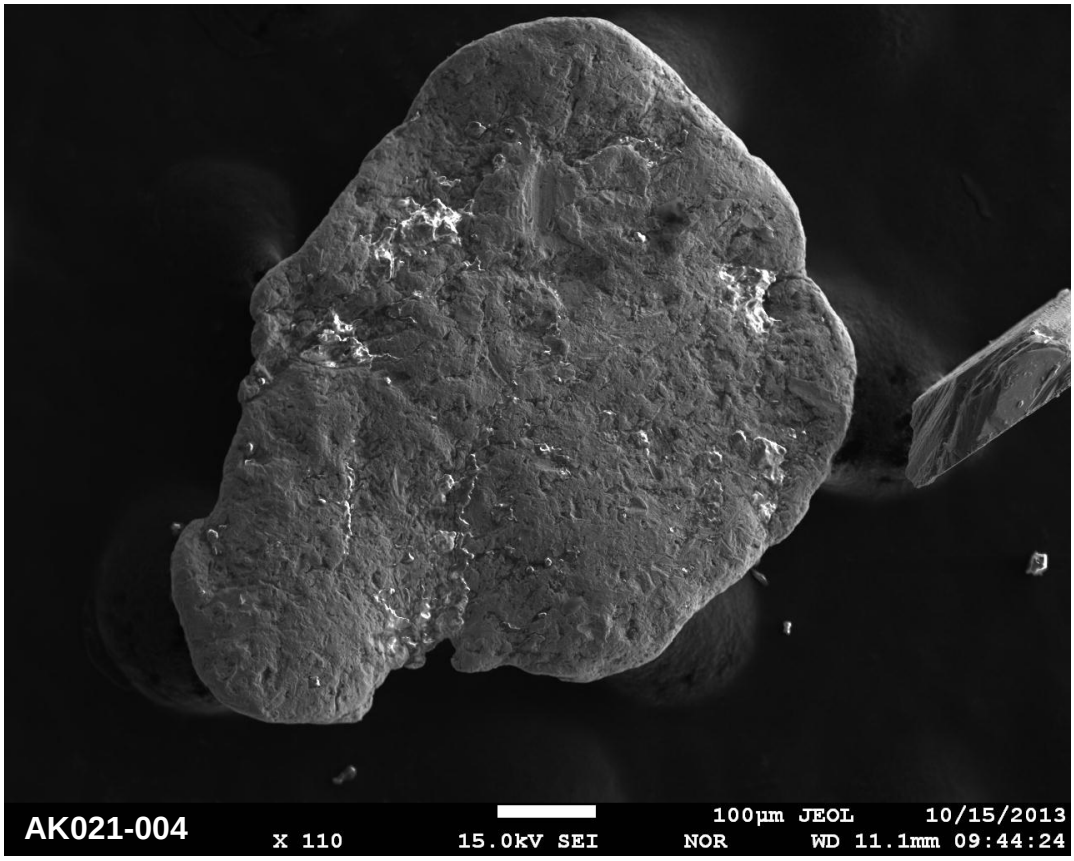
AK021-004
X 110
15.0kV SEI
100µm JEOL
NOR
10/15/2013
WD 11.1mm 09:44:24

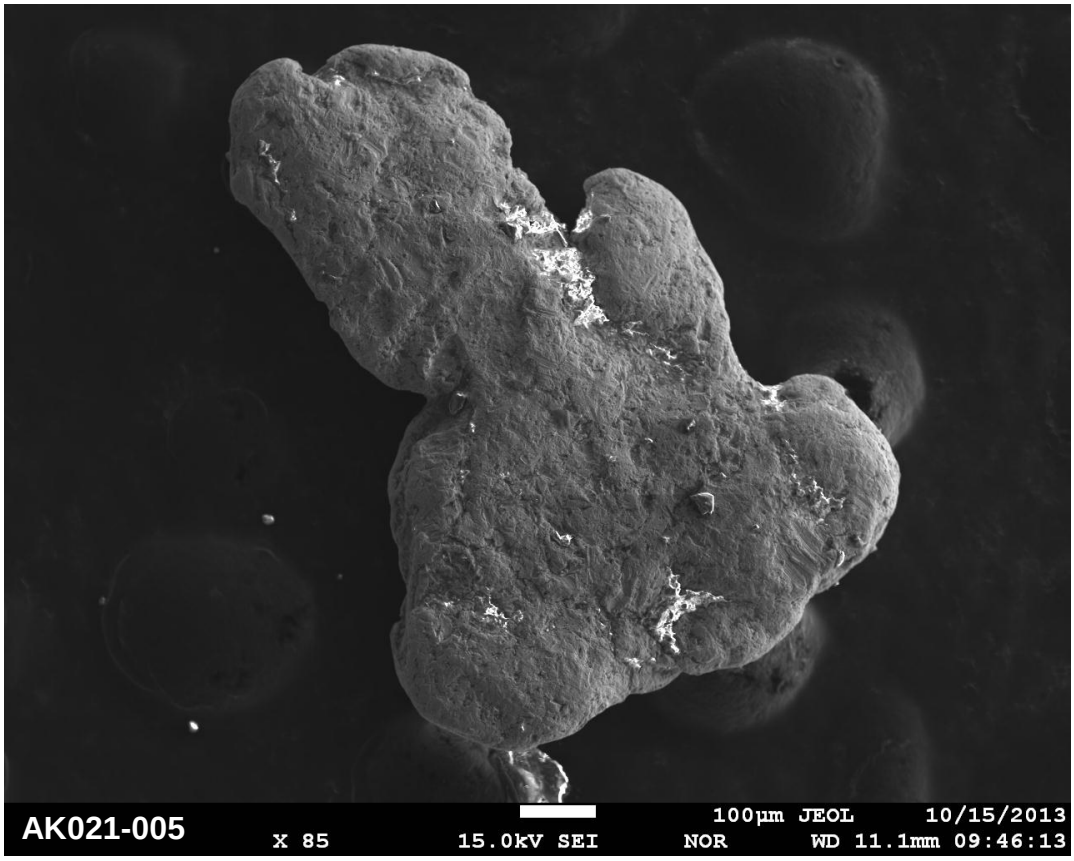
AK021-005
X 85
15.0kV SEI
100µm JEOL
NOR
10/15/2013
WD 11.1mm 09:46:13

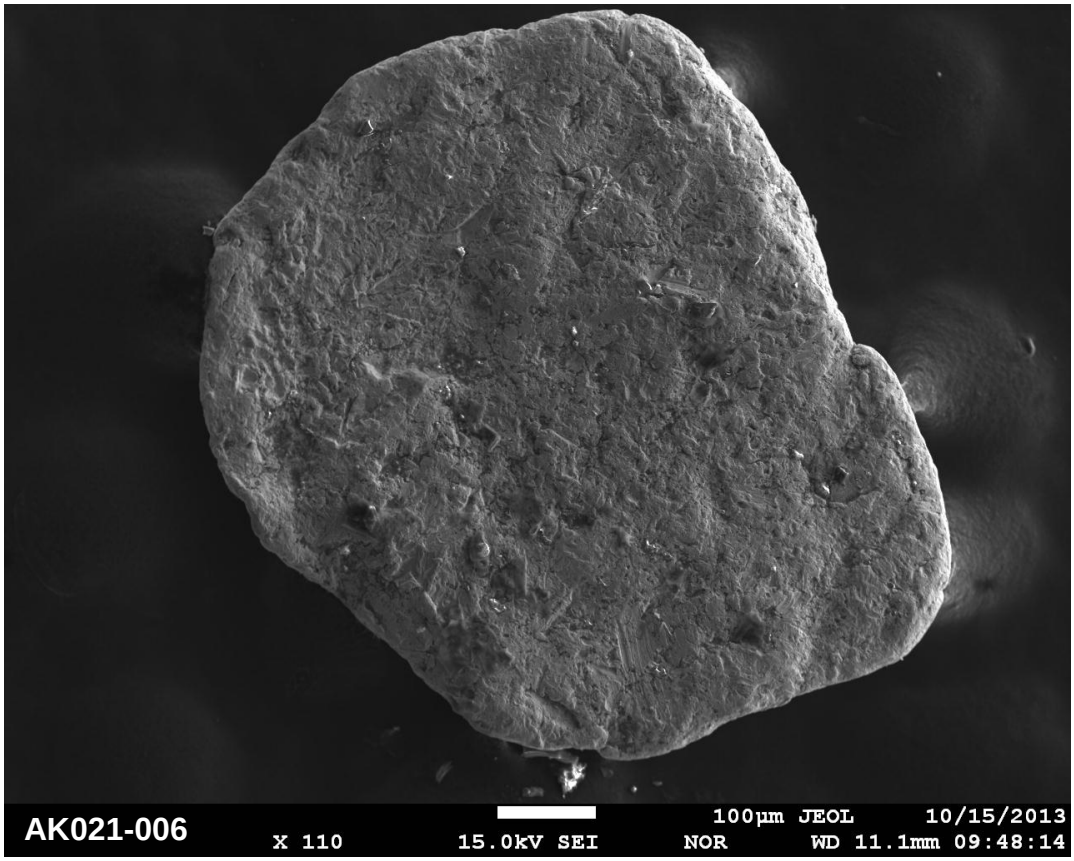
AK021-006
X 110
15.0kV SEI
100µm JEOL
NOR
10/15/2013
WD 11.1mm 09:48:14

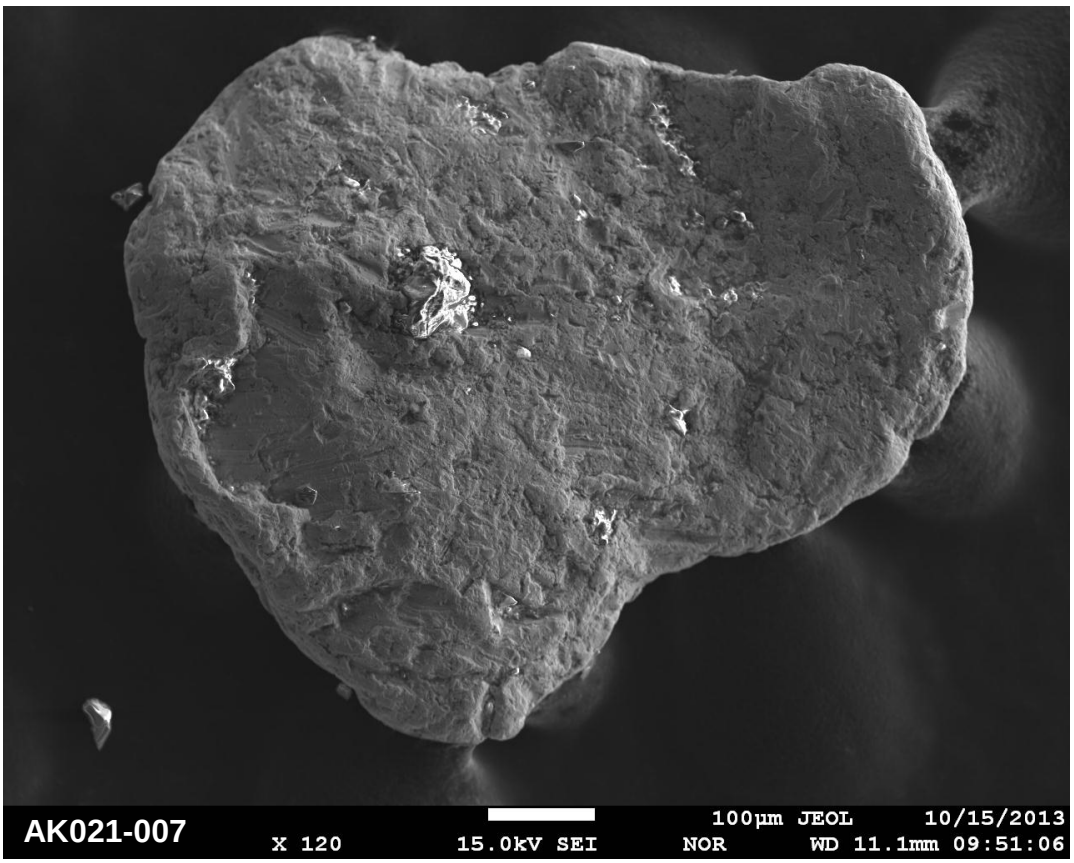
AK021-007
X 120
15.0kV SEI
100µm JEOL
NOR
10/15/2013
WD 11.1mm 09:51:06

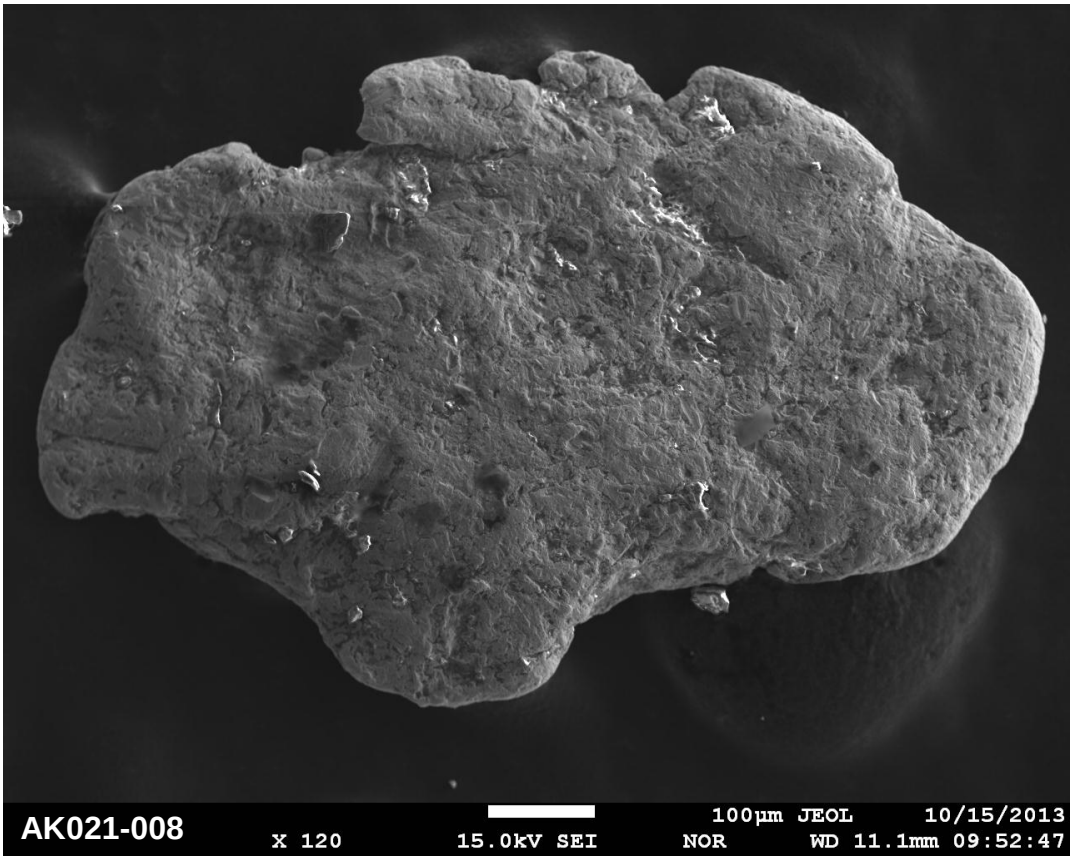
AK021-008
X 120
15.0kV SEI
100µm JEOL
NOR
10/15/2013
WD 11.1mm 09:52:47

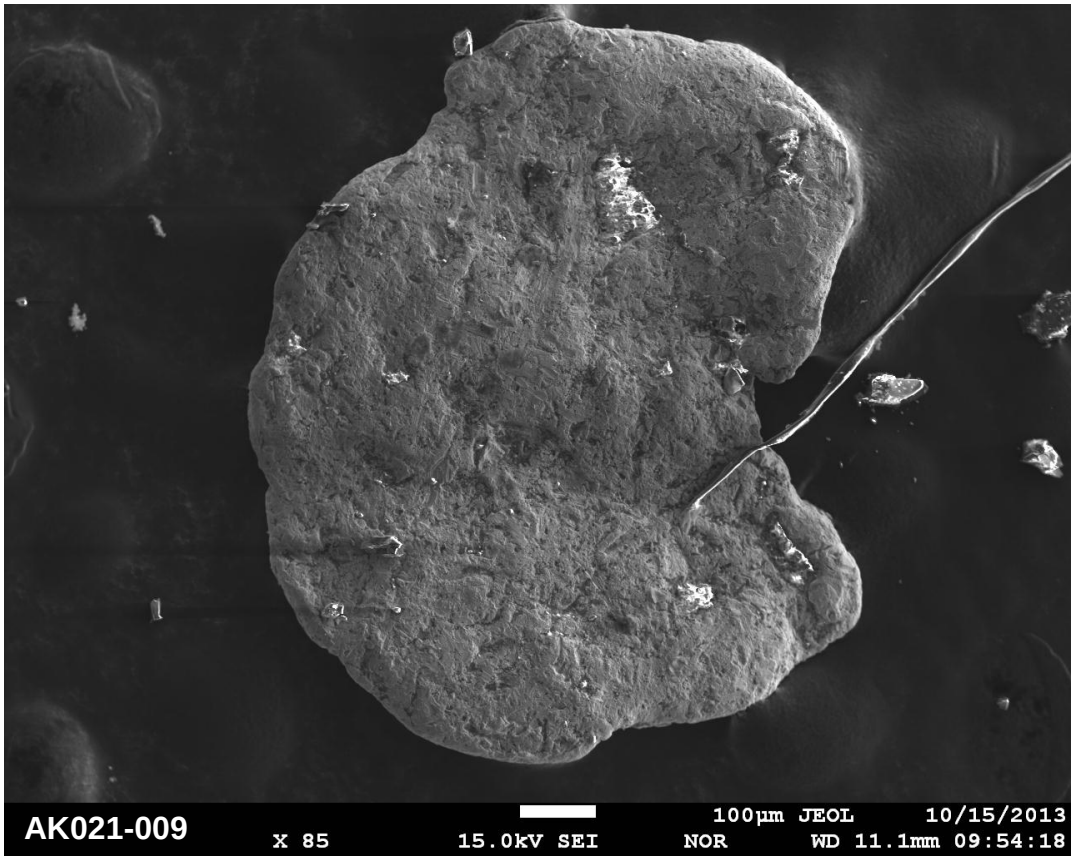
AK021-009
X 85
15.0kV SEI
100µm JEOL
NOR
10/15/2013
WD 11.1mm 09:54:18

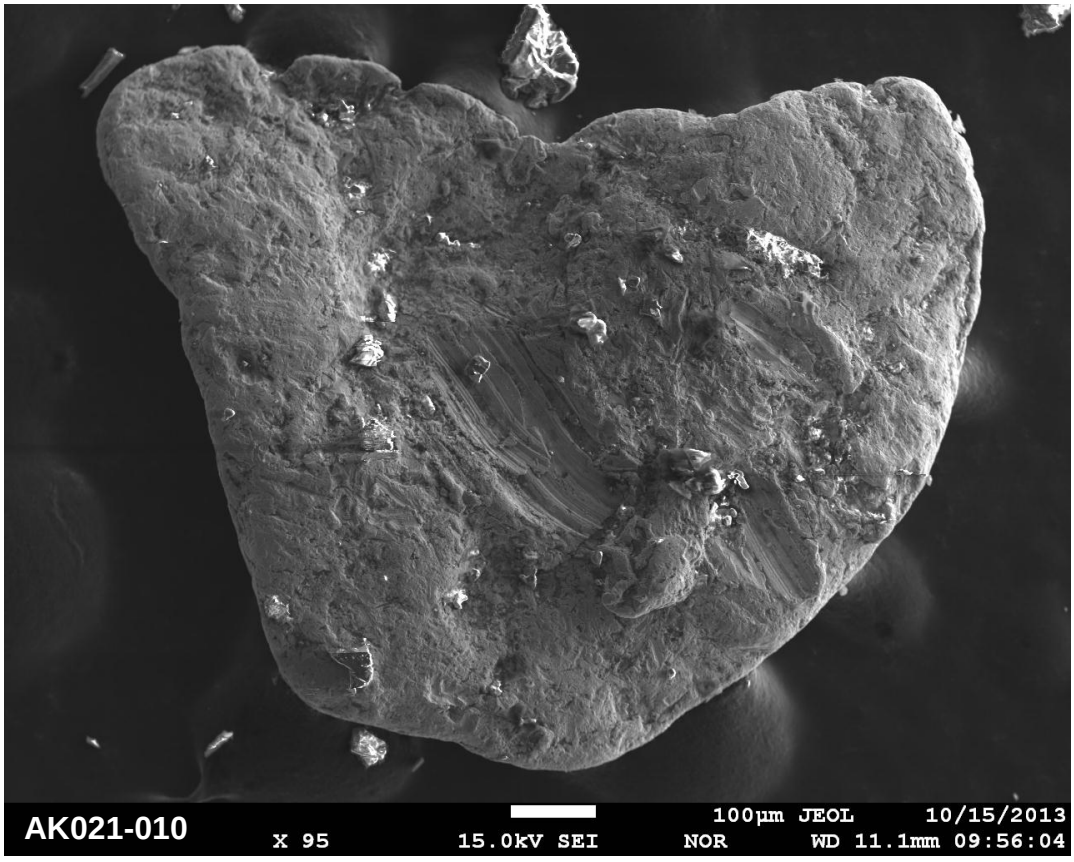
AK021-010
X 95
15.0kV SEI
100µm JEOL
NOR
10/15/2013
WD 11.1mm 09:56:04

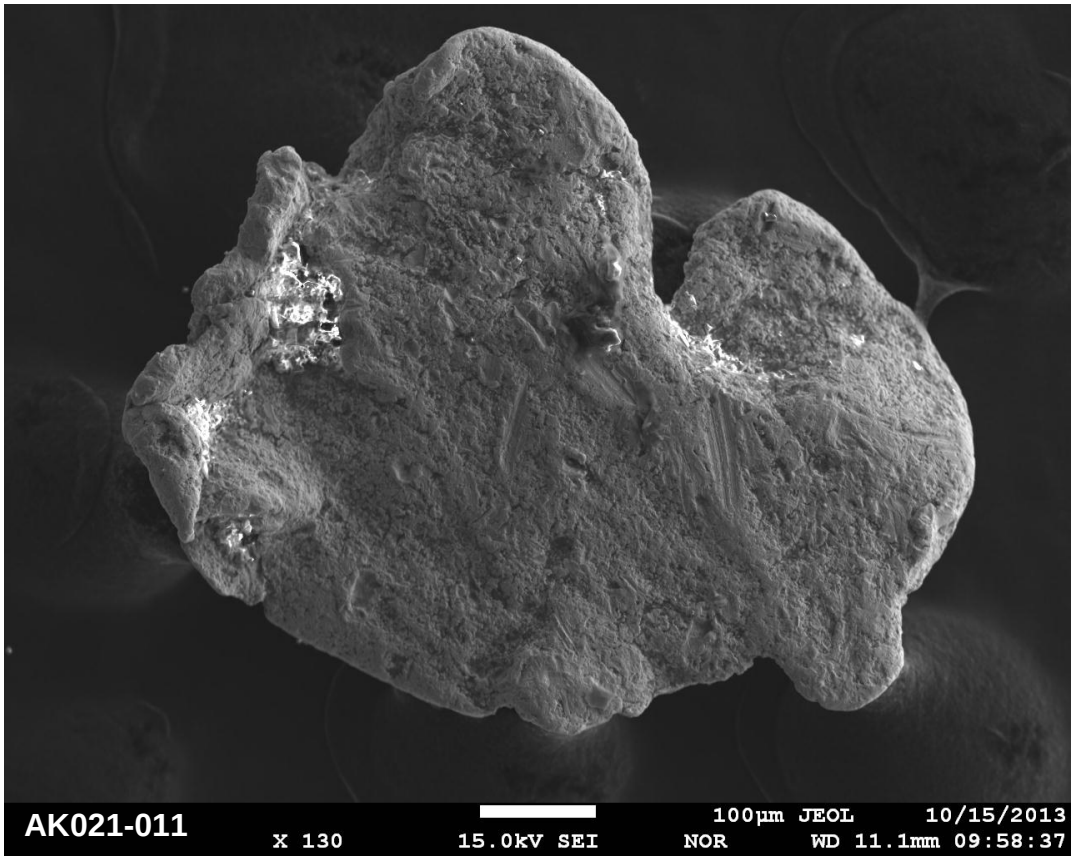
AK021-011
X 130
15.0kV SEI
100µm JEOL
NOR
10/15/2013
WD 11.1mm 09:58:37

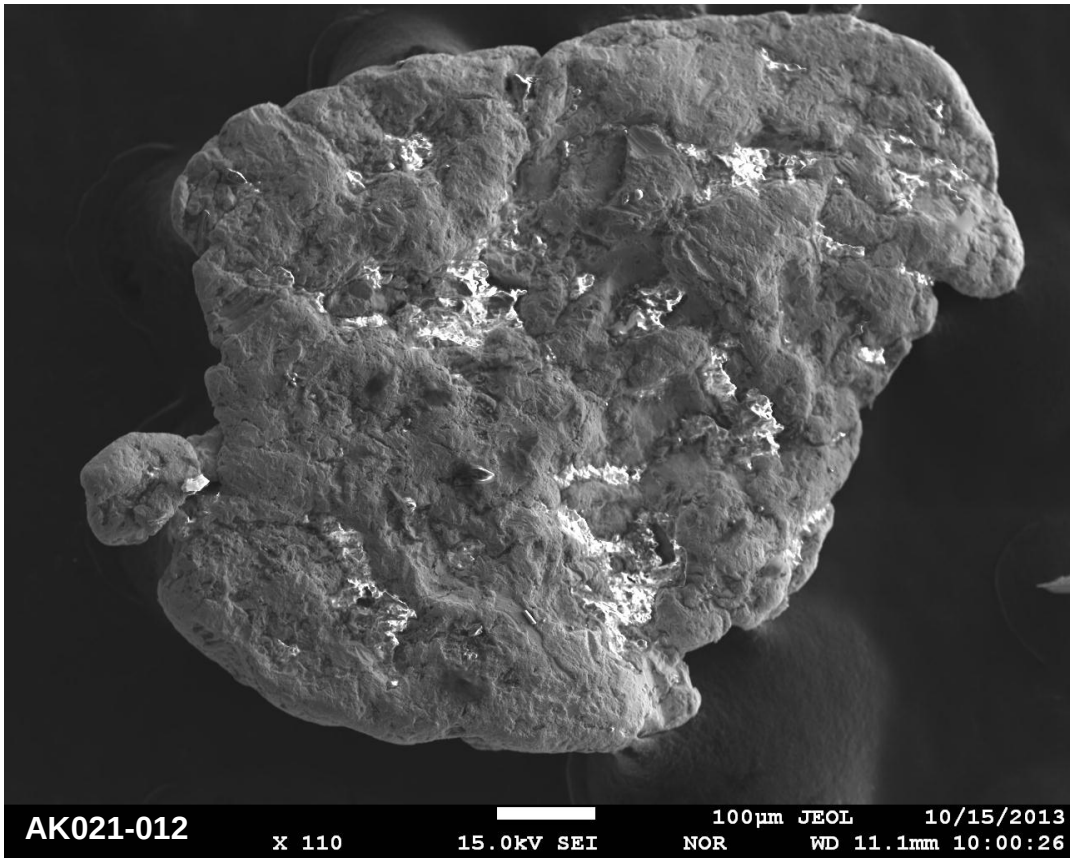
AK021-012
X 110
15.0kV SEI
100µm JEOL
NOR
10/15/2013
WD 11.1mm 10:00:26

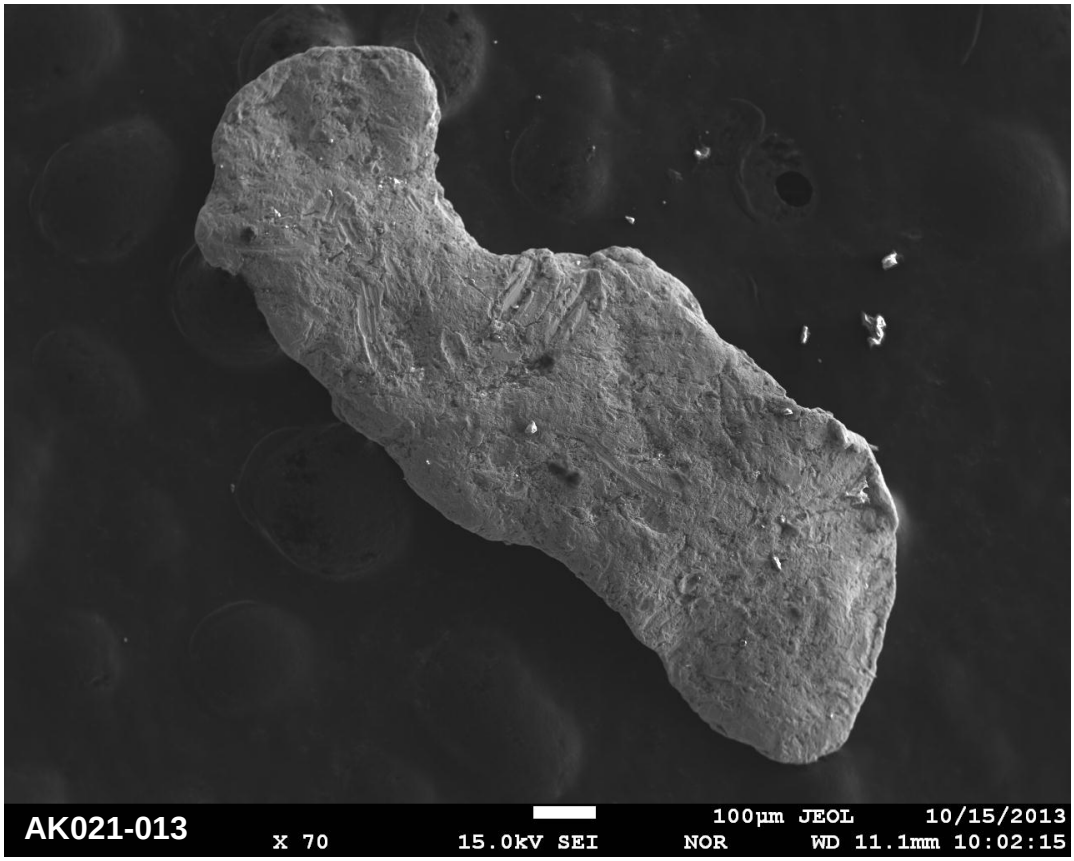
AK021-013
X 70
15.0kV SEI
100µm JEOL
NOR
10/15/2013
WD 11.1mm 10:02:15

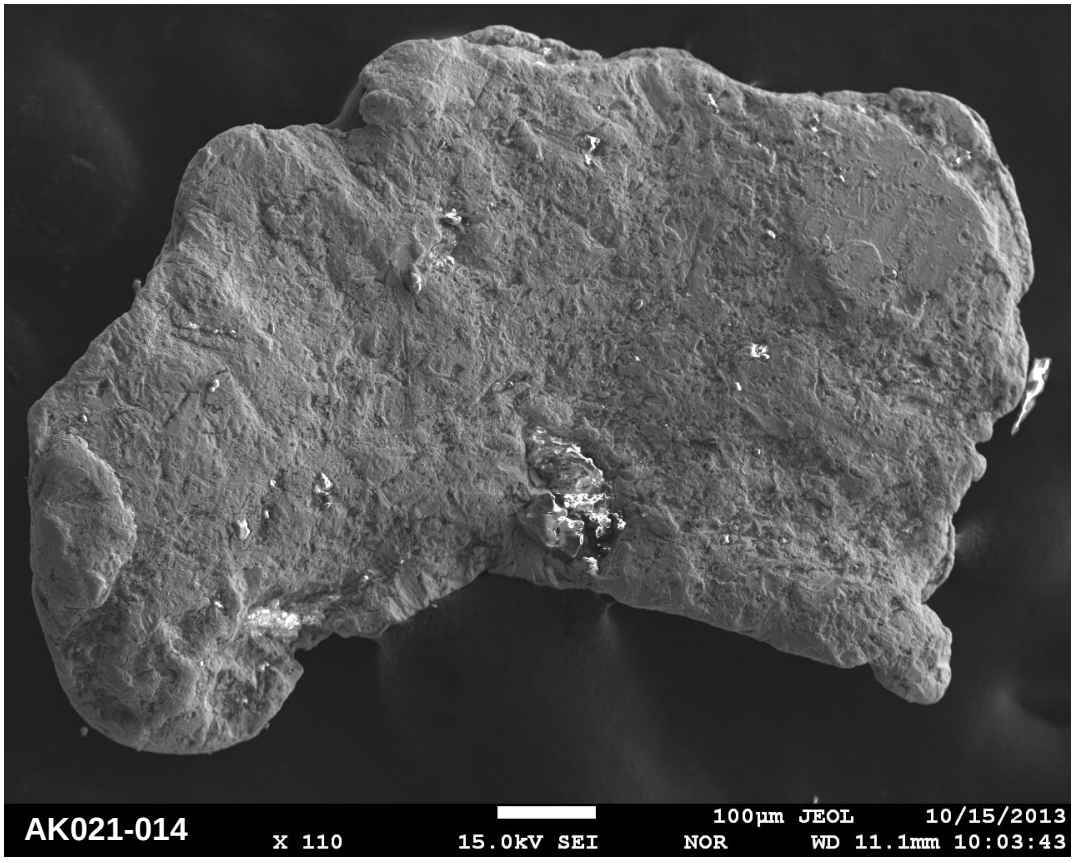
AK021-014
X 110
15.0kV SEI
100µm JEOL
NOR
10/15/2013
WD 11.1mm 10:03:43

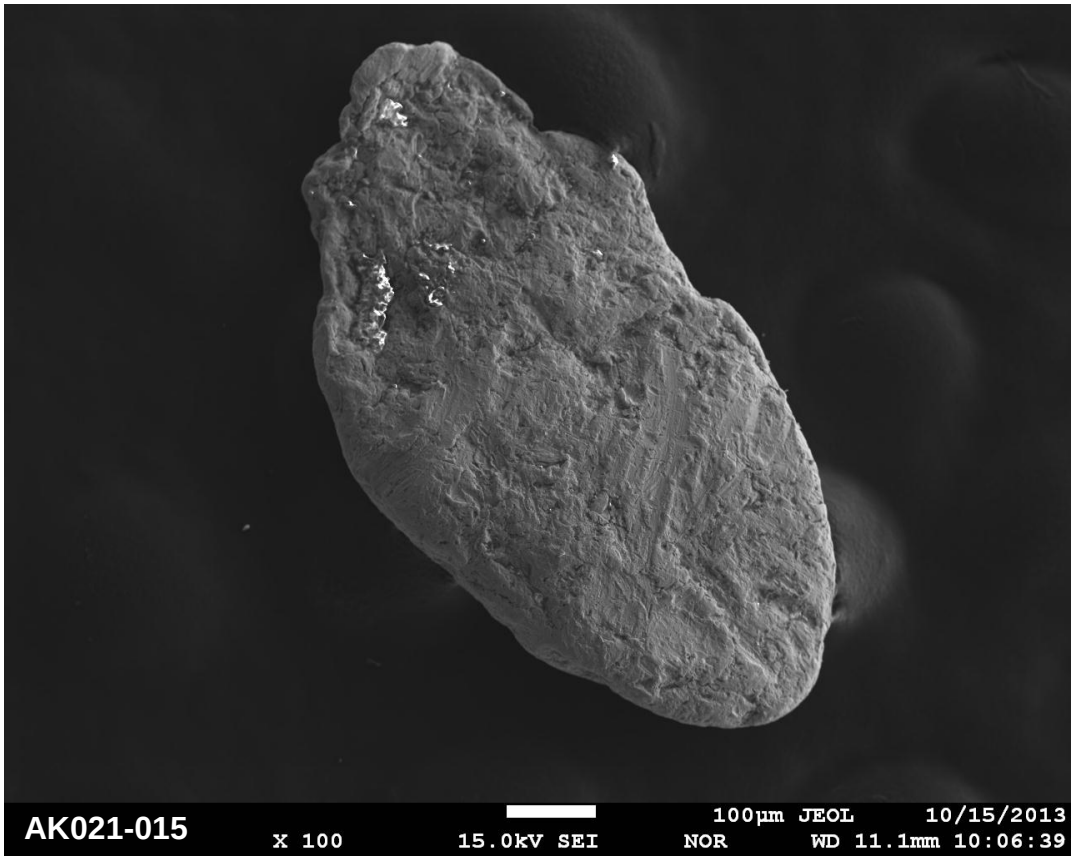
AK021-015
X 100
15.0kV SEI
100µm JEOL
NOR
10/15/2013
WD 11.1mm 10:06:39

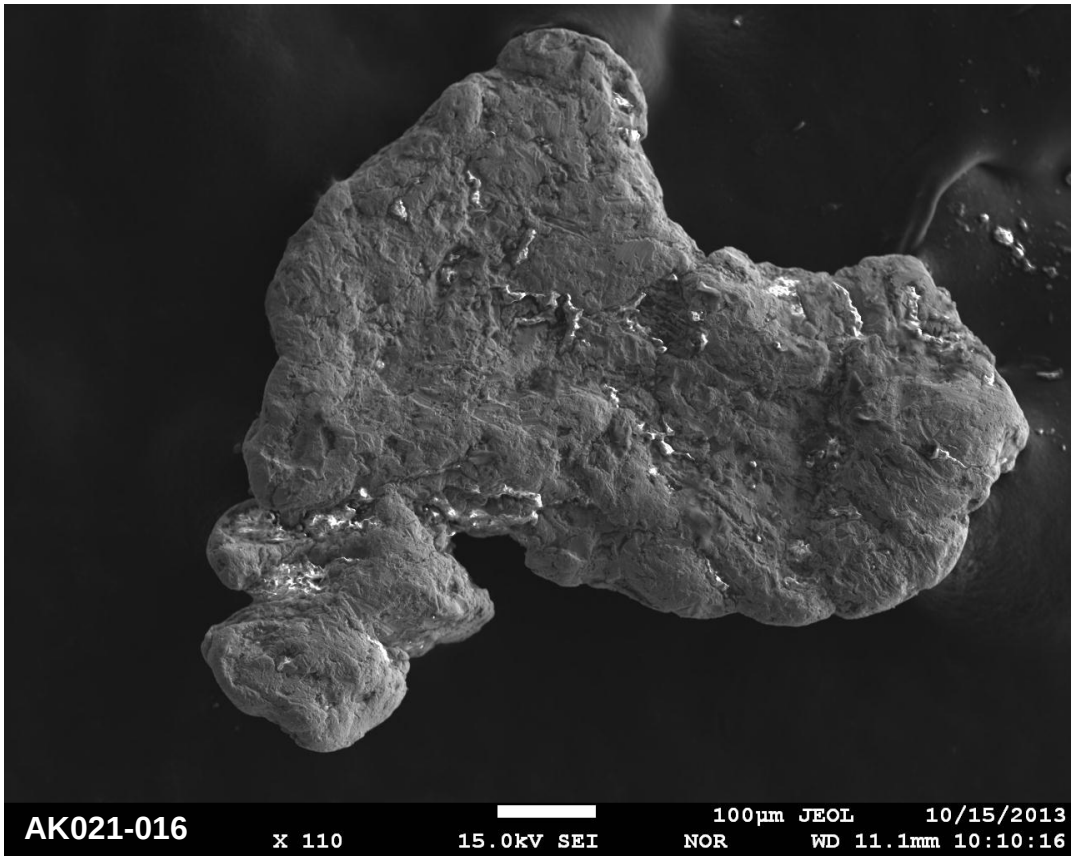
AK021-016
X 110
15.0kV SEI
100µm JEOL
NOR
10/15/2013
WD 11.1mm 10:10:16

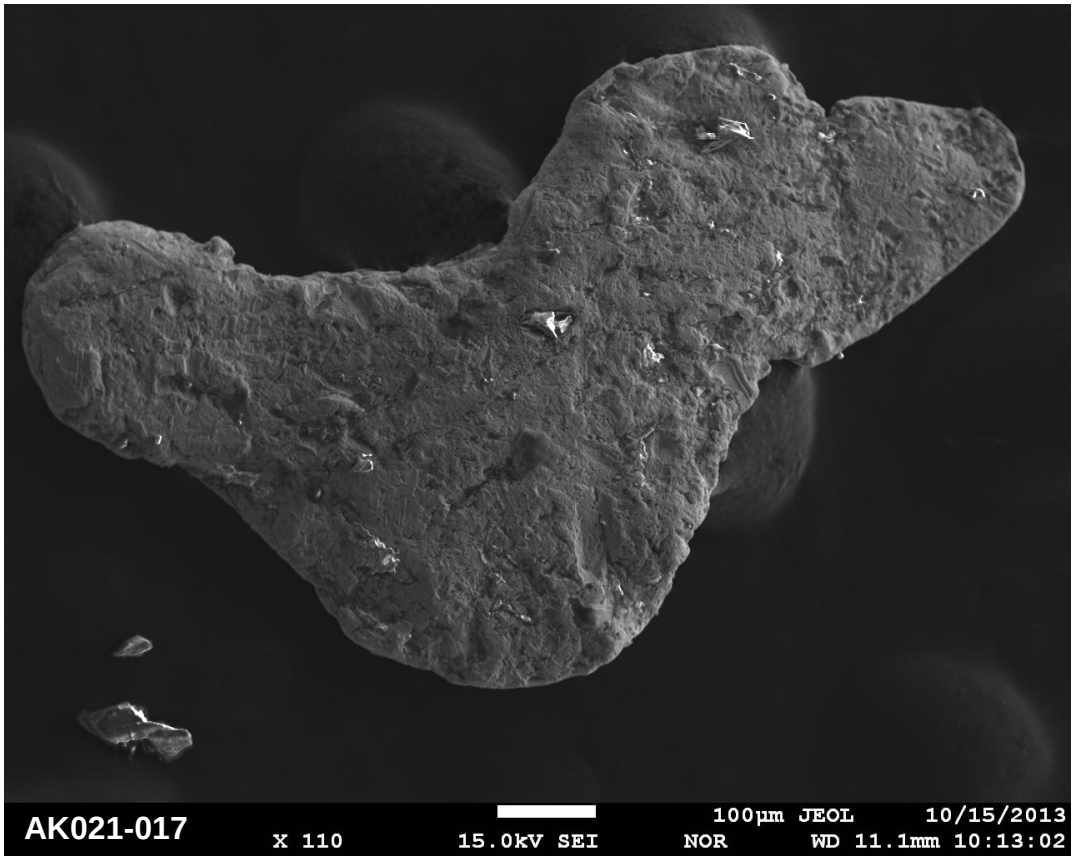
AK021-017
X 110
15.0kV SEI
100µm JEOL
NOR
10/15/2013
WD 11.1mm 10:13:02

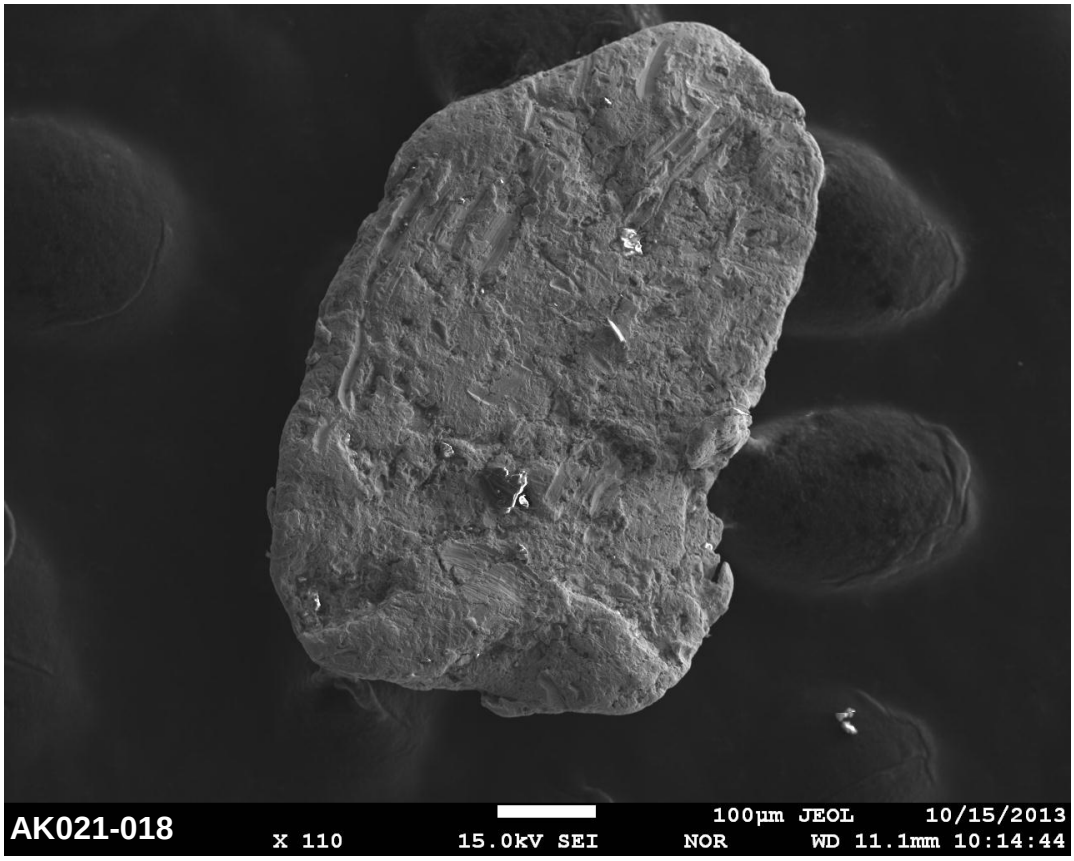
AK021-018
X 110
15.0kV SEI
100µm JEOL
NOR
10/15/2013
WD 11.1mm 10:14:44

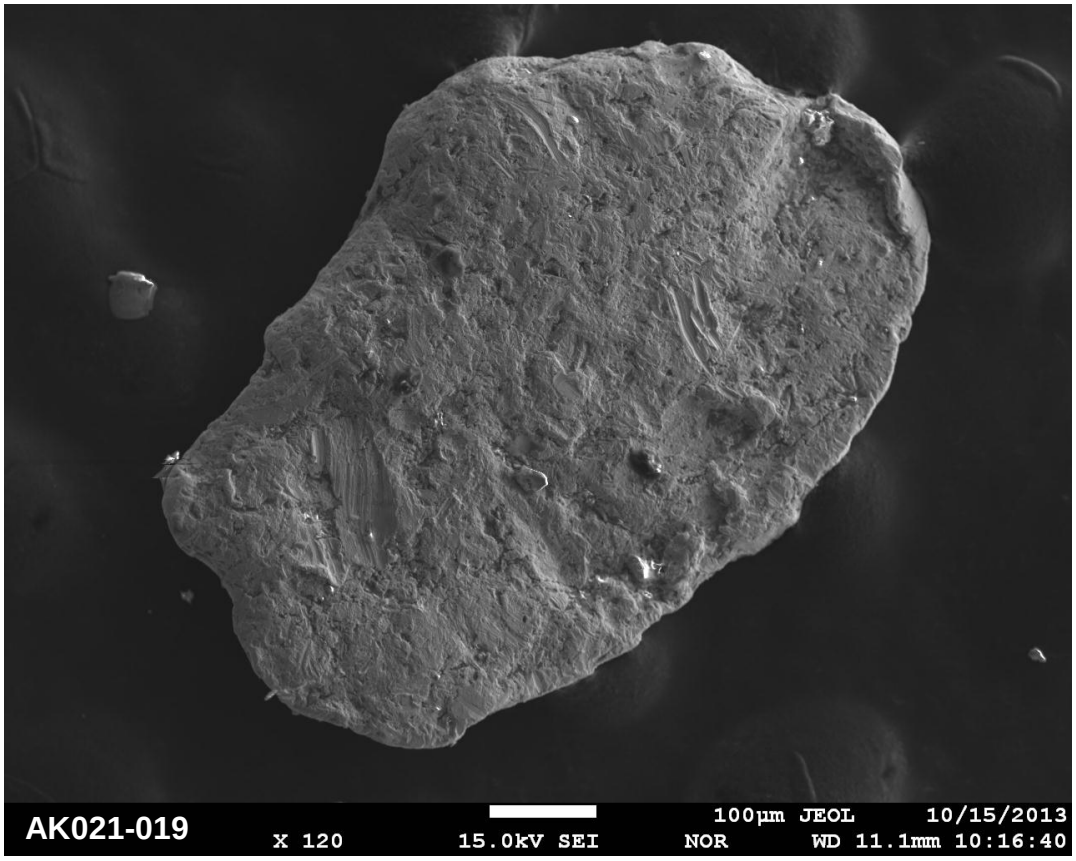
AK021-019
X 120
15.0kV SEI
100µm JEOL
NOR
10/15/2013
WD 11.1mm 10:16:40

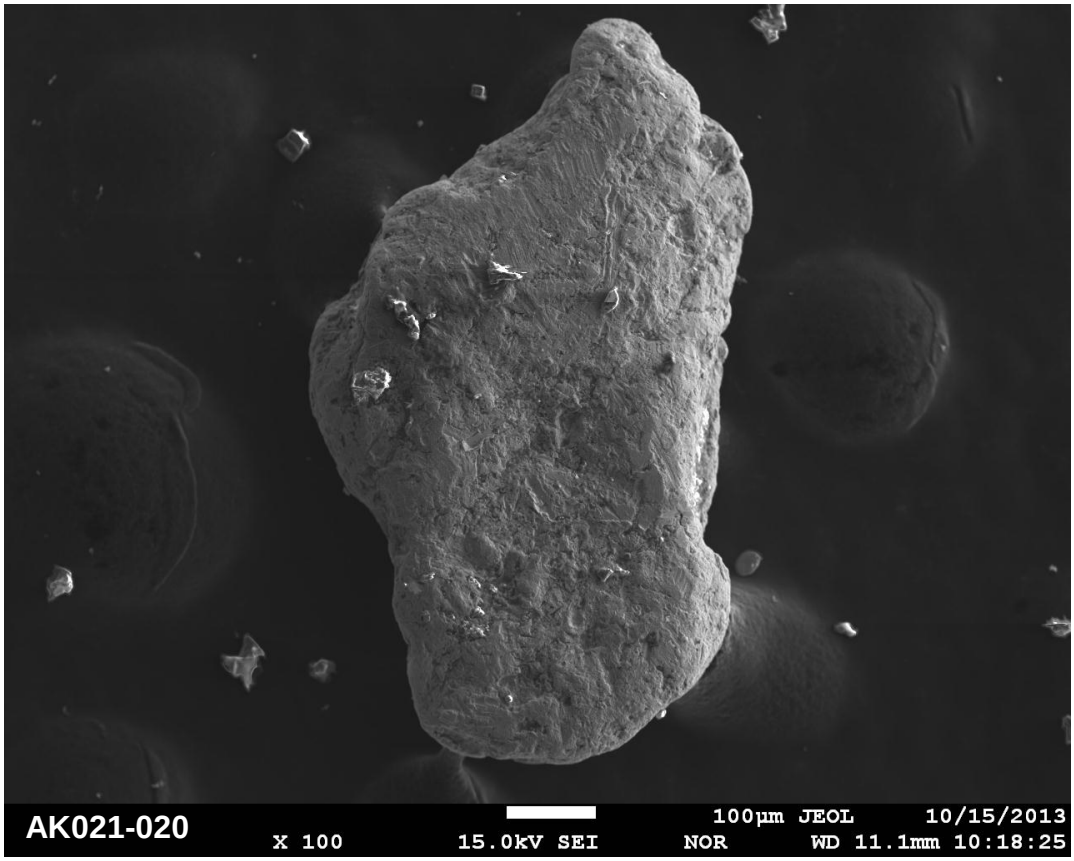
AK021-020
X 100
15.0kV SEI
100µm JEOL
NOR
10/15/2013
WD 11.1mm 10:18:25

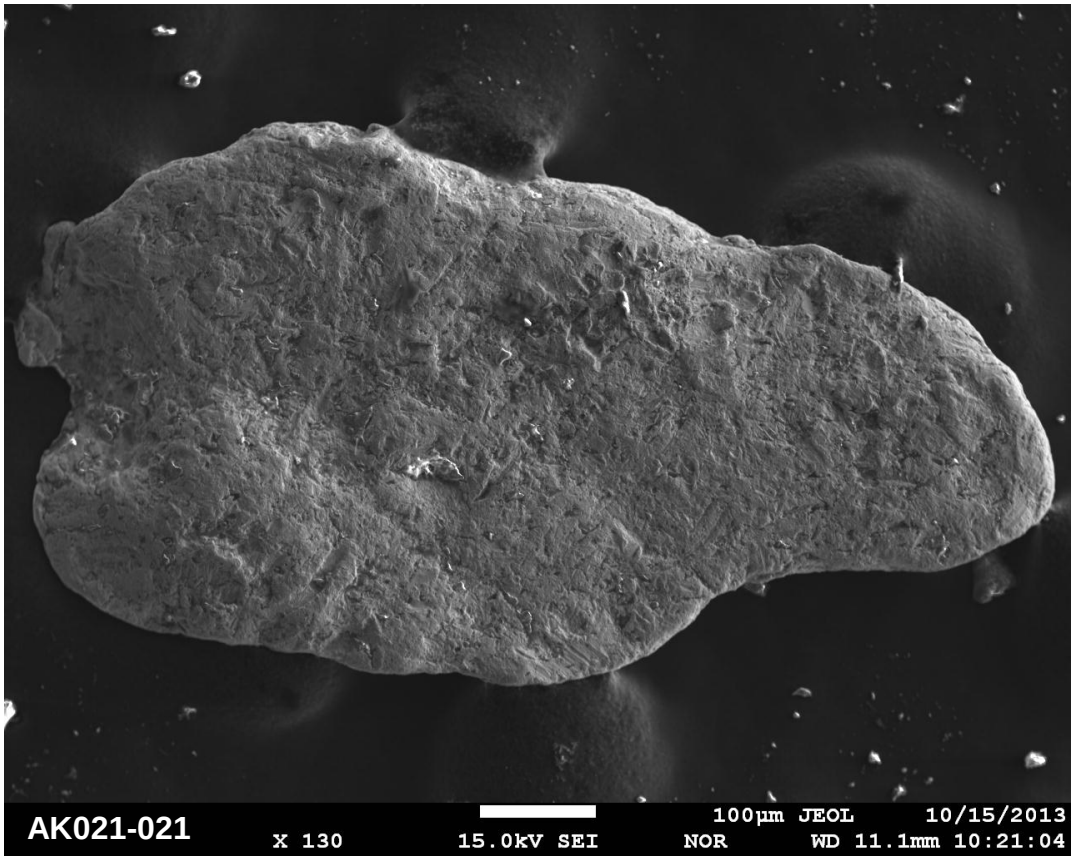
AK021-021
X 130
15.0kV SEI
100µm JEOL
NOR
10/15/2013
WD 11.1mm 10:21:04

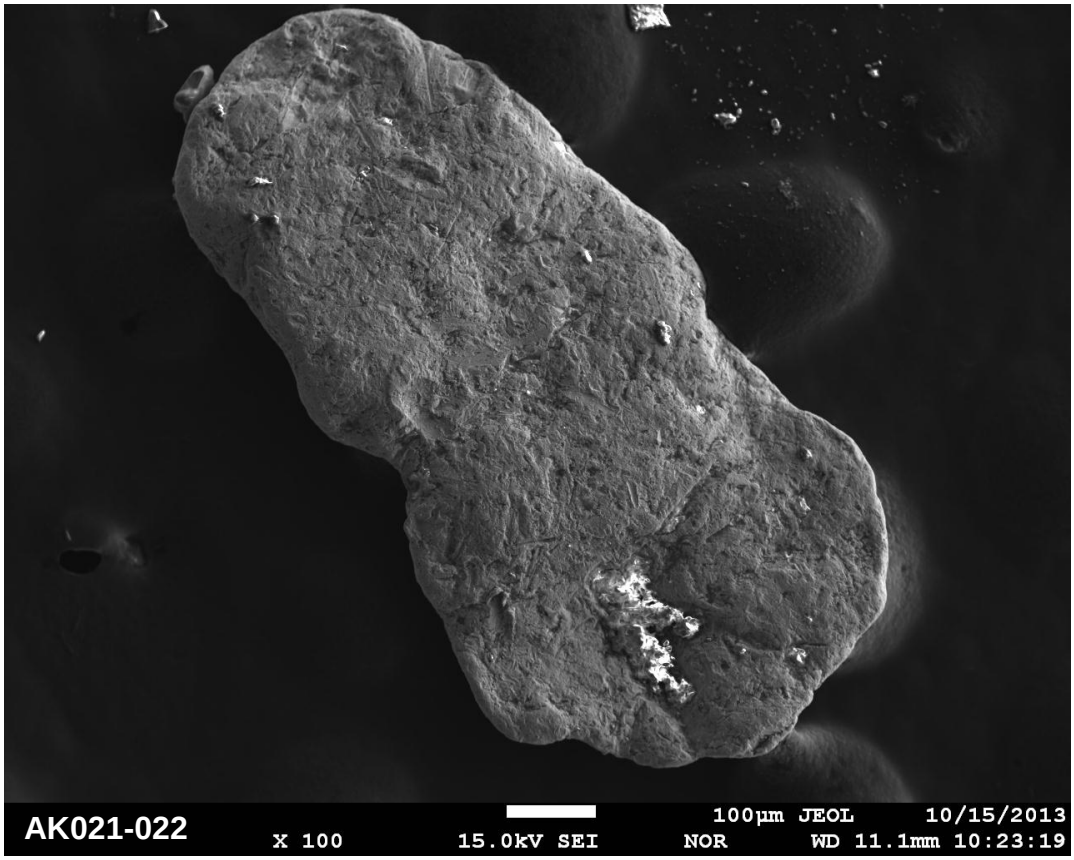
AK021-022
X 100
15.0kV SEI
100µm JEOL
NOR
10/15/2013
WD 11.1mm 10:23:19

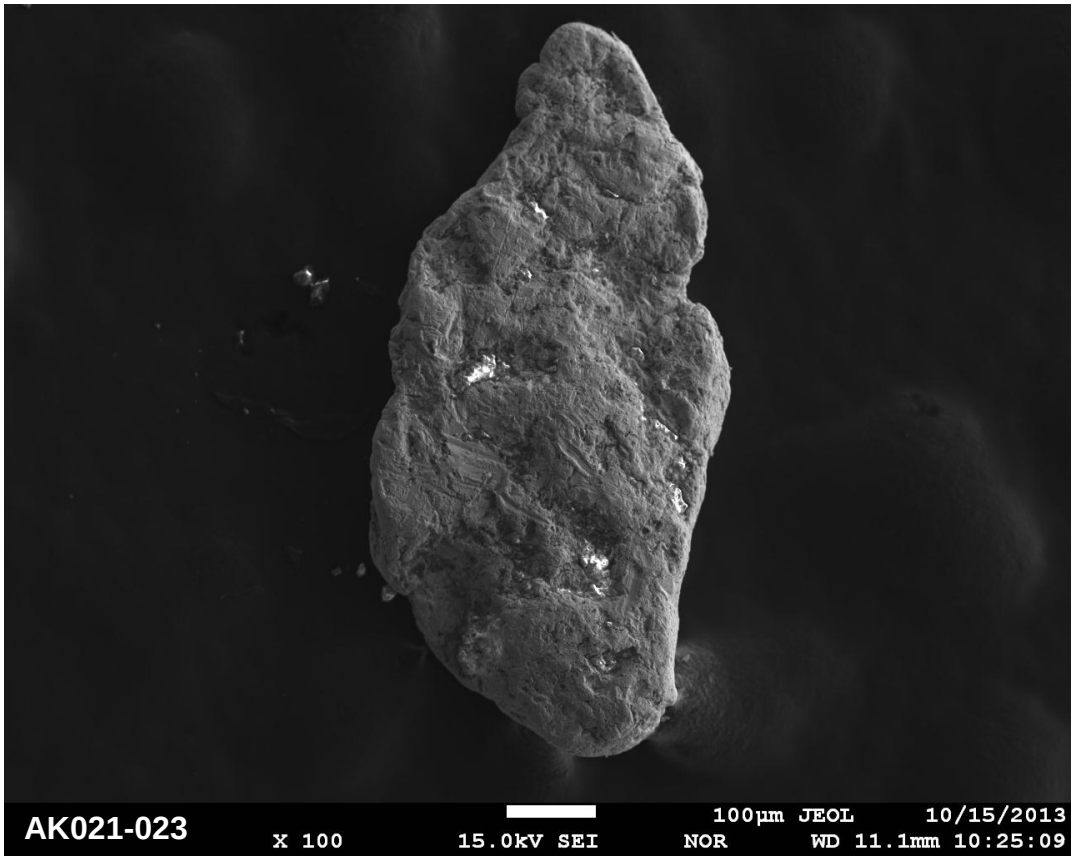
AK021-023
X 100
15.0kV SEI
100µm JEOL
NOR
10/15/2013
WD 11.1mm 10:25:09

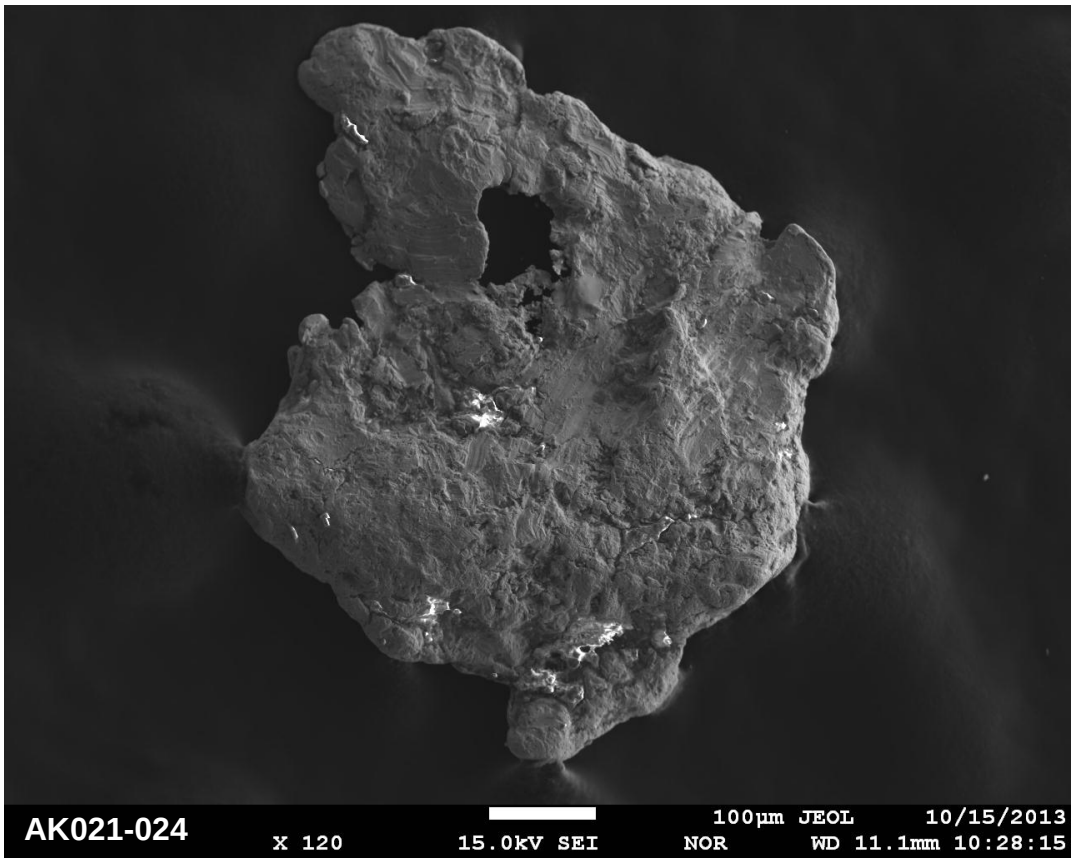
AK021-024
X 120
15.0kV SEI
100µm JEOL
NOR
10/15/2013
WD 11.1mm 10:28:15

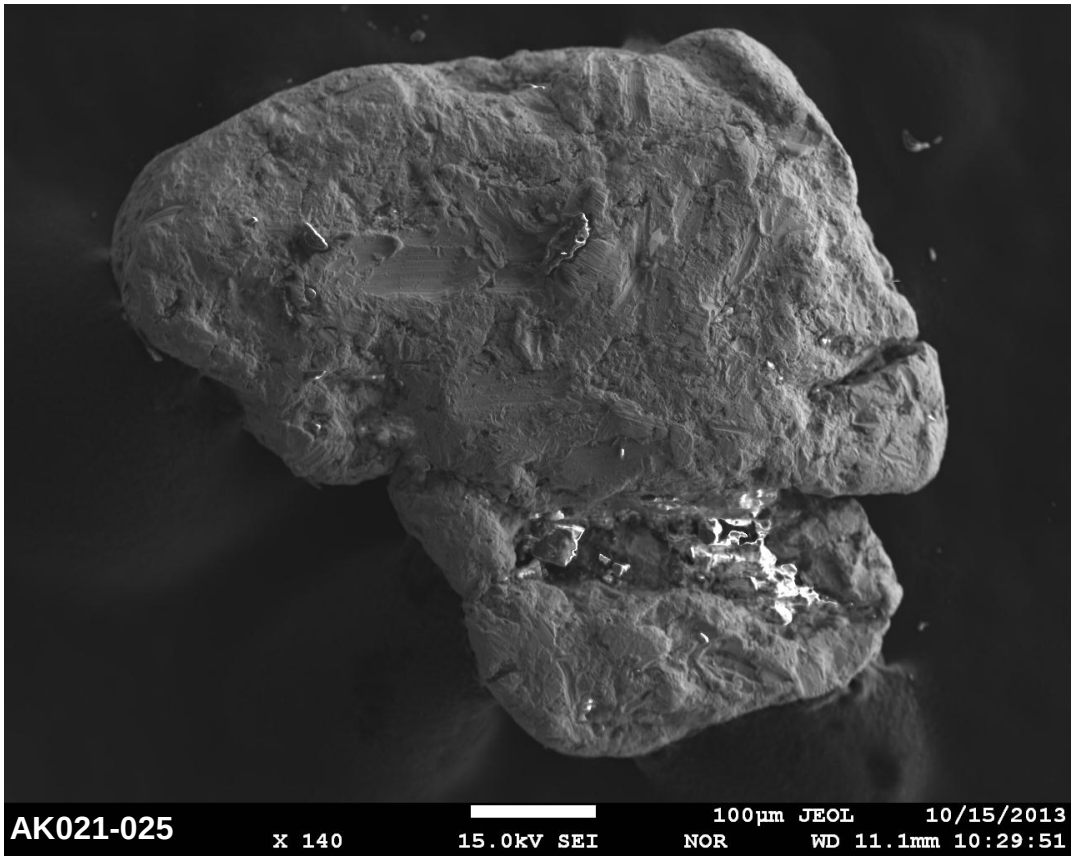
AK021-025
X 140
15.0kV SEI
100µm JEOL
NOR
10/15/2013
WD 11.1mm 10:29:51

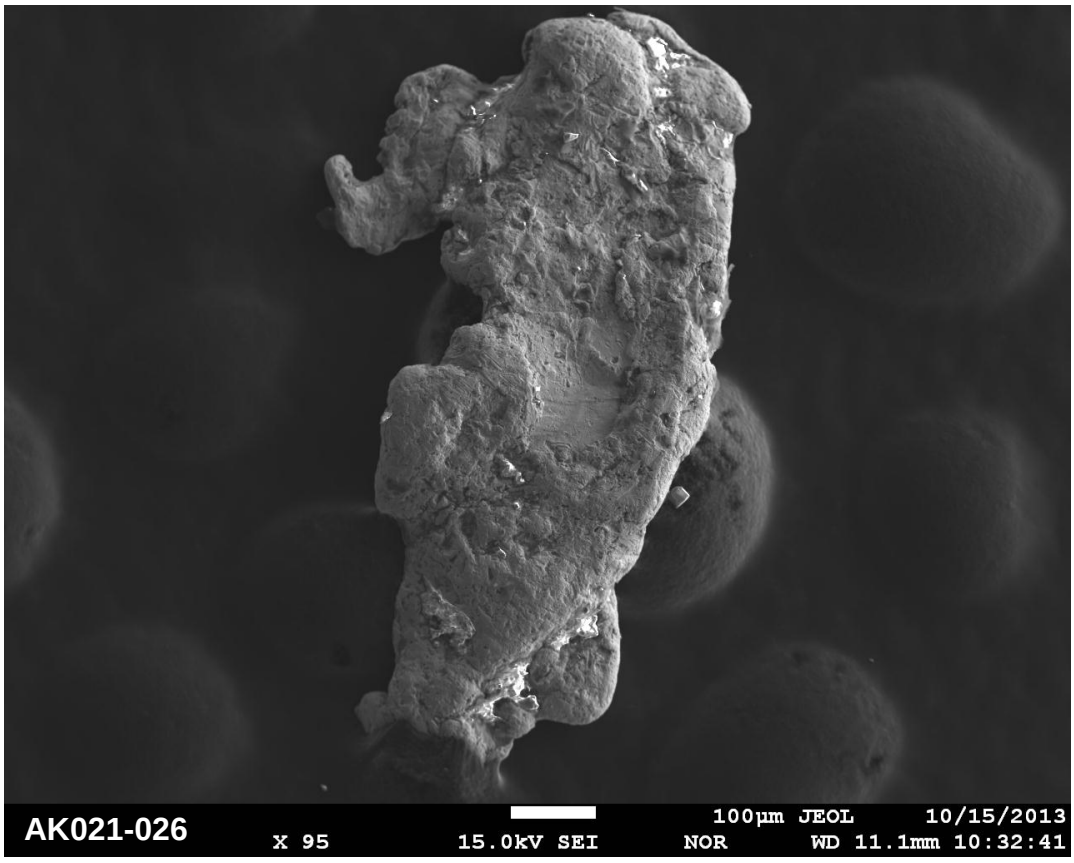
AK021-026
X 95
15.0kV SEI
100µm JEOL
NOR
10/15/2013
WD 11.1mm 10:32:41

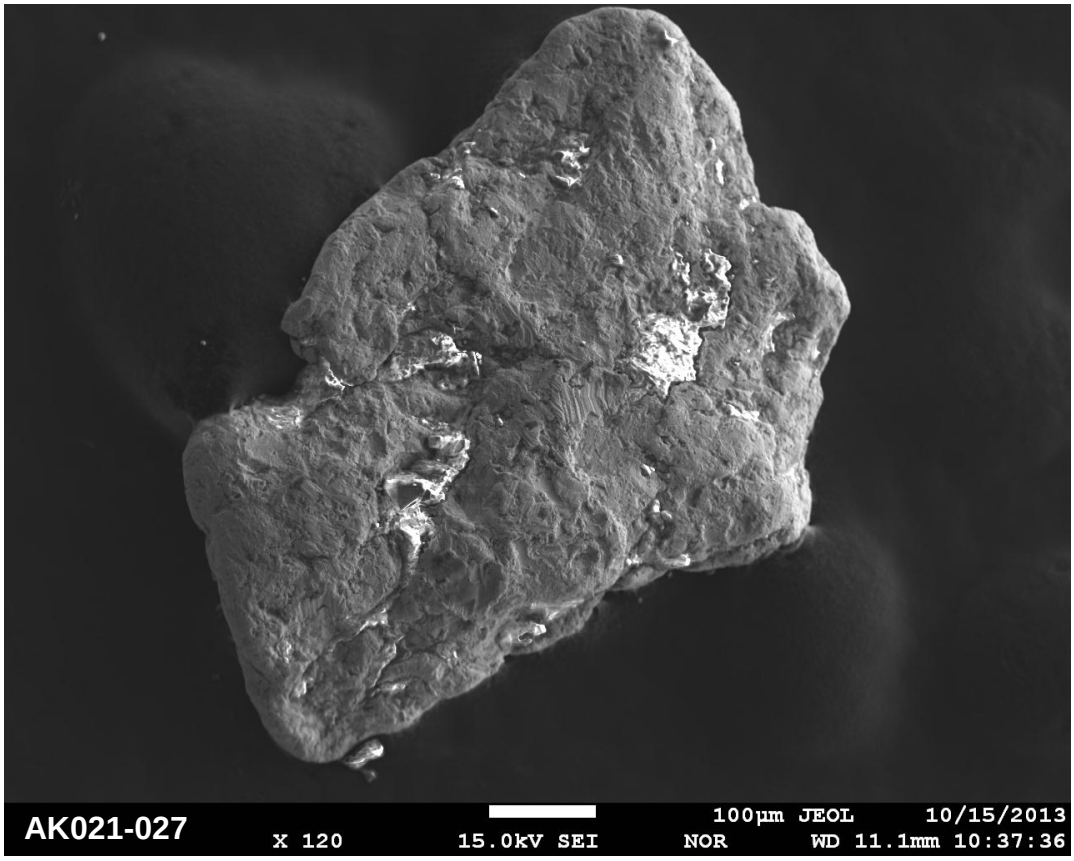
AK021-027
X 120
15.0kV SEI
100µm JEOL
NOR
10/15/2013
WD 11.1mm 10:37:36

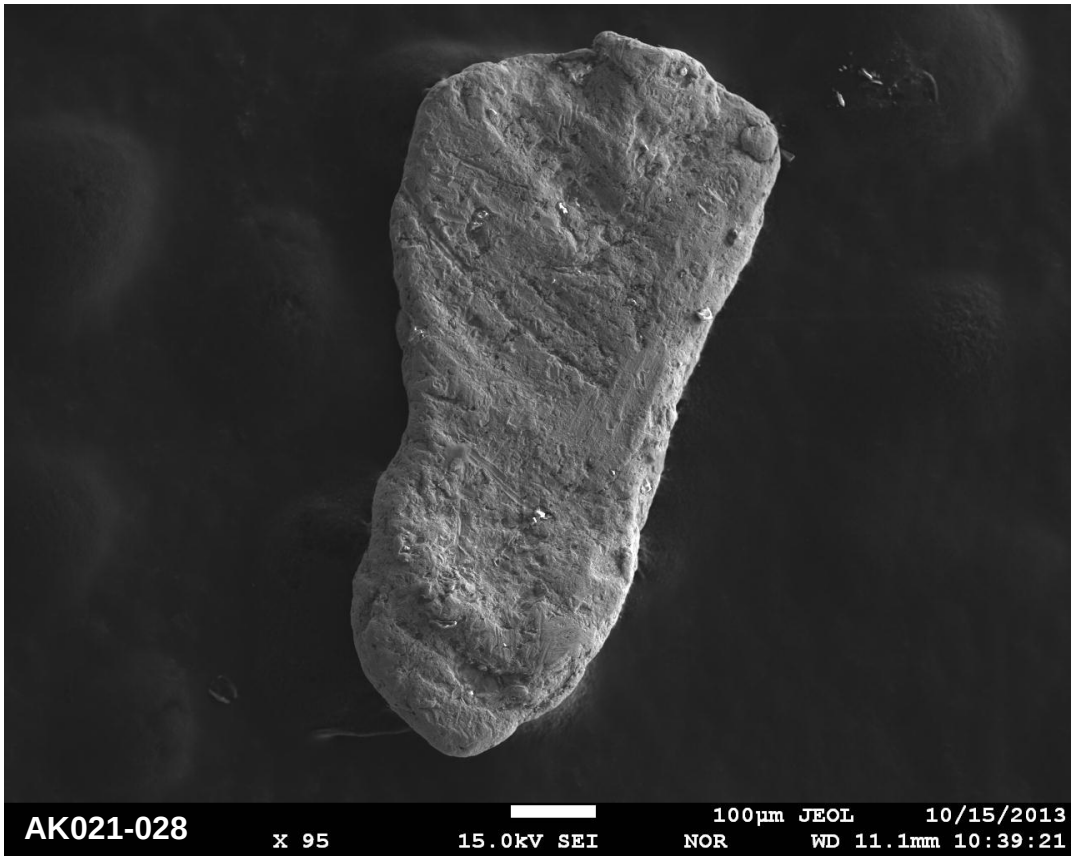
AK021-028
X 95
15.0kV SEI
100µm JEOL
NOR
10/15/2013
WD 11.1mm 10:39:21

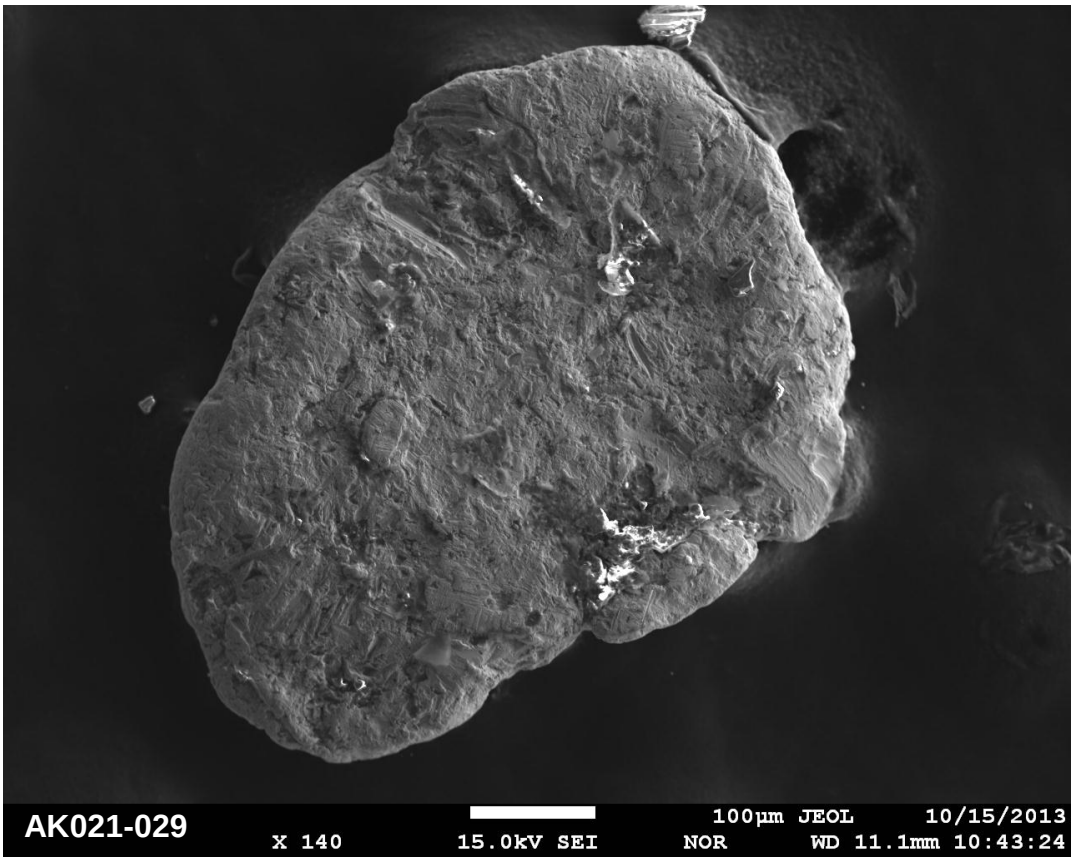
AK021-029
X 140
15.0kV SEI
100µm JEOL
NOR
10/15/2013
WD 11.1mm 10:43:24

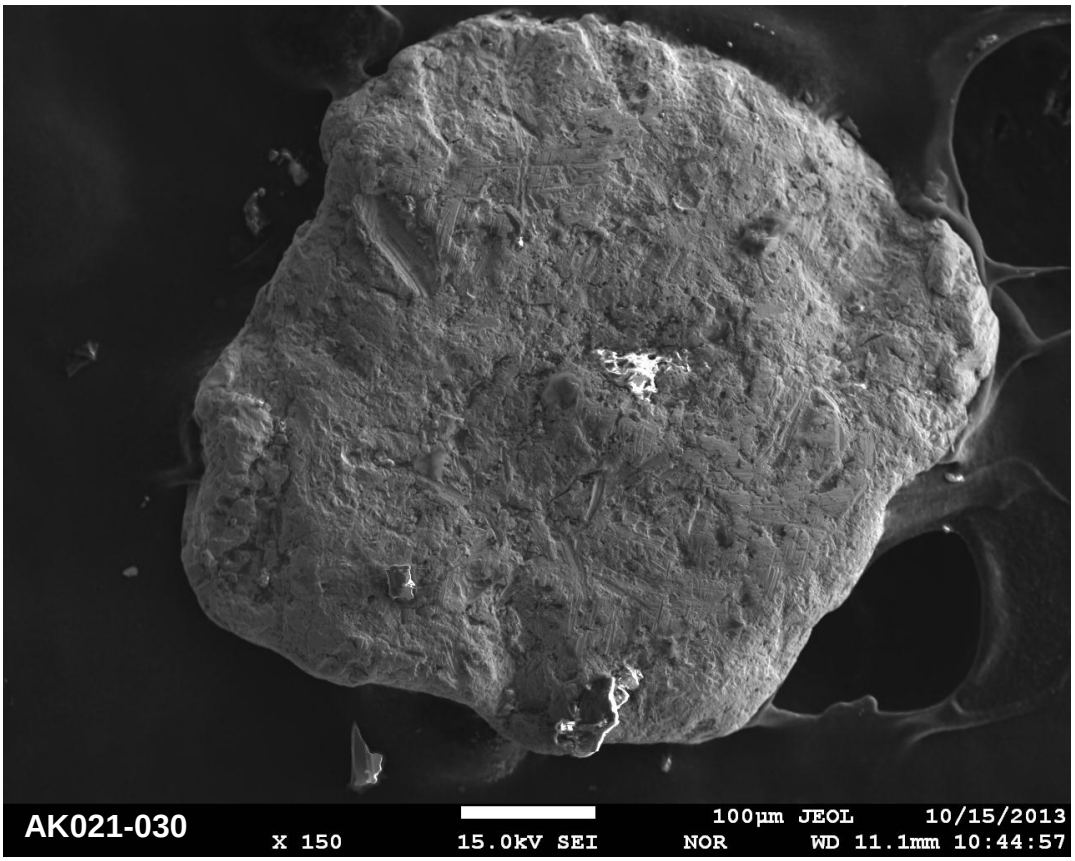
AK021-030
X 150
15.0kV SEI
100µm JEOL
NOR
10/15/2013
WD 11.1mm 10:44:57

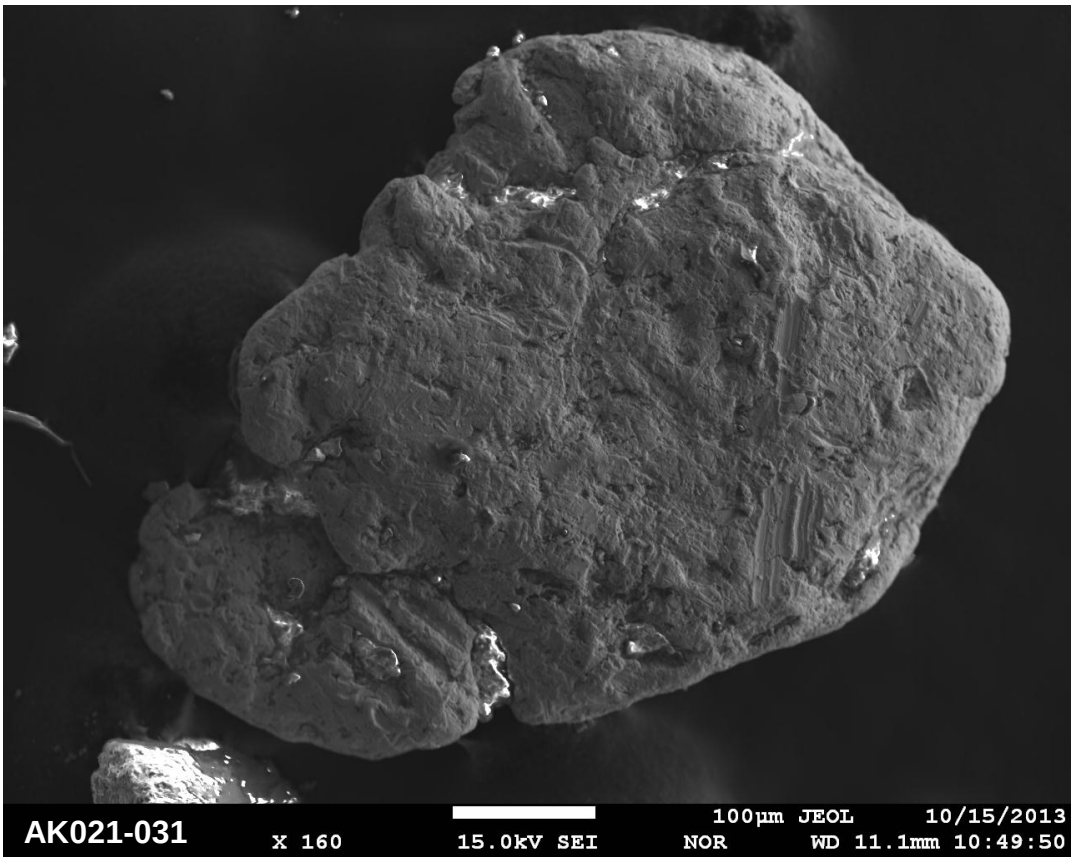
AK021-031
X 160
15.0kV SEI
100µm JEOL
NOR
10/15/2013
WD 11.1mm 10:49:50

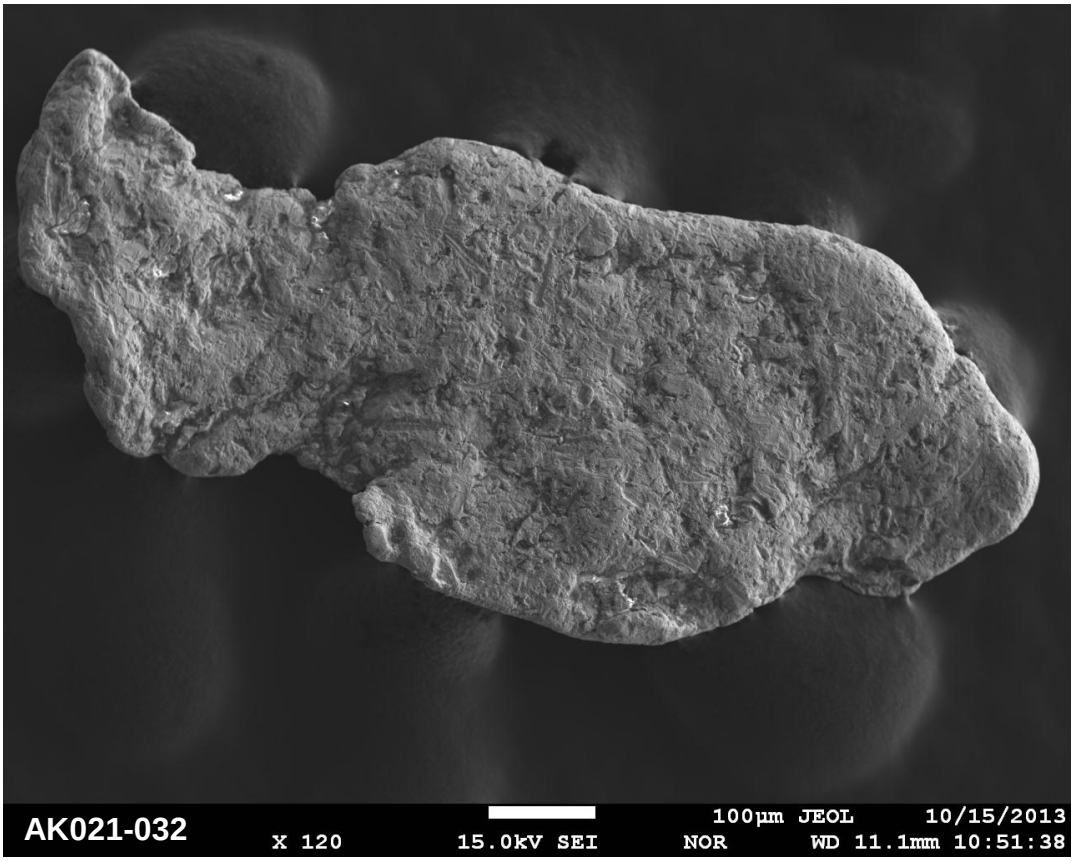
AK021-032
X 120
15.0kV SEI
100µm JEOL
NOR
10/15/2013
WD 11.1mm 10:51:38

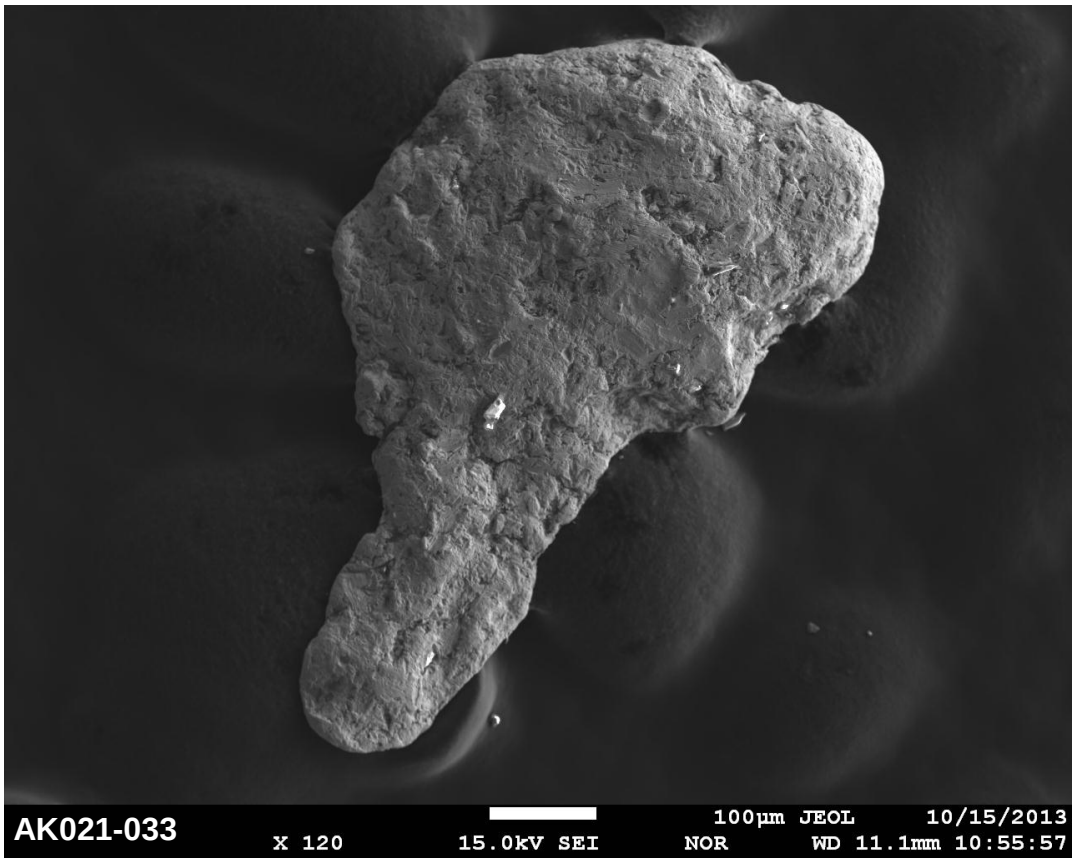
AK021-033
X 120
15.0kV SEI
100µm JEOL
NOR
10/15/2013
WD 11.1mm 10:55:57

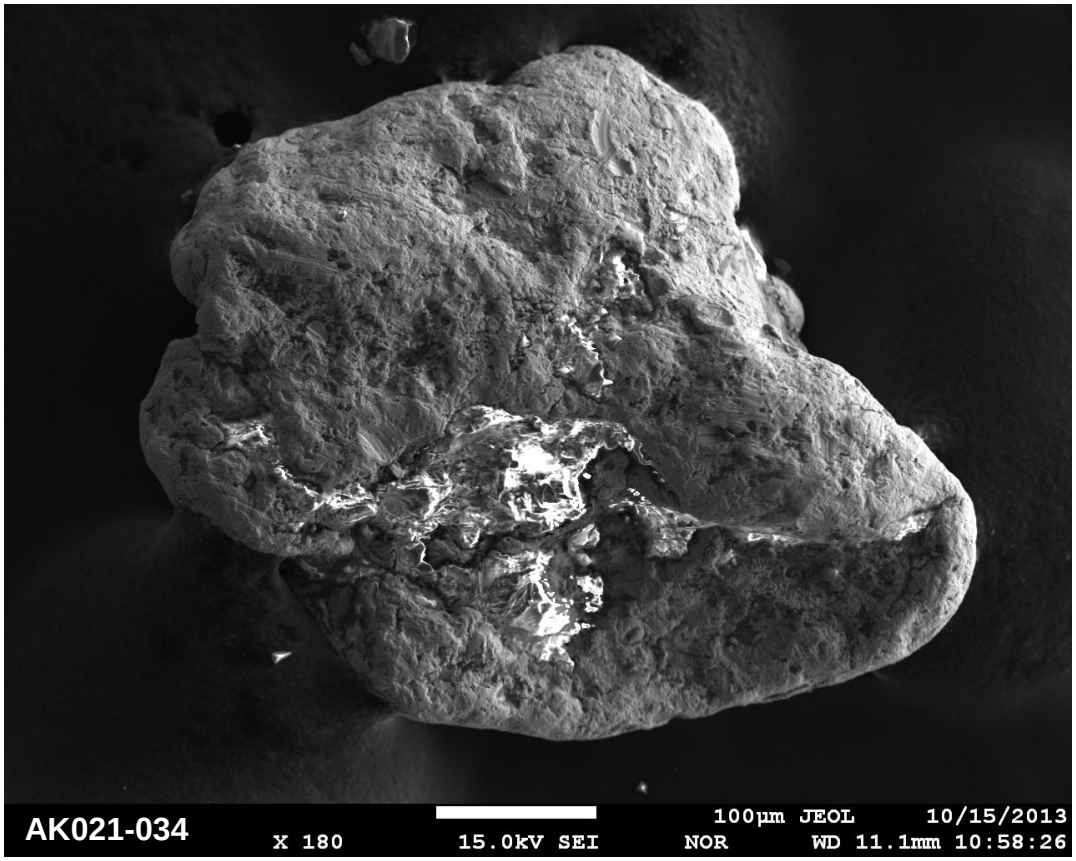
AK021-034
X 180
15.0kV SEI
100µm JEOL
NOR
10/15/2013
WD 11.1mm 10:58:26

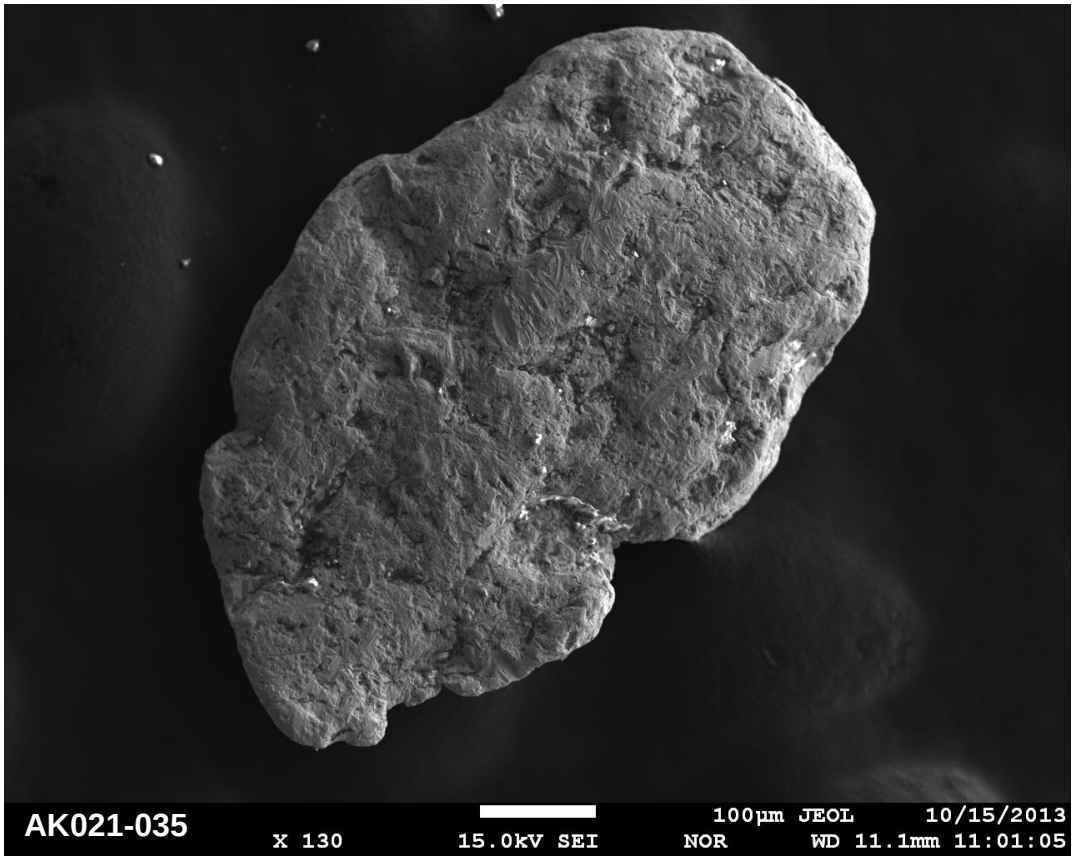
AK021-035
X 130
15.0kV SEI
100µm JEOL
NOR
10/15/2013
WD 11.1mm 11:01:05

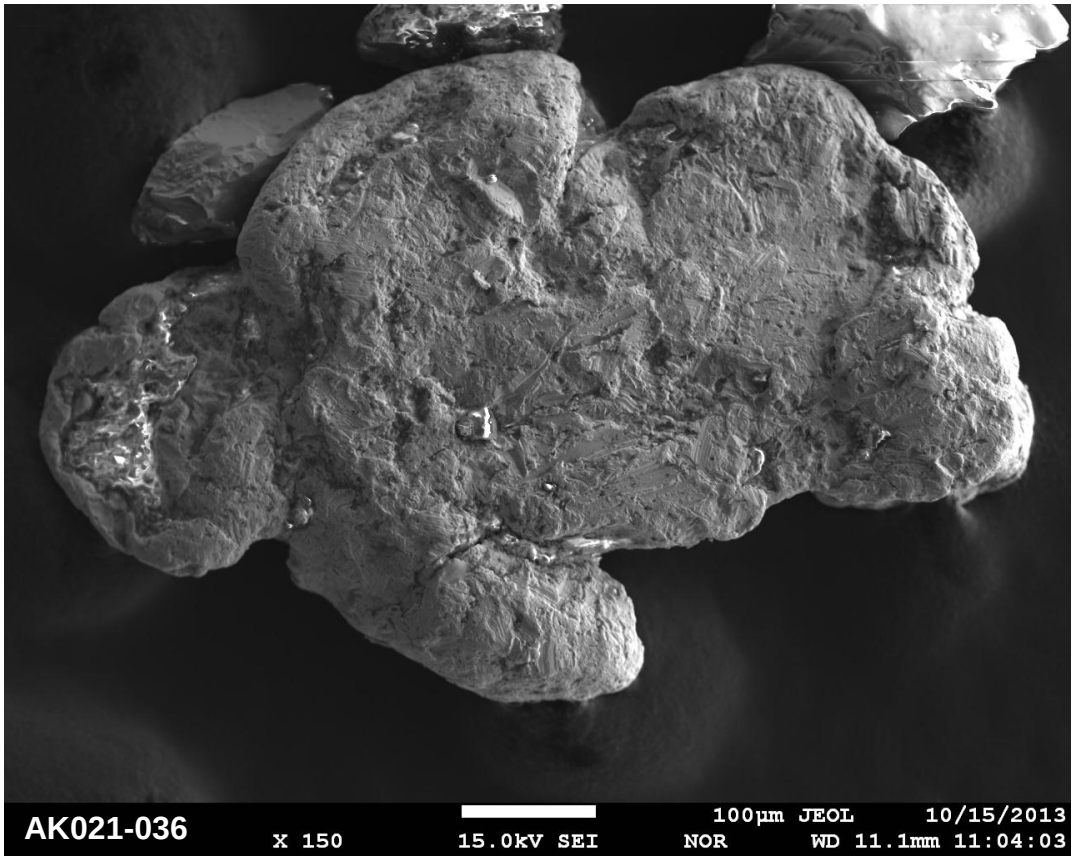
AK021-036
X 150
15.0kV SEI
100µm JEOL
NOR
10/15/2013
WD 11.1mm 11:04:03

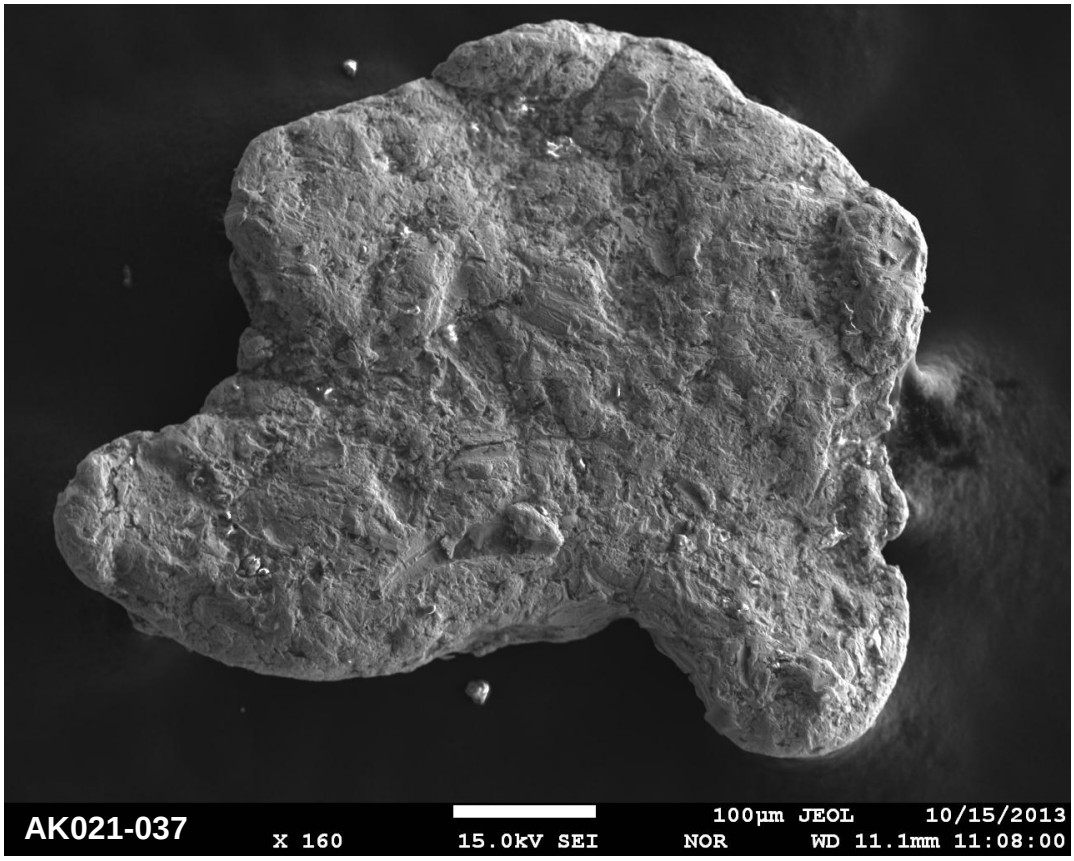
AK021-037
X 160
15.0kV SEI
100µm JEOL
NOR
10/15/2013
WD 11.1mm 11:08:00

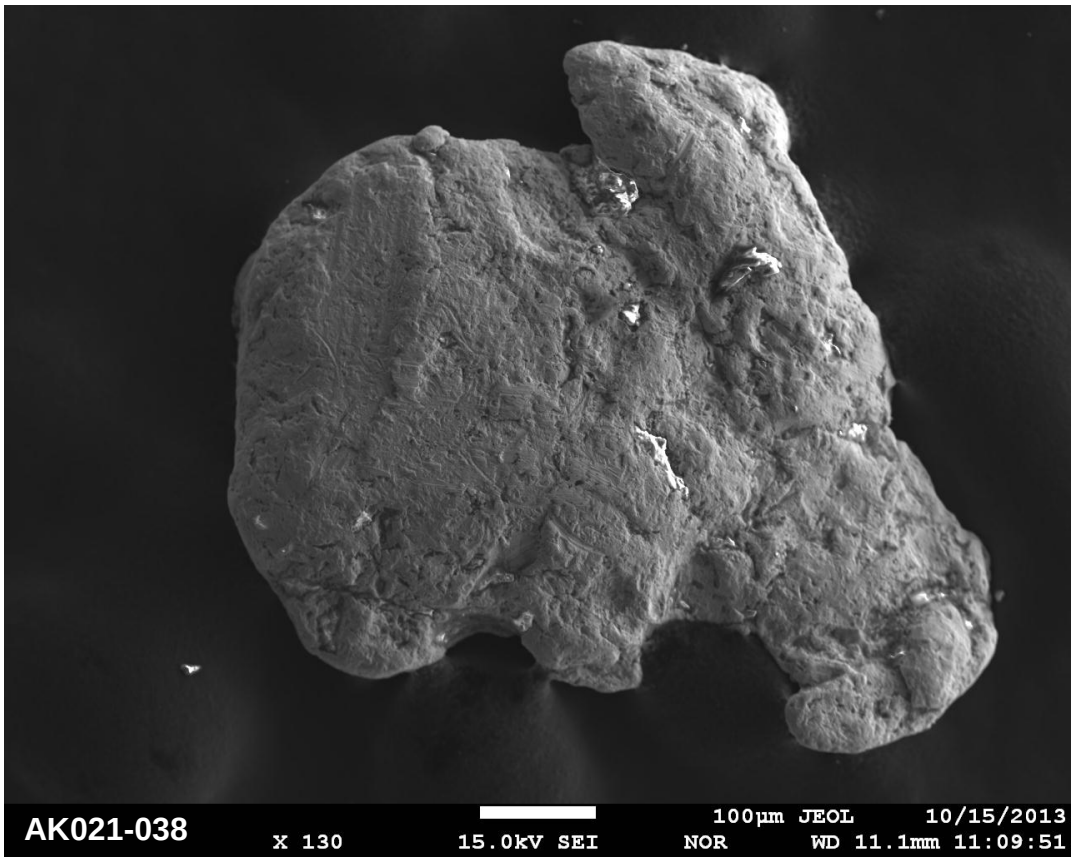
AK021-038
X 130
15.0kV SEI
100µm JEOL
NOR
10/15/2013
WD 11.1mm 11:09:51

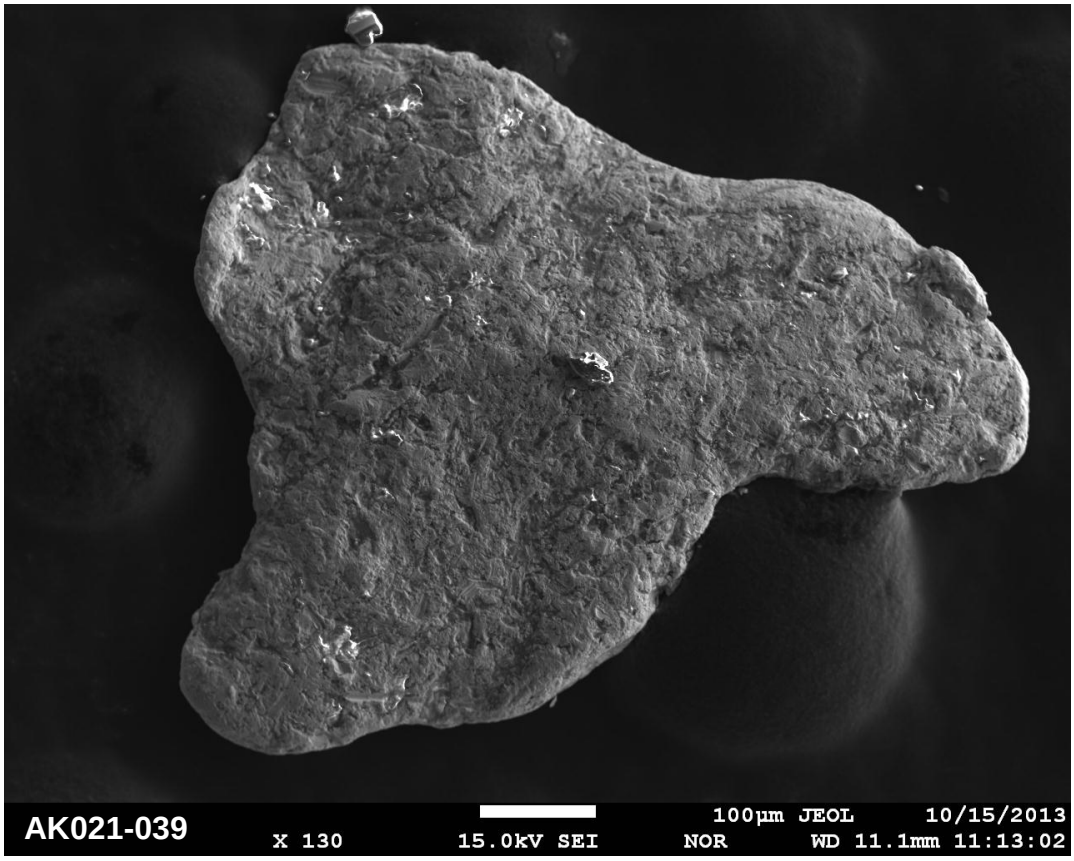
AK021-039
X 130
15.0kV SEI
100µm JEOL
NOR
10/15/2013
WD 11.1mm 11:13:02

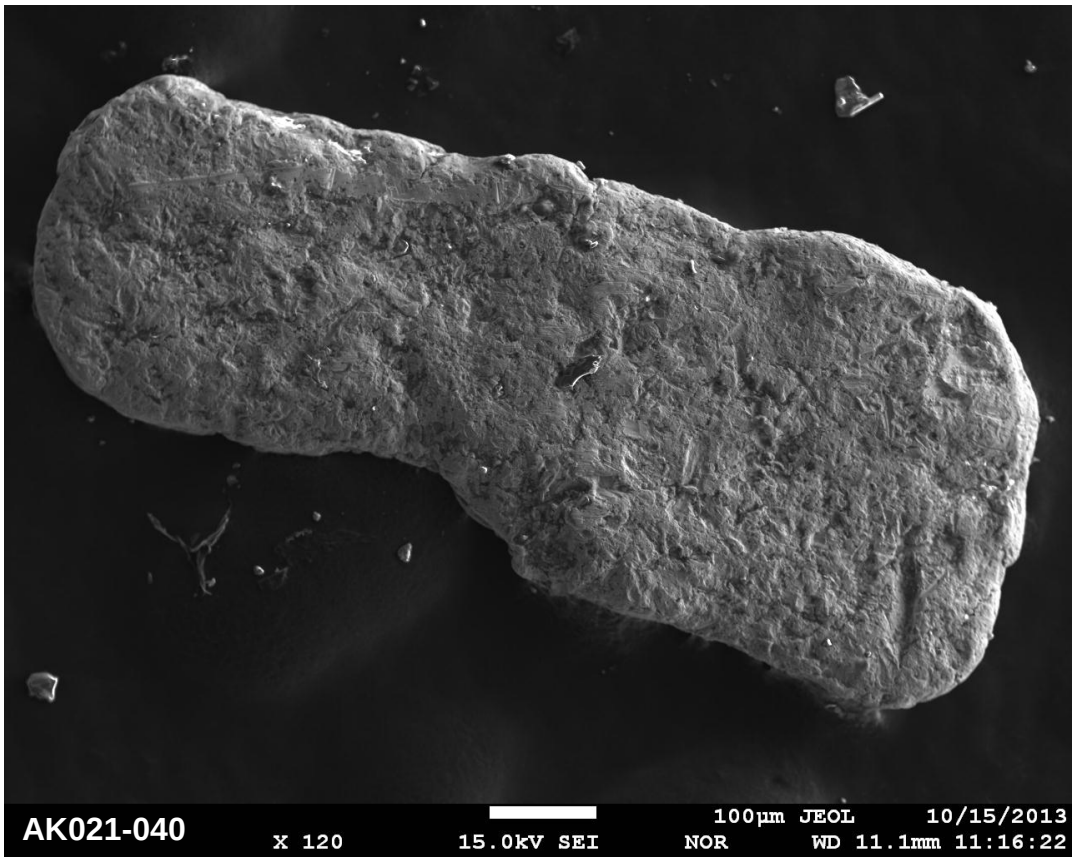
AK021-040
X 120
15.0kV SEI
100µm JEOL
NOR
10/15/2013
WD 11.1mm 11:16:22

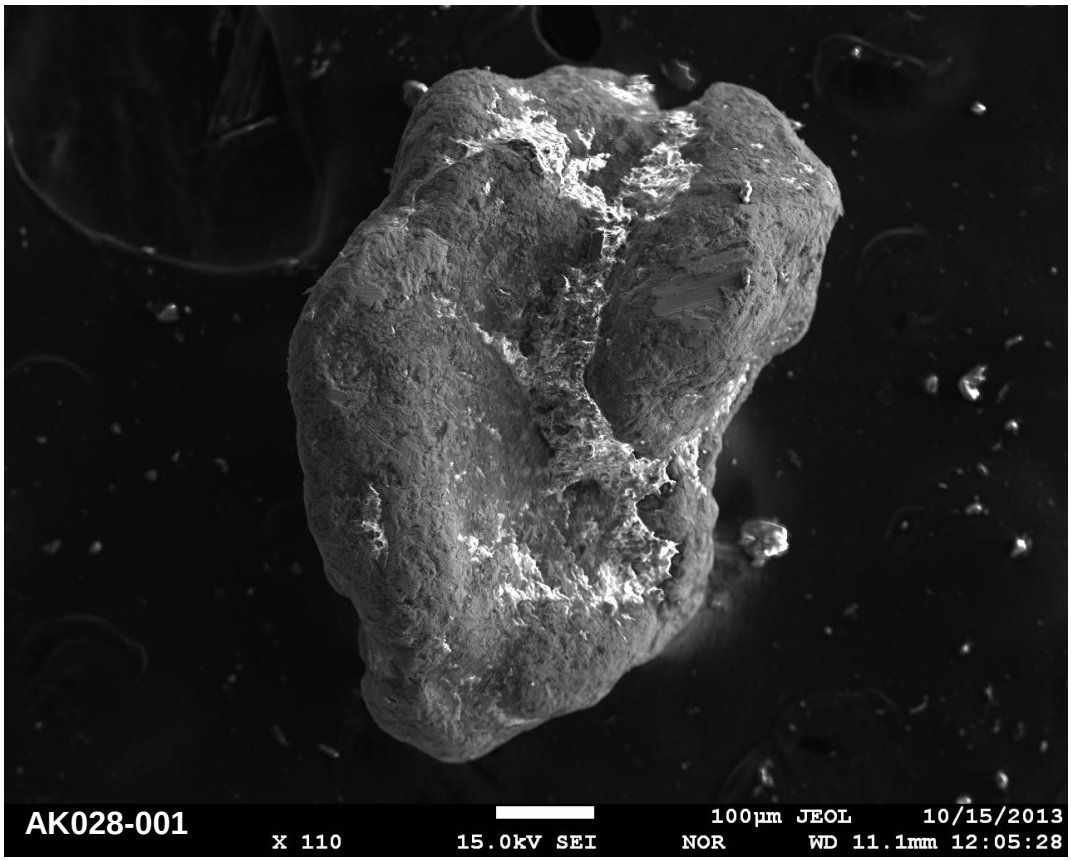
AK028-001
X 110
15.0kV SEI
100µm JEOL
NOR
10/15/2013
WD 11.1mm 12:05:28

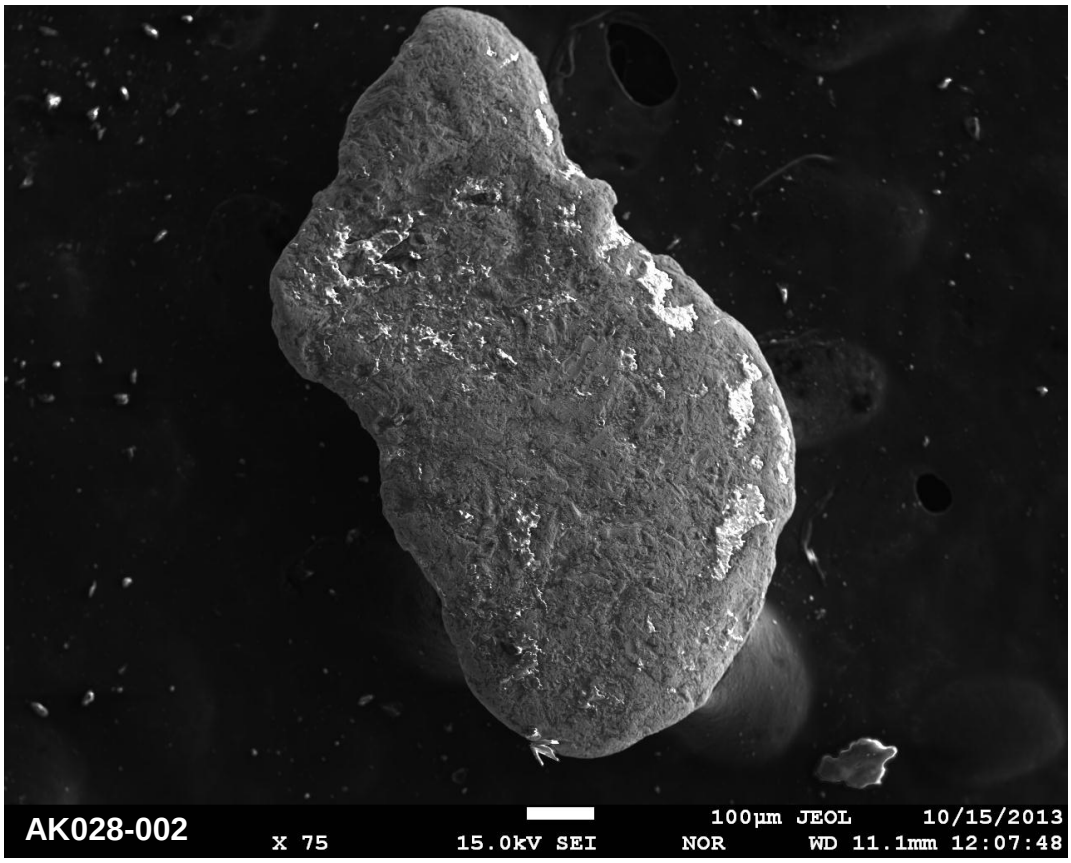
AK028-002
X 75
15.0kV SEI
100µm JEOL
NOR
10/15/2013
WD 11.1mm 12:07:48

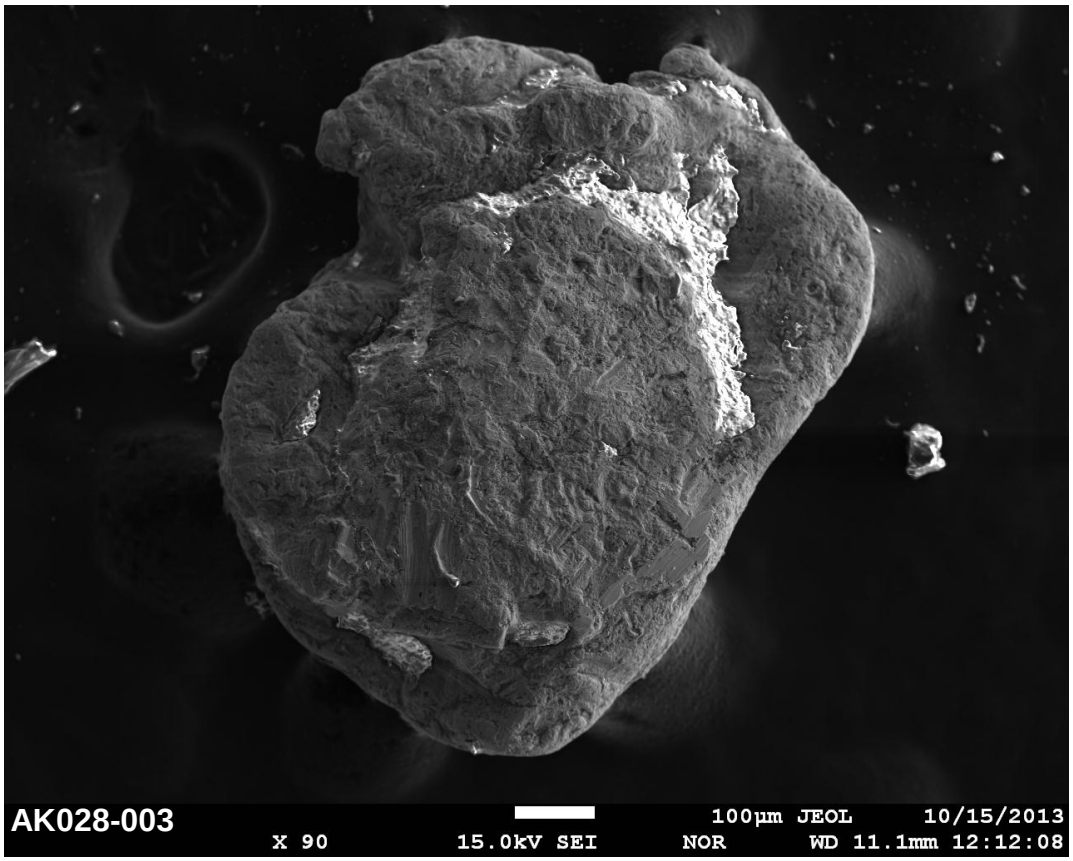
AK028-003
X 90
15.0kV SEI
100µm JEOL
NOR
10/15/2013
WD 11.1mm 12:12:08

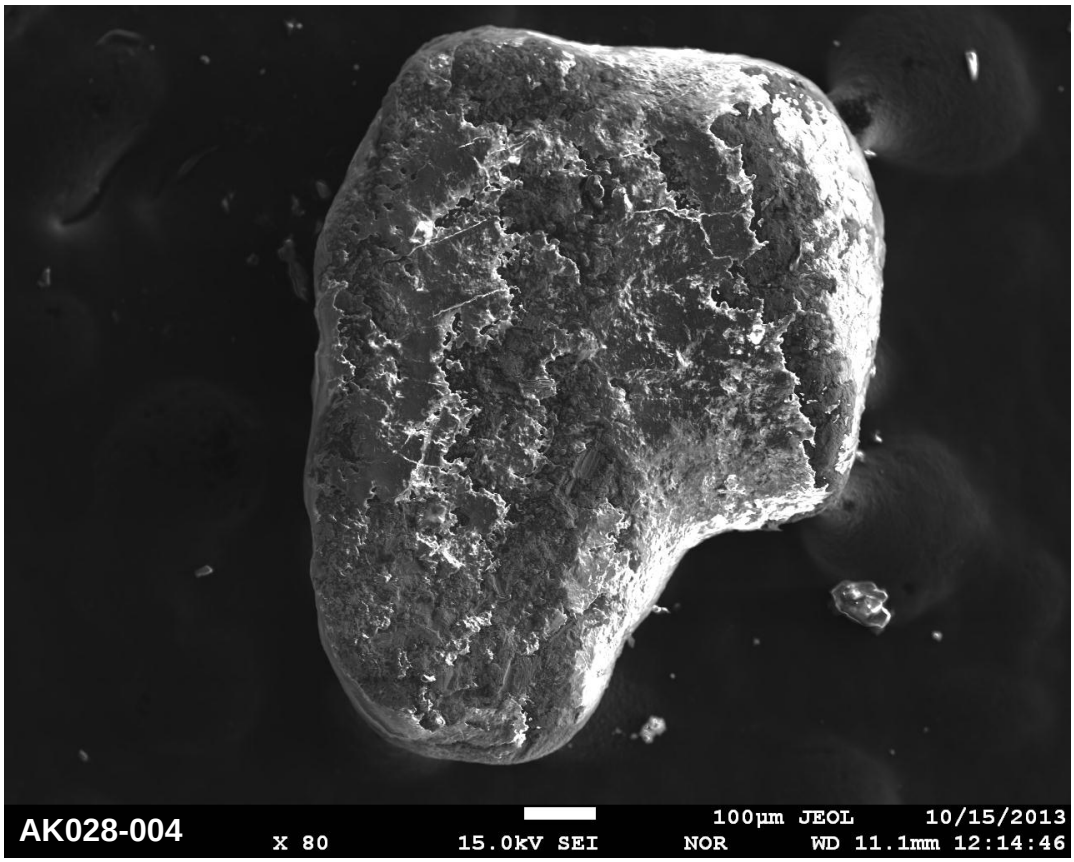
AK028-004
X 80
15.0kV SEI
100µm JEOL
NOR
10/15/2013
WD 11.1mm 12:14:46

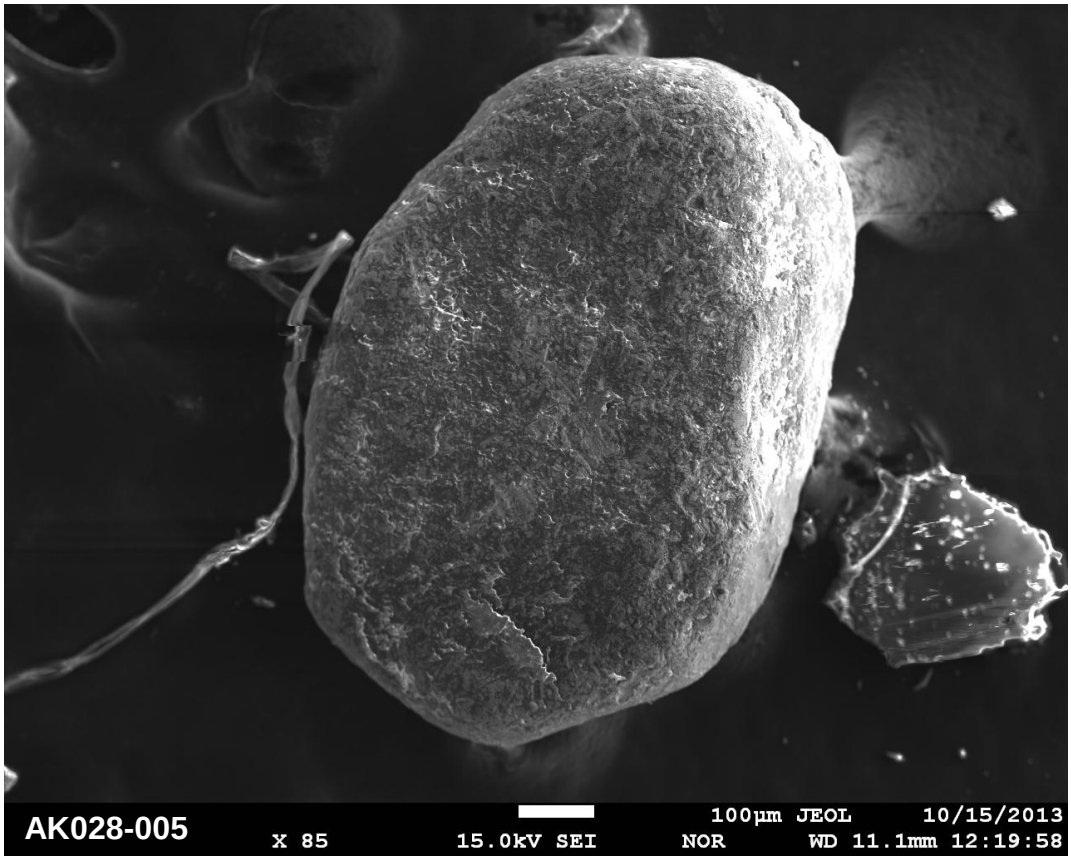
AK028-005
X 85
15.0kV SEI
100µm JEOL
NOR
10/15/2013
WD 11.1mm 12:19:58

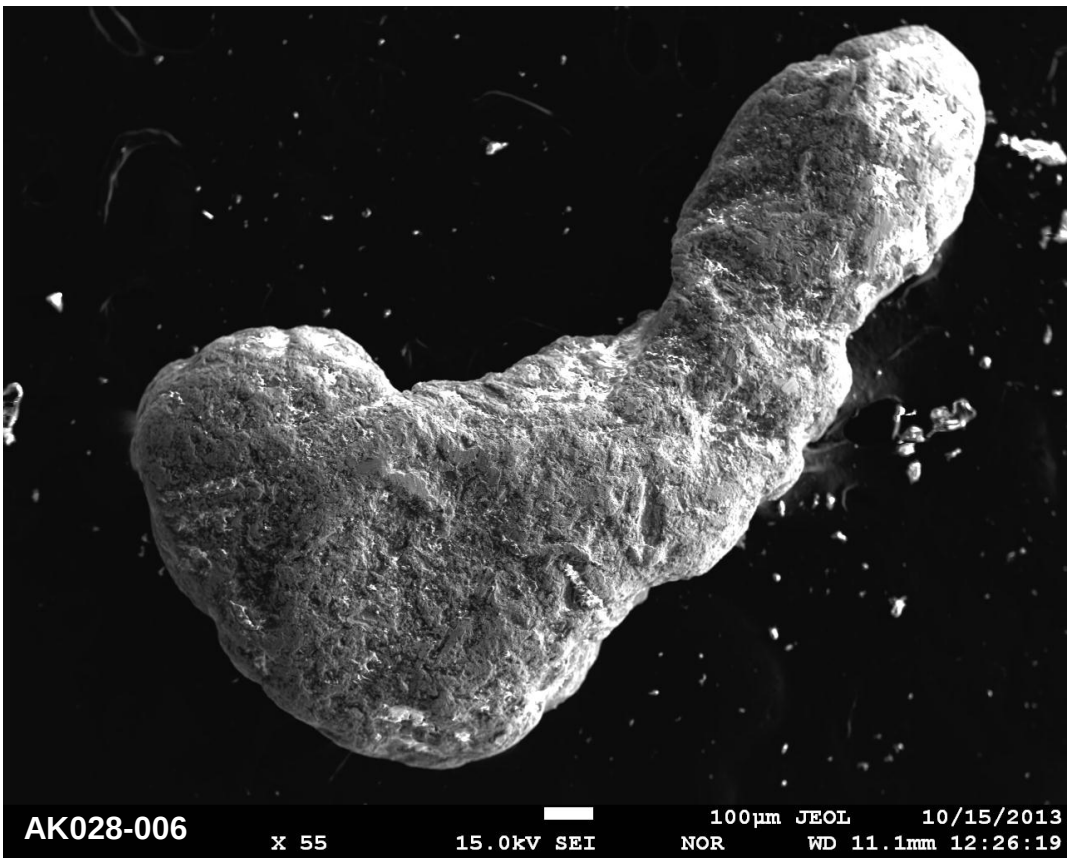
AK028-006
X 55
15.0kV SEI
100µm JEOL
NOR
10/15/2013
WD 11.1mm 12:26:19

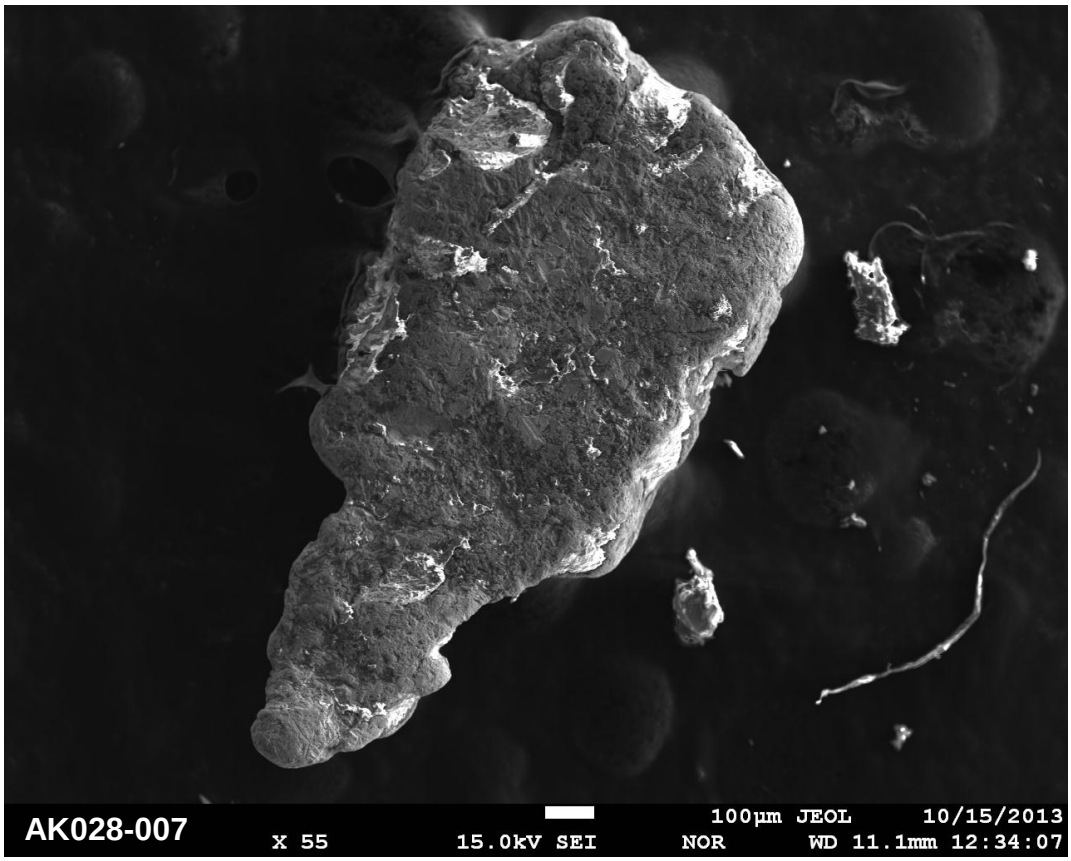
AK028-007
X 55
15.0kV SEI
100µm JEOL
NOR
10/15/2013
WD 11.1mm 12:34:07

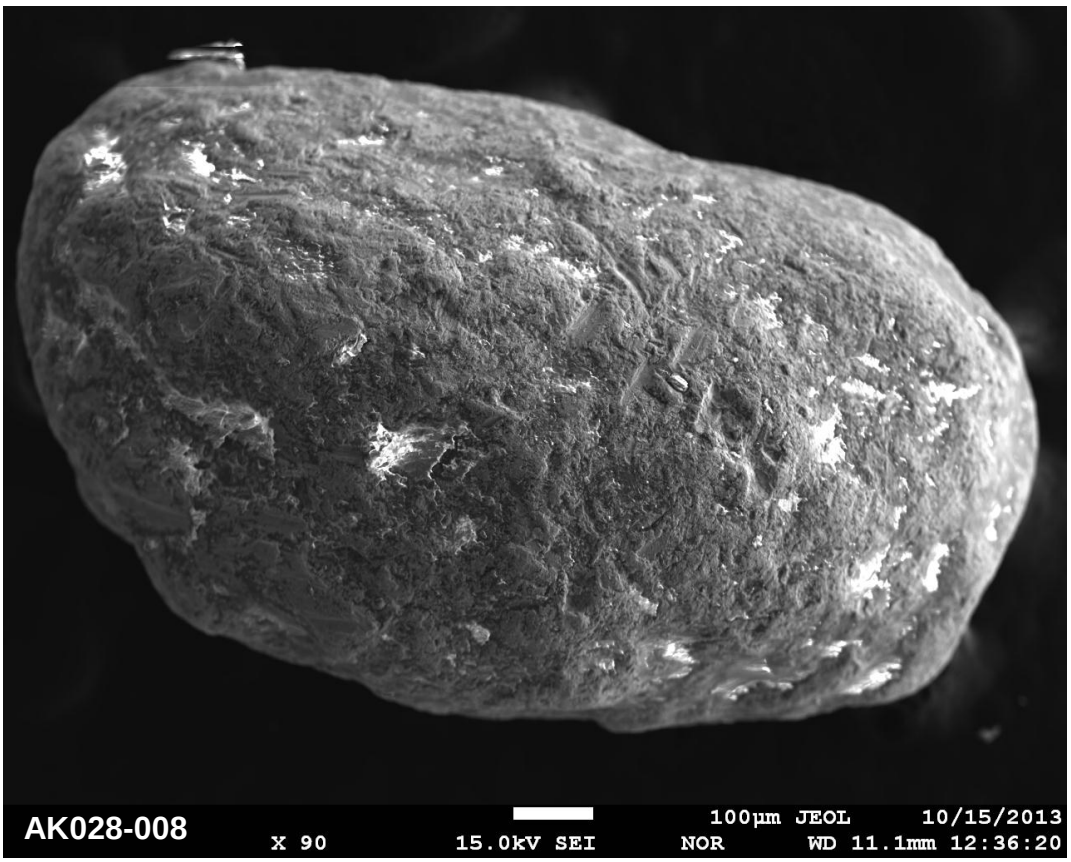
AK028-008
X 90
15.0kV SEI
100µm JEOL
NOR
10/15/2013
WD 11.1mm 12:36:20

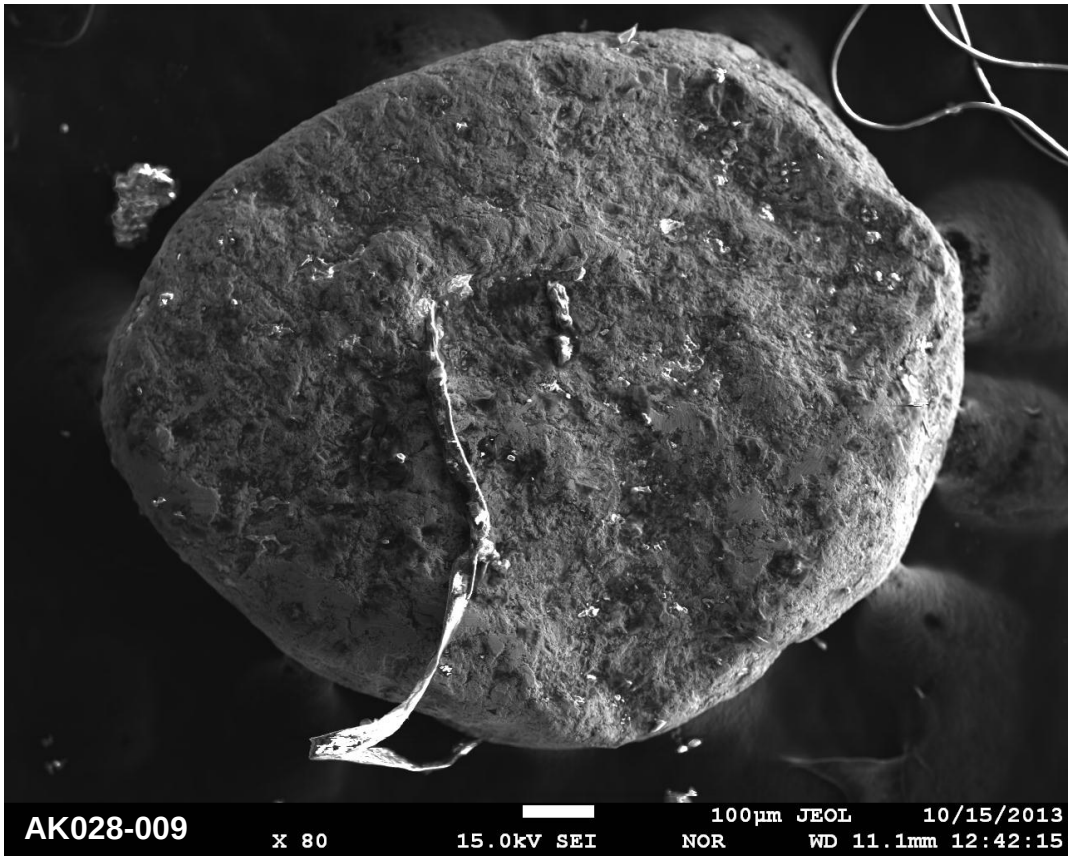
AK028-009
X 80
15.0kV SEI
100µm JEOL
NOR
10/15/2013
WD 11.1mm 12:42:15

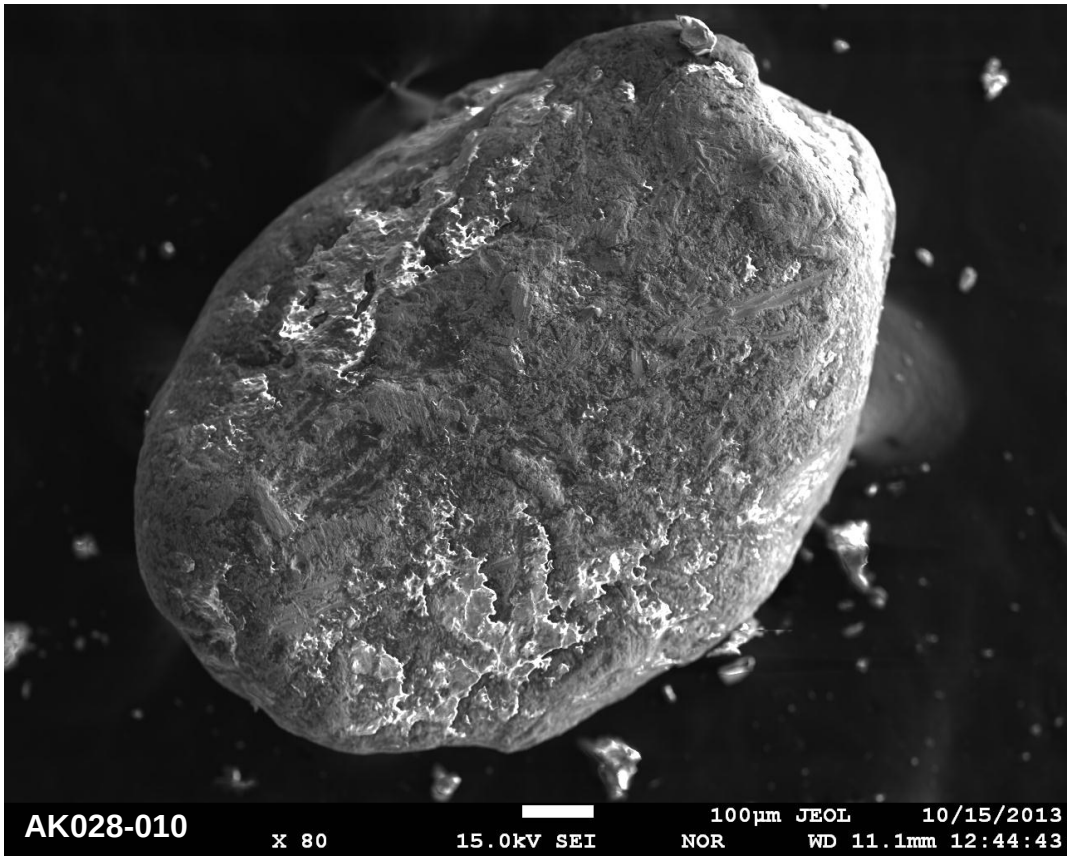
AK028-010
X 80
15.0kV SEI
100µm JEOL
NOR
10/15/2013
WD 11.1mm 12:44:43

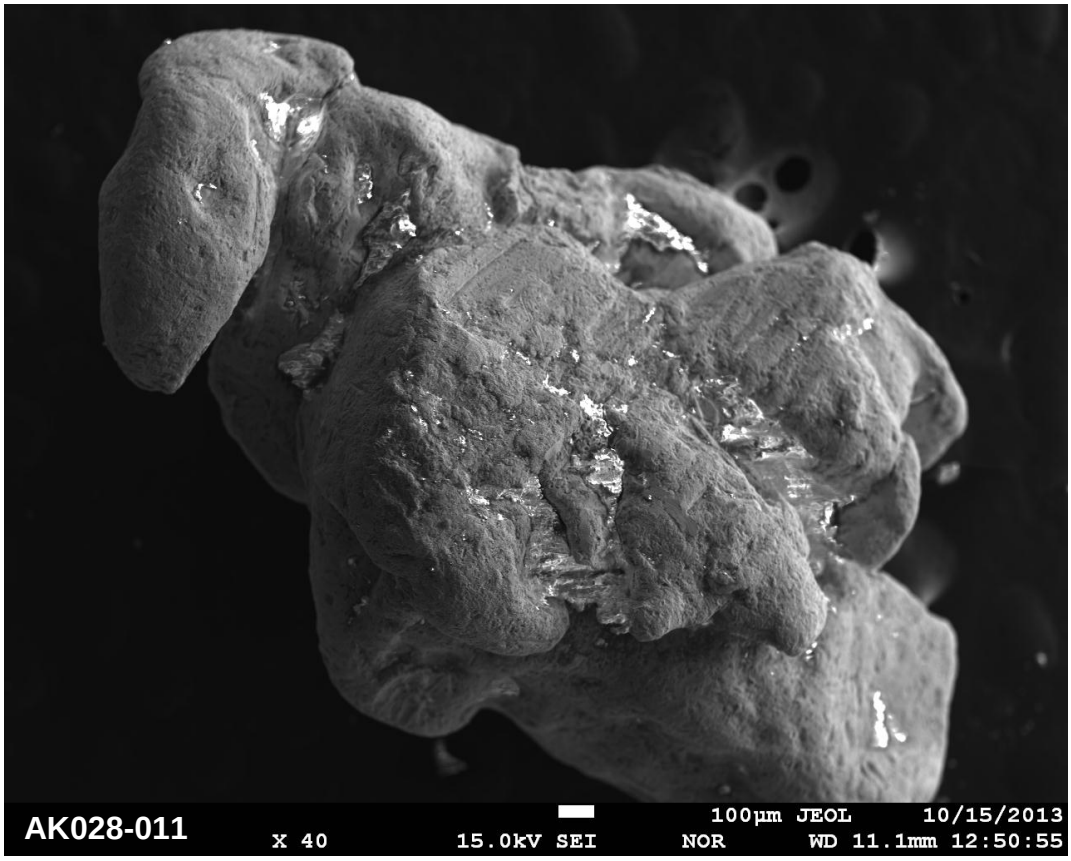
AK028-011
X 40
15.0kV SEI
100µm JEOL
NOR
10/15/2013
WD 11.1mm 12:50:55

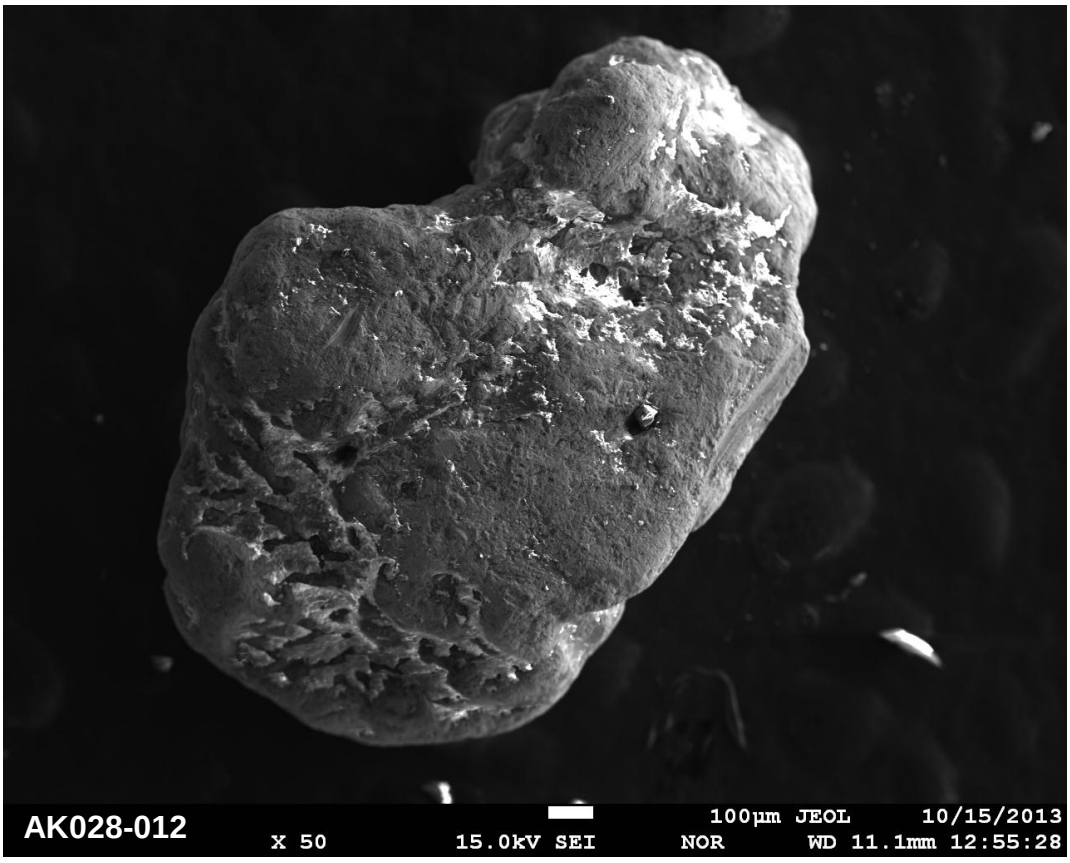
AK028-012
X 50
15.0kV SEI
100µm JEOL
NOR
10/15/2013
WD 11.1mm 12:55:28

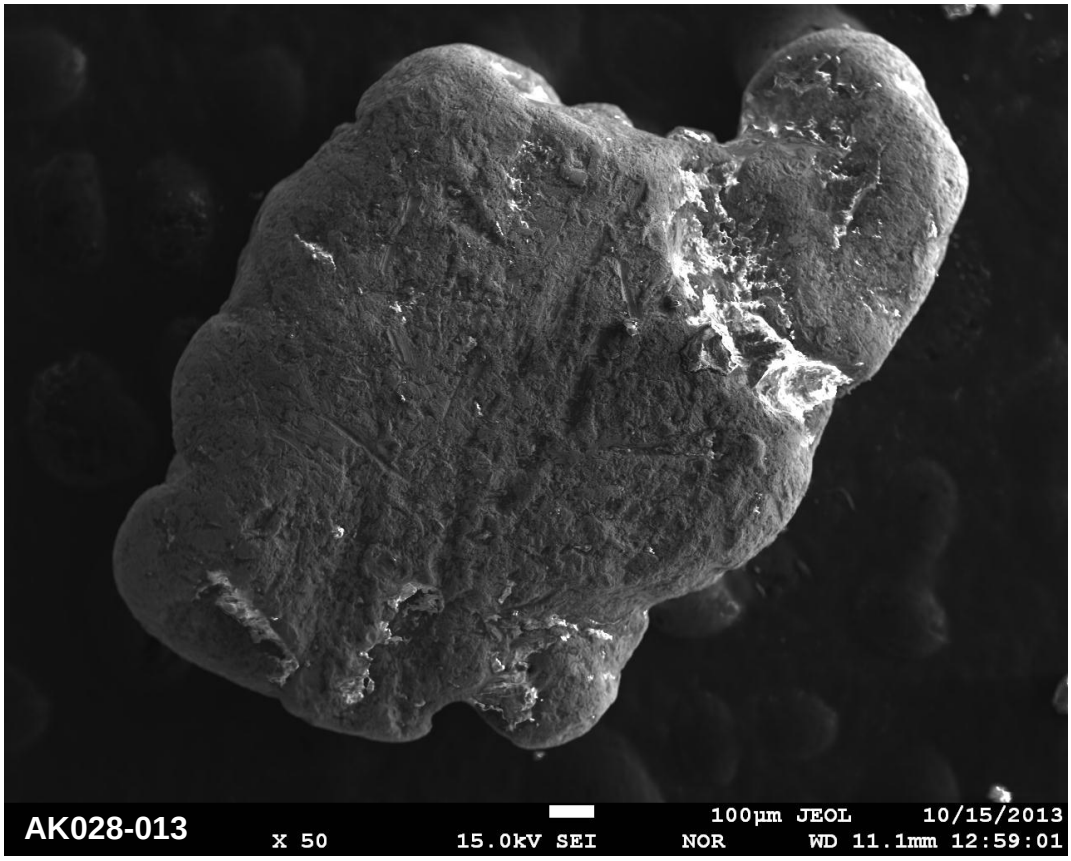
AK028-013
X 50
15.0kV SEI
100µm JEOL
NOR
10/15/2013
WD 11.1mm 12:59:01


AK028-014
X 43
15.0kV SEI
100µm JEOL
NOR
10/15/2013
WD 11.1mm 13:04:44

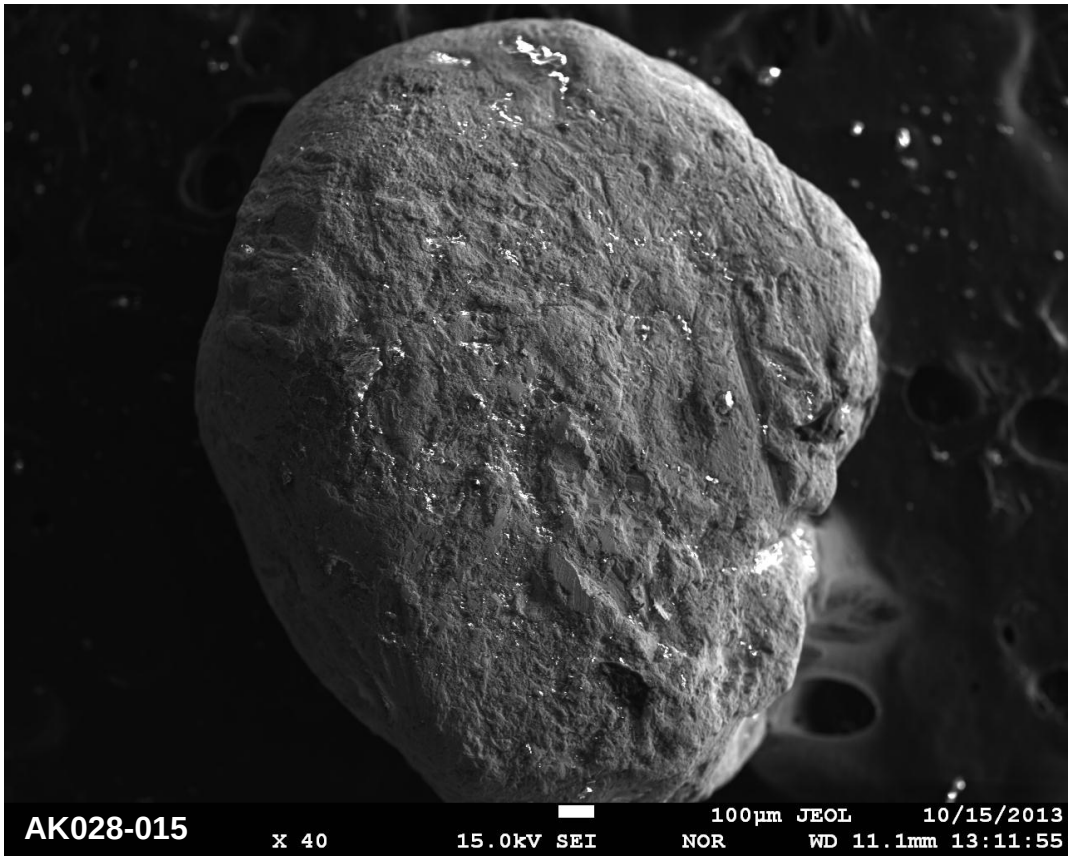
AK028-015
X 40
15.0kV SEI
100µm JEOL
NOR
10/15/2013
WD 11.1mm 13:11:55

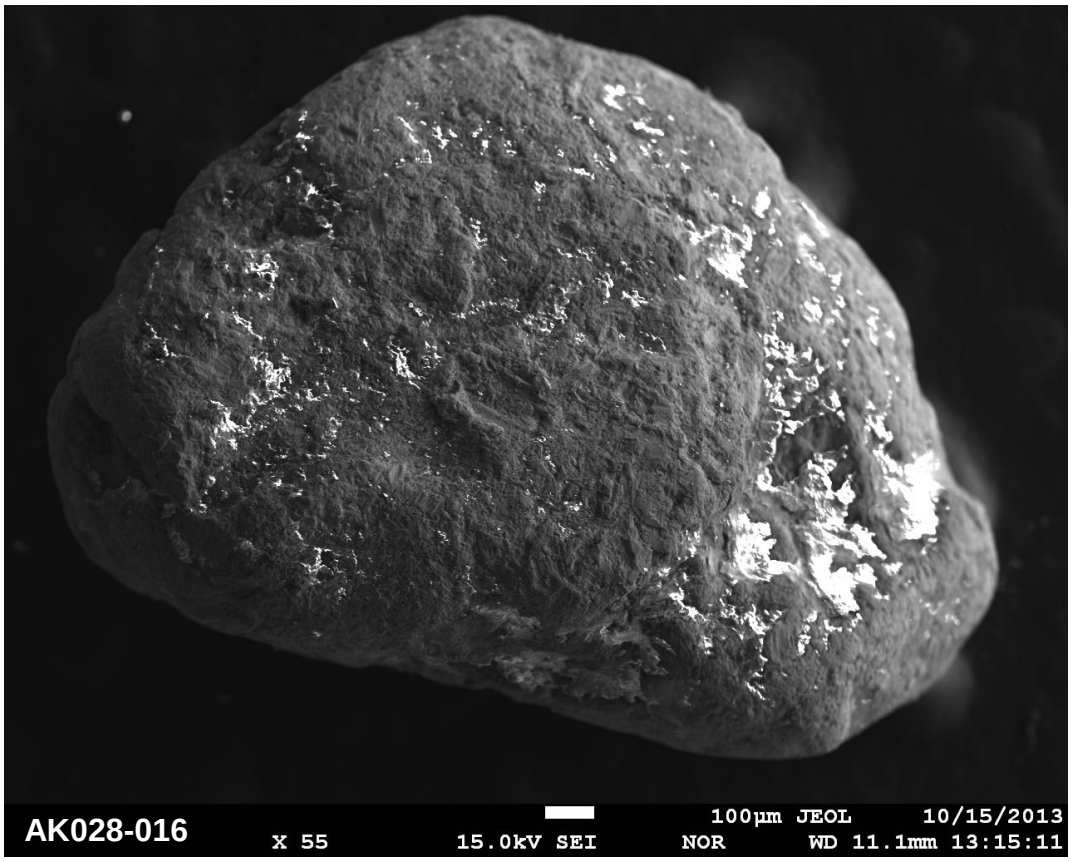
AK028-016
X 55
15.0kV SEI
100µm JEOL
NOR
10/15/2013
WD 11.1mm 13:15:11

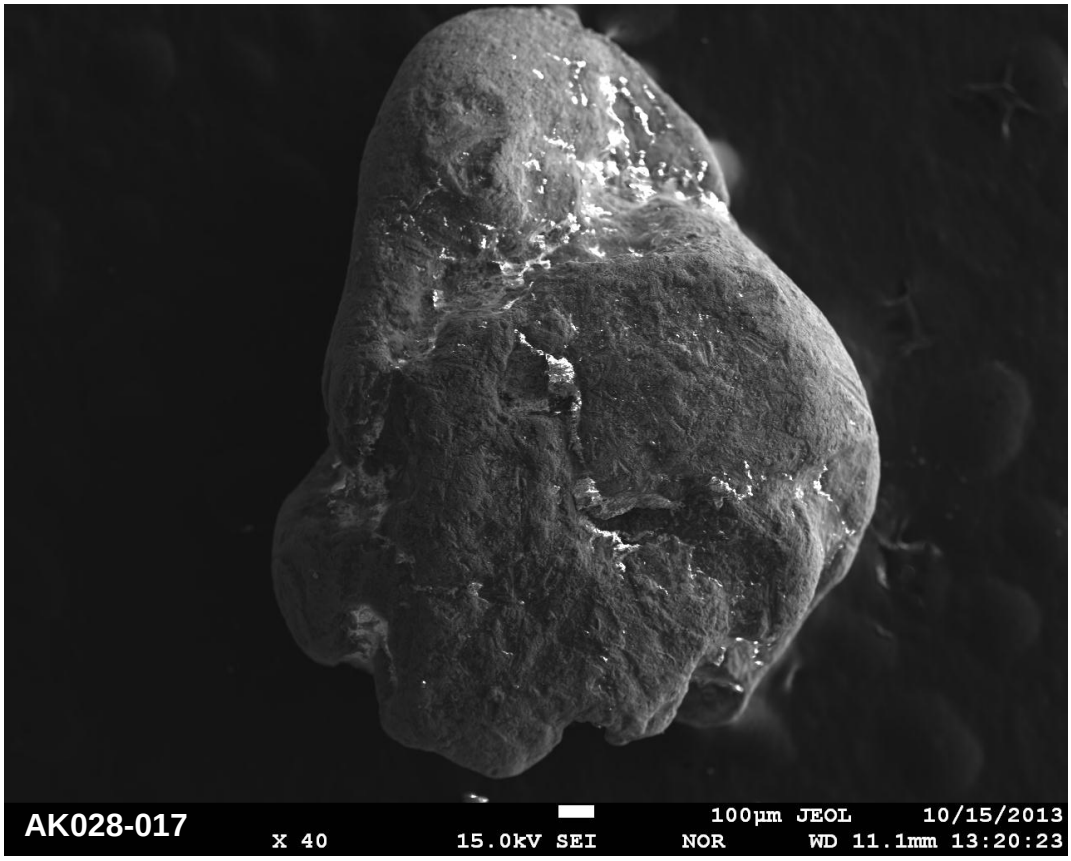
AK028-017
X 40
15.0kV SEI
100µm JEOL
NOR
10/15/2013
WD 11.1mm 13:20:23

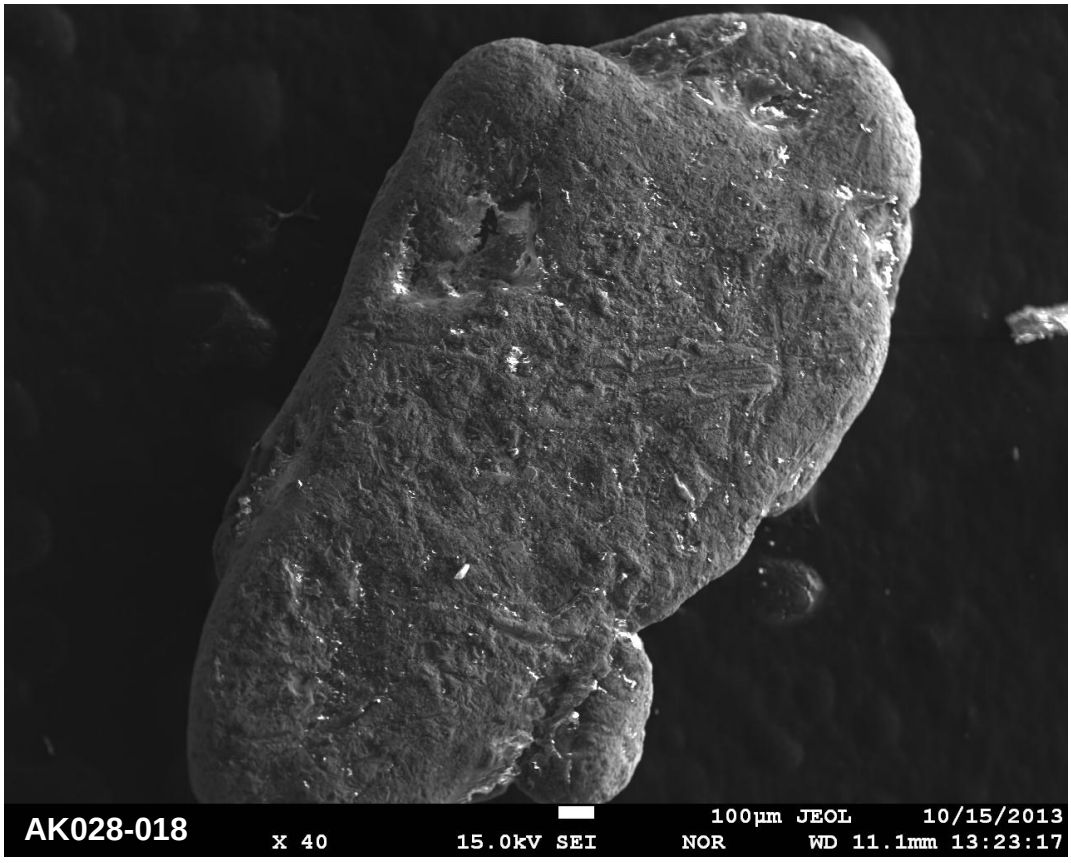
AK028-018
X 40
15.0kV SEI
100µm JEOL
NOR
10/15/2013
WD 11.1mm 13:23:17

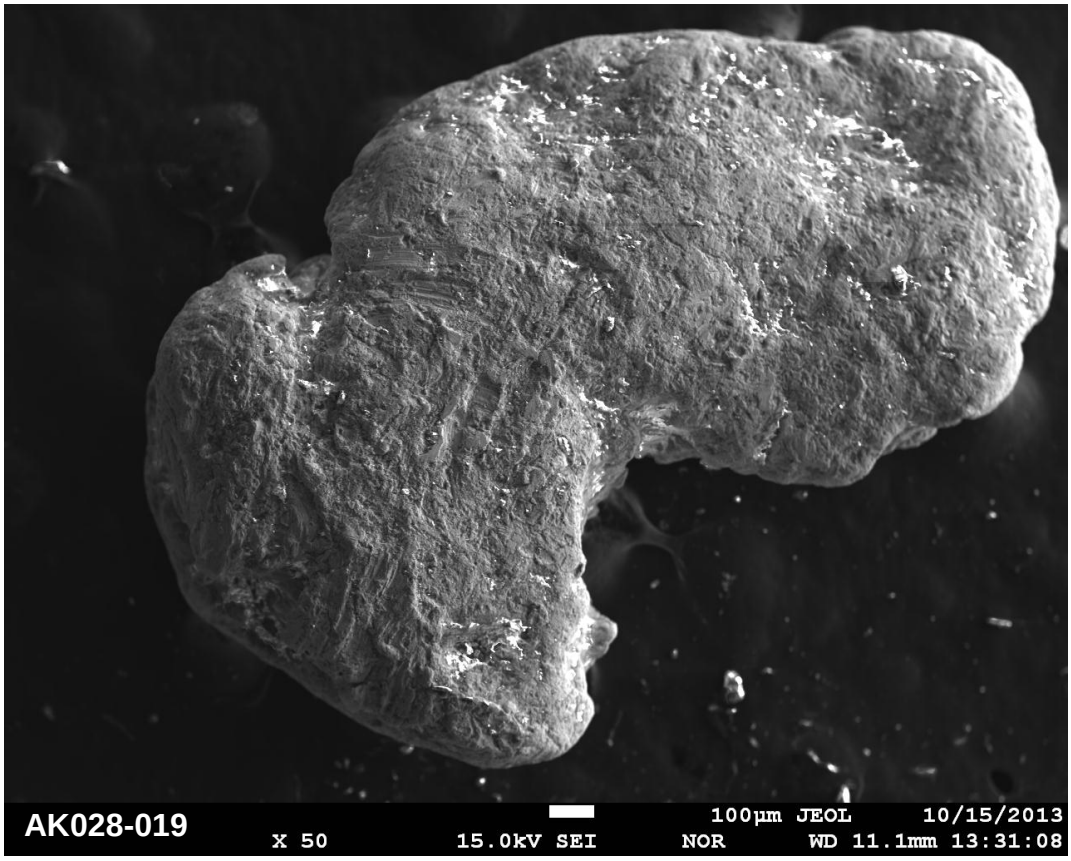
AK028-019
X 50
15.0kV SEI
100µm JEOL
NOR
10/15/2013
WD 11.1mm 13:31:08

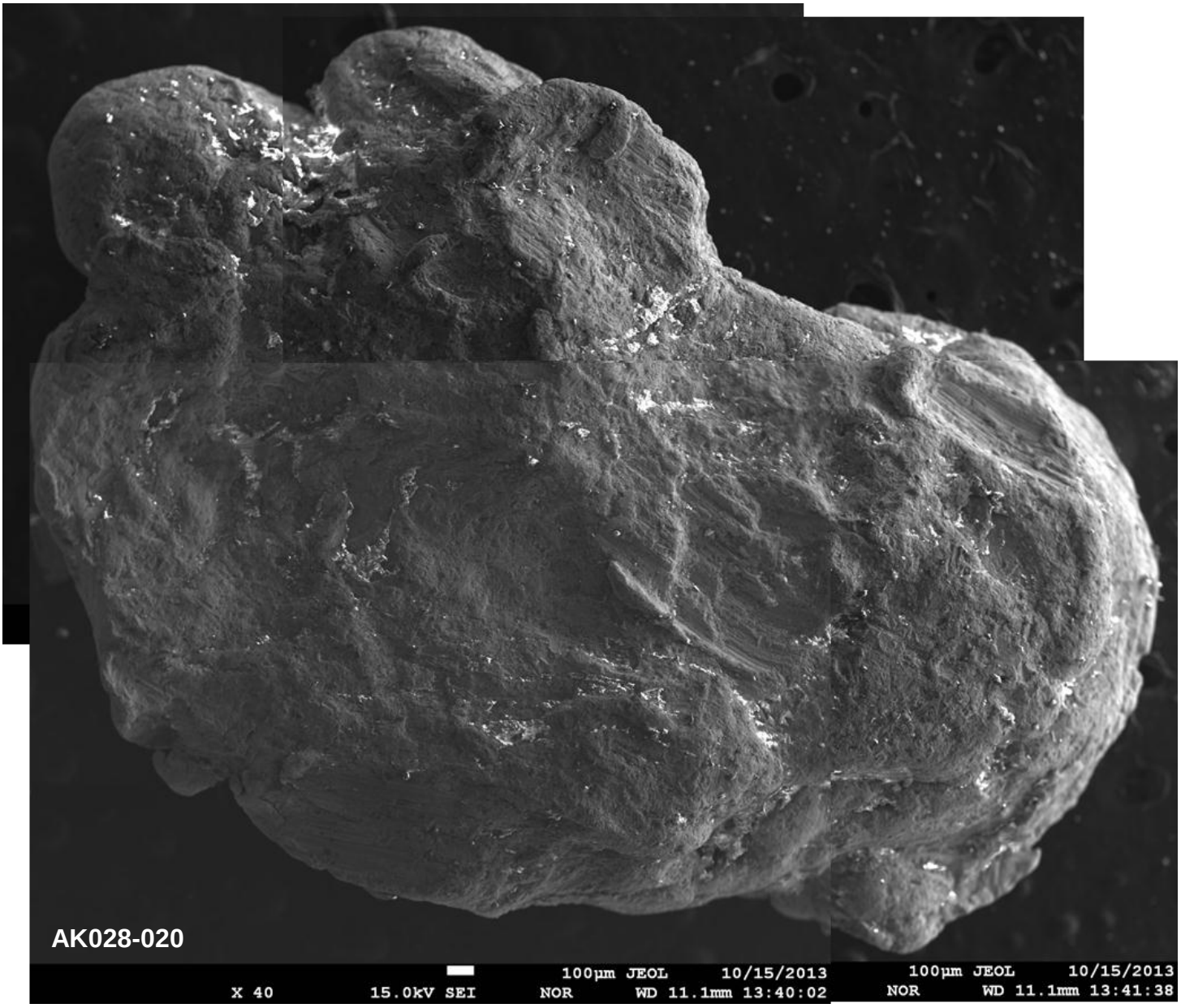
AK028-020
X 40 15.0kV SEI 100µm JEOL NOR 10/15/2013 WD 11.1mm 13:40:02
100µm JEOL NOR 10/15/2013 WD 11.1mm 13:41:38

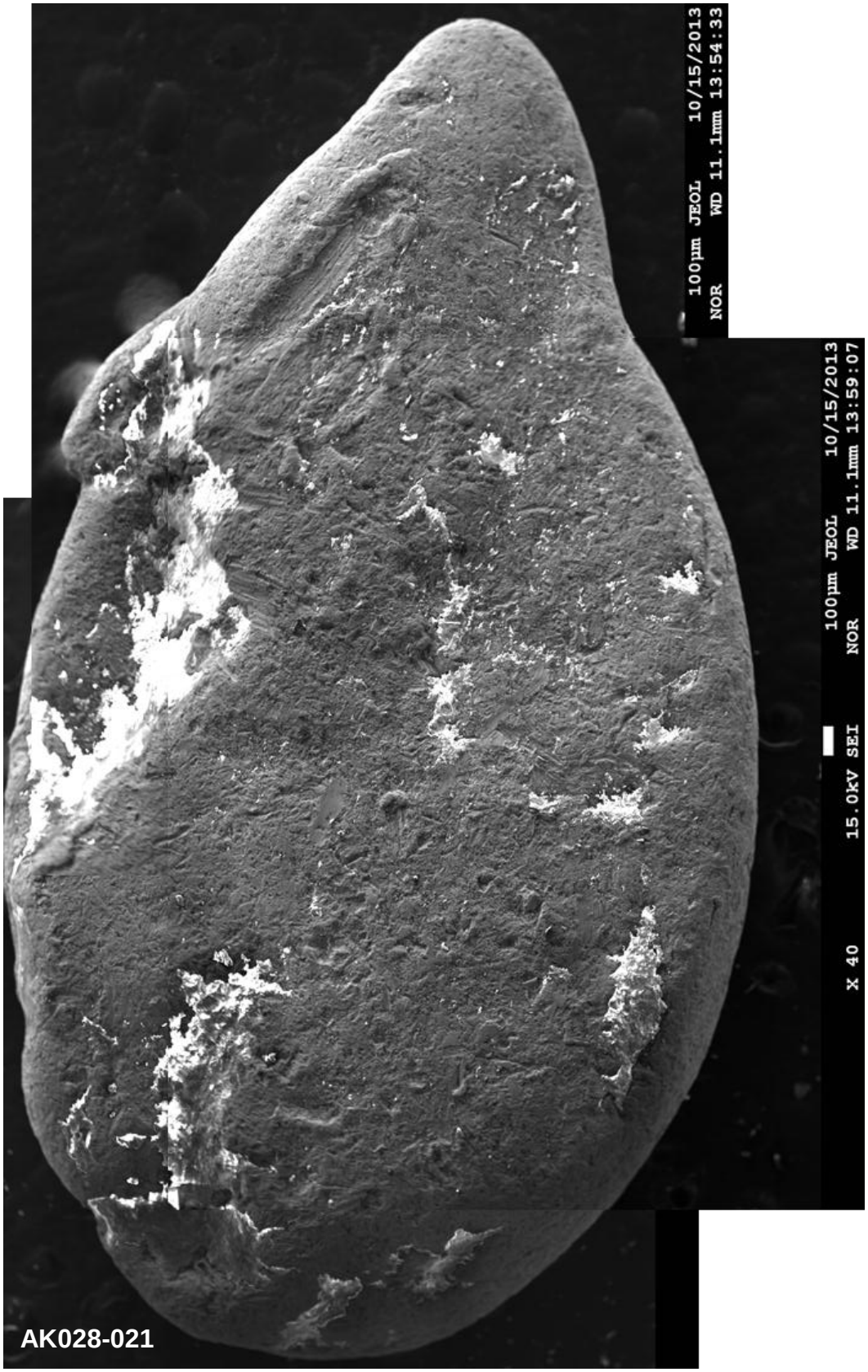
100µm JEOL 10/15/2013
NOR WD 11.1mm 13:54:33
100µm JEOL 10/15/2013
X 40 15.0kV SEI NOR WD 11.1mm 13:59:07
AK028-021

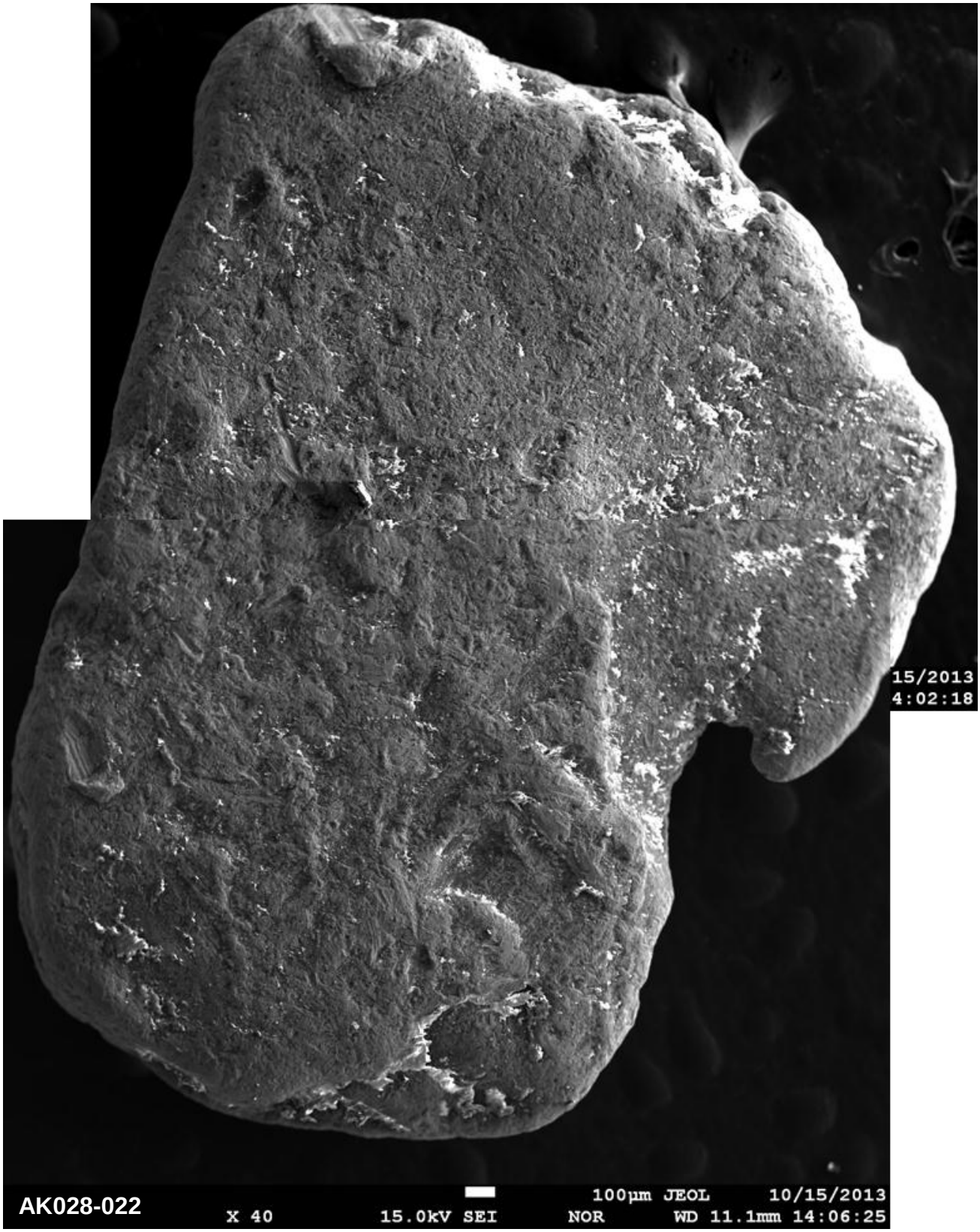
15/2013
4:02:18
AK028-022
X 40
15.0kV SEI
100µm JEOL
NOR
10/15/2013
WD 11.1mm 14:06:25


AK028-023
X 40
15.0kV SEI
100µm JEOL
NOR
10/15/2013
WD 11.1mm 14:15:11

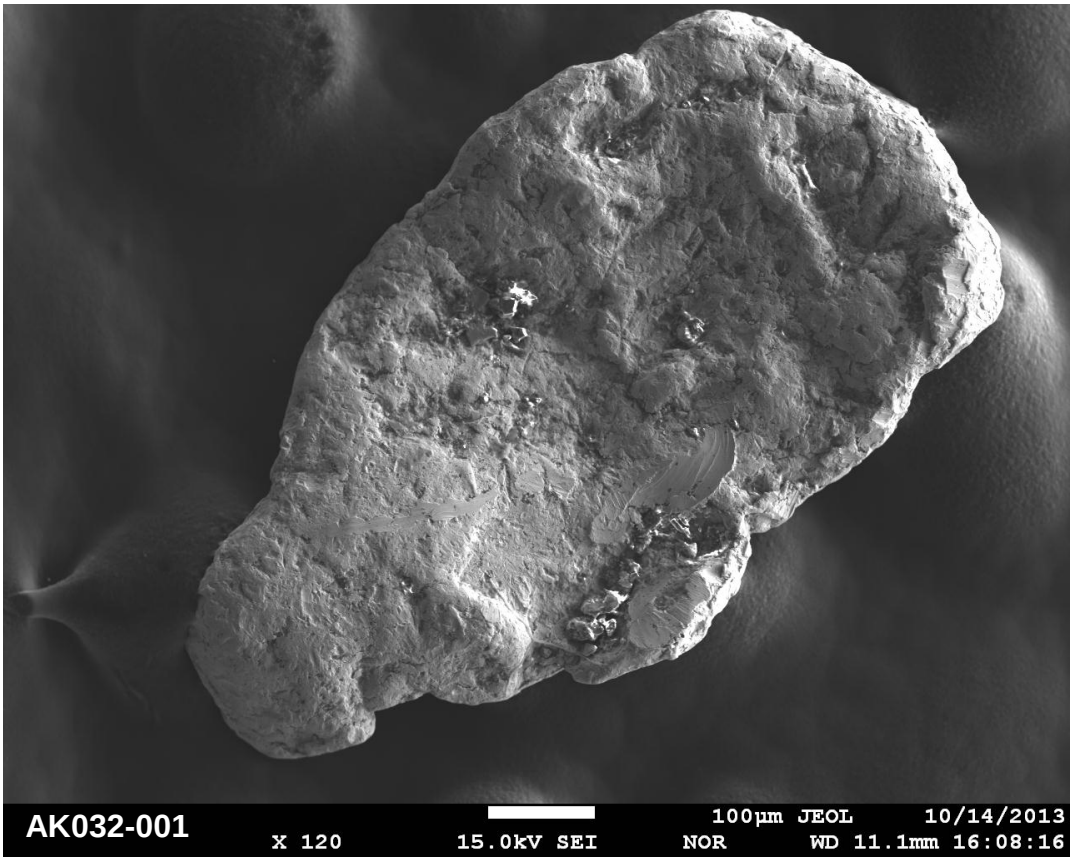
AK032-001
X 120
15.0kV SEI
100µm JEOL
NOR
10/14/2013
WD 11.1mm 16:08:16

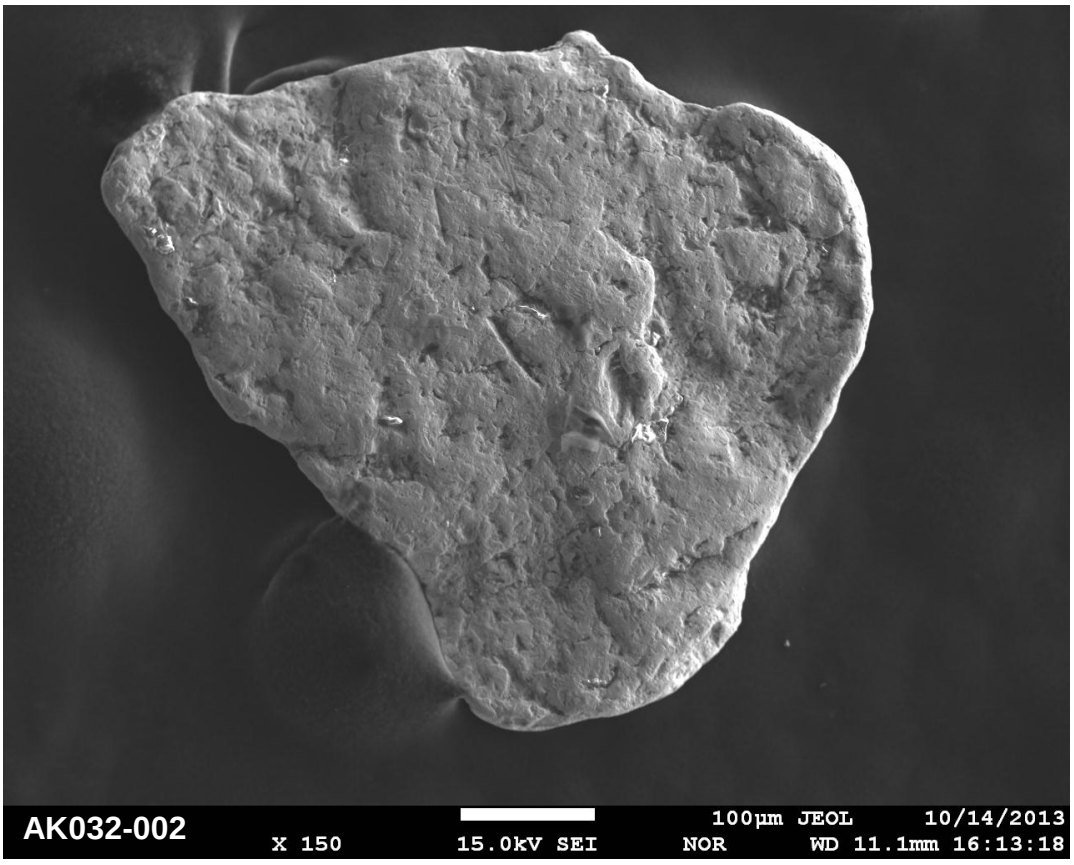
AK032-002
X 150
15.0kV SEI
100µm JEOL
NOR
10/14/2013
WD 11.1mm 16:13:18

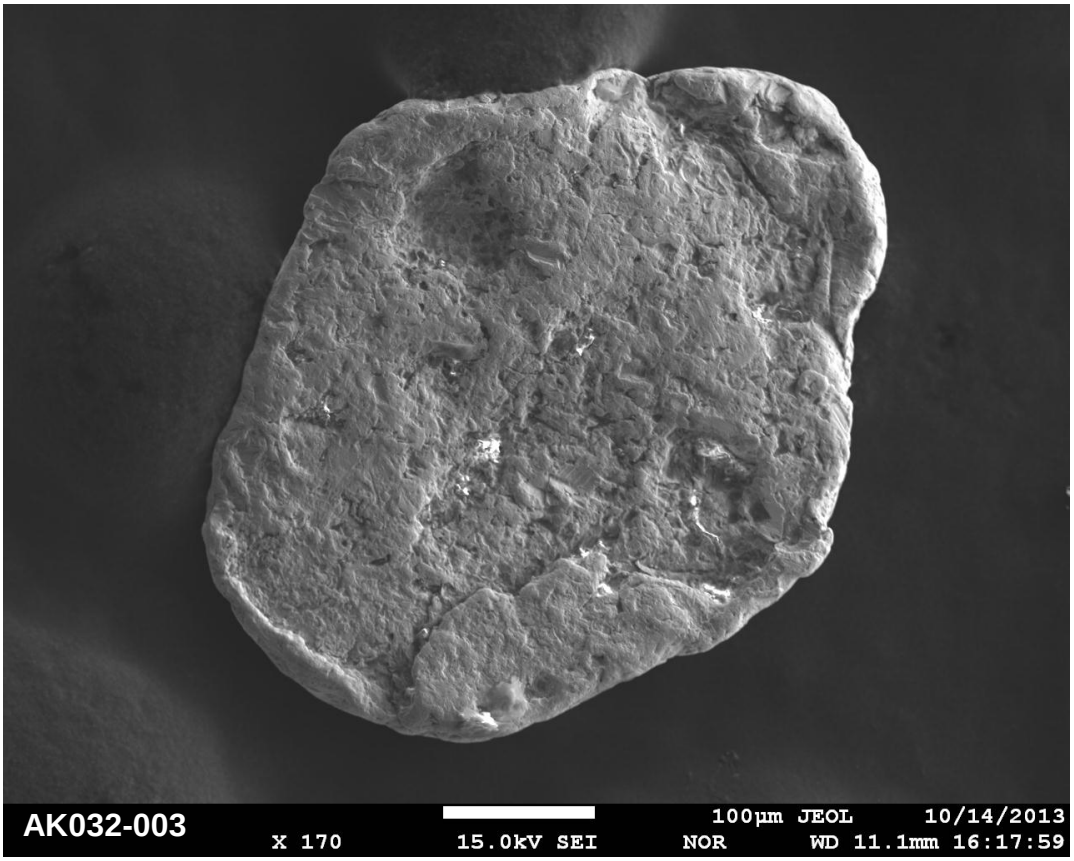
AK032-003
X 170
15.0kV SEI
100µm JEOL
NOR
10/14/2013
WD 11.1mm 16:17:59

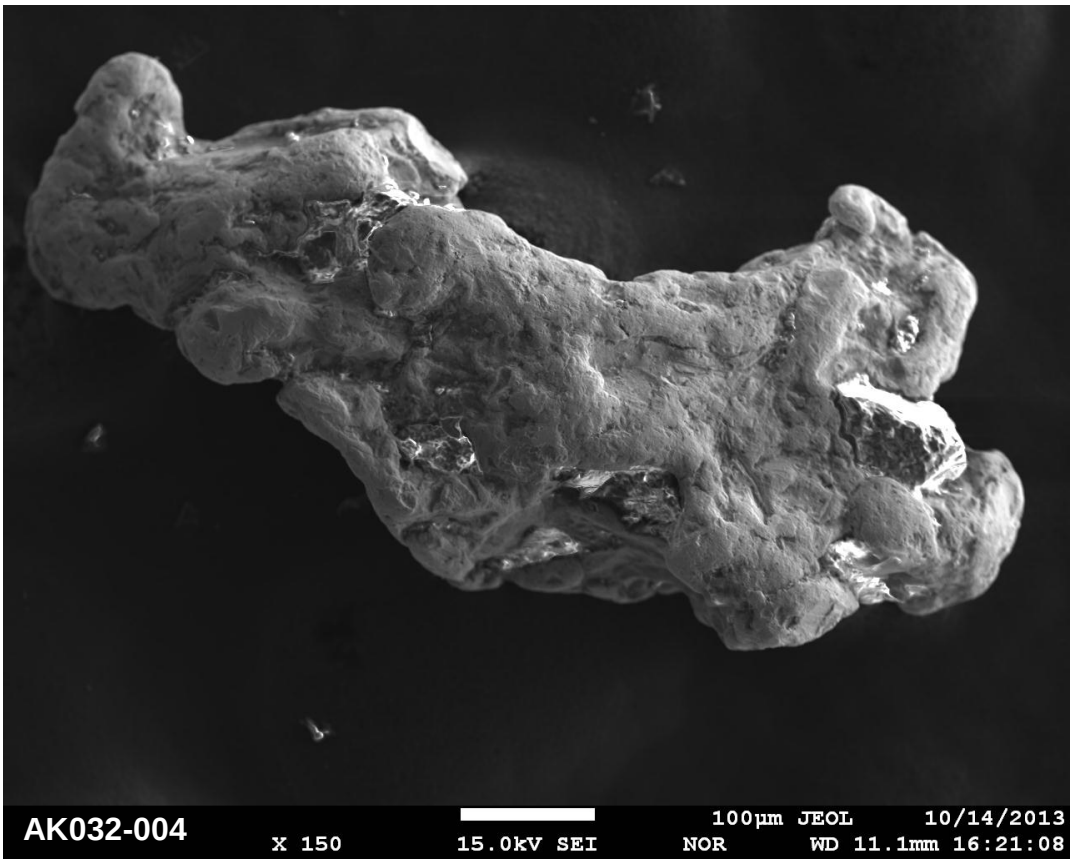
AK032-004
X 150
15.0kV SEI
100µm JEOL
NOR
10/14/2013
WD 11.1mm 16:21:08

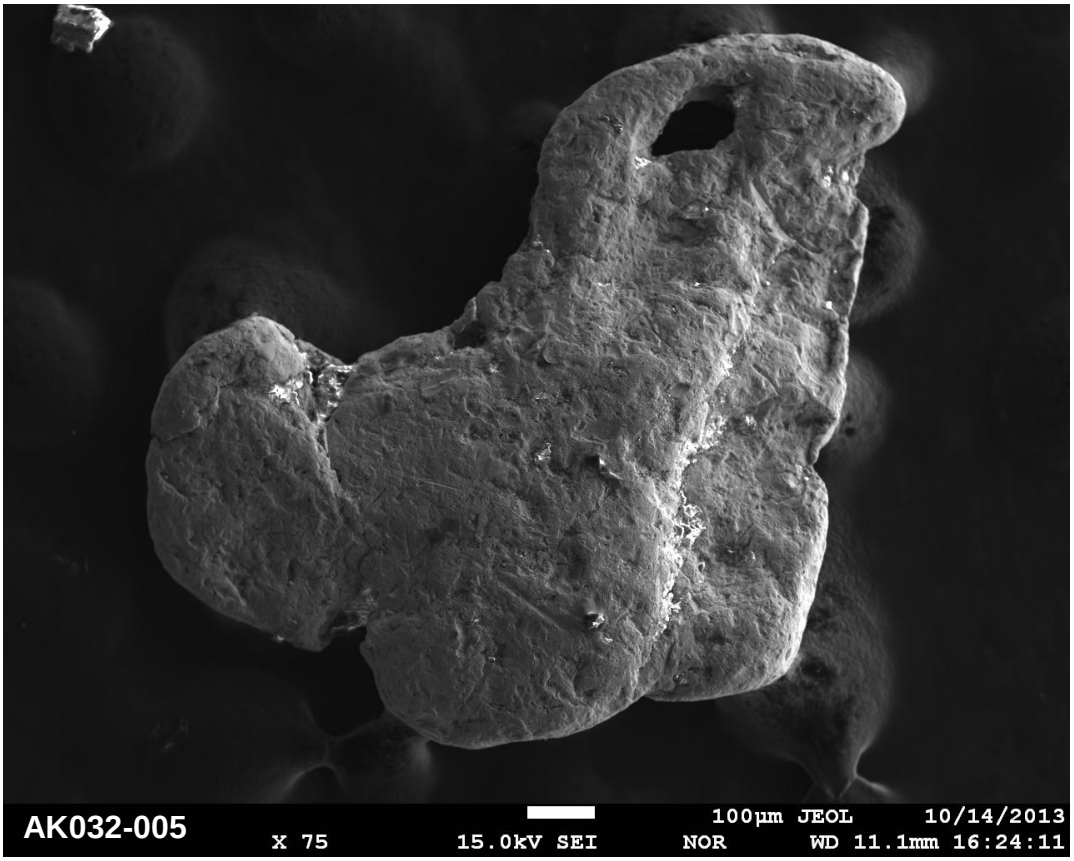
AK032-005
X 75
15.0kV SEI
100µm JEOL
NOR
10/14/2013
WD 11.1mm 16:24:11

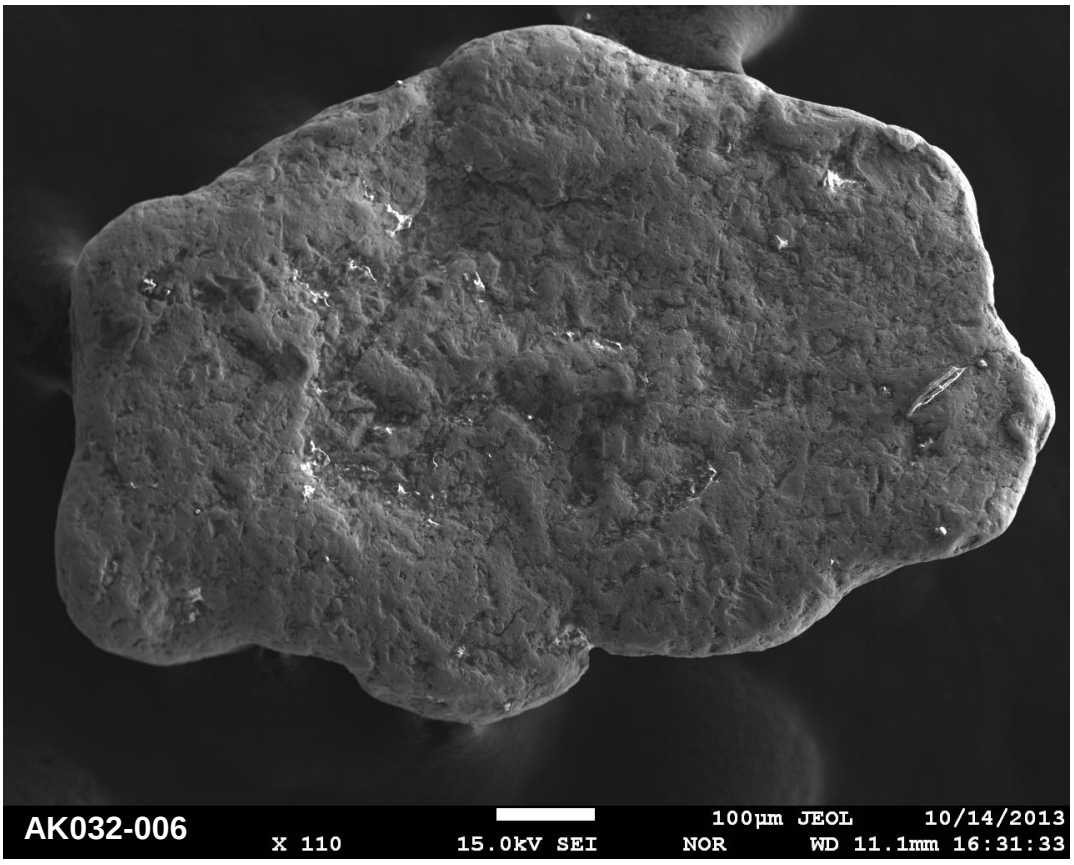
AK032-006
X 110
15.0kV SEI
100µm JEOL
NOR
10/14/2013
WD 11.1mm 16:31:33

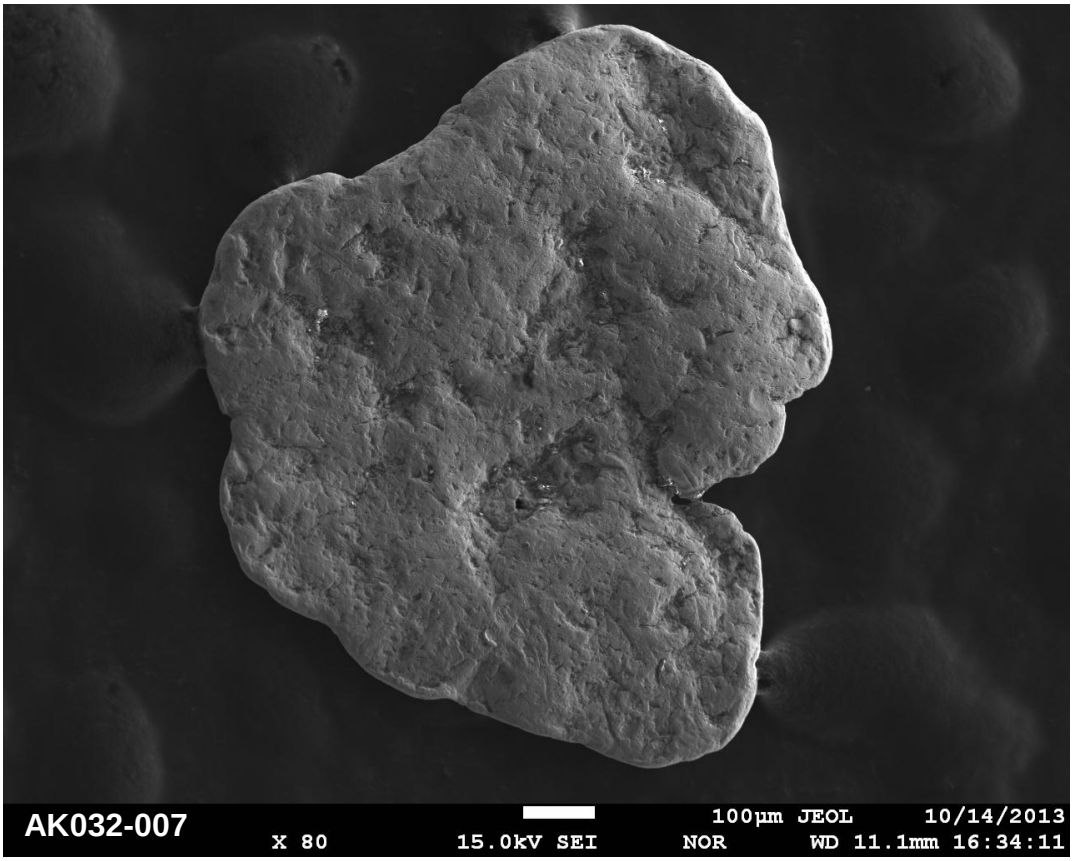
AK032-007
X 80
15.0kV SEI
100µm JEOL
NOR
10/14/2013
WD 11.1mm 16:34:11

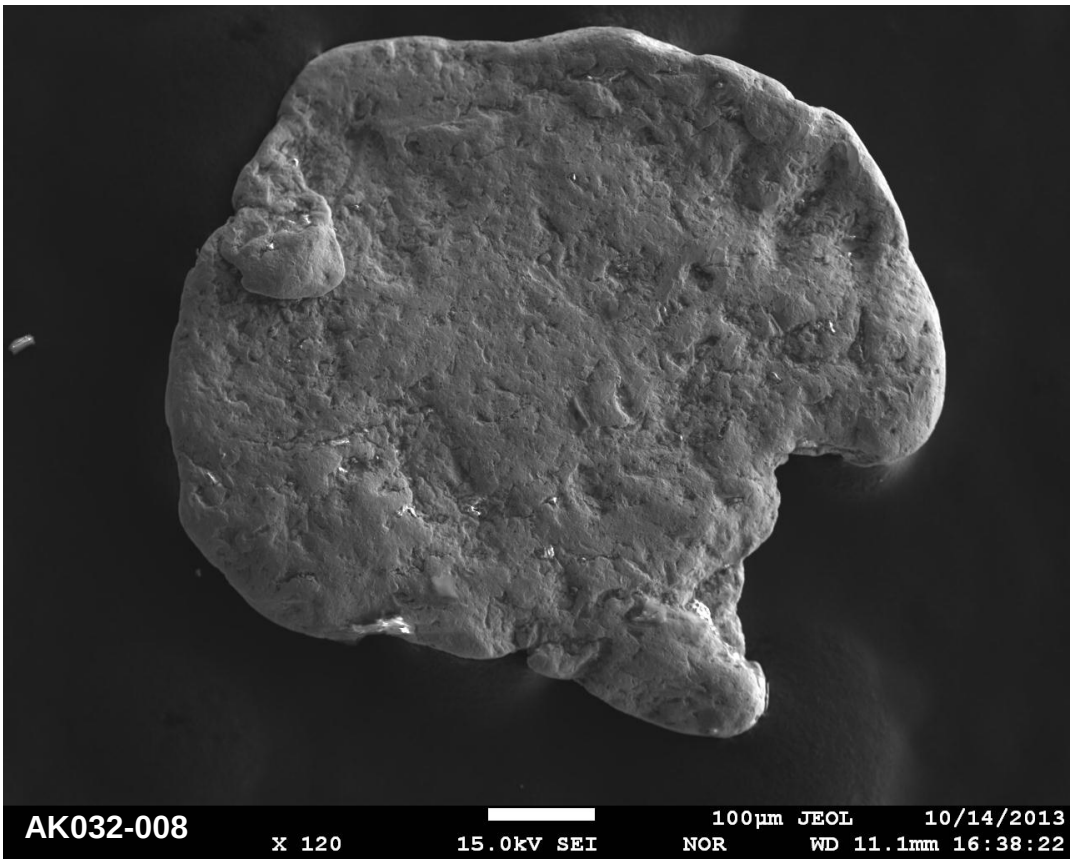
AK032-008
X 120
15.0kV SEI
100µm JEOL
NOR
10/14/2013
WD 11.1mm 16:38:22

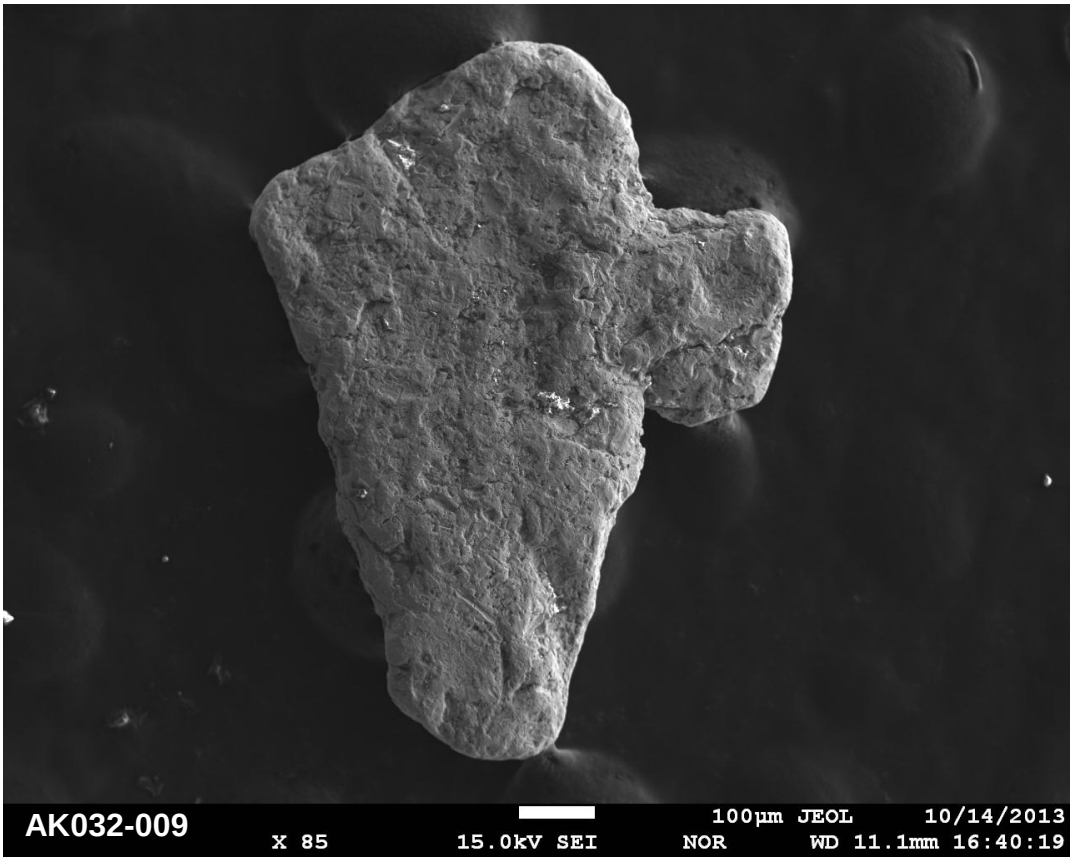
AK032-009
X 85
15.0kV SEI
100µm JEOL
NOR
10/14/2013
WD 11.1mm 16:40:19

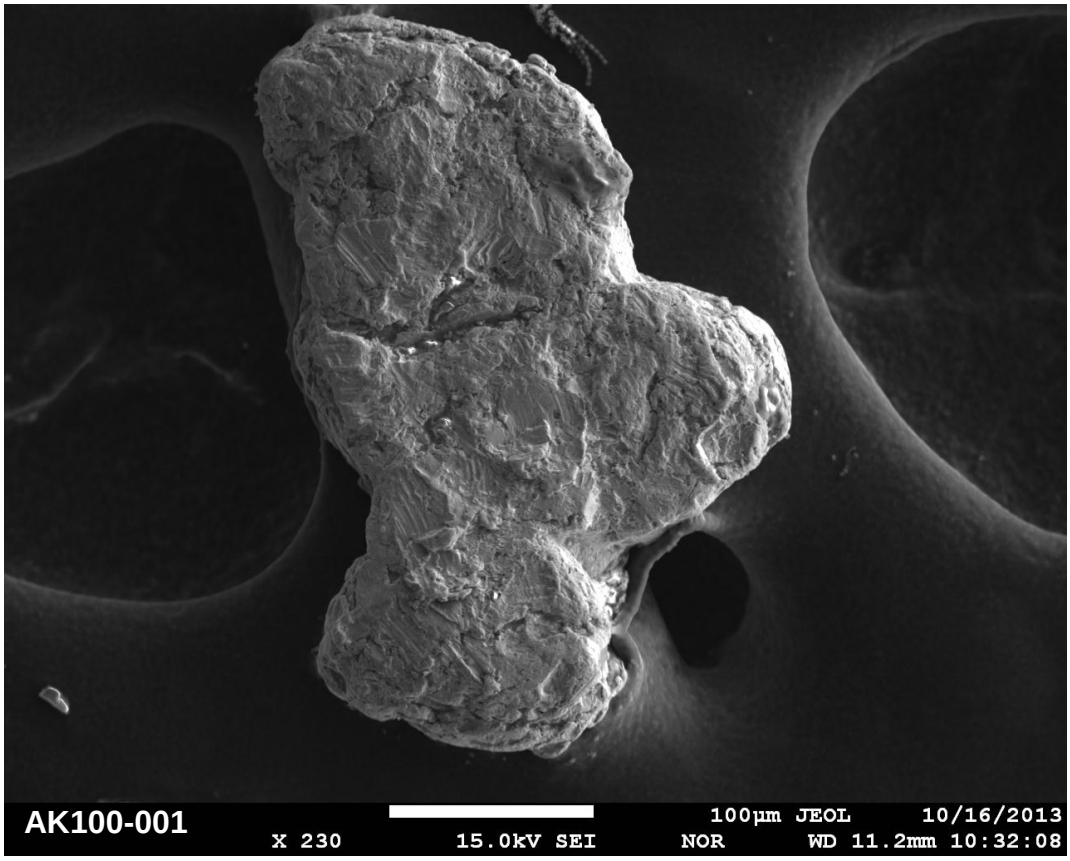
AK100-001
X 230
15.0kV SEI
100µm JEOL
NOR
10/16/2013
WD 11.2mm 10:32:08

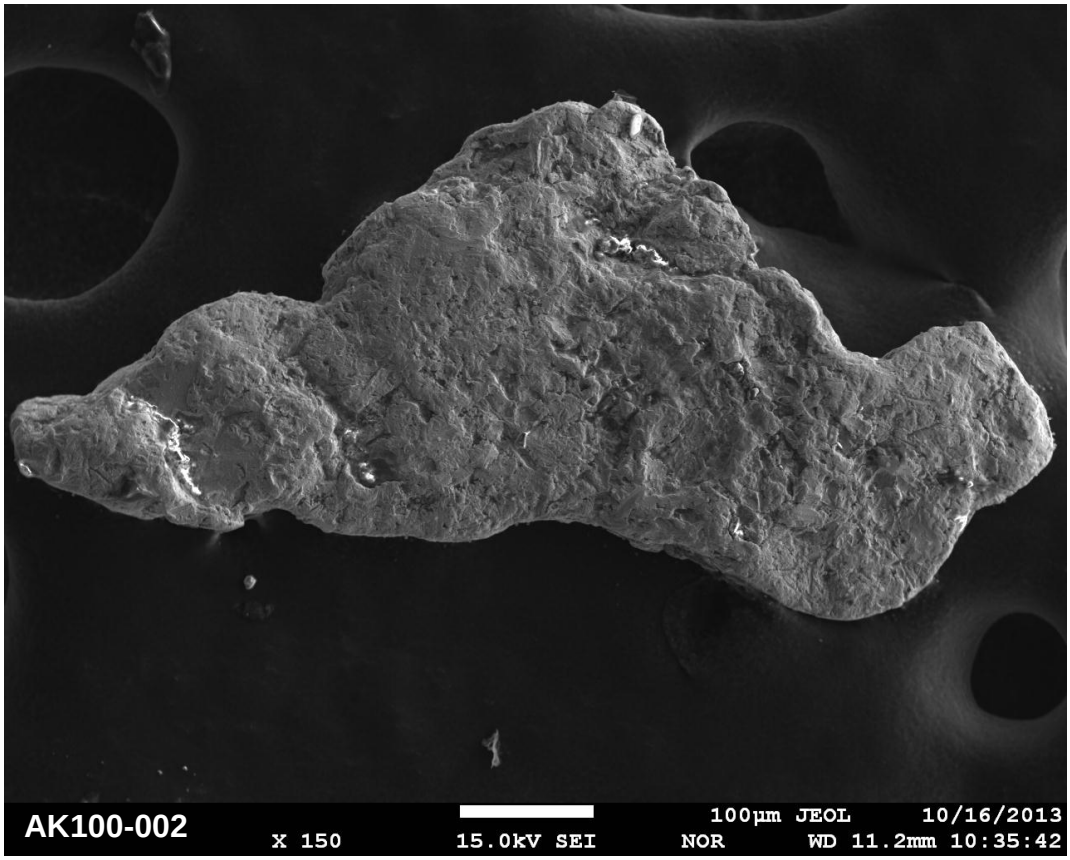
AK100-002
X 150
15.0kV SEI
100µm JEOL
NOR
10/16/2013
WD 11.2mm 10:35:42

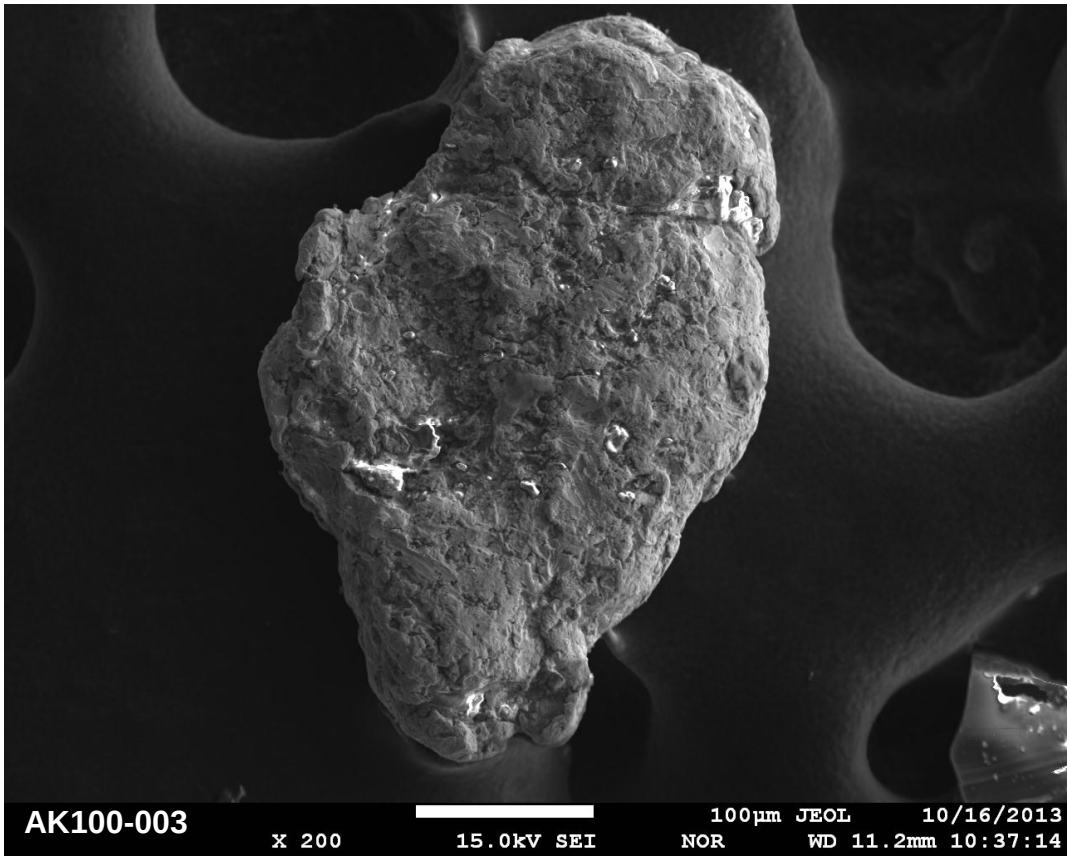
AK100-003
X 200
15.0kV SEI
100µm JEOL
NOR
10/16/2013
WD 11.2mm 10:37:14

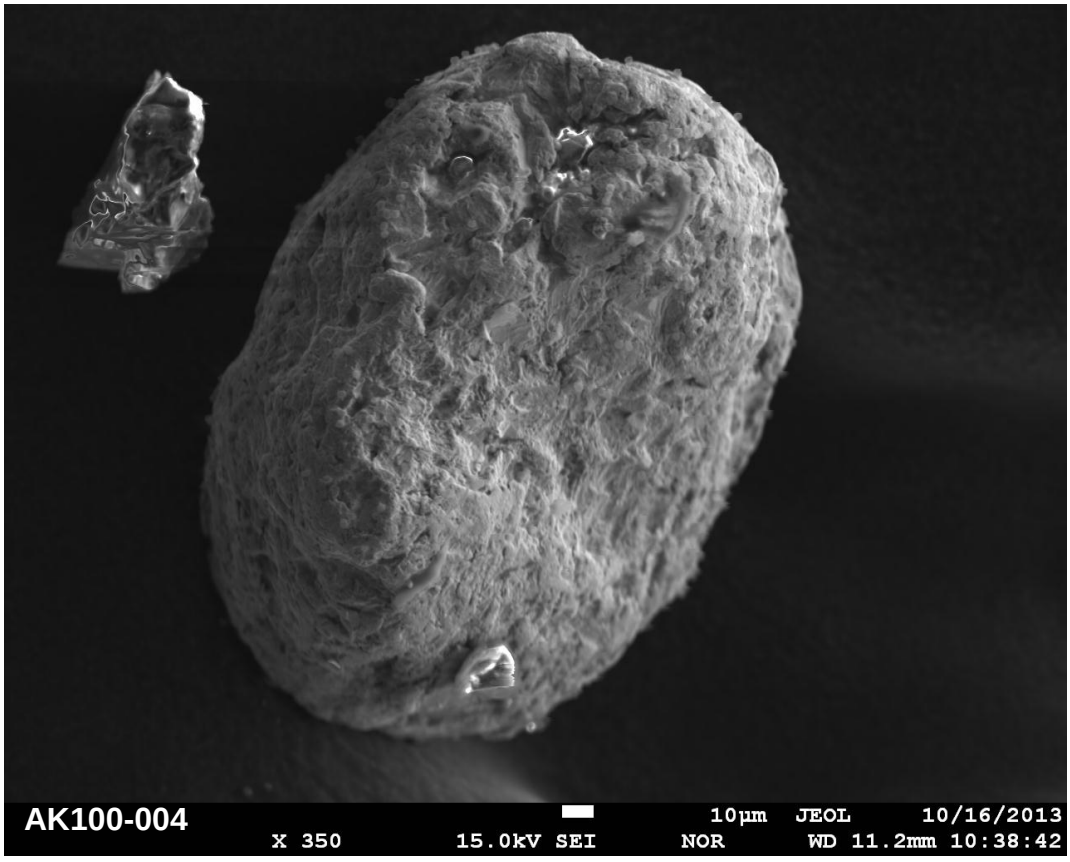
AK100-004
X 350
15.0kV SEI
10µm JEOL
NOR
10/16/2013
WD 11.2mm 10:38:42

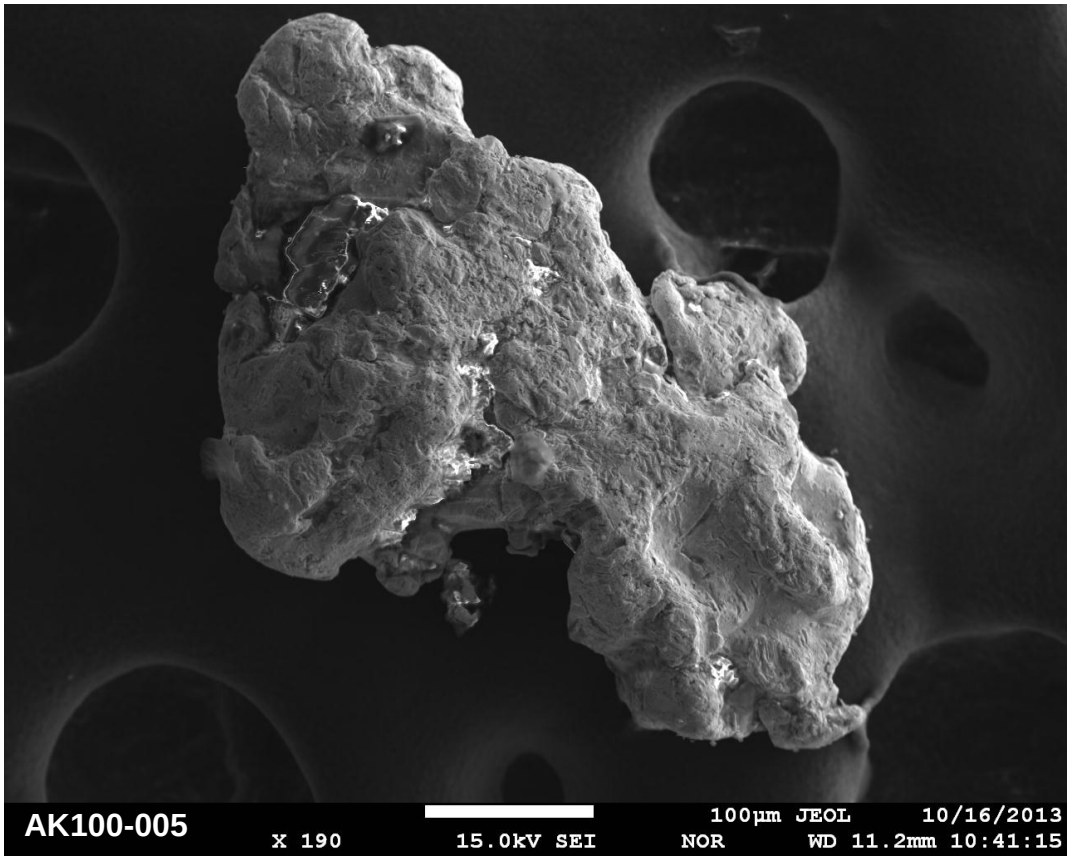
AK100-005
X 190
15.0kV SEI
100µm JEOL
NOR
10/16/2013
WD 11.2mm 10:41:15

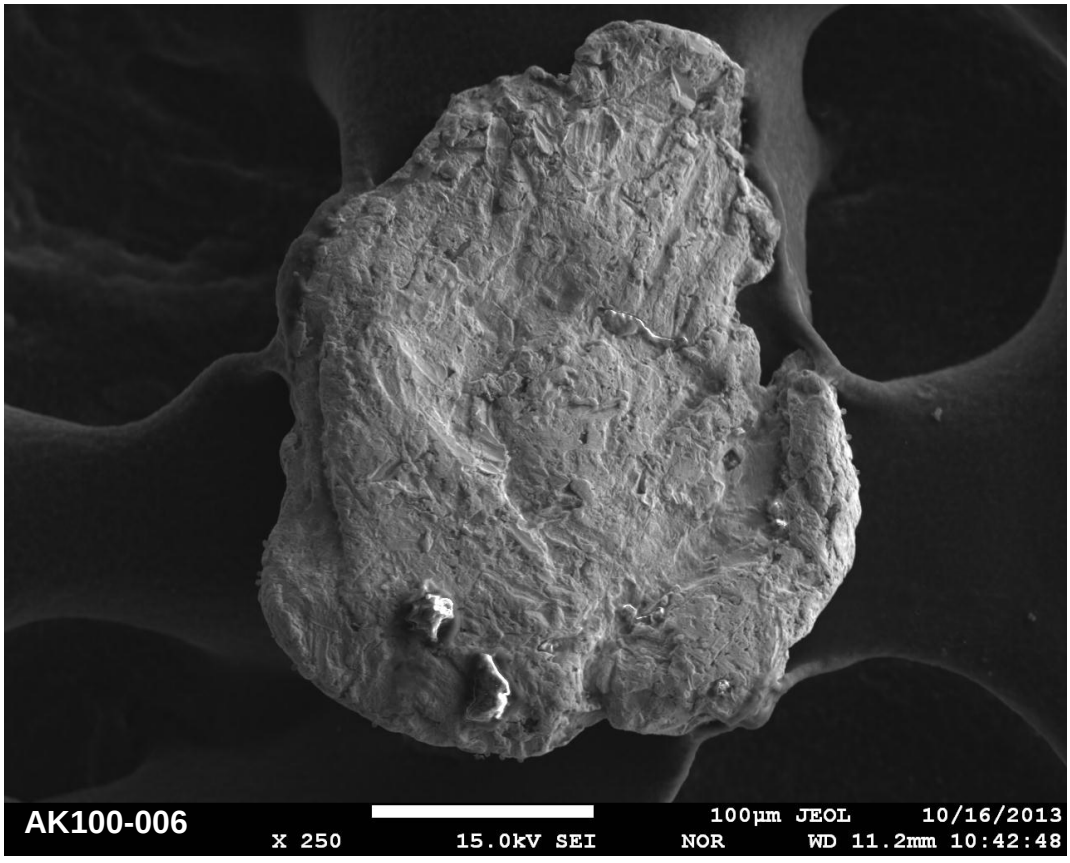
AK100-006
X 250
15.0kV SEI
100µm JEOL
NOR
10/16/2013
WD 11.2mm 10:42:48

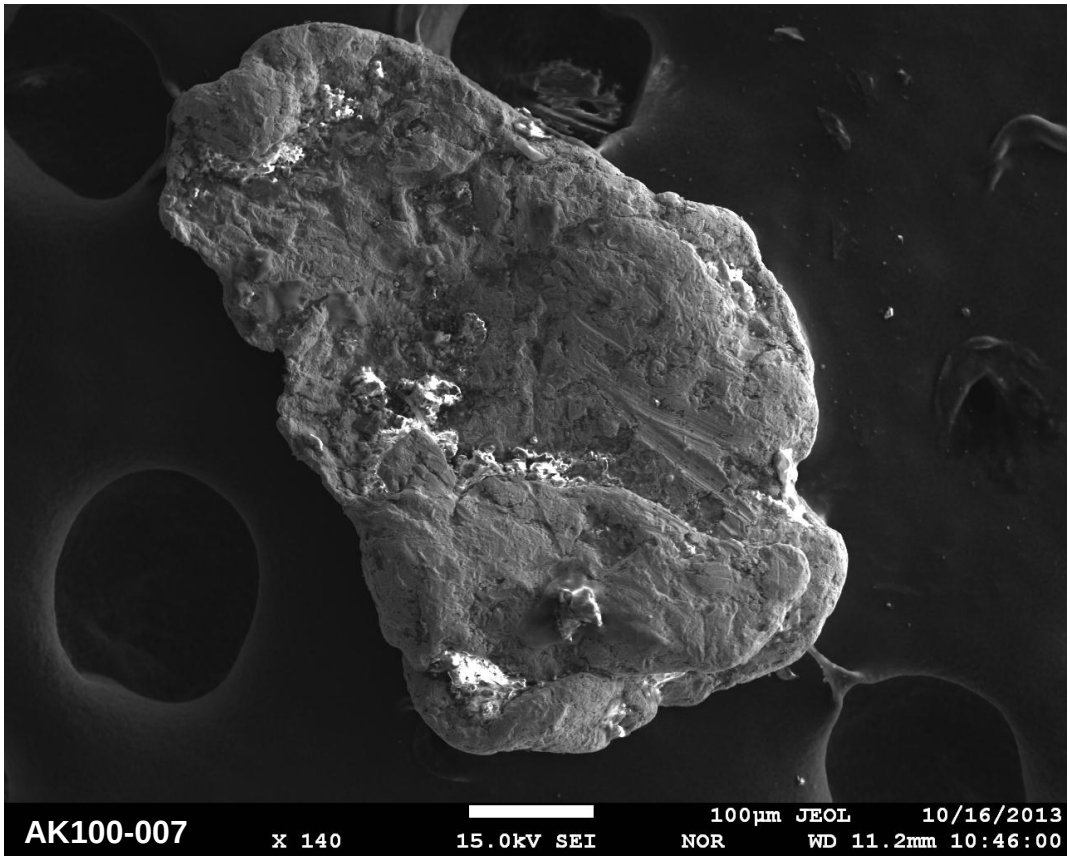
AK100-007
X 140
15.0kV SEI
100µm JEOL
NOR
10/16/2013
WD 11.2mm 10:46:00

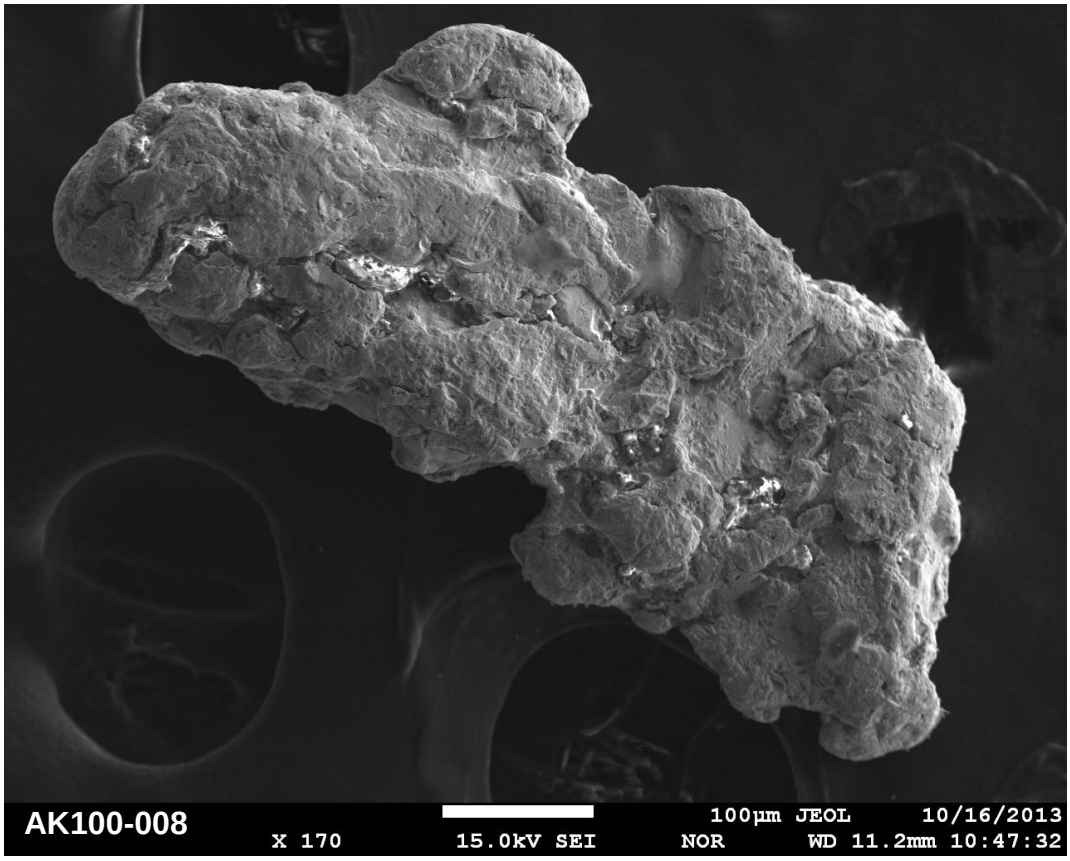
AK100-008
X 170
15.0kV SEI
100µm JEOL
NOR
10/16/2013
WD 11.2mm 10:47:32

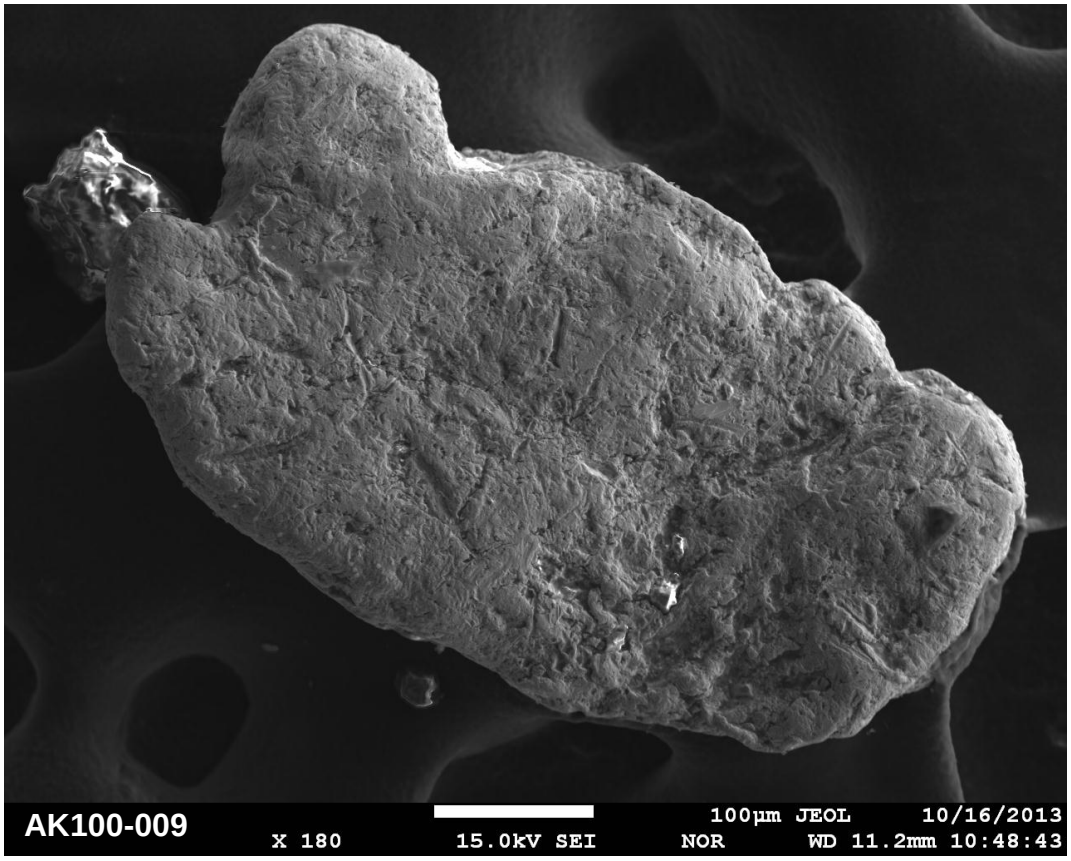
AK100-009
X 180
15.0kV SEI
100µm JEOL
NOR
10/16/2013
WD 11.2mm 10:48:43

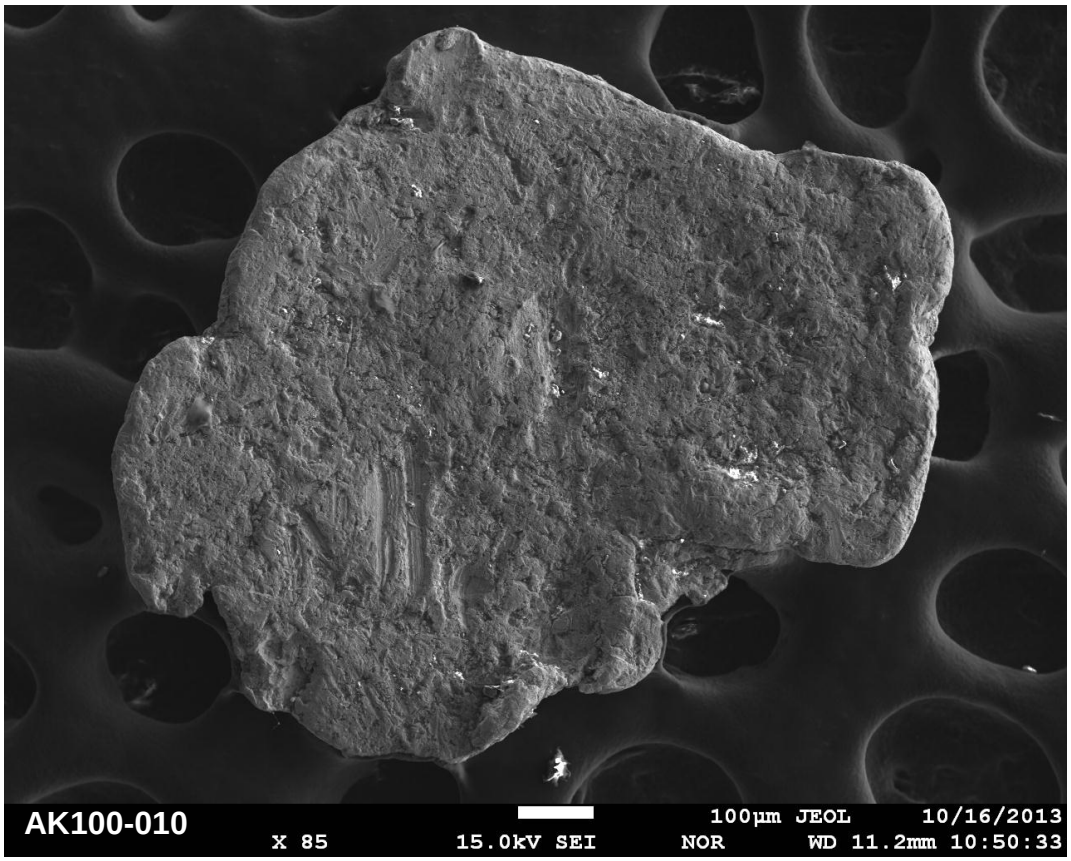
AK100-010
X 85
15.0kV SEI
100µm JEOL
NOR
10/16/2013
WD 11.2mm 10:50:33

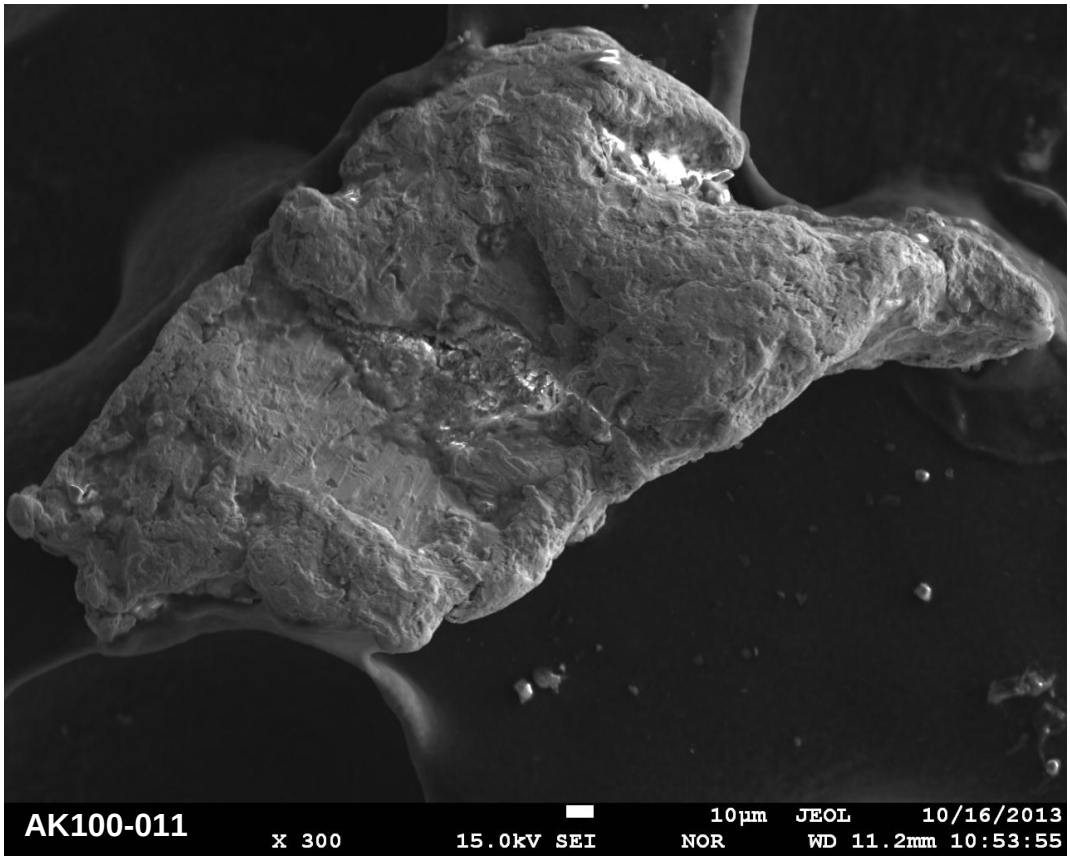
AK100-011
X 300
15.0kV SEI
10µm
NOR
JEOL
WD 11.2mm
10/16/2013
10:53:55

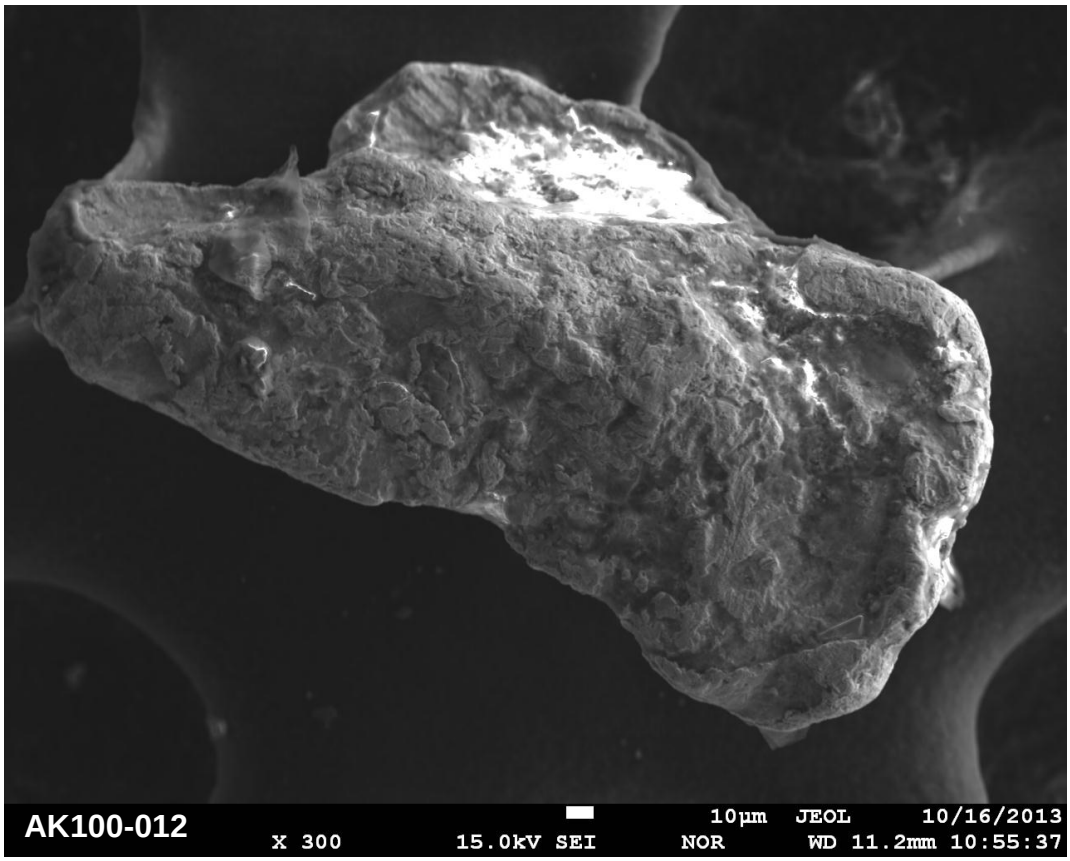
AK100-012
X 300
15.0kV SEI
10µm
NOR
JEOL
WD 11.2mm
10/16/2013
10:55:37

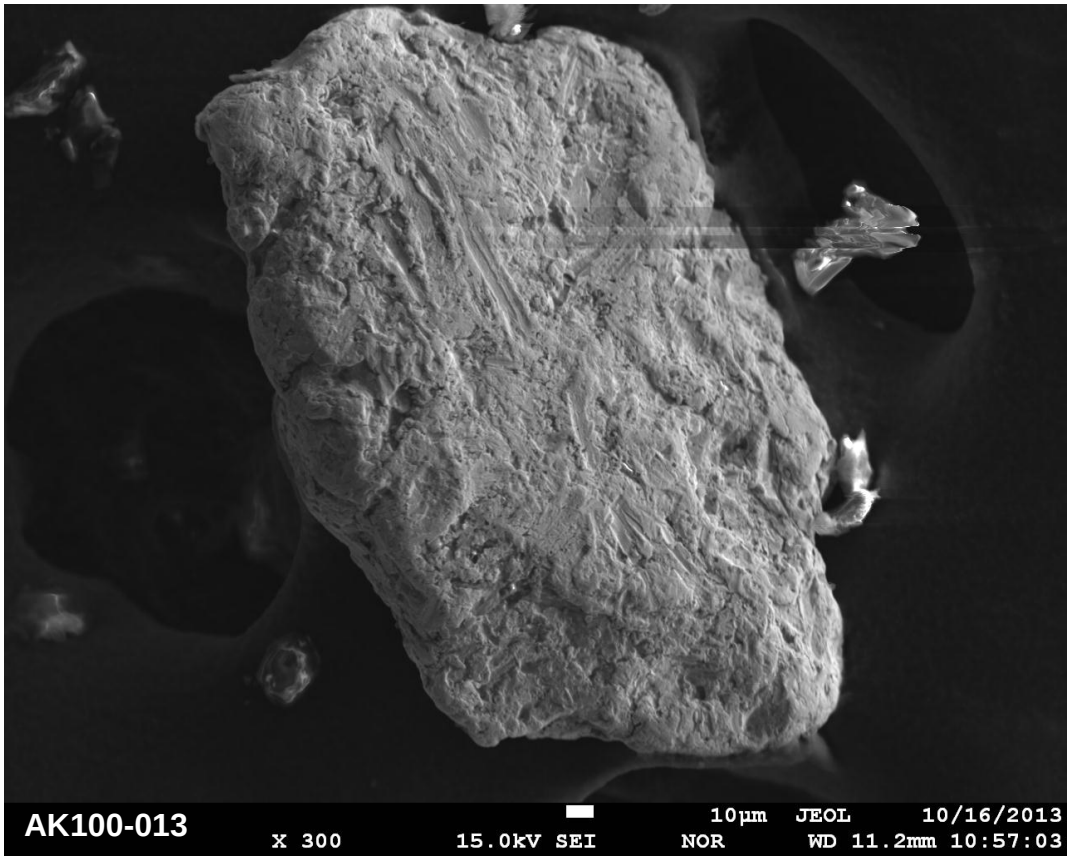
AK100-013
X 300
15.0kV SEI
10µm JEOL
NOR
10/16/2013
WD 11.2mm 10:57:03

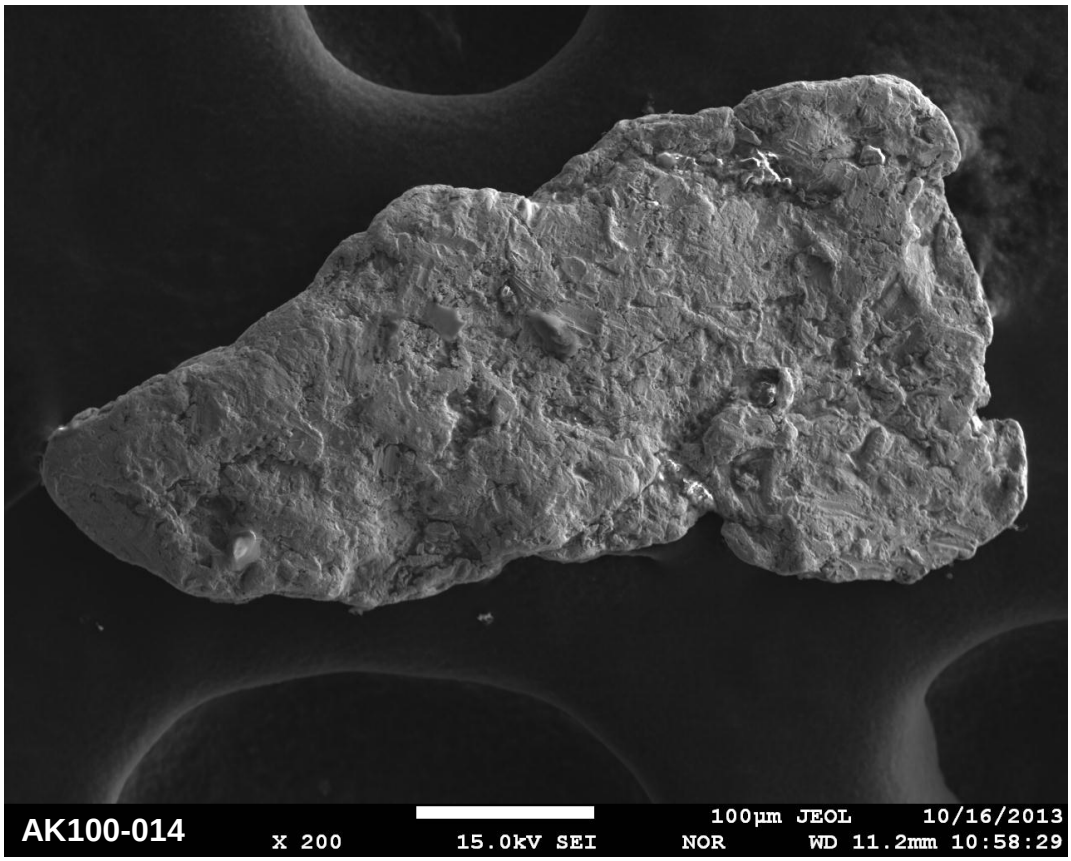
AK100-014
X 200
15.0kV SEI
100µm JEOL
NOR
10/16/2013
WD 11.2mm 10:58:29

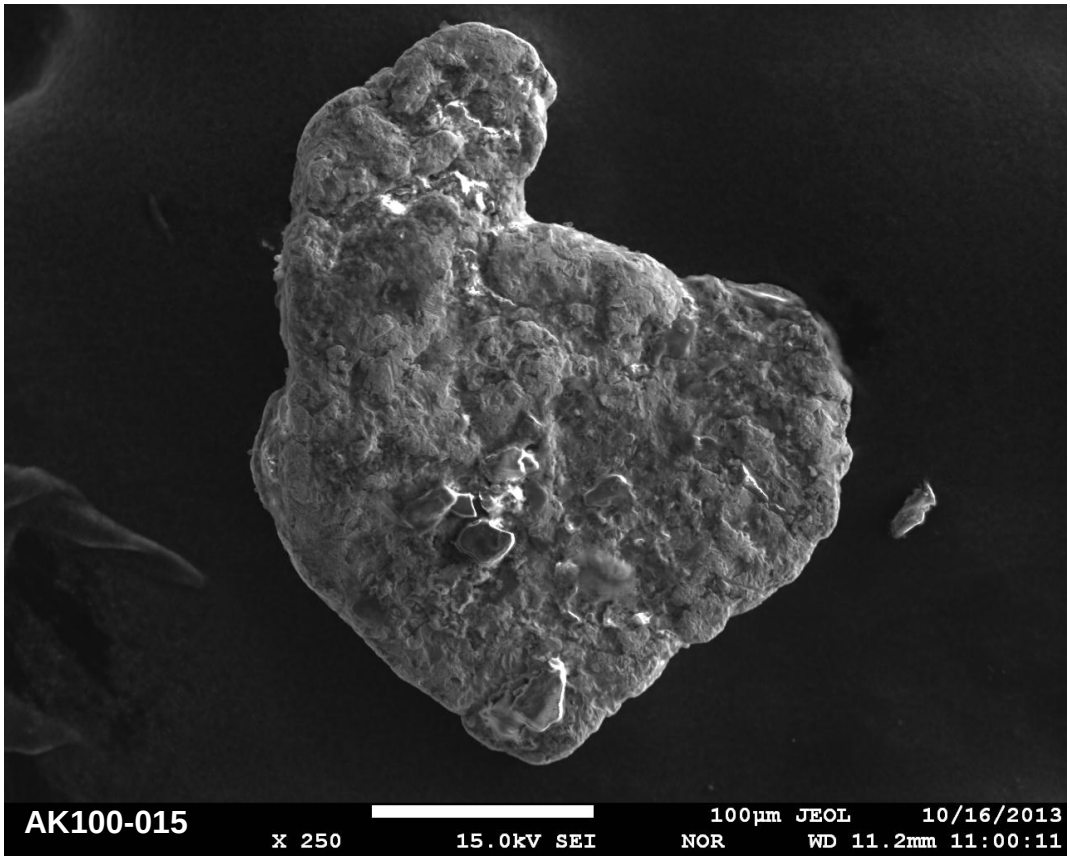
AK100-015
X 250
15.0kV SEI
100µm JEOL
NOR
10/16/2013
WD 11.2mm 11:00:11

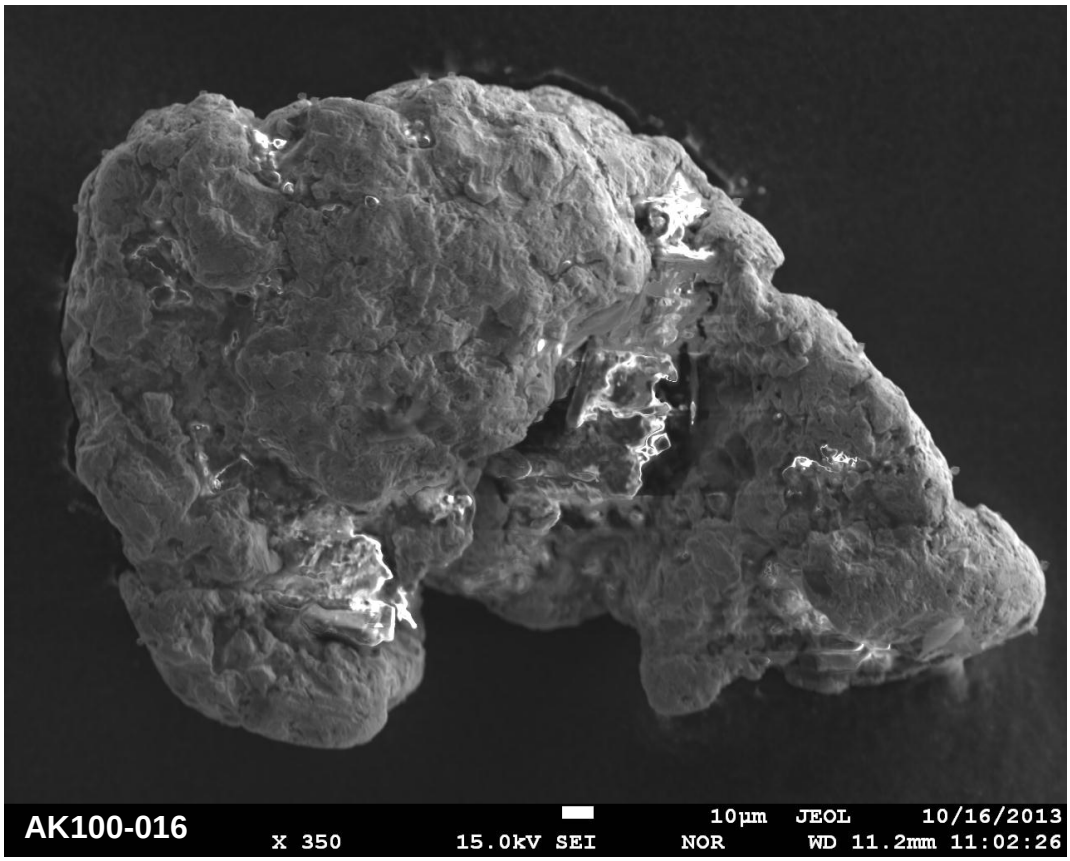
AK100-016
X 350
15.0kV SEI
10µm JEOL
NOR
10/16/2013
WD 11.2mm 11:02:26

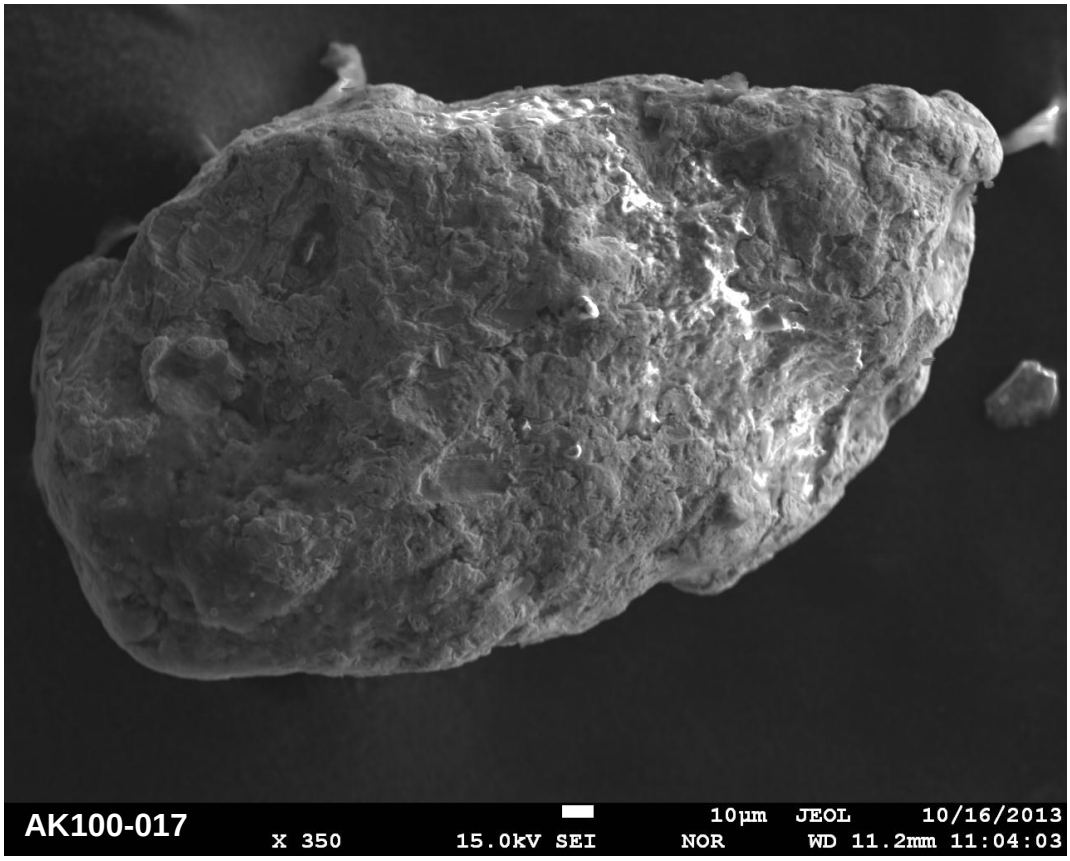
AK100-017
X 350
15.0kV SEI
10µm JEOL
NOR
10/16/2013
WD 11.2mm 11:04:03

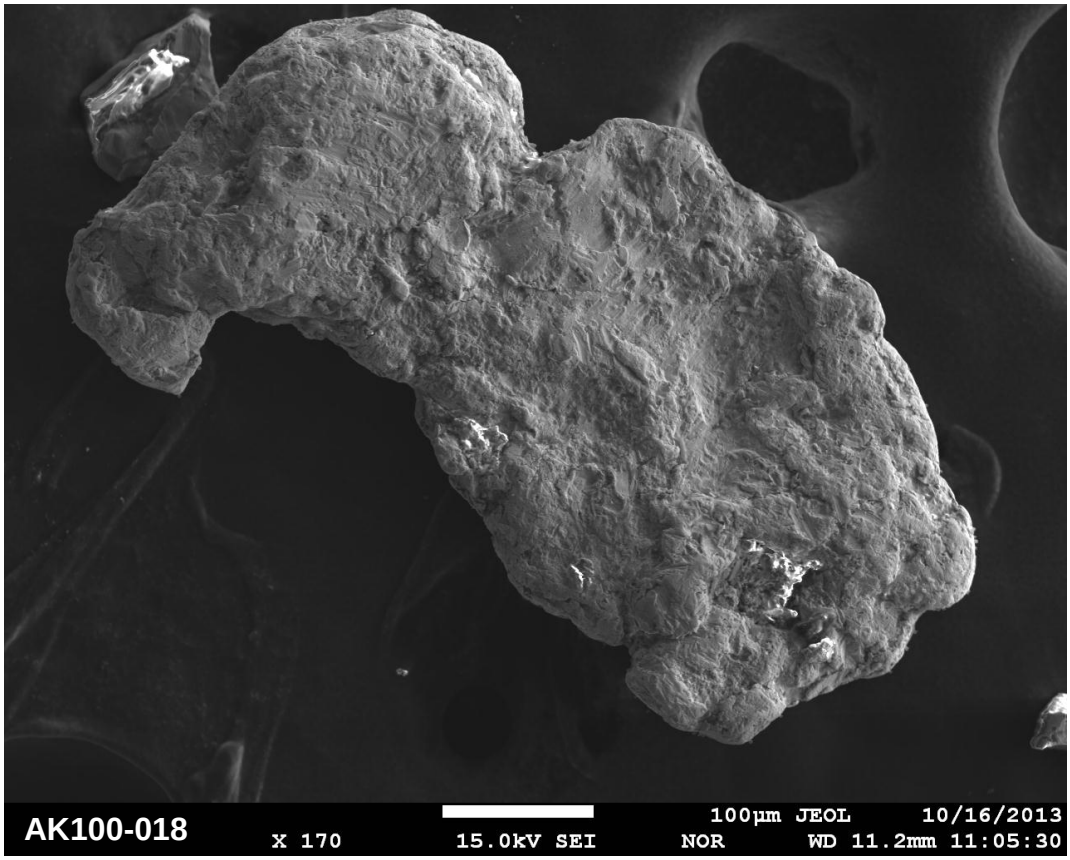
AK100-018
X 170
15.0kV SEI
100µm JEOL
NOR
10/16/2013
WD 11.2mm 11:05:30

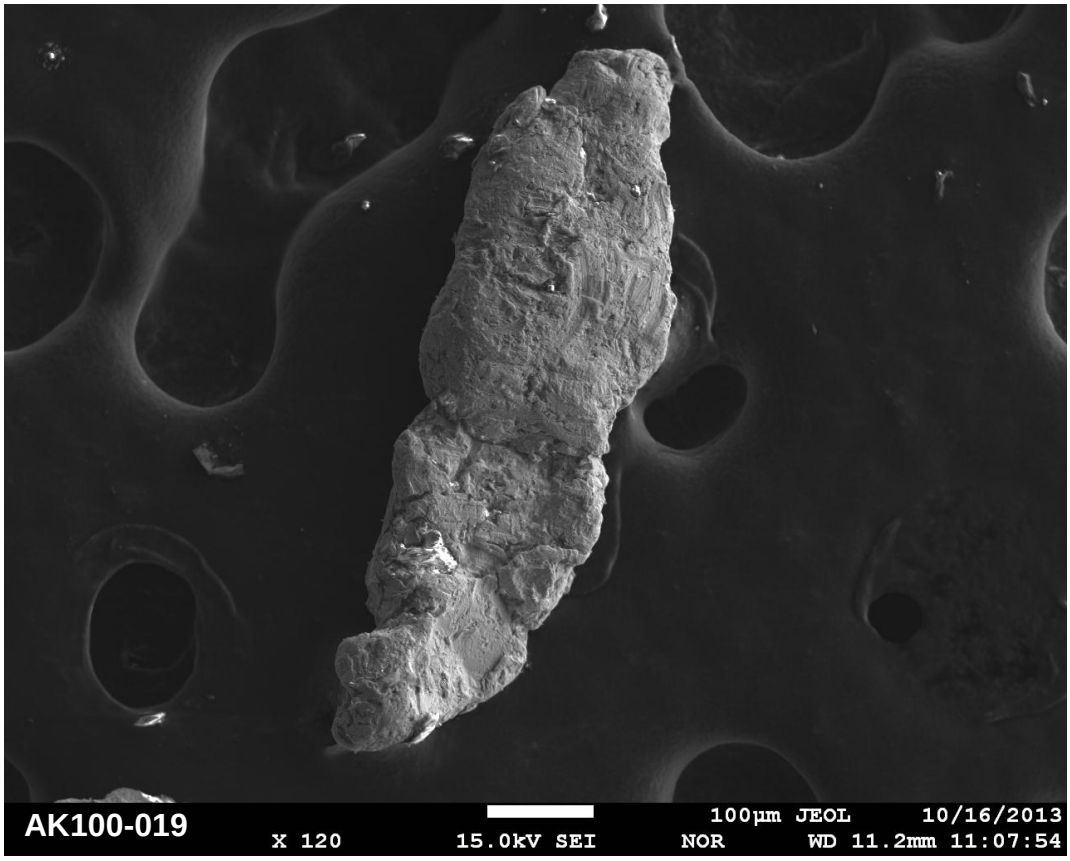
AK100-019
X 120
15.0kV SEI
100µm JEOL
NOR
10/16/2013
WD 11.2mm 11:07:54

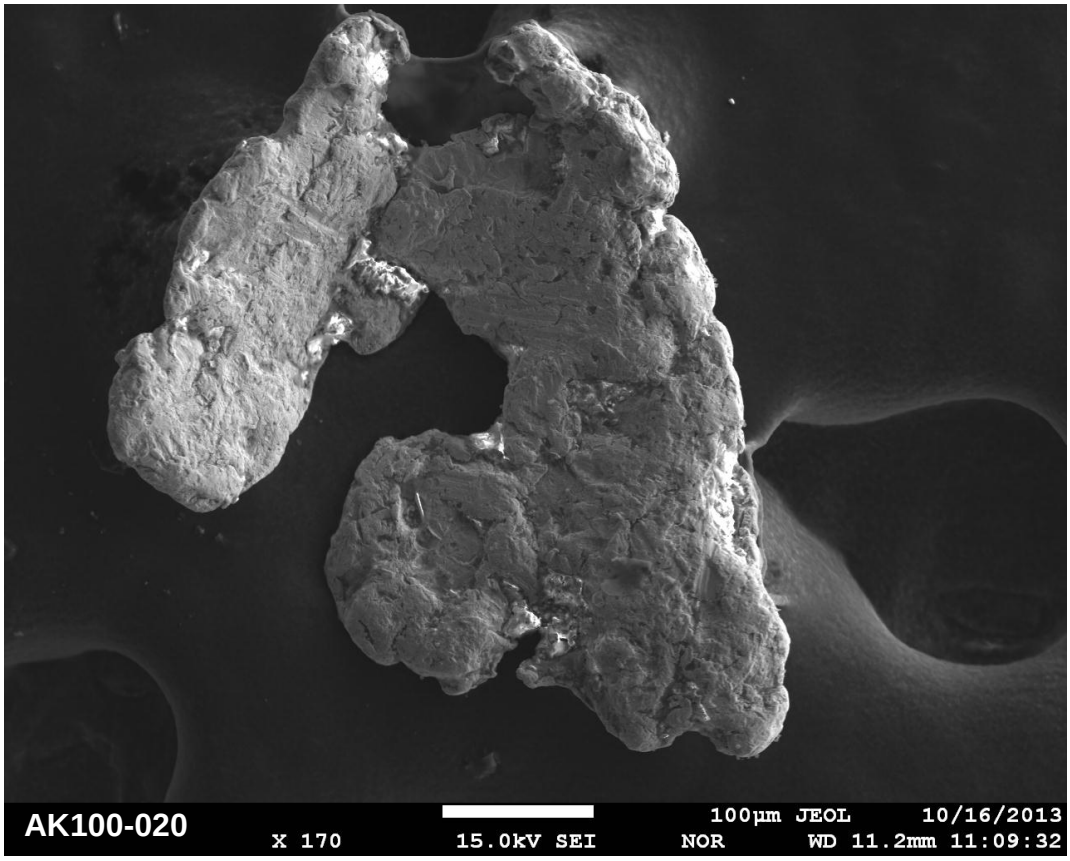
AK100-020
X 170
15.0kV SEI
100µm JEOL
NOR
10/16/2013
WD 11.2mm 11:09:32

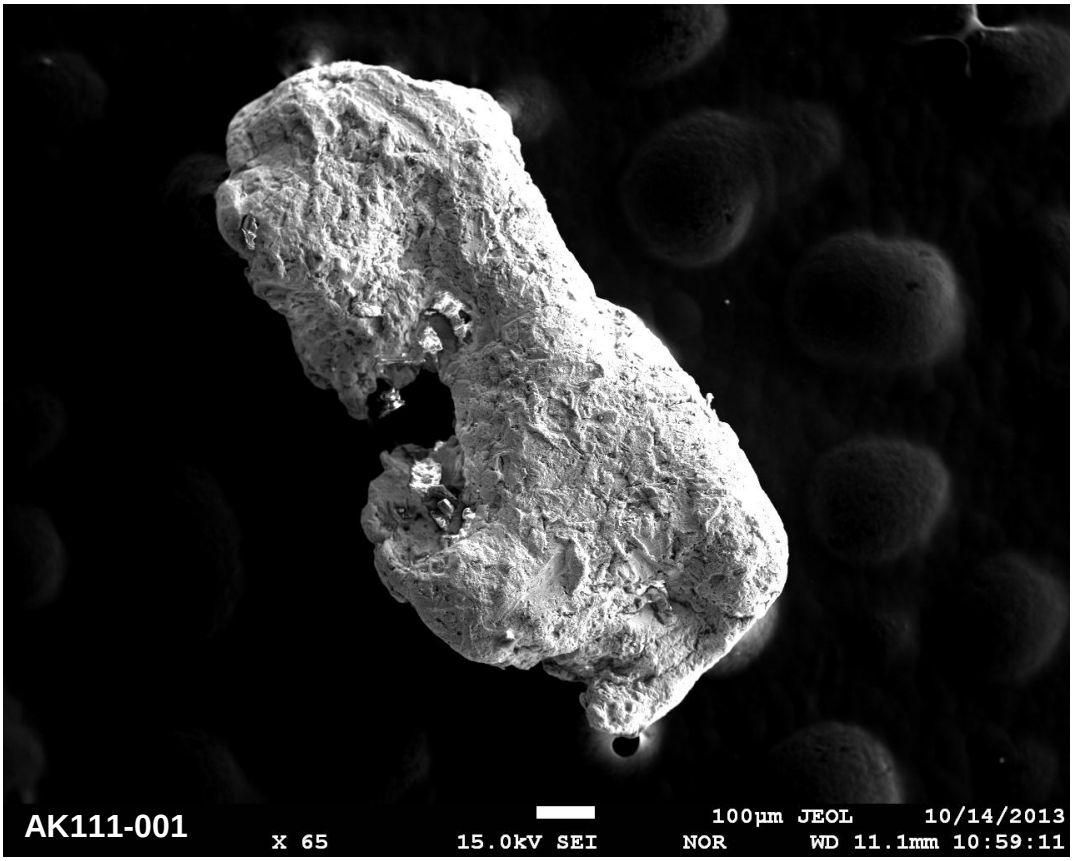
AK111-001
X 65
15.0kV SEI
100µm JEOL
NOR
10/14/2013
WD 11.1mm 10:59:11

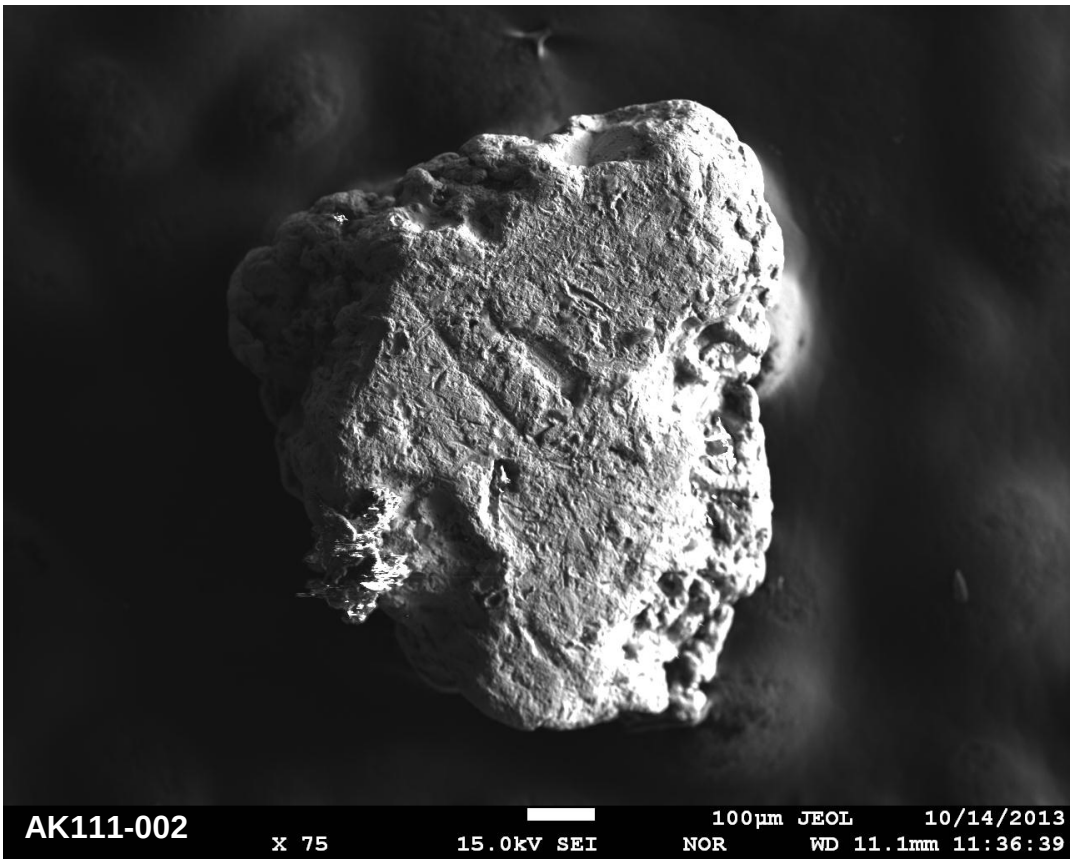
AK111-002
X 75
15.0kV SEI
100µm JEOL
NOR
10/14/2013
WD 11.1mm 11:36:39

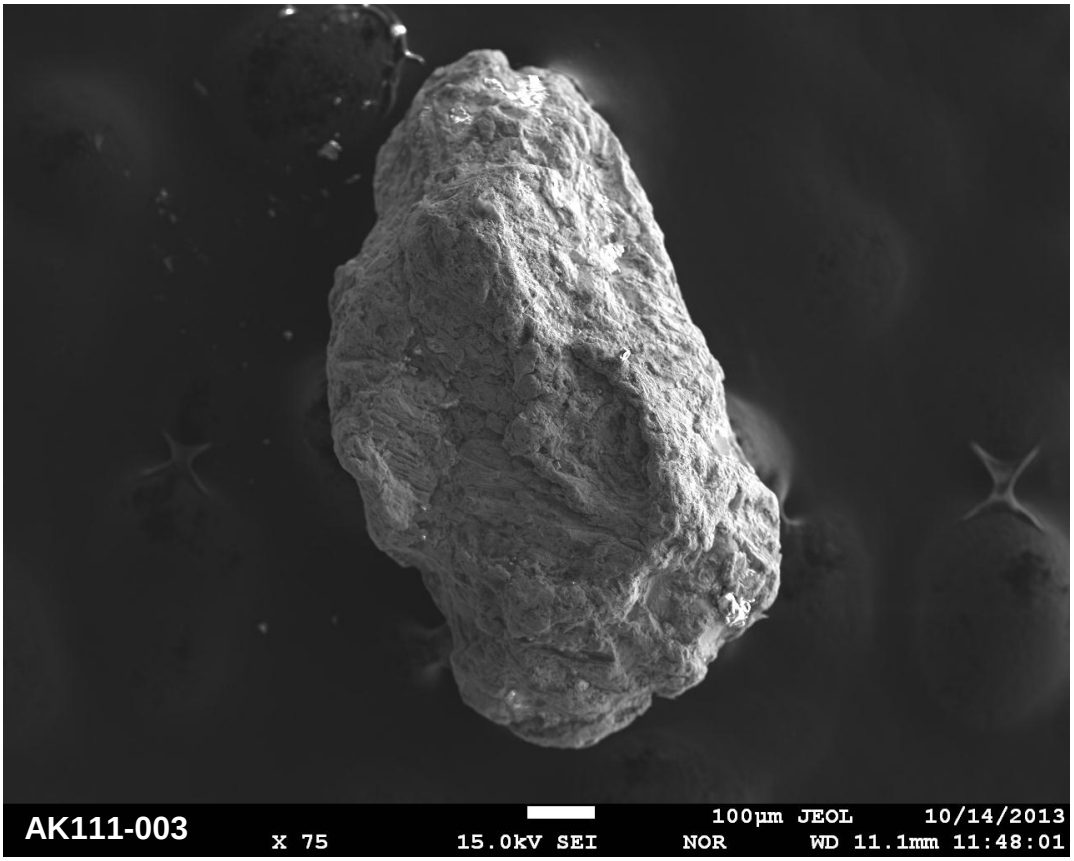
AK111-003
X 75
15.0kV SEI
100µm JEOL
NOR
10/14/2013
WD 11.1mm 11:48:01

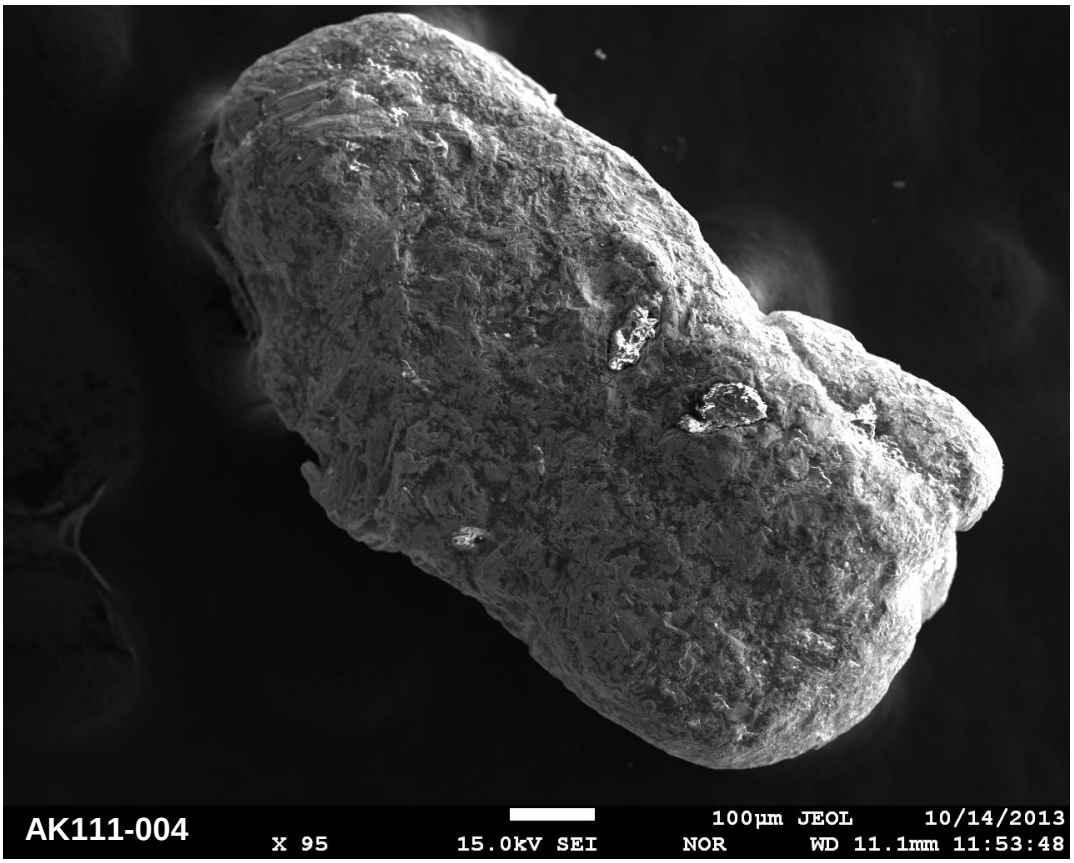
AK111-004
X 95
15.0kV SEI
100µm JEOL
NOR
10/14/2013
WD 11.1mm 11:53:48

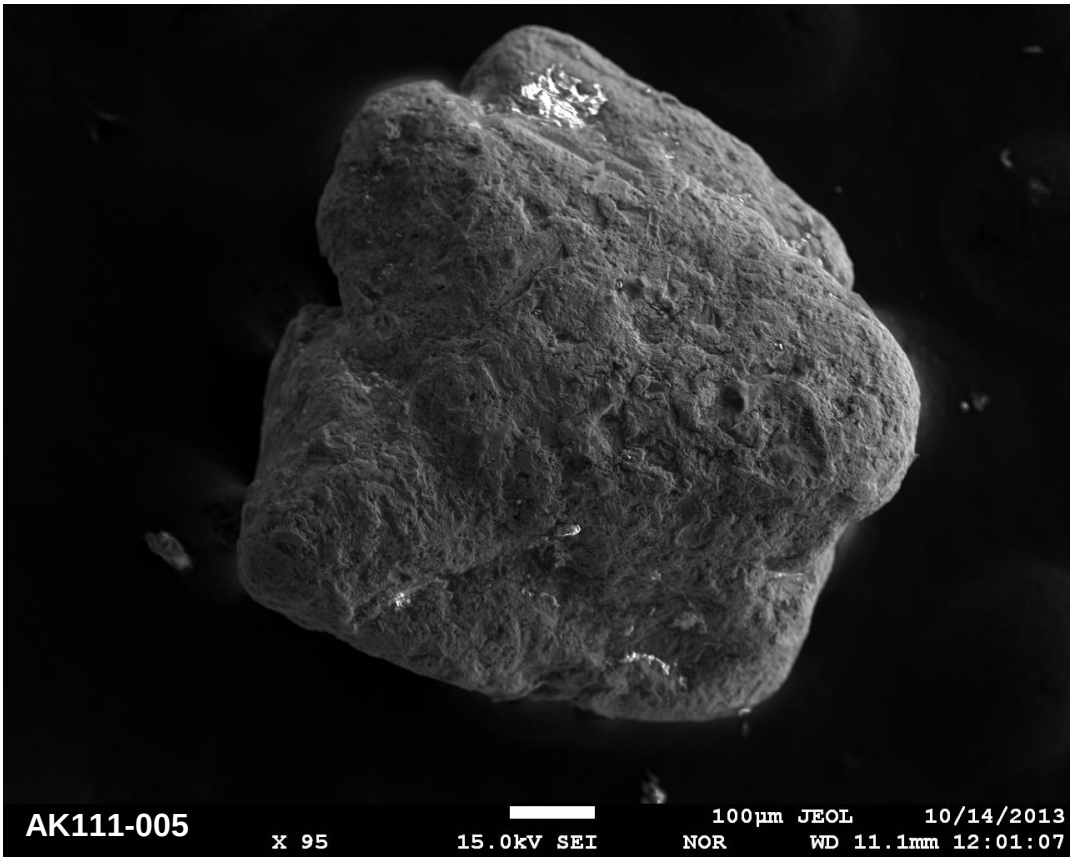
AK111-005
X 95
15.0kV SEI
100µm JEOL
NOR
10/14/2013
WD 11.1mm 12:01:07

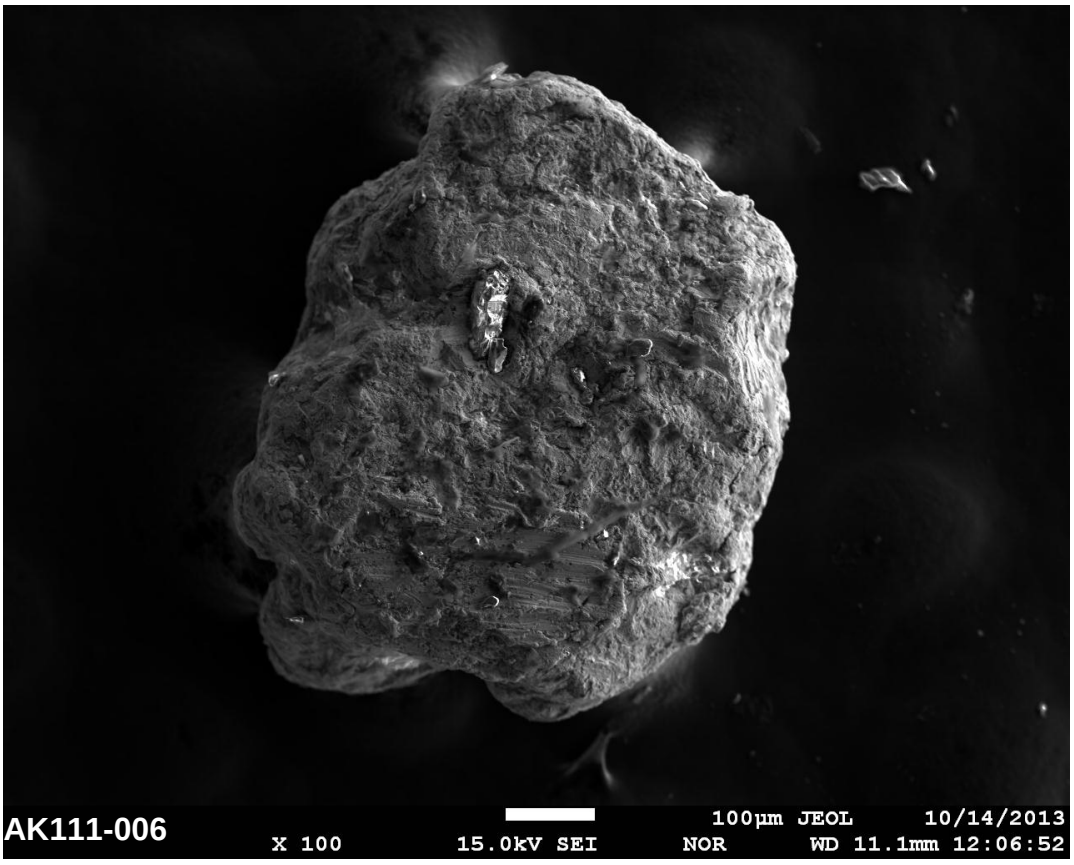
AK111-006
X 100
15.0kV SEI
100µm JEOL
NOR
10/14/2013
WD 11.1mm 12:06:52

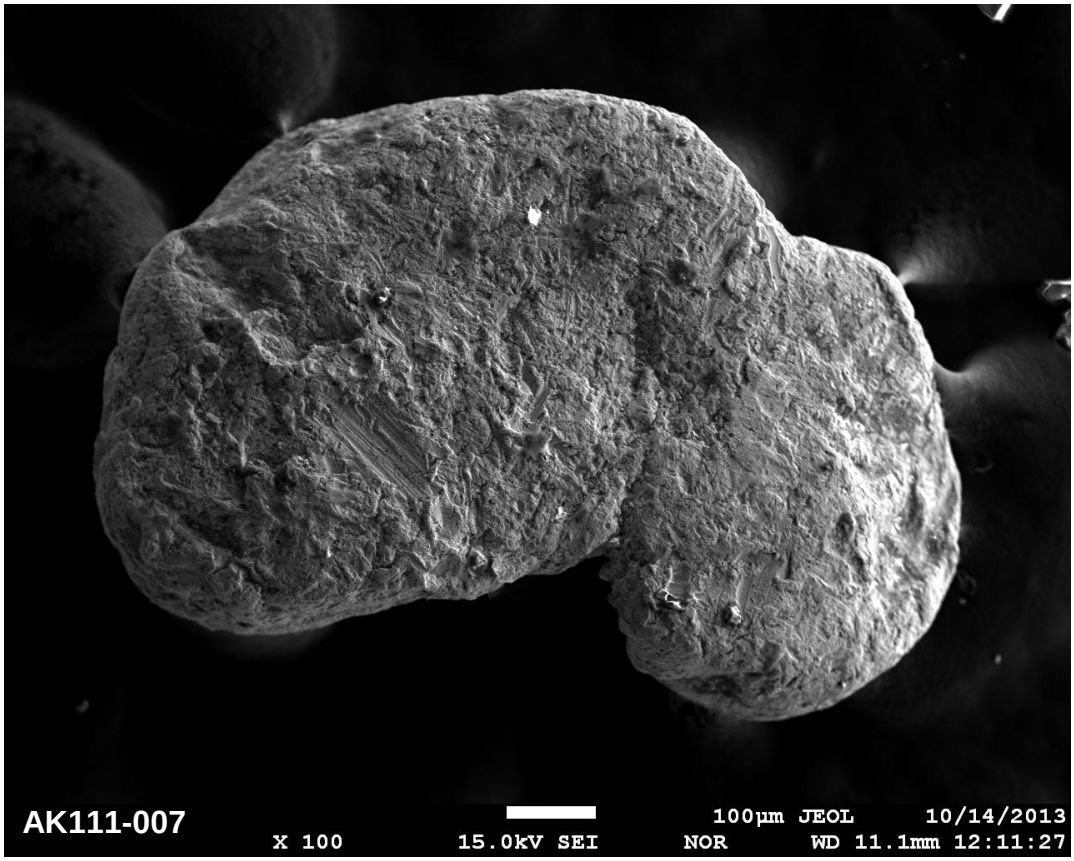
AK111-007
X 100
15.0kV SEI
100µm JEOL
NOR
10/14/2013
WD 11.1mm 12:11:27

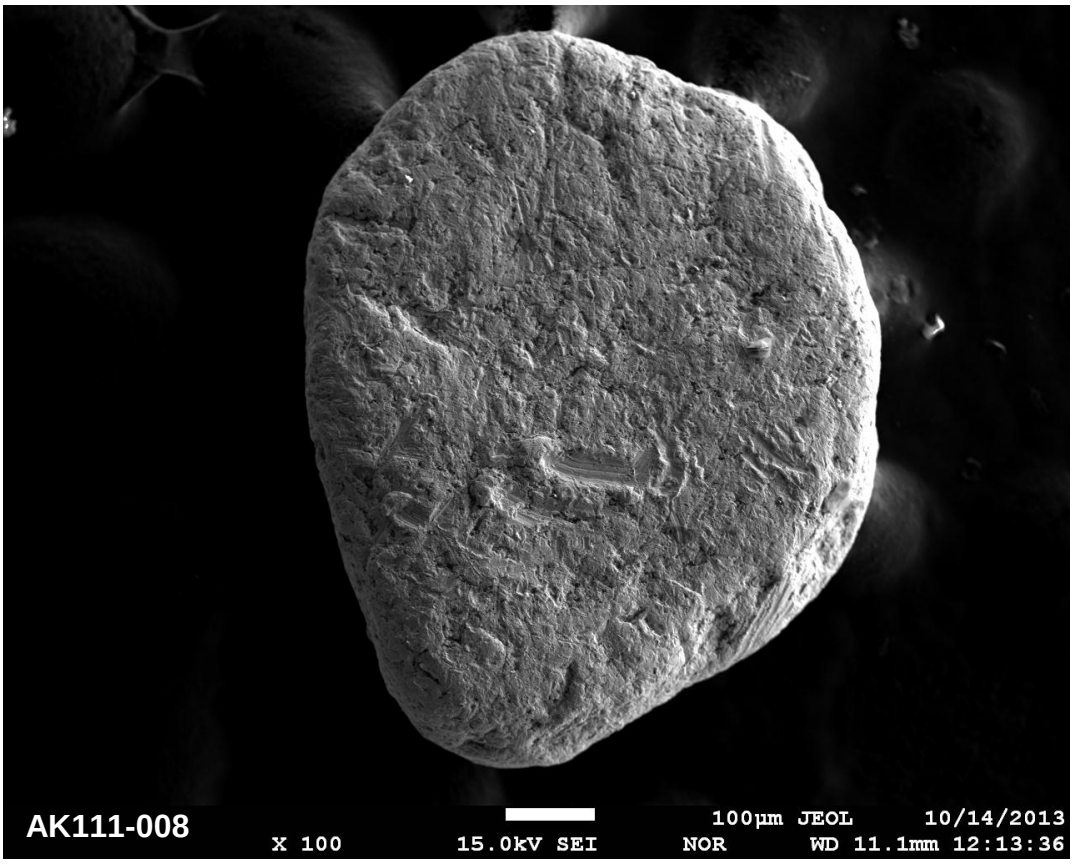
AK111-008
X 100
15.0kV SEI
100µm JEOL
NOR
10/14/2013
WD 11.1mm 12:13:36

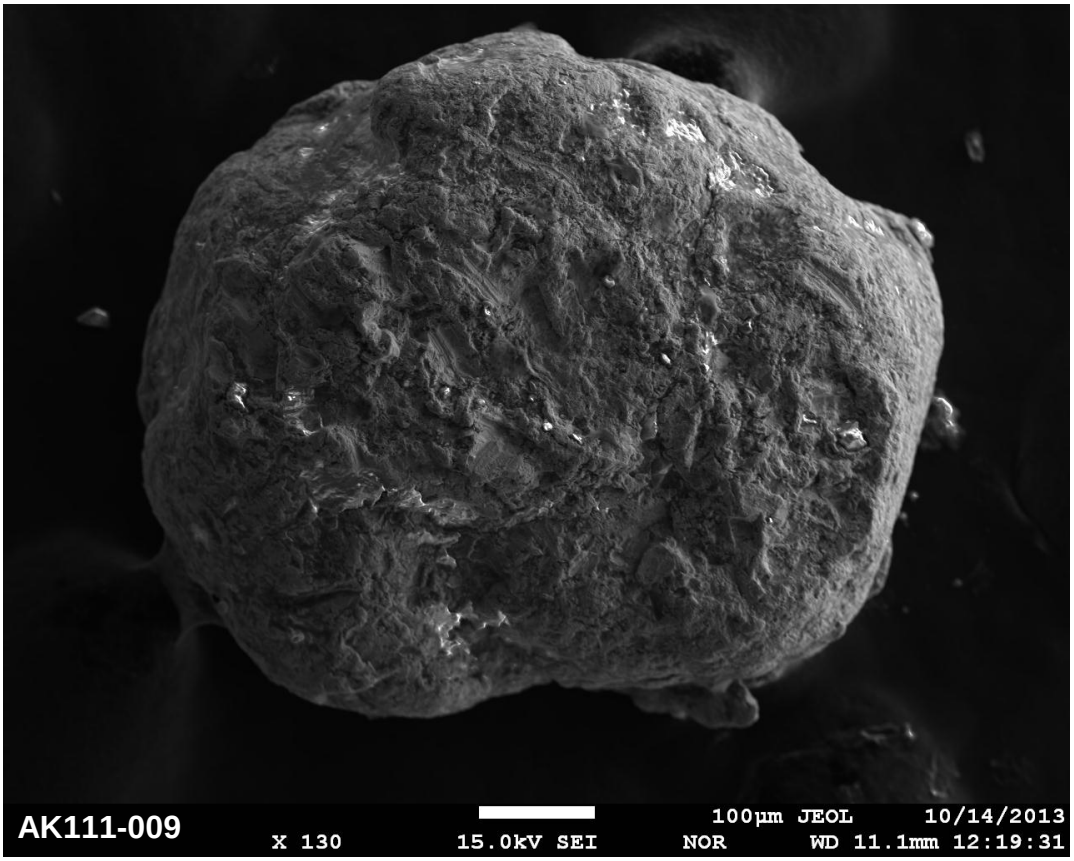
AK111-009
X 130
15.0kV SEI
100µm JEOL
NOR
10/14/2013
WD 11.1mm 12:19:31

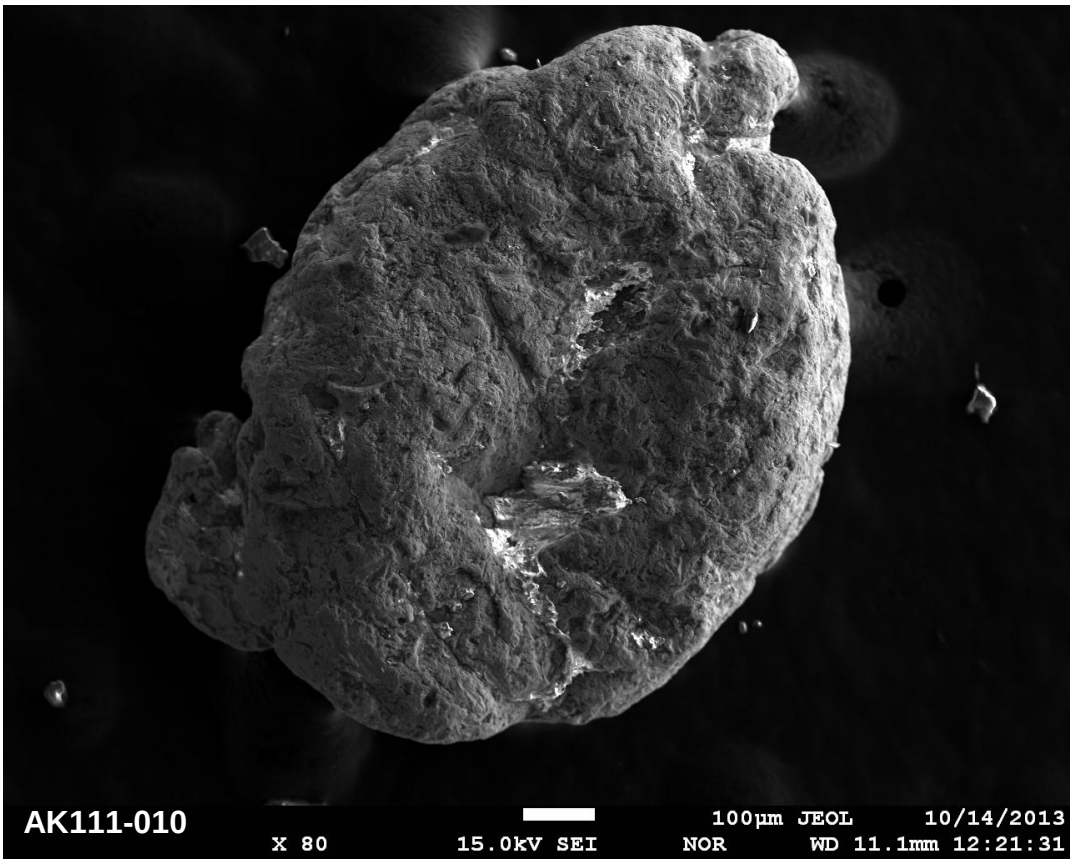
AK111-010
X 80
15.0kV SEI
100µm JEOL
NOR
10/14/2013
WD 11.1mm 12:21:31

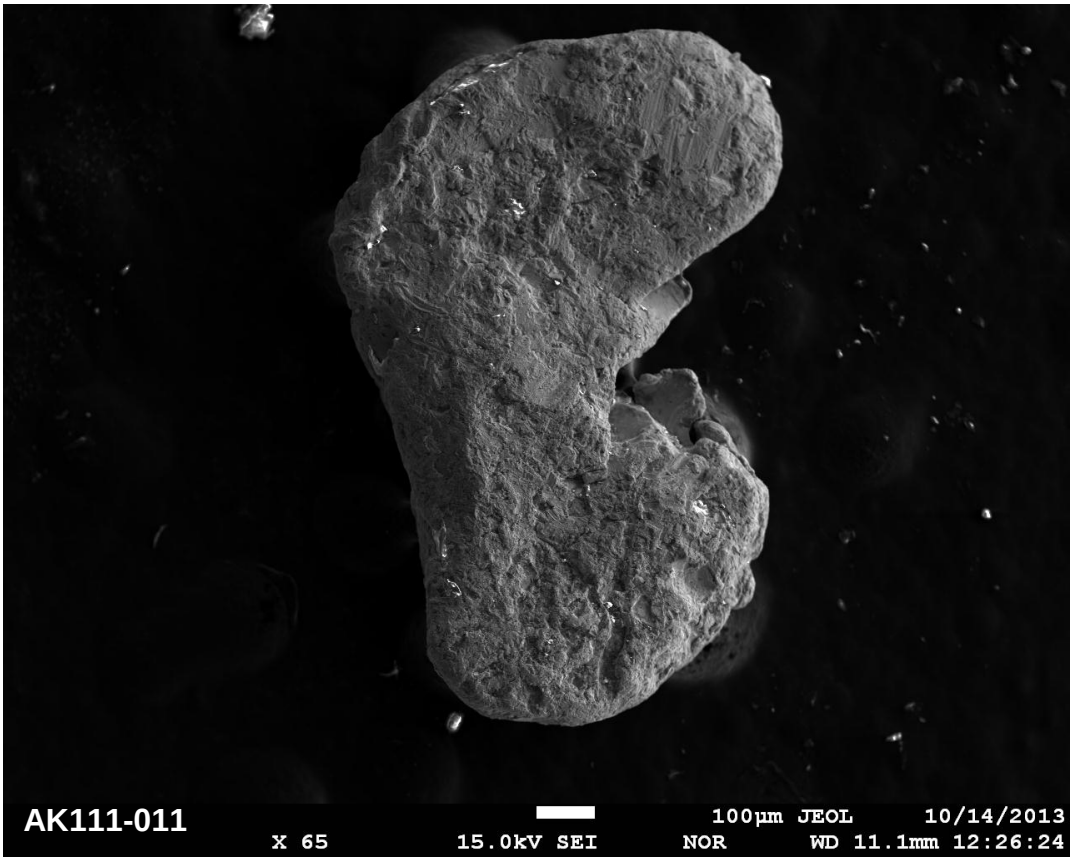
AK111-011
X 65
15.0kV SEI
100µm JEOL
NOR
10/14/2013
WD 11.1mm 12:26:24

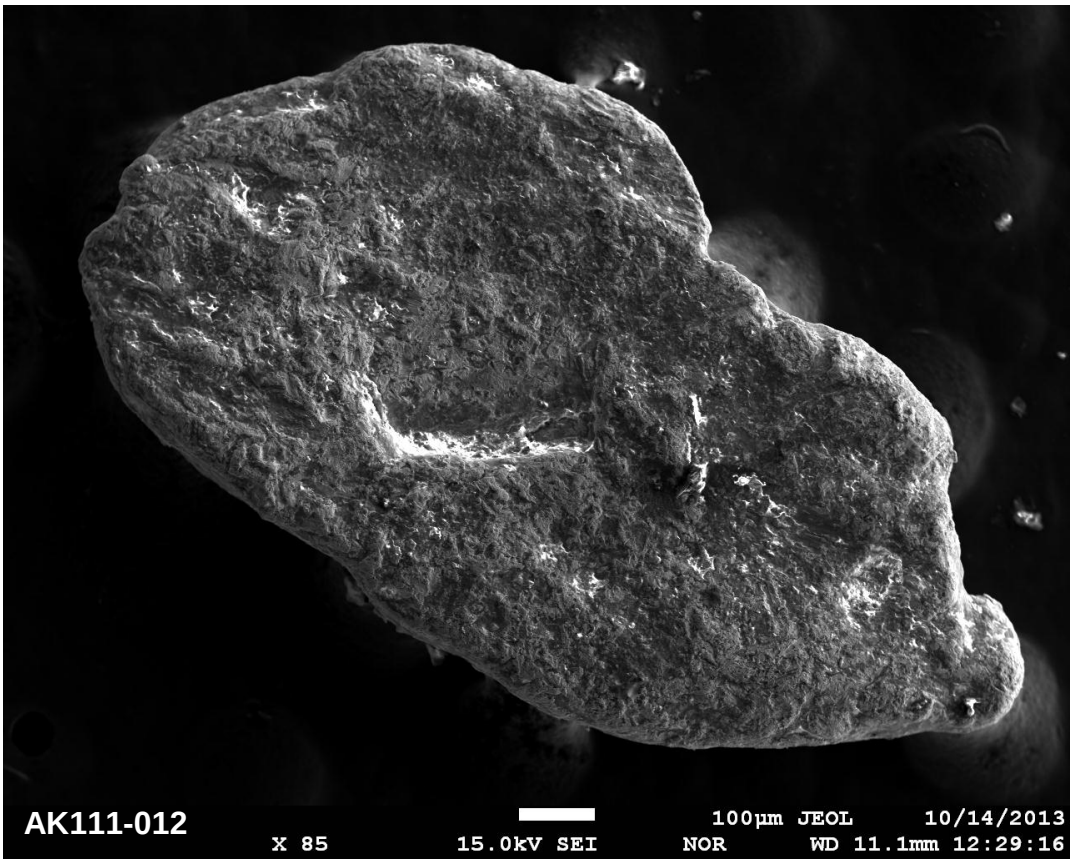
AK111-012
X 85
15.0kV SEI
100µm JEOL
NOR
10/14/2013
WD 11.1mm 12:29:16

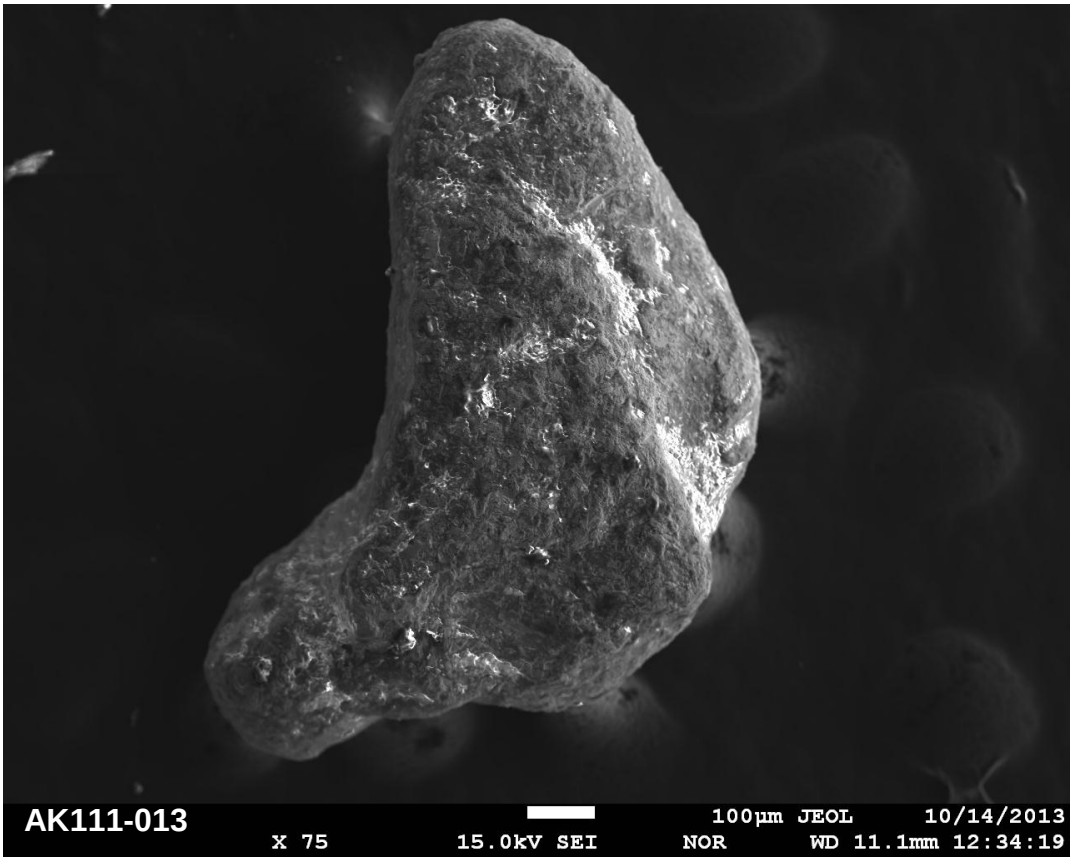
AK111-013
X 75
15.0kV SEI
100µm JEOL
NOR
10/14/2013
WD 11.1mm 12:34:19

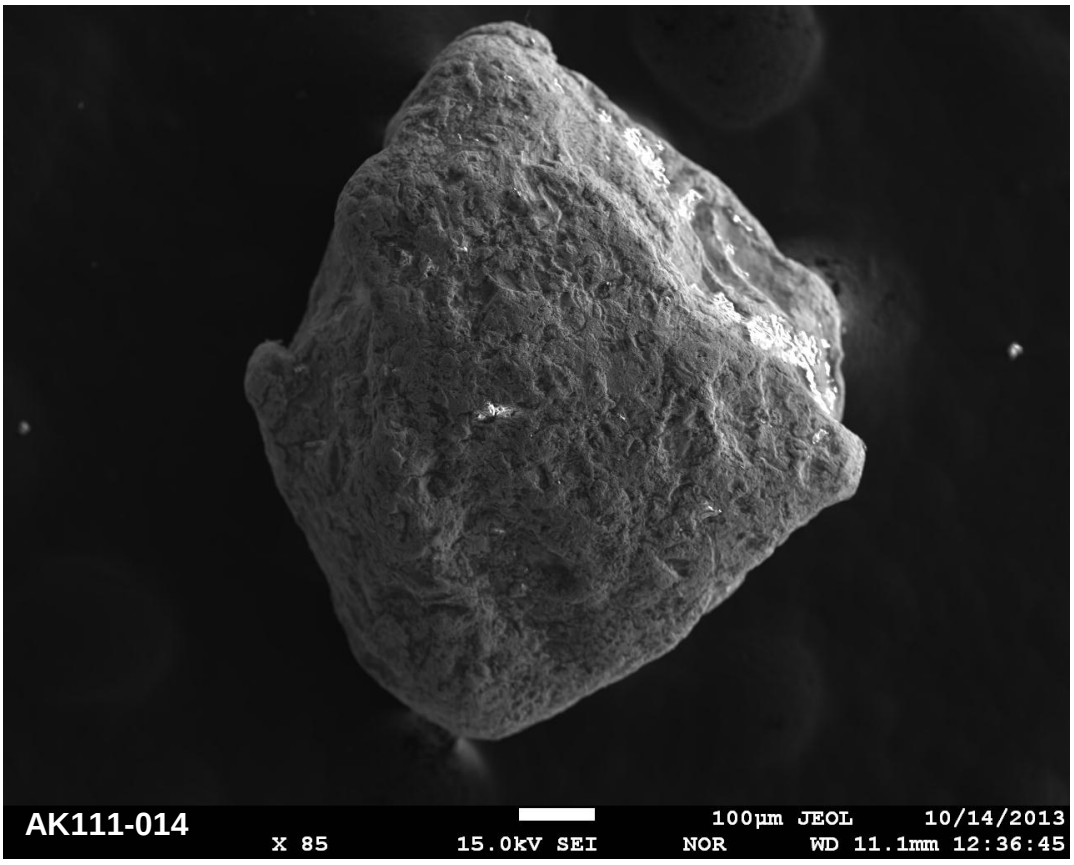
AK111-014
X 85
15.0kV SEI
100µm JEOL
NOR
10/14/2013
WD 11.1mm 12:36:45

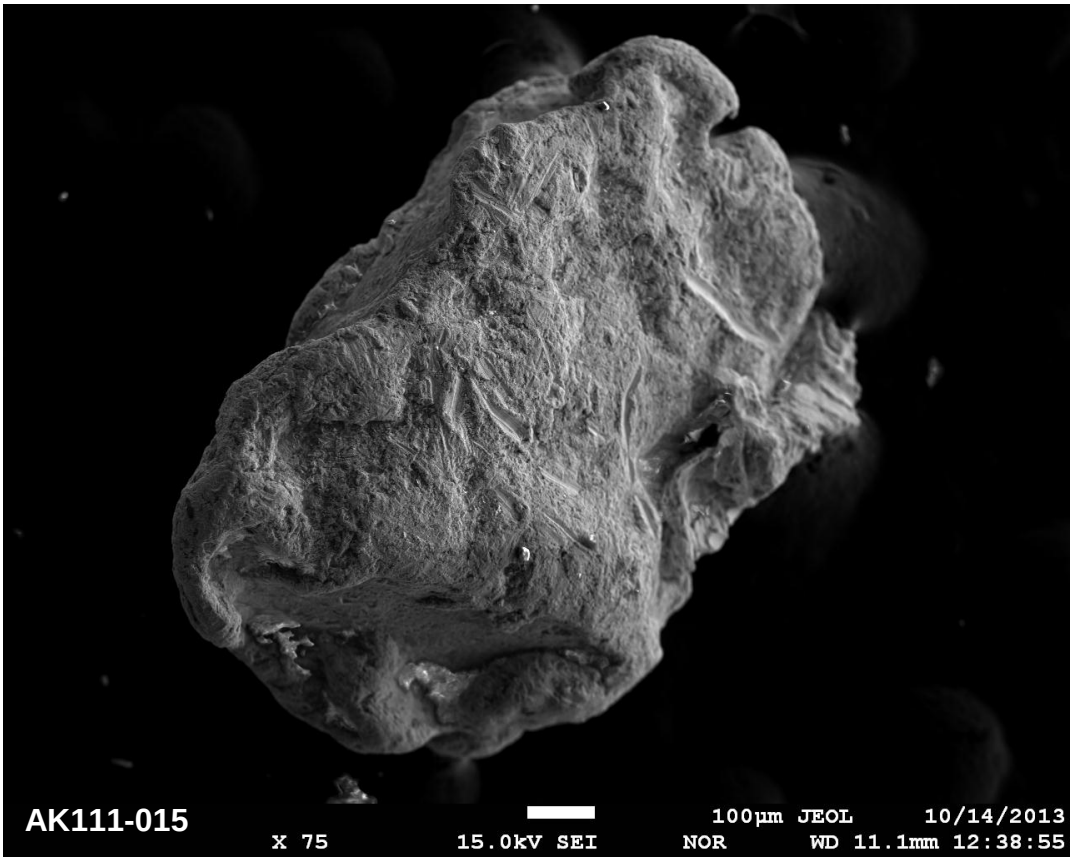
AK111-015
X 75
15.0kV SEI
100µm JEOL
NOR
10/14/2013
WD 11.1mm 12:38:55

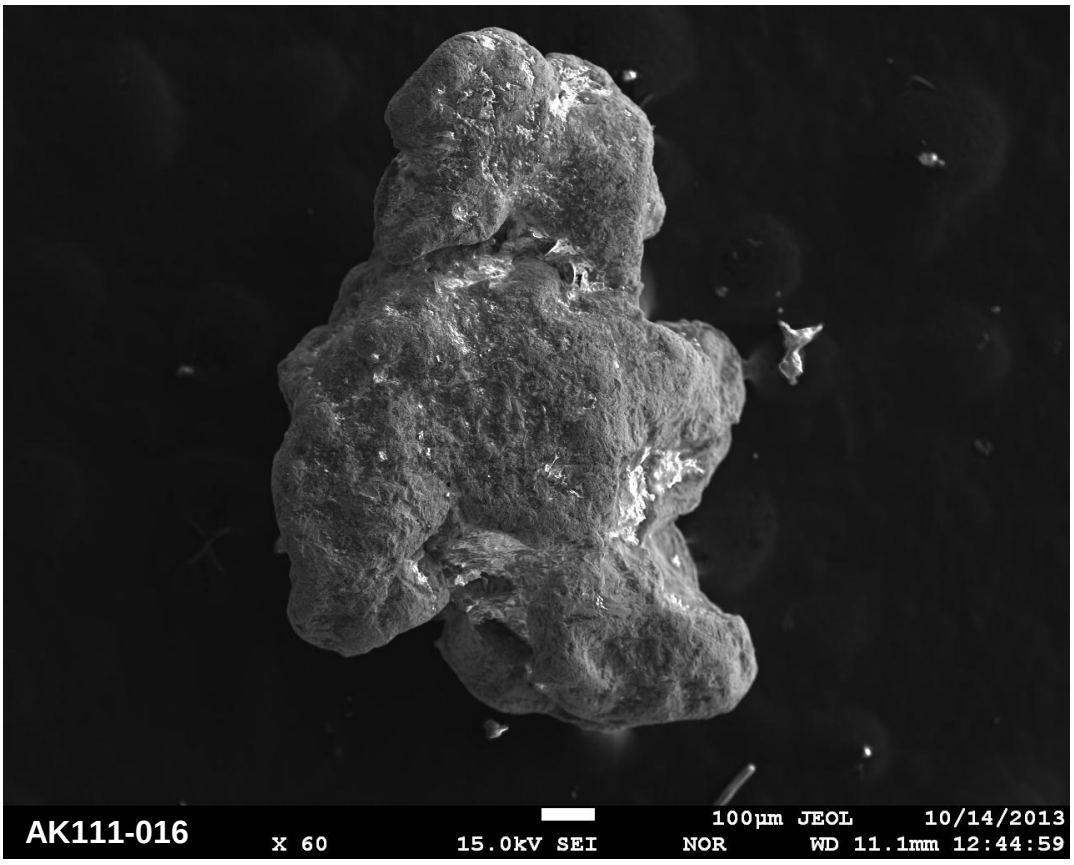
AK111-016
X 60
15.0kV SEI
100µm JEOL
NOR
10/14/2013
WD 11.1mm 12:44:59

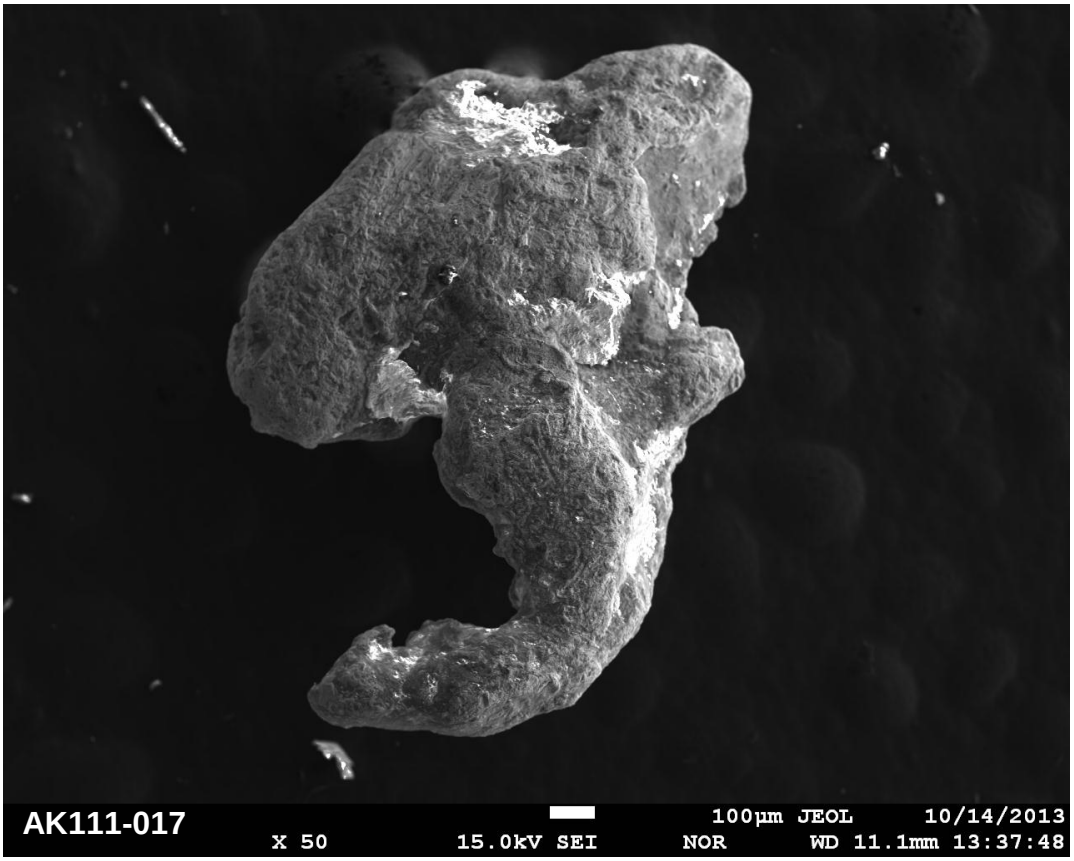
AK111-017
X 50
15.0kV SEI
100µm JEOL
NOR
10/14/2013
WD 11.1mm 13:37:48

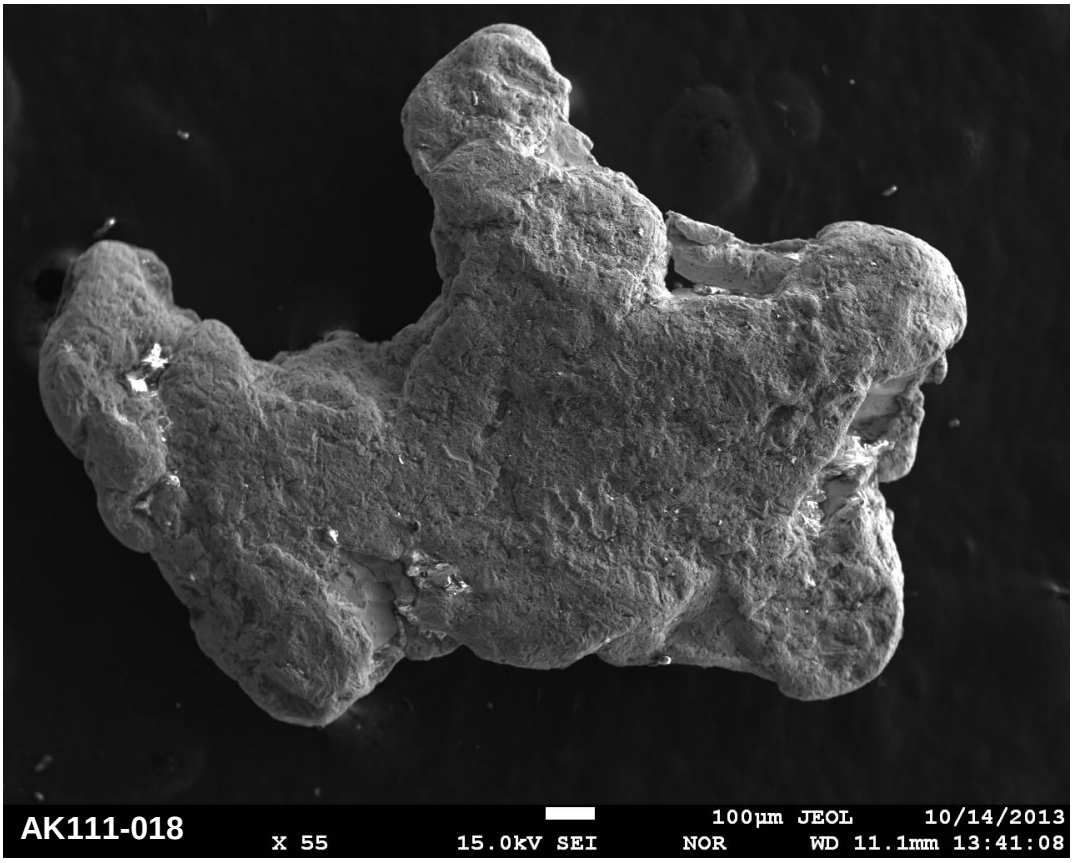
AK111-018
X 55
15.0kV SEI
100µm JEOL
NOR
10/14/2013
WD 11.1mm 13:41:08

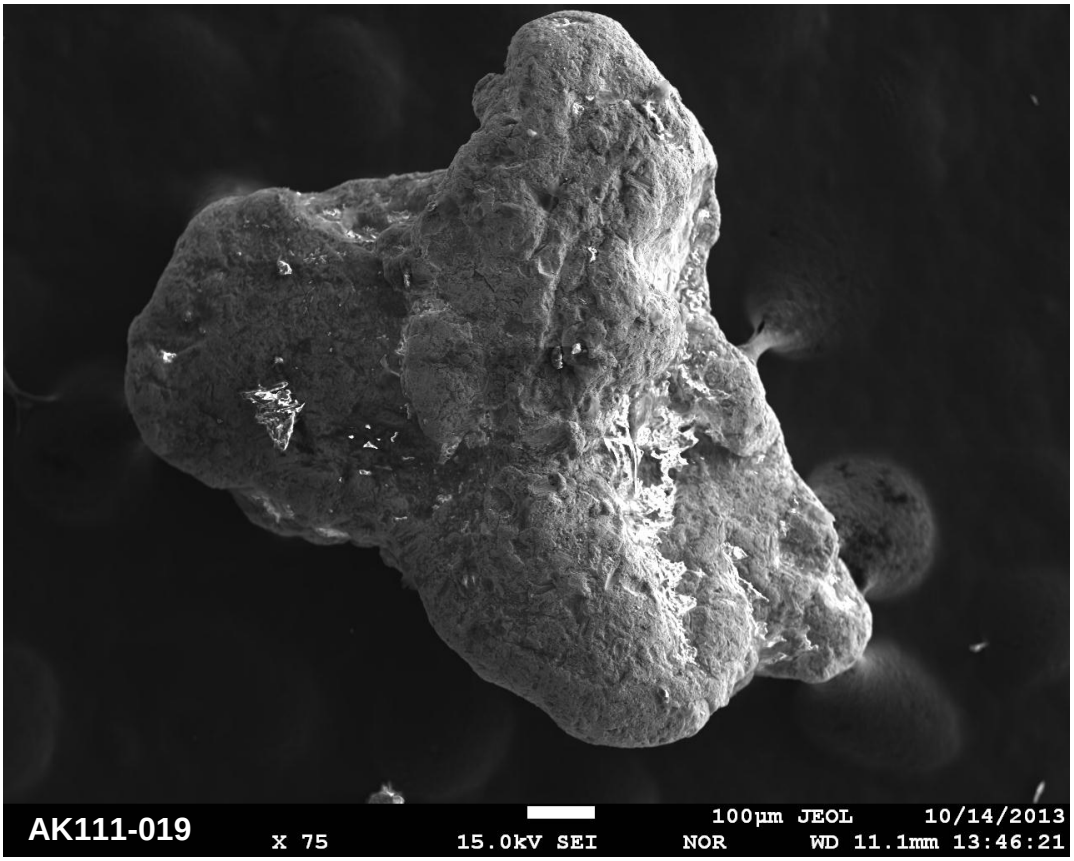
AK111-019
X 75
15.0kV SEI
100µm JEOL
NOR
10/14/2013
WD 11.1mm 13:46:21

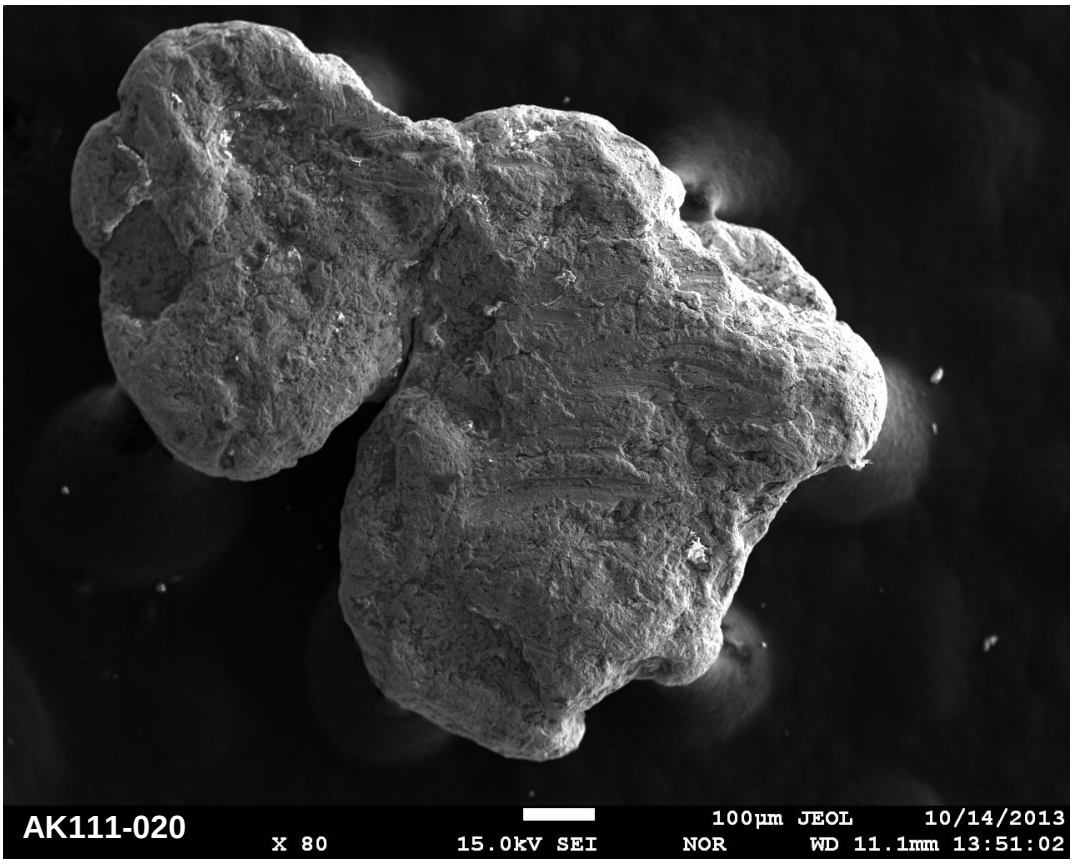
AK111-020
X 80
15.0kV SEI
100µm JEOL
NOR
10/14/2013
WD 11.1mm 13:51:02


AK117-001
X 90
15.0kV SEI
100µm JEOL
NOR
10/15/2013
WD 11.1mm 15:33:22

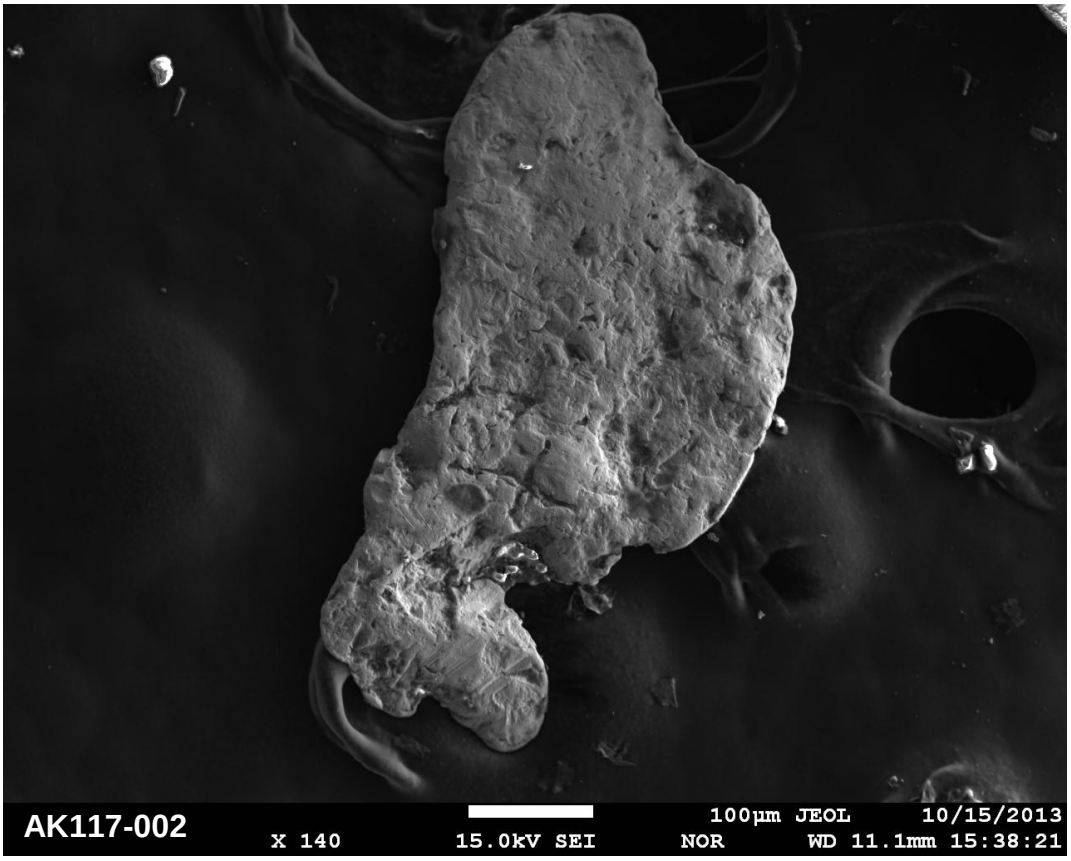
AK117-002
X 140
15.0kV SEI
100µm JEOL
NOR
10/15/2013
WD 11.1mm 15:38:21

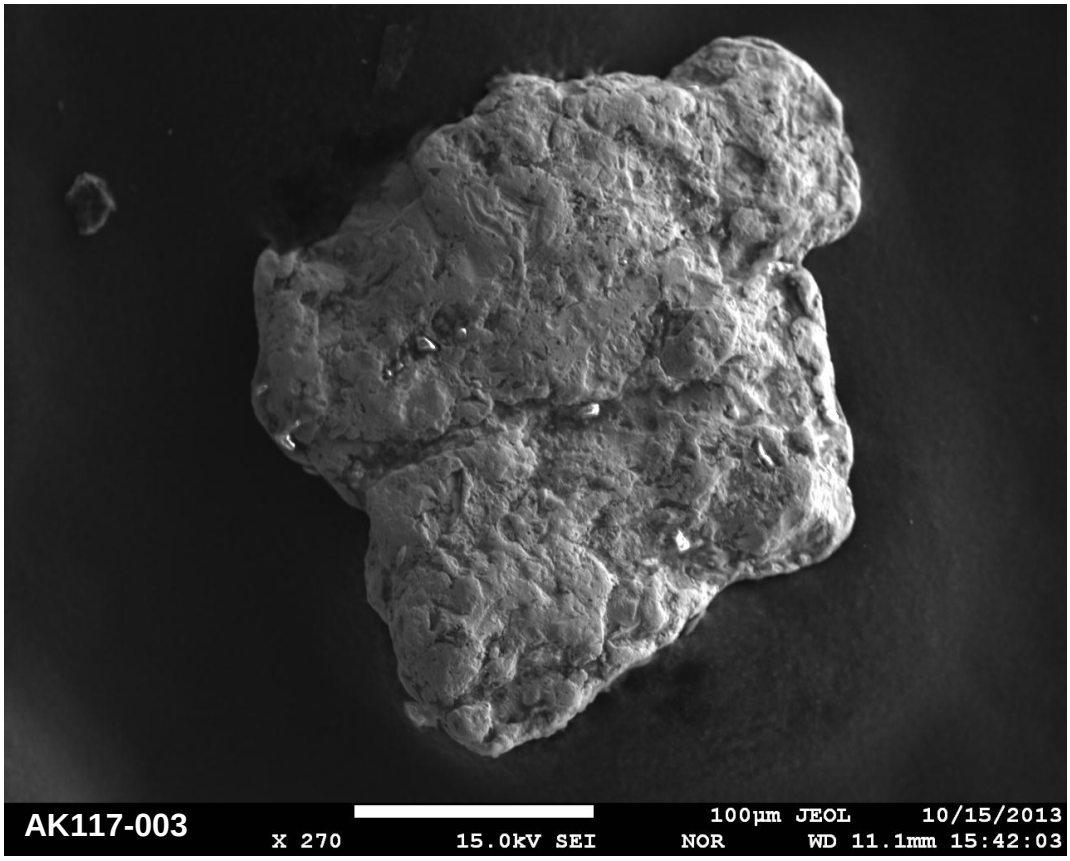
AK117-003
X 270
15.0kV SEI
100µm JEOL
NOR
10/15/2013
WD 11.1mm 15:42:03

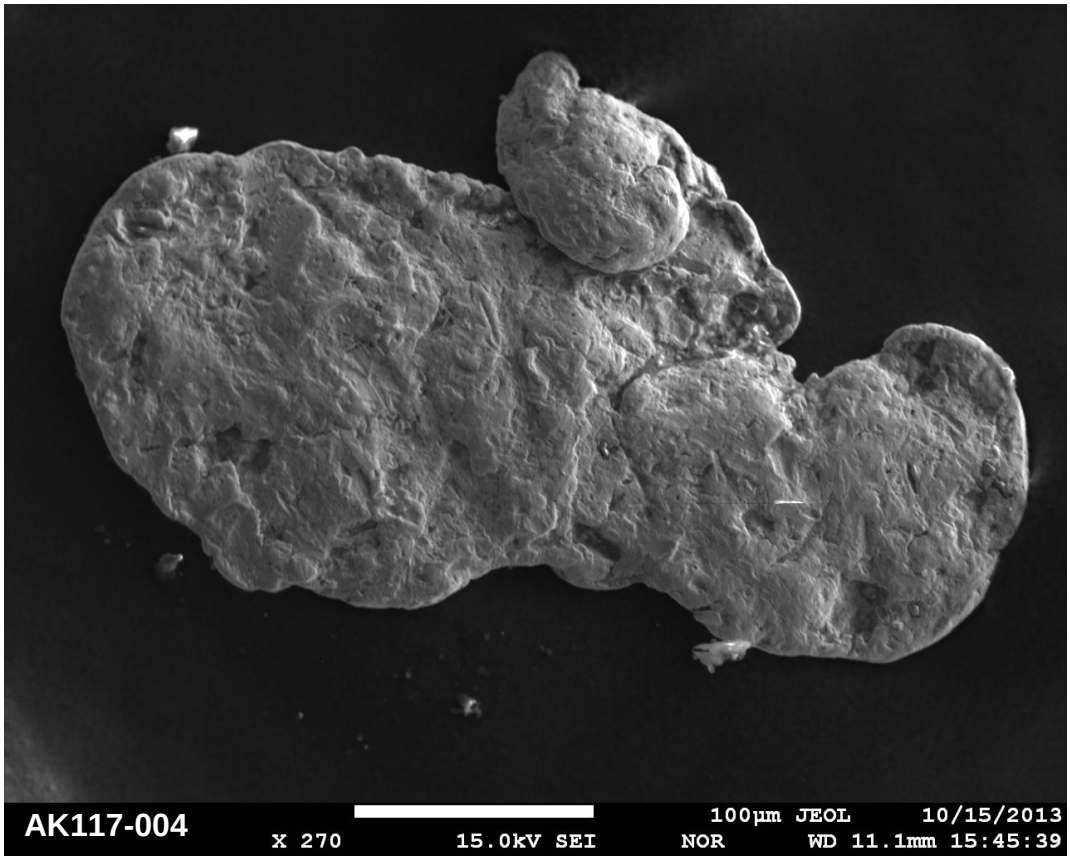
AK117-004
X 270
15.0kV SEI
100µm JEOL
NOR
10/15/2013
WD 11.1mm 15:45:39

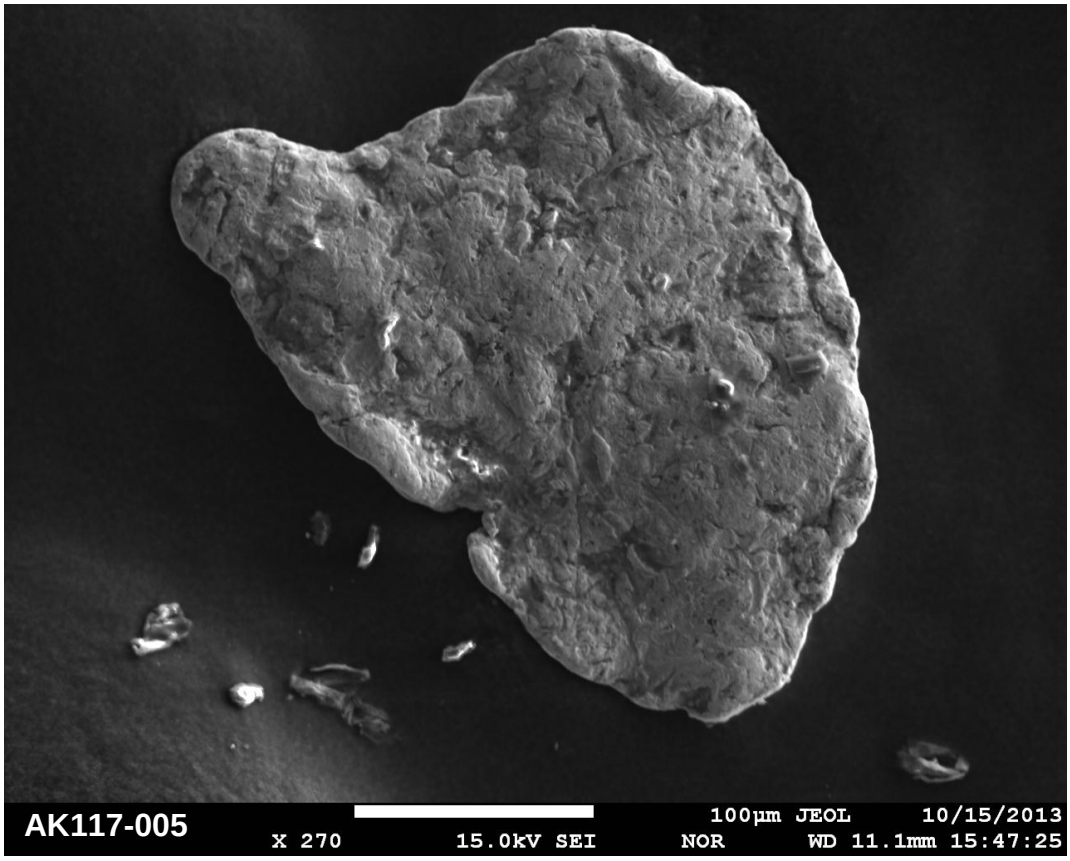
AK117-005
X 270
15.0kV SEI
100µm JEOL
NOR
10/15/2013
WD 11.1mm 15:47:25

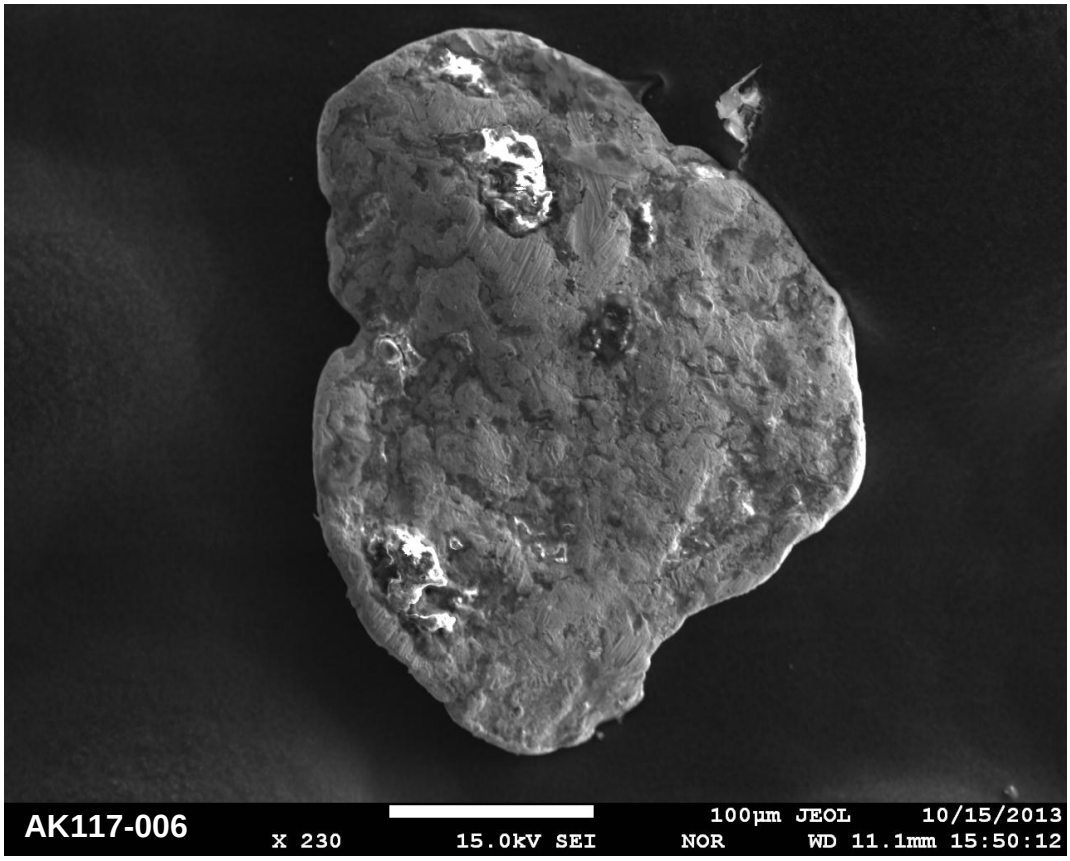
AK117-006
X 230
15.0kV SEI
100µm JEOL
NOR
10/15/2013
WD 11.1mm 15:50:12

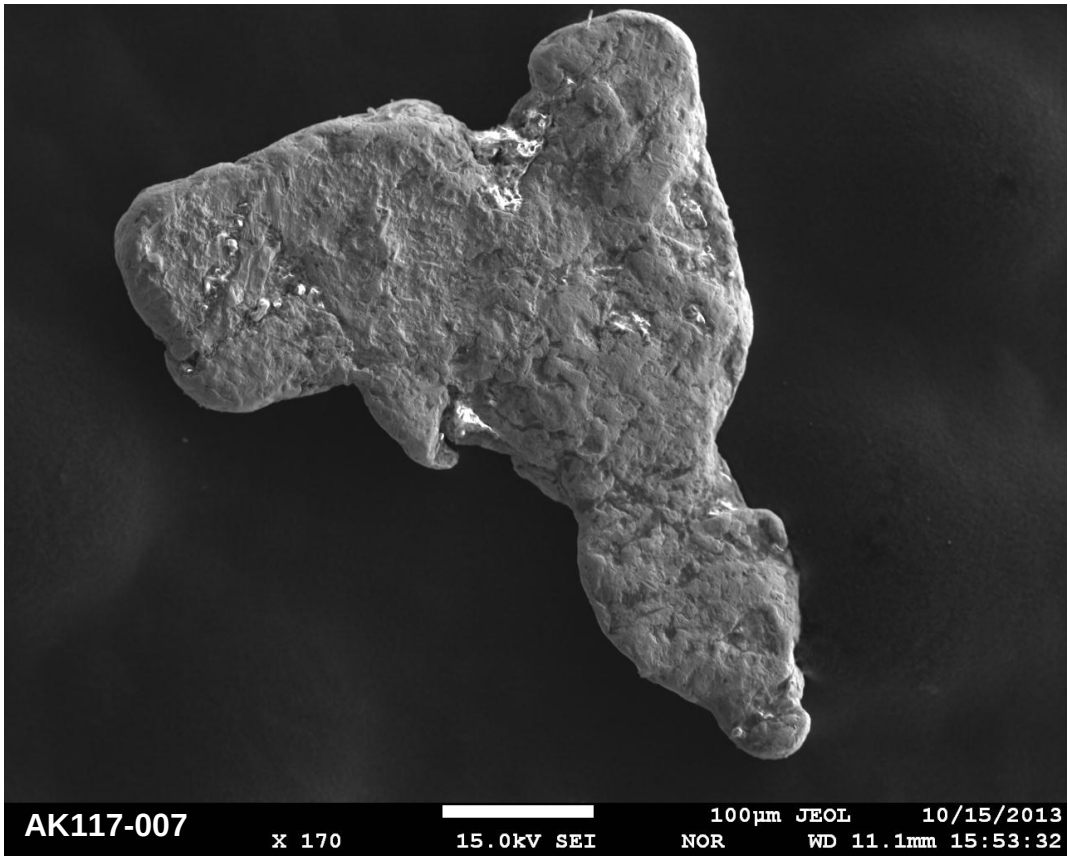
AK117-007
X 170
15.0kV SEI
100µm JEOL
NOR
10/15/2013
WD 11.1mm 15:53:32

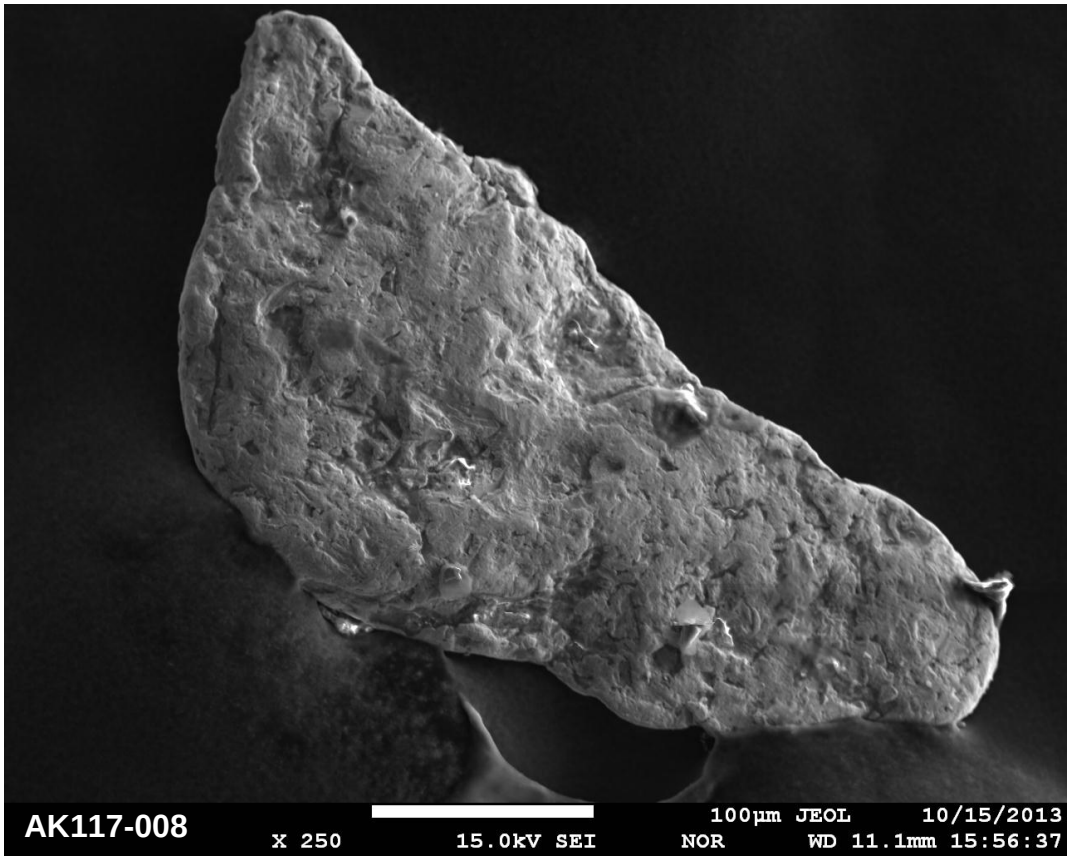
AK117-008
X 250
15.0kV SEI
100µm JEOL
NOR
10/15/2013
WD 11.1mm 15:56:37

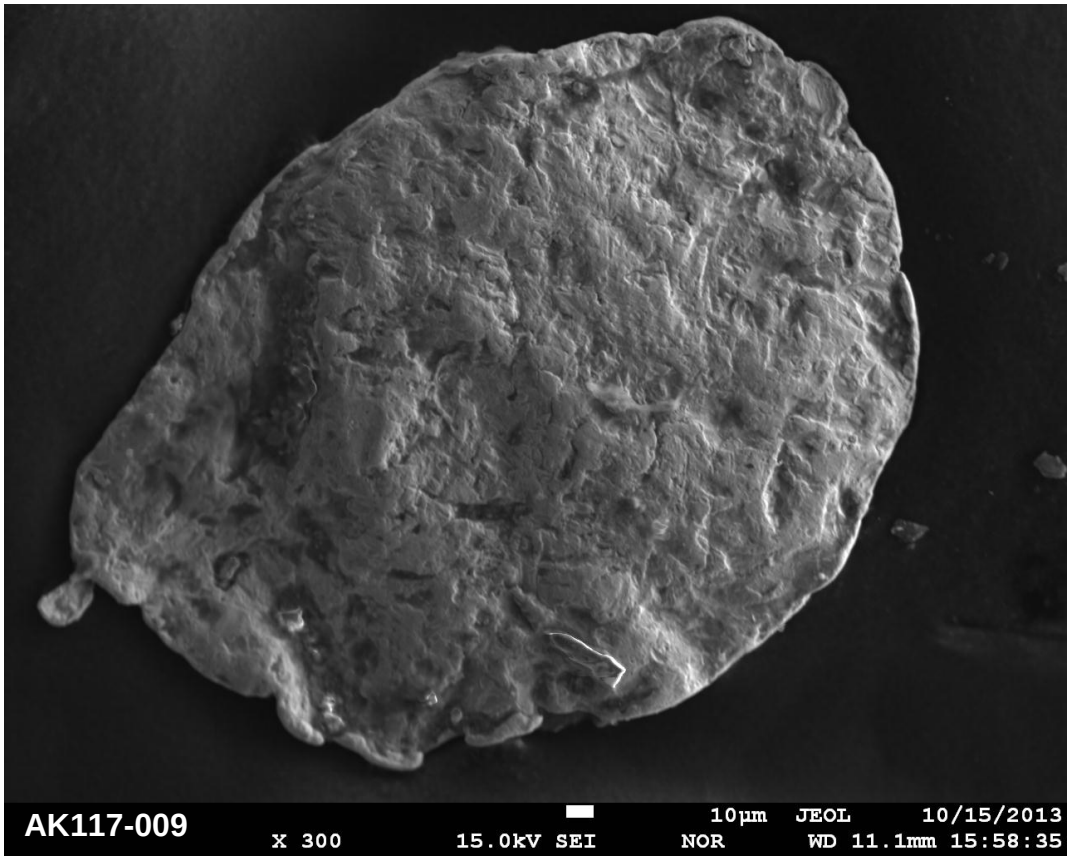
AK117-009
X 300
15.0kV SEI
10µm
NOR
JEOL
10/15/2013
WD 11.1mm 15:58:35

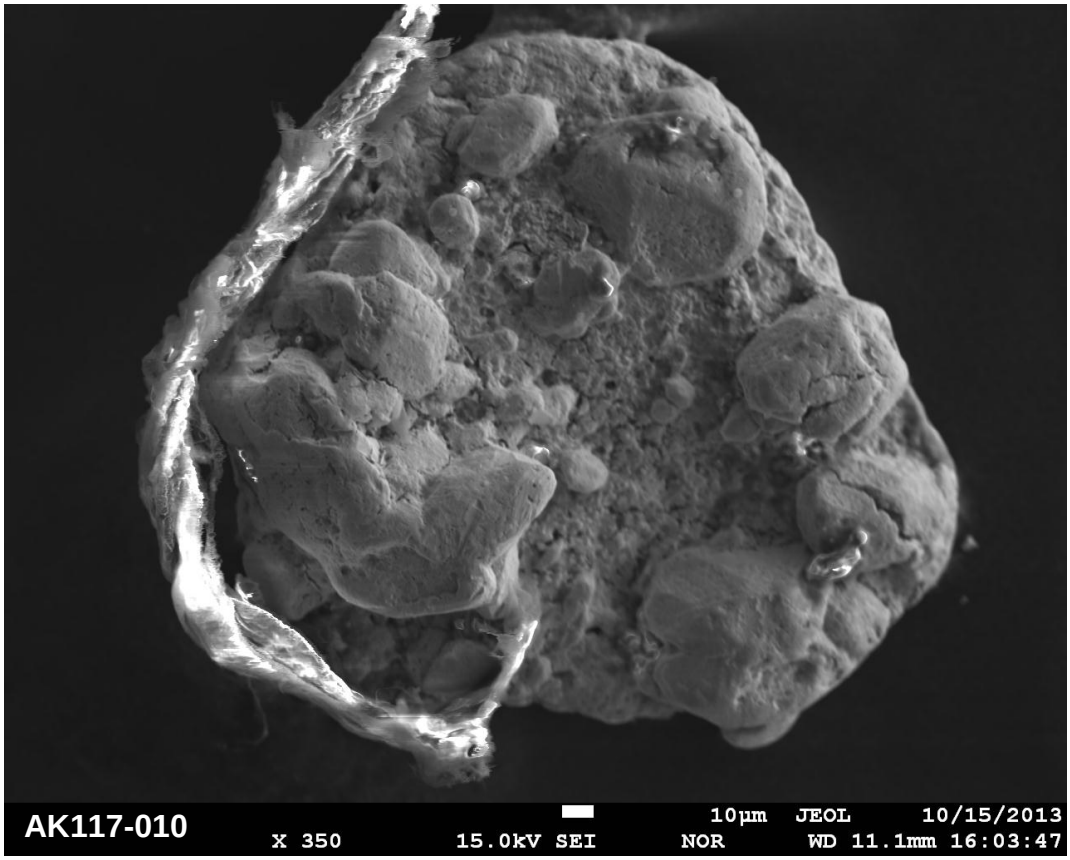
AK117-010
X 350
15.0kV SEI
10µm
NOR
JEOL
10/15/2013
WD 11.1mm 16:03:47

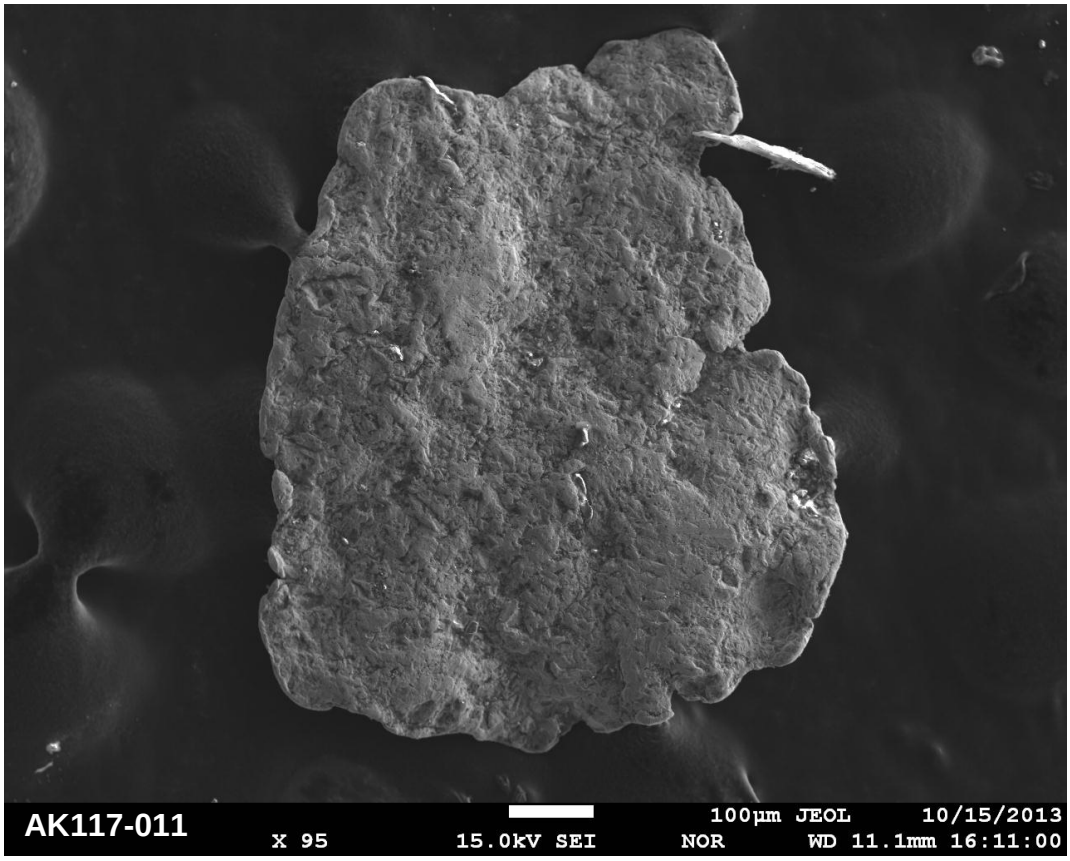
AK117-011
X 95
15.0kV SEI
100µm JEOL
NOR
10/15/2013
WD 11.1mm 16:11:00

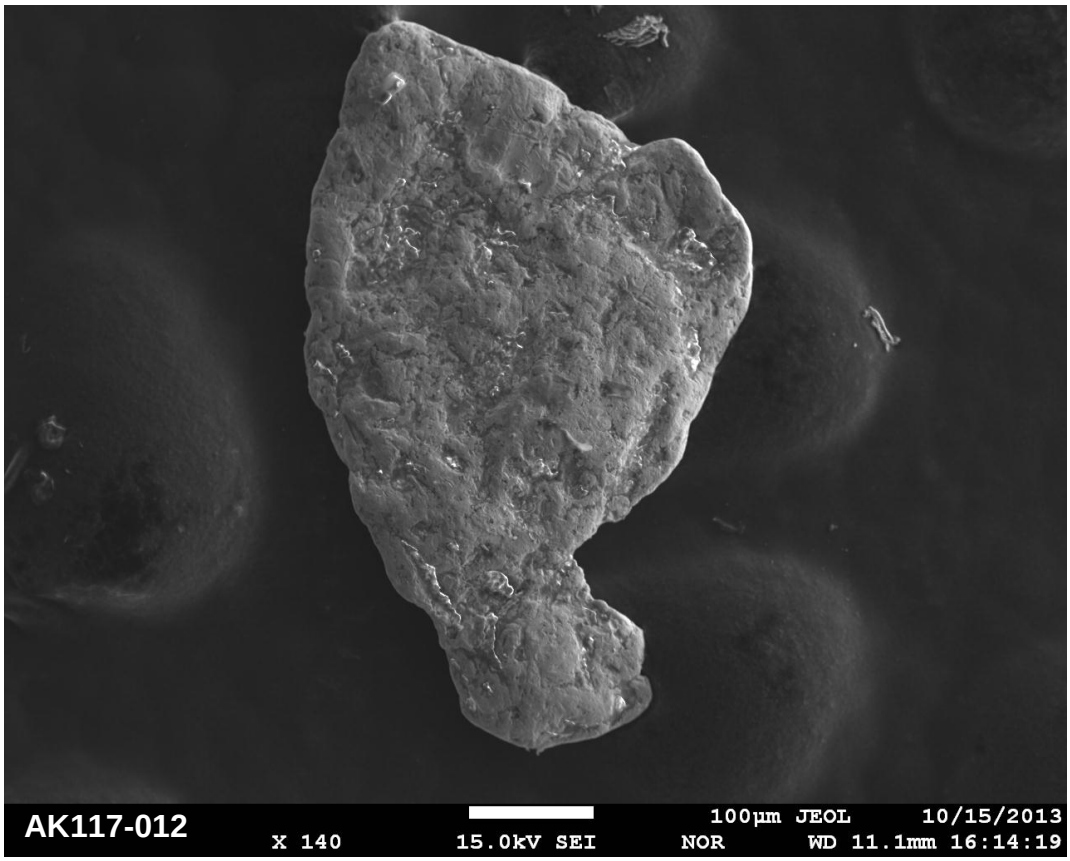
AK117-012
X 140
15.0kV SEI
100µm JEOL
NOR
10/15/2013
WD 11.1mm 16:14:19

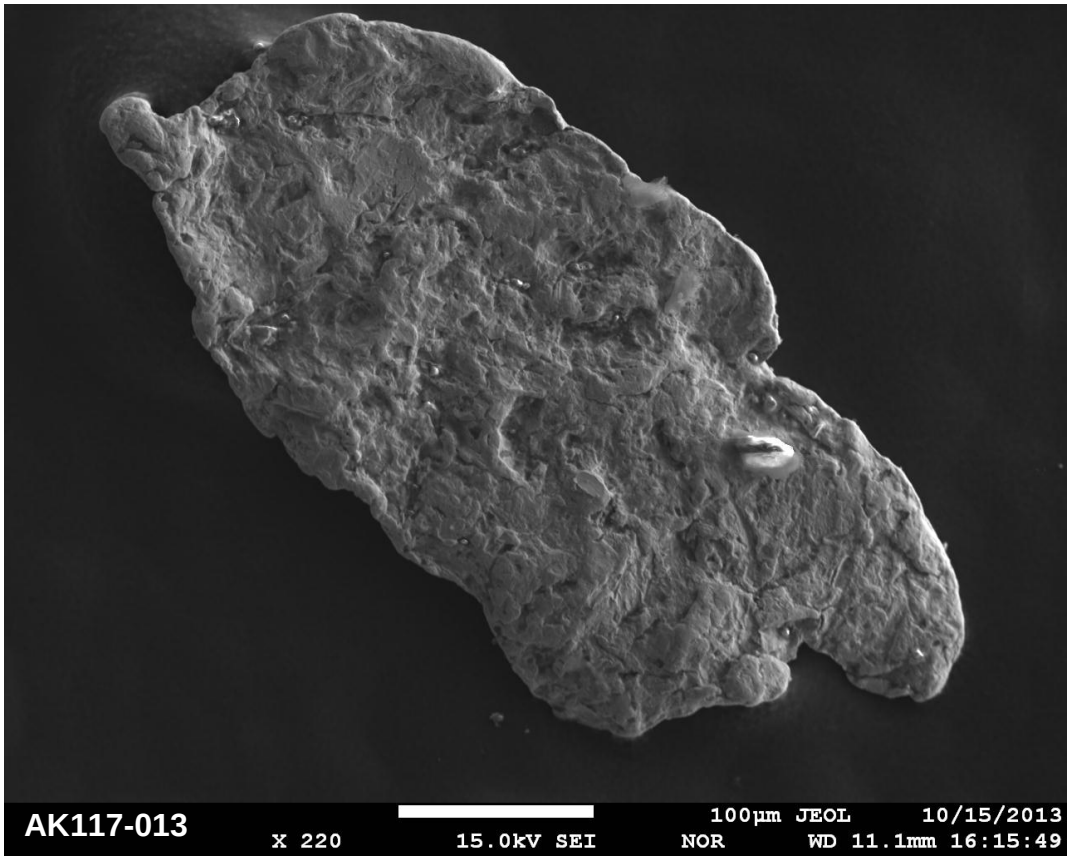
AK117-013
X 220
15.0kV SEI
100µm JEOL
NOR
10/15/2013
WD 11.1mm 16:15:49

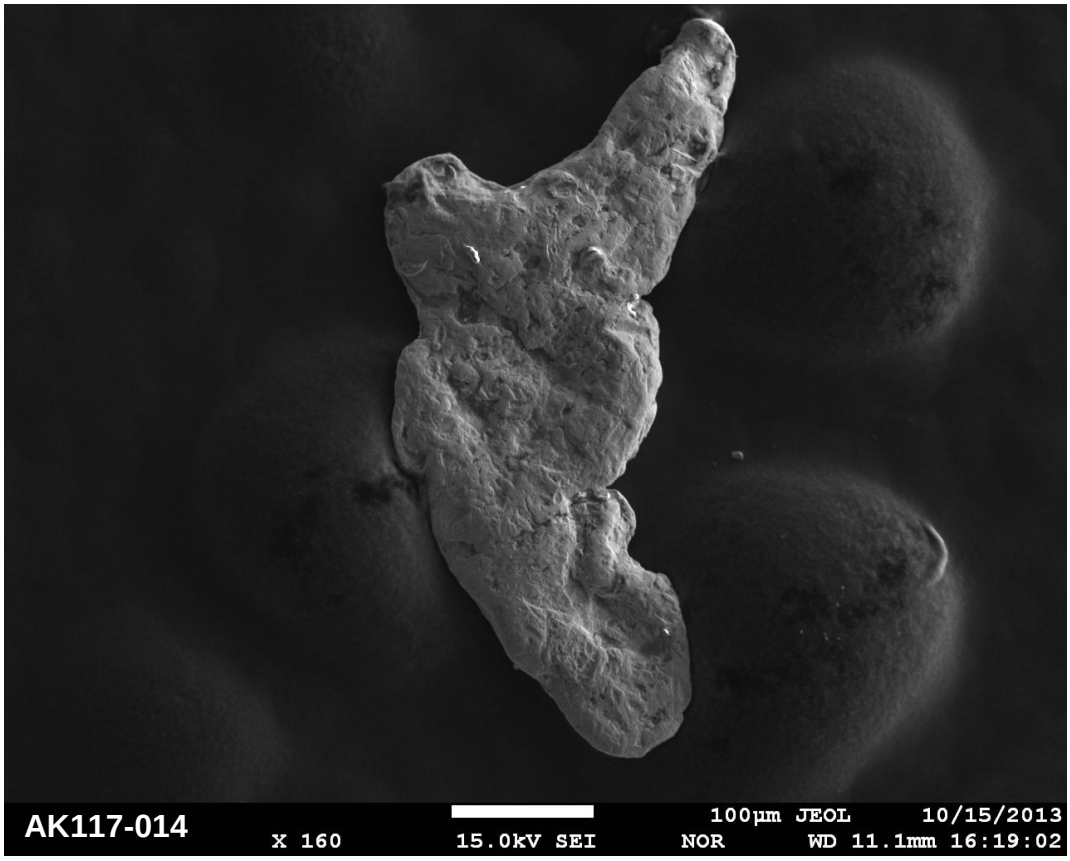
AK117-014
X 160
15.0kV SEI
100µm JEOL
NOR
10/15/2013
WD 11.1mm 16:19:02

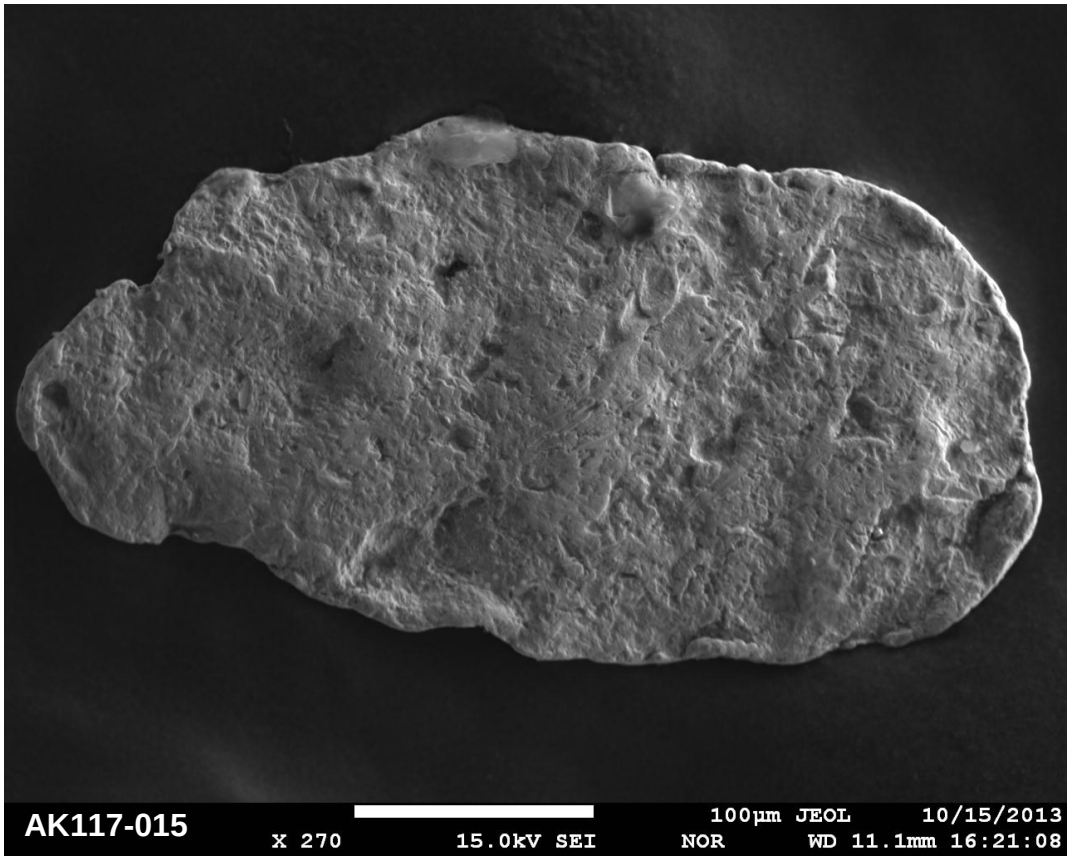
AK117-015
X 270
15.0kV SEI
100µm JEOL
NOR
10/15/2013
WD 11.1mm 16:21:08

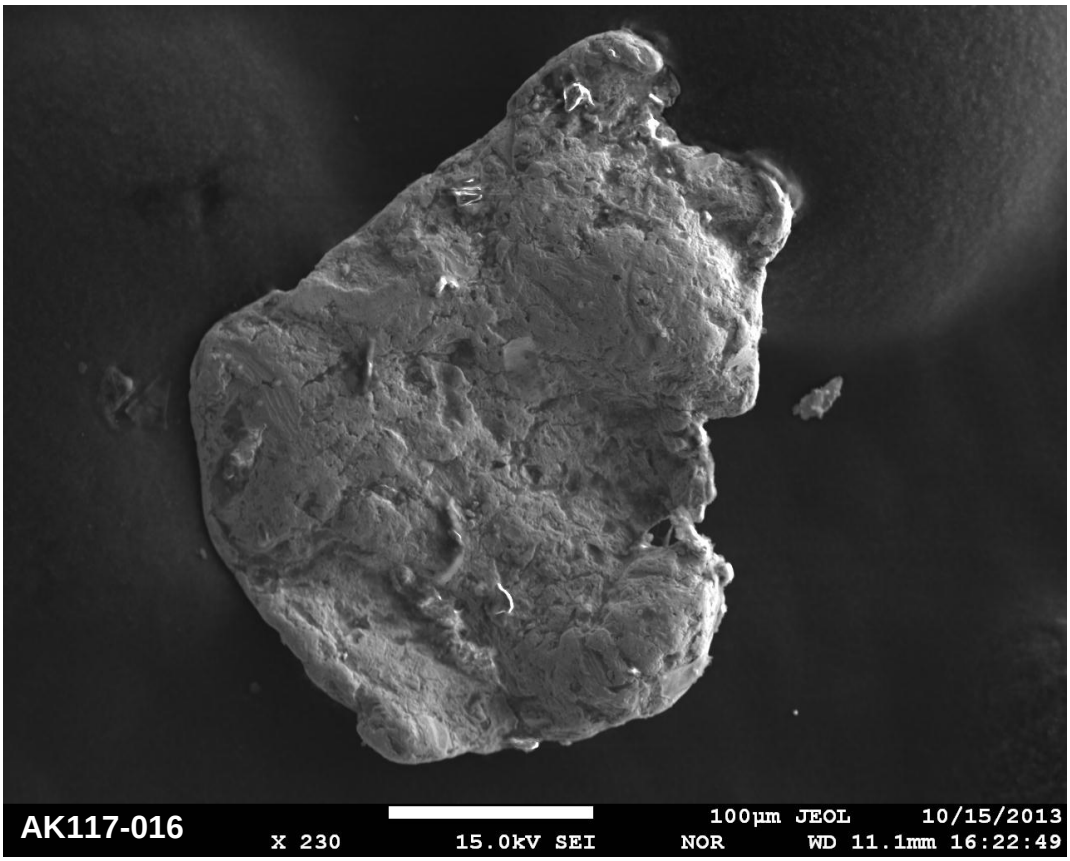
AK117-016
X 230
15.0kV SEI
100µm JEOL
NOR
10/15/2013
WD 11.1mm 16:22:49

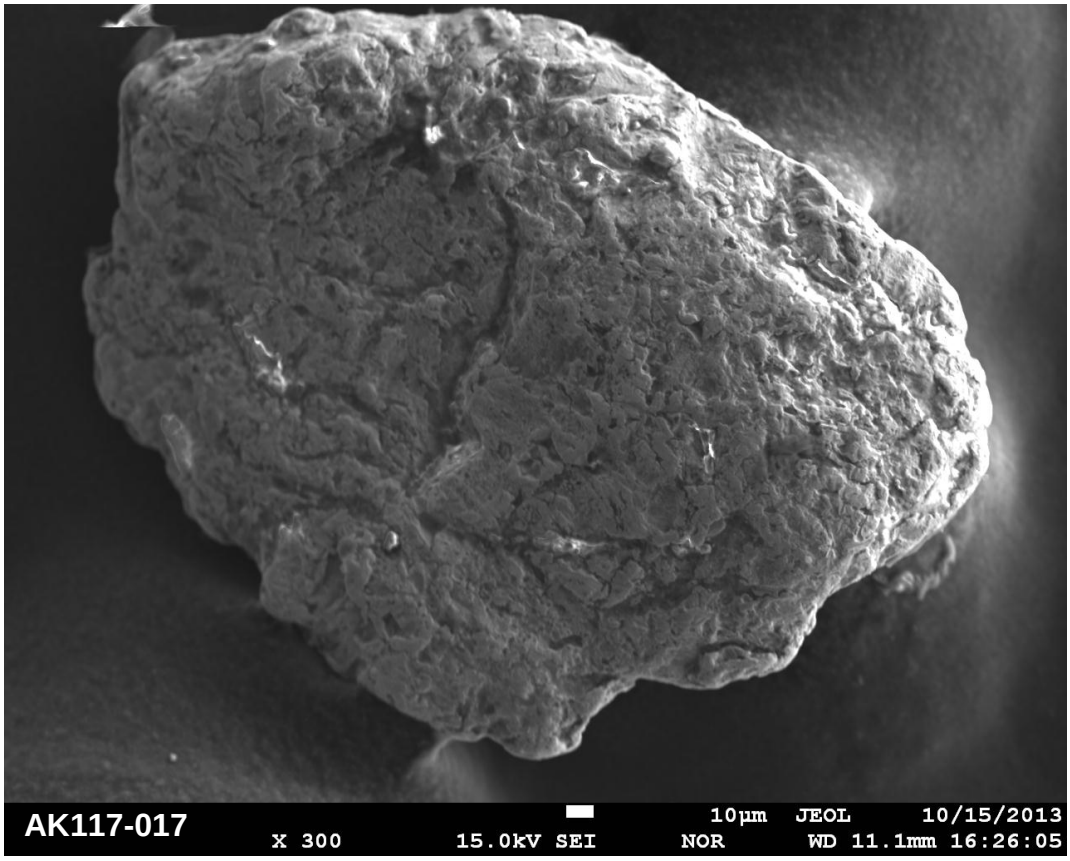
AK117-017
X 300
15.0kV SEI
10µm
NOR
JEOL
WD 11.1mm
10/15/2013
16:26:05

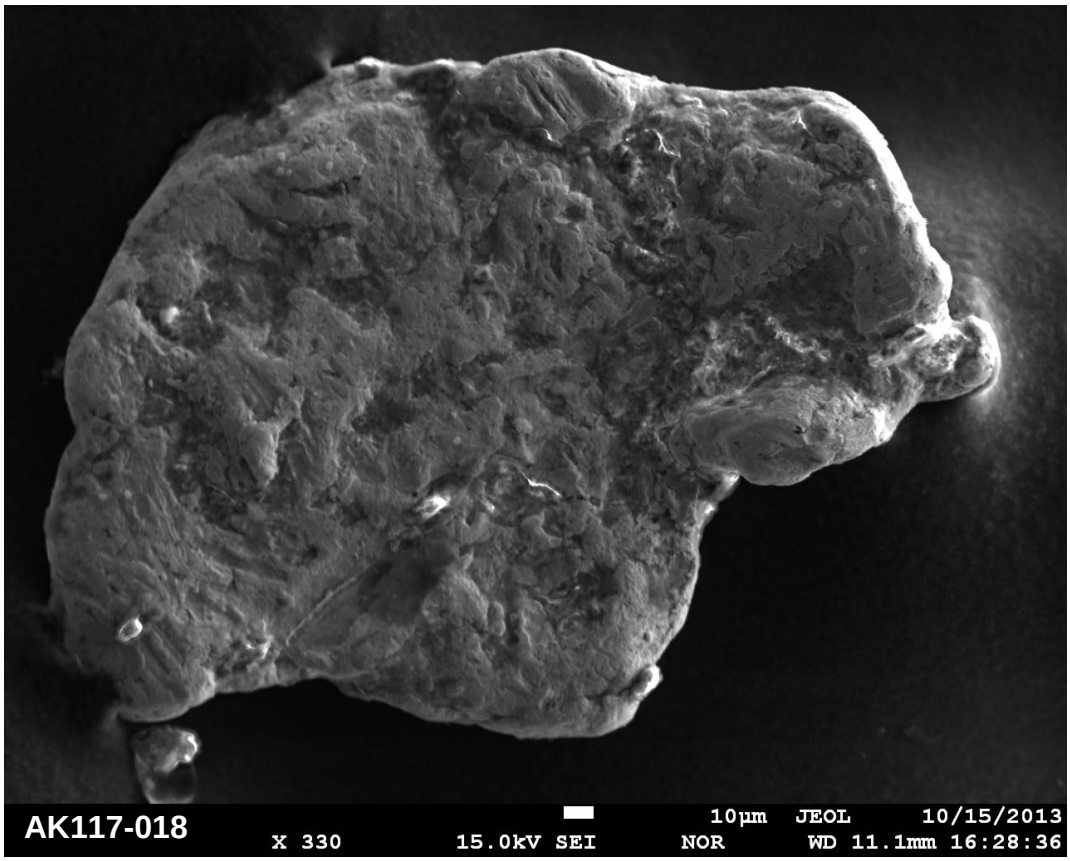
AK117-018
X 330
15.0kV SEI
10µm
NOR
JEOL
WD 11.1mm
10/15/2013
16:28:36

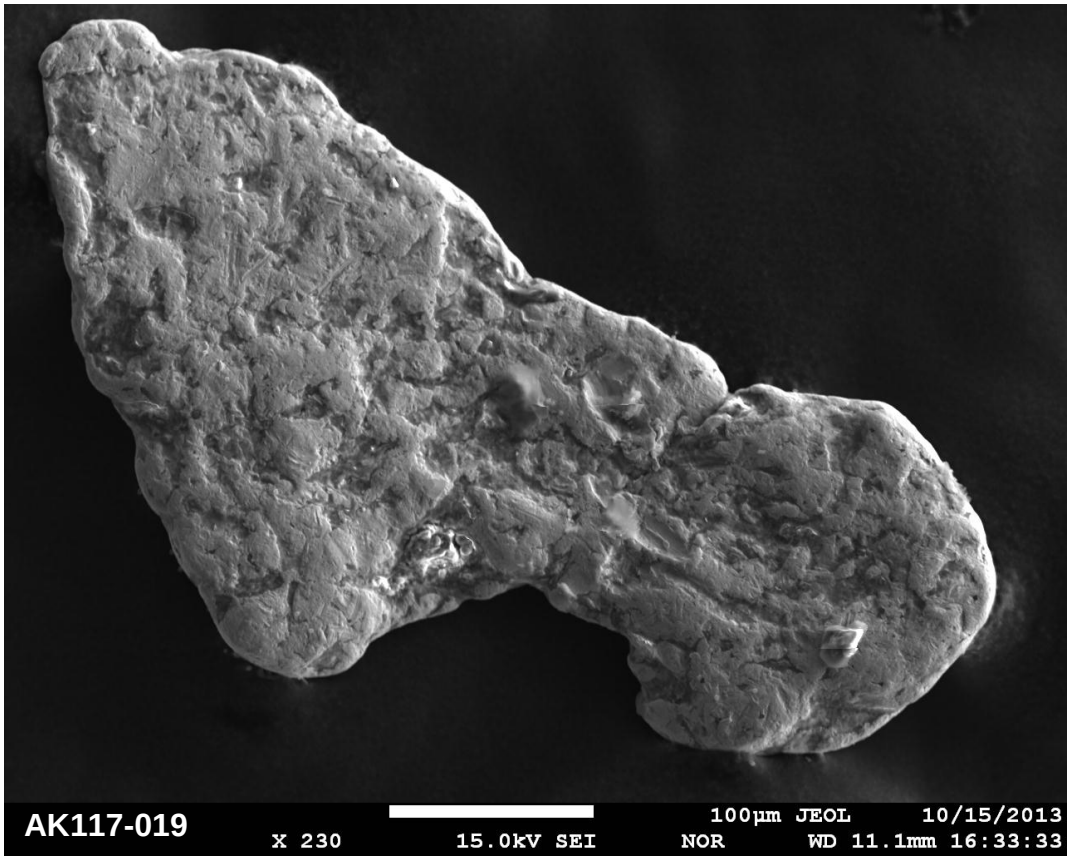
AK117-019
X 230
15.0kV SEI
100µm JEOL
NOR
10/15/2013
WD 11.1mm 16:33:33

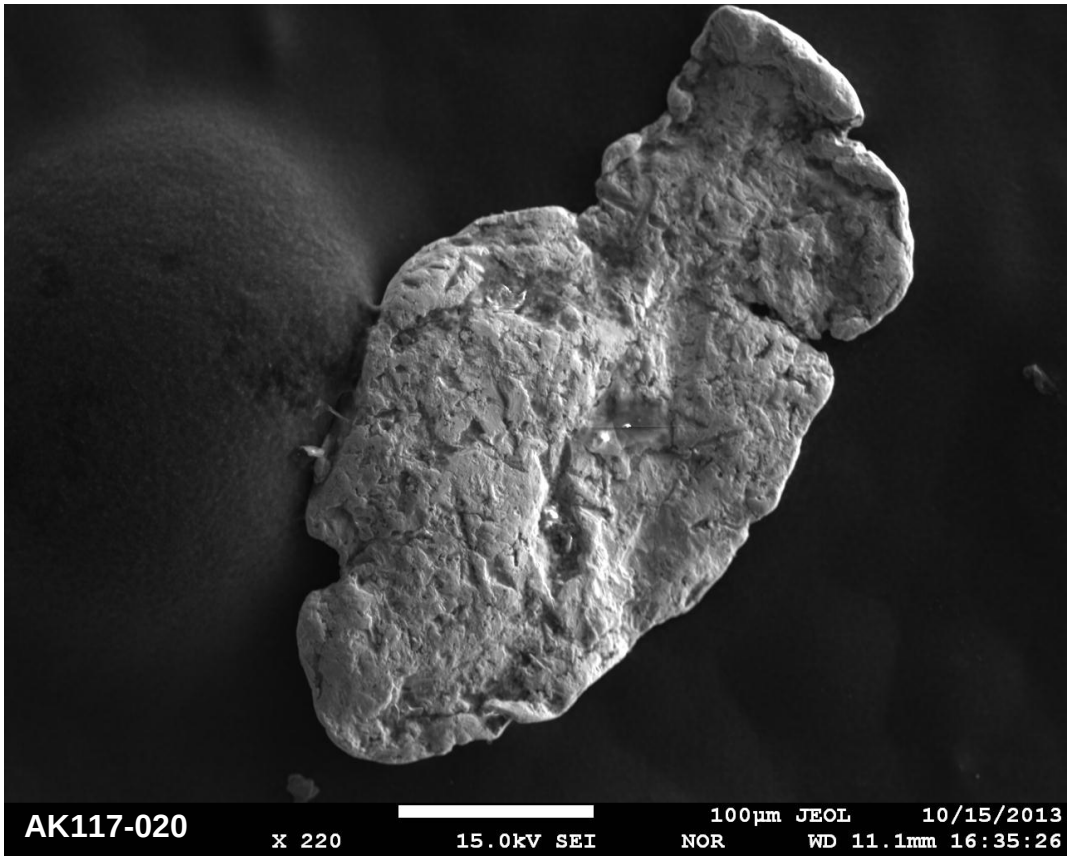
AK117-020
X 220
15.0kV SEI
100µm JEOL
NOR
10/15/2013
WD 11.1mm 16:35:26

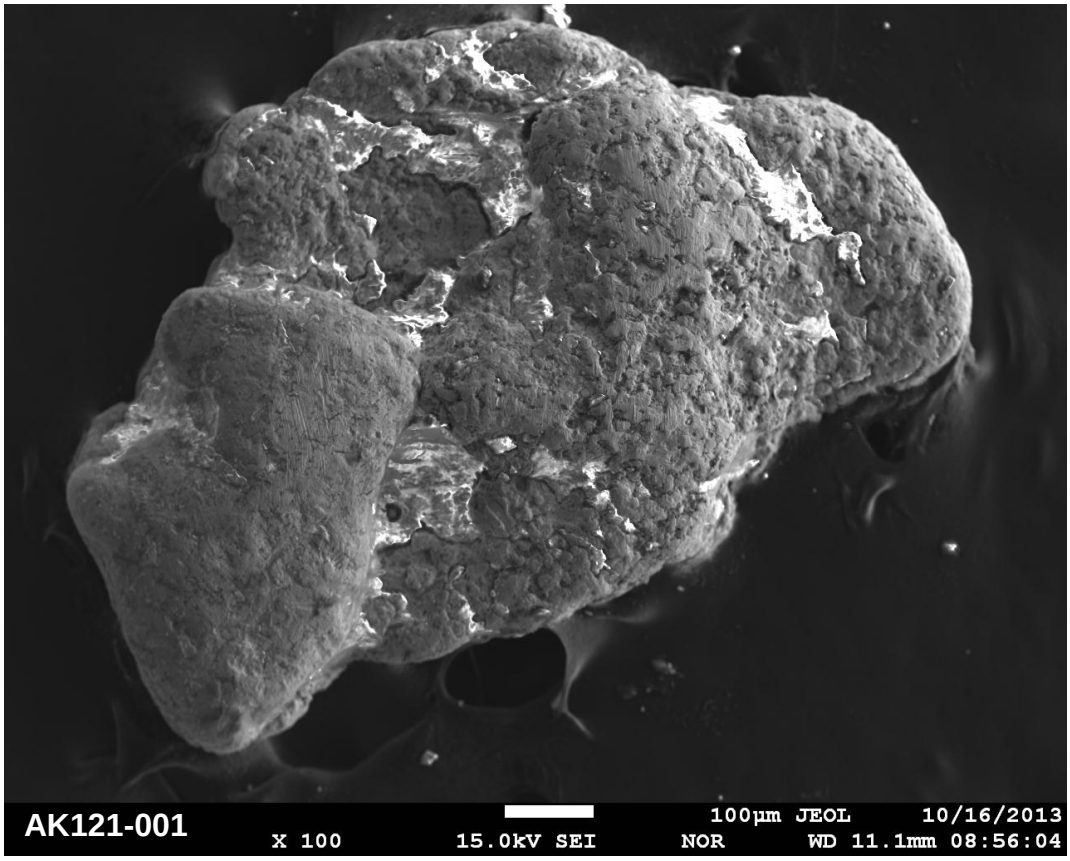
AK121-001
X 100
15.0kV SEI
100µm JEOL
NOR
10/16/2013
WD 11.1mm 08:56:04

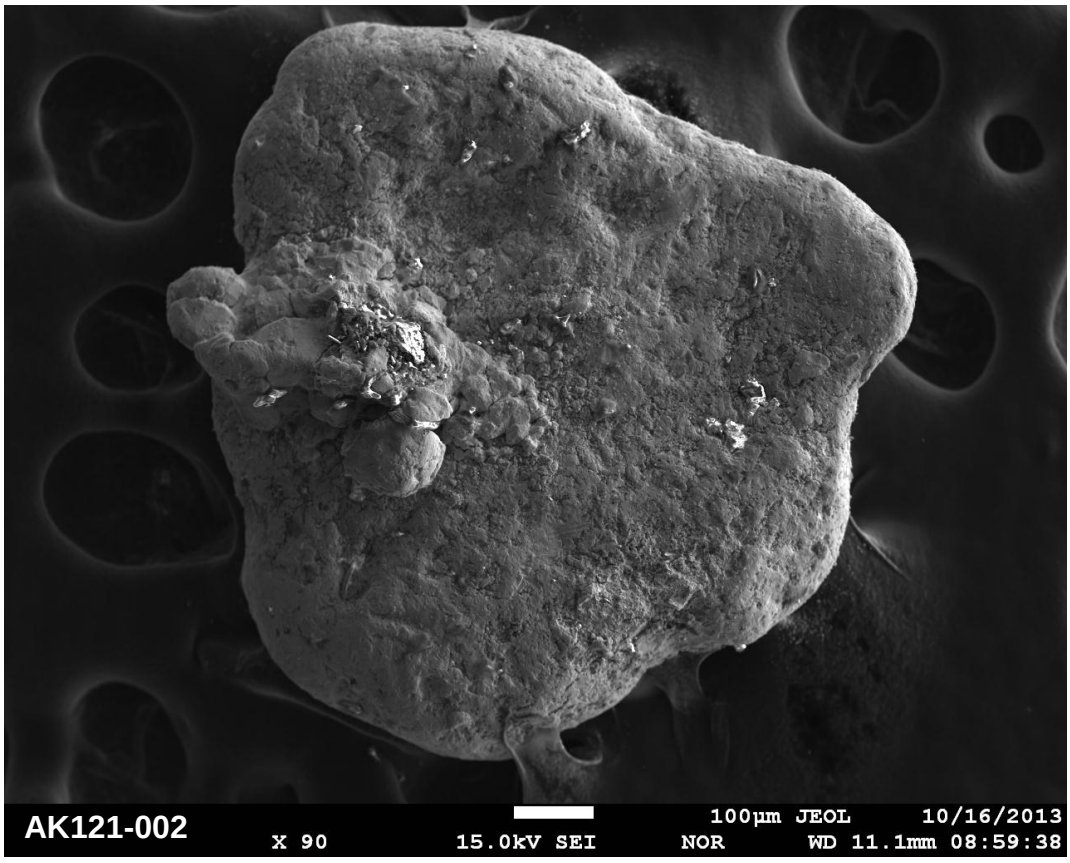
AK121-002
X 90
15.0kV SEI
100µm JEOL
NOR
10/16/2013
WD 11.1mm 08:59:38

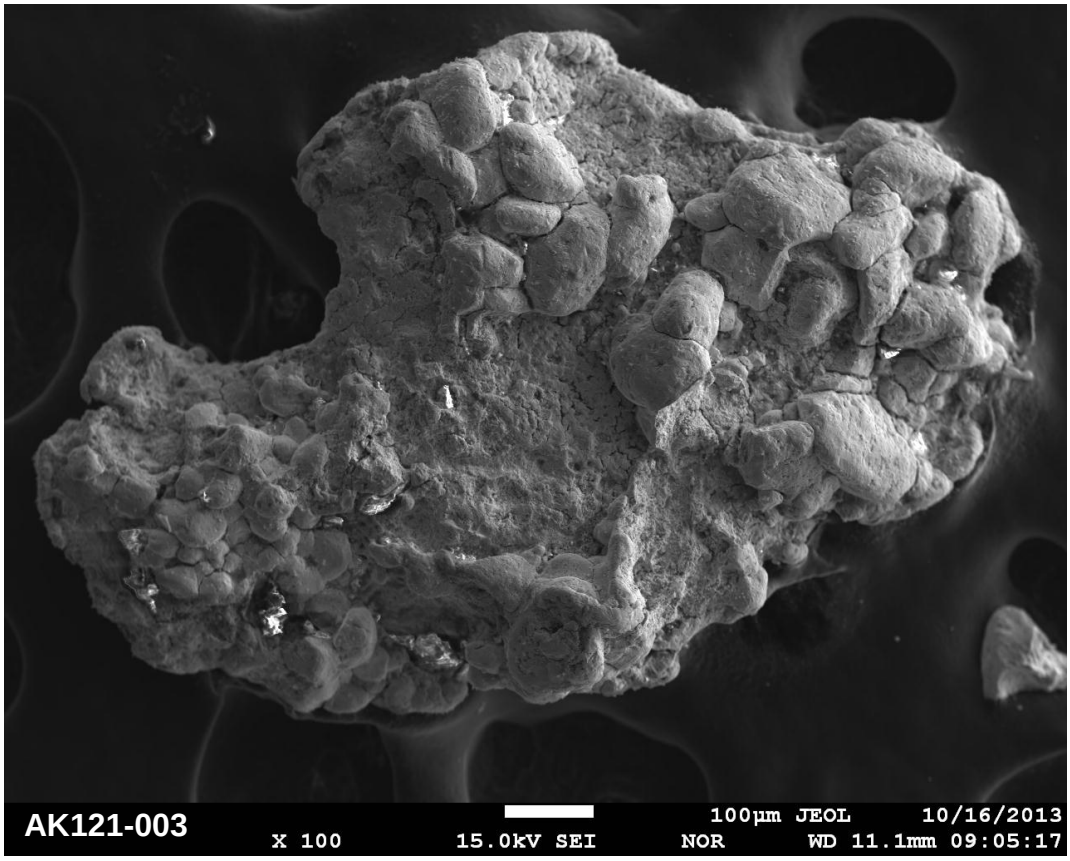
AK121-003
X 100
15.0kV SEI
100µm JEOL
NOR
10/16/2013
WD 11.1mm 09:05:17

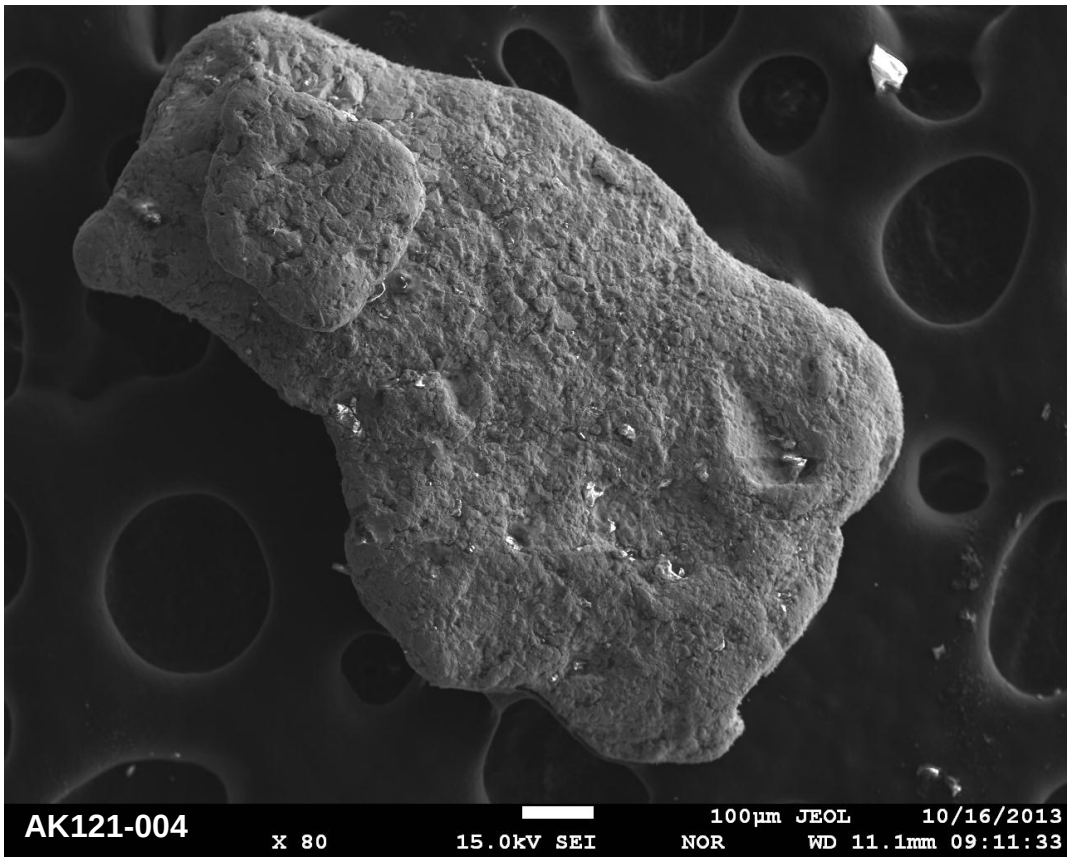
AK121-004
X 80
15.0kV SEI
100µm JEOL
NOR
10/16/2013
WD 11.1mm 09:11:33

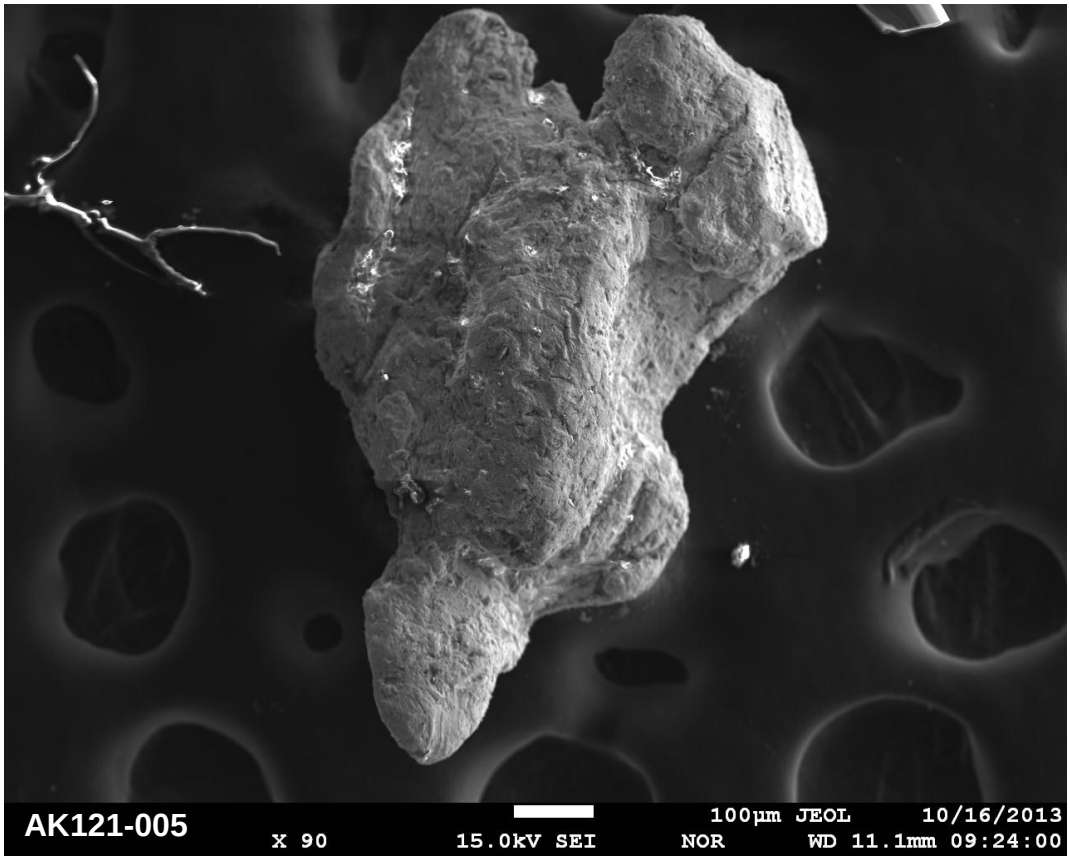
AK121-005
X 90
15.0kV SEI
100µm JEOL
NOR
10/16/2013
WD 11.1mm 09:24:00

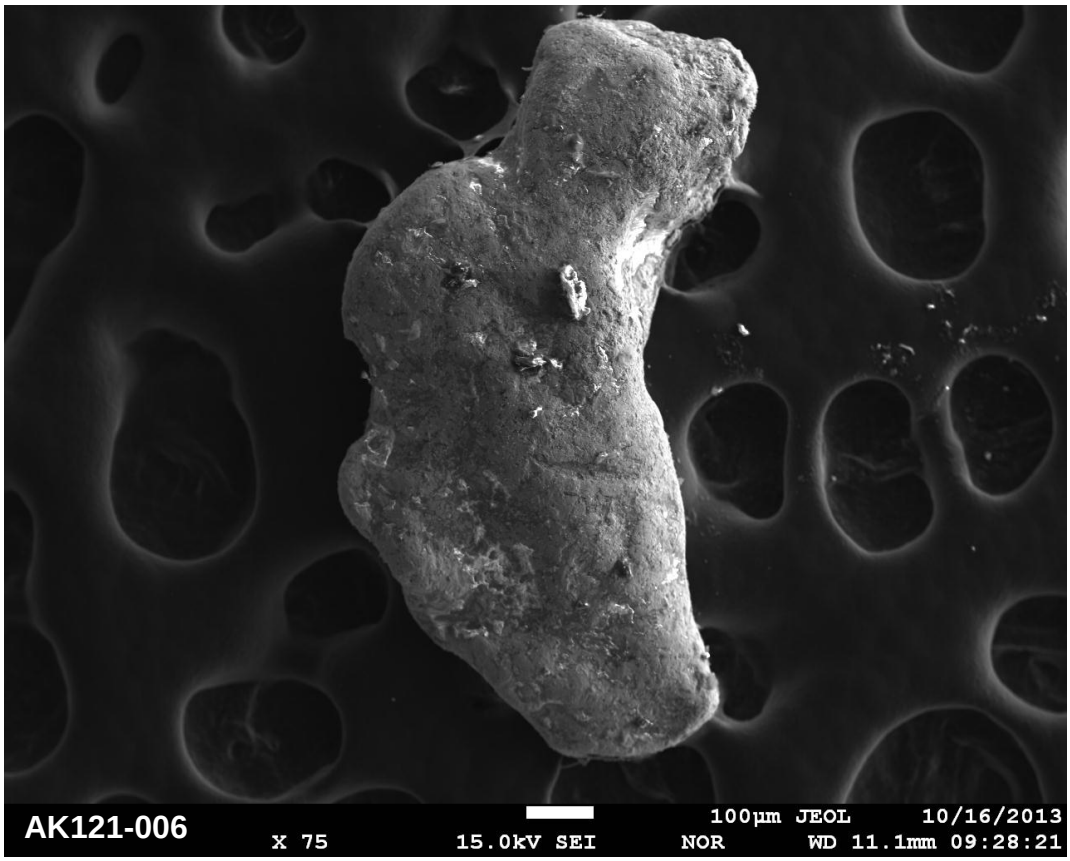
AK121-006
X 75
15.0kV SEI
100µm JEOL
NOR
10/16/2013
WD 11.1mm 09:28:21

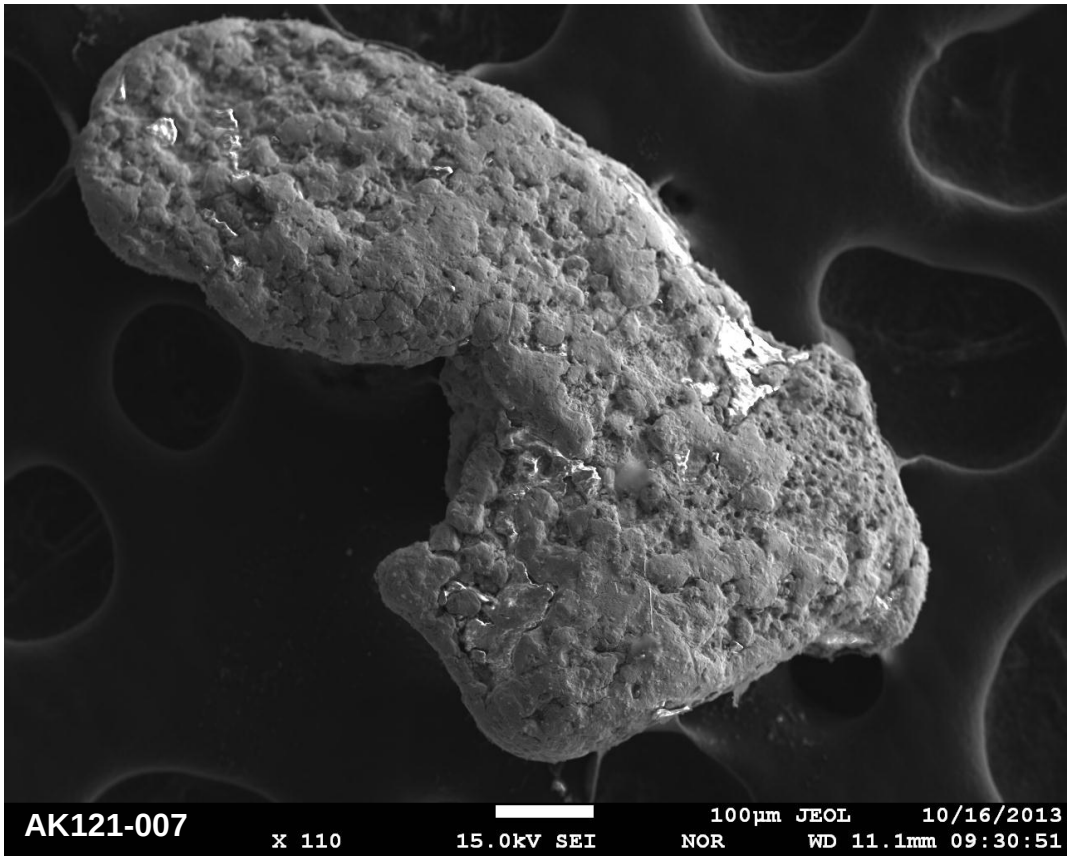
AK121-007
X 110
15.0kV SEI
100µm JEOL
NOR
10/16/2013
WD 11.1mm 09:30:51

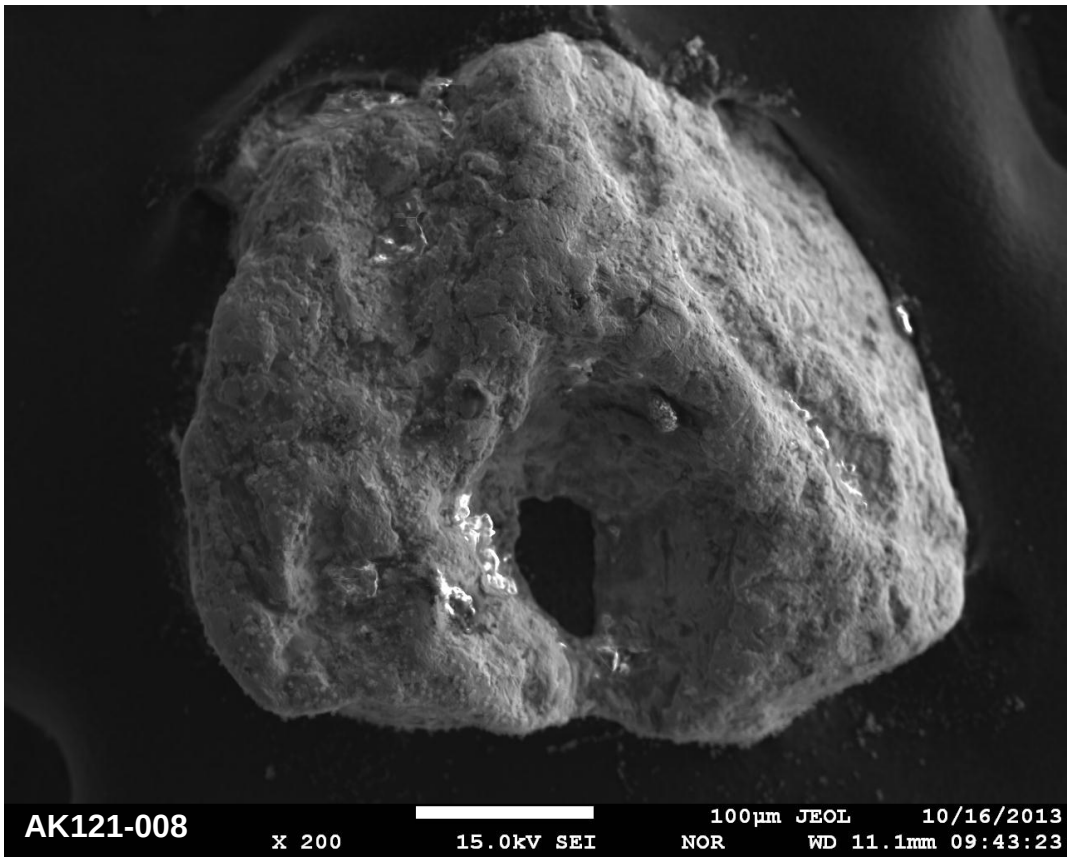
AK121-008
X 200
15.0kV SEI
100µm JEOL
NOR
10/16/2013
WD 11.1mm 09:43:23

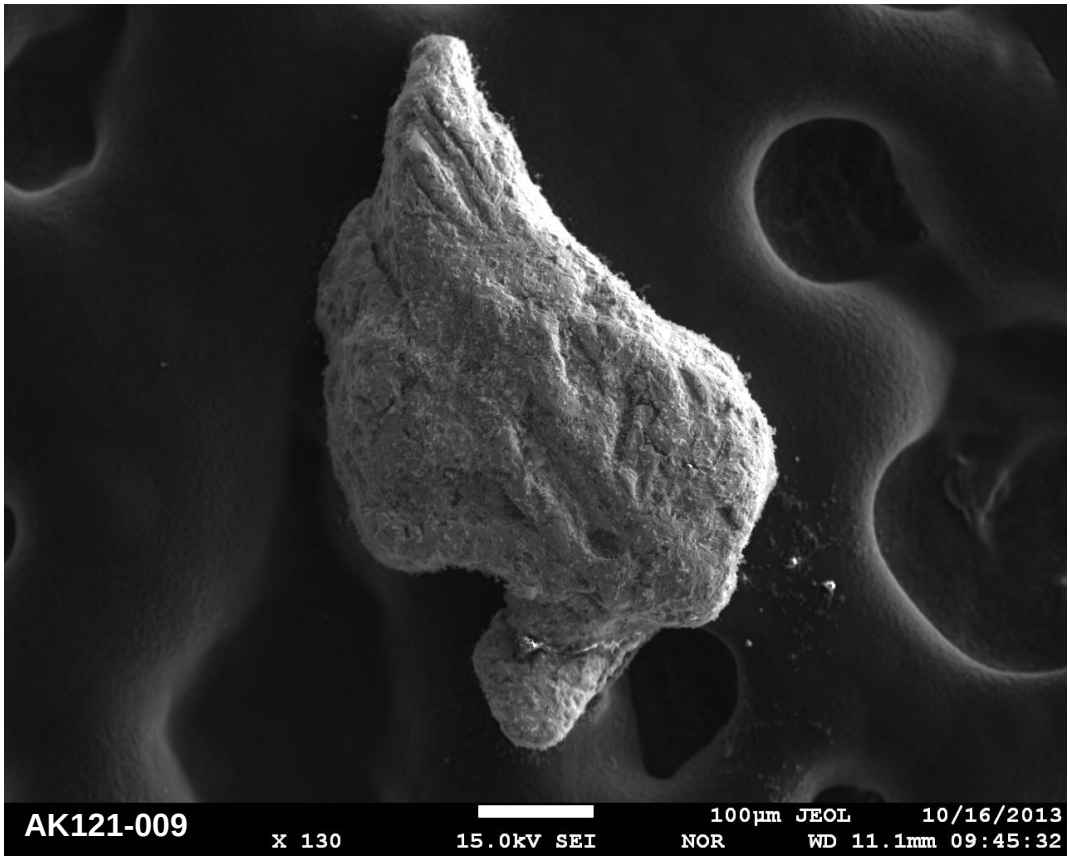
AK121-009
X 130
15.0kV SEI
100µm JEOL
NOR
10/16/2013
WD 11.1mm 09:45:32

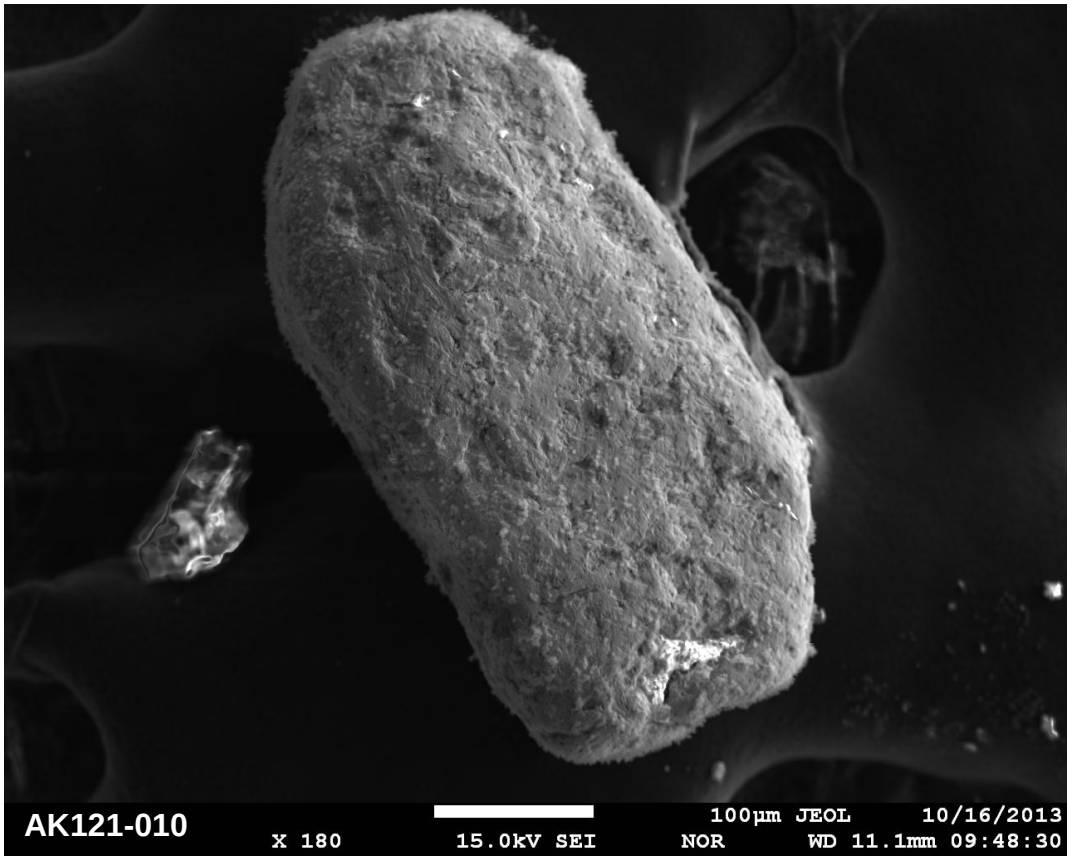
AK121-010
X 180
15.0kV SEI
100µm JEOL
NOR
10/16/2013
WD 11.1mm 09:48:30

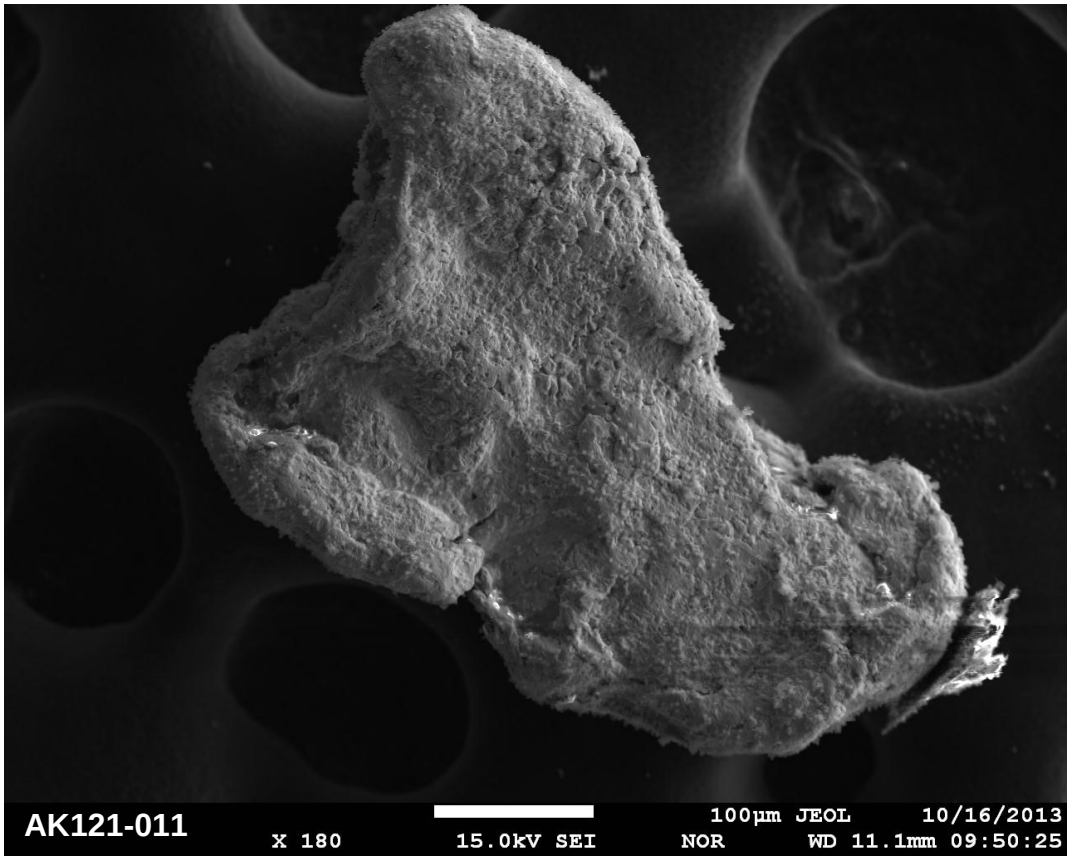
AK121-011
X 180
15.0kV SEI
100µm JEOL
NOR
10/16/2013
WD 11.1mm 09:50:25

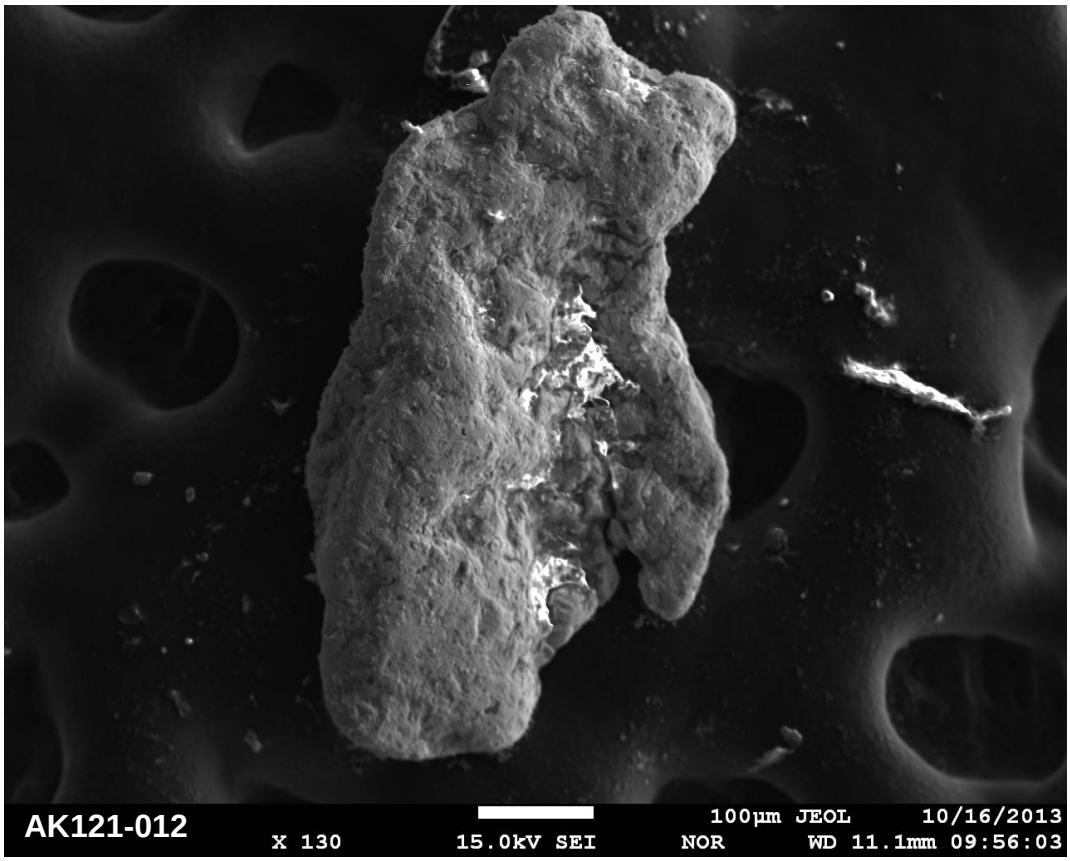
AK121-012
X 130
15.0kV SEI
100µm JEOL
NOR
10/16/2013
WD 11.1mm 09:56:03

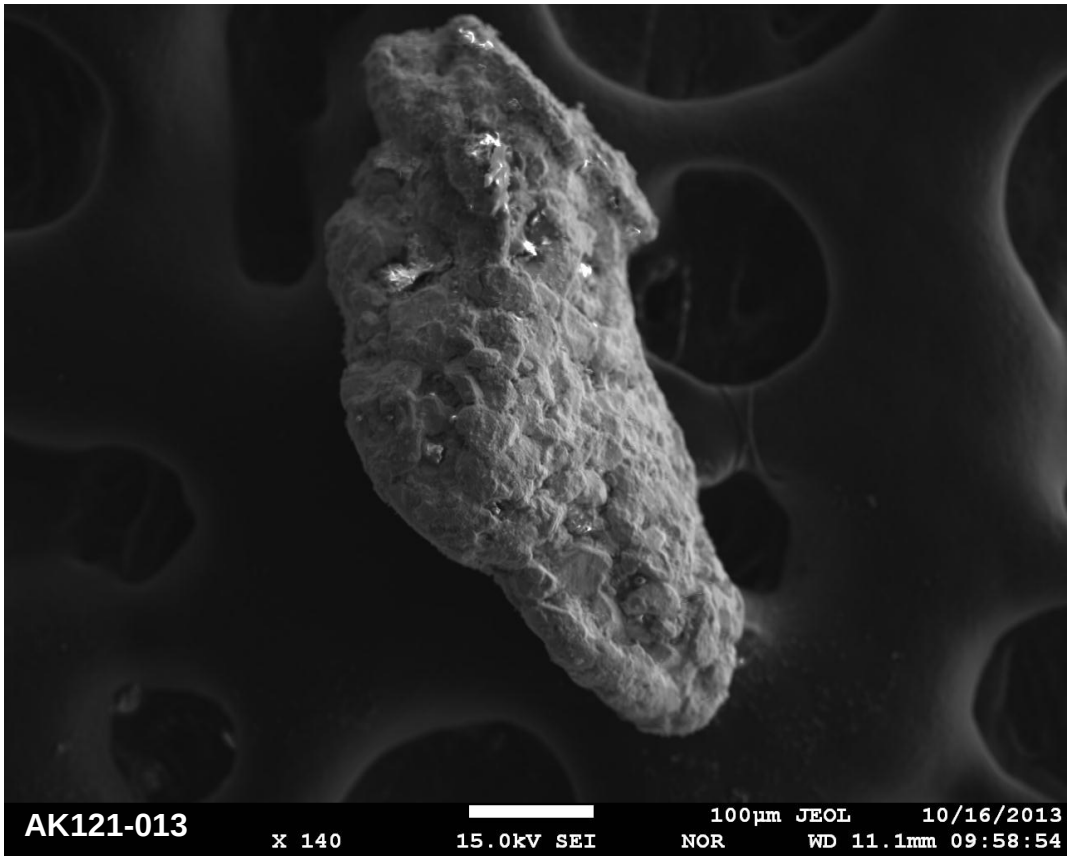
AK121-013
X 140
15.0kV SEI
100µm JEOL
NOR
10/16/2013
WD 11.1mm 09:58:54

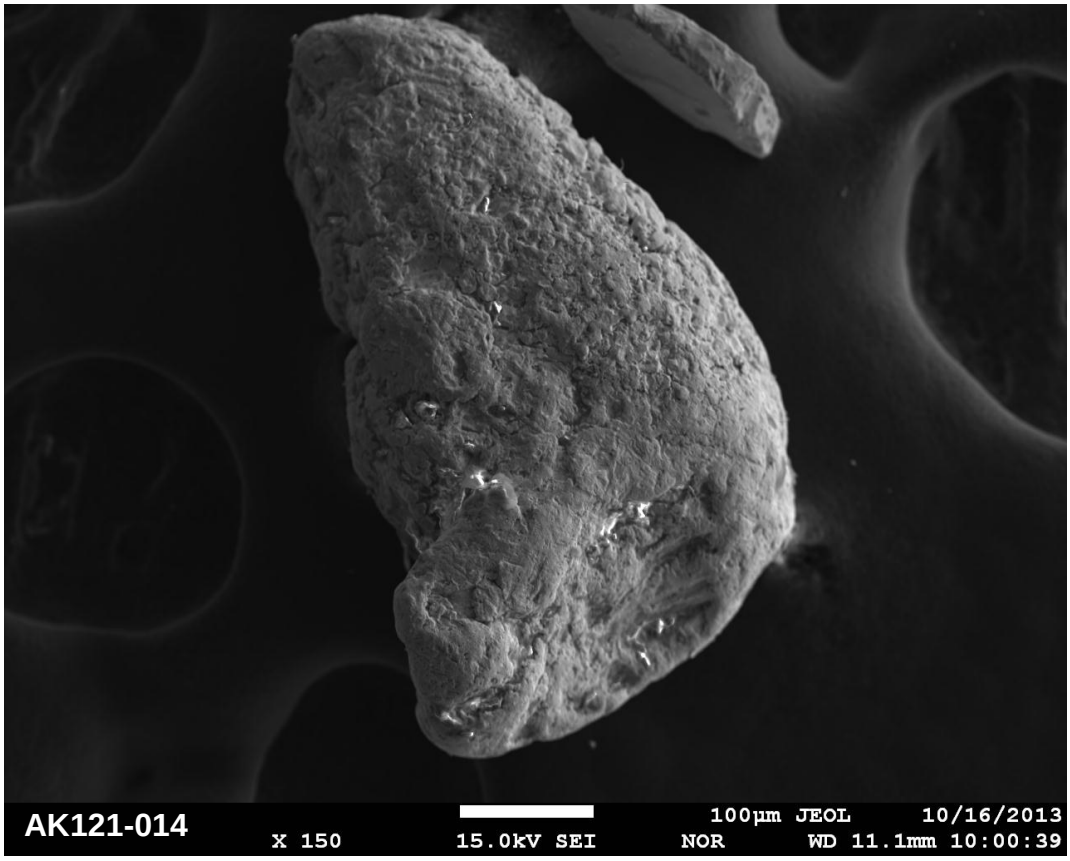
AK121-014
X 150
15.0kV SEI
100µm JEOL
NOR
10/16/2013
WD 11.1mm 10:00:39

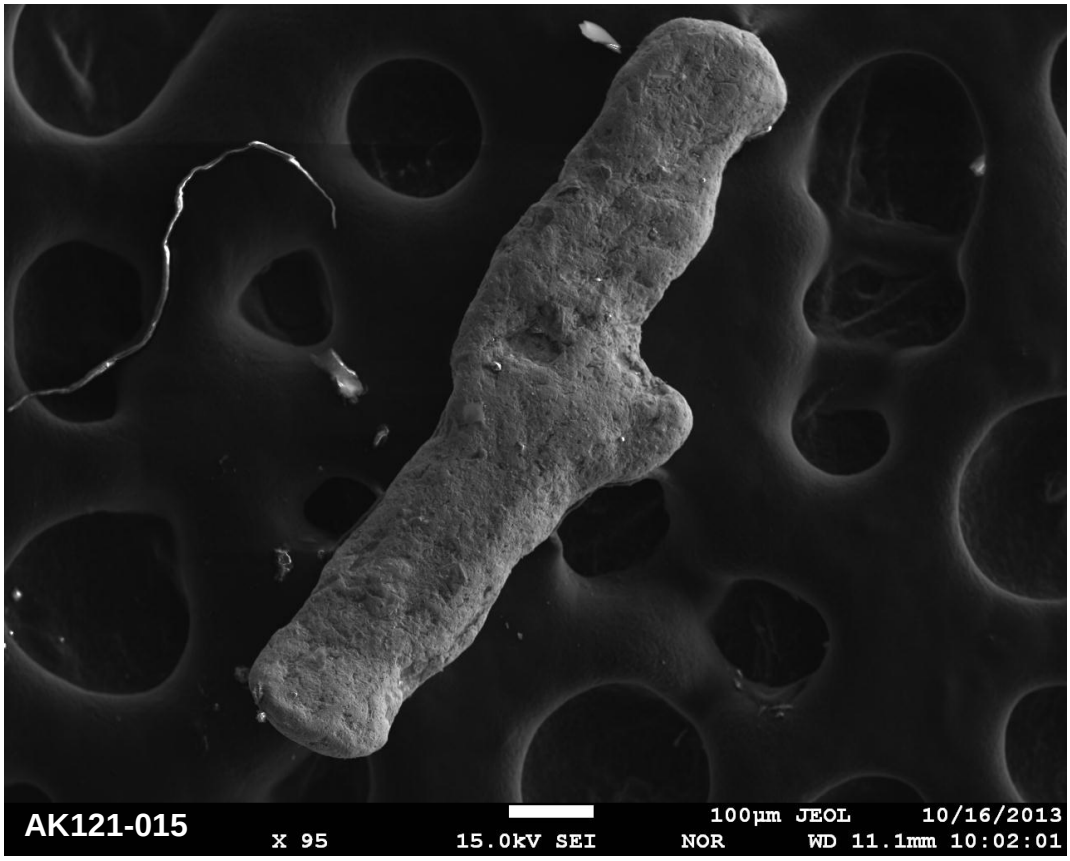
AK121-015
X 95
15.0kV SEI
100µm JEOL
NOR
10/16/2013
WD 11.1mm 10:02:01

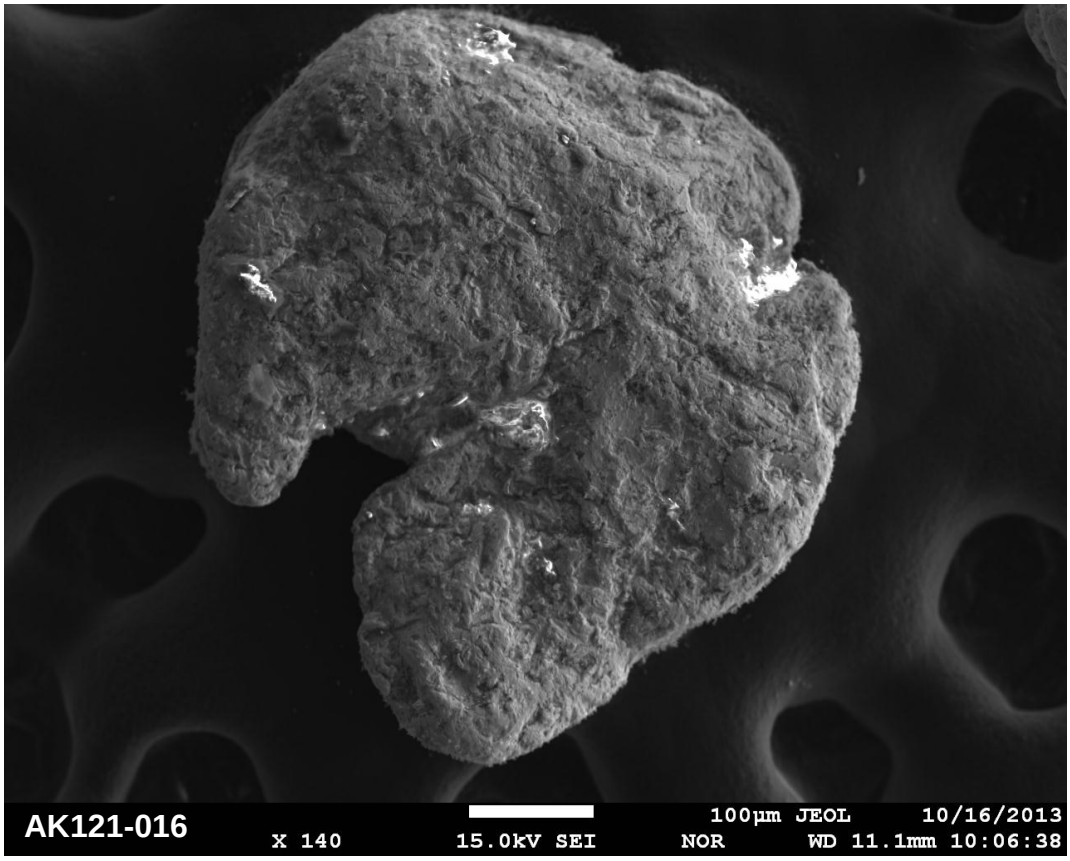
AK121-016
X 140
15.0kV SEI
100µm JEOL
NOR
10/16/2013
WD 11.1mm 10:06:38

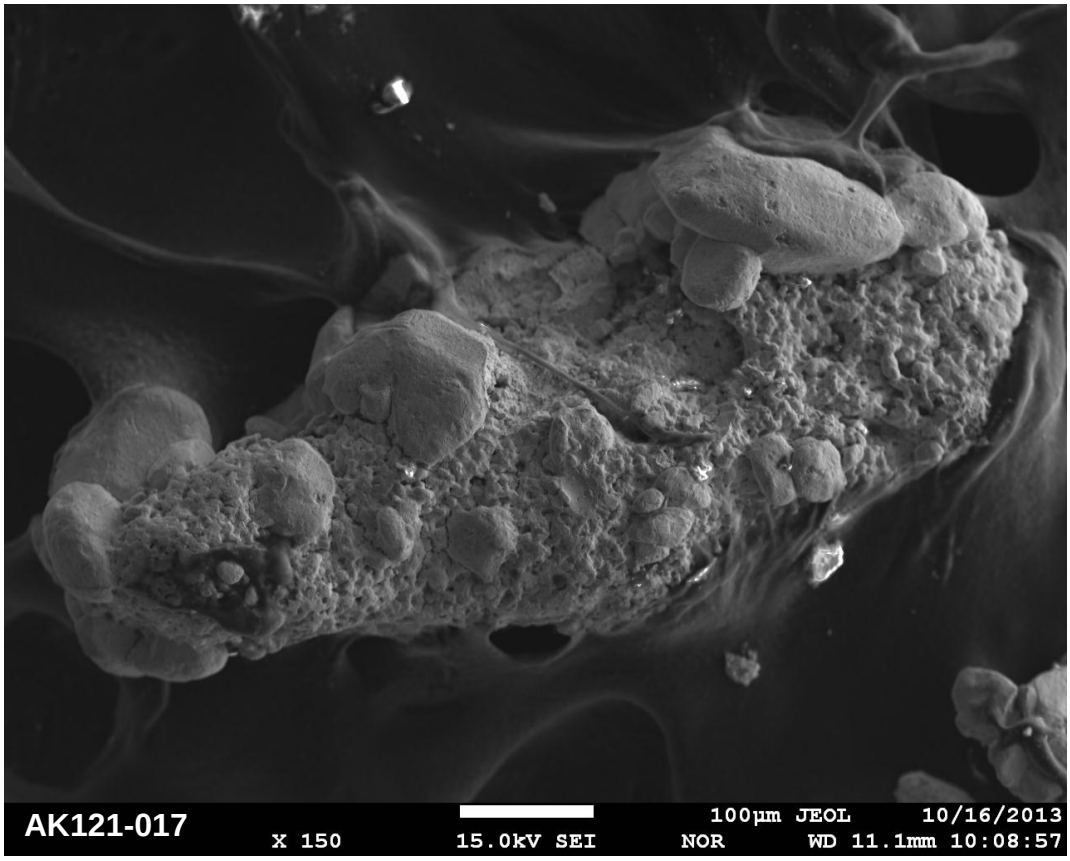
AK121-017
X 150
15.0kV SEI
100µm JEOL
NOR
10/16/2013
WD 11.1mm 10:08:57

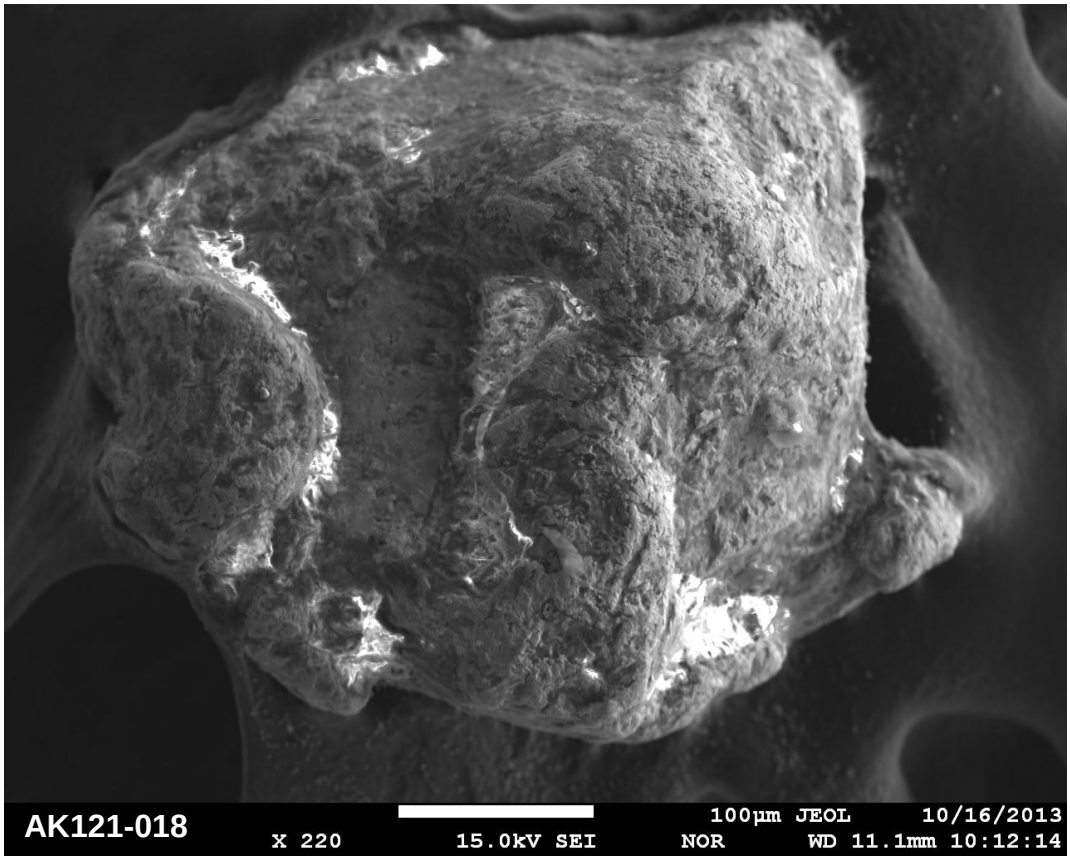
AK121-018
X 220
15.0kV SEI
100µm JEOL
NOR
10/16/2013
WD 11.1mm 10:12:14

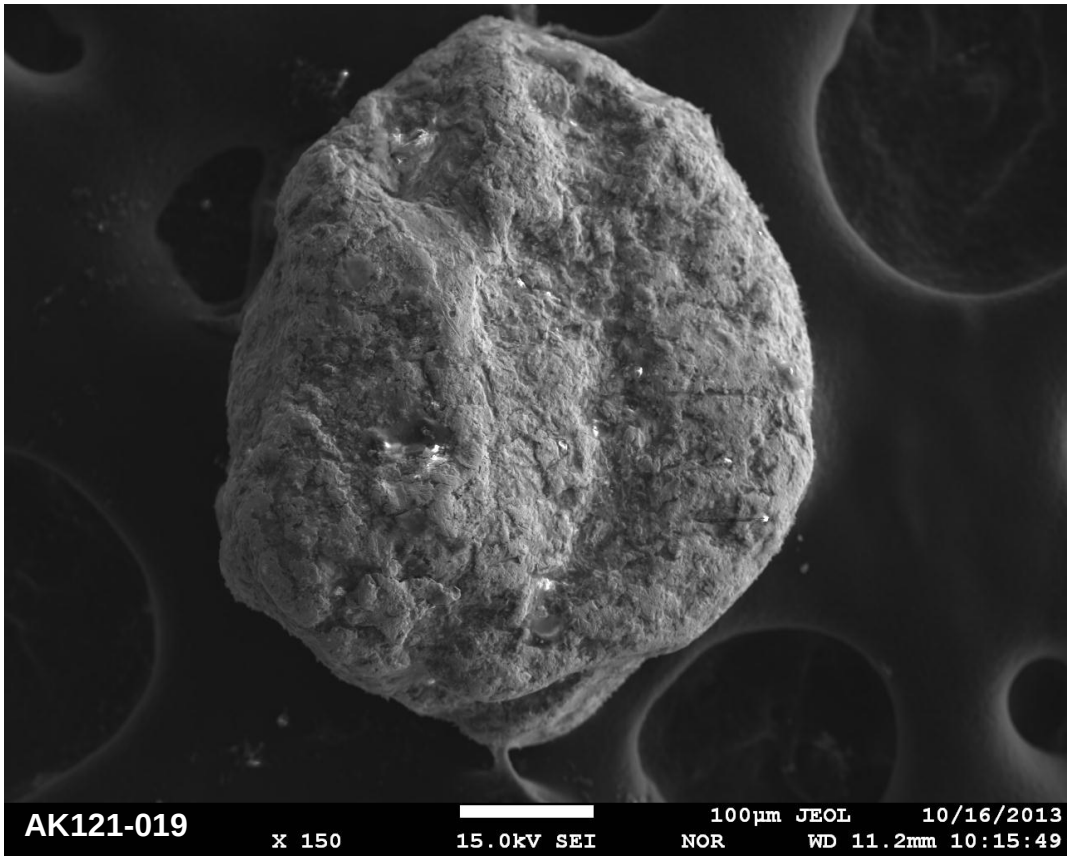
AK121-019
X 150
15.0kV SEI
100µm JEOL
NOR
10/16/2013
WD 11.2mm 10:15:49

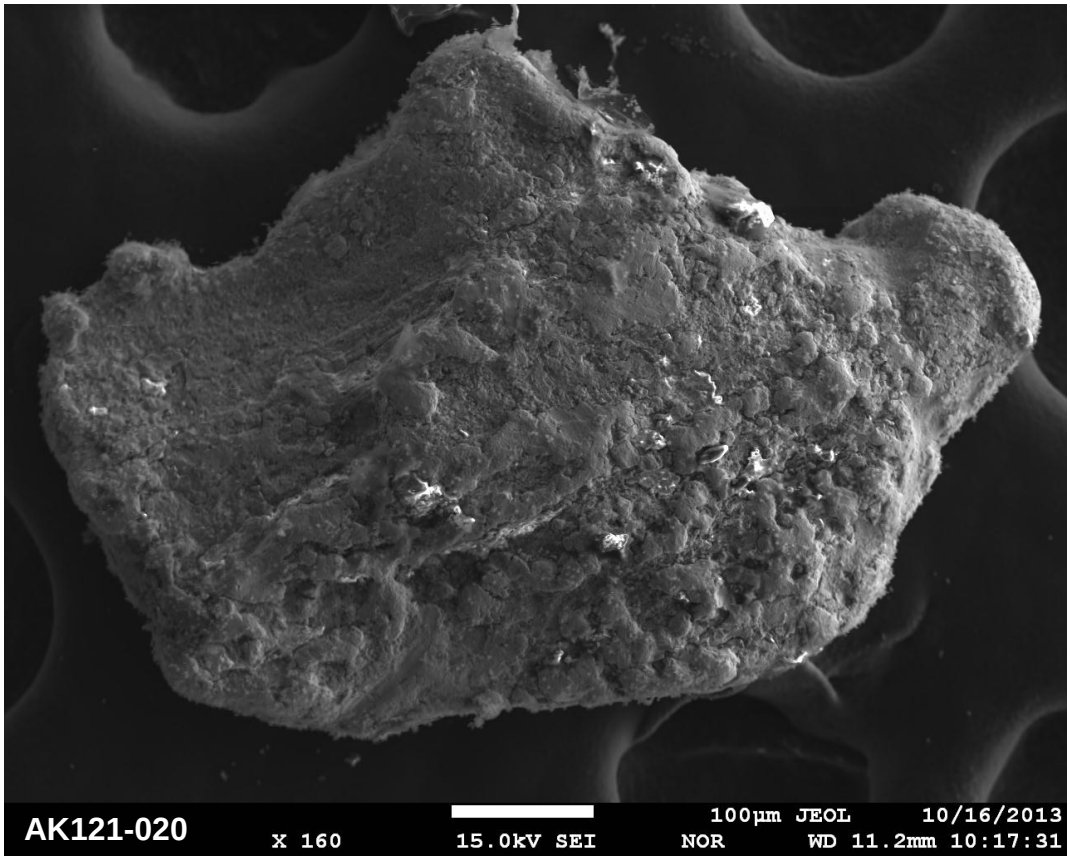
AK121-020
X 160
15.0kV SEI
100µm JEOL
NOR
10/16/2013
WD 11.2mm 10:17:31

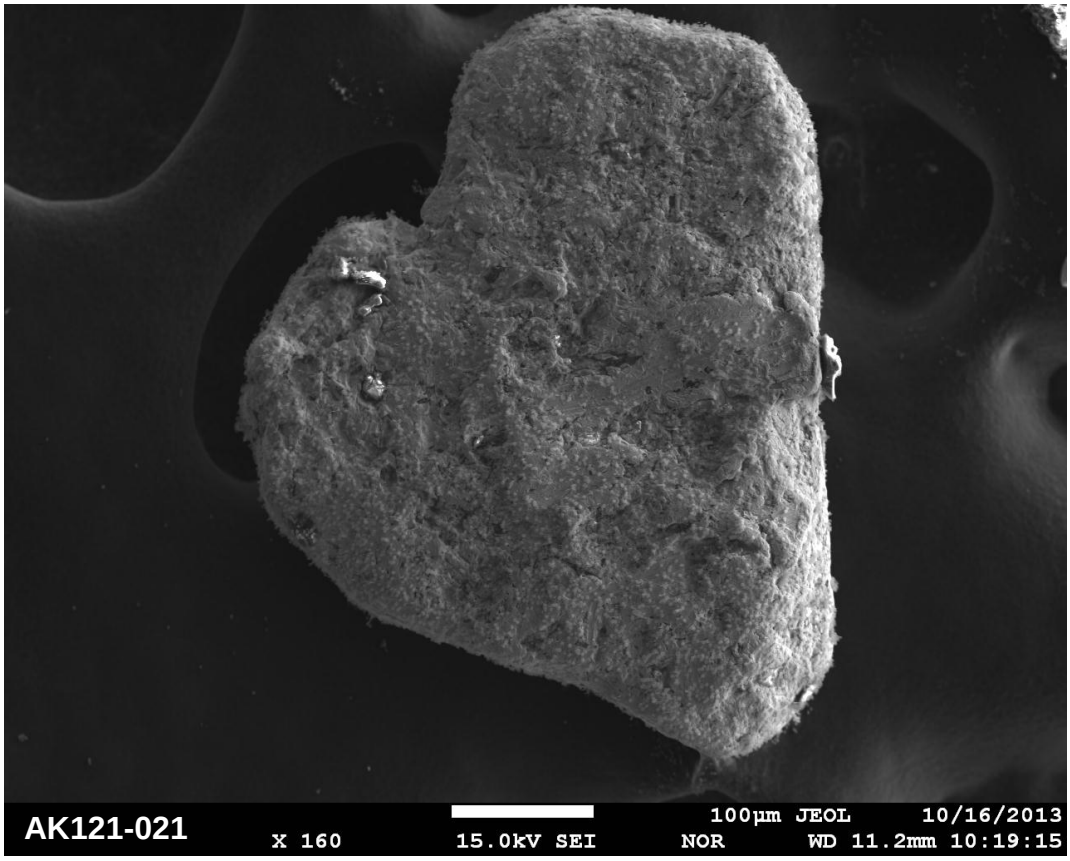
AK121-021
X 160
15.0kV SEI
100µm JEOL
NOR
10/16/2013
WD 11.2mm 10:19:15

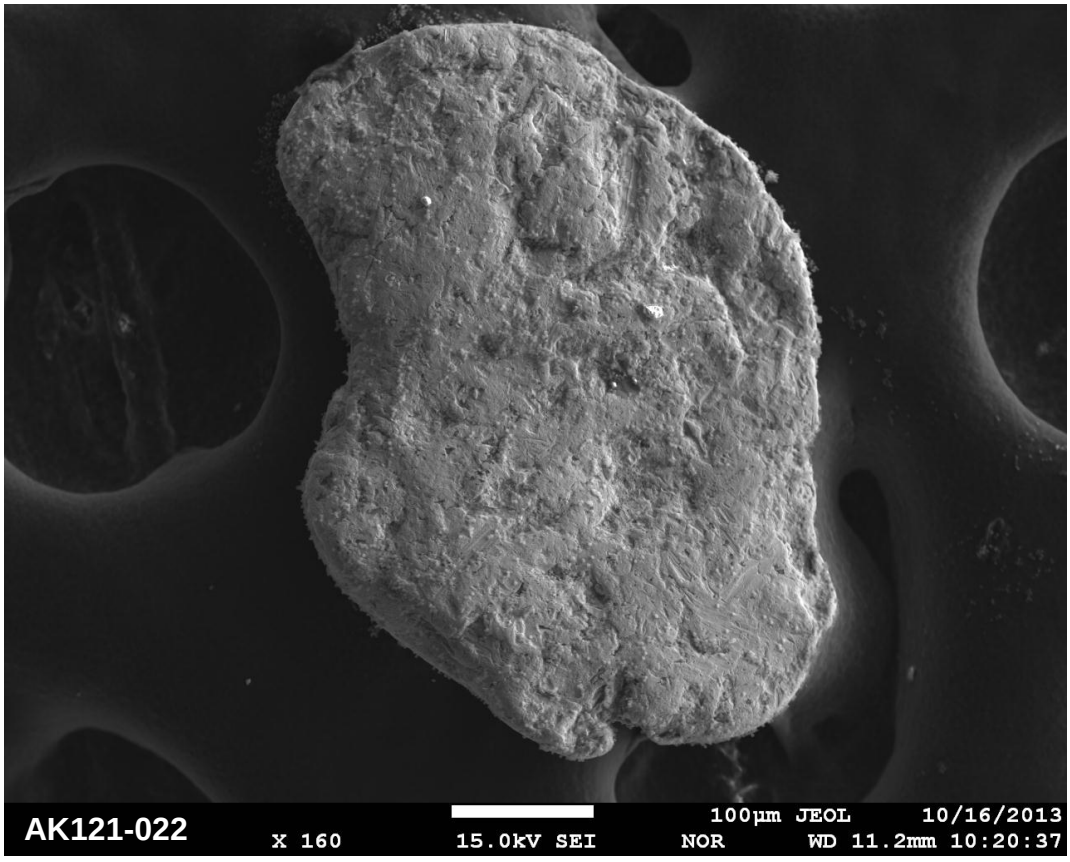
AK121-022
X 160
15.0kV SEI
100µm JEOL
NOR
10/16/2013
WD 11.2mm 10:20:37

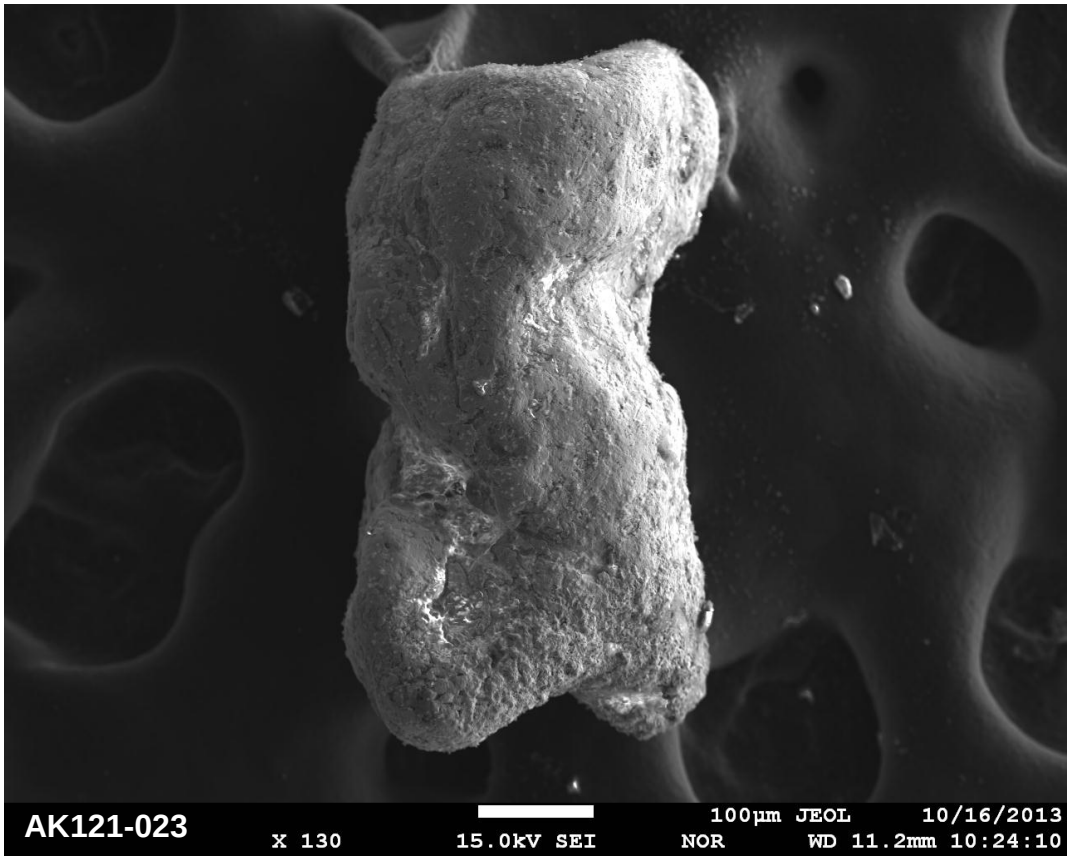
AK121-023
X 130
15.0kV SEI
100µm JEOL
NOR
10/16/2013
WD 11.2mm 10:24:10

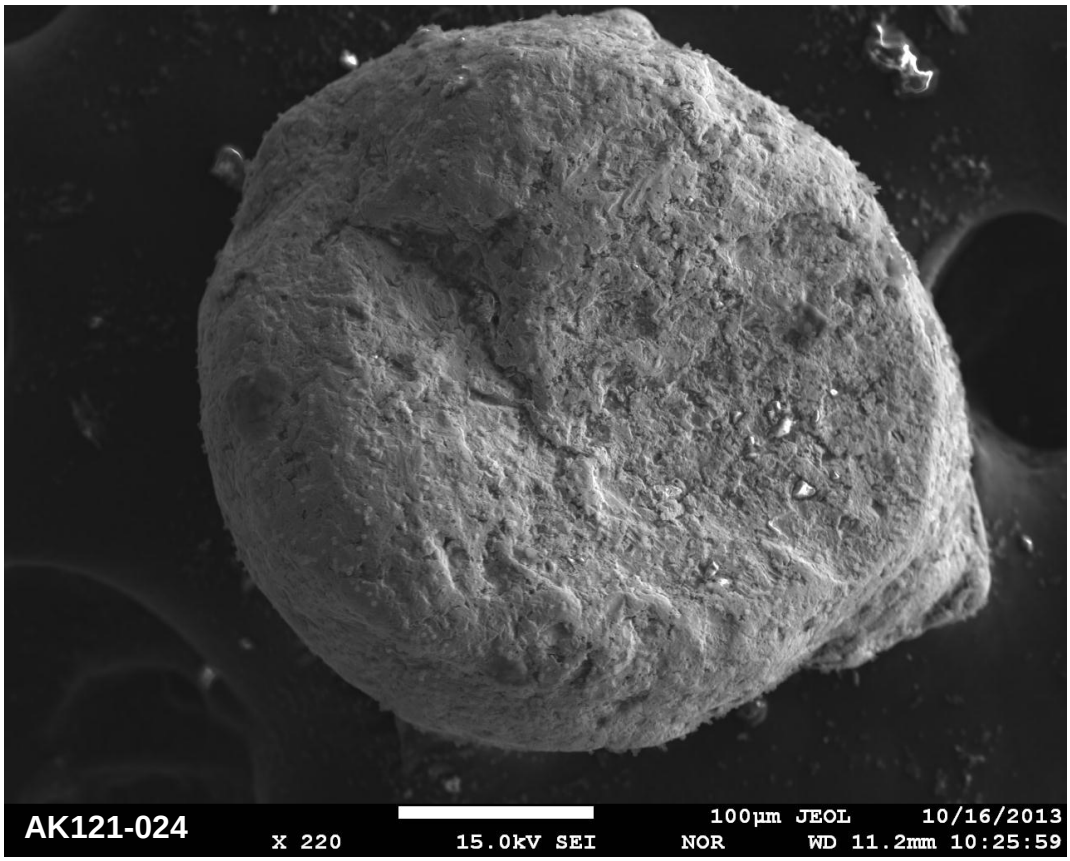
AK121-024
X 220
15.0kV SEI
100µm JEOL
NOR
10/16/2013
WD 11.2mm 10:25:59

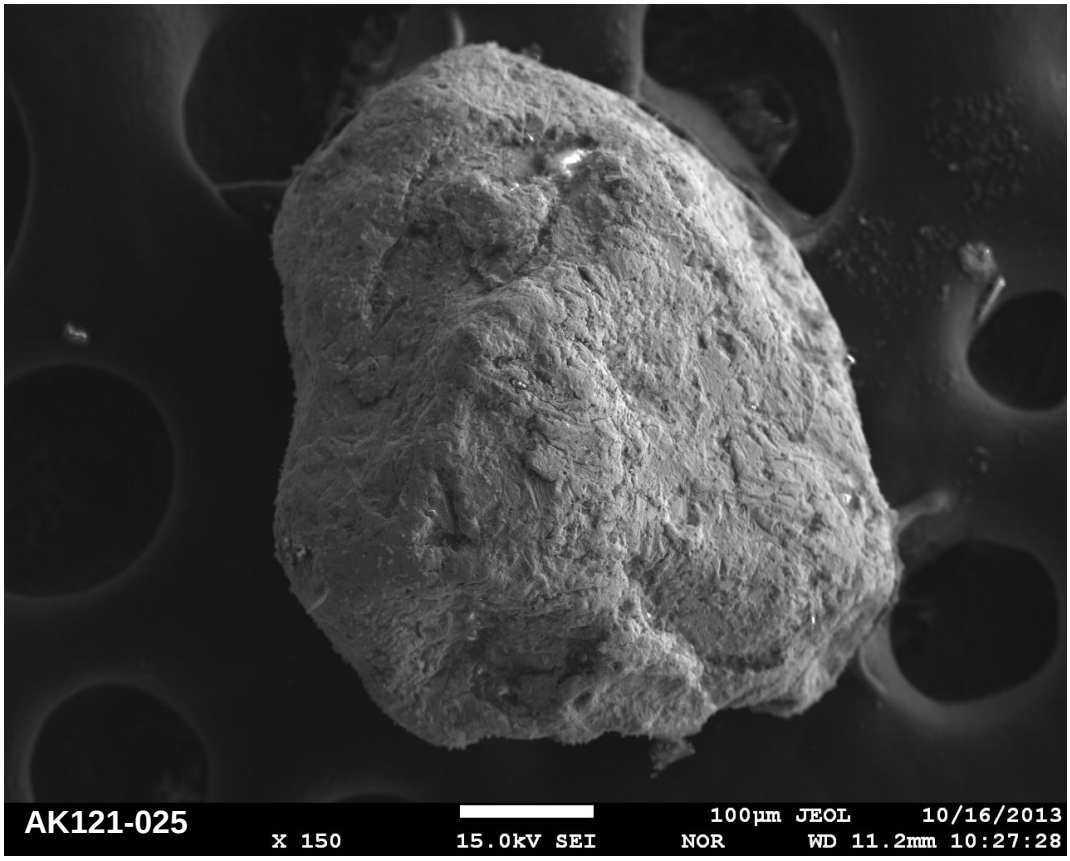
AK121-025
X 150
15.0kV SEI
100µm JEOL
NOR
10/16/2013
WD 11.2mm 10:27:28

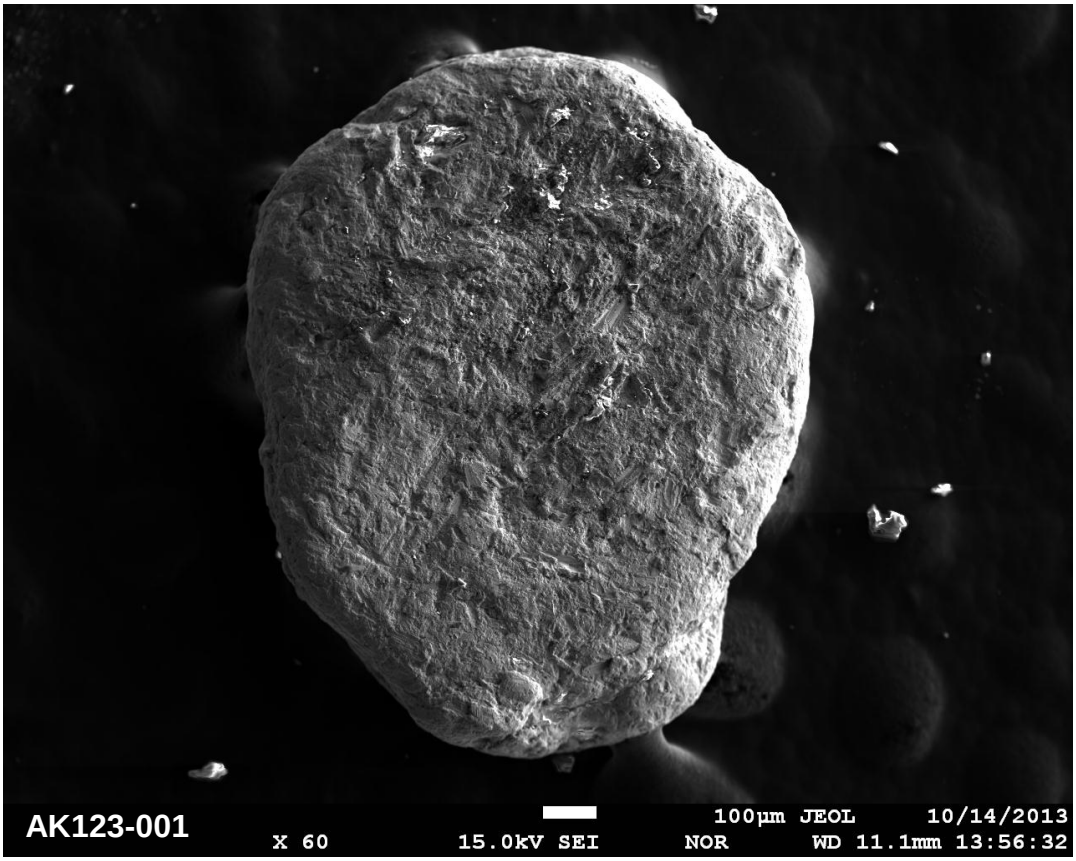
AK123-001
X 60
15.0kV SEI
100µm JEOL
NOR
10/14/2013
WD 11.1mm 13:56:32

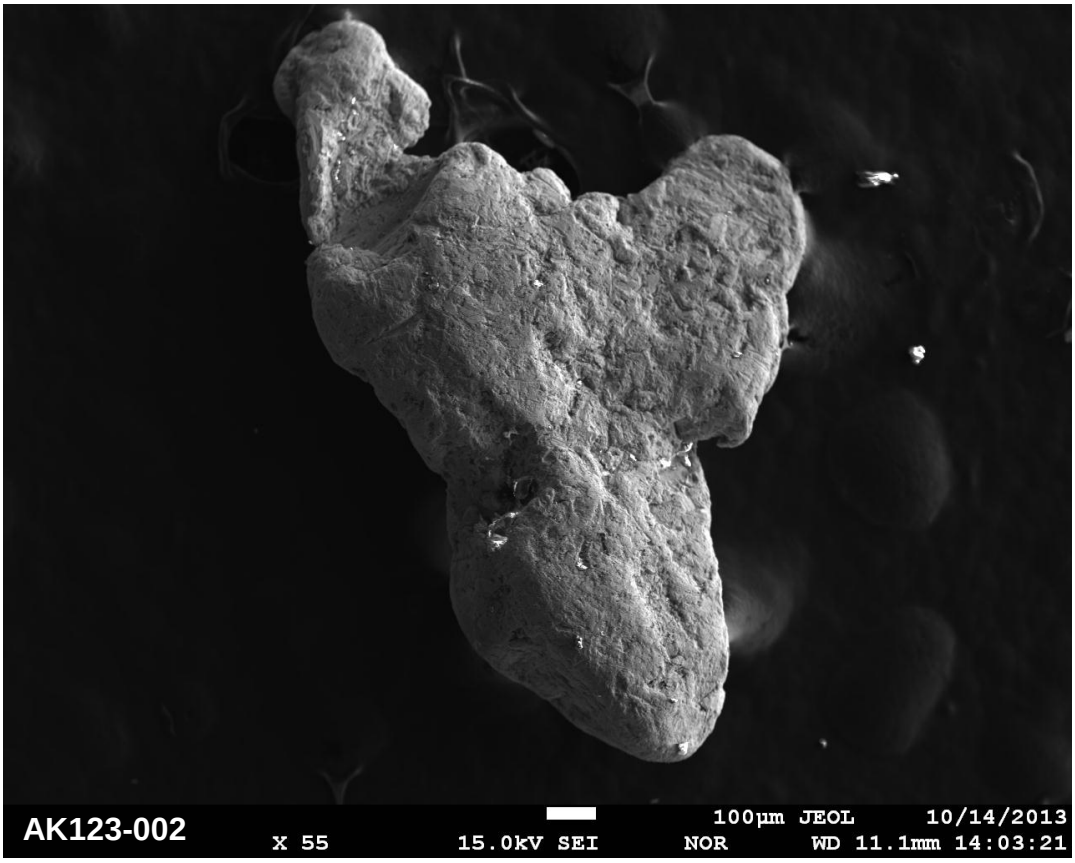
AK123-002
X 55
15.0kV SEI
100µm JEOL
NOR
10/14/2013
WD 11.1mm 14:03:21

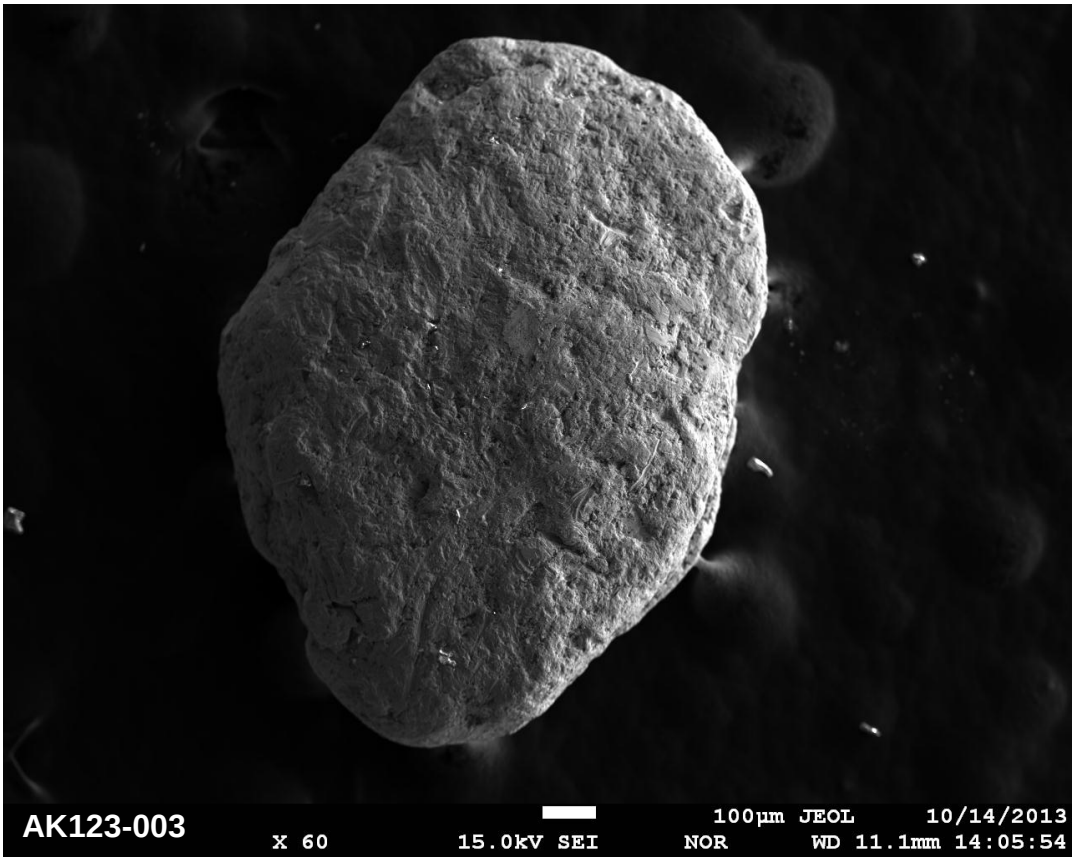
AK123-003
X 60
15.0kV SEI
100µm JEOL
NOR
10/14/2013
WD 11.1mm 14:05:54

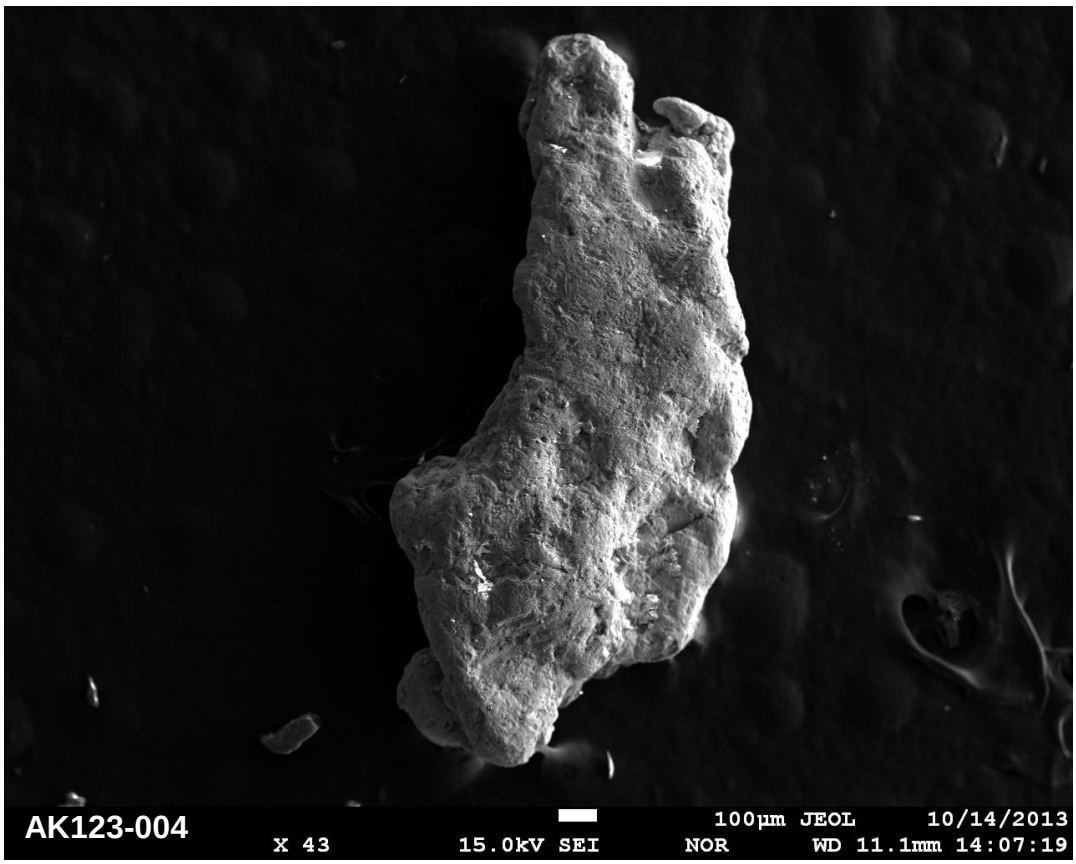
AK123-004
X 43
15.0kV SEI
100µm JEOL
NOR
10/14/2013
WD 11.1mm 14:07:19

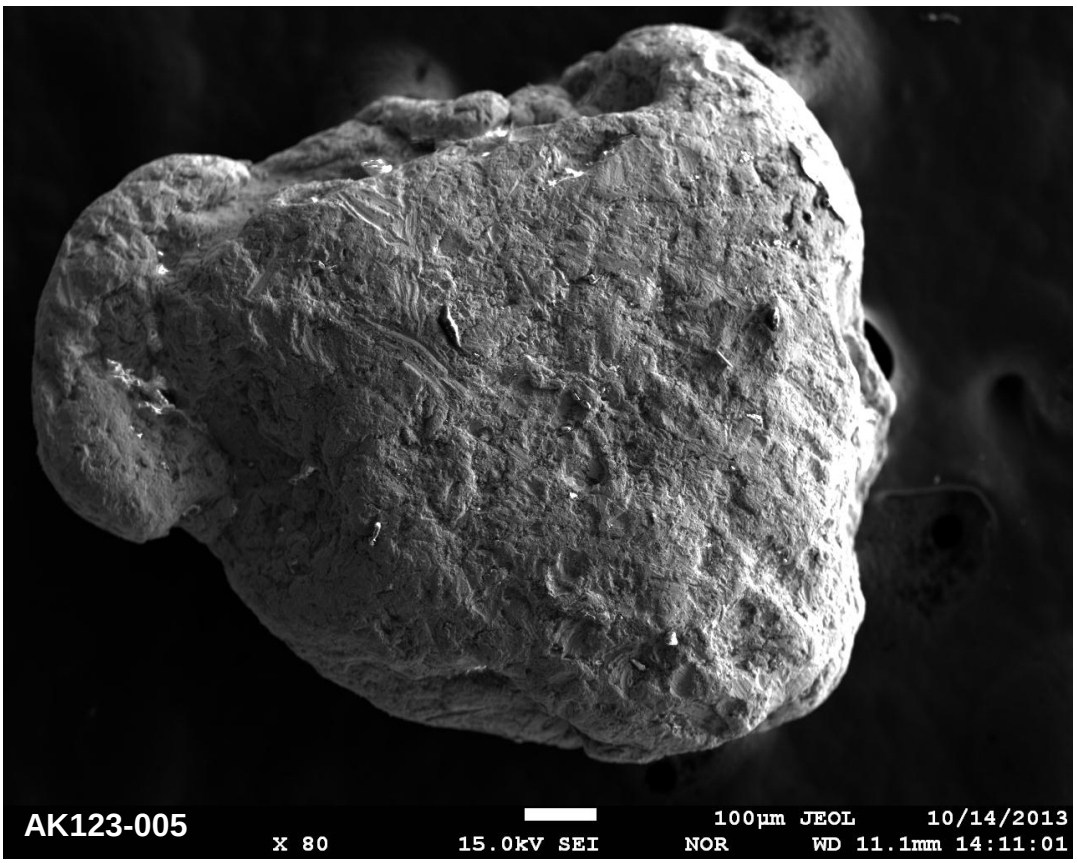
AK123-005
X 80
15.0kV SEI
100µm JEOL
NOR
10/14/2013
WD 11.1mm 14:11:01

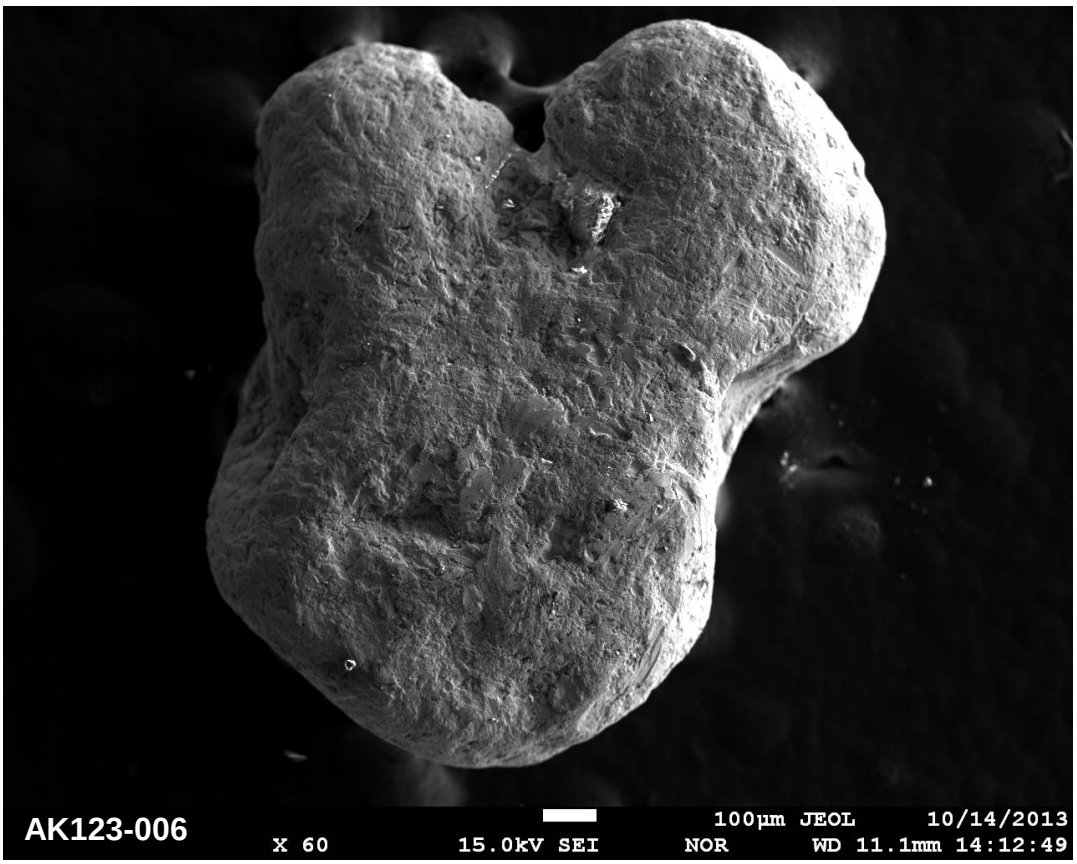
AK123-006
X 60
15.0kV SEI
100µm JEOL
NOR
10/14/2013
WD 11.1mm 14:12:49

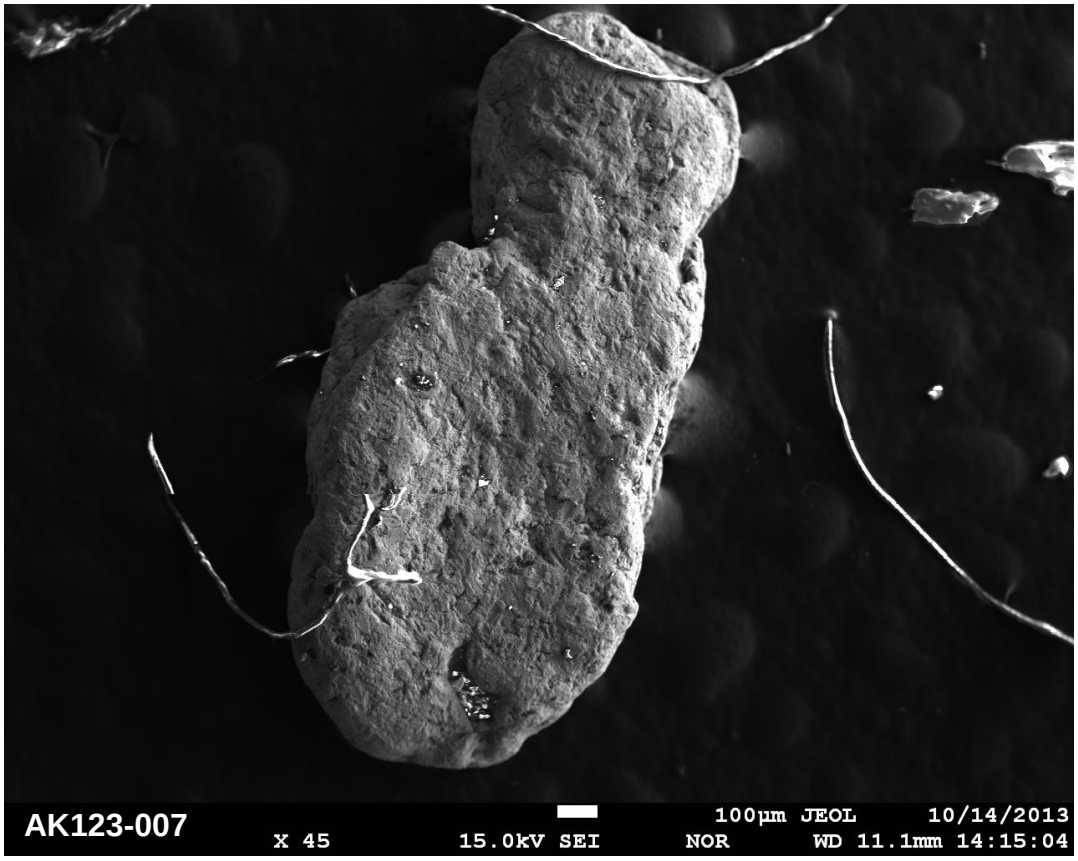
AK123-007
X 45
15.0kV SEI
100µm JEOL
NOR
10/14/2013
WD 11.1mm 14:15:04

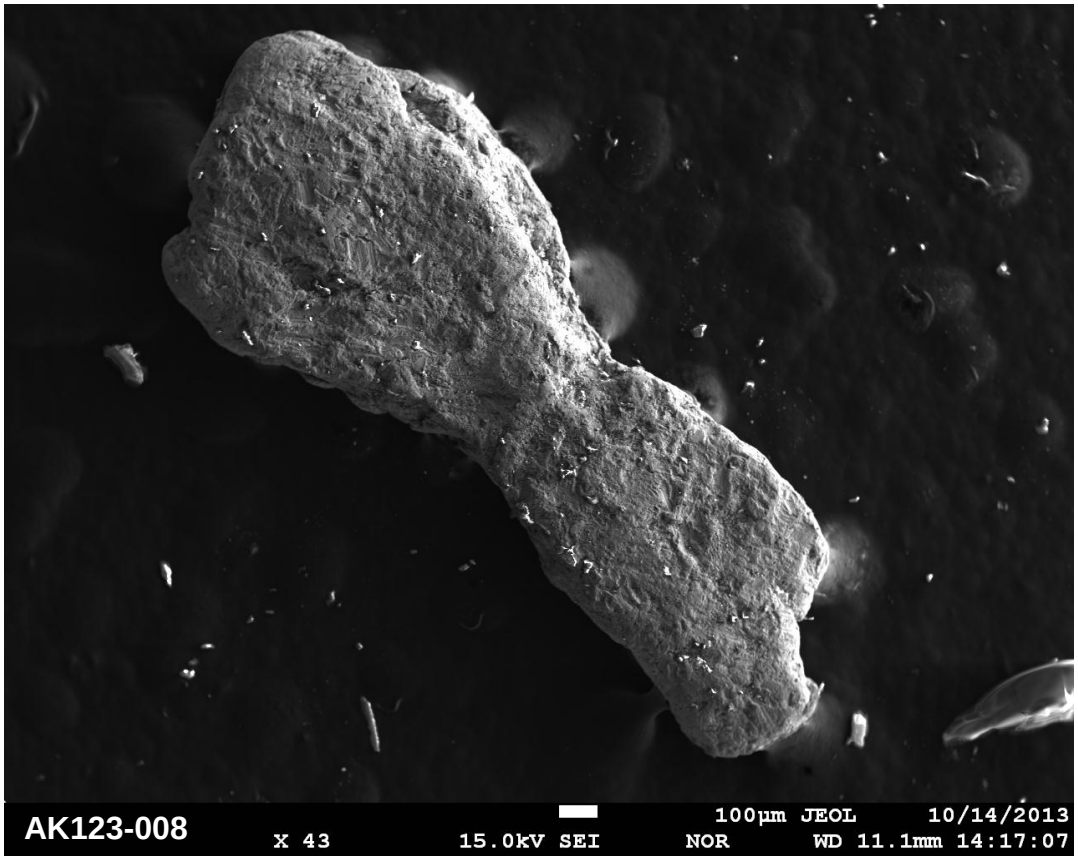
AK123-008
X 43
15.0kV SEI
100µm JEOL
NOR
10/14/2013
WD 11.1mm 14:17:07

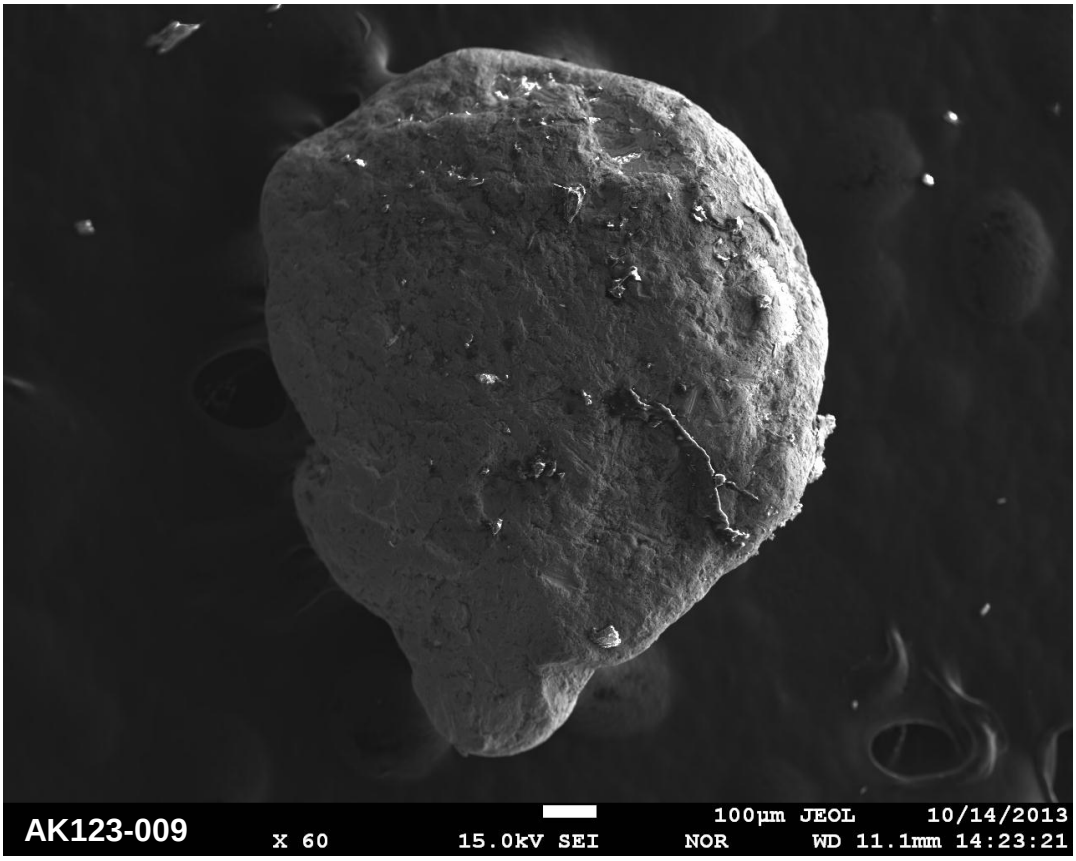
AK123-009
X 60
15.0kV SEI
100µm JEOL
NOR
10/14/2013
WD 11.1mm 14:23:21

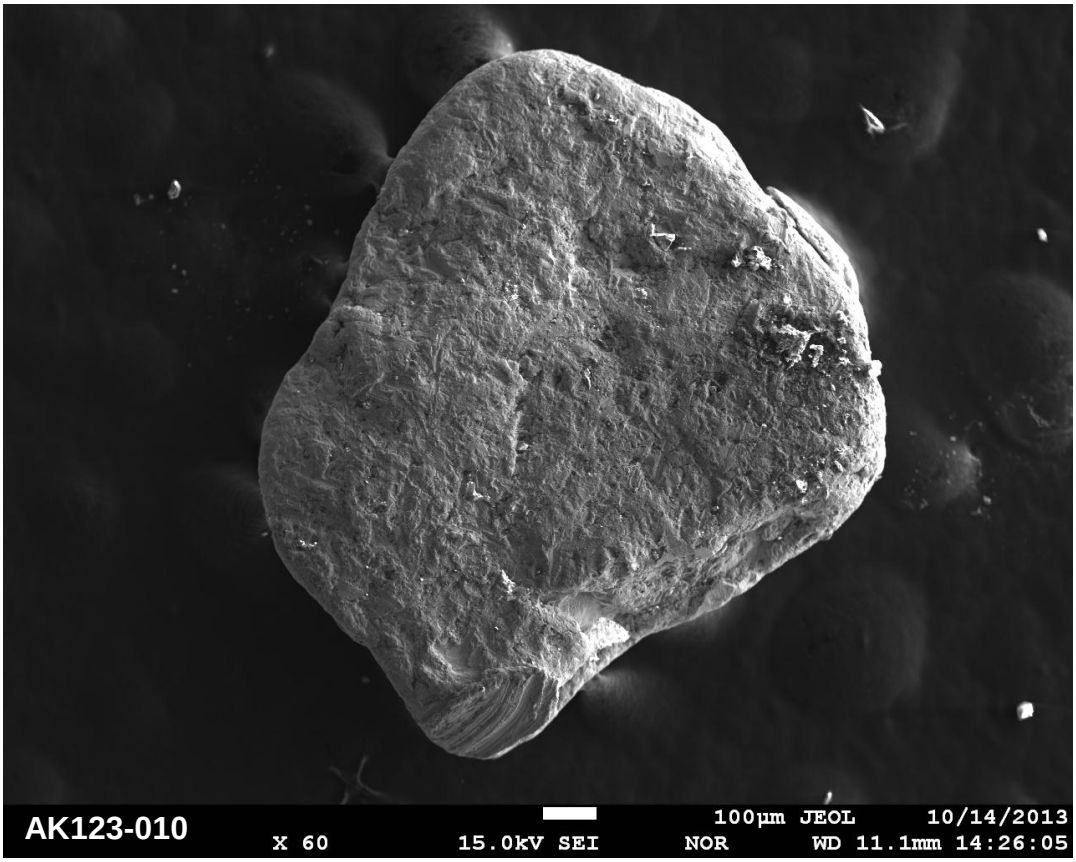
AK123-010
X 60
15.0kV SEI
100µm JEOL
NOR
10/14/2013
WD 11.1mm 14:26:05

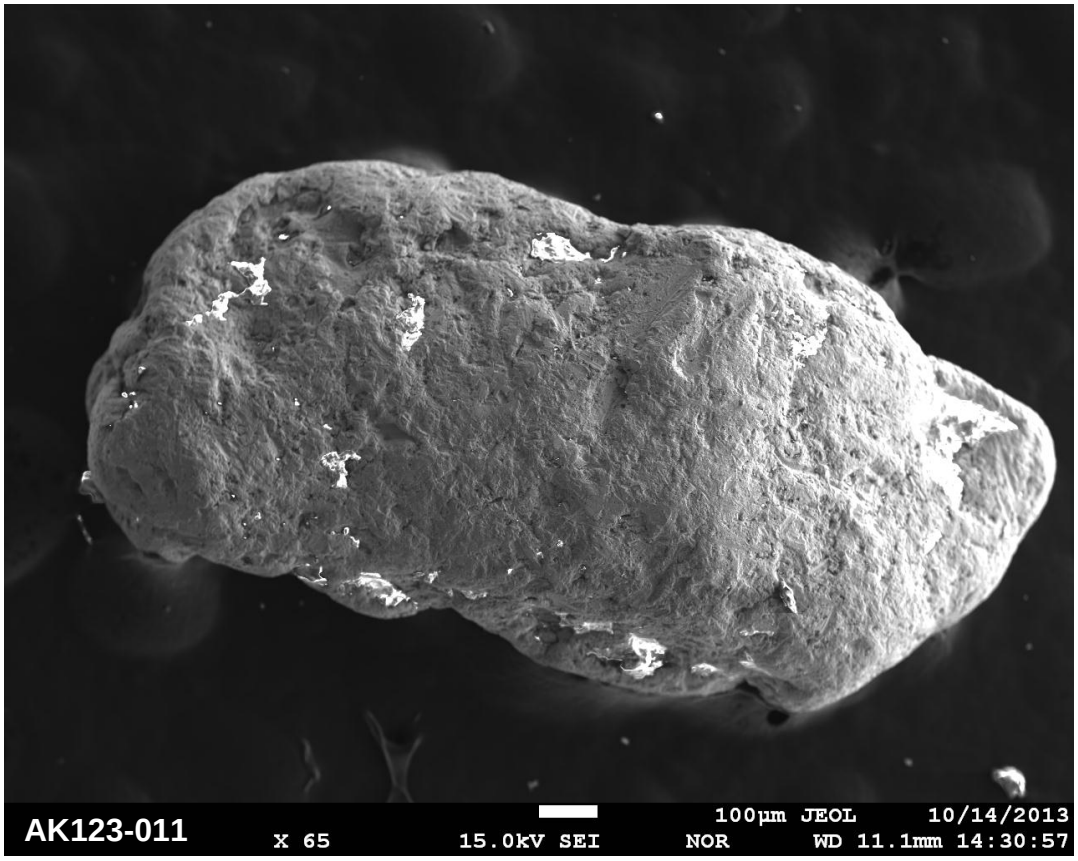
AK123-011
X 65
15.0kV SEI
100µm JEOL
NOR
10/14/2013
WD 11.1mm 14:30:57

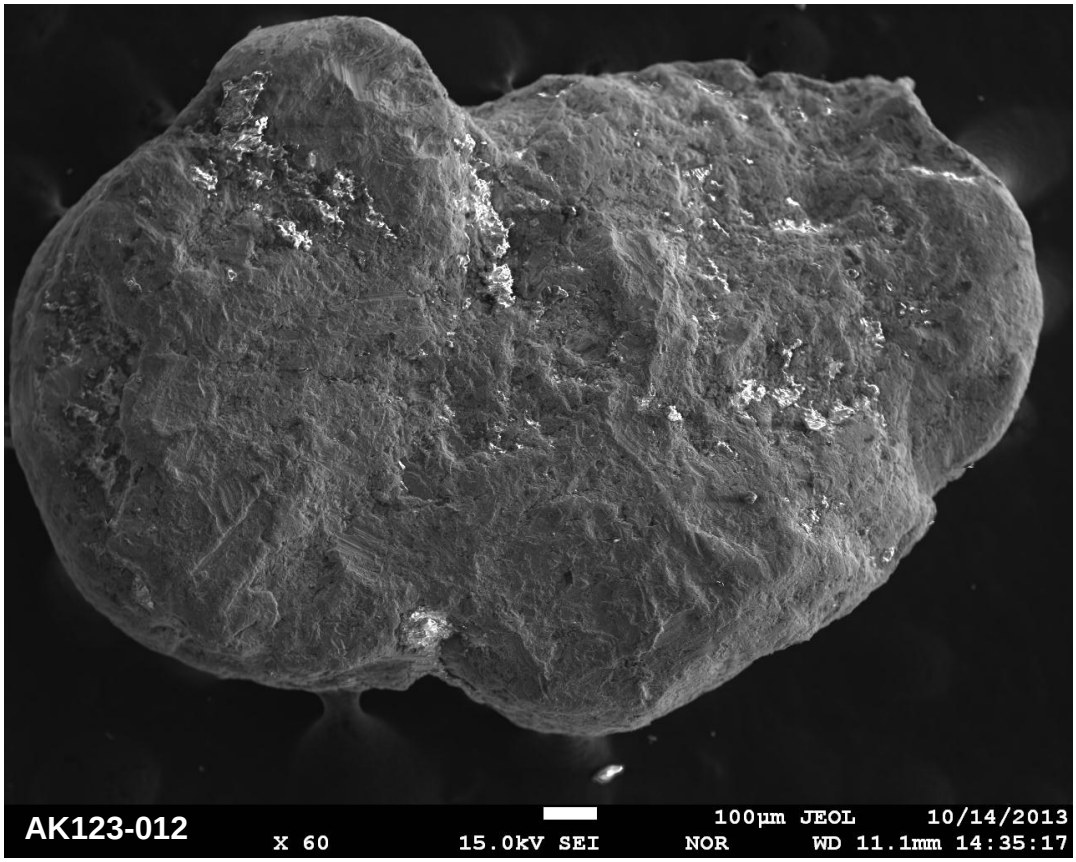
AK123-012
X 60
15.0kV SEI
100µm JEOL
NOR
10/14/2013
WD 11.1mm 14:35:17

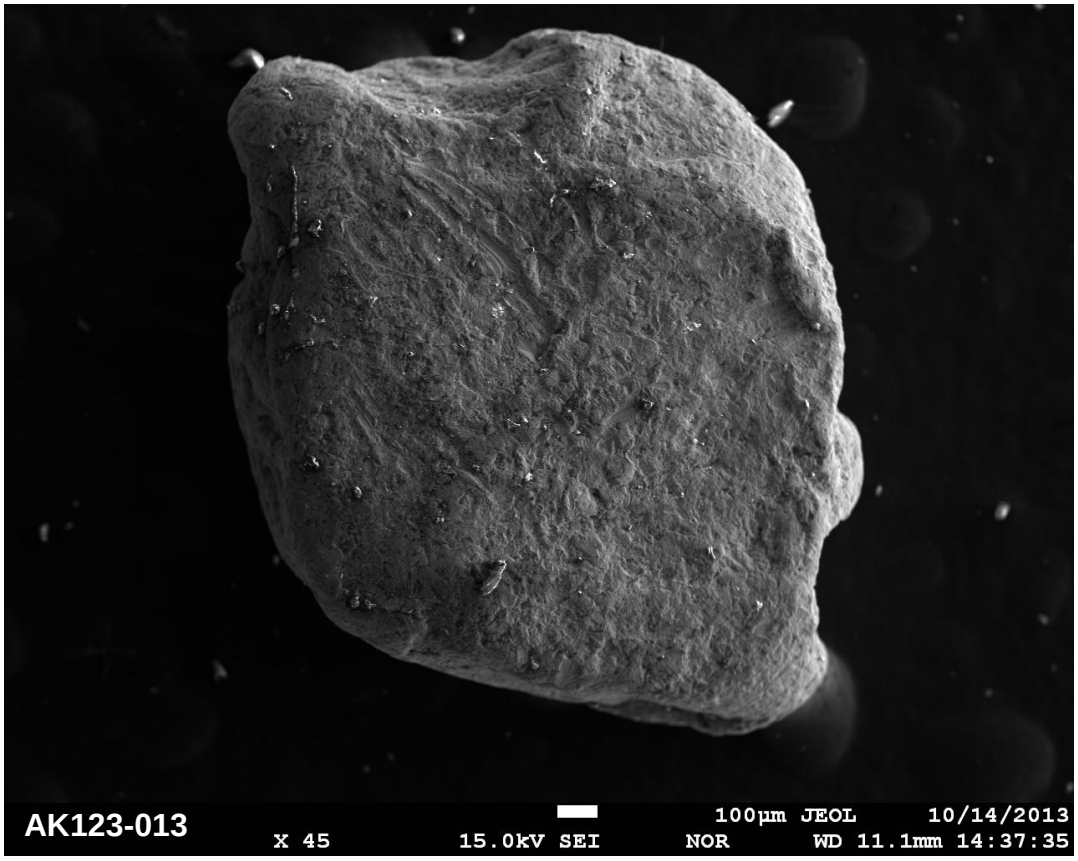
AK123-013
X 45
15.0kV SEI
100µm JEOL
NOR
10/14/2013
WD 11.1mm 14:37:35

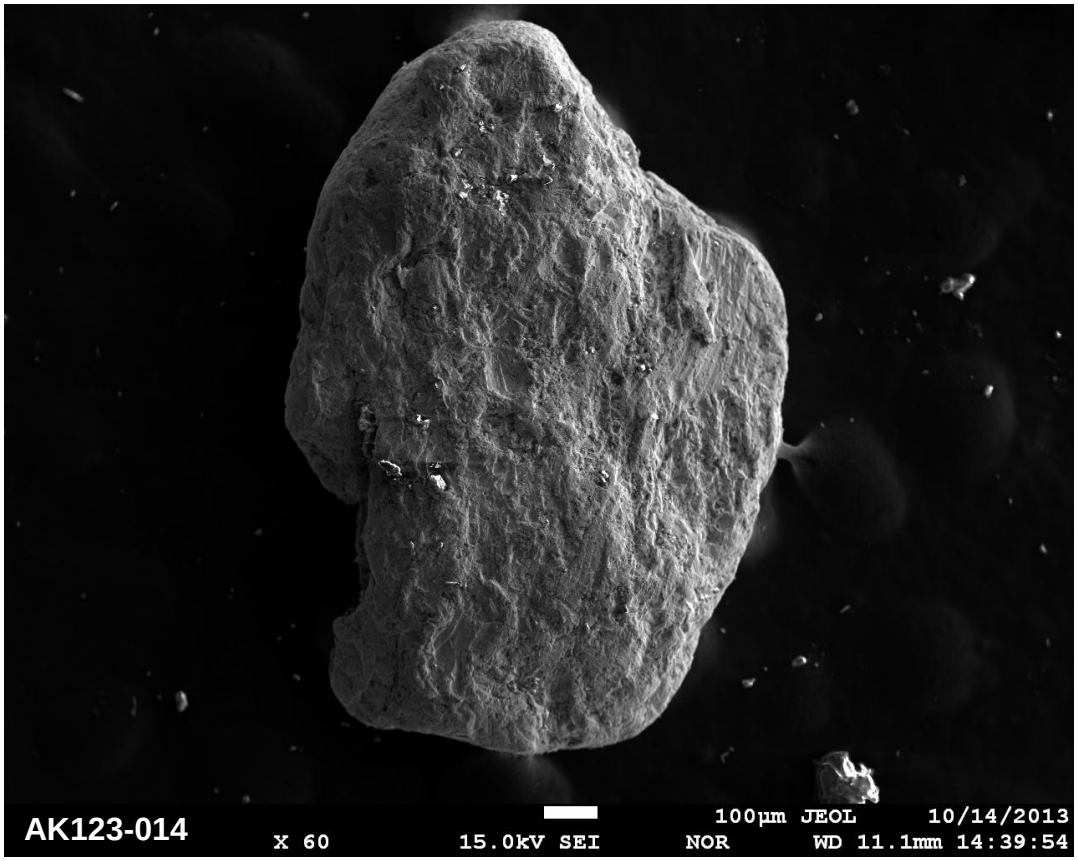
AK123-014
X 60
15.0kV SEI
100µm JEOL
NOR
10/14/2013
WD 11.1mm 14:39:54

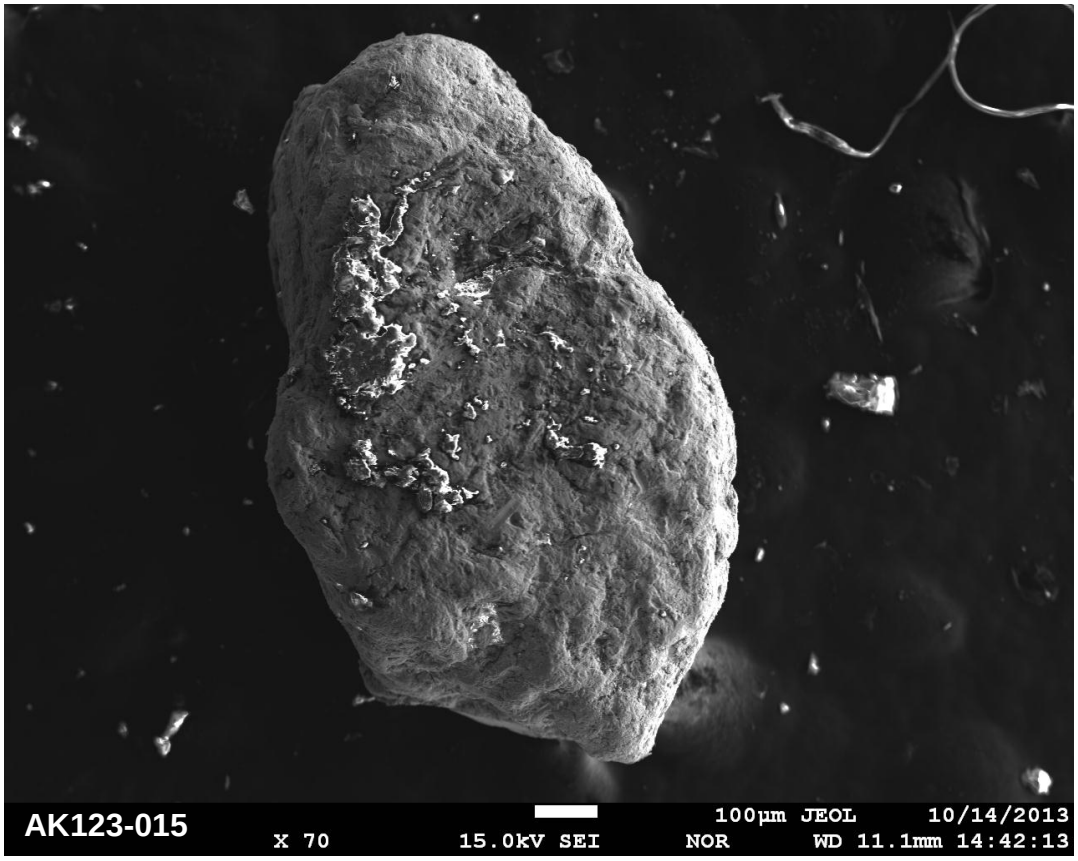
AK123-015
X 70
15.0kV SEI
100µm JEOL
NOR
10/14/2013
WD 11.1mm 14:42:13

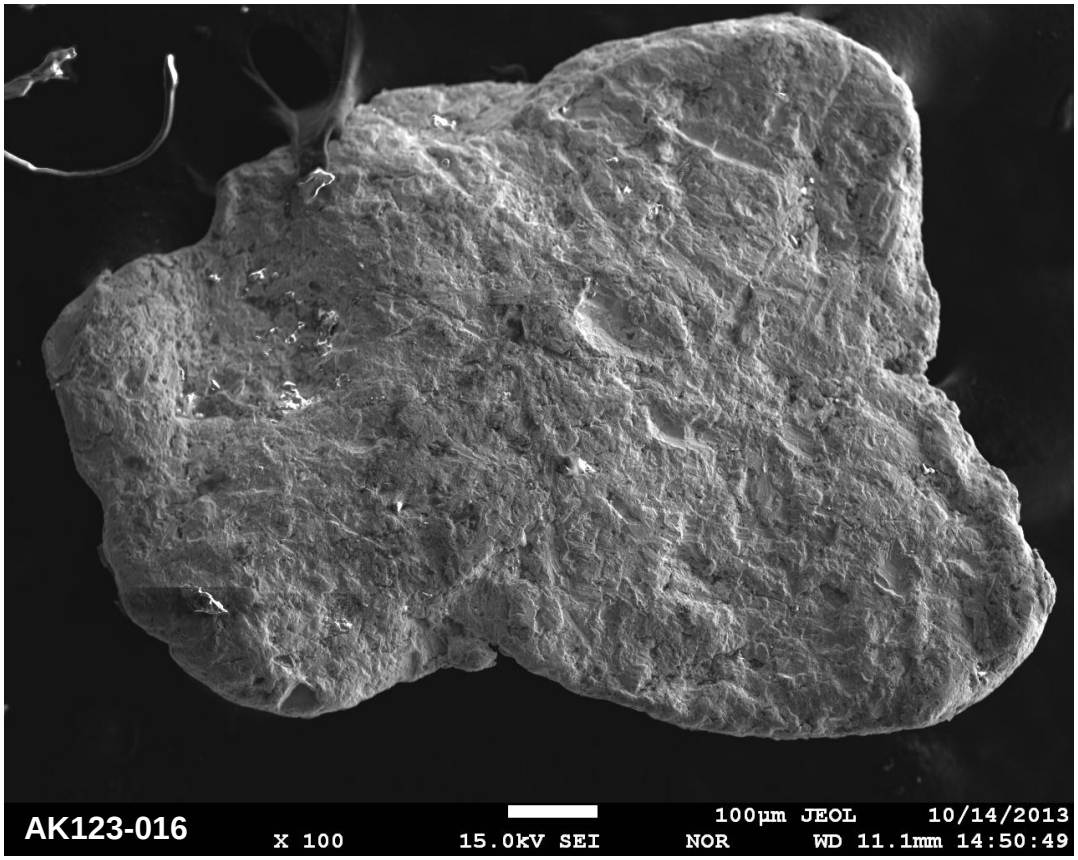
AK123-016
X 100
15.0kV SEI
100µm JEOL
NOR
10/14/2013
WD 11.1mm 14:50:49

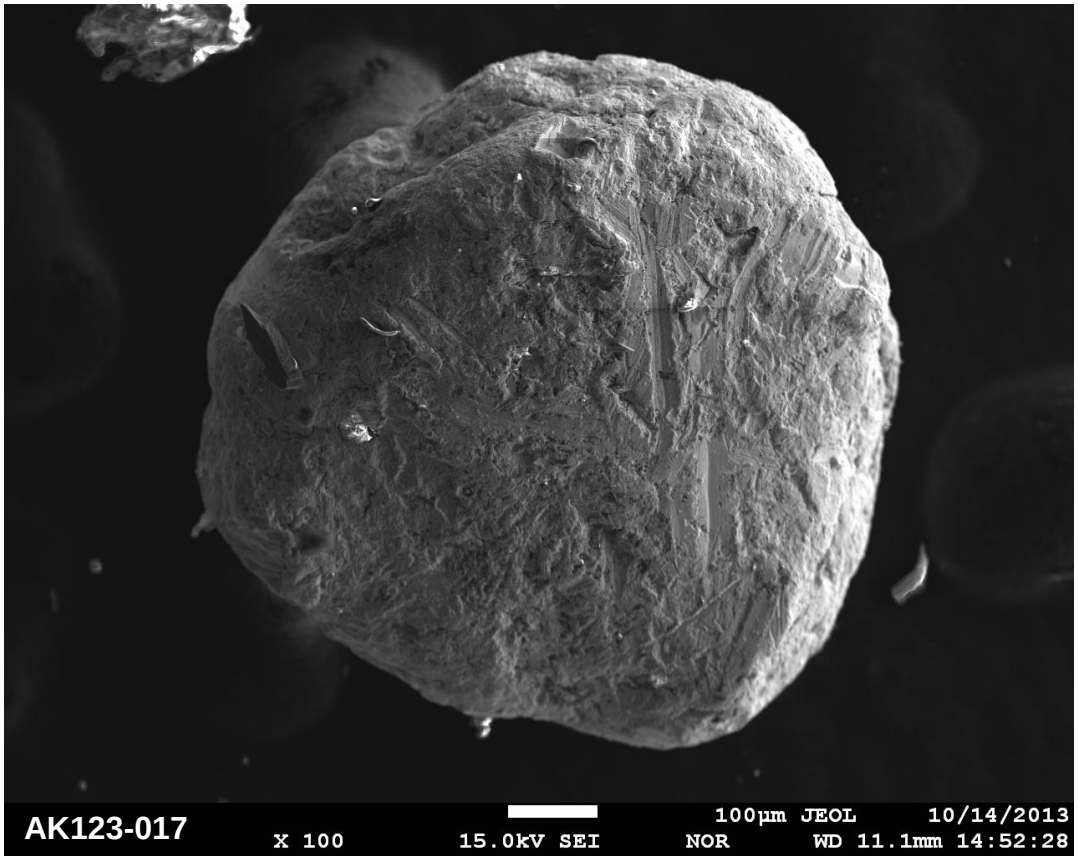
AK123-017
X 100
15.0kV SEI
100µm JEOL
NOR
10/14/2013
WD 11.1mm 14:52:28

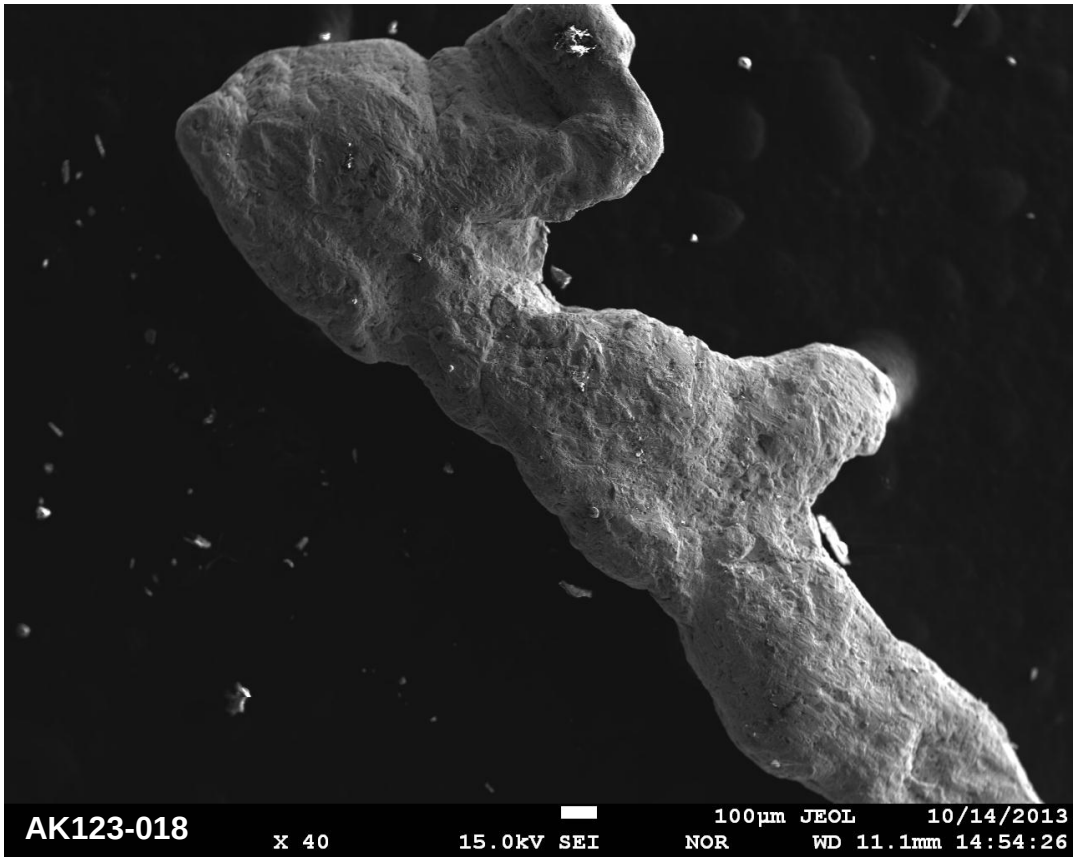
AK123-018
X 40
15.0kV SEI
100µm JEOL
NOR
10/14/2013
WD 11.1mm 14:54:26

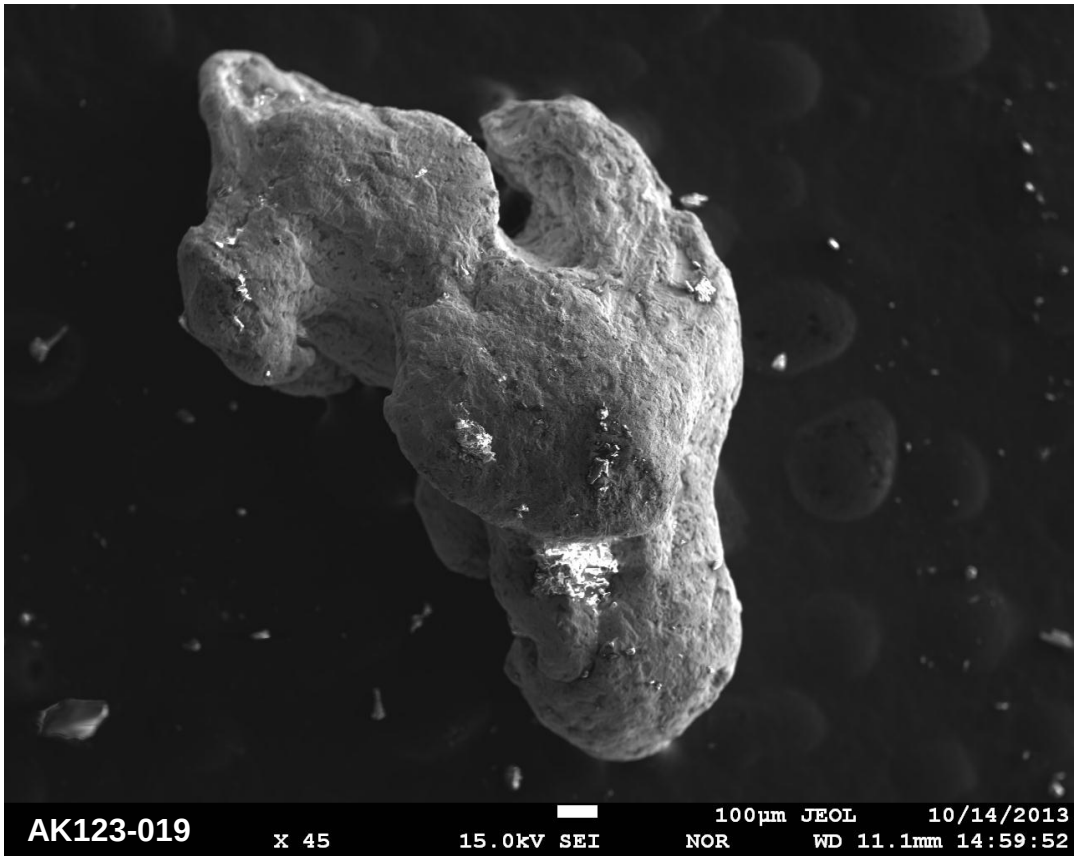
AK123-019
X 45
15.0kV SEI
100µm JEOL
NOR
10/14/2013
WD 11.1mm 14:59:52

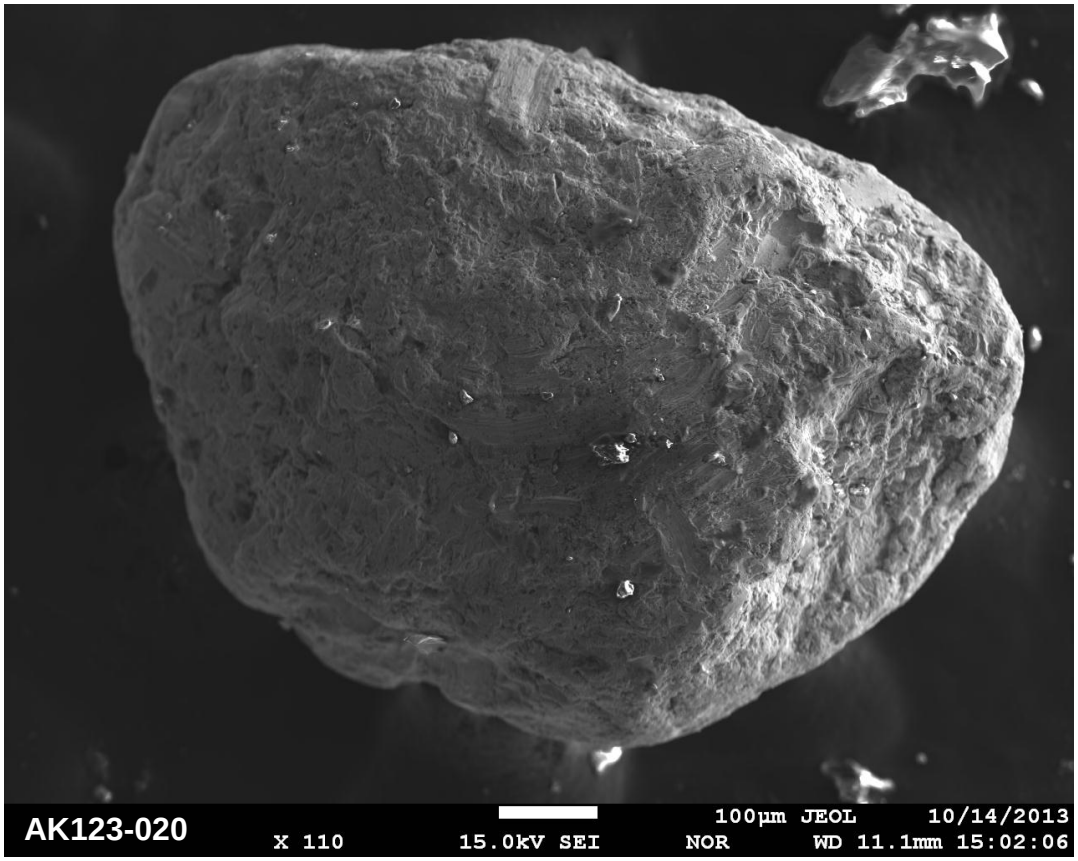
AK123-020
X 110
15.0kV SEI
100µm JEOL
NOR
10/14/2013
WD 11.1mm 15:02:06

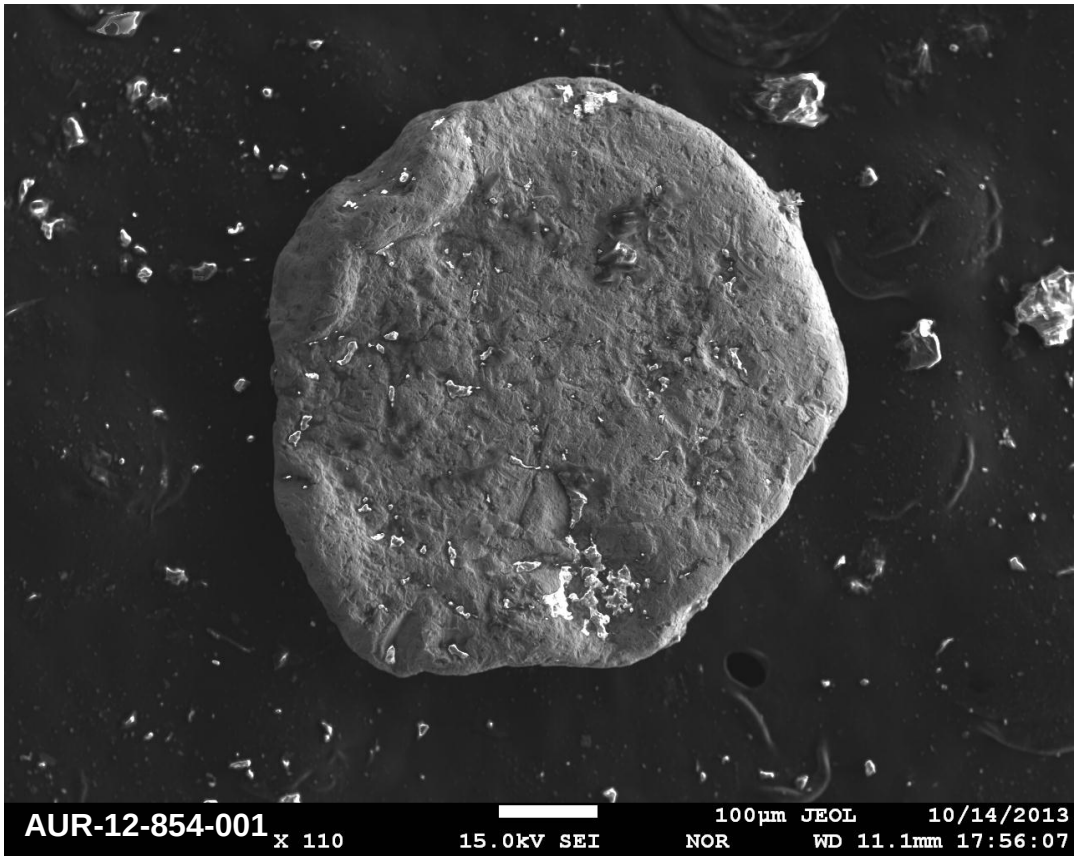
AUR-12-854-001
X 110
15.0kV SEI
100µm JEOL
NOR
10/14/2013
WD 11.1mm 17:56:07

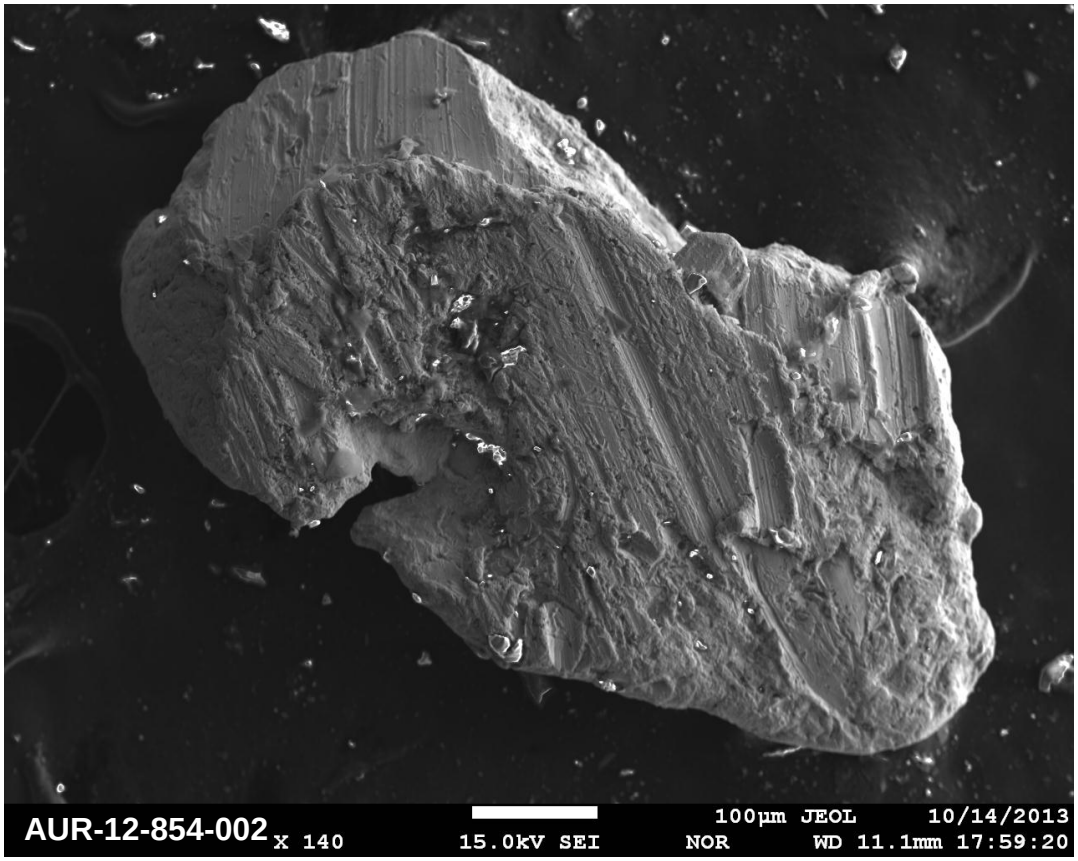
AUR-12-854-002
X 140
15.0kV SEI
100µm JEOL
NOR
10/14/2013
WD 11.1mm 17:59:20

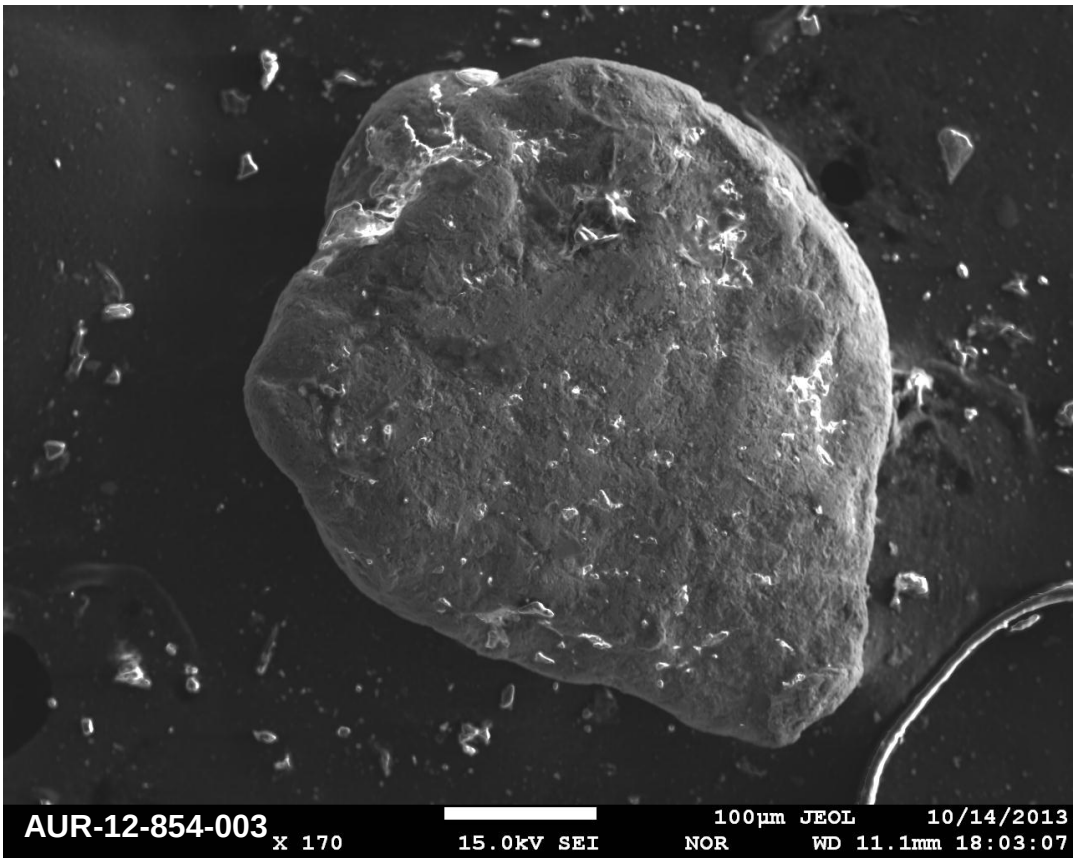
AUR-12-854-003
X 170
15.0kV SEI
100µm JEOL
NOR
10/14/2013
WD 11.1mm 18:03:07

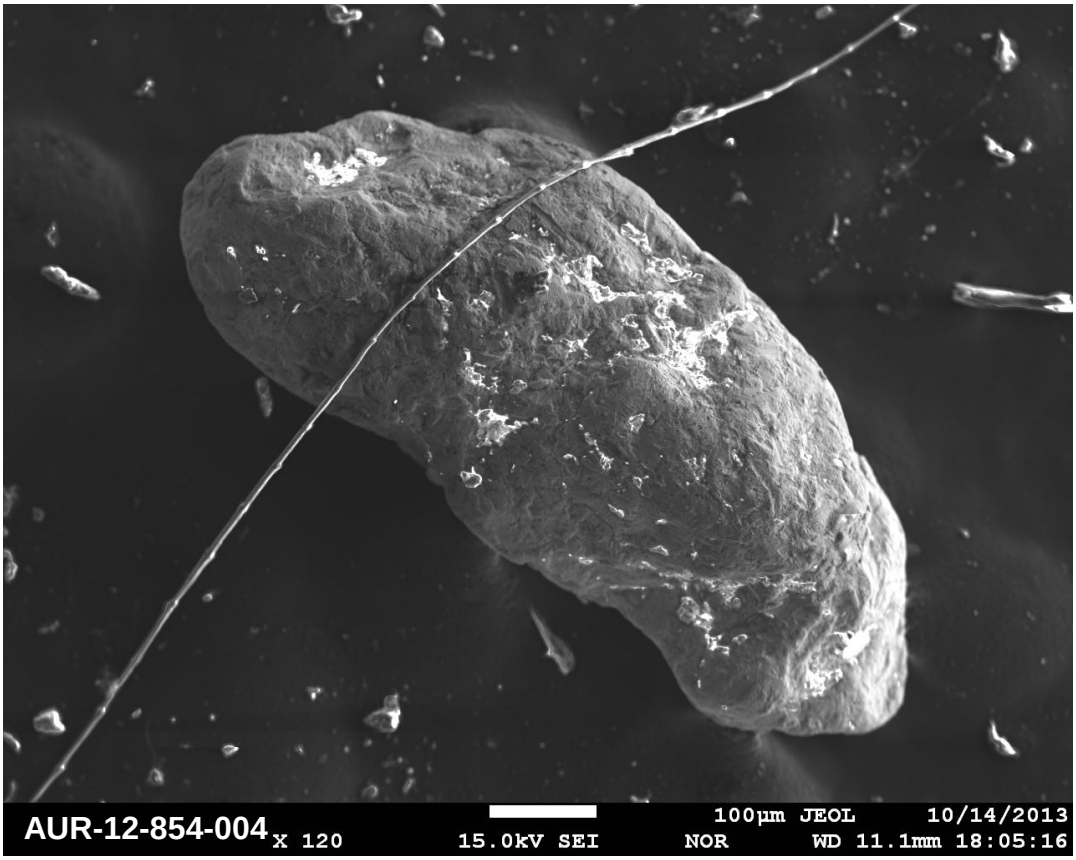
AUR-12-854-004
X 120
15.0kV SEI
100µm JEOL
NOR
10/14/2013
WD 11.1mm 18:05:16

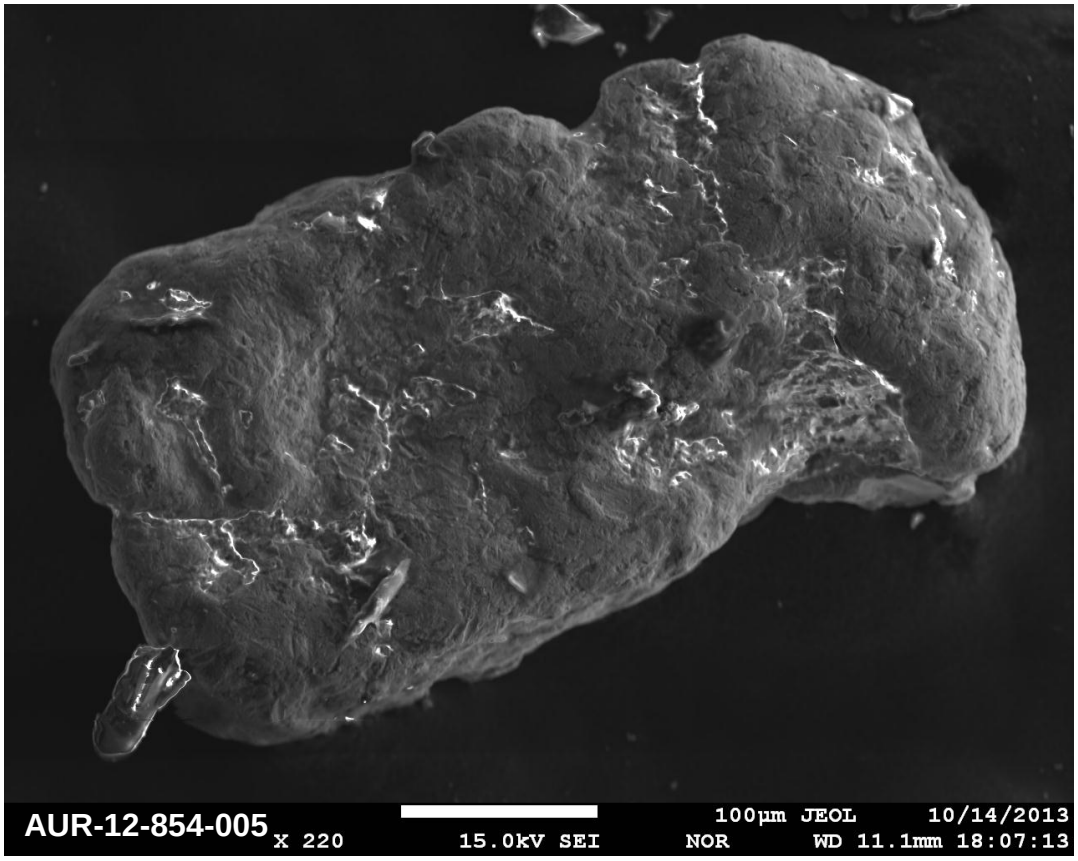
AUR-12-854-005
X 220
15.0kV SEI
100µm JEOL
NOR
10/14/2013
WD 11.1mm 18:07:13

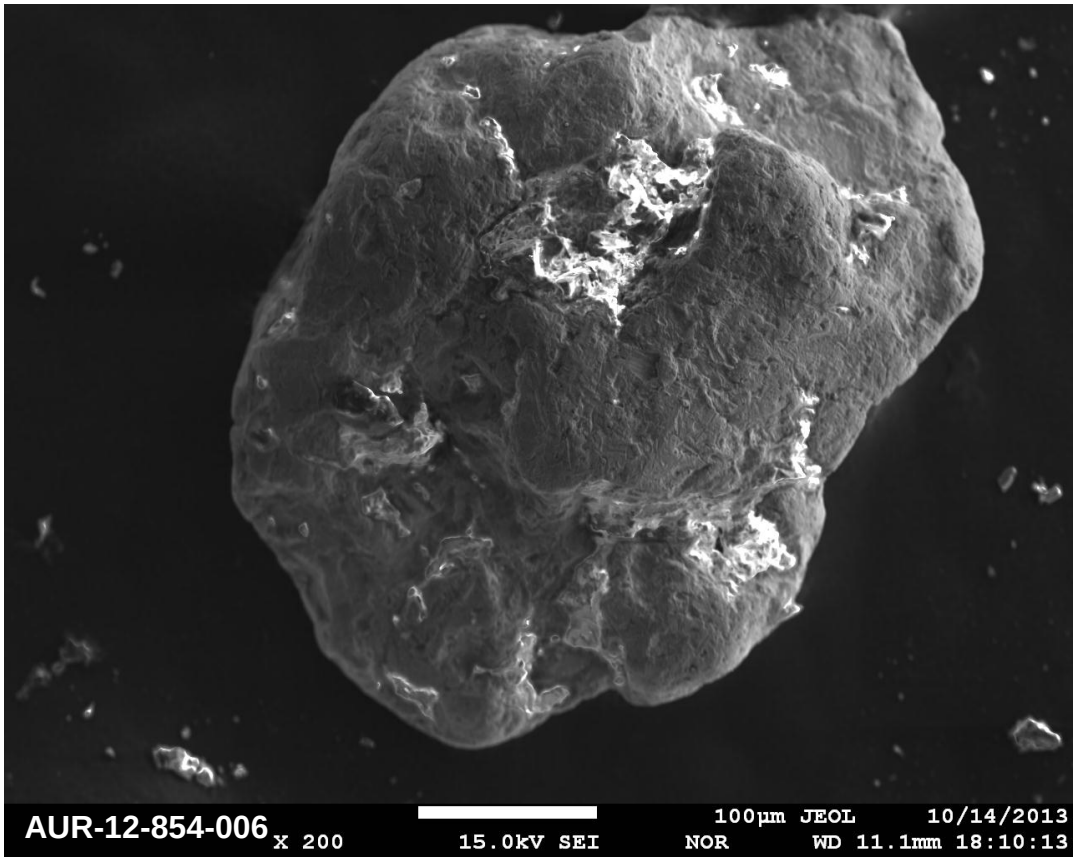
AUR-12-854-006
X 200
15.0kV SEI
100µm JEOL
NOR
10/14/2013
WD 11.1mm 18:10:13

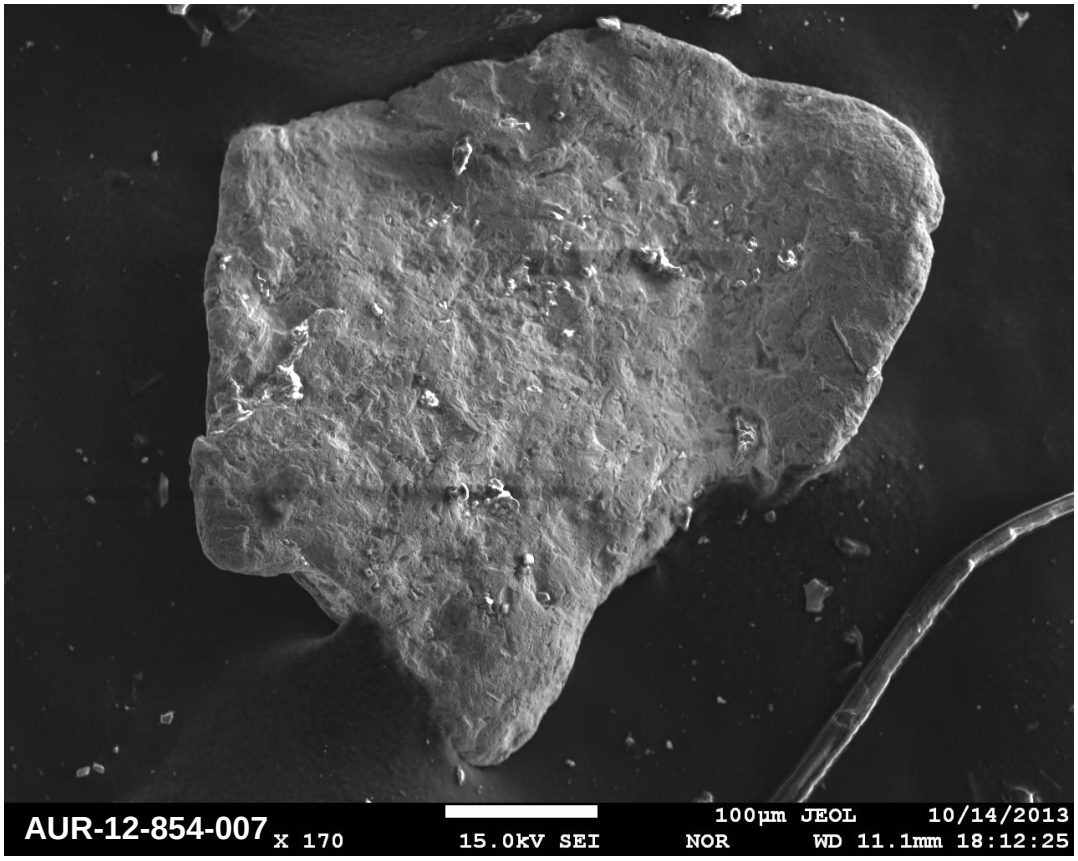
AUR-12-854-007 X 170
15.0kV SEI
100µm JEOL
NOR
10/14/2013
WD 11.1mm 18:12:25

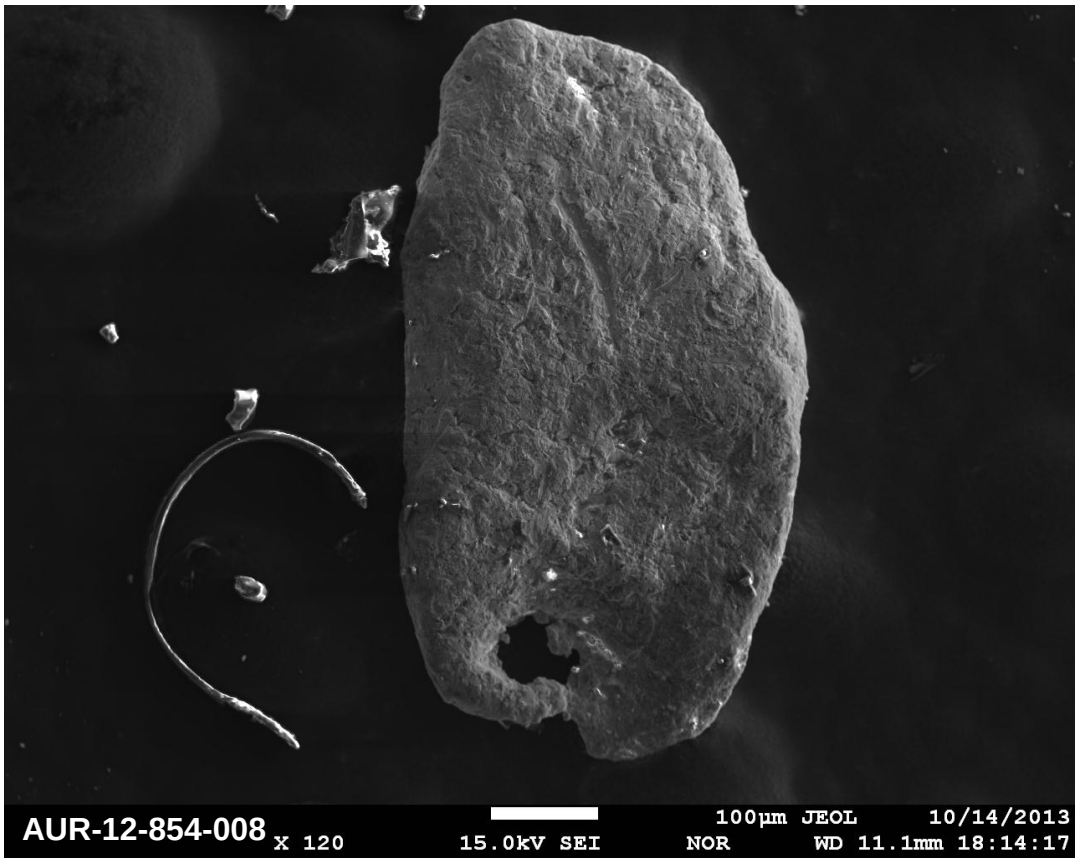
AUR-12-854-008 X 120
15.0kV SEI
100µm JEOL
NOR
10/14/2013
WD 11.1mm 18:14:17

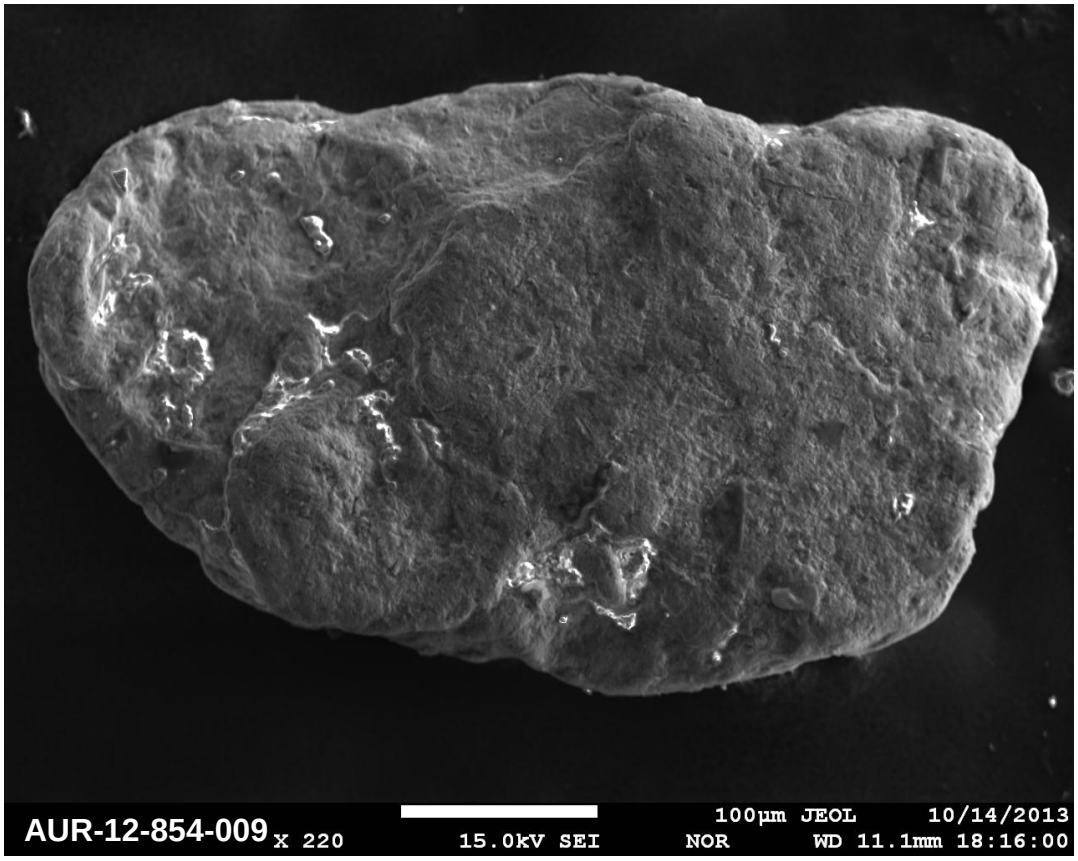
AUR-12-854-009 X 220
15.0kV SEI
100µm JEOL
NOR
10/14/2013
WD 11.1mm 18:16:00

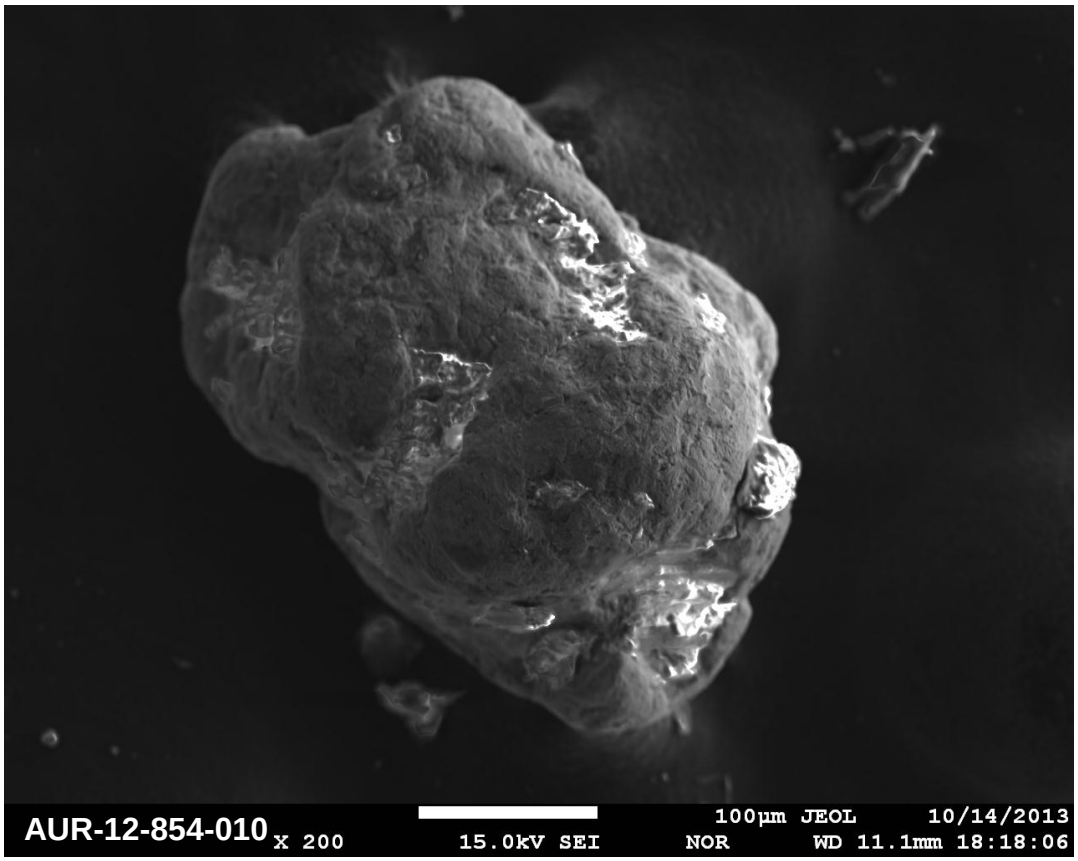
AUR-12-854-010 X 200
15.0kV SEI
100µm JEOL
NOR
10/14/2013
WD 11.1mm 18:18:06

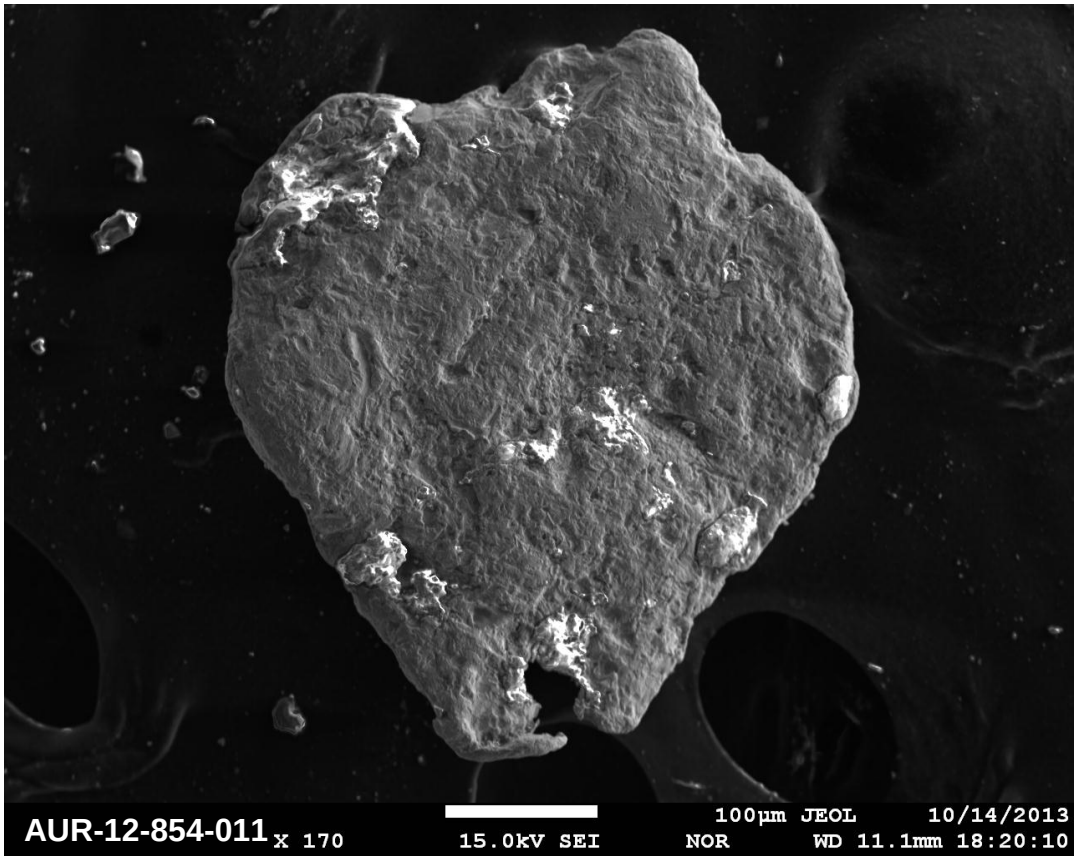
AUR-12-854-011 X 170
15.0kV SEI
100µm JEOL
NOR
10/14/2013
WD 11.1mm 18:20:10

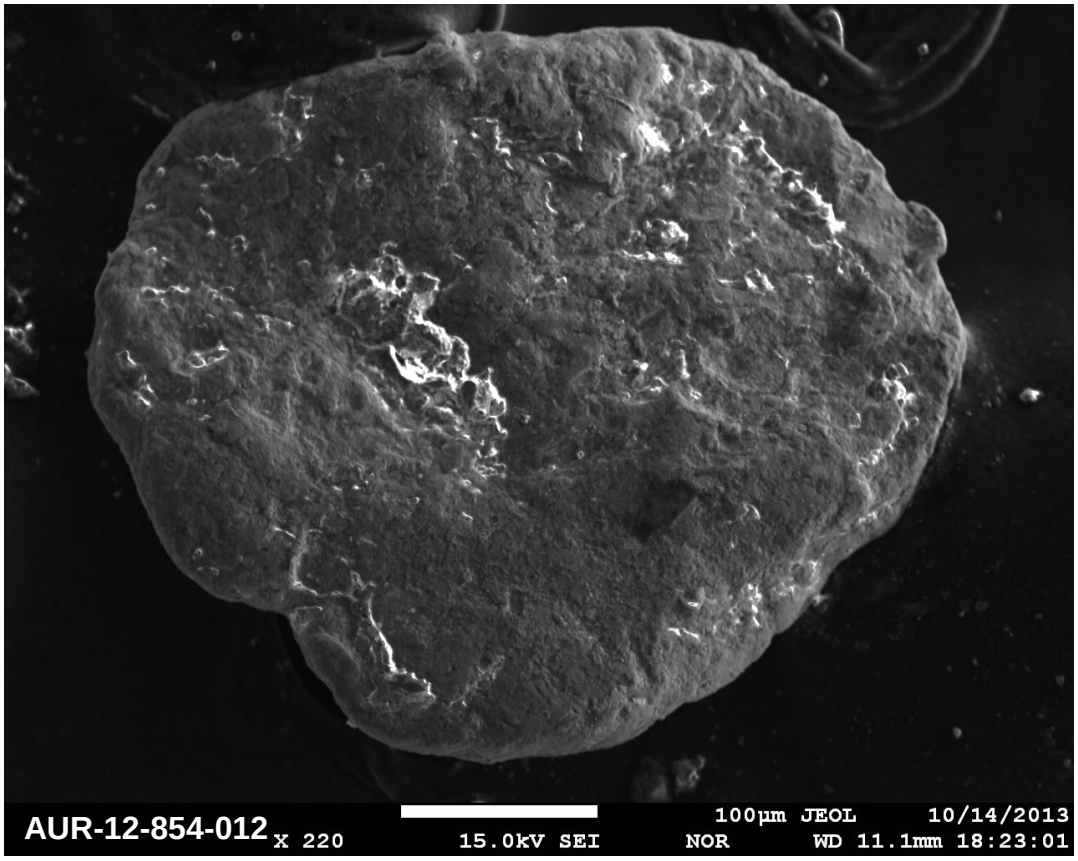
AUR-12-854-012 X 220
15.0kV SEI
100µm JEOL
NOR
10/14/2013
WD 11.1mm 18:23:01

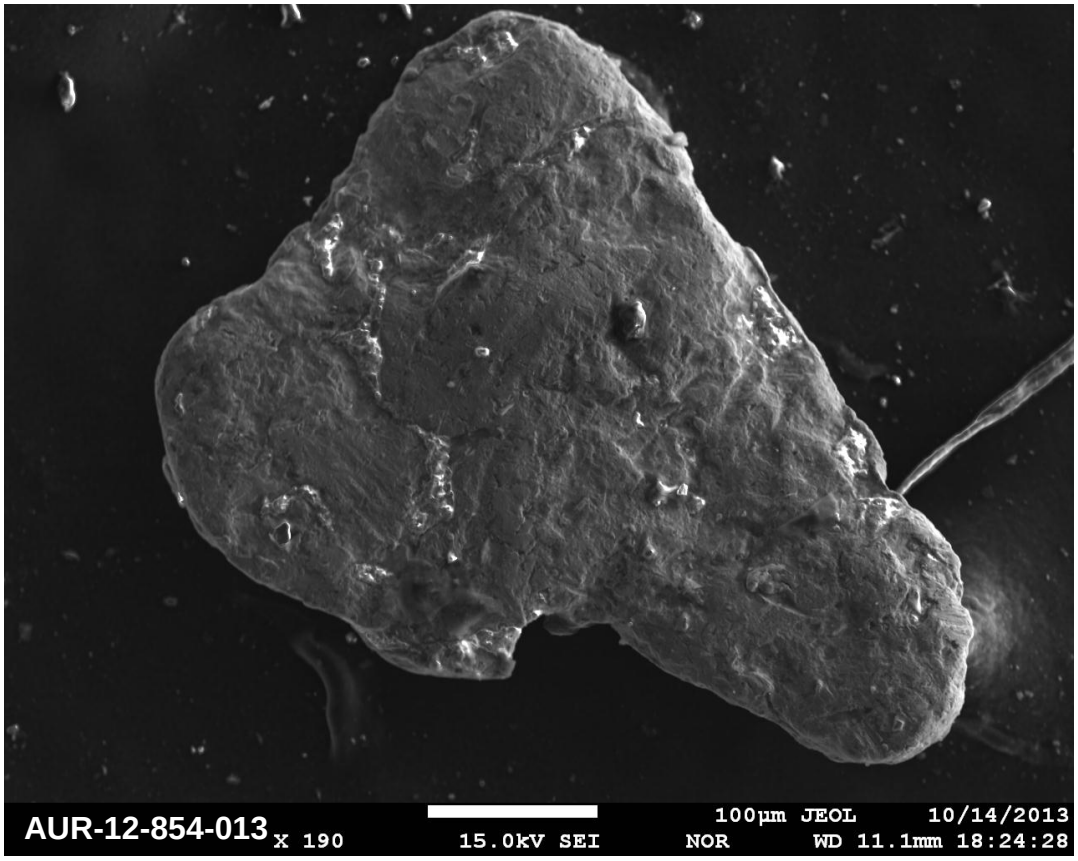
AUR-12-854-013 X 190
15.0kV SEI
100µm JEOL
NOR
10/14/2013
WD 11.1mm 18:24:28

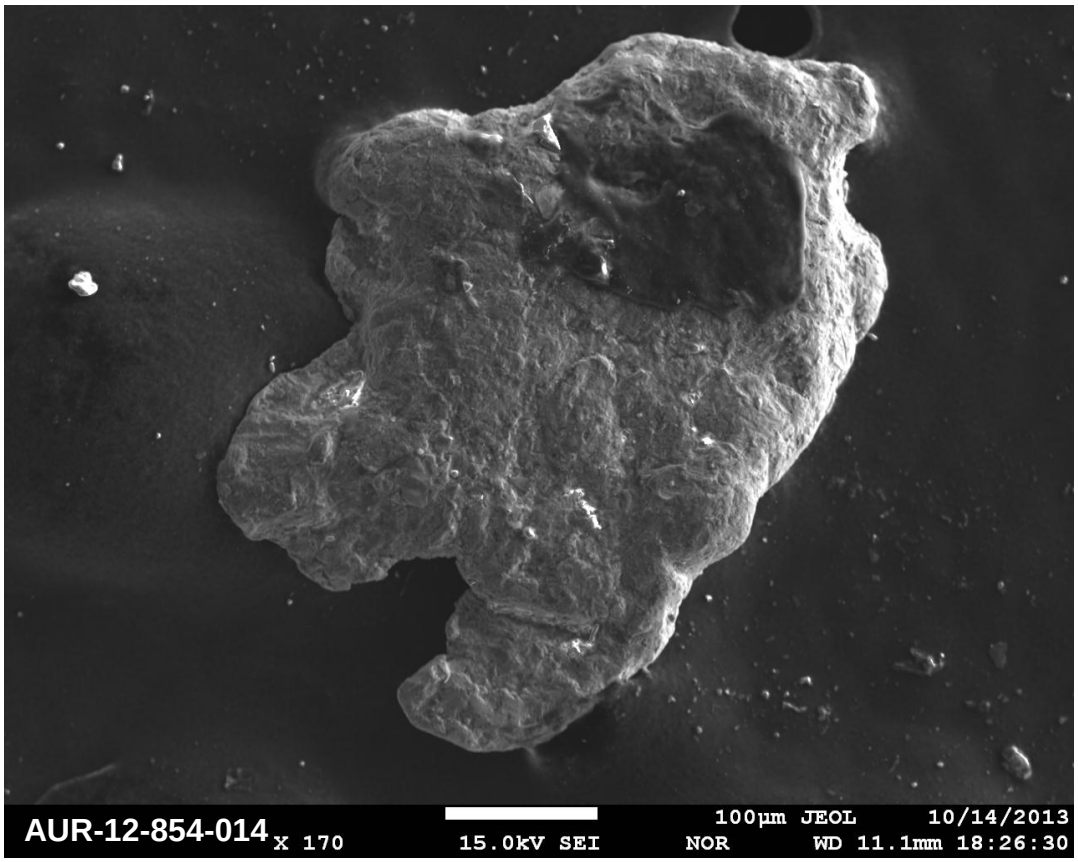
AUR-12-854-014 X 170
15.0kV SEI
100µm JEOL
NOR
10/14/2013
WD 11.1mm 18:26:30

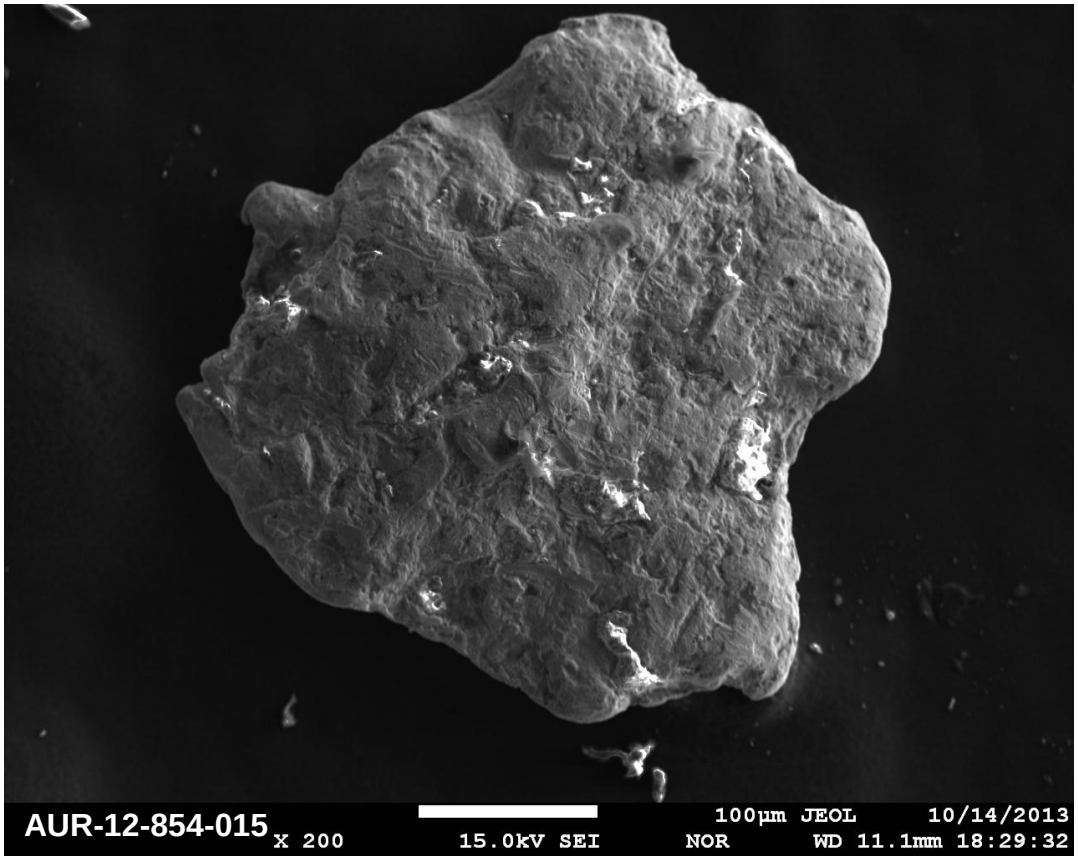
AUR-12-854-015
X 200
15.0kV SEI
100µm JEOL
NOR
10/14/2013
WD 11.1mm 18:29:32

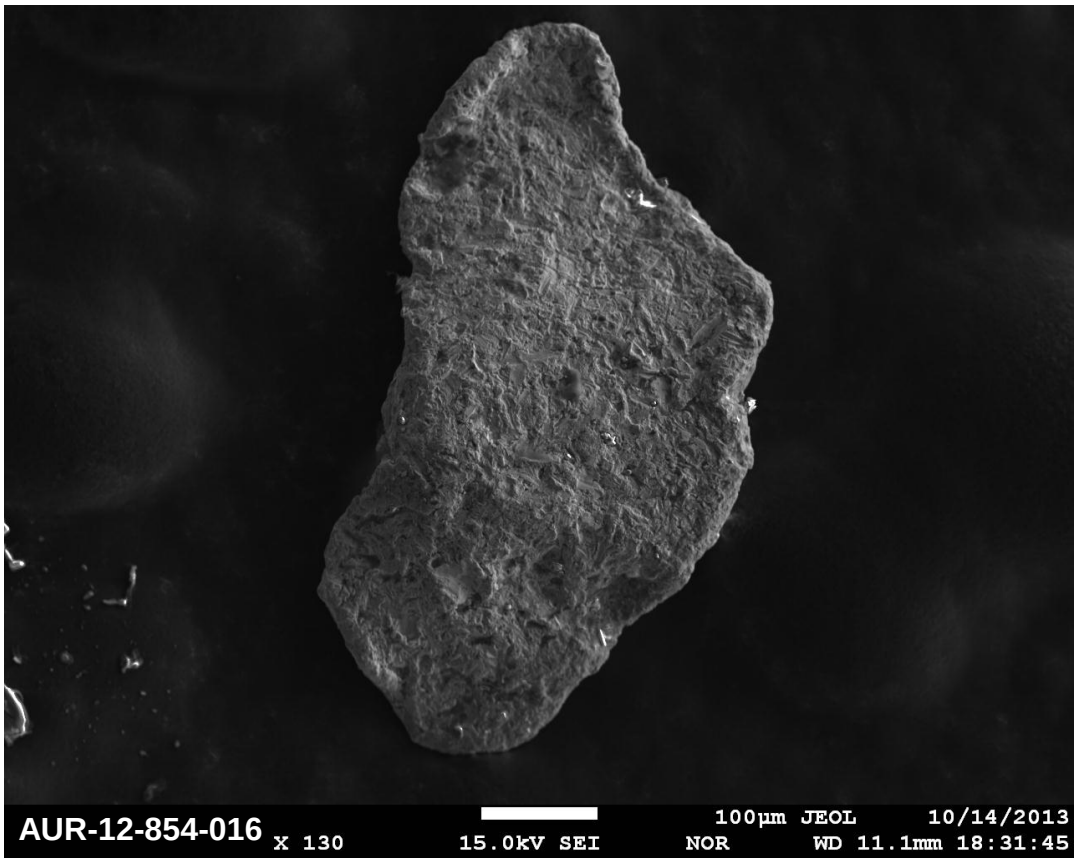
AUR-12-854-016
X 130
15.0kV SEI
100µm JEOL
NOR
10/14/2013
WD 11.1mm 18:31:45

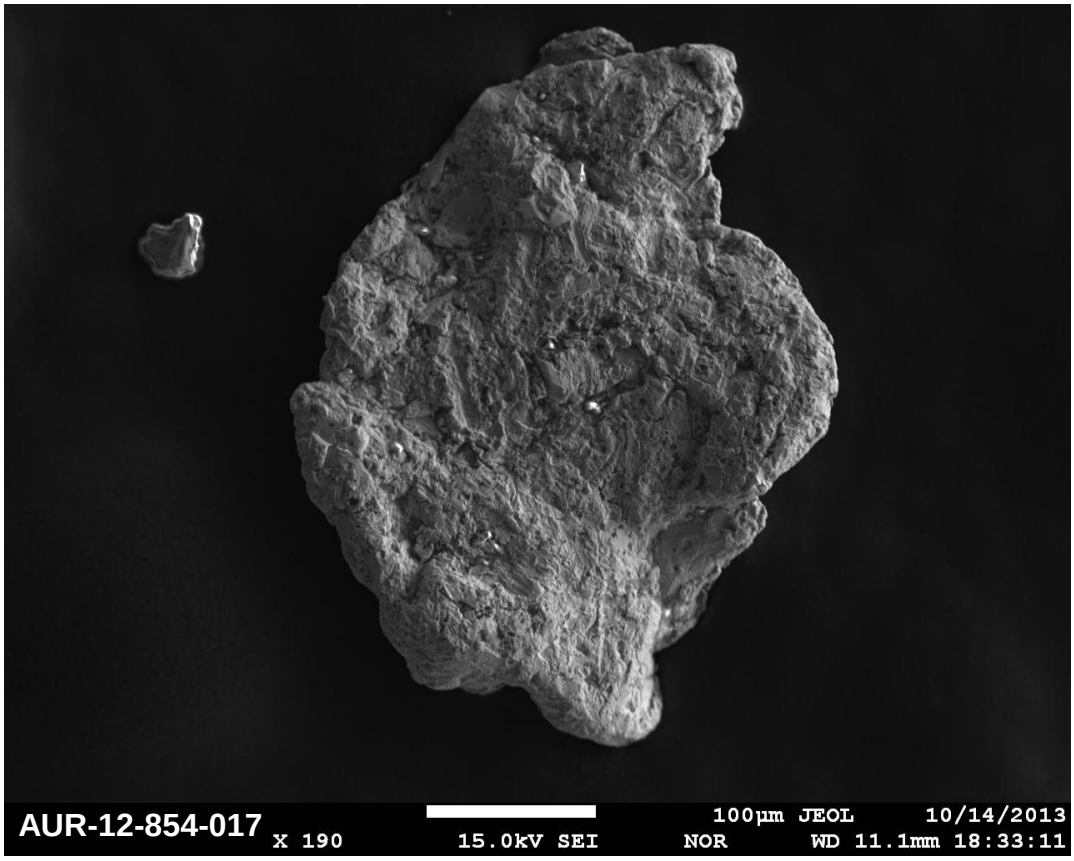
AUR-12-854-017
X 190
15.0kV SEI
100µm JEOL
NOR
10/14/2013
WD 11.1mm 18:33:11

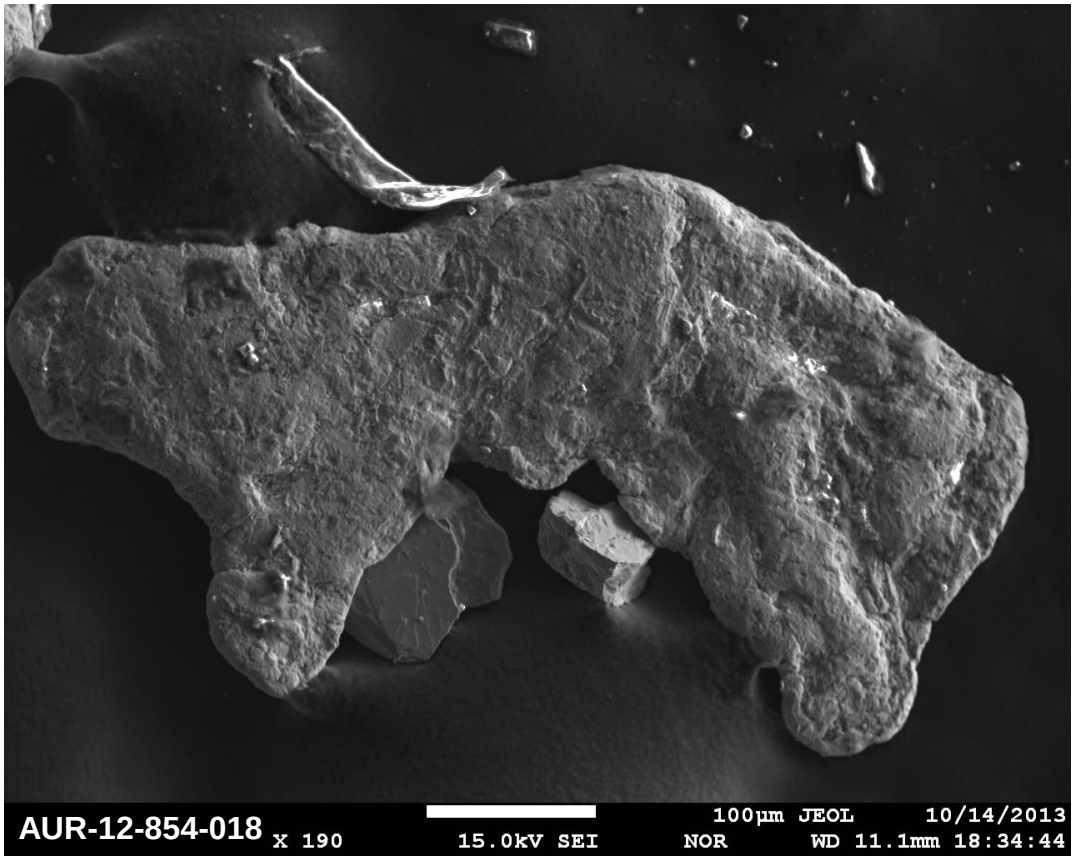
AUR-12-854-018
X 190
15.0kV SEI
100µm JEOL
NOR
10/14/2013
WD 11.1mm 18:34:44

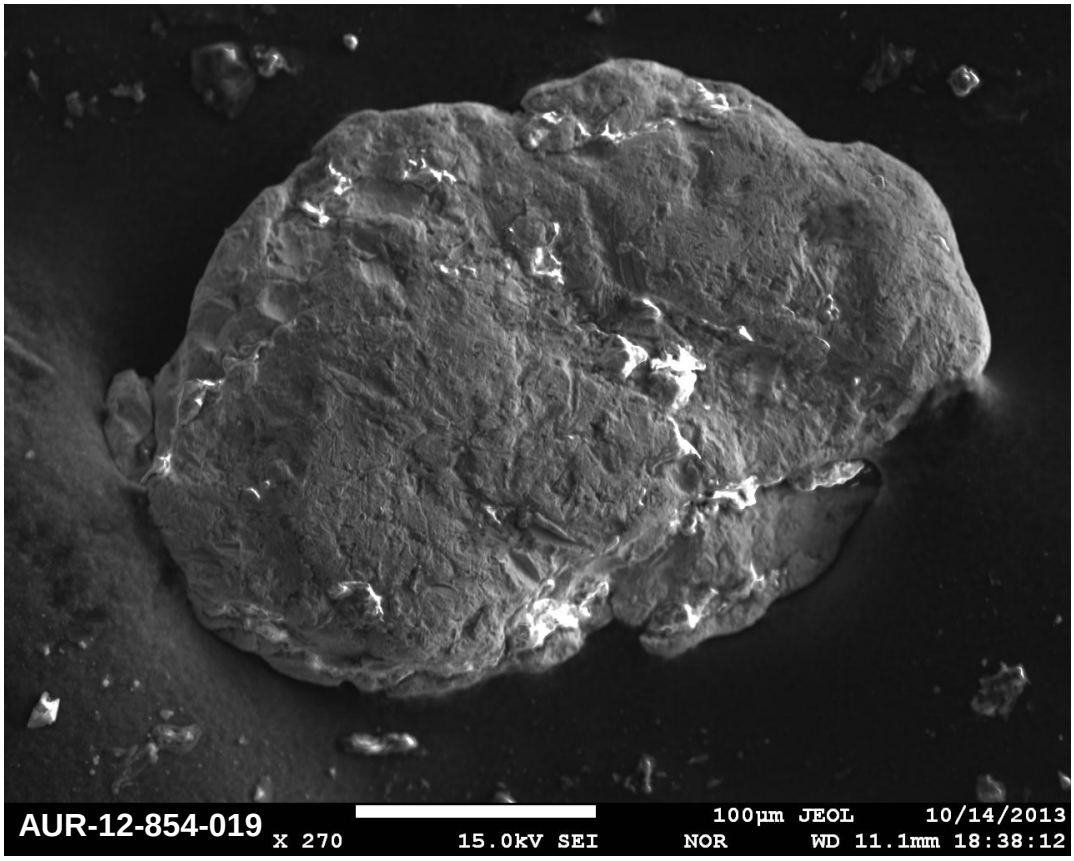
AUR-12-854-019
X 270
15.0kV SEI
100µm JEOL
NOR
10/14/2013
WD 11.1mm 18:38:12

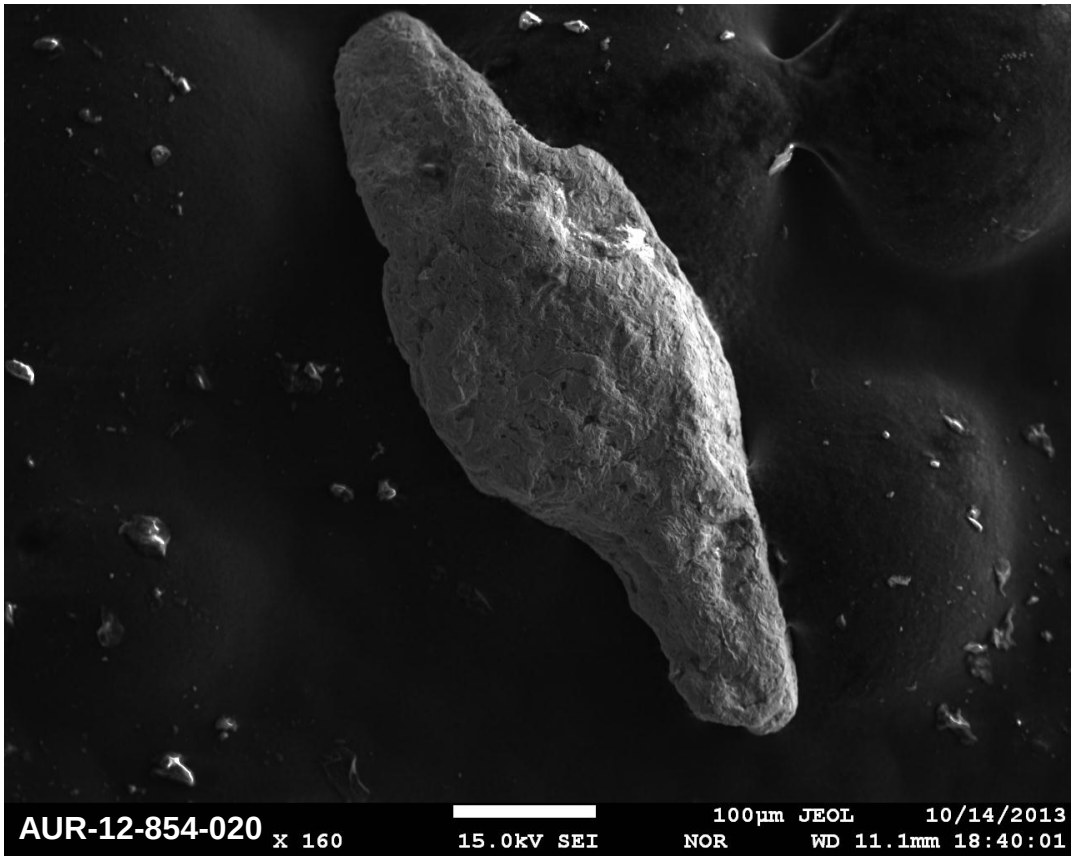
AUR-12-854-020
X 160
15.0kV SEI
100µm JEOL
NOR
10/14/2013
WD 11.1mm 18:40:01

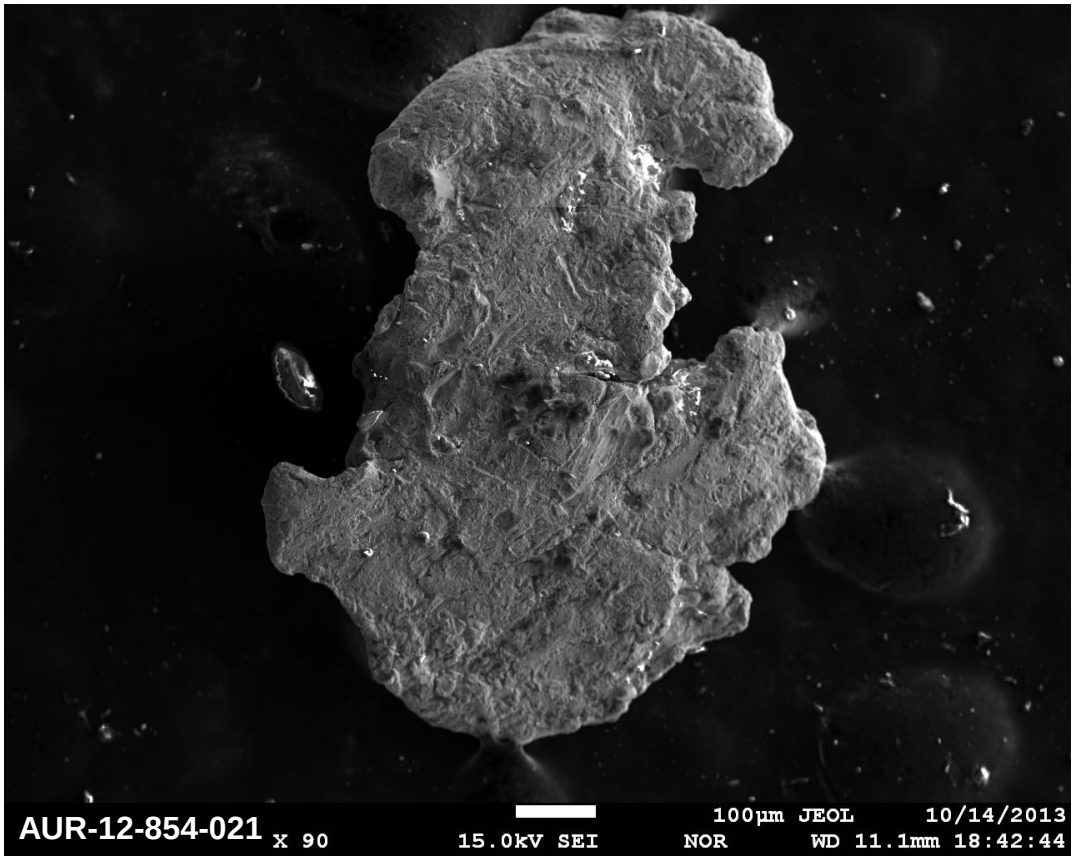
AUR-12-854-021 X 90
15.0kV SEI
100µm JEOL
NOR
10/14/2013
WD 11.1mm 18:42:44

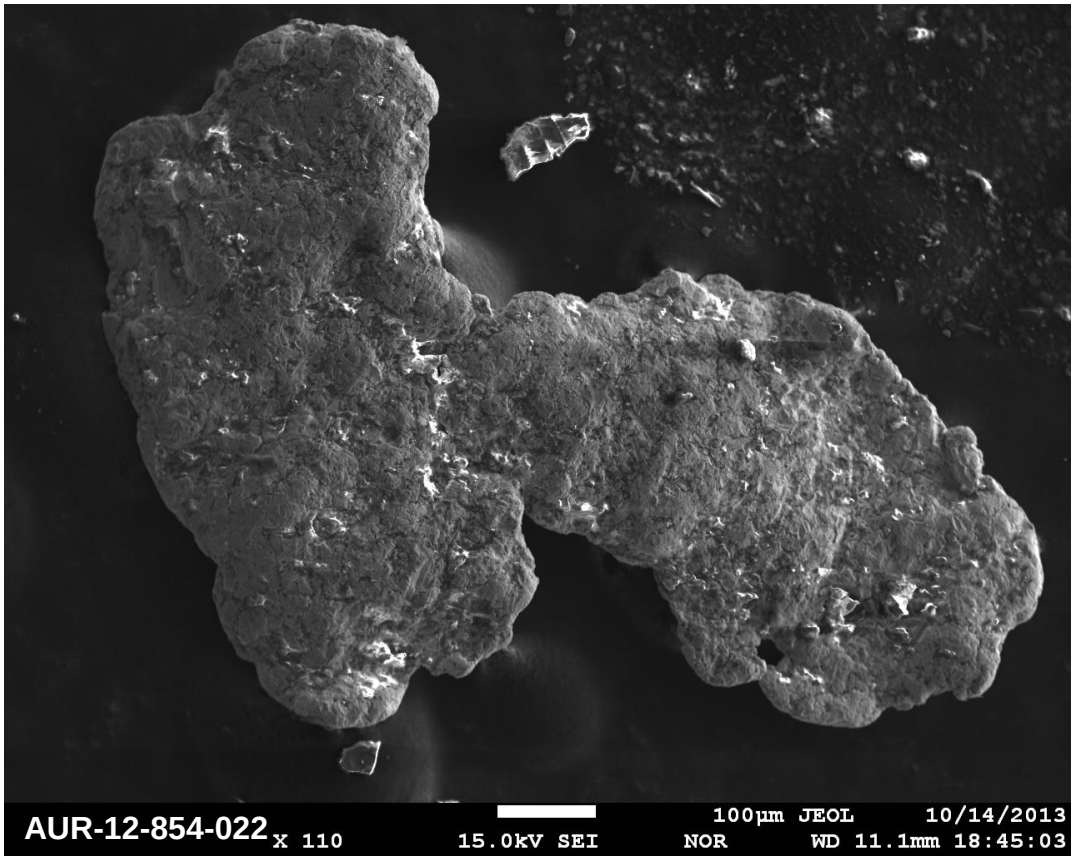
AUR-12-854-022 X 110
15.0kV SEI
100µm JEOL
NOR
10/14/2013
WD 11.1mm 18:45:03

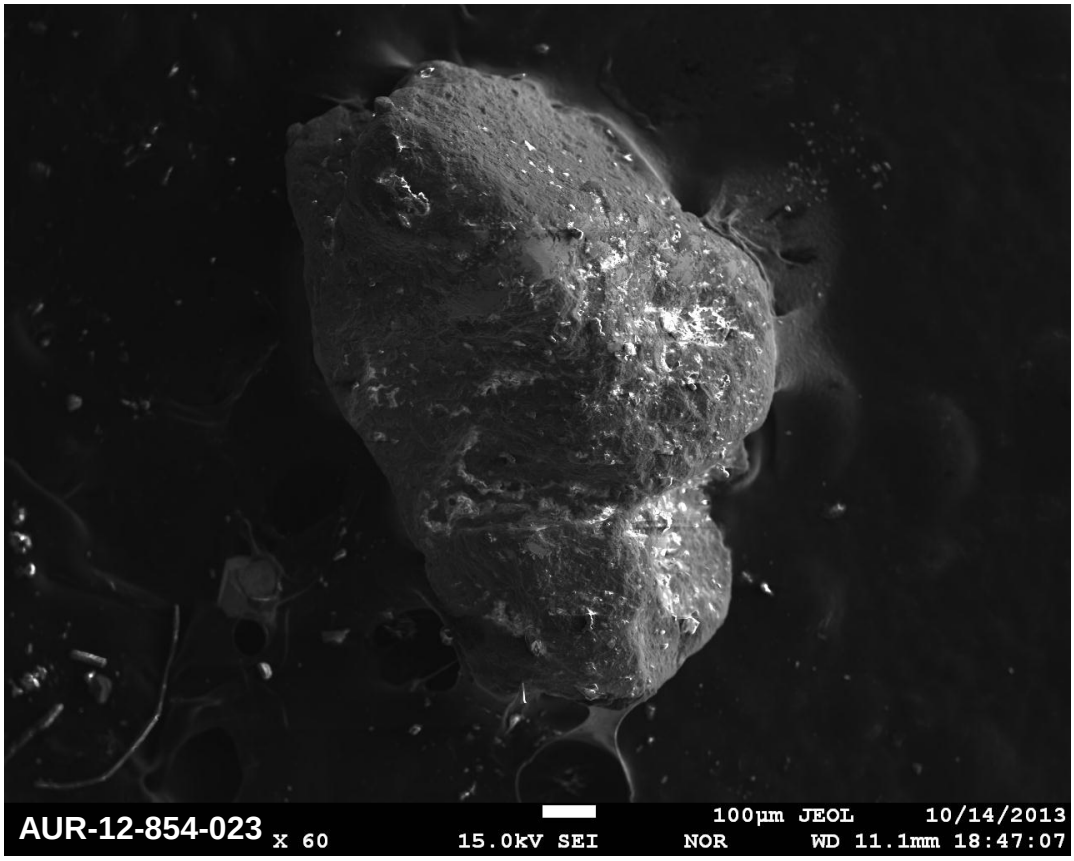
AUR-12-854-023 X 60
15.0kV SEI
100µm JEOL
NOR
10/14/2013
WD 11.1mm 18:47:07

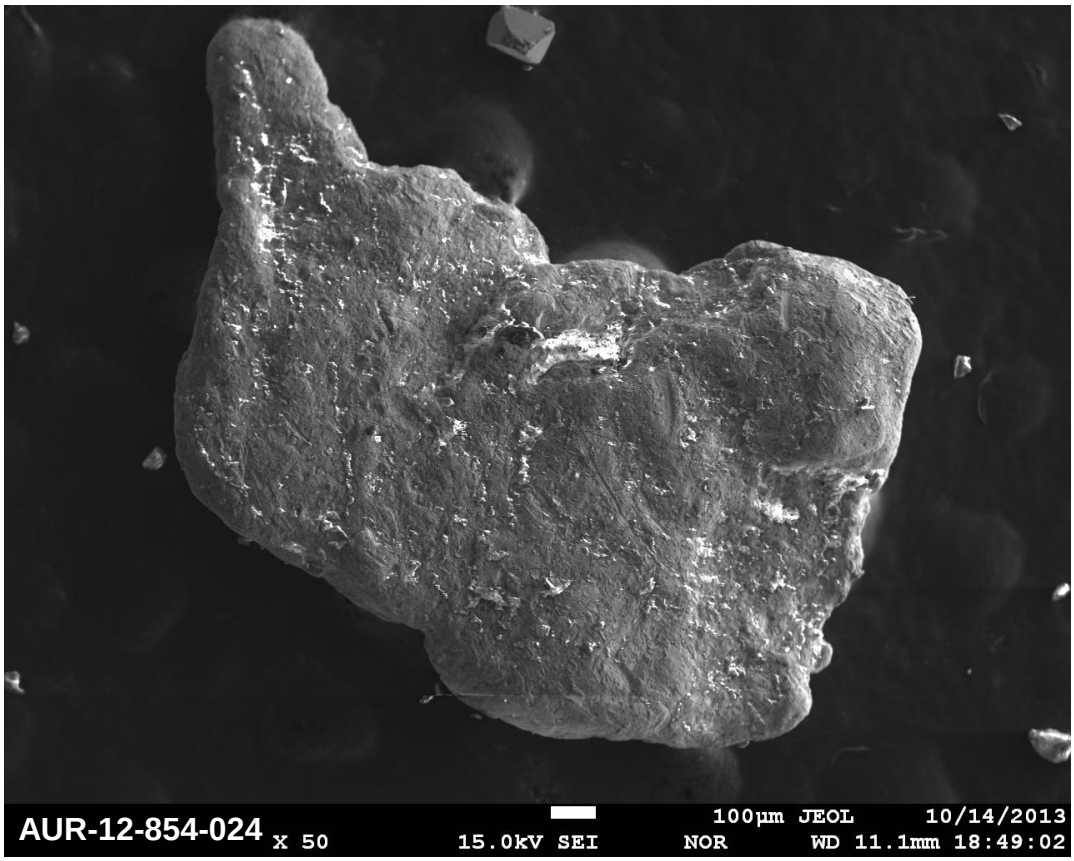
AUR-12-854-024 X 50
15.0kV SEI
100µm JEOL
NOR
10/14/2013
WD 11.1mm 18:49:02

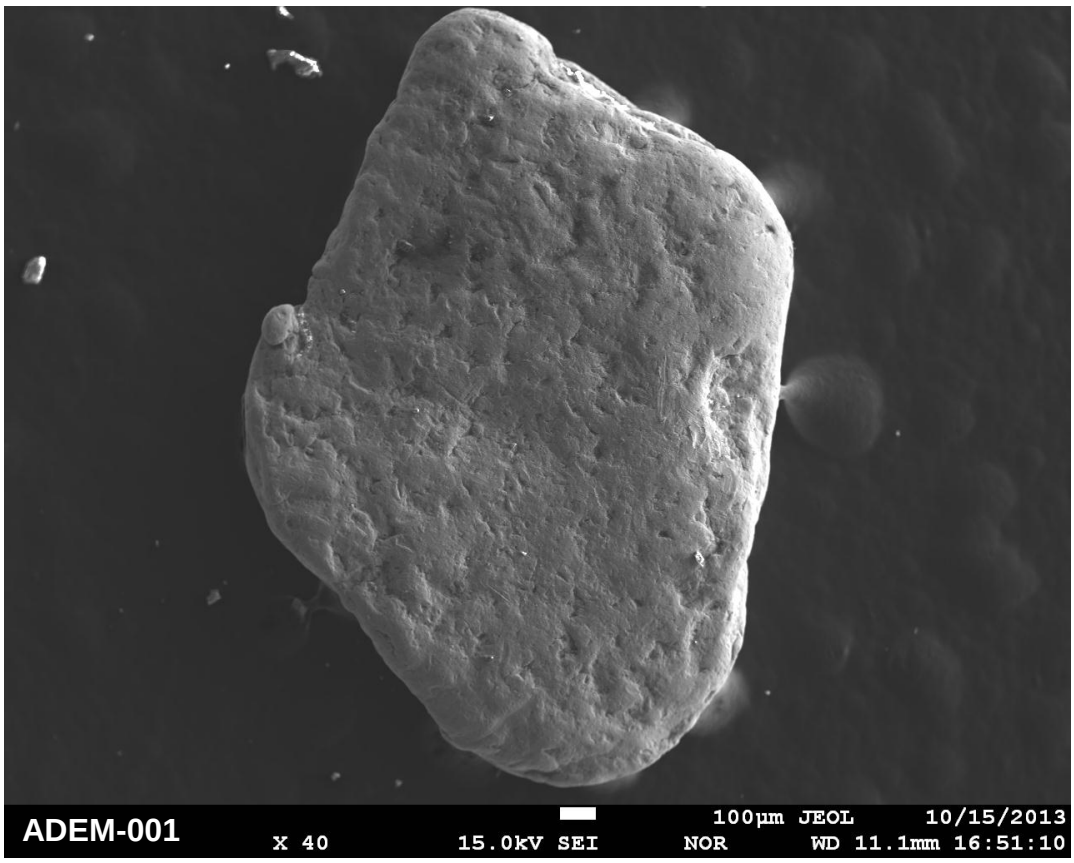
ADEM-001
X 40
15.0kV SEI
100µm JEOL
NOR
10/15/2013
WD 11.1mm 16:51:10

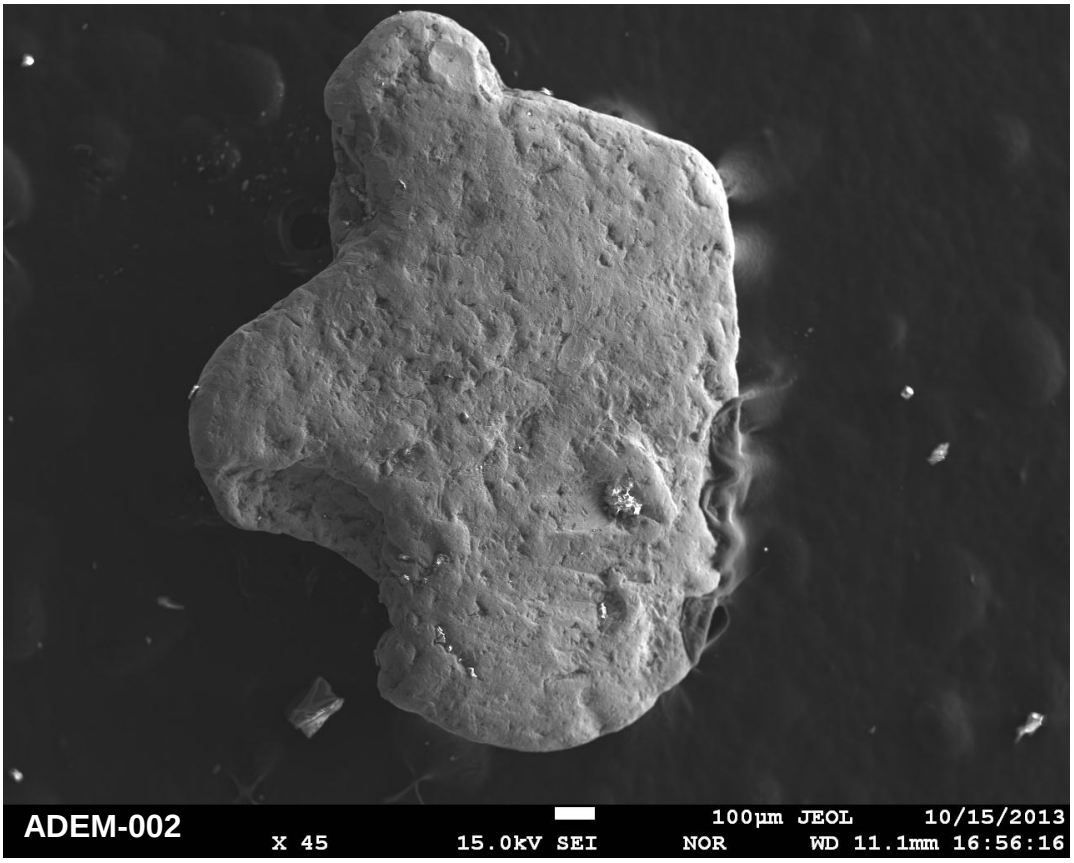
ADEM-002
X 45
15.0kV SEI
100µm JEOL
NOR
10/15/2013
WD 11.1mm 16:56:16

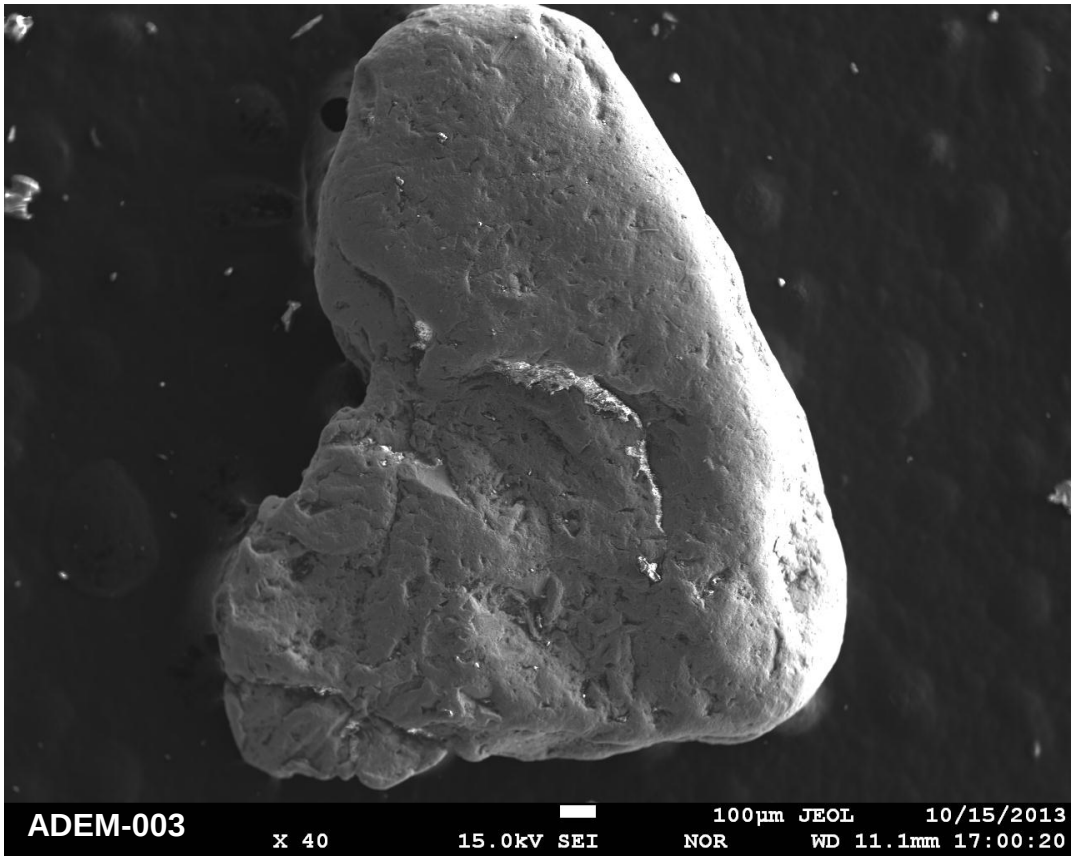
ADEM-003
X 40
15.0kV SEI
100µm JEOL
NOR
10/15/2013
WD 11.1mm 17:00:20

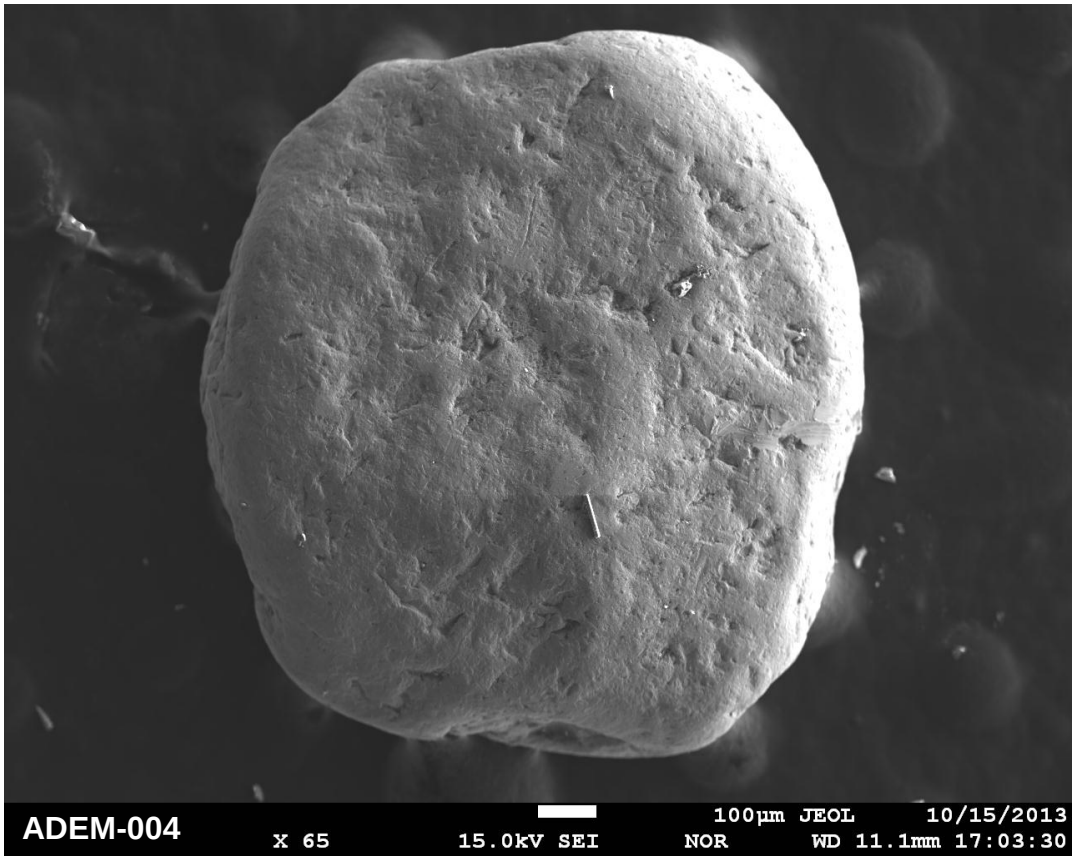
ADEM-004
X 65
15.0kV SEI
100µm JEOL
NOR
10/15/2013
WD 11.1mm 17:03:30

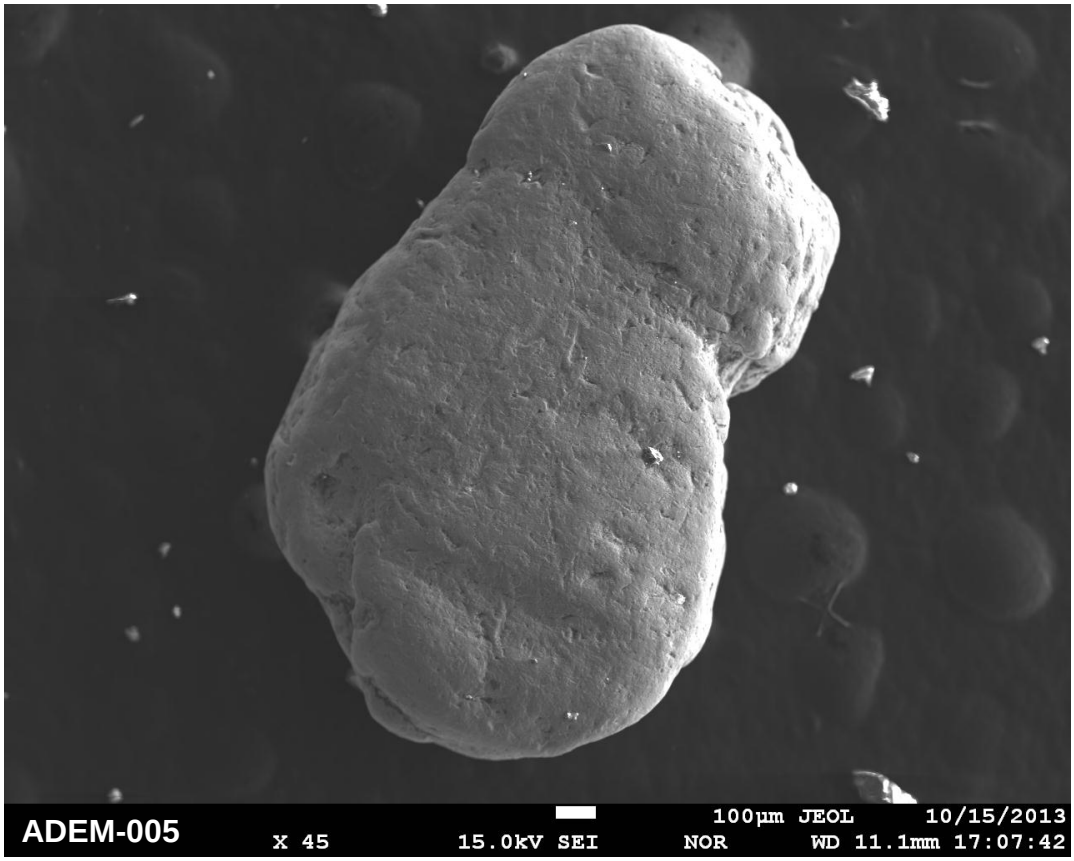
ADEM-005
X 45
15.0kV SEI
100µm JEOL
NOR
10/15/2013
WD 11.1mm 17:07:42

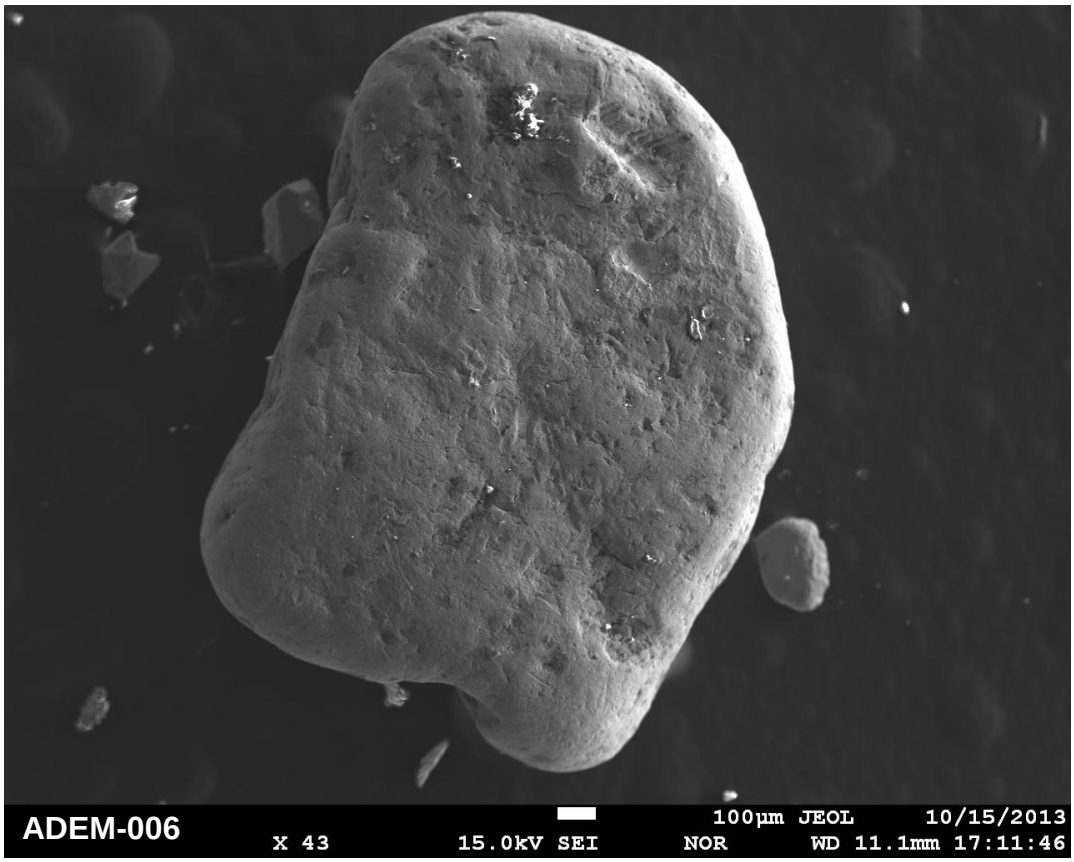
ADEM-006
X 43
15.0kV SEI
100µm JEOL
NOR
10/15/2013
WD 11.1mm 17:11:46

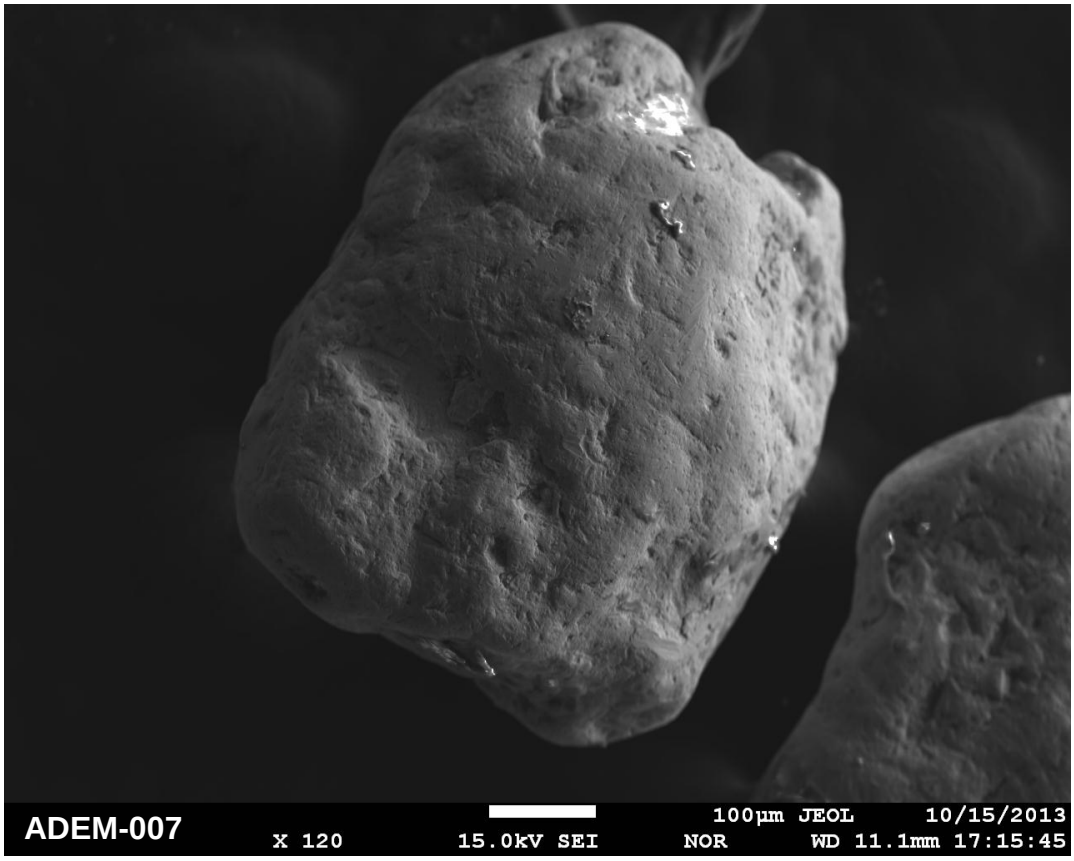
ADEM-007
X 120
15.0kV SEI
100µm JEOL
NOR
10/15/2013
WD 11.1mm 17:15:45

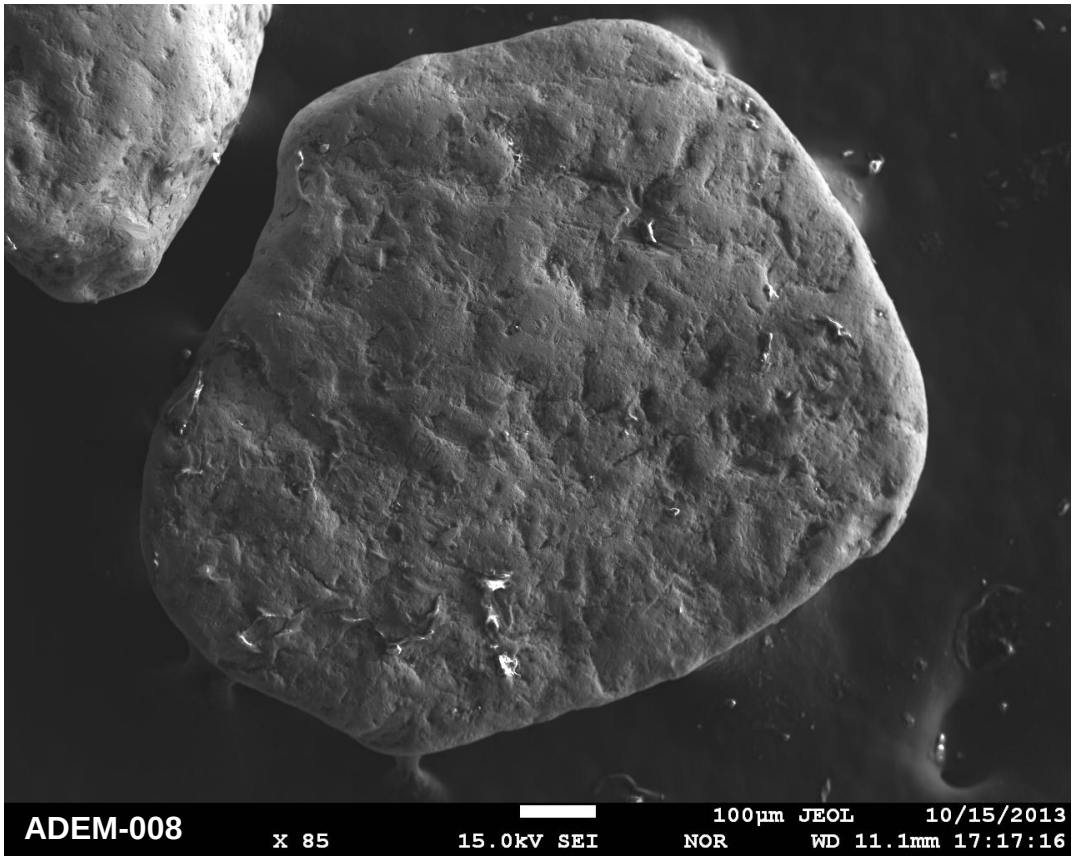
ADEM-008
X 85
15.0kV SEI
100µm JEOL
NOR
10/15/2013
WD 11.1mm 17:17:16

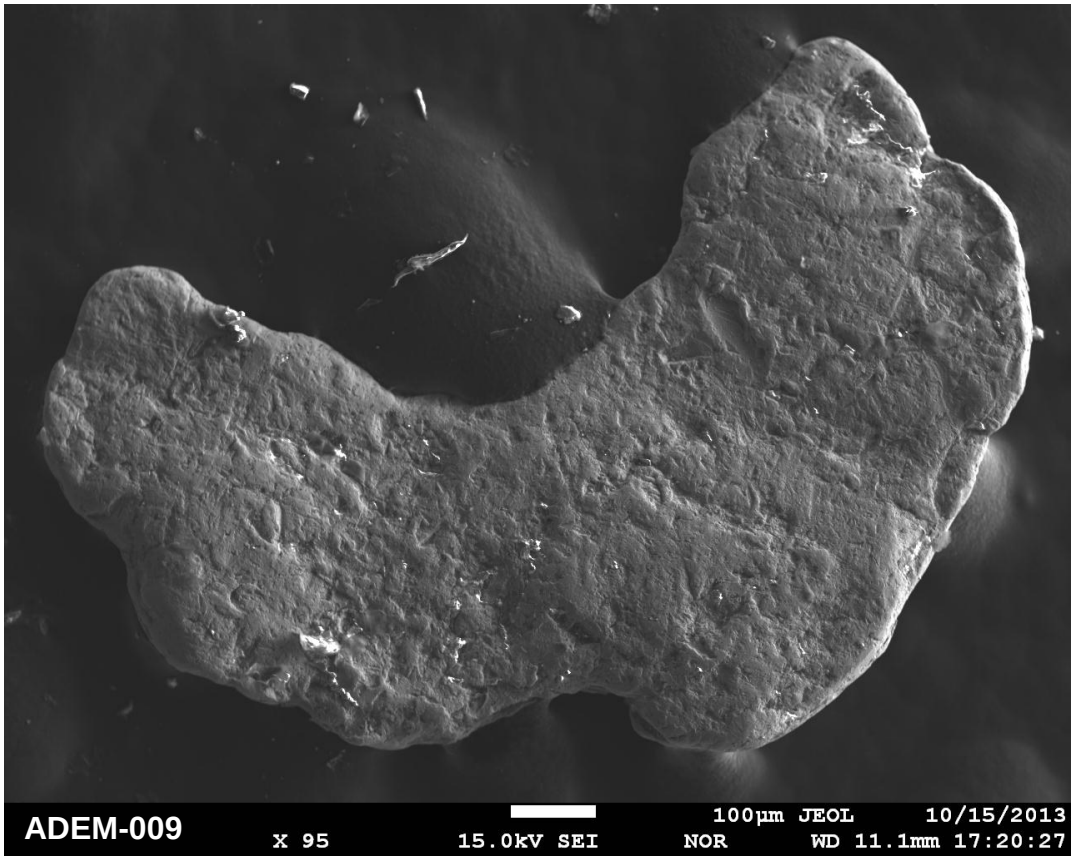
ADEM-009
X 95
15.0kV SEI
100µm JEOL
NOR
10/15/2013
WD 11.1mm 17:20:27

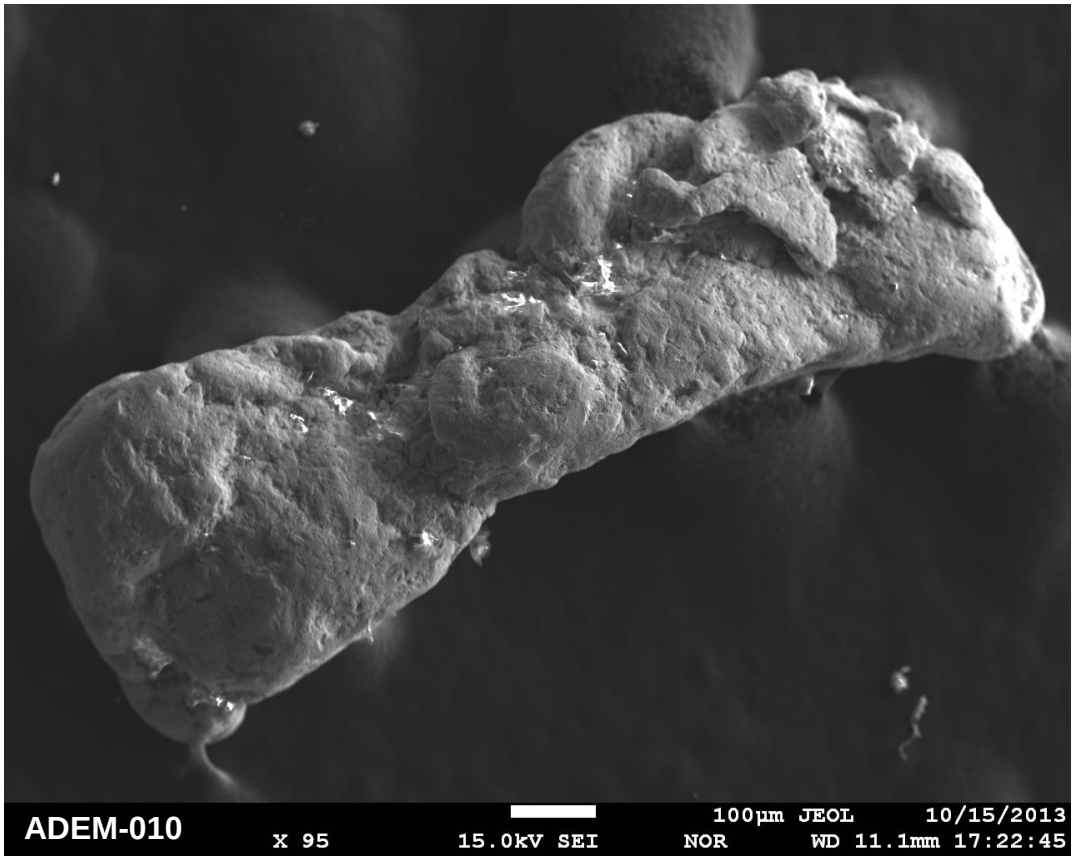
ADEM-010
X 95
15.0kV SEI
100µm JEOL
NOR
10/15/2013
WD 11.1mm 17:22:45

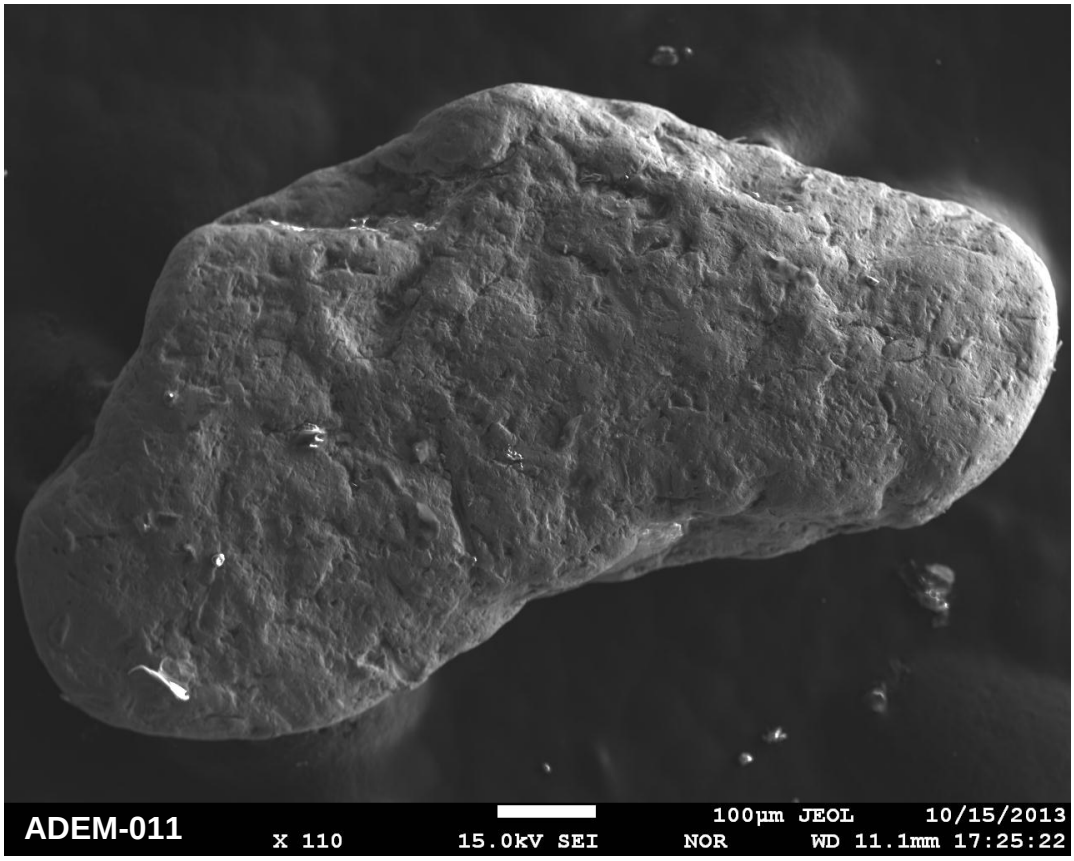
ADEM-011
X 110
15.0kV SEI
100µm JEOL
NOR
10/15/2013
WD 11.1mm 17:25:22

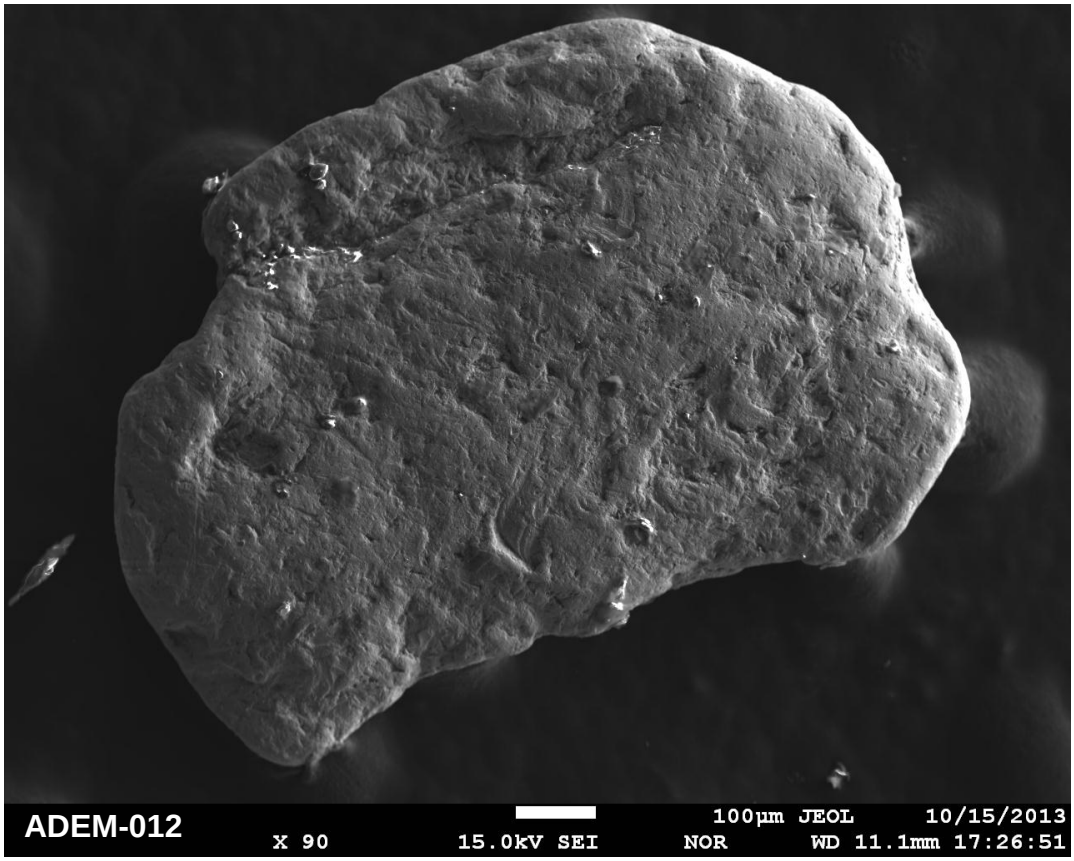
ADEM-012
X 90
15.0kV SEI
100µm JEOL
NOR
10/15/2013
WD 11.1mm 17:26:51

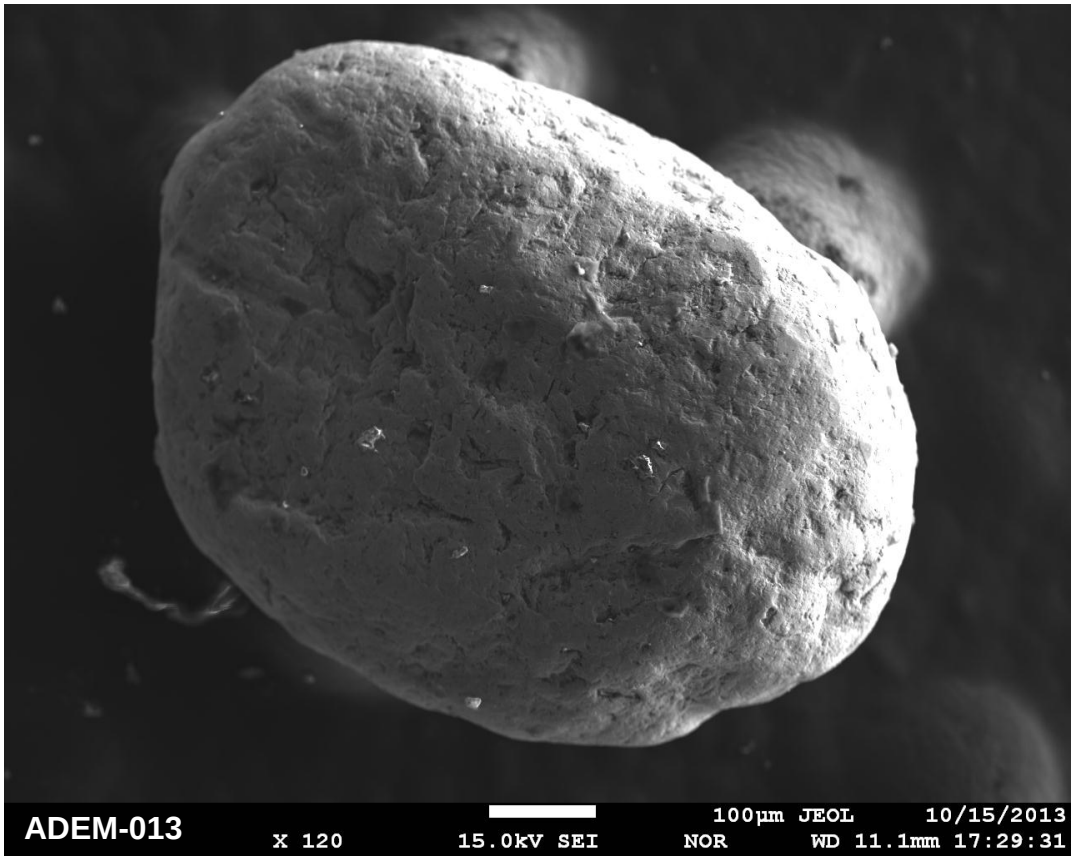
ADEM-013
X 120
15.0kV SEI
100µm JEOL
NOR
10/15/2013
WD 11.1mm 17:29:31

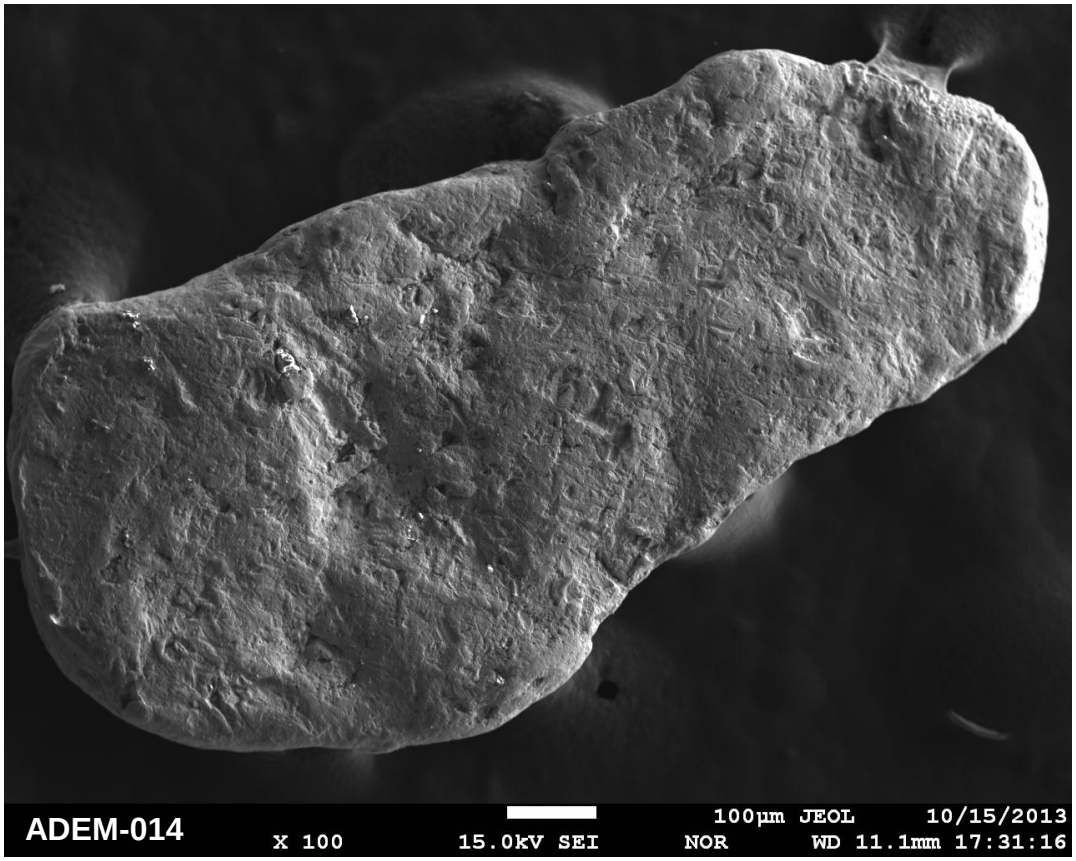
ADEM-014
X 100
15.0kV SEI
100µm JEOL
NOR
10/15/2013
WD 11.1mm 17:31:16

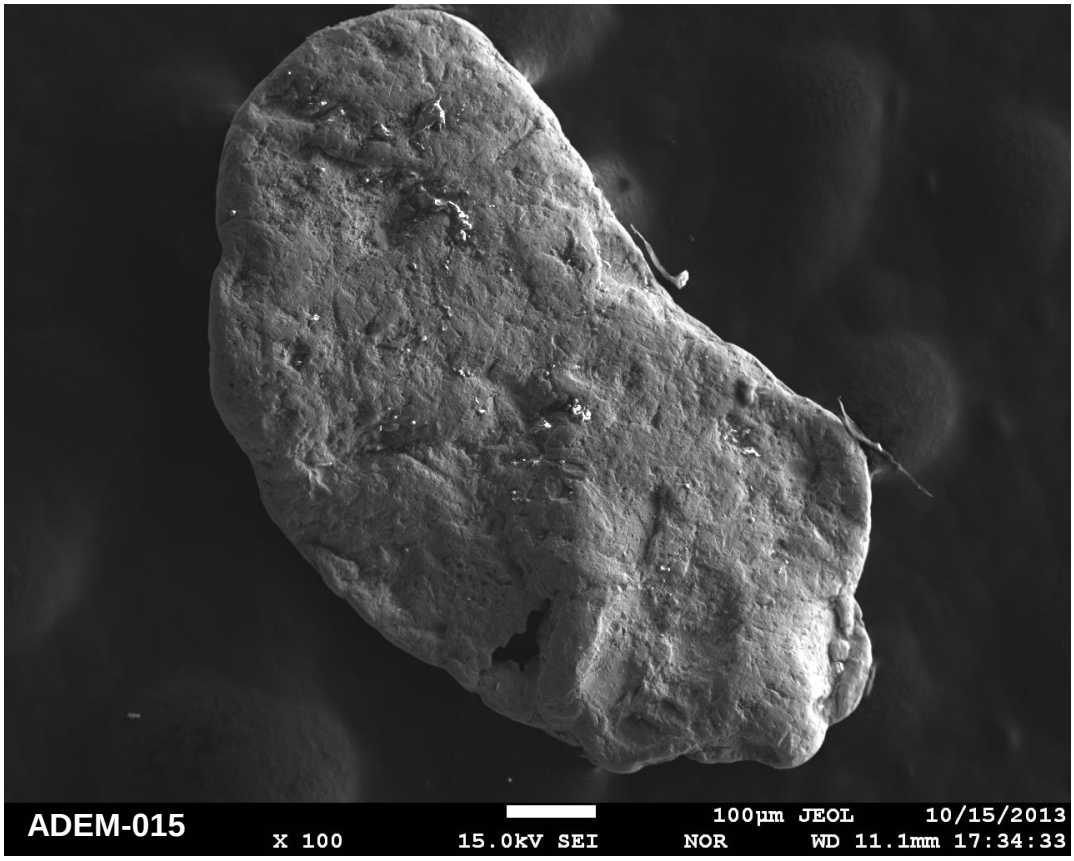
ADEM-015
X 100
15.0kV SEI
100µm JEOL
NOR
10/15/2013
WD 11.1mm 17:34:33

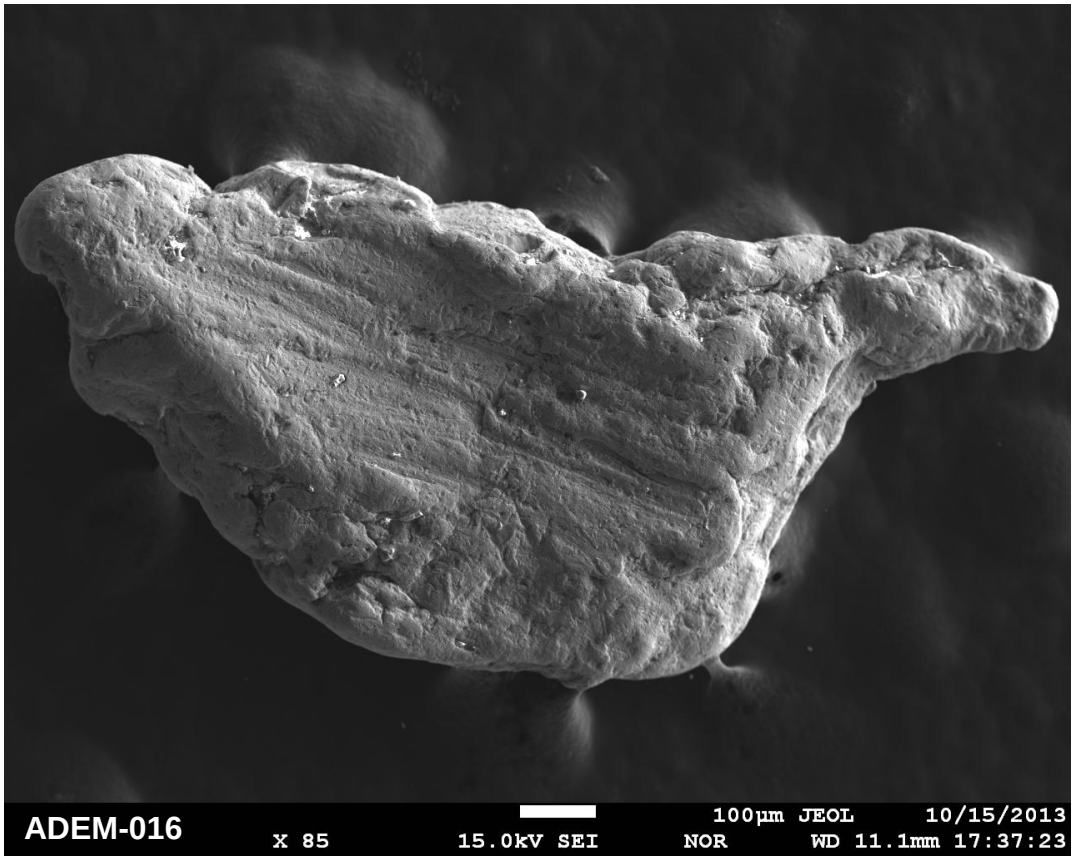
ADEM-016
X 85
15.0kV SEI
100µm JEOL
NOR
10/15/2013
WD 11.1mm 17:37:23

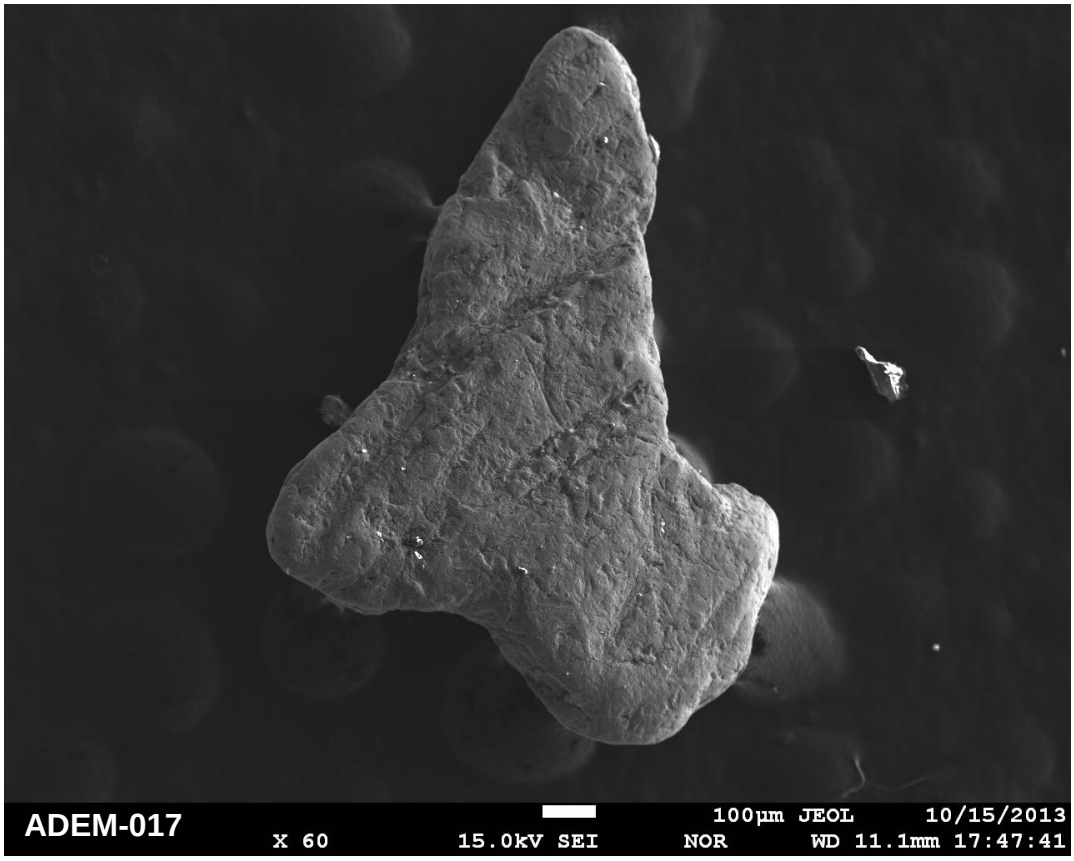
ADEM-017
X 60
15.0kV SEI
100µm JEOL
NOR
10/15/2013
WD 11.1mm 17:47:41

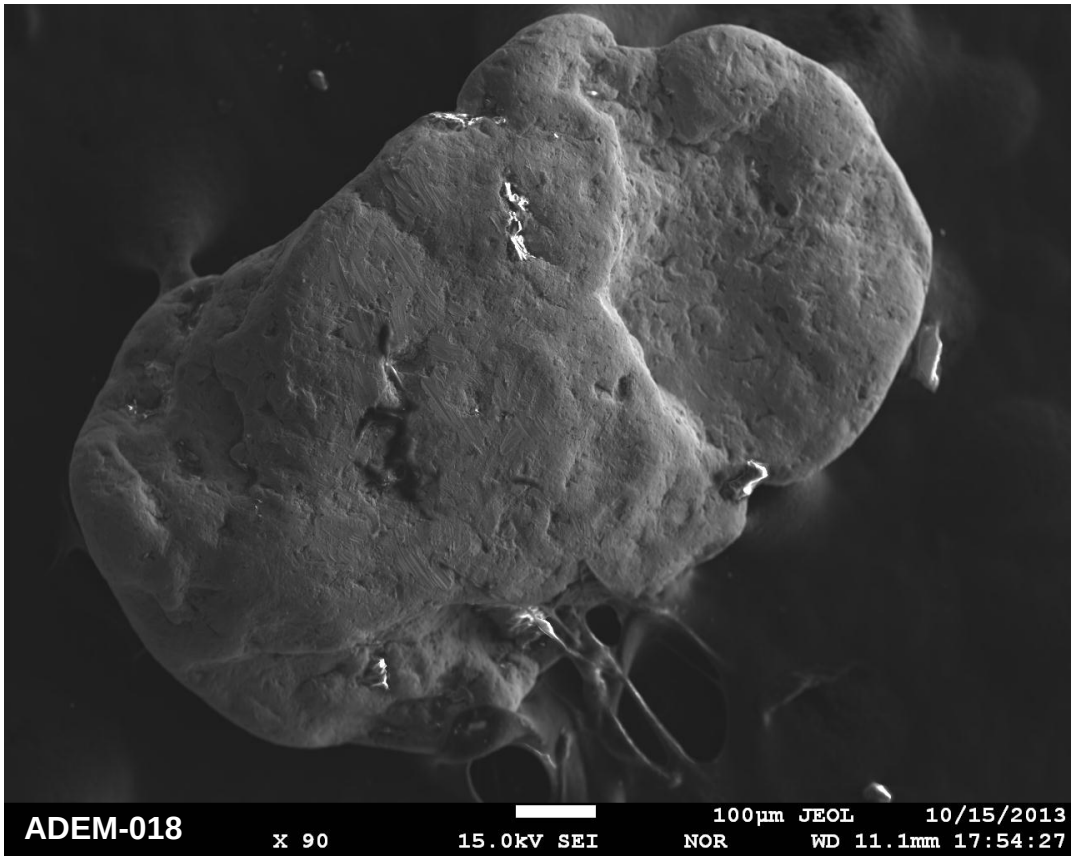
ADEM-018
X 90
15.0kV SEI
100µm JEOL
NOR
10/15/2013
WD 11.1mm 17:54:27

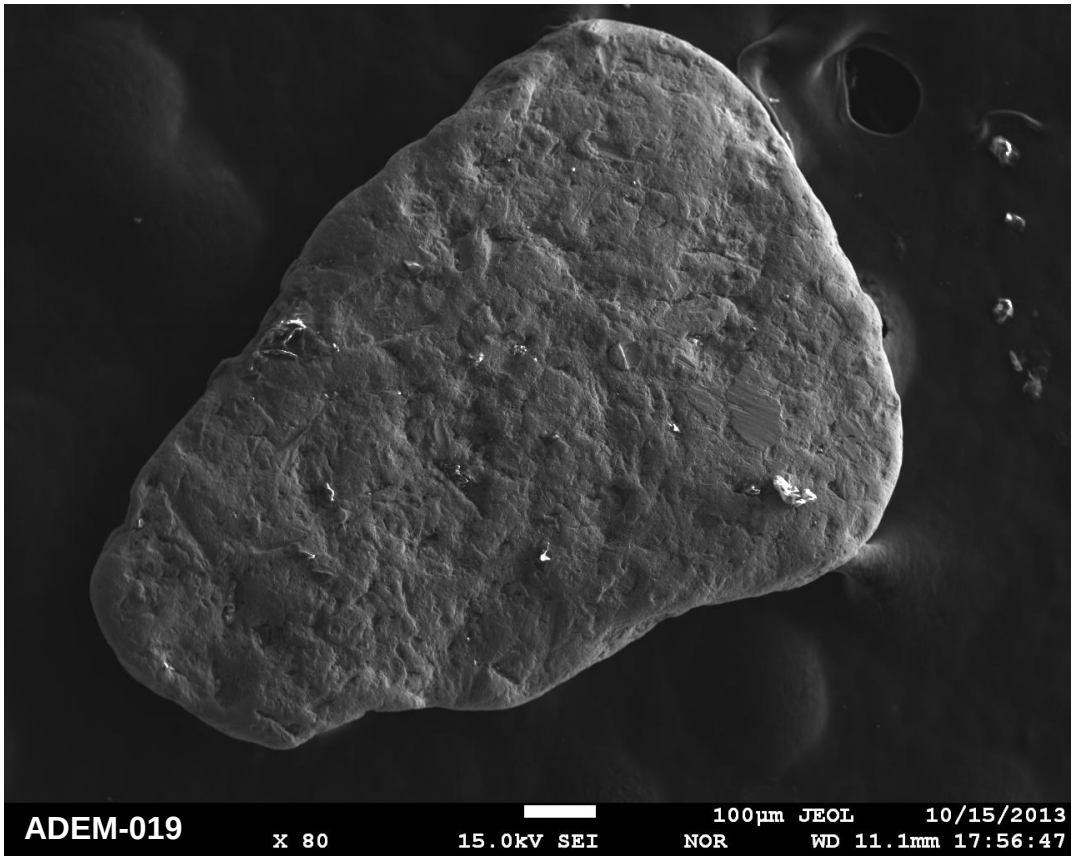
ADEM-019
X 80
15.0kV SEI
100µm JEOL
NOR
10/15/2013
WD 11.1mm 17:56:47

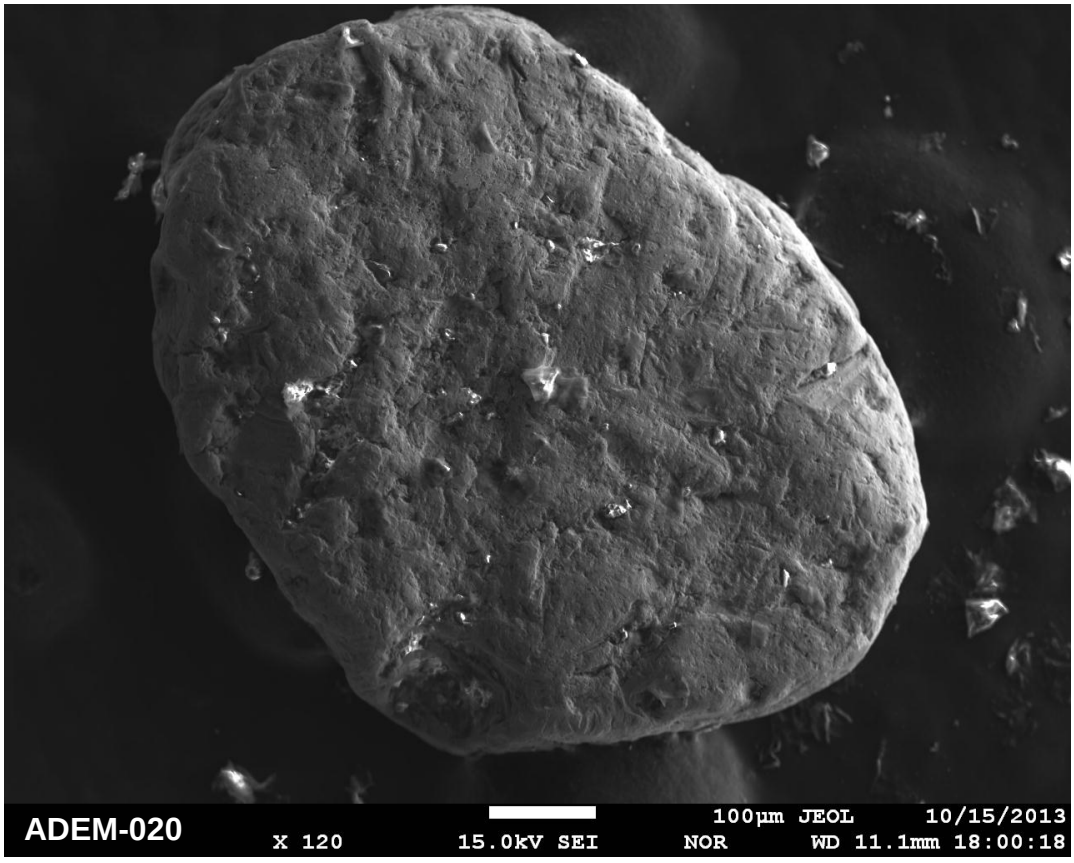
ADEM-020
X 120
15.0kV SEI
100µm JEOL
NOR
10/15/2013
WD 11.1mm 18:00:18

APPENDIX B

Gold grain particle statistics, morphology and textures for all grains from placer sites across the southern Seward Peninsula, Nome, Alaska

Site	Grain #	A-axis (µm)	B-axis (µm)	Elongation (a/b)	Ellipsoidal Area (mm²)	Primary features	Abrasion	Rounding	Flattening	Folding	Aeolian	Au Accretion	Au Dissolution / Pitting
AK015	AK015-1	1077	391	2.75	1.32	r	r	wr	uf	x	x	x	r
AK015	AK015-2	1033	838	1.23	2.72	c	r	r	wf	✓	✓	r	r
AK015	AK015-3	1690	902	1.87	4.79	r	c	wr	wf	✓	x	r	a
AK015	AK015-4	1055	818	1.29	2.71	c	c	sr	uf	x	x	x	r
AK015	AK015-5	1422	801	1.78	3.58	r	c	wr	wf	x	?	r	a
AK015	AK015-6	1483	777	1.91	3.62	r	r	wr	wf	✓	?	r	c
AK015	AK015-7	1250	661	1.89	2.60	a	r	sr	mf	x	x	x	r
AK015	AK015-8	1436	551	2.61	2.49	c	c	wr	mf	x	x	r	r
AK015	AK015-9	1507	649	2.32	3.07	c	c	sr	mf	x	x	r	c
AK015	AK015-10	2169	1035	2.10	7.05	c	r	r	mf	x	x	r	r
AK015	AK015-11	1038	578	1.80	1.88	c	a	r	mf	x	x	r	r
AK015	AK015-12	1035	631	1.64	2.05	r	r	wr	mf	x	x	x	r
AK015	AK015-13	936	644	1.45	1.89	r	c	r	mf	✓	x	r	c
AK015	AK015-14	1642	492	3.34	2.54	c	c	sr	uf	x	x	c	c
AK015	AK015-15	930	799	1.16	2.33	c	r	r	uf	x	x	r	r
AK015	AK015-16	772	742	1.04	1.80	r	r	r	mf	x	x	r	c
AK015	AK015-17	949	725	1.31	2.16	r	a	wr	mf	x	x	r	r
AK015	AK015-18	1059	685	1.55	2.28	r	a	r	mf	x	x	c	c
AK015	AK015-19	862	799	1.08	2.16	r	r	r	mf	x	x	c	a
AK015	AK015-20	945	648	1.46	1.92	r	a	r	mf	x	x	c	r
AK021	AK021-1	878	480	1.83	1.32	r	a	sr	wf	x	x	r	r
AK021	AK021-2	726	701	1.04	1.60	c	a	sr	mf	x	x	c	c
AK021	AK021-3	840	785	1.07	2.07	c	r	r	mf	x	x	r	c
AK021	AK021-4	668	604	1.11	1.27	r	c	wr	wf	✓	x	r	r
AK021	AK021-5	1000	666	1.50	2.09	c	c	r	uf	✓	x	r	r
AK021	AK021-6	761	592	1.29	1.42	r	c	wr	wf	✓	x	r	r
AK021	AK021-7	780	657	1.19	1.61	r	c	wr	wf	✓	x	r	r
AK021	AK021-8	948	608	1.56	1.81	c	c	sr	wf	x	x	r	c
AK021	AK021-9	968	784	1.23	2.38	r	c	wr	wf	x	x	r	c
AK021	AK021-10	1030	998	1.03	3.23	r	a	wr	wf	x	x	c	r
AK021	AK021-11	735	596	1.23	1.38	c	a	wr	wf	✓	x	c	c
AK021	AK021-12	942	696	1.35	2.06	a	c	sr	mf	✓	x	c	r
AK021	AK021-13	1374	525	2.62	2.27	r	c	wr	wf	✓	x	r	r
AK021	AK021-14	1049	731	1.44	2.41	c	r	sr	mf	✓	x	c	c
AK021	AK021-15	877	440	1.99	1.21	c	a	wr	mf	✓	x	c	c
AK021	AK021-16	752	720	1.04	1.70	c	c	sr	mf	✓	x	c	c
AK021	AK021-17	1013	440	2.30	1.40	r	c	sr	wf	✓	x	c	c
AK021	AK021-18	714	437	1.63	0.98	r	a	wr	wf	✓	x	r	c
AK021	AK021-19	740	497	1.49	1.16	r	a	wr	wf	✓	x	r	c
AK021	AK021-20	834	444	1.88	1.16	r	a	wr	wf	✓	x	r	c
AK021	AK021-21	898	433	2.07	1.22	r	c	wr	wf	✓	x	r	c
AK021	AK021-22	973	501	1.94	1.53	r	c	wr	wf	x	x	r	c
AK021	AK021-23	820	376	2.18	0.97	c	a	wr	mf	✓	x	c	c
AK021	AK021-24	704	581	1.21	1.28	a	a	sa	mf	✓	?	c	c
AK021	AK021-25	569	568	1.00	1.02	r	a	wr	wf	✓	x	r	r
AK021	AK021-26	875	412	2.12	1.13	a	c	sa	uf	x	x	c	c
AK021	AK021-27	758	516	1.47	1.23	r	c	r	mf	x	x	r	c
AK021	AK021-28	863	419	2.06	1.14	r	a	wr	wf	x	x	r	r
AK021	AK021-29	633	489	1.29	0.97	r	a	wr	wf	x	x	r	r
AK021	AK021-30	540	491	1.10	0.83	r	a	wr	wf	x	x	c	c
AK021	AK021-31	585	451	1.30	0.83	c	c	r	mf	x	x	a	c
AK021	AK021-32	730	406	1.80	0.93	r	r	wr	wf	x	x	r	c
AK021	AK021-33	519	435	1.19	0.71	c	c	sr	mf	✓	x	a	a
AK021	AK021-34	716	450	1.59	1.01	c	c	r	uf	x	x	a	a
AK021	AK021-35	739	483	1.53	1.12	r	c	wr	mf	✓	x	a	a
AK021	AK021-36	645	554	1.16	1.12	c	a	r	mf	✓	?	a	r
AK021	AK021-37	663	575	1.15	1.20	c	a	r	mf	x	x	c	c
AK021	AK021-38	739	563	1.31	1.31	r	r	r	mf	x	x	r	c
AK021	AK021-39	932	398	2.34	1.17	r	r	wr	wf	✓	x	a	a
AK021	AK021-40	766	573	1.34	1.38	r	c	wr	wf	x	x	a	a
AK028	AK028-1	754	485	1.55	1.15	r	c	r	mf	x	x	x	r
AK028	AK028-2	1149	606	1.90	2.19	r	r	r	mf	x	x	c	c
AK028	AK028-3	930	830	1.12	2.42	r	c	r	mf	✓	x	r	r
AK028	AK028-4	1008	783	1.29	2.48	r	c	wr	mf	x	x	a	a
AK028	AK028-5	966	663	1.46	2.01	r	r	wr	uf	x	x	r	c
AK028	AK028-6	1961	1033	1.90	6.36	r	r	r	uf	x	c	c	a
AK028	AK028-7	1645	832	1.98	4.30	c	c	sr	mf	✓	x	r	c
AK028	AK028-8	1298	770	1.69	3.14	r	c	wr	uf	x	x	r	c
AK028	AK028-9	1212	991	1.22	3.77	r	c	wr	mf	x	x	c	a
AK028	AK028-10	1145	860	1.33	3.09	r	c	wr	uf	x	x	r	c

Site	Grain #	A-axis (µm)	B-axis (µm)	Elongation (a/b)	Ellipsoidal Area (mm²)	Primary features	Abrasion	Rounding	Flattening	Folding	Aeolian	Au Accretion	Au Dissolution / Pitting
AK028	AK028-11	3069	1876	1.64	18.09	a	r	sa	uf	x	x	x	x
AK028	AK028-12	1695	1192	1.42	6.35	c	r	sr	uf	x	x	x	x
AK028	AK028-13	1932	1318	1.47	8.00	c	c	sr	mf	x	x	r	c
AK028	AK028-14	2153	933	2.31	6.31	r	r	wr	uf	✓	x	x	r
AK028	AK028-15	2291	1855	1.24	13.35	r	c	wr	mf	x	x	r	a
AK028	AK028-16	1920	1342	1.43	8.09	r	r	wr	mf	x	x	r	a
AK028	AK028-17	2100	1552	1.35	10.24	c	r	r	uf	x	x	r	c
AK028	AK028-18	2785	1439	1.94	12.59	r	c	r	mf	x	x	c	c
AK028	AK028-19	2140	1160	1.84	7.80	c	a	sr	mf	x	x	r	c
AK028	AK028-20	4329	2876	1.51	39.11	r	a	sr	mf	x	x	r	c
AK028	AK028-21	4577	2534	1.81	36.44	r	c	wr	mf	x	x	r	c
AK028	AK028-22	3532	2668	1.32	29.60	c	c	sr	mf	x	x	r	c
AK028	AK028-23	5417	3395	1.60	57.78	r	r	wr	uf	x	x	x	r
AK032	AK032-1	856	462	1.85	1.24	c	c	sr	mf	x	x	a	r
AK032	AK032-2	580	455	1.27	0.83	r	r	sr	wf	x	x	a	r
AK032	AK032-3	521	401	1.30	0.66	r	r	r	wf	✓	x	a	a
AK032	AK032-4	776	327	2.37	0.80	a	r	sa	uf	x	x	a	r
AK032	AK032-5	1175	998	1.18	3.68	c	c	r	mf	✓	✓	r	r
AK032	AK032-6	1017	646	1.57	2.06	r	r	r	wf	x	x	a	c
AK032	AK032-7	1034	866	1.19	2.81	r	r	r	wf	✓	x	a	c
AK032	AK032-8	724	633	1.14	1.44	r	r	r	wf	✓	x	a	c
AK032	AK032-9	944	702	1.34	2.08	r	c	sr	mf	x	x	a	a
AK100	AK100-1	370	226	1.64	0.26	r	a	r	mf	x	x	r	r
AK100	AK100-2	777	330	2.35	0.81	c	c	sr	mf	x	x	c	c
AK100	AK100-3	428	266	1.61	0.36	c	c	r	uf	x	x	a	a
AK100	AK100-4	228	160	1.43	0.11	x	a	wr	uf	x	x	a	a
AK100	AK100-5	531	285	1.86	0.48	a	c	sa	uf	x	x	c	c
AK100	AK100-6	341	272	1.25	0.29	r	a	sr	mf	x	x	r	r
AK100	AK100-7	674	435	1.55	0.92	r	a	r	mf	✓	x	r	r
AK100	AK100-8	674	293	2.30	0.62	a	r	sr	uf	x	x	r	r
AK100	AK100-9	546	319	1.71	0.55	r	c	r	wf	x	x	c	c
AK100	AK100-10	365	164	2.23	0.19	r	c	r	wf	x	x	c	c
AK100	AK100-11	376	166	2.27	0.20	a	r	sa	uf	x	x	a	c
AK100	AK100-12	341	150	2.27	0.16	a	r	sa	uf	x	x	a	a
AK100	AK100-13	301	171	1.76	0.16	r	a	sr	mf	x	x	a	a
AK100	AK100-14	543	282	1.93	0.48	r	a	r	mf	x	x	a	a
AK100	AK100-15	332	272	1.22	0.28	r	a	r	wf	x	x	a	a
AK100	AK100-16	306	208	1.47	0.20	c	r	sr	uf	x	x	a	a
AK100	AK100-17	323	184	1.76	0.19	c	r	wr	uf	x	x	a	a
AK100	AK100-18	564	305	1.85	0.54	c	a	sr	mf	x	x	c	c
AK100	AK100-19	706	214	3.30	0.47	c	a	sr	uf	x	x	r	r
AK100	AK100-20	506	409	1.24	0.65	a	c	sa	uf	x	x	a	a
AK111	AK111-1	1231	605	2.03	2.34	c	a	sr	uf	x	?	c	c
AK111	AK111-2	870	814	1.07	2.22	c	a	sr	uf	x	x	c	c
AK111	AK111-3	1048	586	1.79	1.93	r	a	sr	uf	x	x	c	c
AK111	AK111-4	1043	501	2.08	1.64	r	a	wr	uf	x	x	c	c
AK111	AK111-5	838	825	1.02	2.17	r	a	r	uf	x	x	c	c
AK111	AK111-6	728	589	1.24	1.35	r	a	sr	uf	x	x	c	c
AK111	AK111-7	980	576	1.70	1.77	r	a	wr	mf	x	x	c	c
AK111	AK111-8	812	631	1.29	1.61	r	a	wr	mf	x	x	c	c
AK111	AK111-9	701	588	1.19	1.29	r	a	wr	uf	x	x	c	a
AK111	AK111-10	1089	805	1.35	2.75	r	c	sr	uf	x	x	c	a
AK111	AK111-11	1159	730	1.59	2.66	r	c	r	mf	x	x	c	c
AK111	AK111-12	1359	734	1.85	3.13	r	c	wr	wf	x	x	a	a
AK111	AK111-13	1102	515	2.14	1.78	r	c	wr	mf	x	x	a	a
AK111	AK111-14	949	802	1.18	2.39	r	r	sr	uf	x	x	a	a
AK111	AK111-15	1113	696	1.60	2.43	a	a	sa	uf	x	x	r	r
AK111	AK111-16	1295	873	1.48	3.55	a	r	sr	uf	x	x	r	r
AK111	AK111-17	1679	974	1.72	5.14	a	c	sr	uf	x	?	c	c
AK111	AK111-18	1820	1305	1.39	7.46	a	c	sr	uf	x	x	r	r
AK111	AK111-19	1221	895	1.36	3.43	c	r	sr	uf	x	x	r	c
AK111	AK111-20	1155	826	1.40	3.00	c	a	r	uf	x	x	r	c
AK117	AK117-1	1346	348	3.87	1.47	x	r	wr	mf	x	x	r	r
AK117	AK117-2	600	290	2.07	0.55	r	r	r	wf	x	x	c	c
AK117	AK117-3	323	265	1.22	0.27	r	r	sr	uf	x	x	a	a
AK117	AK117-4	412	222	1.86	0.29	x	r	wr	wf	✓	x	r	c
AK117	AK117-5	340	221	1.54	0.24	r	r	wr	wf	✓	x	r	c
AK117	AK117-6	358	274	1.31	0.31	r	r	wr	wf	✓	x	a	a
AK117	AK117-7	571	332	1.72	0.60	c	c	sr	mf	x	x	a	a
AK117	AK117-8	448	196	2.29	0.28	r	r	r	wf	✓	x	a	a
AK117	AK117-9	311	244	1.27	0.24	r	r	wr	wf	✓	x	a	a
AK117	AK117-10	228	216	1.06	0.15	r	x	wr	wf	x	x	a	c

Site	Grain #	A-axis (µm)	B-axis (µm)	Elongation (a/b)	Ellipsoidal Area (mm²)	Primary features	Abrasion	Rounding	Flattening	Folding	Aeolian	Au Accretion	Au Dissolution / Pitting
AK117	AK117-11	939	750	1.25	2.21	x	c	wr	wf	✓	?	c	c
AK117	AK117-12	593	366	1.62	0.68	r	r	sr	mf	x	x	c	c
AK117	AK117-13	525	230	2.28	0.38	r	r	wr	wf	x	x	c	a
AK117	AK117-14	524	205	2.56	0.34	r	r	sr	mf	x	x	r	c
AK117	AK117-15	426	219	1.95	0.29	r	c	wr	wf	✓	?	r	c
AK117	AK117-16	378	261	1.45	0.31	r	r	sr	mf	x	x	r	r
AK117	AK117-17	347	263	1.32	0.29	r	r	r	uf	x	x	a	a
AK117	AK117-18	313	236	1.33	0.23	r	c	r	mf	x	x	a	a
AK117	AK117-19	540	242	2.23	0.41	c	c	r	mf	x	x	a	a
AK117	AK117-20	432	230	1.88	0.31	r	c	r	mf	✓	x	a	a
AK121	AK121-1	1039	689	1.51	2.25	r	c	r	uf	x	x	a	c
AK121	AK121-2	932	908	1.03	2.66	r	r	wr	mf	x	x	a	c
AK121	AK121-3	1100	720	1.53	2.49	r	r	wr	wf	x	x	a	c
AK121	AK121-4	1175	726	1.62	2.68	r	r	wr	mf	x	x	a	c
AK121	AK121-5	992	500	1.98	1.56	a	c	r	uf	x	x	c	r
AK121	AK121-6	1078	501	2.15	1.70	r	r	wr	mf	x	x	r	r
AK121	AK121-7	990	505	1.96	1.57	r	r	wr	mf	x	x	a	a
AK121	AK121-8	467	405	1.15	0.59	r	r	r	uf	x	x	c	c
AK121	AK121-9	623	374	1.67	0.73	c	c	sr	uf	x	x	r	r
AK121	AK121-10	485	242	2.00	0.37	r	c	wr	mf	x	x	r	r
AK121	AK121-11	520	303	1.72	0.49	r	c	r	mf	✓	x	c	c
AK121	AK121-12	660	355	1.86	0.74	c	r	sr	uf	x	x	c	c
AK121	AK121-13	602	241	2.50	0.46	r	r	sr	mf	x	x	a	c
AK121	AK121-14	557	314	1.77	0.55	r	r	wr	mf	✓	x	a	c
AK121	AK121-15	980	350	2.80	1.08	r	r	wr	mf	x	x	r	r
AK121	AK121-16	601	330	1.82	0.62	r	c	wr	mf	x	?	c	a
AK121	AK121-17	740	218	3.39	0.51	r	r	wr	uf	x	x	a	a
AK121	AK121-18	425	372	1.14	0.50	r	r	wr	uf	x	x	r	c
AK121	AK121-19	500	455	1.10	0.71	r	r	wr	uf	x	x	c	c
AK121	AK121-20	670	486	1.38	1.02	r	c	sr	wf	x	x	a	c
AK121	AK121-21	543	406	1.34	0.69	r	c	wr	wf	x	x	r	c
AK121	AK121-22	553	403	1.37	0.70	r	c	wr	wf	x	x	r	c
AK121	AK121-23	591	289	2.04	0.54	c	c	wr	uf	x	x	c	c
AK121	AK121-24	380	419	0.91	0.50	r	r	wr	uf	x	x	c	c
AK121	AK121-25	537	442	1.21	0.75	r	r	wr	uf	x	x	r	c
AK123	AK123-1	1330	1030	1.29	4.30	r	c	wr	wf	x	x	r	c
AK123	AK123-2	1720	986	1.74	5.33	c	r	sr	uf	x	x	r	r
AK123	AK123-3	1360	995	1.37	4.25	r	c	wr	mf	x	x	r	c
AK123	AK123-4	1920	1306	1.47	7.88	c	r	sr	uf	x	x	r	c
AK123	AK123-5	1175	1026	1.15	3.79	r	a	r	uf	x	x	c	c
AK123	AK123-6	1460	1140	1.28	5.23	r	c	r	mf	x	x	r	r
AK123	AK123-7	1942	877	2.21	5.35	r	c	r	mf	x	x	r	r
AK123	AK123-8	2190	878	2.49	6.04	r	c	r	mf	x	x	r	r
AK123	AK123-9	1315	1036	1.27	4.28	r	c	wr	mf	x	x	c	r
AK123	AK123-10	1312	1125	1.17	4.64	r	c	wr	mf	x	x	r	r
AK123	AK123-11	1607	800	2.01	4.04	r	c	wr	uf	x	x	c	r
AK123	AK123-12	1906	1252	1.52	7.50	r	c	wr	mf	x	x	r	r
AK123	AK123-13	2059	1600	1.29	10.35	r	c	wr	mf	x	x	r	r
AK123	AK123-14	1381	590	2.34	2.56	r	a	wr	wf	x	x	r	a
AK123	AK123-15	1227	716	1.71	2.76	r	c	wr	uf	x	x	r	a
AK123	AK123-16	1165	803	1.45	2.94	r	a	wr	wf	x	x	r	r
AK123	AK123-17	767	747	1.03	1.80	r	a	wr	mf	x	x	r	r
AK123	AK123-18	3090	1179	2.62	11.45	a	r	sr	uf	x	x	r	r
AK123	AK123-19	2057	905	2.27	5.85	a	r	sr	uf	x	x	r	r
AK123	AK123-20	930	690	1.35	2.02	r	a	wr	wf	x	x	r	r
AUR-12-854	AUR-12-854-1	606	586	1.03	1.12	r	c	wr	wf	✓	x	x	c
AUR-12-854	AUR-12-854-2	760	395	1.92	0.94	r	c	sa	mf	x	x	x	r
AUR-12-854	AUR-12-854-3	475	400	1.19	0.60	r	r	wr	mf	x	x	r	r
AUR-12-854	AUR-12-854-4	830	340	2.44	0.89	r	r	wr	uf	x	x	c	r
AUR-12-854	AUR-12-854-5	467	256	1.82	0.38	r	r	r	mf	x	x	r	r
AUR-12-854	AUR-12-854-6	475	330	1.44	0.49	r	r	wr	uf	x	x	r	r
AUR-12-854	AUR-12-854-7	498	448	1.11	0.70	r	r	wr	wf	x	x	c	r
AUR-12-854	AUR-12-854-8	703	369	1.91	0.81	r	c	wr	mf	x	?	c	r
AUR-12-854	AUR-12-854-9	520	302	1.72	0.49	r	r	wr	mf	x	x	r	r
AUR-12-854	AUR-12-854-10	378	273	1.38	0.32	r	r	wr	uf	x	x	c	r
AUR-12-854	AUR-12-854-11	461	408	1.13	0.59	r	a	wr	wf	x	x	c	c
AUR-12-854	AUR-12-854-12	440	366	1.20	0.51	r	r	wr	mf	x	x	c	c
AUR-12-854	AUR-12-854-13	496	359	1.38	0.56	r	c	r	wf	x	x	r	r
AUR-12-854	AUR-12-854-14	512	353	1.45	0.57	r	r	sr	mf	x	x	r	r
AUR-12-854	AUR-12-854-15	395	360	1.10	0.45	r	r	sr	mf	x	x	c	c

Site	Grain #	A-axis (µm)	B-axis (µm)	Elongation (a/b)	Ellipsoidal Area (mm²)	Primary features	Abrasion	Rounding	Flattening	Folding	Aeolian	Au Accretion	Au Dissolution / Pitting
AUR-12-854	AUR-12-854-16	634	319	1.99	0.64	r	a	wr	wf	✓	x	c	c
AUR-12-854	AUR-12-854-17	426	324	1.31	0.43	r	c	sr	mf	x	x	c	a
AUR-12-854	AUR-12-854-18	606	277	2.19	0.53	c	r	sr	mf	x	x	r	c
AUR-12-854	AUR-12-854-19	506	343	1.48	0.55	r	c	r	mf	x	x	r	r
AUR-12-854	AUR-12-854-20	571	204	2.80	0.37	r	c	wr	uf	x	x	r	c
AUR-12-854	AUR-12-854-21	928	581	1.60	1.69	r	a	sr	wf	x	x	r	r
AUR-12-854	AUR-12-854-22	1061	503	2.11	1.68	c	a	sr	mf	x	x	c	a
AUR-12-854	AUR-12-854-23	1265	825	1.53	3.28	c	r	sa	uf	x	x	r	r
AUR-12-854	AUR-12-854-24	2020	1339	1.51	8.50	r	c	sr	mf	x	x	r	r
ADEM	ADEM-1	2254	1552	1.45	10.99	r	r	wr	mf	x	x	c	c
ADEM	ADEM-2	1960	1470	1.33	9.05	r	r	wr	mf	x	x	c	r
ADEM	ADEM-3	2126	1766	1.20	11.80	r	r	wr	mf	x	x	c	r
ADEM	ADEM-4	1265	1150	1.10	4.57	r	r	wr	mf	x	x	c	r
ADEM	ADEM-5	1868	1203	1.55	7.06	r	r	wr	mf	x	x	c	r
ADEM	ADEM-6	1800	1256	1.43	7.10	r	r	wr	mf	x	x	c	c
ADEM	ADEM-7	634	495	1.28	0.99	r	r	wr	mf	x	x	c	c
ADEM	ADEM-8	1020	957	1.07	3.07	r	r	wr	mf	x	x	c	c
ADEM	ADEM-9	1156	750	1.54	2.72	r	c	wr	wf	x	x	c	c
ADEM	ADEM-10	1212	342	3.54	1.30	c	r	sr	uf	x	x	c	c
ADEM	ADEM-11	1103	524	2.10	1.82	r	c	wr	mf	x	x	c	c
ADEM	ADEM-12	1061	722	1.47	2.41	r	c	wr	mf	x	x	c	c
ADEM	ADEM-13	738	596	1.24	1.38	r	r	wr	uf	x	x	c	c
ADEM	ADEM-14	1214	590	2.06	2.25	r	c	wr	mf	x	x	c	c
ADEM	ADEM-15	965	497	1.94	1.51	r	c	wr	uf	x	x	c	c
ADEM	ADEM-16	1340	605	2.21	2.55	r	a	wr	mf	x	x	c	c
ADEM	ADEM-17	1291	913	1.41	3.70	r	c	r	mf	x	x	r	c
ADEM	ADEM-18	1085	623	1.74	2.12	r	c	wr	mf	x	x	c	c
ADEM	ADEM-19	1188	829	1.43	3.09	r	c	wr	mf	x	x	c	c
ADEM	ADEM-20	820	602	1.36	1.55	r	c	wr	mf	x	x	c	c

Explanation:

A-axis (major axis) and B-axis (minor axis) are measured quantitatively in microns. Elongation is defined as the major axis divided by the minor axis and is thus always greater than unity.

Ellipsoidal area is a semi-quantitative expression of grain area defined by Area = π(a-axis)(b-axis). This is expressed in mm².

Relative abundance of primary features, abrasion features, gold accretion and gold dissolution/pitting are expressed as absent (x), rare (r), common (c), or abundant (a).

Rounding is expressed qualitatively as very angular (va), angular (a), sub-angular (sa), sub-rounded (sr), rounded (r), and well rounded (wr).

Flattening is expressed qualitatively as un-flattened (uf), moderately flattened (mf), or well flattened (wf).

Significant folding and aeolian signatures are expressed as present (✓) or absent (x).

APPENDIX C

Major and Minor Element data for gold grains from the southern Seward Peninsula, Nome, Alaska

Site	Sample	Total (Mass%)	Au (Norm%) LLD = 0.065%	Ag (Norm%) LLD = 0.035%	Hg (Norm%) LLD = 0.030%	Cu (Norm%) LLD = 0.017%	Au (Error%)	Ag (Error%)	Hg (Error%)	Cu (Error%)	Fineness
AK015	AK015-1a	100.45	97.843	1.984	0.173	0.000	0.53	2.81	25.76	-	980
	AK015-1b	101.21	93.588	6.123	0.289	0.000	0.54	1.21	15.77	-	939
	AK015-1c	102.64	93.301	6.458	0.242	0.000	0.53	1.13	17.82	-	935
	AK015-1d	101.45	93.409	6.543	0.035	0.013	0.54	1.14	123.85	108.89	935
	AK015-5a	100.80	93.884	5.923	0.192	0.001	0.54	1.21	23.01	1264.45	941
	AK015-5b	99.60	93.493	6.178	0.313	0.016	0.54	1.24	14.89	85.42	938
	AK015-5c	99.34	93.509	6.223	0.268	0.000	0.54	1.18	16.26	-	938
	AK015-5d	102.50	94.067	5.805	0.116	0.012	0.53	1.21	36.51	111.74	942
	AK015-10a	101.19	94.719	5.217	0.000	0.064	0.53	1.32	-	21.44	948
	AK015-10c	103.22	94.946	4.992	0.062	0.000	0.53	1.33	63.84	-	950
	AK015-10d	102.15	95.092	4.908	0.000	0.000	0.53	1.33	-	-	951
	AK015-12a	103.89	95.164	4.799	0.000	0.037	0.52	1.33	-	35.83	952
	AK015-12b	102.39	94.899	5.057	0.000	0.044	0.53	1.28	-	30.00	949
	AK015-12c	102.94	95.109	4.885	0.007	0.000	0.53	1.33	580.44	-	951
	AK015-13a	100.61	90.268	7.853	1.875	0.005	0.55	1.01	3.12	301.35	920
	AK015-13b	100.79	91.057	7.654	1.289	0.000	0.55	1.03	4.11	-	922
	AK015-13c	97.95	90.158	8.021	1.820	0.000	0.56	1.02	3.21	-	918
	AK015-17a	101.86	93.295	6.529	0.162	0.015	0.54	1.11	25.69	92.08	935
	AK015-17b	101.58	95.739	4.261	0.000	0.000	0.53	1.46	-	-	957
AK021	AK021-1a	95.08	80.865	19.135	0.000	0.000	0.60	0.60	-	-	809
	AK021-1b	96.46	81.078	18.915	0.000	0.007	0.60	0.60	-	201.61	811
	AK021-1c_rim	96.64	82.248	17.717	0.035	0.000	0.59	0.62	111.96	-	823
	AK021-2a	99.68	83.397	16.603	0.000	0.000	0.58	0.63	-	-	834
	AK021-2b	100.60	83.322	16.677	0.000	0.001	0.58	0.63	-	1675.91	833
	AK021-2c_rim	101.34	83.086	16.914	0.000	0.000	0.58	0.62	-	-	831
	AK021-3a	100.77	83.760	16.240	0.000	0.000	0.57	0.64	-	-	838
	AK021-3b	101.33	83.253	16.738	0.000	0.010	0.58	0.63	-	137.29	833
	AK021-3c_rim	100.61	83.093	16.907	0.000	0.000	0.58	0.63	-	-	831
	AK021-4a	100.81	83.046	16.940	0.000	0.014	0.58	0.62	-	96.39	831
	AK021-4b	100.78	82.330	17.670	0.000	0.000	0.58	0.61	-	-	823
	AK021-4c_rim	98.25	82.026	17.974	0.000	0.000	0.59	0.61	-	-	820
	AK021-5a	97.77	79.654	20.318	0.000	0.029	0.60	0.56	-	49.46	797
	AK021-5b	98.54	78.511	21.489	0.000	0.000	0.60	0.55	-	-	785
	AK021-5c_rim	99.55	78.650	21.350	0.000	0.000	0.60	0.55	-	-	787
	AK021-6a	99.84	84.475	15.489	0.028	0.008	0.58	0.66	139.13	179.76	845
	AK021-6c_rim	98.24	83.660	16.333	0.000	0.007	0.58	0.65	-	197.34	837
	AK021-7a	99.37	84.637	15.356	0.000	0.007	0.58	0.67	-	213.03	846
	AK021-7b	97.79	84.398	15.602	0.000	0.000	0.58	0.67	-	-	844
	AK021-7c_rim	98.93	84.298	15.686	0.003	0.013	0.58	0.66	1166.32	108.86	843
	AK021-8a	102.71	85.991	14.008	0.000	0.001	0.56	0.69	-	1245.75	860
	AK021-8b	101.19	85.273	14.723	0.000	0.004	0.57	0.68	-	317.19	853
	AK021-9a	97.17	89.986	10.008	0.000	0.005	0.56	0.87	-	303.53	900
	AK021-9b	98.61	86.814	13.186	0.000	0.000	0.57	0.74	-	-	868
	AK021-10a	96.70	78.453	21.547	0.000	0.000	0.61	0.56	-	-	785
	AK021-10b	100.42	78.675	21.312	0.000	0.013	0.60	0.55	-	108.52	787
	AK021-10c_rim	99.51	76.051	23.949	0.000	0.000	0.61	0.51	-	-	761
	AK021-12a	99.07	87.934	11.814	0.252	0.000	0.56	0.79	18.27	-	882
	AK021-12b	100.45	88.391	11.232	0.374	0.003	0.56	0.81	11.72	450.40	887
	AK021-12c_rim	101.65	88.580	11.025	0.378	0.018	0.55	0.81	11.54	76.95	889
	AK021-13a	100.70	81.116	18.884	0.000	0.000	0.59	0.59	-	-	811
	AK021-13b	100.27	80.740	19.251	0.000	0.009	0.59	0.59	-	152.07	807
	AK021-13c_rim	98.50	81.767	18.233	0.000	0.000	0.59	0.61	-	-	818
	AK021-14a	96.89	82.922	16.995	0.074	0.008	0.59	0.64	54.87	164.77	830
	AK021-14b	100.44	82.810	17.190	0.000	0.000	0.58	0.62	-	-	828
	AK021-14c_rim	96.35	81.722	18.203	0.076	0.000	0.60	0.62	55.04	-	818
	AK021-15a	98.29	88.014	11.986	0.000	0.000	0.56	0.79	-	-	880
	AK021-15b	100.94	88.665	11.325	0.000	0.010	0.56	0.81	-	139.79	887
	AK021-15c_rim	101.47	87.803	12.197	0.000	0.000	0.56	0.76	-	-	878
	AK021-16a	99.65	89.632	10.356	0.000	0.012	0.56	0.85	-	114.39	896
	AK021-16b_rim	100.19	89.511	10.361	0.128	0.000	0.55	0.85	33.33	-	896
	AK021-16c_rim	100.49	89.533	10.444	0.023	0.000	0.55	0.84	189.38	-	896
	AK021-17a	101.37	84.531	15.469	0.000	0.000	0.57	0.66	-	-	845
	AK021-17b	99.99	83.906	16.047	0.000	0.047	0.58	0.66	-	29.81	839
	AK021-17c	100.68	85.142	14.858	0.000	0.000	0.57	0.67	-	-	851
	AK021-18b	100.43	84.185	15.815	0.000	0.000	0.57	0.66	-	-	842
	AK021-18c	98.99	83.674	16.326	0.000	0.000	0.58	0.65	-	-	837
	AK021-19a	103.11	86.034	13.967	0.000	0.000	0.56	0.67	-	-	860
	AK021-19b	99.40	83.520	16.480	0.000	0.000	0.58	0.64	-	-	835
	AK021-19c	100.80	84.906	15.083	0.000	0.011	0.57	0.66	-	128.25	849
	AK021-20a	98.89	76.230	23.754	0.013	0.003	0.61	0.52	311.52	486.22	762
	AK021-20b	99.04	74.757	25.243	0.000	0.000	0.62	0.50	-	-	748
	AK021-21a	100.91	81.272	18.718	0.000	0.010	0.59	0.59	-	135.72	813
	AK021-21b	98.70	81.327	18.649	0.022	0.002	0.59	0.60	180.39	591.07	813
	AK021-22a	99.79	86.410	13.590	0.000	0.000	0.57	0.70	-	-	864
	AK021-22b	98.32	87.260	12.740	0.000	0.000	0.57	0.74	-	-	873

Site	Sample	Total (Mass%)	Au (Norm%) LLD = 0.065%	Ag (Norm%) LLD = 0.035%	Hg (Norm%) LLD = 0.030%	Cu (Norm%) LLD = 0.017%	Au (Error%)	Ag (Error%)	Hg (Error%)	Cu (Error%)	Fineness
AK021	AK021-24a	101.01	85.960	14.037	0.003	0.000	0.57	0.70	1275.50	-	860
	AK021-24b	100.28	85.766	14.234	0.000	0.000	0.57	0.70	-	-	858
	AK021-23a	97.61	82.581	17.403	0.000	0.015	0.59	0.62	-	89.05	826
	AK021-23b	101.86	82.423	17.577	0.000	0.000	0.58	0.61	-	-	824
	AK021-23c	100.73	82.168	17.832	0.000	0.000	0.58	0.61	-	-	822
	AK021-25a	98.10	80.756	19.221	0.022	0.000	0.60	0.59	181.17	-	808
	AK021-25b	97.67	80.537	19.463	0.000	0.000	0.60	0.59	-	-	805
	AK021-25c	101.41	81.391	18.609	0.000	0.000	0.58	0.59	-	-	814
	AK021-26a	100.52	84.495	15.505	0.000	0.000	0.57	0.66	-	-	845
	AK021-26b	101.78	84.398	15.602	0.000	0.000	0.57	0.65	-	-	844
	AK021-31a	99.46	81.004	18.996	0.000	0.000	0.59	0.59	-	-	810
	AK021-32b	99.65	83.124	16.876	0.000	0.000	0.58	0.62	-	-	831
	AK021-31b	101.61	81.284	18.710	0.000	0.006	0.58	0.59	-	212.02	813
	AK021-33a	101.99	88.332	11.646	0.000	0.022	0.55	0.79	-	64.15	884
	AK021-33b	98.27	89.328	10.637	0.035	0.000	0.56	0.82	113.03	-	894
	AK021-34a	101.03	84.841	15.159	0.000	0.000	0.57	0.67	-	-	848
	AK021-34c	100.50	83.735	16.234	0.000	0.031	0.58	0.65	-	43.92	838
	AK021-35a	102.13	83.448	16.552	0.000	0.000	0.57	0.63	-	-	834
	AK021-35b	100.67	82.298	17.688	0.000	0.014	0.58	0.61	-	98.84	823
	AK021-36a	99.19	82.382	17.618	0.000	0.000	0.59	0.62	-	-	824
	AK021-36b	101.07	81.254	18.736	0.000	0.010	0.58	0.60	-	142.48	813
	AK021-37a	101.01	83.051	16.949	0.000	0.000	0.58	0.63	-	-	831
	AK021-37b	101.51	83.459	16.507	0.000	0.034	0.57	0.63	-	39.14	835
	AK021-37c	100.85	82.801	17.177	0.000	0.022	0.58	0.62	-	63.06	828
	AK021-38a	101.55	92.445	7.519	0.000	0.036	0.54	1.05	-	38.27	925
	AK021-38b	102.06	93.476	6.524	0.000	0.000	0.54	1.08	-	-	935
	AK021-39a	103.45	87.389	12.611	0.000	0.000	0.55	0.73	-	-	874
	AK021-39b	101.81	86.659	13.341	0.000	0.000	0.56	0.71	-	-	867
	AK021-39c	97.68	87.094	12.902	0.000	0.004	0.57	0.74	-	336.29	871
	AK021-40a	101.07	85.255	14.695	0.000	0.049	0.57	0.68	-	27.38	853
	AK021-40b	99.17	85.164	14.836	0.000	0.000	0.57	0.69	-	-	852
	AK021-40c	102.74	85.559	14.441	0.000	0.000	0.56	0.69	-	-	856
AK028	AK028_1a	96.81	80.475	17.944	1.521	0.061	0.60	0.63	3.69	23.69	818
	AK028_1b	96.32	84.493	14.354	1.151	0.002	0.58	0.70	4.51	580.38	855
	AK028_1c_rim	99.24	80.948	17.646	1.406	0.000	0.59	0.62	3.84	-	821
	AK028_2a	98.15	89.801	9.294	0.906	0.000	0.56	0.91	5.58	-	906
	AK028_3b	96.95	89.918	9.359	0.696	0.027	0.56	0.90	6.65	51.86	906
	AK028_3c	95.68	85.137	11.516	3.347	0.000	0.58	0.83	2.11	-	881
	AK028_4a	98.87	88.079	11.204	0.717	0.000	0.56	0.83	6.72	-	887
	AK028_4b	98.13	88.716	10.537	0.747	0.000	0.56	0.83	6.12	-	894
	AK028_4c_rim	98.53	91.766	7.668	0.558	0.008	0.55	1.02	8.53	31.79	923
	AK028_5a	100.70	87.783	11.379	0.812	0.026	0.56	0.79	5.98	52.87	885
	AK028_5b	100.90	88.511	10.602	0.887	0.000	0.56	0.82	5.56	-	893
	AK028_5c_rim	103.68	88.991	10.444	0.564	0.000	0.55	0.82	8.07	-	895
	AK028_6a	101.34	91.443	7.534	1.022	0.000	0.54	0.98	4.56	-	924
	AK028_6b_rim	101.64	89.170	9.843	0.964	0.023	0.55	0.88	5.22	61.74	901
	AK028_6c_rim	99.37	88.263	10.004	1.723	0.010	0.56	0.90	3.37	145.41	898
	AK028_9a_rim	98.38	89.617	10.040	0.343	0.000	0.56	0.87	12.69	-	899
	AK028_9b_rim	99.64	93.212	6.631	0.158	0.000	0.54	1.03	24.26	-	934
	AK028_9c	97.71	90.506	9.273	0.221	0.000	0.56	0.89	18.52	-	907
	AK028_10a	99.34	79.664	16.951	3.386	0.000	0.60	0.64	2.05	-	825
	AK028_10b	99.33	82.259	16.289	1.453	0.000	0.59	0.64	3.77	-	835
	AK028_10c_rim	100.89	77.532	15.951	6.517	0.000	0.60	0.65	1.30	-	829
	AK028-11a	96.09	92.477	7.195	0.279	0.049	0.55	1.10	17.14	29.23	928
	AK028-11b	98.86	92.335	7.190	0.470	0.005	0.55	1.07	9.69	288.59	928
	AK028-11c	99.89	92.740	7.101	0.159	0.000	0.54	1.05	25.50	-	929
	AK028-11d_rim	99.59	90.334	7.139	2.522	0.004	0.55	1.08	2.49	306.04	927
	AK028-12a	100.87	86.351	12.755	0.893	0.000	0.56	0.74	5.58	-	871
	AK028-12b	99.48	83.884	13.353	2.763	0.000	0.58	0.73	2.30	-	863
	AK028-12c_rim	98.93	85.591	11.204	3.199	0.005	0.57	0.79	2.14	255.64	884
	AK028-13a	101.01	82.273	9.049	8.678	0.000	0.57	0.91	1.09	-	901
	AK028-13b	101.72	83.053	9.143	7.804	0.000	0.57	0.91	1.15	-	901
	AK028-13c_rim	97.24	83.514	9.397	7.089	0.000	0.58	0.92	1.28	-	899
	AK028-14a	97.74	86.685	12.881	0.434	0.000	0.57	0.76	11.20	-	871
	AK028-14b	99.21	87.783	11.882	0.336	0.000	0.56	0.78	13.73	-	881
	AK028-14c_rim	98.96	87.943	10.996	1.056	0.005	0.56	0.82	4.82	253.07	889
	AK028-15a	100.65	90.721	9.171	0.108	0.000	0.55	0.92	39.71	-	908
	AK028-15b	100.17	90.918	8.859	0.223	0.000	0.55	0.94	19.66	-	911
	AK028-15c_rim	100.53	90.407	9.372	0.221	0.000	0.55	0.90	20.20	-	906
	AK028-16a	99.00	85.808	13.790	0.386	0.016	0.57	0.71	11.32	83.40	862
	AK028-16b	100.19	85.752	13.839	0.409	0.000	0.57	0.70	10.62	-	861
	AK028-16c	100.43	85.178	14.333	0.489	0.000	0.57	0.69	9.50	-	856
	AK028-16d	97.98	84.742	14.795	0.415	0.047	0.58	0.70	11.37	30.29	851
	AK028-17a	98.51	93.502	4.387	0.448	1.663	0.55	1.57	10.65	1.12	955
	AK028-17b	98.81	93.727	5.200	0.257	0.816	0.54	1.33	18.16	1.99	947

Site	Sample	Total (Mass%)	Au (Norm%) LLD = 0.065%	Ag (Norm%) LLD = 0.035%	Hg (Norm%) LLD = 0.030%	Cu (Norm%) LLD = 0.017%	Au (Error%)	Ag (Error%)	Hg (Error%)	Cu (Error%)	Fineness
AK028	AK028-17c	99.12	93.713	3.920	0.460	1.907	0.54	1.70	10.67	1.01	960
	AK028-17d	99.84	93.475	4.168	0.553	1.805	0.54	1.64	8.60	1.05	957
	AK028-18a	95.23	92.487	6.531	0.982	0.000	0.55	1.19	5.33	-	934
	AK028-18b	95.47	93.026	6.579	0.395	0.000	0.55	1.21	12.30	-	934
	AK028-18c	100.65	93.510	6.007	0.483	0.000	0.54	1.22	9.48	-	940
	AK028-19a	100.92	85.111	5.632	9.233	0.024	0.56	1.26	1.05	55.77	938
	AK028-19b	101.88	88.370	5.710	5.921	0.000	0.55	1.25	1.39	-	939
	AK028-19c_rim	96.42	89.745	4.998	5.257	0.000	0.56	1.29	1.49	-	947
	AK028-20a	99.00	89.127	10.220	0.654	0.000	0.56	0.86	7.31	-	897
	AK028-20b	100.70	89.352	10.552	0.078	0.018	0.55	0.84	54.81	77.33	894
	AK028-20c	102.07	89.854	10.118	0.028	0.000	0.55	0.86	151.53	-	899
	AK028-21a	103.19	93.223	6.364	0.407	0.006	0.53	1.13	10.62	213.54	936
	AK028-21c	101.75	93.167	6.481	0.303	0.049	0.54	1.15	14.39	27.76	935
	AK028-21d	102.36	93.202	6.412	0.386	0.000	0.54	1.14	11.90	-	936
	AK028-21e_rim	101.00	92.816	6.796	0.373	0.014	0.54	1.10	12.46	97.69	932
	AK028-22a	100.77	92.928	6.140	0.892	0.040	0.54	1.20	5.80	35.00	938
	AK028-22b	98.46	93.135	6.007	0.858	0.000	0.55	1.24	6.02	-	939
	AK028-22c_rim	102.77	95.592	3.866	0.542	0.000	0.53	1.58	8.52	-	961
	AK028-22d	103.00	93.286	5.950	0.710	0.054	0.53	1.21	7.00	24.94	940
	AK028-23a	100.48	89.447	9.962	0.551	0.039	0.55	0.86	8.39	35.73	900
	AK028-23b	99.54	89.331	10.107	0.558	0.004	0.56	0.86	8.45	390.26	898
	AK028-23c	100.42	89.121	10.307	0.571	0.001	0.56	0.84	8.29	1032.62	896
	AK028-23d	102.62	89.159	10.351	0.487	0.003	0.55	0.83	9.26	485.31	896
	AK028-23e_rim	101.09	88.939	10.444	0.608	0.009	0.55	0.83	7.82	161.61	895
AK032	AK032-1a	96.28	94.357	5.627	0.017	0.000	0.55	1.17	211.90	-	944
	AK032-1b	96.65	92.897	6.663	0.440	0.000	0.55	1.11	10.73	-	933
	AK032-1c	101.18	93.100	6.900	0.000	0.000	0.54	1.10	-	-	931
	AK032-2a	99.60	94.847	4.409	0.635	0.109	0.54	1.44	7.35	12.83	956
	AK032-2b	101.35	95.164	4.133	0.620	0.083	0.53	1.45	7.22	16.56	958
	AK032-2c	99.12	94.465	4.643	0.807	0.085	0.54	1.38	6.32	16.99	953
	AK032-7a	100.94	77.984	21.999	0.000	0.017	0.60	0.54	-	83.79	780
	AK032-7c_rim	99.45	78.248	21.752	0.000	0.000	0.60	0.54	-	-	782
	AK032-8a	98.65	83.424	16.576	0.000	0.000	0.58	0.63	-	-	834
	AK032-8c_rim	100.21	83.037	16.959	0.000	0.004	0.58	0.62	-	322.94	830
	AK032-8d	99.65	82.705	17.295	0.000	0.000	0.58	0.62	-	-	827
	AK032-9a	98.00	88.626	11.002	0.310	0.061	0.56	0.83	13.82	23.19	890
	AK032-9b	100.36	89.293	10.646	0.049	0.012	0.55	0.83	81.45	118.53	893
	AK032-9c_rim	100.07	89.139	10.601	0.260	0.000	0.56	0.84	16.72	-	894
AK100	AK100-1a	95.12	97.366	2.634	0.000	0.000	0.54	2.35	-	-	974
	AK100-1b	103.18	94.466	5.534	0.000	0.000	0.53	1.21	-	-	945
	AK100-2a	98.90	81.086	18.906	0.008	0.000	0.59	0.59	474.26	-	811
	AK100-2b	99.71	83.453	16.547	0.000	0.000	0.58	0.62	-	-	835
	AK100-2c	99.33	81.323	18.673	0.000	0.004	0.59	0.59	-	372.82	813
	AK100-3a	100.46	92.267	7.710	0.000	0.023	0.54	1.00	-	58.20	923
	AK100-3b	99.31	92.031	7.969	0.000	0.000	0.55	0.99	-	-	920
	AK100-3c	101.96	92.348	7.641	0.000	0.011	0.54	1.01	-	131.66	924
	AK100-4b	102.60	96.042	3.955	0.000	0.003	0.52	1.56	-	438.23	960
	AK100-4c	99.06	95.498	4.499	0.000	0.003	0.54	1.48	-	479.54	955
	AK100-9a	97.70	78.966	21.034	0.000	0.000	0.60	0.56	-	-	790
	AK100-9b	99.62	80.593	19.407	0.000	0.000	0.59	0.57	-	-	806
	AK100-9c	97.98	79.360	20.640	0.000	0.000	0.60	0.56	-	-	794
	AK100-10a_rim	98.00	91.576	8.424	0.000	0.000	0.55	0.94	-	-	916
	AK100-13a	99.95	97.807	2.193	0.000	0.000	0.52	2.56	-	-	978
	AK100-13b	99.33	97.759	2.235	0.006	0.000	0.53	2.53	696.93	-	978
	AK100-13c	104.11	98.129	1.871	0.000	0.000	0.51	2.55	-	-	981
	AK100-14b	97.54	77.363	22.618	0.000	0.019	0.61	0.53	-	71.87	774
	AK100-14c	97.66	73.272	26.712	0.016	0.000	0.63	0.49	253.87	-	733
	AK100-15a	100.44	90.647	9.353	0.000	0.000	0.55	0.86	-	-	906
	AK100-15b	100.31	90.315	9.657	0.000	0.028	0.55	0.88	-	48.37	903
	AK100-15c	100.83	90.271	9.729	0.000	0.000	0.55	0.85	-	-	903
	AK100-18a	97.05	96.025	3.975	0.000	0.000	0.54	1.60	-	-	960
	AK100-18b	100.43	95.682	4.311	0.000	0.007	0.53	1.49	-	201.56	957
	AK100-18c	100.99	96.447	3.553	0.000	0.000	0.53	1.63	-	-	964
	AK100-19a	97.75	93.095	6.689	0.193	0.023	0.55	1.09	22.27	61.50	933
	AK100-19c	101.14	93.275	6.546	0.179	0.000	0.54	1.10	22.53	-	934
AK111	AK111-1a	97.87	89.590	10.358	0.000	0.052	0.56	0.86	-	26.90	896
	AK111-1b	98.50	89.208	10.792	0.000	0.000	0.56	0.83	-	-	892
	AK111-1c_rim	95.83	89.227	10.769	0.003	0.000	0.57	0.85	1596.84	-	892
	AK111-2a	95.06	79.580	20.418	0.000	0.002	0.61	0.58	-	757.71	796
	AK111-2b	97.72	79.382	20.602	0.000	0.016	0.60	0.57	-	84.19	794
	AK111-2c_rim	96.69	79.532	20.370	0.094	0.004	0.61	0.58	45.59	68.40	796
	AK111-3a	100.38	97.448	2.552	0.000	0.000	0.53	2.15	-	-	974
	AK111-3b	100.56	97.241	2.693	0.066	0.000	0.53	2.08	59.29	-	973
	AK111-3c_rim	100.68	97.165	2.784	0.007	0.044	0.53	2.09	587.36	31.61	972
	AK111-4a	95.00	87.478	12.522	0.000	0.000	0.58	0.76	-	-	875

Site	Sample	Total (Mass%)	Au (Norm%) LLD = 0.065%	Ag (Norm%) LLD = 0.035%	Hg (Norm%) LLD = 0.030%	Cu (Norm%) LLD = 0.017%	Au (Error%)	Ag (Error%)	Hg (Error%)	Cu (Error%)	Fineness
AK111	AK111-4b	95.79	87.476	12.519	0.000	0.005	0.58	0.77	-	291.11	875
	AK111-4c_rim	95.87	87.117	12.883	0.000	0.000	0.58	0.74	-	-	871
	AK111-5a	99.14	90.141	9.858	0.000	0.001	0.56	0.88	-	1069.59	901
	AK111-5b	102.24	89.825	10.119	0.056	0.000	0.55	0.83	67.66	-	899
	AK111-5c_rim	100.98	88.760	11.191	0.050	0.000	0.56	0.79	79.97	-	888
	AK111-6a	102.92	93.919	6.081	0.000	0.000	0.53	1.14	-	-	939
	AK111-6b	99.91	93.836	6.076	0.088	0.000	0.54	1.18	46.25	-	939
	AK111-6c_rim	101.88	94.284	5.716	0.000	0.000	0.53	1.22	-	-	943
	AK111-7a	100.62	93.392	6.608	0.000	0.000	0.54	1.13	-	-	934
	AK111-7b	98.57	93.486	6.503	0.000	0.011	0.55	1.17	-	130.10	935
	AK111-7c_rim	99.56	96.760	3.240	0.000	0.000	0.53	1.91	-	-	968
	AK111-8a	98.40	91.784	8.200	0.000	0.016	0.55	0.99	-	84.33	918
	AK111-8b	97.55	91.537	8.463	0.000	0.000	0.55	0.98	-	-	915
	AK111-8c_rim	96.99	91.642	8.358	0.000	0.000	0.56	0.98	-	-	916
	AK111-9a	98.84	92.544	7.456	0.000	0.000	0.55	1.07	-	-	925
	AK111-9b	100.52	92.339	7.661	0.000	0.000	0.54	1.02	-	-	923
	AK111-9c_rim	98.69	92.774	7.201	0.000	0.024	0.55	1.09	-	56.22	928
	AK111-10a	100.47	89.476	10.500	0.000	0.024	0.55	0.84	-	57.03	895
	AK111-10b	98.93	89.501	10.499	0.000	0.000	0.56	0.84	-	-	895
	AK111-10c_rim	96.60	90.073	9.927	0.000	0.000	0.56	0.87	-	-	901
	AK111-11a	100.87	89.579	10.354	0.066	0.000	0.55	0.85	61.20	-	896
	AK111-11b	98.48	98.301	1.693	0.000	0.006	0.53	3.22	-	234.72	983
	AK111-11c_rim	99.95	88.928	10.875	0.159	0.038	0.56	0.83	27.20	36.32	891
	AK111-12a	101.24	90.499	9.501	0.000	0.000	0.55	0.87	-	-	905
	AK111-12b	100.19	90.140	9.860	0.000	0.000	0.55	0.88	-	-	901
	AK111-12c_rim	97.90	90.239	9.699	0.000	0.062	0.56	0.89	-	22.73	903
	AK111-13a	97.70	84.123	15.833	0.031	0.013	0.58	0.66	133.17	107.71	842
	AK111-13b	98.80	84.640	15.360	0.000	0.000	0.58	0.68	-	-	846
	AK111-13c_rim	99.88	84.547	15.453	0.000	0.000	0.58	0.66	-	-	845
	AK111-14b	101.26	92.014	7.986	0.000	0.000	0.54	0.97	-	-	920
	AK111-14c_rim	100.30	94.516	5.450	0.000	0.034	0.54	1.22	-	40.69	945
	AK111-15a	101.53	93.328	6.631	0.040	0.000	0.54	1.11	96.26	-	934
	AK111-15b	95.37	92.218	7.752	0.000	0.030	0.56	1.09	-	48.24	922
	AK111-15c_rim	99.06	93.873	6.120	0.000	0.007	0.54	1.16	-	188.70	939
	AK111-16a	101.15	91.217	8.767	0.000	0.016	0.55	0.92	-	87.88	912
	AK111-16b	101.67	91.209	8.758	0.018	0.016	0.55	0.92	220.44	85.94	912
	AK111-16c	95.76	90.048	9.952	0.000	0.000	0.57	0.90	-	-	900
	AK111-16d_rim	99.72	91.428	8.572	0.000	0.000	0.55	0.96	-	-	914
	AK111-17b	100.32	94.892	5.101	0.000	0.007	0.53	1.33	-	191.81	949
	AK111-17c_rim	101.30	94.480	5.506	0.000	0.014	0.53	1.27	-	95.48	945
	AK111-18a	99.26	93.427	6.573	0.000	0.000	0.54	1.17	-	-	934
	AK111-18b	98.46	93.578	6.414	0.000	0.008	0.54	1.18	-	181.10	936
	AK111-18c_rim	102.23	93.932	6.068	0.000	0.000	0.53	1.17	-	-	939
	AK111-19a	100.61	90.037	9.963	0.000	0.000	0.55	0.87	-	-	900
	AK111-19c_rim	98.71	90.030	9.970	0.000	0.000	0.56	0.87	-	-	900
	AK111-19b	100.15	90.231	9.769	0.000	0.000	0.55	0.88	-	-	902
	AK111-20a	97.80	93.128	6.843	0.000	0.030	0.55	1.13	-	48.43	932
	AK111-20b	99.47	92.892	7.108	0.000	0.000	0.54	1.08	-	-	929
	AK111-20c_rim	98.73	97.578	2.422	0.000	0.000	0.53	2.42	-	-	976
AK121	AK121-1b	99.28	86.099	13.901	0.000	0.000	0.57	0.71	-	-	861
	AK121-1c_rim	98.74	85.802	14.198	0.000	0.000	0.57	0.71	-	-	858
	AK121-2a	96.77	88.893	11.087	0.000	0.021	0.57	0.84	-	67.77	889
	AK121-2c_rim	100.65	89.757	10.243	0.000	0.000	0.55	0.85	-	-	898
	AK121-3a	99.38	90.835	9.141	0.000	0.024	0.55	0.91	-	56.57	909
	AK121-3b	97.96	90.909	9.082	0.000	0.008	0.55	0.91	-	176.75	909
	AK121-4a	97.48	93.955	6.045	0.000	0.000	0.54	1.15	-	-	940
	AK121-4b	96.98	93.220	6.780	0.000	0.000	0.55	1.14	-	-	932
	AK121-4c_rim	97.63	93.361	6.598	0.000	0.041	0.55	1.14	-	34.04	934
	AK121-5a	98.54	94.616	5.349	0.003	0.031	0.54	1.25	1065.42	43.65	946
	AK121-5b	102.00	93.525	6.462	0.006	0.007	0.54	1.13	725.20	194.00	935
	AK121-5c_rim	95.92	93.090	6.814	0.096	0.000	0.55	1.14	45.51	-	932
	AK121-6b	100.15	89.833	10.167	0.000	0.000	0.55	0.85	-	-	898
	AK121-7a	100.47	88.988	10.769	0.243	0.000	0.55	0.81	17.11	-	892
	AK121-7a	98.10	92.073	7.927	0.000	0.000	0.55	1.07	-	-	921
	AK121-7c_rim	99.96	89.610	10.390	0.000	0.000	0.55	0.81	-	-	896
	AK121-8a	101.06	91.852	8.042	0.106	0.000	0.54	0.96	35.25	-	919
	AK121-8b	97.12	89.371	10.605	0.024	0.000	0.56	0.88	183.51	-	894
	AK121-8c	98.18	92.288	7.678	0.000	0.034	0.55	0.97	-	40.63	923
	AK121-8d	96.61	94.797	5.141	0.061	0.000	0.54	1.31	64.18	-	949
	AK121-9a	98.65	89.956	10.038	0.000	0.006	0.56	0.87	-	221.81	900
	AK121-9b	101.02	91.147	8.853	0.000	0.000	0.55	0.92	-	-	911
	AK121-9c	100.21	90.674	9.304	0.000	0.022	0.55	0.88	-	61.18	907
	AK121-10c_rim	98.09	85.991	13.858	0.151	0.000	0.57	0.71	26.92	-	861
	AK121-11a	100.78	91.478	8.502	0.020	0.000	0.54	0.92	187.80	-	915
	AK121-11b_rim	96.02	90.767	9.233	0.000	0.000	0.56	0.93	-	-	908

Site	Sample	Total (Mass%)	Au (Norm%) LLD = 0.065%	Ag (Norm%) LLD = 0.035%	Hg (Norm%) LLD = 0.030%	Cu (Norm%) LLD = 0.017%	Au (Error%)	Ag (Error%)	Hg (Error%)	Cu (Error%)	Fineness
AK121	AK121-11c	98.63	98.102	1.884	0.000	0.014	0.53	1.97	-	85.46	981
	AK121-12a	99.21	94.824	4.561	0.611	0.004	0.54	1.46	7.55	351.15	954
	AK121-12b	98.48	95.205	4.795	0.000	0.000	0.54	1.44	-	-	952
	AK121-13a	100.93	93.133	6.855	0.000	0.013	0.54	1.09	-	103.87	931
	AK121-13b	98.10	93.715	6.236	0.049	0.000	0.54	1.15	85.33	-	938
	AK121-13c_rim	98.98	71.100	3.963	24.928	0.009	0.62	1.60	0.59	154.47	947
	AK121-14a	101.02	93.737	6.241	0.000	0.022	0.54	1.11	-	61.32	938
	AK121-14c_rim	97.70	93.036	6.964	0.000	0.000	0.55	1.06	-	-	930
	AK121-15a	102.29	90.880	9.086	0.034	0.000	0.54	0.88	112.06	-	909
	AK121-15b	97.63	89.761	10.226	0.013	0.000	0.56	0.86	309.79	-	898
	AK121-15c	97.10	87.282	12.718	0.000	0.000	0.57	0.76	-	-	873
	AK121-16a	99.80	91.330	8.659	0.000	0.011	0.55	0.95	-	130.63	913
	AK121-16b	97.35	99.650	0.350	0.000	0.000	0.53	5.44	-	-	997
	AK121-16c	102.40	91.584	8.416	0.000	0.000	0.54	0.93	-	-	916
	AK121-17c_growth	96.23	75.589	6.080	18.331	0.000	0.61	1.23	0.72	-	926
	AK121-17a	100.93	94.839	5.147	0.000	0.014	0.53	1.19	-	93.64	949
	AK121-17c	99.84	93.981	5.681	0.339	0.000	0.54	1.17	11.17	-	943
	AK121-18a	99.61	93.272	6.728	0.000	0.000	0.54	1.10	-	-	933
	AK121-18b	100.44	93.231	6.769	0.000	0.000	0.54	1.14	-	-	932
	AK121-19a	96.31	91.754	8.244	0.000	0.002	0.56	0.96	-	692.58	918
	AK121-19b_rim	101.91	91.118	8.804	0.078	0.000	0.54	0.90	46.90	-	912
	AK121-19c	99.80	90.276	9.724	0.000	0.000	0.55	0.88	-	-	903
	AK121-20a	95.74	97.677	2.319	0.000	0.004	0.54	2.31	-	314.48	977
	AK121-20b	97.29	96.563	2.057	1.354	0.027	0.54	2.95	4.16	53.89	979
	AK121-20c	100.42	97.799	2.127	0.074	0.000	0.52	2.42	50.98	-	979
	AK121-21a	101.61	94.955	4.946	0.098	0.000	0.53	1.25	37.32	-	950
	AK121-21b	102.43	94.555	5.367	0.053	0.025	0.53	1.26	78.44	52.94	946
	AK121-21c	100.49	94.451	5.453	0.087	0.009	0.54	1.27	47.96	146.98	945
	AK121-22b	101.12	91.801	8.178	0.000	0.022	0.54	0.97	-	63.32	918
	AK121-22c_rim	95.17	90.850	9.092	0.058	0.000	0.56	0.92	76.37	-	909
	AK121-23b	96.60	89.635	10.365	0.000	0.000	0.56	0.87	-	-	896
	AK121-23c	96.75	90.282	9.718	0.000	0.000	0.56	0.88	-	-	903
	AK121-24a	99.74	87.801	12.198	0.000	0.001	0.56	0.77	-	1036.01	878
	AK121-24b	95.54	86.955	13.045	0.000	0.000	0.58	0.76	-	-	870
AK123	AK123-1a	102.20	91.367	8.633	0.000	0.000	0.54	0.93	-	-	914
	AK123-1b	99.49	91.205	8.763	0.000	0.032	0.55	0.95	-	43.41	912
	AK123-1c_rim	99.16	91.284	8.716	0.000	0.000	0.55	0.95	-	-	913
	AK123-2a	95.79	89.713	10.287	0.000	0.000	0.57	0.88	-	-	897
	AK123-2b	99.20	90.336	9.664	0.000	0.000	0.55	0.88	-	-	903
	AK123-2c_rim	99.73	90.020	9.980	0.000	0.000	0.55	0.87	-	-	900
	AK123-3a	100.11	92.140	7.739	0.056	0.066	0.54	1.01	69.90	20.89	923
	AK123-3b	97.88	91.700	8.300	0.000	0.000	0.55	1.00	-	-	917
	AK123-3c_rim	101.19	92.057	7.893	0.000	0.049	0.54	0.99	-	27.46	921
	AK123-4a	99.11	91.140	8.859	0.000	0.001	0.55	0.95	-	2348.12	911
	AK123-4b	98.97	91.132	8.860	0.000	0.008	0.55	0.94	-	169.92	911
	AK123-4c_rim	100.07	91.446	8.554	0.000	0.000	0.55	0.95	-	-	914
	AK123-5a	100.36	91.346	8.646	0.000	0.008	0.55	0.95	-	180.56	914
	AK123-5b	100.43	91.484	8.516	0.000	0.000	0.55	0.96	-	-	915
	AK123-5c_rim	96.46	91.035	8.950	0.000	0.016	0.56	0.96	-	90.00	910
	AK123-6a	98.59	87.783	12.210	0.000	0.007	0.57	0.77	-	202.35	878
	AK123-6b	97.00	87.527	12.473	0.000	0.000	0.57	0.78	-	-	875
	AK123-6c_rim	95.84	88.021	11.941	0.039	0.000	0.57	0.80	106.92	-	881
	AK123-7a	98.77	88.285	11.680	0.000	0.035	0.56	0.78	-	39.94	883
	AK123-7b	97.26	87.272	12.712	0.000	0.016	0.57	0.76	-	87.98	873
	AK123-7c_rim	97.50	87.802	12.198	0.000	0.000	0.57	0.77	-	-	878
	AK123-8a	97.39	83.690	16.310	0.000	0.000	0.58	0.65	-	-	837
	AK123-8b	98.63	82.380	17.620	0.000	0.000	0.59	0.62	-	-	824
	AK123-8c_rim	97.21	77.821	22.179	0.000	0.000	0.61	0.54	-	-	778
	AK123-9a	97.63	91.134	8.862	0.000	0.004	0.56	0.95	-	368.77	911
	AK123-9b	101.58	91.692	8.306	0.000	0.002	0.54	0.94	-	566.39	917
	AK123-9c_rim	99.46	91.399	8.579	0.000	0.022	0.55	0.96	-	61.75	914
	AK123-10a	99.26	90.816	9.184	0.000	0.000	0.55	0.92	-	-	908
	AK123-10b	98.97	90.746	9.244	0.010	0.000	0.55	0.91	401.34	-	908
	AK123-10c_rim	98.16	91.566	8.409	0.025	0.000	0.55	0.98	153.71	-	916
	AK123-12a	99.22	90.802	9.198	0.000	0.000	0.55	0.92	-	-	908
	AK123-12b	100.53	90.641	9.317	0.000	0.042	0.55	0.91	-	33.28	907
	AK123-12c_rim	99.23	91.079	8.921	0.000	0.000	0.55	0.93	-	-	911
	AK123-13a	101.65	92.983	7.014	0.000	0.004	0.54	1.08	-	69.99	930
	AK123-13b	96.31	92.652	7.348	0.000	0.000	0.55	1.10	-	-	927
	AK123-13c_rim	98.81	93.225	6.745	0.030	0.000	0.55	1.13	140.60	-	933
	AK123-14a	99.08	91.621	8.379	0.000	0.000	0.55	0.98	-	-	916
	AK123-14b	100.03	91.608	8.377	0.000	0.015	0.55	0.96	-	89.28	916
	AK123-14b	100.19	91.541	8.456	0.000	0.003	0.55	0.97	-	443.45	915
	AK123-14c_rim	100.08	91.549	8.451	0.000	0.000	0.55	0.96	-	-	915
	AK123-15a	97.10	86.357	13.624	0.000	0.019	0.58	0.73	-	78.59	864

Site	Sample	Total (Mass%)	Au (Norm%) LLD = 0.065%	Ag (Norm%) LLD = 0.035%	Hg (Norm%) LLD = 0.030%	Cu (Norm%) LLD = 0.017%	Au (Error%)	Ag (Error%)	Hg (Error%)	Cu (Error%)	Fineness
AK123	AK123-15b	100.71	86.674	13.302	0.025	0.000	0.56	0.72	162.85	-	867
	AK123-15c_rim	100.11	86.364	13.636	0.000	0.000	0.57	0.72	-	-	864
	AK123-16a	99.71	93.822	6.153	0.025	0.000	0.54	1.17	164.48	-	938
	AK123-16b	97.96	97.430	2.570	0.000	0.000	0.53	2.30	-	-	974
	AK123-16c	100.72	94.148	5.852	0.000	0.000	0.54	1.22	-	-	941
	AK123-17a	99.66	96.952	3.048	0.000	0.000	0.53	2.01	-	-	970
	AK123-17b	101.63	96.674	3.326	0.000	0.000	0.52	1.83	-	-	967
	AK123-17c_rim	98.69	97.024	2.976	0.000	0.000	0.53	2.04	-	-	970
	AK123-18c_rim	98.62	93.848	6.152	0.000	0.000	0.54	1.20	-	-	938
	AK123-18a	98.90	94.187	5.770	0.000	0.043	0.54	1.27	-	32.78	942
	AK123-18b	101.91	94.145	5.855	0.000	0.000	0.53	1.21	-	-	941
	AK123-19a	101.91	92.763	7.225	0.000	0.012	0.54	1.05	-	111.08	928
	AK123-19b	101.32	92.826	7.168	0.000	0.006	0.54	1.05	-	220.28	928
	AK123-19c_rim	98.59	93.050	6.926	0.000	0.024	0.55	1.08	-	56.87	931
	AK123-20a	96.84	93.927	6.068	0.000	0.005	0.55	1.25	-	299.22	939
	AK123-20b	102.90	94.020	5.963	0.000	0.017	0.53	1.19	-	77.90	940
	AK123-20c_rim	101.16	94.380	5.620	0.000	0.000	0.53	1.26	-	-	944
AUR-12-854	AUR-12-854-21a	100.29	84.378	15.622	0.000	0.000	0.57	0.66	-	-	844
	AUR-12-854-21b_rim	100.25	84.742	15.258	0.000	0.000	0.57	0.66	-	-	847
	AUR-12-854-21c	99.33	83.836	16.164	0.000	0.000	0.58	0.65	-	-	838
	AUR-12-854-21d_rim	100.73	83.868	16.132	0.000	0.000	0.57	0.64	-	-	839
	AUR-12-854-22a	99.98	95.410	4.354	0.074	0.162	0.53	1.53	59.06	8.71	956
	AUR-12-854-22b	98.16	95.130	4.580	0.206	0.084	0.54	1.50	21.16	17.20	954
	AUR-12-854-22c_rim	103.17	95.882	4.083	0.016	0.019	0.52	1.54	247.64	69.03	959
	AUR-12-854-23a	100.66	91.301	8.602	0.096	0.000	0.55	0.94	42.17	-	914
	AUR-12-854-23b	98.33	91.375	8.532	0.094	0.000	0.55	0.95	45.63	-	915
	AUR-12-854-23c	98.59	91.587	8.323	0.090	0.000	0.55	0.95	44.11	-	917
	AUR-12-854-23d_rim	99.61	91.608	8.295	0.097	0.000	0.55	0.96	43.29	-	917
	AUR-12-854-24a	99.22	91.190	8.810	0.000	0.000	0.55	0.96	-	-	912
	AUR-12-854-24b	97.65	92.035	7.908	0.052	0.005	0.55	0.99	72.33	266.81	921
	AUR-12-854-24c	101.14	92.716	7.249	0.005	0.030	0.54	1.01	778.37	45.60	927
	AUR-12-854-24d_rim	97.32	93.810	6.179	0.000	0.011	0.55	1.10	-	117.53	938
ADEM	ADEM-1d_rim	104.72	99.391	0.609	0.000	0.000	0.51	7.11	-	-	994
	ADEM-2a	102.10	91.764	8.218	0.000	0.019	0.54	0.96	-	71.68	918
	ADEM-2b	102.75	91.804	8.180	0.000	0.016	0.54	0.96	-	84.30	918
	ADEM-2c_rim	96.75	92.097	7.893	0.000	0.009	0.55	1.01	-	149.32	921
	ADEM-2d_rim	101.66	97.604	2.138	0.241	0.018	0.52	2.65	19.19	76.01	979
	ADEM-3a	101.67	90.170	9.804	0.014	0.012	0.55	0.87	293.05	109.23	902
	ADEM-3b	98.94	90.968	9.032	0.000	0.000	0.55	0.92	-	-	910
	ADEM-3c_rim	98.73	89.067	10.820	0.112	0.001	0.56	0.83	39.23	1515.97	892
	ADEM-4b	100.93	90.505	9.474	0.021	0.000	0.55	0.88	195.17	-	905
	ADEM-4c_rim	99.10	99.853	0.147	0.000	0.000	0.52	29.95	-	22001.27	999
	ADEM-5a	98.58	91.344	8.623	0.032	0.000	0.55	0.95	130.89	-	914
	ADEM-5b	98.98	91.185	8.750	0.066	0.000	0.55	0.94	64.95	-	912
	ADEM-5c_rim	99.92	98.313	1.687	0.000	0.000	0.52	3.12	-	-	983
	ADEM-6a	99.35	80.862	18.696	0.422	0.020	0.59	0.59	10.66	67.93	812
	ADEM-6b	97.33	81.126	18.497	0.374	0.003	0.59	0.60	11.79	465.58	814
	ADEM-6c_rim	99.30	99.201	0.790	0.000	0.009	0.52	6.10	-	156.64	992
	ADEM-7a	101.48	87.443	12.526	0.000	0.031	0.56	0.74	-	43.91	875
	ADEM-7b	99.86	87.253	12.735	0.000	0.012	0.56	0.74	-	118.33	873
	ADEM-7c_rim	100.28	87.366	12.629	0.005	0.000	0.56	0.74	797.00	-	874
	ADEM-8b	100.28	91.257	8.740	0.000	0.003	0.55	0.93	-	466.91	913
	ADEM-8c_rim	101.39	91.048	8.952	0.000	0.000	0.55	0.92	-	-	910
	ADEM-9a	102.51	90.198	9.797	0.000	0.005	0.54	0.88	-	304.61	902
	ADEM-9b	101.76	89.546	10.264	0.191	0.000	0.55	0.85	22.47	-	897
	ADEM-9c	101.16	90.160	9.772	0.055	0.013	0.55	0.88	78.48	105.34	902
	ADEM-11a	99.47	88.545	11.277	0.158	0.020	0.56	0.81	26.10	71.02	887
	ADEM-11b	96.91	89.591	10.353	0.056	0.000	0.56	0.88	80.62	87237.64	896
	ADEM-11c_rim	99.74	89.226	10.738	0.035	0.000	0.56	0.83	121.33	-	893
	ADEM-13a	100.50	87.706	12.260	0.000	0.034	0.56	0.76	-	40.25	877
	ADEM-13b_rim	97.65	93.077	6.870	0.000	0.053	0.55	1.01	-	25.03	931
	ADEM-13c	96.90	86.835	13.165	0.000	0.000	0.57	0.74	-	-	868
	ADEM-14a	100.73	91.305	8.679	0.007	0.009	0.55	0.93	548.66	153.34	913
	ADEM-14b_rim	101.45	99.533	0.467	0.000	0.000	0.52	8.70	-	-	995
	ADEM-14c	103.89	91.441	8.533	0.000	0.026	0.54	0.93	-	51.08	915
	ADEM-18a	100.99	90.988	8.912	0.100	0.000	0.55	0.92	41.15	-	911
	ADEM-18b	101.48	90.977	9.023	0.000	0.000	0.54	0.91	-	-	910
	ADEM-18c	101.35	90.648	9.341	0.000	0.011	0.55	0.91	-	124.62	907
	ADEM-18d_rim	100.48	90.506	9.432	0.063	0.000	0.55	0.90	68.64	-	906
RC4	RC4-1a	99.04	78.476	21.524	0.000	0.000	0.60	0.54	-	-	785
	RC4-1b	99.54	76.879	23.105	0.016	0.000	0.61	0.53	251.65	-	769
	RC4-1c	97.03	75.477	24.509	0.000	0.013	0.62	0.51	-	104.62	755
	RC4-3a	100.73	76.458	23.536	0.000	0.006	0.61	0.52	-	216.29	765
	RC4-3b	101.78	74.712	25.288	0.000	0.000	0.61	0.49	-	-	747

APPENDIX D

Filtered Major and Minor Element data for gold grains from the southern Seward Peninsula, Nome, Alaska

Site	Sample	Total (Mass%)	Au (Norm%) LLD = 0.065%	Ag (Norm%) LLD = 0.035%	Hg (Norm%) LLD = 0.030%	Cu (Norm%) LLD = 0.017%	Au (Error%)	Ag (Error%)	Hg (Error%)	Cu (Error%)	Fineness
AK015	AK015-1b	101.21	93.588	6.123	0.289	0.000	0.54	1.21	15.77	-	939
	AK015-5b	99.60	93.493	6.178	0.313	0.016	0.54	1.24	14.89	85.42	938
	AK015-10a	101.19	94.719	5.217	0.000	0.064	0.53	1.32	-	21.44	948
	AK015-12c	102.94	95.109	4.885	0.007	0.000	0.53	1.33	580.44	-	951
	AK015-13a	100.61	90.268	7.853	1.875	0.005	0.55	1.01	3.12	301.35	920
	AK015-17a	101.86	93.295	6.529	0.162	0.015	0.54	1.11	25.69	92.08	935
AK021	AK021-1b	96.46	81.078	18.915	0.000	0.007	0.60	0.60	-	201.61	811
	AK021-2b	100.60	83.322	16.677	0.000	0.001	0.58	0.63	-	1675.91	833
	AK021-3b	101.33	83.253	16.738	0.000	0.010	0.58	0.63	-	137.29	833
	AK021-4a	100.81	83.046	16.940	0.000	0.014	0.58	0.62	-	96.39	831
	AK021-5a	97.77	79.654	20.318	0.000	0.029	0.60	0.56	-	49.46	797
	AK021-6a	99.84	84.475	15.489	0.028	0.008	0.58	0.66	139.13	179.76	845
	AK021-7a	99.37	84.637	15.356	0.000	0.007	0.58	0.67	-	213.03	846
	AK021-8b	101.19	85.273	14.723	0.000	0.004	0.57	0.68	-	317.19	853
	AK021-9b	98.61	86.814	13.186	0.000	0.000	0.57	0.74	-	-	868
	AK021-10b	100.42	78.675	21.312	0.000	0.013	0.60	0.55	-	108.52	787
	AK021-12b	100.45	88.391	11.232	0.374	0.003	0.56	0.81	11.72	450.40	887
	AK021-13b	100.27	80.740	19.251	0.000	0.009	0.59	0.59	-	152.07	807
	AK021-14b	100.44	82.810	17.190	0.000	0.000	0.58	0.62	-	-	828
	AK021-15b	100.94	88.665	11.325	0.000	0.010	0.56	0.81	-	139.79	887
	AK021-16a	99.65	89.632	10.356	0.000	0.012	0.56	0.85	-	114.39	896
	AK021-17b	99.99	83.906	16.047	0.000	0.047	0.58	0.66	-	29.81	839
	AK021-18b	100.43	84.185	15.815	0.000	0.000	0.57	0.66	-	-	842
	AK021-19c	100.80	84.906	15.083	0.000	0.011	0.57	0.66	-	128.25	849
	AK021-20a	98.89	76.230	23.754	0.013	0.003	0.61	0.52	311.52	486.22	762
	AK021-21b	98.70	81.327	18.649	0.022	0.002	0.59	0.60	180.39	591.07	813
	AK021-22a	99.79	86.410	13.590	0.000	0.000	0.57	0.70	-	-	864
	AK021-23c	100.73	82.168	17.832	0.000	0.000	0.58	0.61	-	-	822
	AK021-24a	101.01	85.960	14.037	0.003	0.000	0.57	0.70	1275.50	-	860
	AK021-25a	98.10	80.756	19.221	0.022	0.000	0.60	0.59	181.17	-	808
	AK021-26a	100.52	84.495	15.505	0.000	0.000	0.57	0.66	-	-	845
	AK021-31a	99.46	81.004	18.996	0.000	0.000	0.59	0.59	-	-	810
	AK021-32b	99.65	83.124	16.876	0.000	0.000	0.58	0.62	-	-	831
	AK021-33a	101.99	88.332	11.646	0.000	0.022	0.55	0.79	-	64.15	884
	AK021-34c	100.50	83.735	16.234	0.000	0.031	0.58	0.65	-	43.92	838
	AK021-35b	100.67	82.298	17.688	0.000	0.014	0.58	0.61	-	98.84	823
	AK021-36b	101.07	81.254	18.736	0.000	0.010	0.58	0.60	-	142.48	813
	AK021-37c	100.85	82.801	17.177	0.000	0.022	0.58	0.62	-	63.06	828
	AK021-38a	101.55	92.445	7.519	0.000	0.036	0.54	1.05	-	38.27	925
	AK021-39b	101.81	86.659	13.341	0.000	0.000	0.56	0.71	-	-	867
	AK021-40a	101.07	85.255	14.695	0.000	0.049	0.57	0.68	-	27.38	853
AK028	AK028-1a	96.81	80.475	17.944	1.521	0.061	0.60	0.63	3.69	23.69	818
	AK028-2a	98.15	89.801	9.294	0.906	0.000	0.56	0.91	5.58	-	906
	AK028-3c	95.68	85.137	11.516	3.347	0.000	0.58	0.83	2.11	-	881
	AK028-4a	98.87	88.079	11.204	0.717	0.000	0.56	0.83	6.72	-	887
	AK028-5a	100.70	87.783	11.379	0.812	0.026	0.56	0.79	5.98	52.87	885
	AK028-6a	101.34	91.443	7.534	1.022	0.000	0.54	0.98	4.56	-	924
	AK028-9c	97.71	90.506	9.273	0.221	0.000	0.56	0.89	18.52	-	907
	AK028-10a	99.34	79.664	16.951	3.386	0.000	0.60	0.64	2.05	-	825
	AK028-11b	98.86	92.335	7.190	0.470	0.005	0.55	1.07	9.69	288.59	928
	AK028-12b	99.48	83.884	13.353	2.763	0.000	0.58	0.73	2.30	-	863
	AK028-13a	101.01	82.273	9.049	8.678	0.000	0.57	0.91	1.09	-	901
	AK028-14b	99.21	87.783	11.882	0.336	0.000	0.56	0.78	13.73	-	881
	AK028-15b	100.17	90.918	8.859	0.223	0.000	0.55	0.94	19.66	-	911
	AK028-16c	100.43	85.178	14.333	0.489	0.000	0.57	0.69	9.50	-	856
	AK028-17d	99.84	93.475	4.168	0.553	1.805	0.54	1.64	8.60	1.05	957
	AK028-18c	100.65	93.510	6.007	0.483	0.000	0.54	1.22	9.48	-	940
	AK028-19a	100.92	85.111	5.632	9.233	0.024	0.56	1.26	1.05	55.77	938
	AK028-20b	100.70	89.352	10.552	0.078	0.018	0.55	0.84	54.81	77.33	894
	AK028-21c	101.75	93.167	6.481	0.303	0.049	0.54	1.15	14.39	27.76	935
	AK028-22a	100.77	92.928	6.140	0.892	0.040	0.54	1.20	5.80	35.00	938
	AK028-23a	100.48	89.447	9.962	0.551	0.039	0.55	0.86	8.39	35.73	900

Site	Sample	Total (Mass%)	Au (Norm%) LLD = 0.065%	Ag (Norm%) LLD = 0.035%	Hg (Norm%) LLD = 0.030%	Cu (Norm%) LLD = 0.017%	Au (Error%)	Ag (Error%)	Hg (Error%)	Cu (Error%)	Fineness
AK032	AK032-1c	101.18	93.100	6.900	0.000	0.000	0.54	1.10	-	-	931
	AK032-2a	99.60	94.847	4.409	0.635	0.109	0.54	1.44	7.35	12.83	956
	AK032-7a	100.94	77.984	21.999	0.000	0.017	0.60	0.54	-	83.79	780
	AK032-8d	99.65	82.705	17.295	0.000	0.000	0.58	0.62	-	-	827
	AK032-9b	100.36	89.293	10.646	0.049	0.012	0.55	0.83	81.45	118.53	893
AK100	AK100-1b	103.18	94.466	5.534	0.000	0.000	0.53	1.21	-	-	945
	AK100-2c	99.33	81.323	18.673	0.000	0.004	0.59	0.59	-	372.82	813
	AK100-3a	100.46	92.267	7.710	0.000	0.023	0.54	1.00	-	58.20	923
	AK100-4c	99.06	95.498	4.499	0.000	0.003	0.54	1.48	-	479.54	955
	AK100-9b	99.62	80.593	19.407	0.000	0.000	0.59	0.57	-	-	806
	AK100-13b	99.33	97.759	2.235	0.006	0.000	0.53	2.53	696.93	-	978
	AK100-14b	97.54	77.363	22.618	0.000	0.019	0.61	0.53	-	71.87	774
	AK100-15b	100.31	90.315	9.657	0.000	0.028	0.55	0.88	-	48.37	903
	AK100-18b	100.43	95.682	4.311	0.000	0.007	0.53	1.49	-	201.56	957
	AK100-19c	101.14	93.275	6.546	0.179	0.000	0.54	1.10	22.53	-	934
AK111	AK111-1a	97.87	89.590	10.358	0.000	0.052	0.56	0.86	-	26.90	896
	AK111-2b	97.72	79.382	20.602	0.000	0.016	0.60	0.57	-	84.19	794
	AK111-3b	100.56	97.241	2.693	0.066	0.000	0.53	2.08	59.29	-	973
	AK111-4b	95.79	87.476	12.519	0.000	0.005	0.58	0.77	-	291.11	875
	AK111-5a	99.14	90.141	9.858	0.000	0.001	0.56	0.88	-	1069.59	901
	AK111-6b	99.91	93.836	6.076	0.088	0.000	0.54	1.18	46.25	-	939
	AK111-7a	100.62	93.392	6.608	0.000	0.000	0.54	1.13	-	-	934
	AK111-8a	98.40	91.784	8.200	0.000	0.016	0.55	0.99	-	84.33	918
	AK111-9b	100.52	92.339	7.661	0.000	0.000	0.54	1.02	-	-	923
	AK111-10a	100.47	89.476	10.500	0.000	0.024	0.55	0.84	-	57.03	895
	AK111-11a	100.87	89.579	10.354	0.066	0.000	0.55	0.85	61.20	-	896
	AK111-12b	100.19	90.140	9.860	0.000	0.000	0.55	0.88	-	-	901
	AK111-13b	98.80	84.640	15.360	0.000	0.000	0.58	0.68	-	-	846
	AK111-14b	101.26	92.014	7.986	0.000	0.000	0.54	0.97	-	-	920
	AK111-15a	101.53	93.328	6.631	0.040	0.000	0.54	1.11	96.26	-	934
	AK111-16b	101.67	91.209	8.758	0.018	0.016	0.55	0.92	220.44	85.94	912
	AK111-17b	100.32	94.892	5.101	0.000	0.007	0.53	1.33	-	191.81	949
	AK111-18a	99.26	93.427	6.573	0.000	0.000	0.54	1.17	-	-	934
	AK111-19b	100.15	90.231	9.769	0.000	0.000	0.55	0.88	-	-	902
	AK111-20b	99.47	92.892	7.108	0.000	0.000	0.54	1.08	-	-	929
AK121	AK121-1b	99.28	86.099	13.901	0.000	0.000	0.57	0.71	-	-	861
	AK121-2a	96.77	88.893	11.087	0.000	0.021	0.57	0.84	-	67.77	889
	AK121-3a	99.38	90.835	9.141	0.000	0.024	0.55	0.91	-	56.57	909
	AK121-4a	97.48	93.955	6.045	0.000	0.000	0.54	1.15	-	-	940
	AK121-5a	98.54	94.616	5.349	0.003	0.031	0.54	1.25	1065.42	43.65	946
	AK121-6b	100.15	89.833	10.167	0.000	0.000	0.55	0.85	-	-	898
	AK121-7a	100.47	88.988	10.769	0.243	0.000	0.55	0.81	17.11	-	892
	AK121-8a	101.06	91.852	8.042	0.106	0.000	0.54	0.96	35.25	-	919
	AK121-9c	100.21	90.674	9.304	0.000	0.022	0.55	0.88	-	61.18	907
	AK121-11a	100.78	91.478	8.502	0.020	0.000	0.54	0.92	187.80	-	915
	AK121-12a	99.21	94.824	4.561	0.611	0.004	0.54	1.46	7.55	351.15	954
	AK121-13a	100.93	93.133	6.855	0.000	0.013	0.54	1.09	-	103.87	931
	AK121-14a	101.02	93.737	6.241	0.000	0.022	0.54	1.11	-	61.32	938
	AK121-15a	102.29	90.880	9.086	0.034	0.000	0.54	0.88	112.06	-	909
	AK121-16a	99.80	91.330	8.659	0.000	0.011	0.55	0.95	-	130.63	913
	AK121-17c	99.84	93.981	5.681	0.339	0.000	0.54	1.17	11.17	-	943
	AK121-18a	99.61	93.272	6.728	0.000	0.000	0.54	1.10	-	-	933
	AK121-19c	99.80	90.276	9.724	0.000	0.000	0.55	0.88	-	-	903
	AK121-20c	100.42	97.799	2.127	0.074	0.000	0.52	2.42	50.98	-	979
	AK121-21c	100.49	94.451	5.453	0.087	0.009	0.54	1.27	47.96	146.98	945
	AK121-22b	101.12	91.801	8.178	0.000	0.022	0.54	0.97	-	63.32	918
	AK121-23c	96.75	90.282	9.718	0.000	0.000	0.56	0.88	-	-	903
	AK121-24a	99.74	87.801	12.198	0.000	0.001	0.56	0.77	-	1036.01	878

Site	Sample	Total (Mass%)	Au (Norm%) LLD = 0.065%	Ag (Norm%) LLD = 0.035%	Hg (Norm%) LLD = 0.030%	Cu (Norm%) LLD = 0.017%	Au (Error%)	Ag (Error%)	Hg (Error%)	Cu (Error%)	Fineness
AK123	AK123-1b	99.49	91.205	8.763	0.000	0.032	0.55	0.95	-	43.41	912
	AK123-2b	99.20	90.336	9.664	0.000	0.000	0.55	0.88	-	-	903
	AK123-3a	100.11	92.140	7.739	0.056	0.066	0.54	1.01	69.90	20.89	923
	AK123-4a	99.11	91.140	8.859	0.000	0.001	0.55	0.95	-	2348.12	911
	AK123-5a	100.36	91.346	8.646	0.000	0.008	0.55	0.95	-	180.56	914
	AK123-6a	98.59	87.783	12.210	0.000	0.007	0.57	0.77	-	202.35	878
	AK123-7a	98.77	88.285	11.680	0.000	0.035	0.56	0.78	-	39.94	883
	AK123-8b	98.63	82.380	17.620	0.000	0.000	0.59	0.62	-	-	824
	AK123-9b	101.58	91.692	8.306	0.000	0.002	0.54	0.94	-	566.39	917
	AK123-10a	99.26	90.816	9.184	0.000	0.000	0.55	0.92	-	-	908
	AK123-12b	100.53	90.641	9.317	0.000	0.042	0.55	0.91	-	33.28	907
	AK123-13a	101.65	92.983	7.014	0.000	0.004	0.54	1.08	-	69.99	930
	AK123-14a	99.08	91.621	8.379	0.000	0.000	0.55	0.98	-	-	916
	AK123-14b	100.03	91.608	8.377	0.000	0.015	0.55	0.96	-	89.28	916
	AK123-15b	100.71	86.674	13.302	0.025	0.000	0.56	0.72	162.85	-	867
	AK123-16a	99.71	93.822	6.153	0.025	0.000	0.54	1.17	164.48	-	938
	AK123-17a	99.66	96.952	3.048	0.000	0.000	0.53	2.01	-	-	970
	AK123-18a	98.90	94.187	5.770	0.000	0.043	0.54	1.27	-	32.78	942
	AK123-19a	101.91	92.763	7.225	0.000	0.012	0.54	1.05	-	111.08	928
	AK123-20b	102.90	94.020	5.963	0.000	0.017	0.53	1.19	-	77.90	940
AUR-12-854	AUR-12-854-21a	100.29	84.378	15.622	0.000	0.000	0.57	0.66	-	-	844
	AUR-12-854-22a	99.98	95.410	4.354	0.074	0.162	0.53	1.53	59.06	8.71	956
	AUR-12-854-23a	100.66	91.301	8.602	0.096	0.000	0.55	0.94	42.17	-	914
	AUR-12-854-24c	101.14	92.716	7.249	0.005	0.030	0.54	1.01	778.37	45.60	927
ADEM	ADEM-2a	102.10	91.764	8.218	0.000	0.019	0.54	0.96	-	71.68	918
	ADEM-3b	98.94	90.968	9.032	0.000	0.000	0.55	0.92	-	-	910
	ADEM-4b	100.93	90.505	9.474	0.021	0.000	0.55	0.88	195.17	-	905
	ADEM-5b	98.98	91.185	8.750	0.066	0.000	0.55	0.94	64.95	-	912
	ADEM-6a	99.35	80.862	18.696	0.422	0.020	0.59	0.59	10.66	67.93	812
	ADEM-7b	99.86	87.253	12.735	0.000	0.012	0.56	0.74	-	118.33	873
	ADEM-8b	100.28	91.257	8.740	0.000	0.003	0.55	0.93	-	466.91	913
	ADEM-9c	101.16	90.160	9.772	0.055	0.013	0.55	0.88	78.48	105.34	902
	ADEM-11a	99.47	88.545	11.277	0.158	0.020	0.56	0.81	26.10	71.02	887
	ADEM-13a	100.50	87.706	12.260	0.000	0.034	0.56	0.76	-	40.25	877
	ADEM-14a	100.73	91.305	8.679	0.007	0.009	0.55	0.93	548.66	153.34	913
	ADEM-18a	100.99	90.988	8.912	0.100	0.000	0.55	0.92	41.15	-	911
RC4	RC4-1a	99.04	78.476	21.524	0.000	0.000	0.60	0.54	-	-	785
	RC4-1b	99.54	76.879	23.105	0.016	0.000	0.61	0.53	251.65	-	769
	RC4-3a	100.73	76.458	23.536	0.000	0.006	0.61	0.52	-	216.29	765
	RC4-3b	101.78	74.712	25.288	0.000	0.000	0.61	0.49	-	-	747

Explanation:

Appendix D represents an extract of the full major and minor element dataset (Appendix C) as per the discussion text in Section 6.4. This table consists of data of 160 individual gold grain analyses from 11 sites across the southern Seward Peninsula (there is no geochemical data available for Site AK117).

"Sample" refers to the particular grain analysis selected to represent each grain (e.g. AK015-1b refers to the fact that the second analysis ("b") was selected to represent grain 1 from site AK015).

Total (Mass %) represents the summation of reported percentages for the four major and minor elements (Au, Ag, Hg and Cu) for an individual analysis.

Au (Norm%) refers to the normalised percentage (Total Mass % = 100%) for gold in an individual analysis. The same applies for Ag, Hg and Cu.

"LLD" refers to the "Lower Limit of Detection" and is the lowest value for which a particular element can be analysed with a degree of certainty (defined as error % < 100%).

"Error %" is the percentage analytical error in the result of an individual analysis.

"Fineness" is a value representing the normalised ratio of gold to silver of an individual analysis. It is calculated by [(Au Norm%) / (Au Norm% + Ag Norm%) X 1000].

APPENDIX E

Comparison between major and minor element core and rim chemistry of gold grains from the southern Seward Peninsula, Nome, Alaska

Site	Sample	Total (Mass%)	Au (Norm%) LLD = 0.065%	Ag (Norm%) LLD = 0.035%	Hg (Norm%) LLD = 0.030%	Cu (Norm%) LLD = 0.017%	Fineness	Au/Au	Ag/Ag	Hg/Hg	Cu/Cu	Fine/Fine
AK021	AK021-1b	96.46	81.078	18.915	0.001	0.007	811	-	-	-	-	-
	AK021-1c_rim	96.64	82.248	17.717	0.035	0.001	823	0.99	1.07	0.03	7.00	1.02
	AK021-2b	100.60	83.322	16.677	0.001	0.001	833	-	-	-	-	-
	AK021-2c_rim	101.34	83.086	16.914	0.001	0.001	831	1.00	0.99	1.00	1.00	1.00
	AK021-3b	101.33	83.253	16.738	0.001	0.010	833	-	-	-	-	-
	AK021-3c_rim	100.61	83.093	16.907	0.001	0.001	831	1.00	0.99	1.00	10.00	1.00
	AK021-4a	100.81	83.046	16.940	0.001	0.014	831	-	-	-	-	-
	AK021-4c_rim	98.25	82.026	17.974	0.001	0.001	820	1.01	0.94	1.00	14.00	0.98
	AK021-5a	97.77	79.654	20.318	0.001	0.029	797	-	-	-	-	-
	AK021-5c_rim	99.55	78.650	21.350	0.001	0.001	787	1.01	0.95	1.00	29.00	1.00
	AK021-6a	99.84	84.475	15.489	0.028	0.008	845	-	-	-	-	-
	AK021-6c_rim	98.24	83.660	16.333	0.001	0.007	837	1.01	0.95	28.00	1.14	1.00
	AK021-7a	99.37	84.637	15.356	0.001	0.007	846	-	-	-	-	-
	AK021-7c_rim	98.93	84.298	15.686	0.003	0.013	843	1.00	0.98	0.33	0.54	1.00
	AK021-10b	100.42	78.675	21.312	0.001	0.013	787	-	-	-	-	-
	AK021-10c_rim	99.51	76.051	23.949	0.001	0.001	761	1.03	0.89	1.00	13.00	0.98
	AK021-12b	100.45	88.391	11.232	0.374	0.003	887	-	-	-	-	-
	AK021-12c_rim	101.65	88.580	11.025	0.378	0.018	889	1.00	1.02	0.99	0.17	1.02
	AK021-13b	100.27	80.740	19.251	0.001	0.009	807	-	-	-	-	-
	AK021-13c_rim	98.50	81.767	18.233	0.001	0.001	818	0.99	1.06	1.00	9.00	1.00
	AK021-14b	100.44	82.810	17.190	0.001	0.001	828	-	-	-	-	-
	AK021-14c_rim	96.35	81.722	18.203	0.076	0.001	818	1.01	0.94	0.01	1.00	0.97
	AK021-15b	100.94	88.665	11.325	0.001	0.010	887	-	-	-	-	-
	AK021-15c_rim	101.47	87.803	12.197	0.001	0.001	878	1.01	0.93	1.00	10.00	1.00
	AK021-16a	99.65	89.632	10.356	0.001	0.012	896	-	-	-	-	-
	AK021-16b_rim	100.19	89.511	10.361	0.128	0.001	896	1.00	1.00	0.01	12.00	1.02
AK028	AK028_1a	96.81	80.475	17.944	1.521	0.061	818	-	-	-	-	-
	AK028_1c_rim	99.24	80.948	17.646	1.406	0.001	821	0.99	1.02	1.08	61.00	1.02
	AK028_4a	98.87	88.079	11.204	0.717	0.001	887	-	-	-	-	-
	AK028_4c_rim	98.53	91.766	7.668	0.558	0.008	923	0.96	1.46	1.28	0.13	1.02
	AK028_5a	100.70	87.783	11.379	0.812	0.026	885	-	-	-	-	-
	AK028_5c_rim	103.68	88.991	10.444	0.564	0.001	895	0.99	1.09	1.44	26.00	1.02
	AK028_6a	101.34	91.443	7.534	1.022	0.001	924	-	-	-	-	-
	AK028_6c_rim	99.37	88.263	10.004	1.723	0.010	898	1.04	0.75	0.59	0.10	0.96
	AK028_9c	97.71	90.506	9.273	0.221	0.001	907	-	-	-	-	-
	AK028_9b_rim	99.64	93.212	6.631	0.158	0.001	934	0.97	1.40	1.40	1.00	1.04
	AK028_10a	99.34	79.664	16.951	3.386	0.001	825	-	-	-	-	-
	AK028_10c_rim	100.89	77.532	15.951	6.517	0.001	829	1.03	1.06	0.52	1.00	1.00
	AK028-11b	98.86	92.335	7.190	0.470	0.005	928	-	-	-	-	-
	AK028-11d_rim	99.59	90.334	7.139	2.522	0.004	927	1.02	1.01	0.19	1.25	1.00
	AK028-12b	99.48	83.884	13.353	2.763	0.001	863	-	-	-	-	-
	AK028-12c_rim	98.93	85.591	11.204	3.199	0.005	884	0.98	1.19	0.86	0.20	1.02
	AK028-13a	101.01	82.273	9.049	8.678	0.001	901	-	-	-	-	-
	AK028-13c_rim	97.24	83.514	9.397	7.089	0.001	899	0.99	0.96	1.22	1.00	0.98
	AK028-14b	99.21	87.783	11.882	0.336	0.001	881	-	-	-	-	-
	AK028-14c_rim	98.96	87.943	10.996	1.056	0.005	889	1.00	1.08	0.32	0.20	1.00
	AK028-15b	100.17	90.918	8.859	0.223	0.001	911	-	-	-	-	-
	AK028-15c_rim	100.53	90.407	9.372	0.221	0.001	906	1.01	0.95	1.01	1.00	1.00
	AK028-19a	100.92	85.111	5.632	9.233	0.024	938	-	-	-	-	-
	AK028-19c_rim	96.42	89.745	4.998	5.257	0.001	947	0.95	1.13	1.76	24.00	1.00
	AK028-21c	101.75	93.167	6.481	0.303	0.049	935	-	-	-	-	-
	AK028-21e_rim	101.00	92.816	6.796	0.373	0.014	932	1.00	0.95	0.81	3.50	1.00
	AK028-22a	100.77	92.928	6.140	0.892	0.040	938	-	-	-	-	-
	AK028-22c_rim	102.77	95.592	3.866	0.542	0.001	961	0.97	1.59	1.65	40.00	1.02
	AK028-23a	100.48	89.447	9.962	0.551	0.039	900	-	-	-	-	-
	AK028-23e_rim	101.09	88.939	10.444	0.608	0.009	895	1.01	0.95	0.91	4.33	1.00
AK032	AK032-7a	100.94	77.984	21.999	0.001	0.017	780	-	-	-	-	-
	AK032-7c_rim	99.45	78.248	21.752	0.001	0.001	782	1.00	1.01	1.00	17.00	1.00
	AK032-8d	99.65	82.705	17.295	0.001	0.001	827	-	-	-	-	-
	AK032-8c_rim	100.21	83.037	16.959	0.001	0.004	830	1.00	1.02	1.00	0.25	1.00
	AK032-9b	100.36	89.293	10.646	0.049	0.012	893	-	-	-	-	-
	AK032-9c_rim	100.07	89.139	10.601	0.260	0.001	894	1.00	1.00	0.19	12.00	0.98

Site	Sample	Total (Mass%)	Au (Norm%) LLD = 0.065%	Ag (Norm%) LLD = 0.035%	Hg (Norm%) LLD = 0.030%	Cu (Norm%) LLD = 0.017%	Fineness	Au/Au	Ag/Ag	Hg/Hg	Cu/Cu	Fine/Fine
AK111	AK111-1a	97.87	89.590	10.358	0.001	0.052	896	-	-	-	-	-
	AK111-1c_rim	95.83	89.227	10.769	0.003	0.001	892	1.00	0.96	0.33	52.00	0.98
	AK111-2b	97.72	79.382	20.602	0.001	0.016	794	-	-	-	-	-
	AK111-2c_rim	96.69	79.532	20.370	0.094	0.004	796	1.00	1.01	0.01	4.00	0.98
	AK111-3b	100.56	97.241	2.693	0.066	0.001	973	-	-	-	-	-
	AK111-3c_rim	100.68	97.165	2.784	0.007	0.044	972	1.00	0.97	9.43	0.02	1.00
	AK111-4b	95.79	87.476	12.519	0.001	0.005	875	-	-	-	-	-
	AK111-4c_rim	95.87	87.117	12.883	0.001	0.001	871	1.00	0.97	1.00	5.00	1.00
	AK111-5a	99.14	90.141	9.858	0.001	0.001	901	-	-	-	-	-
	AK111-5c_rim	100.98	88.760	11.191	0.050	0.001	888	1.02	0.88	0.02	1.00	1.00
	AK111-6b	99.91	93.836	6.076	0.088	0.001	939	-	-	-	-	-
	AK111-6c_rim	101.88	94.284	5.716	0.001	0.001	943	1.00	1.06	88.00	1.00	1.02
	AK111-7a	100.62	93.392	6.608	0.001	0.001	934	-	-	-	-	-
	AK111-7c_rim	99.56	96.760	3.240	0.001	0.001	968	0.97	2.04	1.00	1.00	1.02
	AK111-8a	98.40	91.784	8.200	0.001	0.016	918	-	-	-	-	-
	AK111-8c_rim	96.99	91.642	8.358	0.001	0.001	916	1.00	0.98	1.00	16.00	0.98
	AK111-9b	100.52	92.339	7.661	0.001	0.001	923	-	-	-	-	-
	AK111-9c_rim	98.69	92.774	7.201	0.001	0.024	928	1.00	1.06	1.00	0.04	0.98
	AK111-10a	100.47	89.476	10.500	0.001	0.024	895	-	-	-	-	-
	AK111-10c_rim	96.60	90.073	9.927	0.001	0.001	901	0.99	1.06	1.00	24.00	0.98
	AK111-11a	100.87	89.579	10.354	0.066	0.001	896	-	-	-	-	-
	AK111-11c_rim	99.95	88.928	10.875	0.159	0.038	891	1.01	0.95	0.42	0.03	0.98
	AK111-12b	100.19	90.140	9.860	0.001	0.001	901	-	-	-	-	-
	AK111-12c_rim	97.90	90.239	9.699	0.001	0.062	903	1.00	1.02	1.00	0.02	0.98
	AK111-13b	98.80	84.640	15.360	0.001	0.001	846	-	-	-	-	-
	AK111-13c_rim	99.88	84.547	15.453	0.001	0.001	845	1.00	0.99	1.00	1.00	1.00
	AK111-14b	101.26	92.014	7.986	0.001	0.001	920	-	-	-	-	-
	AK111-14c_rim	100.30	94.516	5.450	0.001	0.034	945	0.97	1.47	1.00	0.03	1.00
	AK111-15a	101.53	93.328	6.631	0.040	0.001	934	-	-	-	-	-
	AK111-15c_rim	99.06	93.873	6.120	0.001	0.007	939	0.99	1.08	40.00	0.14	1.00
	AK111-16b	101.67	91.209	8.758	0.018	0.016	912	-	-	-	-	-
	AK111-16d_rim	99.72	91.428	8.572	0.001	0.001	914	1.00	1.02	18.00	16.00	1.00
	AK111-17b	100.32	94.892	5.101	0.001	0.007	949	-	-	-	-	-
	AK111-17c_rim	101.30	94.480	5.506	0.001	0.014	945	1.00	0.93	1.00	0.50	1.00
	AK111-18a	99.26	93.427	6.573	0.001	0.001	934	-	-	-	-	-
	AK111-18c_rim	102.23	93.932	6.068	0.001	0.001	939	0.99	1.08	1.00	1.00	1.02
	AK111-19b	100.15	90.231	9.769	0.001	0.001	902	-	-	-	-	-
	AK111-19c_rim	98.71	90.030	9.970	0.001	0.001	900	1.00	0.98	1.00	1.00	0.98
	AK111-20b	99.47	92.892	7.108	0.001	0.001	929	-	-	-	-	-
	AK111-20c_rim	98.73	97.578	2.422	0.001	0.001	976	0.95	2.93	1.00	1.00	1.02
AK121	AK121-1b	99.28	86.099	13.901	0.001	0.001	861	-	-	-	-	-
	AK121-1c_rim	98.74	85.802	14.198	0.001	0.001	858	1.00	0.98	1.00	1.00	1.00
	AK121-22b	101.12	91.801	8.178	0.001	0.022	918	-	-	-	-	-
	AK121-22c_rim	95.17	90.850	9.092	0.058	0.001	909	1.01	0.90	0.02	22.00	0.96
	AK121-2a	96.77	88.893	11.087	0.001	0.021	889	-	-	-	-	-
	AK121-2c_rim	100.65	89.757	10.243	0.001	0.001	898	0.99	1.08	1.00	21.00	1.04
	AK121-4a	97.48	93.955	6.045	0.001	0.001	940	-	-	-	-	-
	AK121-4c_rim	97.63	93.361	6.598	0.001	0.041	934	1.01	0.92	1.00	0.02	0.98
	AK121-5a	98.54	94.616	5.349	0.003	0.031	946	-	-	-	-	-
	AK121-5c_rim	95.92	93.090	6.814	0.096	0.001	932	1.02	0.79	0.03	31.00	0.98
	AK121-7a	100.47	88.988	10.769	0.243	0.001	892	-	-	-	-	-
	AK121-7c_rim	99.96	89.610	10.390	0.001	0.001	896	0.99	1.04	243.00	1.00	1.00
	AK121-11a	100.78	91.478	8.502	0.020	0.001	915	-	-	-	-	-
	AK121-11b_rim	96.02	90.767	9.233	0.001	0.001	908	1.01	0.92	20.00	1.00	0.96
	AK121-13a	100.93	93.133	6.855	0.001	0.013	931	-	-	-	-	-
	AK121-13c_rim	98.98	71.100	3.963	24.928	0.009	947	1.31	1.73	0.00	1.44	0.87
	AK121-14a	101.02	93.737	6.241	0.001	0.022	938	-	-	-	-	-
	AK121-14c_rim	97.70	93.036	6.964	0.001	0.001	930	1.01	0.90	1.00	22.00	0.98
	AK121-17c	99.84	93.981	5.681	0.339	0.001	943	-	-	-	-	-
	AK121-17c_growth	96.23	75.589	6.080	18.331	0.001	926	1.24	0.93	0.02	1.00	0.89
	AK121-19c	99.80	90.276	9.724	0.001	0.001	903	-	-	-	-	-
	AK121-19b_rim	101.91	91.118	8.804	0.078	0.001	912	0.99	1.10	0.01	1.00	1.02

Site	Sample	Total (Mass%)	Au (Norm%) LLD = 0.065%	Ag (Norm%) LLD = 0.035%	Hg (Norm%) LLD = 0.030%	Cu (Norm%) LLD = 0.017%	Fineness	Au/Au	Ag/Ag	Hg/Hg	Cu/Cu	Fine/Fine
AK123	AK123-1b	99.49	91.205	8.763	0.001	0.032	912	-	-	-	-	-
	AK123-1c_rim	99.16	91.284	8.716	0.001	0.001	913	1.00	1.01	1.00	32.00	1.00
	AK123-2b	99.20	90.336	9.664	0.001	0.001	903	-	-	-	-	-
	AK123-2c_rim	99.73	90.020	9.980	0.001	0.001	900	1.00	0.97	1.00	1.00	1.00
	AK123-3a	100.11	92.140	7.739	0.056	0.066	923	-	-	-	-	-
	AK123-3c_rim	101.19	92.057	7.893	0.001	0.049	921	1.00	0.98	56.00	1.35	1.00
	AK123-4a	99.11	91.140	8.859	0.001	0.001	911	-	-	-	-	-
	AK123-4c_rim	100.07	91.446	8.554	0.001	0.001	914	1.00	1.04	1.00	1.00	1.00
	AK123-5a	100.36	91.346	8.646	0.001	0.008	914	-	-	-	-	-
	AK123-5c_rim	96.46	91.035	8.950	0.001	0.016	910	1.00	0.97	1.00	0.50	0.98
	AK123-6a	98.59	87.783	12.210	0.001	0.007	878	-	-	-	-	-
	AK123-6c_rim	95.84	88.021	11.941	0.039	0.001	881	1.00	1.02	0.03	7.00	1.00
	AK123-7a	98.77	88.285	11.680	0.001	0.035	883	-	-	-	-	-
	AK123-7c_rim	97.50	87.802	12.198	0.001	0.001	878	1.01	0.96	1.00	35.00	0.98
	AK123-8b	98.63	82.380	17.620	0.001	0.001	824	-	-	-	-	-
	AK123-8c_rim	97.21	77.821	22.179	0.001	0.001	778	1.06	0.79	1.00	1.00	0.97
	AK123-9b	101.58	91.692	8.306	0.001	0.002	917	-	-	-	-	-
	AK123-9c_rim	99.46	91.399	8.579	0.001	0.022	914	1.00	0.97	1.00	0.09	0.98
	AK123-10a	99.26	90.816	9.184	0.001	0.001	908	-	-	-	-	-
	AK123-10c_rim	98.16	91.566	8.409	0.025	0.001	916	0.99	1.09	0.04	1.00	1.00
	AK123-12b	100.53	90.641	9.317	0.001	0.042	907	-	-	-	-	-
	AK123-12c_rim	99.23	91.079	8.921	0.001	0.001	911	1.00	1.04	1.00	42.00	1.00
	AK123-13a	101.65	92.983	7.014	0.001	0.004	930	-	-	-	-	-
	AK123-13c_rim	98.81	93.225	6.745	0.030	0.001	933	1.00	1.04	0.03	4.00	0.98
	AK123-14b	100.03	91.608	8.377	0.001	0.015	916	-	-	-	-	-
	AK123-14c_rim	100.08	91.549	8.451	0.001	0.001	915	1.00	0.99	1.00	15.00	1.00
	AK123-15b	100.71	86.674	13.302	0.025	0.001	867	-	-	-	-	-
	AK123-15c_rim	100.11	86.364	13.636	0.001	0.001	864	1.00	0.98	25.00	1.00	0.98
	AK123-17a	99.66	96.952	3.048	0.001	0.001	970	-	-	-	-	-
	AK123-17c_rim	98.69	97.024	2.976	0.001	0.001	970	1.00	1.02	1.00	1.00	1.00
	AK123-18a	98.90	94.187	5.770	0.001	0.043	942	-	-	-	-	-
	AK123-18c_rim	98.62	93.848	6.152	0.001	0.001	938	1.00	0.94	1.00	43.00	1.00
	AK123-19a	101.91	92.763	7.225	0.001	0.012	928	-	-	-	-	-
	AK123-19c_rim	98.59	93.050	6.926	0.001	0.024	931	1.00	1.04	1.00	0.50	0.98
	AK123-20b	102.90	94.020	5.963	0.001	0.017	940	-	-	-	-	-
	AK123-20c_rim	101.16	94.380	5.620	0.001	0.001	944	1.00	1.06	1.00	17.00	1.00
AUR-12-854	AUR-12-854-21a	100.29	84.378	15.622	0.001	0.001	844	-	-	-	-	-
	AUR-12-854-21b_rim	100.25	84.742	15.258	0.001	0.001	847	1.00	1.02	1.00	1.00	1.00
	AUR-12-854-22a	99.98	95.410	4.354	0.074	0.162	956	-	-	-	-	-
	AUR-12-854-22c_rim	103.17	95.882	4.083	0.016	0.019	959	1.00	1.07	4.63	8.53	1.02
	AUR-12-854-23a	100.66	91.301	8.602	0.096	0.001	914	-	-	-	-	-
	AUR-12-854-23d_rim	99.61	91.608	8.295	0.097	0.001	917	1.00	1.04	0.99	1.00	1.00
	AUR-12-854-24c	101.14	92.716	7.249	0.005	0.030	927	-	-	-	-	-
	AUR-12-854-24d_rim	97.32	93.810	6.179	0.001	0.011	938	0.99	1.17	5.00	2.73	0.98
ADEM	ADEM-2a	102.10	91.764	8.218	0.001	0.019	918	-	-	-	-	-
	ADEM-2d_rim	101.66	97.604	2.138	0.241	0.018	979	0.94	3.84	0.00	1.06	1.04
	ADEM-3b	98.94	90.968	9.032	0.001	0.001	910	-	-	-	-	-
	ADEM-3c_rim	98.73	89.067	10.820	0.112	0.001	892	1.02	0.83	0.01	1.00	0.98
	ADEM-4b	100.93	90.505	9.474	0.021	0.001	905	-	-	-	-	-
	ADEM-4c_rim	99.10	99.853	0.147	0.001	0.001	999	0.91	64.45	21.00	1.00	1.06
	ADEM-5b	98.98	91.185	8.750	0.066	0.001	912	-	-	-	-	-
	ADEM-5c_rim	99.92	98.313	1.687	0.001	0.001	983	0.93	5.19	66.00	1.00	1.06
	ADEM-6a	99.35	80.862	18.696	0.422	0.020	812	-	-	-	-	-
	ADEM-6c_rim	99.30	99.201	0.790	0.001	0.009	992	0.82	23.67	422.00	2.22	1.13
	ADEM-7b	99.86	87.253	12.735	0.001	0.012	873	-	-	-	-	-
	ADEM-7c_rim	100.28	87.366	12.629	0.005	0.001	874	1.00	1.01	0.20	12.00	1.00
	ADEM-8b	100.28	91.257	8.740	0.001	0.003	913	-	-	-	-	-
	ADEM-8c_rim	101.39	91.048	8.952	0.001	0.001	910	1.00	0.98	1.00	3.00	1.00
	ADEM-11a	99.47	88.545	11.277	0.158	0.020	887	-	-	-	-	-
	ADEM-11c_rim	99.74	89.226	10.738	0.035	0.001	893	0.99	1.05	4.51	20.00	1.00
	ADEM-13a	100.50	87.706	12.260	0.001	0.034	877	-	-	-	-	-
	ADEM-13b_rim	97.65	93.077	6.870	0.001	0.053	931	0.94	1.78	1.00	0.64	1.02
	ADEM-14a	100.73	91.305	8.679	0.007	0.009	913	-	-	-	-	-
	ADEM-14b_rim	101.45	99.533	0.467	0.001	0.001	995	0.92	18.58	7.00	9.00	1.06
	ADEM-18a	100.99	90.988	8.912	0.100	0.001	911	-	-	-	-	-
	ADEM-18d_rim	100.48	90.506	9.432	0.063	0.001	906	1.01	0.94	1.59	1.00	1.00

Explanation:

Appendix E represents an extract of the full major and minor element dataset (Appendix C) as per the discussion text in Section 6.4.2. This table consists of data of 195 individual gold grain analyses from 8 sites across the southern Seward Peninsula.

"Sample" refers to the particular grain analysis selected to represent each grain (e.g. AK015-1b refers to the fact that the second analysis ("b") was selected to represent grain 1 from site AK015). The suffix "_rim" refers to an analysis taken within 10µm of the edge of a polished grain.

Total (Mass %) represents the summation of reported percentages for the four major and minor elements (Au, Ag, Hg and Cu) for an individual analysis.

Au (Norm%) refers to the normalised percentage (Total Mass % = 100%) for gold in an individual analysis. The same applies for Ag, Hg and Cu. For Hg and Cu in **Error! Reference source not found.** only, values of 0.000% have been changed to 0.001% to prevent dividing by zero in calculations.

"LLD" refers to the "Lower Limit of Detection" and is the lowest value for which a particular element can be analysed with a degree of certainty (defined as error % < 100%).

"Fineness" is a value representing the normalised ratio of gold to silver of an individual analysis. It is calculated by [(Au Norm%) / (Au Norm% + Ag Norm%) X 1000].

[Au/Au] (similarly for [Ag/Ag], [Hg/Hg] and [Cu/Cu]) refers to the ratio of the core/rim percentage of the particular element being assessed. For a particular element, values >1 indicate rim depletion relative to the core whereas values <1 indicate rim is enrichment relative to the core.

APPENDIX F

Trace Element data of gold grains from the southern Seward Peninsula, Nome, Alaska

Site	Sample ID	Cu (Mass%) LLD = 0.003	Te (Mass%) LLD = 0.003	Hg (Mass%) LLD = 0.004	W (Mass%) LLD = 0.008	As (Mass%) LLD = 0.004	Sb (Mass%) LLD = 0.002	Cu (Error%)	Te (Error%)	Hg (Error%)	W (Error%)	As (Error%)	Sb (Error%)
AK015	AK015-1a	0.004	0.002	0.282	0	0	0	67	238.19	2.73	100	100	100
	AK015-1b	0.001	0.009	0.326	0	0	0	339.82	52.35	2.39	100	100	100
	AK015-5a	0	0	0	0	0	0	100	100	100	100	100	100
	AK015-5b	0.014	0.009	0.1	0	0.002	0	21.24	51.56	7.85	100	247.02	100
	AK015-10a	0.036	0	0	0	0.002	0	10.11	100	100	100	430.1	100
	AK015-10b	0	0	0	0	0.004	0	100	100	100	100	67.28	100
AK021	AK021-1a	0	0.007	0	0	0.033	0	2489.73	59.2	100	100	10.3	100
	AK021-2a	0	0.011	0	0	0	0	100	34.69	100	100	100	100
	AK021-3	0	0	0	0	0.017	0	100	100	100	100	16.51	100
	AK021-4	0	0.015	0	0	0.006	0	100	25.96	100	100	86.29	100
	AK021-5	0	0.021	0	0	0	0	100	17.96	100	100	100	100
	AK021-6	0.011	0.015	0	0	0	0	30.43	25.57	100	100	1160000	100
	AK021-7	0.002	0	0	0	0	0	208.09	100	100	100	100	100
	AK021-8	0	0.02	0	0	0.993	0	100	21.54	100	100	0.32	100
	AK021-9	0	0.02	0	0	0	0	100	19.14	100	100	100	100
	AK021-10	0	0.015	0	0	0	0	100	23.84	100	100	100	100
	AK021-12a	0	0.007	0.177	0	0	0	100	60.91	4.22	100	100	100
	AK021-12b	0	0.011	0.096	0	0.032	0	100	39.39	8.43	100	10.37	100
	AK021-13a	0	0.013	0	0	0	0	100	27.68	100	100	100	100
	AK021-14	0	0.007	0	0	0.018	0	100	57.22	100	100	20.85	100
	AK021-15	0	0.008	0	0	0	0	100	46.75	100	100	100	100
	AK021-16	0.001	0	0	0	0.016	0	556.69	14196.5	100	100	18.77	100
	AK021-16b	0.002	0	0	0	0	0	200.53	100	100	100	100	100
	AK021-17	0.004	0.009	0	0	0	0.04	71.02	41.5	100	100	322.12	5.14
	AK021-18	0.014	0	0	0	0.005	0	25.16	100	100	100	115.93	100
	AK021-19	0	0.011	0	0	0	0	100	32.62	100	100	100	100
	AK021-20	0	0.015	0	0	0	0	100	24.96	100	100	100	100
	AK021-21	0	0.004	0	0	0	0	100	88.61	100	100	100	100
	AK021-22	0	0.019	0	0	0	0	100	19.38	100	100	100	100
	AK021-23	0	0.007	0	0	0.013	0	100	54.76	100	100	30.9	100
	AK021-24	0	0	0	0	0	0	100	100	100	100	100	100
	AK021-25	0	0.011	0	0	0	0	100	32.44	100	100	100	100
	AK021-26	0	0.008	0	0	0.012	0	100	52.39	100	100	31.58	100
	AK021-31	0	0.016	0	0	0.003	0	100	25.07	100	100	148.64	100
	AK021-32	0	0	0	0	0	0	100	100	100	100	100	100
	AK021-33	0	0.008	0	0	0.002	0	100	47.26	100	100	251.98	100
	AK021-34	0	0.008	0	0	0	0	100	45.25	100	100	100	100
	AK021-35	0	0.003	0	0	0.01	0	100	134.55	100	100	33.05	100
	AK021-36	0	0.006	0	0	0	0	100	61.63	100	100	100	100
	AK021-37	0	0.016	0	0	0	0	100	22.54	100	100	100	100
	AK021-38	0	0.006	0	0	0	0	100	63.11	100	100	100	100
	AK021-39	0	0.015	0	0	0.007	0	100	26.31	100	106000	63.87	100
	AK021-40	0	0	0.004	0	0	0	100	100	148.68	100	100	100
AK028	AK028-1	0	0.004	0.932	0	0	0.001	100	119.21	0.95	100	100	308.07
	AK028-2	0	0	0.603	0	0	0	100	100	1.36	100	100	100
	AK028-3	0.002	0.01	1.604	0	0	0	160.05	43.16	0.62	100	100	100
	AK028-4	0	0.026	0.613	0	0	0	100	17.86	1.36	100	100	100
	AK028-5	0.006	0	0.583	0	0	0	44.02	100	1.4	100	100	100
	AK028-5b	0	0.005	0.473	0	0	0	100	98.15	1.72	100	100	100
	AK028-6	0	0.011	0.603	0	0	0	1084.02	41.24	1.38	100	100	100
	AK028-9	0.011	0.007	0.064	0	0.002	0	25.8	62.05	12	100	185.77	100
	AK028-10	0	0	4.29	0	0	0	100	1840.16	0.32	100	100	100
	AK028-10b	0.004	0.002	3.898	0	0	0	69.64	203.59	0.34	100	100	100
	AK028-11c	0.01	0	0	0	0	0	36.79	100	100	100	100	100
	AK028-12b	0	0	1.693	0	0	0	2126.12	100	0.6	100	100	100
	AK028-13a	0	0.015	6.031	0	0	0	100	30.11	0.26	100	100	100
	AK028-14b	0	0.014	0.187	0	0	0	100	30.05	3.87	100	100	100
	AK028-15a	0.016	0.005	0.045	0.004	0	0.001	18.72	89.2	17.72	137.32	100	186.55
	AK028-16b	0.007	0.009	0.106	0.008	0	0.003	41.02	49.4	7.43	61.55	100	88.34
	AK028-17c	2.162	0	0.446	0.003	0	0.002	0.22	100	2.45	215.69	100	146.32
	AK028-17d	2.176	0	0.514	0	0	0	0.21	100	2.08	100	100	100
	AK028-18c	0.054	0.004	0.226	0	0	0	5.53	114.29	3.6	100	100	100
	AK028-19a	0	0	6.301	0	0	0	100	100	0.25	100	100	716.96
	AK028-21	0.01	0.013	0.166	0	0.005	0	28.22	34.34	4.62	100	74.61	100
	AK028-22a	0.04	0.009	0.168	0	0	0	7.5	49	4.7	100	100	100
	AK028-22b	0.066	0.012	0.065	0	0	0	4.92	38.72	13.43	100	100	100
	AK028-23	0	0	0.324	0	0.006	0	100	1176.45	2.4	100	48.52	100
	AK028-24a	0.037	0.006	0.337	0	0.001	0	7.85	78.92	2.38	100	626.14	100
	AK028-24b	0.029	0.014	0.324	0.001	0	0	9.77	31.91	2.39	1231.71	100	100
	AK028-24c	0	0.004	0.321	0	0	0	100	113.28	2.38	100	100	100

Site	Sample ID	Cu (Mass%) LLD = 0.003	Te (Mass%) LLD = 0.003	Hg (Mass%) LLD = 0.004	W (Mass%) LLD = 0.008	As (Mass%) LLD = 0.004	Sb (Mass%) LLD = 0.002	Cu (Error%)	Te (Error%)	Hg (Error%)	W (Error%)	As (Error%)	Sb (Error%)
AK032	AK032-1	0.002	0.004	0	0	0	0	149.94	102.36	100	100	100	100
	AK032-1b	0.011	0	0	0	0	0	32.07	100	100	100	100	100
	AK032-2a	0.146	0.014	0.366	0	0.032	0	2.16	31.2	2.37	100	13.23	100
	AK032-2b	0.144	0	0.311	0	0.061	0	2.17	100	2.73	100	6.1	100
	AK032-7a	0	0.004	0	0	0	0	100	103.93	100	100	100	100
	AK032-7b	0.013	0.006	0	0.003	0	0	24.94	76.07	100	255.47	100	100
	AK032-8a	0.001	0.005	0	0	0	0.002	255.27	77.44	100	100	100	78.63
	AK032-9a	0	0	0.022	0	0	0	100	100	30.99	100	100	100
AK100	AK100-1	0	0	0	0.005	0	0	100	100	100	181.42	100	100
	AK100-2	0	0	0	0	0.009	0	100	100	100	100	32.33	100
	AK100-3	0.02	0.008	0	0.008	0.03	0	16.14	54.79	100	112.39	13.55	100
	AK100-3b	0.023	0.023	0	0	0.064	0	14.53	19	100	100	7	100
	AK100-4	0.021	0.002	0	0	0	0	16.76	242.35	100	100	100	100
	AK100-9	0	0.015	0	0	0.013	0	100	26.85	100	100	29.76	100
	AK100-10a	0.012	0	0	0	0	0	28.41	100	100	100	100	100
	AK100-10b	0.012	0	0	0	0.045	0	25.86	100	100	100	6.65	100
	AK100-13a	0.028	0.002	0	0	0.005	0	12.94	273.01	100	100	130.05	100
	AK100-13b	0.027	0	0	0	0.05	0	12.59	100	100	100	8.84	100
	AK100-14	0	0.017	0	0	0.042	0	100	23.88	100	100	8.24	100
	AK100-15	0.003	0.003	0	0	0.006	0	93.5	130.46	100	100	73.82	100
	AK100-18a	0	0	0	0.015	0	0.004	100	100	100	64.67	138.53	52.68
	AK100-18b	0.027	0	0	0	0.032	0	12.64	100	100	100	15.81	100
	AK100-19	0.027	0.012	0	0	0	0	12.56	32.39	100	100	100	100
	AK100-20	0.012	0.007	0	0.008	0	0	27.98	62.18	100	103.78	100	100
AK111	AK111-1a	0.008	0.015	0	0	0	0	41	25.67	100	100	100	100
	AK111-2a	0.002	0	0	0	0	0	155.35	100	100	100	100	100
	AK111-2b	0	0.003	0	0	0	0	100	103.43	100	100	100	100
	AK111-3a	0.013	0	0	0	0	0.003	27.85	100	100	100	100	68.62
	AK111-4a	0	0.013	0	0	0	0	710.44	28.72	100	100	100	100
	AK111-5a	0.007	0.006	0	0	0	0	50.43	65.39	100	100	100	100
	AK111-6a	0.003	0	0	0	0	0	134.41	100	100	100	100	100
	AK111-7a	0.004	0.01	0	0	0	0	81.96	39.41	100	100	100	100
	AK111-8a	0.03	0.012	0	0	0	0	11.52	35.94	100	100	100	100
	AK111-9a	0.032	0.019	0	0	0	0	10.65	22.15	100	100	100	100
	AK111-9b	0.001	0	0	0	0	0	342.82	100	100	100	100	100
	AK111-10a	0	0.002	0	0	0	0	100	236.4	100	100	100	100
	AK111-10b	0	0.004	0	0	0	0	100	83.69	100	100	100	100
	AK111-11a	0.009	0.01	0.006	0	0	0	34.67	41.11	137.36	100	100	100
	AK111-12a	0	0	0	0.005	0	0	100	100	100	184.29	100	100
	AK111-13a	0	0.015	0	0	0	0	100	25.05	100	100	100	100
	AK111-14a	0	0.018	0	0	0.002	0	100	20.93	100	100	211.59	100
	AK111-15a	0.008	0.004	0	0	0.011	0	44.7	110.66	100	100	45.82	100
	AK111-16a	0.018	0.004	0	0	0	0	19.43	108.63	100	100	100	100
	AK111-16b	0	0.003	0	0	0.014	0	100	160.19	100	100	23.57	100
	AK111-17a	0.024	0.011	0	0.008	0	0	14.33	36.4	100	106.34	100	100
	AK111-18a	0	0	0	0	0	0	100	100	100	100	100	100
	AK111-18b	0.007	0	0	0	0	0	54.8	100	100	100	100	100
	AK111-19a	0.008	0.01	0	0.001	0	0	43.14	42.4	100	1588.24	3393.61	100
	AK111-19b	0.018	0.005	0	0	0	0	19.06	87.96	100	100	4248.65	100
	AK111-20a	0	0.01	0	0	0	0	100	36.52	100	100	1346.52	100
AK121	AK121-1b	0.002	0.009	0	0.008	0.024	0	170.94	45.61	100	86.09	14.63	100
	AK121-2a	0	0	0	0.006	0	0	100	100	100	73.42	100	100
	AK121-2c_rim	0.002	0.01	0	0	0	0	188.12	39.7	100	100	100	100
	AK121-3a	0.001	0.001	0	0.002	0	0.001	238.94	562.8	100	373.95	100	254.1
	AK121-4a	0.024	0	0	0	0	0	15.01	100	100	100	100	100
	AK121-5a	0	0.012	0	0	0.001	0	100	31.35	100	100	866	100
	AK121-6b	0	0	0	0	0.002	0	100	3552.58	100	100	152.94	100
	AK121-7a	0	0.006	0	0	0.003	0	100	62.59	100	100	163.89	100
	AK121-8a	0	0.001	0	0	0	0	100	443.37	100	100	100	100
	AK121-8c	0.013	0	0	0	0	0	27.19	100	100	100	100	100
	AK121-9c	0	0	0	0	0	0	100	100	100	100	100	100
	AK121-10a	0	0	0	0	0.005	0	100	100	100	100	56.07	100
	AK121-11a	0	0	0	0.004	0	0	100	100	100	100.27	100	100
	AK121-12a	0	0.005	0	0.007	0.002	0	100	65.74	100	64.52	220.64	100
	AK121-13a	0.02	0	0	0	0	0	18.01	100	100	100	100	100
	AK121-14a	0.01	0.002	0	0	0	0	36.4	202.15	100	100	100	100
	AK121-15b	0	0	0	0	0	0	100	100	100	100	100	100
	AK121-16a	0	0.006	0	0	0.004	0	100	71.4	100	100	127.65	100
	AK121-17a_growth	0	0.004	7.407	0	0	0	100	115.23	0.23	100	100	100
	AK121-17c_growth	0	0.003	10.977	0	0	0	100	155.81	0.18	100	100	100
	AK121-17c	0.007	0.005	0.041	0	0	0	45.77	98.94	19.2	100	100	100
	AK121-18a	0	0	0	0	0	0	100	100	100	100	100	100
	AK121-19c	0	0.011	0	0	0	0	100	34.94	100	100	100	100
	AK121-20c	0.011	0.006	0	0	0	0	31.43	70.68	100	100	100	100
	AK121-21c	0.005	0	0	0	0	0	71.36	100	100	100	100	100
	AK121-22b	0.007	0	0	0	0.005	0	48.36	100	100	100	110.02	100
	AK121-23c	0.004	0.004	0	0.008	0	0	71.88	117.82	100	64.92	100	100
	AK121-24a	0	0	0	0.001	0	0	100	100	100	336.74	100	100

Site	Sample ID	Cu (Mass%) LLD = 0.003	Te (Mass%) LLD = 0.003	Hg (Mass%) LLD = 0.004	W (Mass%) LLD = 0.008	As (Mass%) LLD = 0.004	Sb (Mass%) LLD = 0.002	Cu (Error%)	Te (Error%)	Hg (Error%)	W (Error%)	As (Error%)	Sb (Error%)
AK123	AK123-1a	0.004	0	0	0	0	0	80.62	100	100	100	100	100
	AK123-2a	0	0.005	0	0	0.009	0	100	84.17	100	100	45.69	100
	AK123-2b	0	0.011	0	0	0	0	100	35.5	100	100	100	100
	AK123-3a	0.008	0.009	0	0	0	0	44.78	45.84	100	100	100	100
	AK123-4a	0	0.009	0	0	0	0	100	41.35	100	100	100	100
	AK123-5a	0.004	0	0	0	0.011	0.001	83.94	100	100	100	33.8	348.39
	AK123-6a	0	0.008	0	0	0	0	100	44.95	100	100	100	100
	AK123-7a	0	0	0	0	0	0	100	100	100	100	100	100
	AK123-8a	0	0.012	0	0	0	0	100	31.48	100	100	100	100
	AK123-8b	0	0.012	0	0	0.001	0	100	31.31	100	100	734.43	100
	AK123-9a	0.021	0.009	0	0	0	0	16.27	44.44	100	100	100	100
	AK123-10a	0.012	0.008	0	0	0	0	29.26	50.4	100	100	100	100
	AK123-11a	0.022	0.003	0	0	0	0.002	15.8	165.3	100	100	100	119.64
	AK123-11b	0.004	0	0	0	0	0.002	83.72	100	100	100	100	154.85
	AK123-12a	0	0	0	0	0.004	0.001	100	100	100	100	85.31	334.68
	AK123-13a	0.02	0.004	0	0	0	0	17.45	124.76	100	100	100	100
	AK123-13b	0.014	0	0	0	0	0	26.49	100	100	100	100	100
	AK123-14a	0.016	0.016	0	0	0	0	21.65	25.99	100	100	100	215.21
	AK123-15a	0	0.016	0	0	0	0	100	23.71	100	100	100	100
	AK123-16a	0	0.014	0	0	0	0	100	27.54	100	100	100	100
	AK123-17a	0.008	0	0	0	0	0	45.12	100	100	100	100	100
	AK123-17b	0.025	0.008	0	0	0.013	0	14.1	52.16	100	100	47.94	100
	AK123-18a	0.007	0.009	0	0	0	0	47.77	44.81	100	100	100	100
	AK123-18b	0.008	0.004	0	0.001	0	0	40.79	97.72	100	1317.37	100	100
	AK123-19a	0.012	0	0	0	0	0	29.37	100	100	100	100	100
	AK123-19b	0.012	0	0	0	0	0	30.1	100	100	100	100	100
	AK123-20a	0.021	0	0	0	0	0	17.37	100	100	100	100	100
	AK123-20b	0	0.003	0	0	0	0	100	127.56	100	100	100	100
AUR-12-854	AUR-12-854-21a	0	0.001	0	0	0	0	100	259.07	100	100	100	100
	AUR-12-854-21b	0.023	0.005	0	0	0	0	15.2	86.46	100	100	100	100
	AUR-12-854-22a	0.153	0	0	0	0.098	0	2.37	100	100	100	6.08	100
	AUR-12-854-22b	0.205	0.008	0	0	0.019	0	1.81	54.31	100	100	40.78	100
	AUR-12-854-22c	0.226	0	0	0	0	0	1.67	100	100	100	100	100
	AUR-12-854-23a	0.007	0.005	0	0	0	0	46.52	84.68	100	100	100	100
	AUR-12-854-23b	0.008	0	0	0	0.015	0	44	100	100	100	30.24	100
	AUR-12-854-24a	0	0.005	0	0	0	0	100	77.29	100	100	100	100
	AUR-12-854-24b	0	0.006	0	0.003	0	0	100	59.69	100	314.68	100	100
ADEM	ADEM-1a	0	0.019	0	0.002	0	0.001	100	19.15	100	213.58	100	94.9
	ADEM-2a	0.025	0.012	0	0.008	0	0	13.01	32.37	100	79.13	100	100
	ADEM-2d_rim	0	0	0	0	0	0	100	100	100	100	100	100
	ADEM-3b	0.02	0.009	0	0.002	0	0	17.38	49.18	100	290.68	100	100
	ADEM-4b	0	0.004	0	0.001	0	0	100	99.69	100	753.22	100	100
	ADEM-5a	0.015	0.006	0	0	0	0	23.6	67.16	100	100	100	100
	ADEM-5c_rim	0.002	0.01	0	0	0	0	152.7	37.43	100	100	100	100
	ADEM-6a	0	0.015	0.199	0	0	0	100	29.57	3.61	100	100	100
	ADEM-6c_rim	0	0	0	0	0	0.003	100	100	100	100	231.96	82.49
	ADEM-7	0.014	0.004	0	0.001	0	0	24.17	118.4	100	991.07	100	100
	ADEM-7b	0.019	0.015	0	0	0	0.007	17.5	27.18	100	100	175.67	27.59
	ADEM-8	0.002	0	0	0	0	0	201.66	100	100	100	100	100
	ADEM-9	0	0.005	0	0	0	0	100	85.09	100	100	100	100
	ADEM-11	0	0	0	0	0	0	100	3739.28	100	100	100	100
	ADEM-13	0	0.003	0	0	0.034	0	100	163.96	100	100	9.46	100
	ADEM-14	0	0.004	0	0	0	0	100	97.48	100	100	100	100
	ADEM-18	0	0.012	0	0	0.037	0	100	34.75	100	100	9.8	100
	ADEM-18b	0.006	0	0	0	0.059	0	52.61	100	100	100	5.65	100

APPENDIX G

Filtered Trace Element data of gold grains from the southern Seward Peninsula, Nome, Alaska

Site	Sample ID	Cu (Mass%) LLD = 0.003	Te (Mass%) LLD = 0.003	Hg (Mass%) LLD = 0.004	W (Mass%) LLD = 0.004	As (Mass%) LLD = 0.004	Sb (Mass%) LLD = 0.002	Cu (Error%)	Te (Error%)	Hg (Error%)	W (Error%)	As (Error%)	Sb (Error%)
AK015	AK015-1a	0.004	0.002	0.282				67	238	3	-	-	-
	AK015-5b	0.014	0.009	0.1		0.002		21	52	8	-	247	-
	AK015-10a	0.036				0.002		10	-	-	-	430	-
AK021	AK021-1a		0.007			0.033		2490	59	-	-	10	-
	AK021-2a		0.011					-	35	-	-	-	-
	AK021-3					0.017		-	-	-	-	17	-
	AK021-4		0.015			0.006		-	26	-	-	86	-
	AK021-5		0.021					-	18	-	-	-	-
	AK021-6	0.011	0.015					30	26	-	-	-	-
	AK021-7	0.002						208	-	-	-	-	-
	AK021-8		0.02			0.993		-	22	-	-	0	-
	AK021-9		0.02					-	19	-	-	-	-
	AK021-10		0.015					-	24	-	-	-	-
	AK021-12b		0.011	0.096		0.032		-	39	8	-	10	-
	AK021-13a		0.013					-	28	-	-	-	-
	AK021-14		0.007			0.018		-	57	-	-	21	-
	AK021-15		0.008					-	47	-	-	-	-
	AK021-16	0.001				0.016		557	-	-	-	19	-
	AK021-17	0.004	0.009				0.04	71	42	-	-	322	5
	AK021-18	0.014				0.005		25	-	-	-	116	-
	AK021-19		0.011					-	33	-	-	-	-
	AK021-20		0.015					-	25	-	-	-	-
	AK021-21		0.004					-	89	-	-	-	-
	AK021-22		0.019					-	19	-	-	-	-
	AK021-23		0.007			0.013		-	55	-	-	31	-
	AK021-24							-	-	-	-	-	-
	AK021-25		0.011					-	32	-	-	-	-
	AK021-26		0.008			0.012		-	52	-	-	32	-
	AK021-31		0.016			0.003		-	25	-	-	149	-
	AK021-33		0.008			0.002		-	47	-	-	252	-
	AK021-34		0.008					-	45	-	-	-	-
	AK021-35		0.003			0.01		-	135	-	-	33	-
	AK021-36		0.006					-	62	-	-	-	-
	AK021-37		0.016					-	23	-	-	-	-
	AK021-38		0.006					-	63	-	-	-	-
	AK021-39		0.015			0.007		-	26	-	-	64	-
	AK021-40			0.004				-	-	149	-	-	-
AK028	AK028-1		0.004	0.932			0.001	-	119	1	-	-	308
	AK028-2			0.603				-	-	1	-	-	-
	AK028-3	0.002	0.01	1.604				160	43	1	-	-	-
	AK028-4		0.026	0.613				-	18	1	-	-	-
	AK028-5	0.006		0.583				44	-	1	-	-	-
	AK028-6		0.011	0.603				1084	41	1	-	-	-
	AK028-9	0.011	0.007	0.064		0.002		26	62	12	-	186	-
	AK028-10b	0.004	0.002	3.898				70	204	0	-	-	-
	AK028-11c	0.01						37	-	-	-	-	-
	AK028-12b			1.693				2126	-	1	-	-	-
	AK028-13a		0.015	6.031				-	30	0	-	-	-
	AK028-14b		0.014	0.187				-	30	4	-	-	-
	AK028-15a	0.016	0.005	0.045	0.004		0.001	19	89	18	137	-	187
	AK028-16b	0.007	0.009	0.106	0.008		0.003	41	49	7	62	-	88
	AK028-17c	2.162		0.446	0.003		0.002	0	-	2	216	-	146
	AK028-18c	0.054	0.004	0.226				6	114	4	-	-	-
	AK028-19a			6.301				-	-	0	-	-	717
	AK028-21	0.01	0.013	0.166		0.005		28	34	5	-	75	-
	AK028-22a	0.04	0.009	0.168				8	49	5	-	-	-
	AK028-23			0.324		0.006		-	1176	2	-	49	-
	AK028-24a	0.037	0.006	0.337		0.001		8	79	2	-	626	-

Site	Sample ID	Cu (Mass%) LLD = 0.003	Te (Mass%) LLD = 0.003	Hg (Mass%) LLD = 0.004	W (Mass%) LLD = 0.004	As (Mass%) LLD = 0.004	Sb (Mass%) LLD = 0.002	Cu (Error%)	Te (Error%)	Hg (Error%)	W (Error%)	As (Error%)	Sb (Error%)
AK032	AK032-1b	0.011						32	-	-	-	-	-
	AK032-2a	0.146	0.014	0.366		0.032		2	31	2	-	13	-
	AK032-7b	0.013	0.006		0.003			25	76	-	255	-	-
	AK032-8a	0.001	0.005				0.002	255	77	-	-	-	79
	AK032-9a			0.022				-	-	31	-	-	-
AK100	AK100-1				0.005			-	-	-	181	-	-
	AK100-2					0.009		-	-	-	-	32	-
	AK100-3b	0.023	0.023			0.064		15	19	-	-	7	-
	AK100-4	0.021	0.002					17	242	-	-	-	-
	AK100-9		0.015			0.013		-	27	-	-	30	-
	AK100-10b	0.012				0.045		26	-	-	-	7	-
	AK100-13b	0.027				0.05		13	-	-	-	9	-
	AK100-14		0.017			0.042		-	24	-	-	8	-
	AK100-15	0.003	0.003			0.006		94	130	-	-	74	-
	AK100-18b	0.027				0.032		13	-	-	-	16	-
	AK100-19	0.027	0.012					13	32	-	-	-	-
	AK100-20	0.012	0.007		0.008			28	62	-	104	-	-
AK111	AK111-1a	0.008	0.015					41	26	-	-	-	-
	AK111-2a	0.002						155	-	-	-	-	-
	AK111-2b		0.003					-	103	-	-	-	-
	AK111-3a	0.013					0.003	28	-	-	-	-	69
	AK111-4a		0.013					710	29	-	-	-	-
	AK111-5a	0.007	0.006					50	65	-	-	-	-
	AK111-6a	0.003						134	-	-	-	-	-
	AK111-7a	0.004	0.01					82	39	-	-	-	-
	AK111-8a	0.03	0.012					12	36	-	-	-	-
	AK111-9a	0.032	0.019					11	22	-	-	-	-
	AK111-9b	0.001						343	-	-	-	-	-
	AK111-10a		0.002					-	236	-	-	-	-
	AK111-10b		0.004					-	84	-	-	-	-
	AK111-11a	0.009	0.01	0.006				35	41	137	-	-	-
	AK111-12a				0.005			-	-	-	184	-	-
	AK111-13a		0.015					-	25	-	-	-	-
	AK111-14a		0.018			0.002		-	21	-	-	212	-
	AK111-15a	0.008	0.004			0.011		45	111	-	-	46	-
	AK111-16b		0.003			0.014		-	160	-	-	24	-
	AK111-17a	0.024	0.011		0.008			14	36	-	106	-	-
	AK111-18b	0.007						55	-	-	-	-	-
	AK111-19a	0.008	0.01		0.001			43	42	-	1588	3394	-
	AK111-20a		0.01					-	37	-	-	1347	-
AK121	AK121-1b	0.002	0.009		0.008	0.024		171	46	-	86	15	-
	AK121-2a				0.006			-	-	-	73	-	-
	AK121-3a	0.001	0.001		0.002		0.001	239	563	-	374	-	254
	AK121-4a	0.024						15	-	-	-	-	-
	AK121-5a		0.012			0.001		-	31	-	-	866	-
	AK121-6b					0.002		-	3553	-	-	153	-
	AK121-7a		0.006			0.003		-	63	-	-	164	-
	AK121-8a		0.001					-	443	-	-	-	-
	AK121-8c	0.013						27	-	-	-	-	-
	AK121-9c							-	-	-	-	-	-
	AK121-10a					0.005		-	-	-	-	56	-
	AK121-11a				0.004			-	-	-	0	-	-
	AK121-12a		0.005		0.007	0.002		-	66	-	65	221	-
	AK121-13a	0.02						18	-	-	-	-	-
	AK121-14a	0.01	0.002					36	202	-	-	-	-
	AK121-15b							-	-	-	-	-	-
	AK121-16a		0.006			0.004		-	71	-	-	128	-
	AK121-17c	0.007	0.005	0.041				46	99	19	-	-	-
	AK121-18a							-	-	-	-	-	-
	AK121-19c		0.011					-	35	-	-	-	-
	AK121-20c	0.011	0.006					31	71	-	-	-	-
	AK121-21c	0.005						71	-	-	-	-	-
	AK121-22b	0.007				0.005		48	-	-	-	110	-
	AK121-23c	0.004	0.004		0.008			72	118	-	65	-	-
	AK121-24a				0.001			-	-	-	337	-	-

Site	Sample ID	Cu (Mass%) LLD = 0.003	Te (Mass%) LLD = 0.003	Hg (Mass%) LLD = 0.004	W (Mass%) LLD = 0.004	As (Mass%) LLD = 0.004	Sb (Mass%) LLD = 0.002	Cu (Error%)	Te (Error%)	Hg (Error%)	W (Error%)	As (Error%)	Sb (Error%)
AK123	AK123-1a	0.004						81	-	-	-	-	-
	AK123-2a		0.005			0.009		-	84	-	-	46	-
	AK123-3a	0.008	0.009					45	46	-	-	-	-
	AK123-4a		0.009					-	41	-	-	-	-
	AK123-5a	0.004				0.011	0.001	84	-	-	-	34	348
	AK123-6a		0.008					-	45	-	-	-	-
	AK123-7a							-	-	-	-	-	-
	AK123-8a		0.012					-	31	-	-	-	-
	AK123-9a	0.021	0.009					16	44	-	-	-	-
	AK123-10a	0.012	0.008					29	50	-	-	-	-
	AK123-11a	0.022	0.003				0.002	16	165	-	-	-	120
	AK123-12a					0.004	0.001	-	-	-	-	85	335
	AK123-13a	0.02	0.004					17	125	-	-	-	-
	AK123-14a	0.016	0.016					22	26	-	-	-	215
	AK123-15a		0.016					-	24	-	-	-	-
	AK123-16a		0.014					-	28	-	-	-	-
	AK123-17b	0.025	0.008			0.013		14	52	-	-	48	-
	AK123-18a	0.007	0.009					48	45	-	-	-	-
	AK123-19b	0.012						30	-	-	-	-	-
	AK123-20a	0.021						17	-	-	-	-	-
AUR-12-854	AUR-12-854-21b	0.023	0.005					15	86	-	-	-	-
	AUR-12-854-22a	0.153				0.098		2	-	-	-	6	-
	AUR-12-854-23b	0.008				0.015		44	-	-	-	30	-
	AUR-12-854-24b		0.006		0.003			-	60	-	315	-	-
ADEM	ADEM-1a		0.019		0.002		0.001	-	19	-	214	-	95
	ADEM-2a	0.025	0.012		0.008			13	32	-	79	-	-
	ADEM-3b	0.02	0.009		0.002			17	49	-	291	-	-
	ADEM-4b		0.004		0.001			-	100	-	753	-	-
	ADEM-5a	0.015	0.006					24	67	-	-	-	-
	ADEM-6a		0.015	0.199				-	30	4	-	-	-
	ADEM-7b	0.019	0.015				0.007	18	27	-	-	176	28
	ADEM-8	0.002						202	-	-	-	-	-
	ADEM-9		0.005					-	85	-	-	-	-
	ADEM-11							-	3739	-	-	-	-
	ADEM-13		0.003			0.034		-	164	-	-	9	-
	ADEM-14		0.004					-	97	-	-	-	-
	ADEM-18b	0.006				0.059		53	-	-	-	6	-

Explanation:

Appendix G represents an extract of the full trace element dataset (Appendix F) as per the discussion text in Section 6.5. This table consists of data of 151 individual gold grain analyses from 10 sites across the southern Seward Peninsula (there is no geochemical data available for Site AK117, nor trace element data for Site RC4). Blank results indicate that the element in question was not detectable.

"Sample" refers to the particular grain analysis selected to represent each grain (e.g. AK015-1a refers to the fact that the first analysis ("a") was selected to represent grain 1 from site AK015).

Te (Mass%) refers to the mass percentage of a particular element (e.g. Te) present in gold at the analysis site. The same applies for Cu, W, As and Sb.

"LLD" refers to the "Lower Limit of Detection" and is the lowest value for which a particular element can be analysed with a degree of certainty (defined as error % < 100%).

"Error %" is the percentage analytical error in the result of an individual analysis. Where "Error%" is greater than 200 the result is not shown in the table as it is deemed too uncertain. Where "Error%" is shown as "-", no result was available.

APPENDIX H

Elemental maps of gold grains from the southern Seward Peninsula, Nome, Alaska

Grain ID: AK015-1

Accelerating Voltage: 15.0 kV

Probe Current: 150 nA

Sample Points: 500 X 600

Sampling Interval (µm): 0.80 X 0.80

Sample Size (µm): 400 X 480

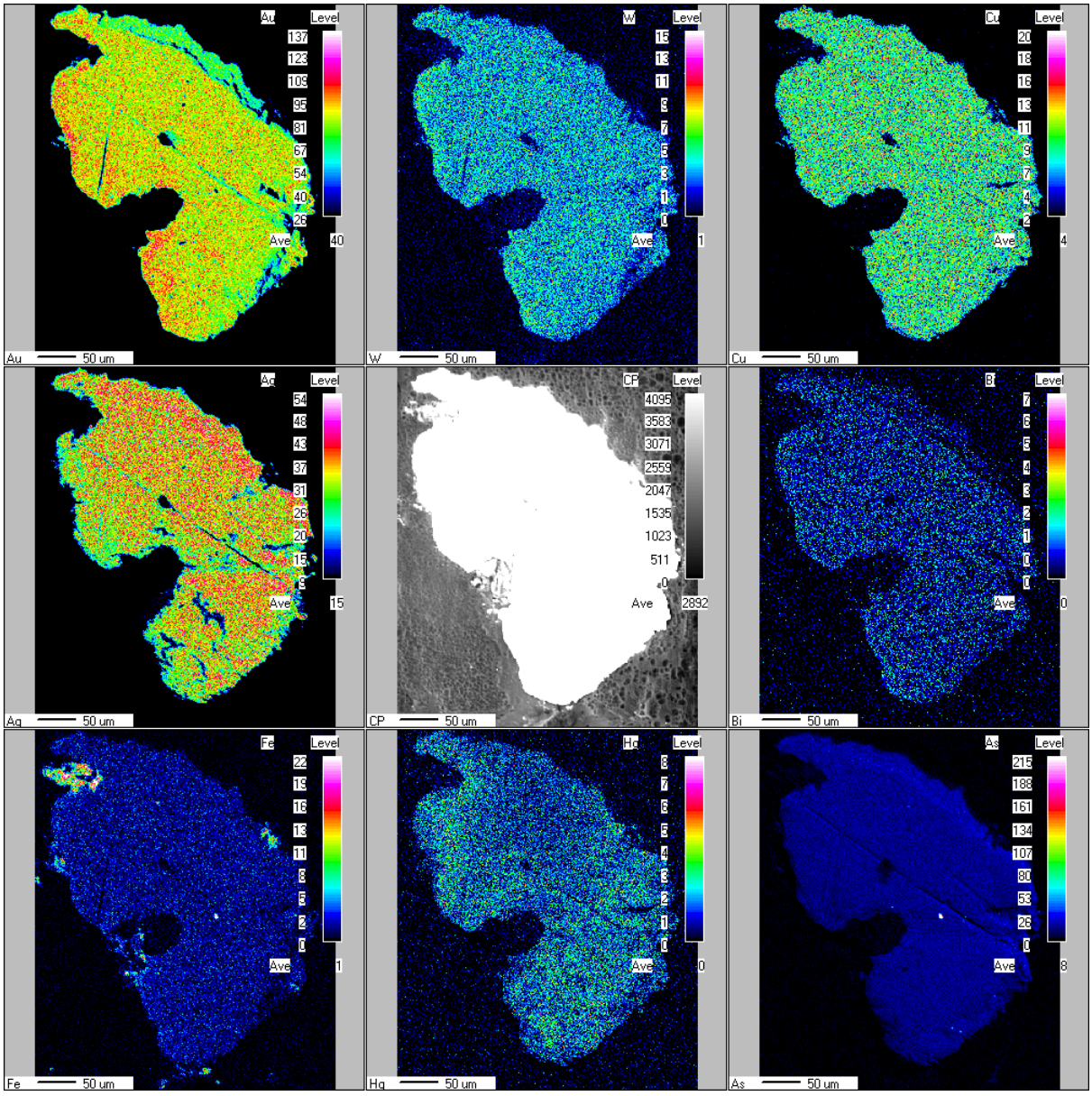

Grain ID: AK021-6

Accelerating Voltage: 15.0 kV

Probe Current: 150 nA

Sample Points: 850 X 850

Sampling Interval (µm): 1.00 X 1.00

Sample Size (µm): 850 X 850

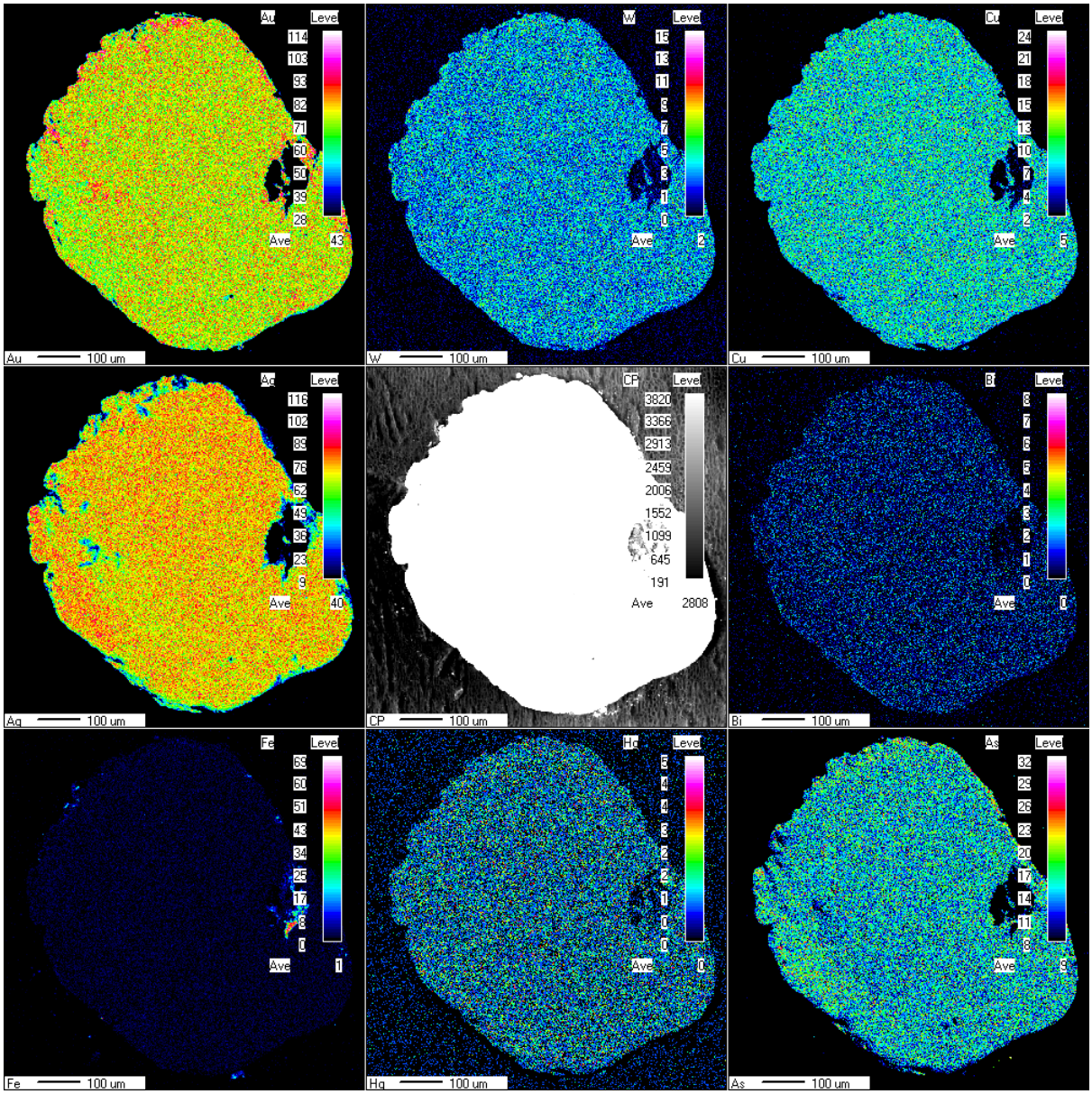

Grain ID: AK028-3

Accelerating Voltage: 15.0 kV

Probe Current: 20 nA

Sample Points: 1100 X 800

Sampling Interval (µm): 1.00 X 1.00

Sample Size (µm): 1100 X 800

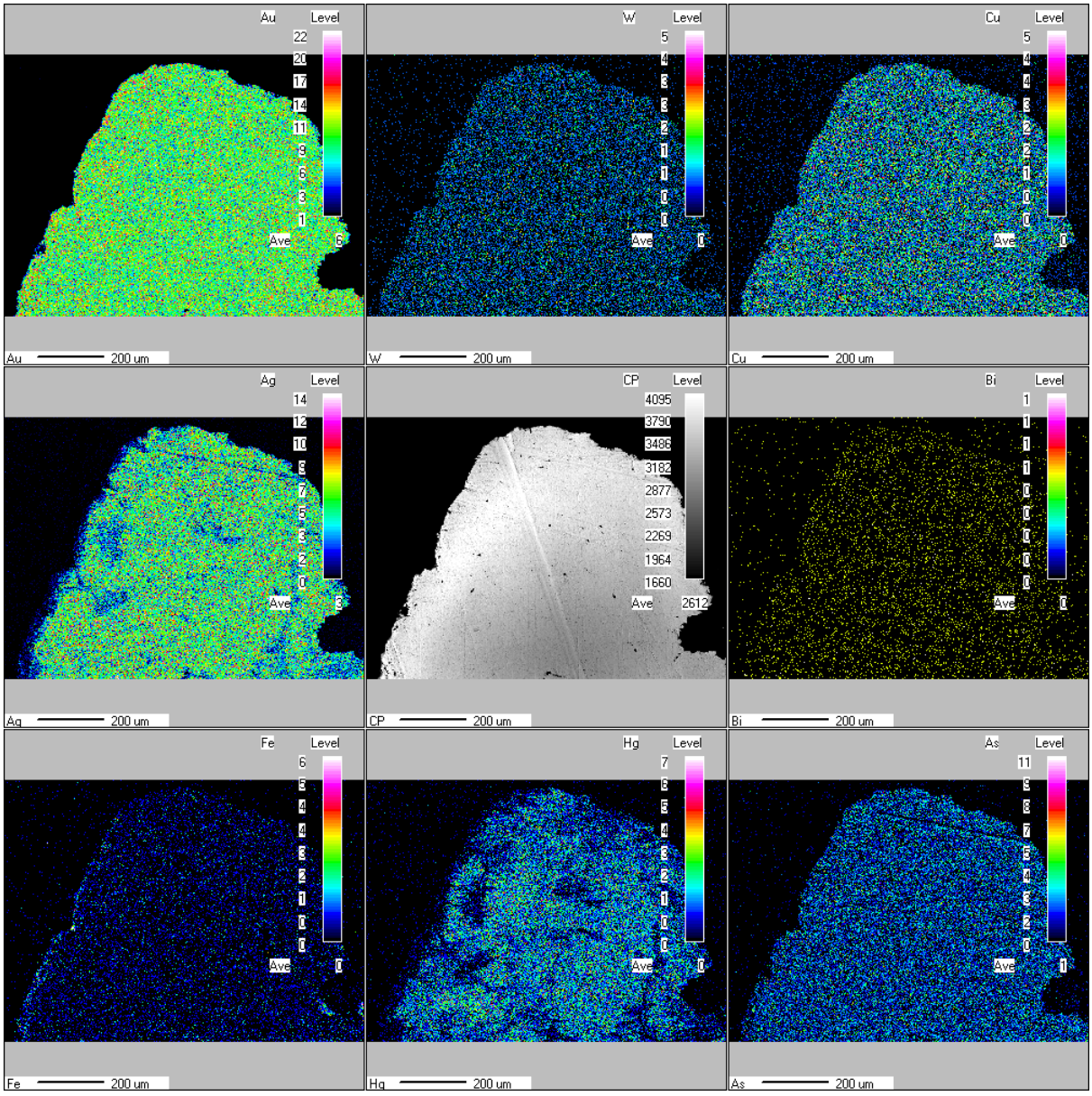

Grain ID: AK032-7

Accelerating Voltage: 15.0 kV

Probe Current: 20 nA

Sample Points: 450 X 500

Sampling Interval (µm): 1.00 X 1.00

Sample Size (µm): 450 X 500

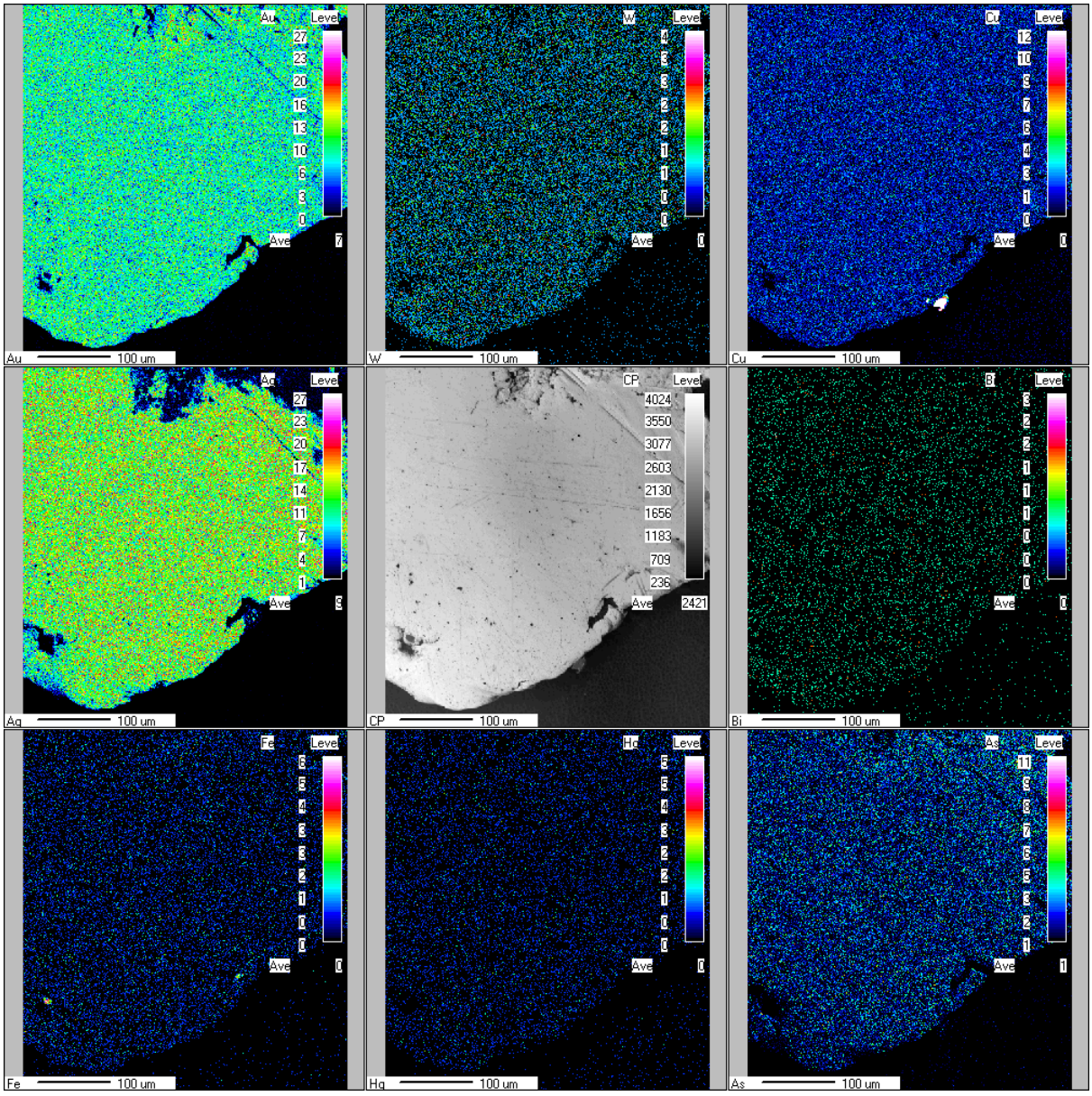

Grain ID: AK100-4

Accelerating Voltage: 15.0 kV

Probe Current: 20 nA

Sample Points: 280 X 320

Sampling Interval (µm): 0.86 X 0.86

Sample Size (µm): 241 X 275

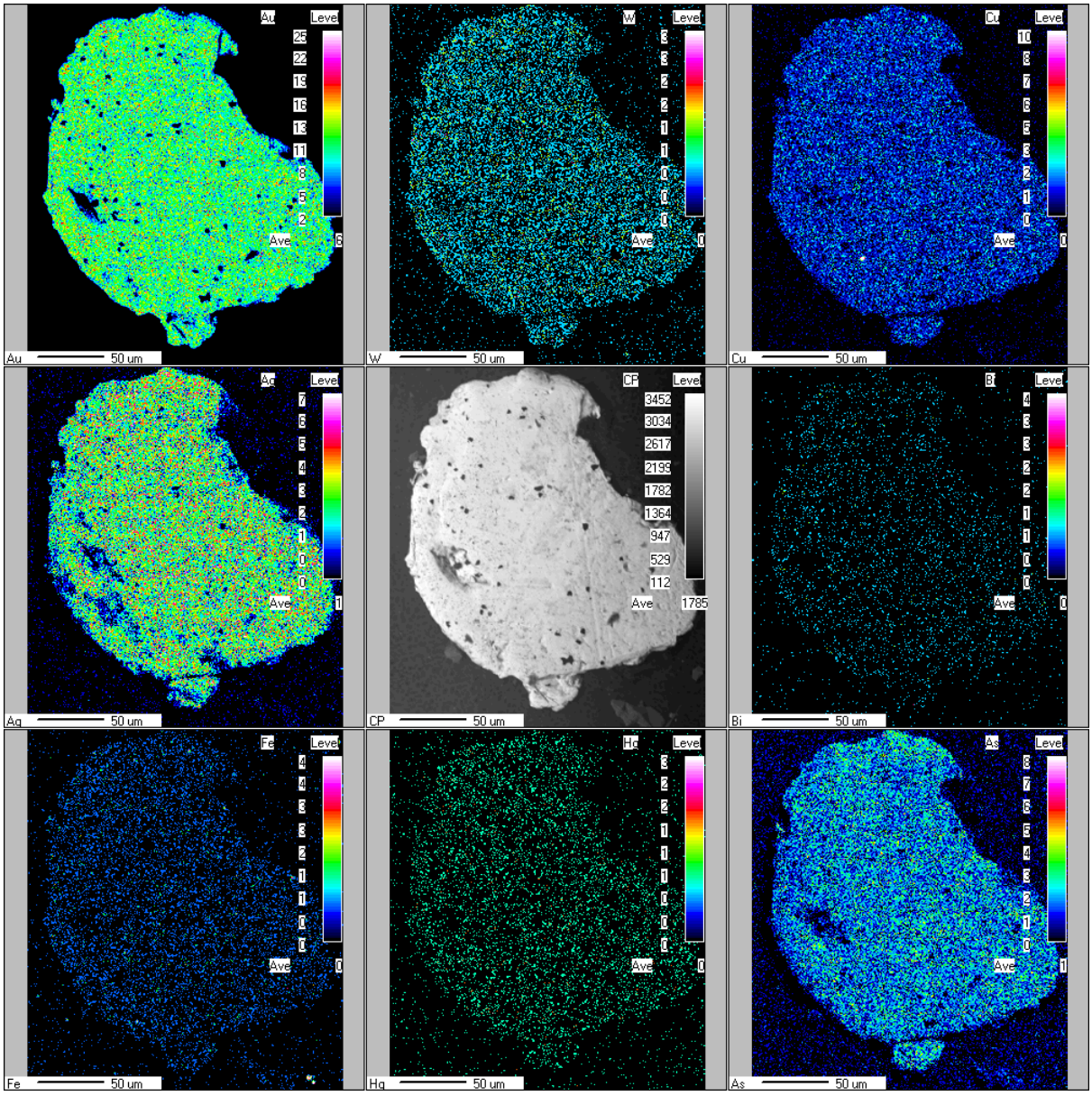

Grain ID: AK100-18

Accelerating Voltage: 15.0 kV

Probe Current: 20 nA

Sample Points: 380 X 450

Sampling Interval (µm): 0.86 X 0.86

Sample Size (µm): 326 X 387

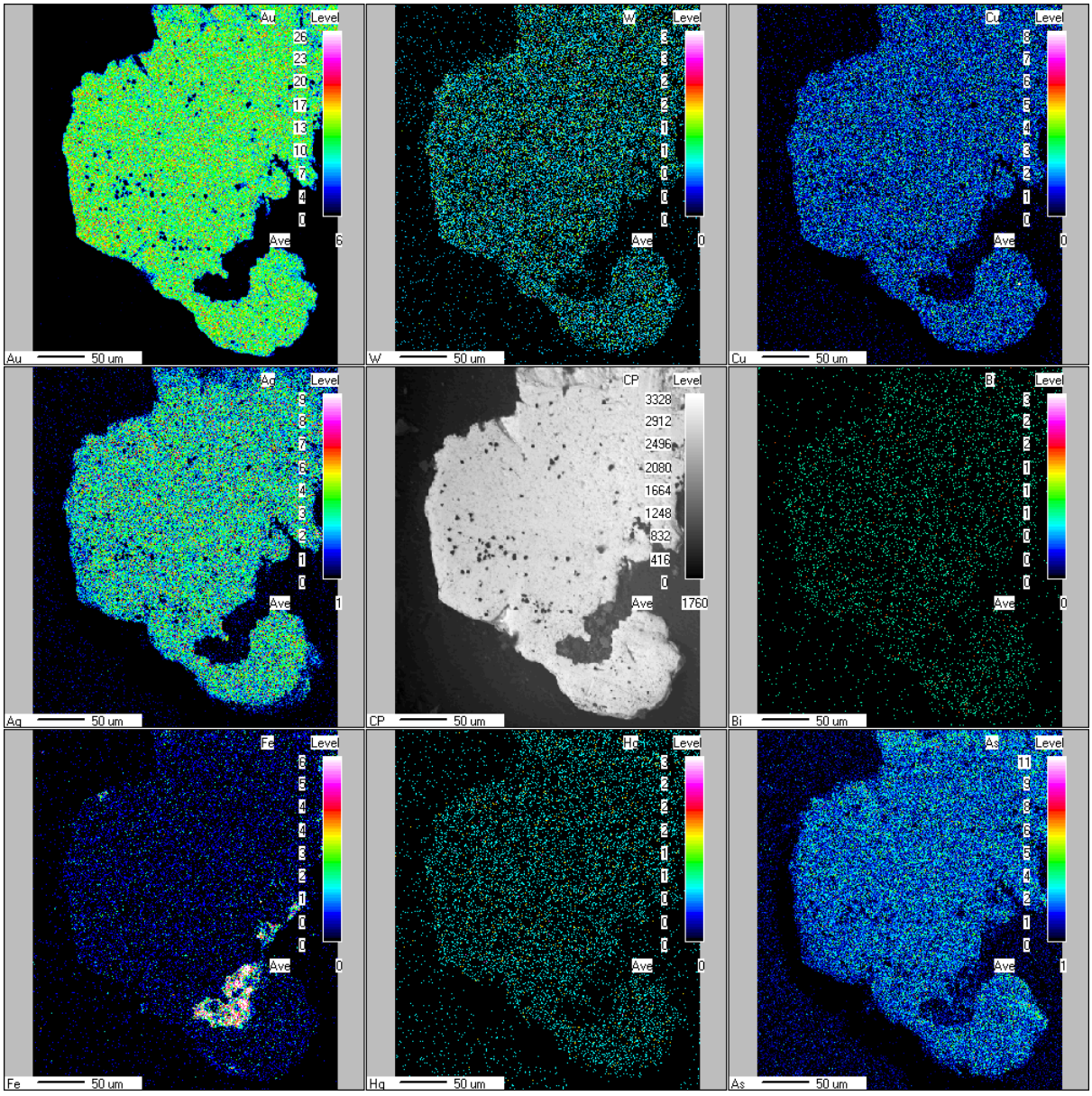

Grain ID: AK111-5

Accelerating Voltage: 15.0 kV

Probe Current: 20 nA

Sample Points: 1000 X 1000

Sampling Interval (µm): 0.76 X 0.76

Sample Size (µm): 760 X 760

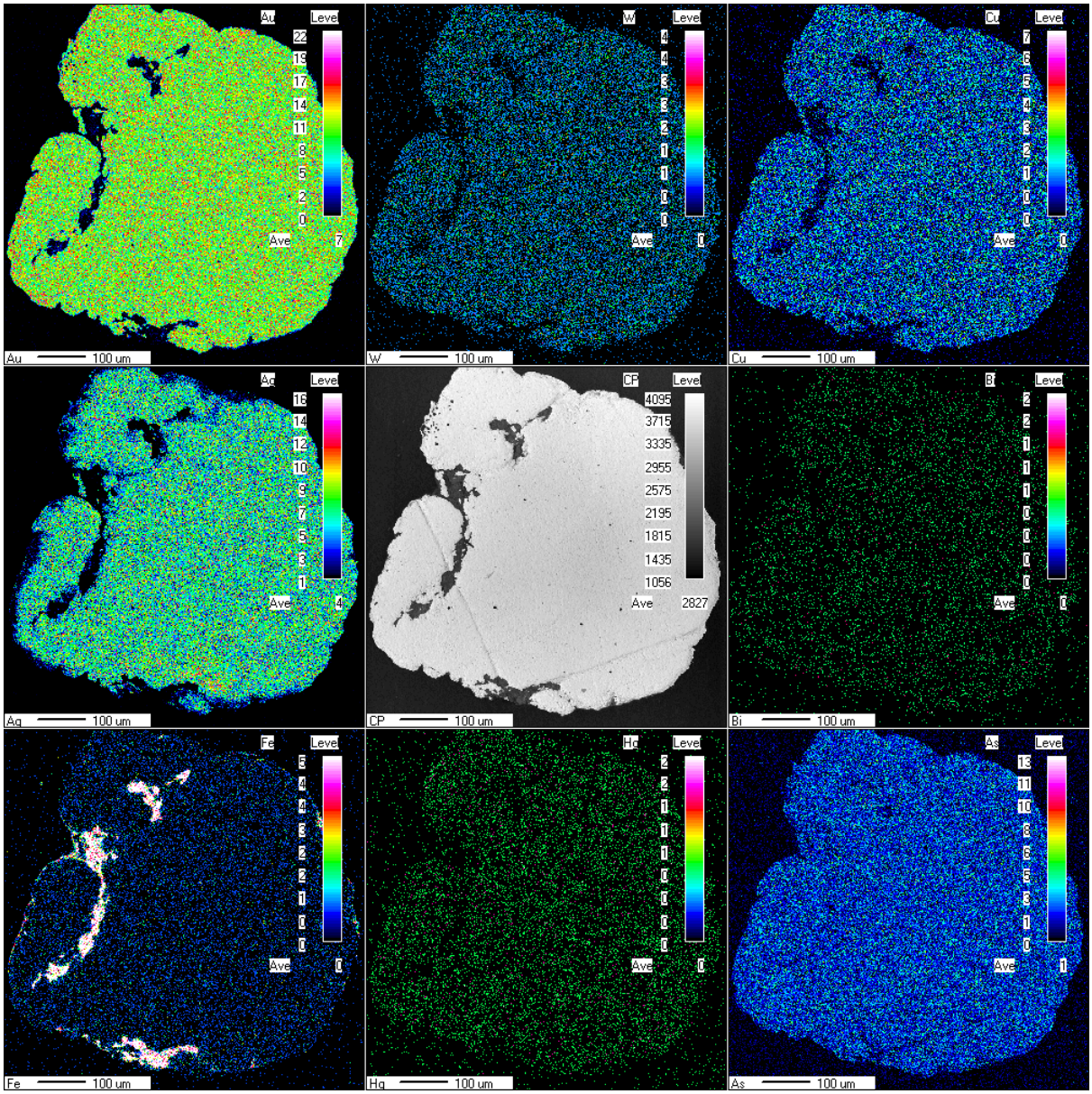

Grain ID: AK121-17

Accelerating Voltage: 15.0 kV

Probe Current: 20 nA

Sample Points: 750 X 450

Sampling Interval (µm): 1.00 X 1.00

Sample Size (µm): 750 X 450

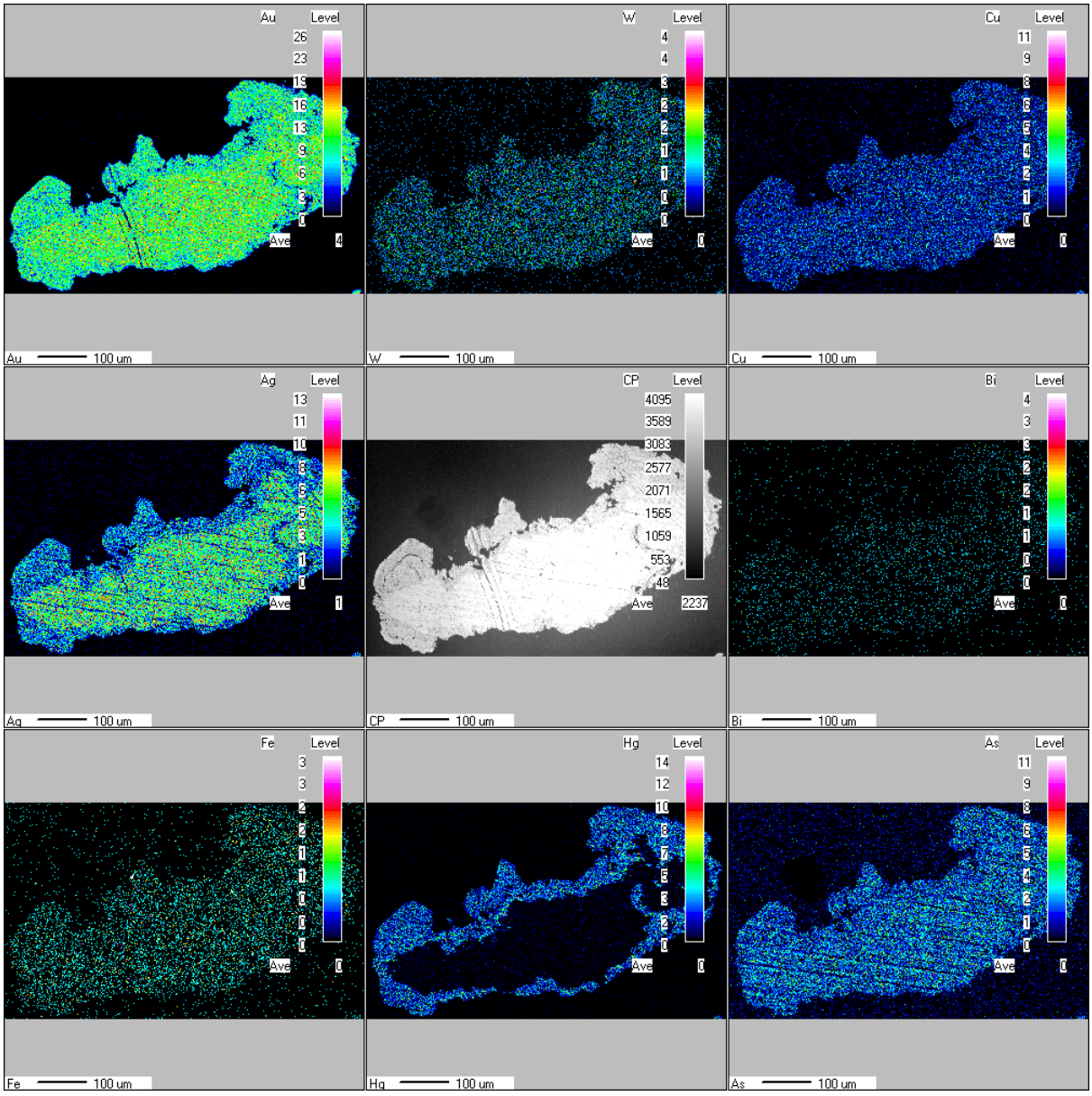

Grain ID: AK123-8

Accelerating Voltage: 15.0 kV

Probe Current: 20 nA

Sample Points: 1100 X 600

Sampling Interval (µm): 0.76 X 0.76

Sample Size (µm): 836 X 456

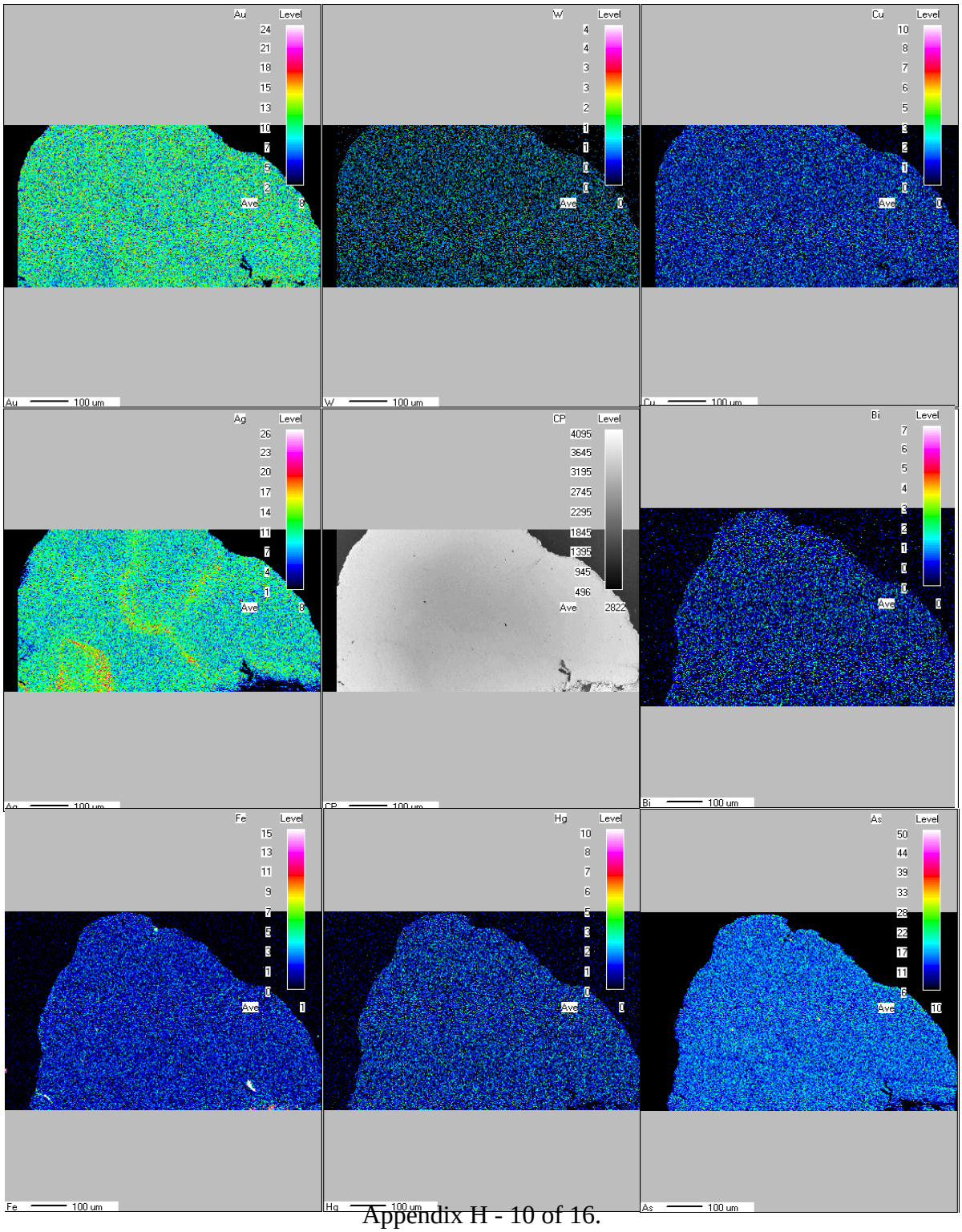

Grain ID: AUR-12-854-21

Accelerating Voltage: 15.0 kV

Probe Current: 20 nA

Sample Points: 750 X 600

Sampling Interval (µm): 0.86 X 0.86

Sample Size (µm): 645 X 516

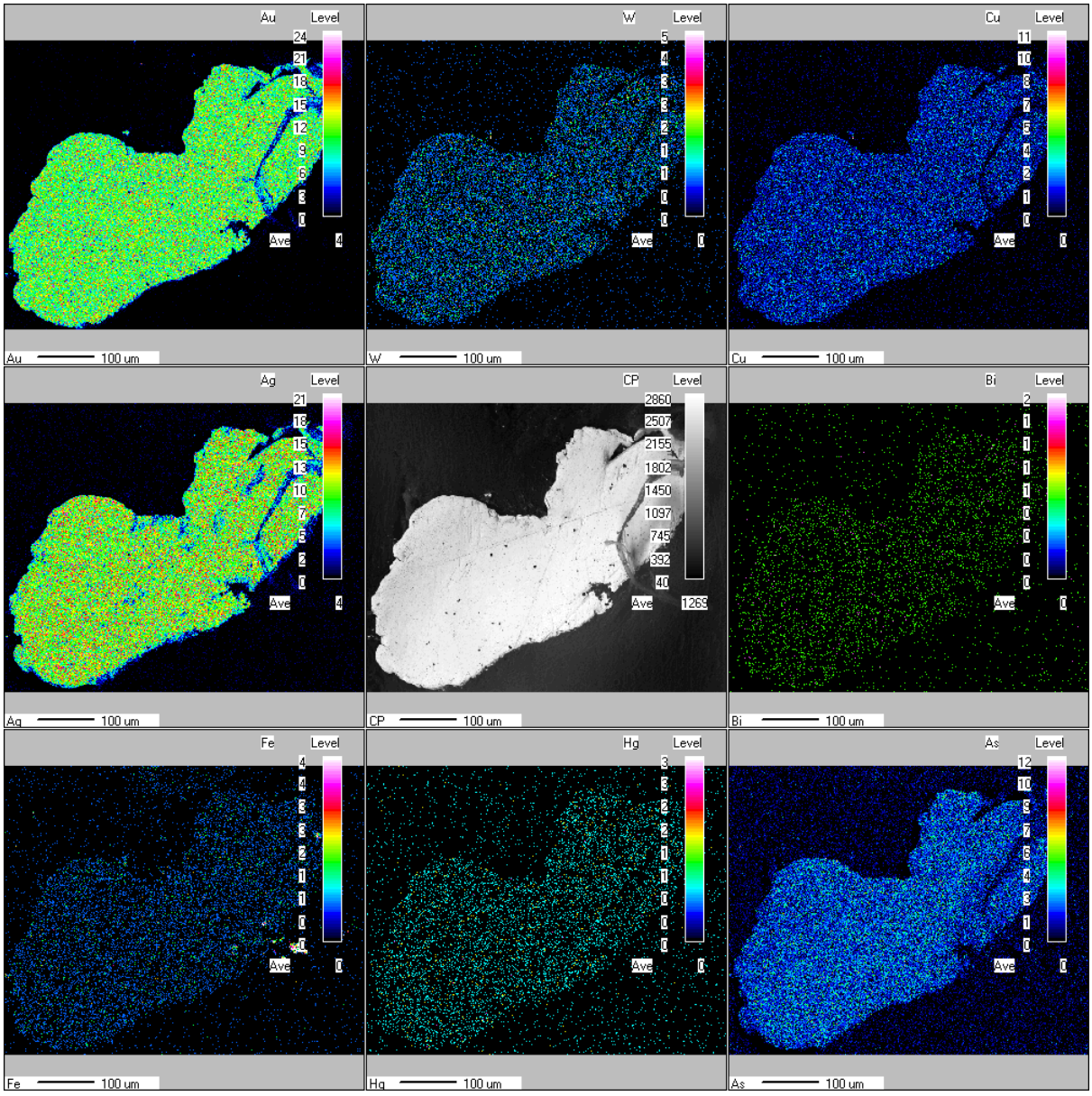

Grain ID: ADEM-4

Accelerating Voltage: 15.0 kV

Probe Current: 150 nA

Sample Points: 1200 X 1200

Sampling Interval (µm): 1.00 X 1.00

Sample Size (µm): 1200 X 1200

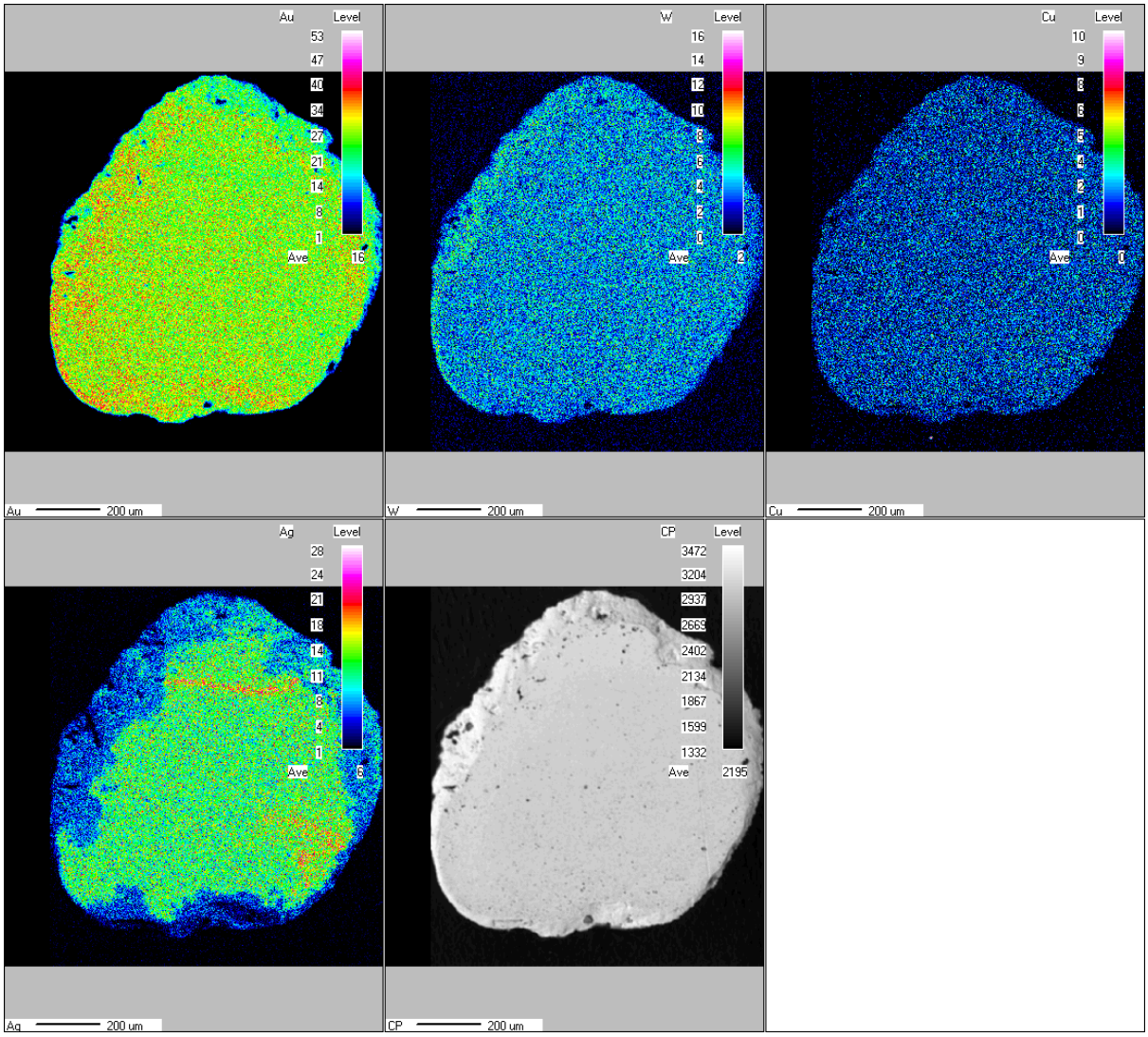

Grain ID: ADEM-7 (Map 1)

Accelerating Voltage: 15.0 kV

Probe Current: 150 nA

Sample Points: 1100 X 1050

Sampling Interval (µm): 1.00 X 1.00

Sample Size (µm): 1100 X 1050

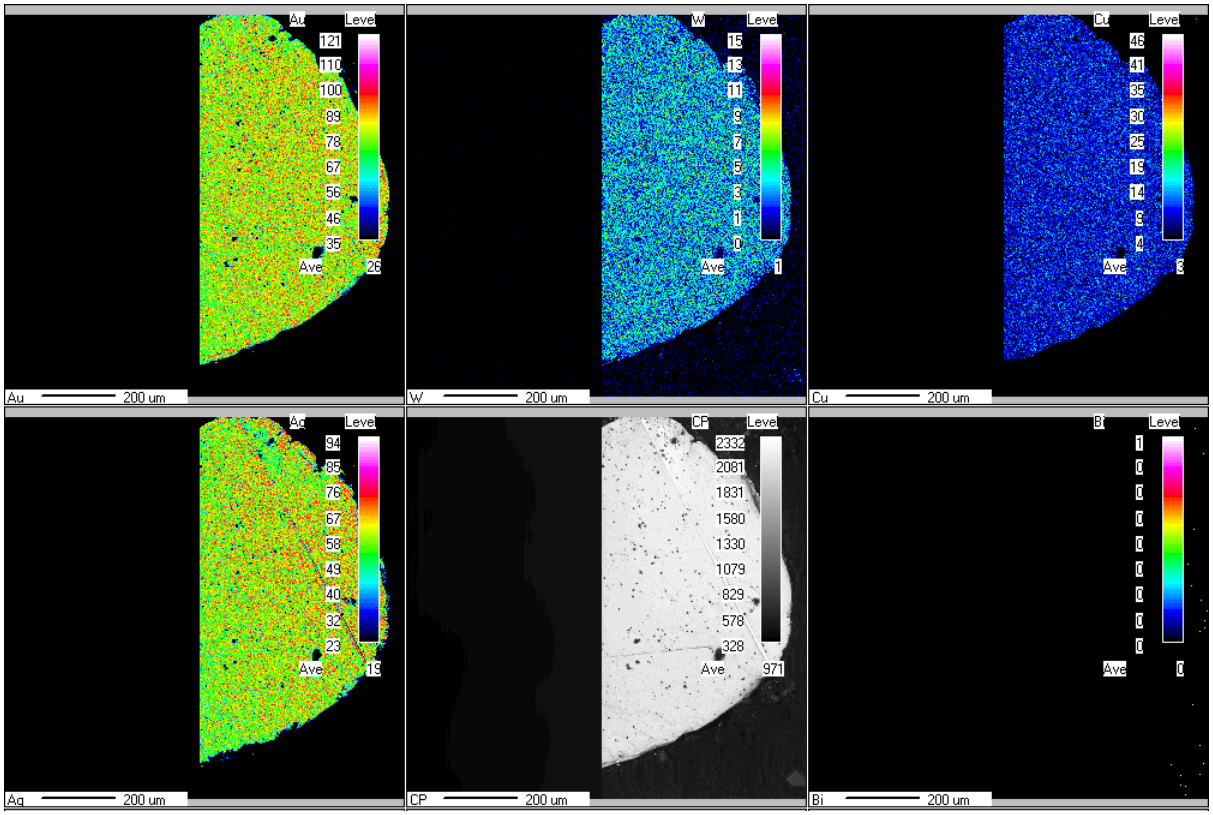

Grain ID: ADEM-7 (Map 2)

Accelerating Voltage: 15.0 kV

Probe Current: 20 nA

Sample Points: 1250 X 1250

Sampling Interval (µm): 0.86 X 0.86

Sample Size (µm): 1075 X 1075

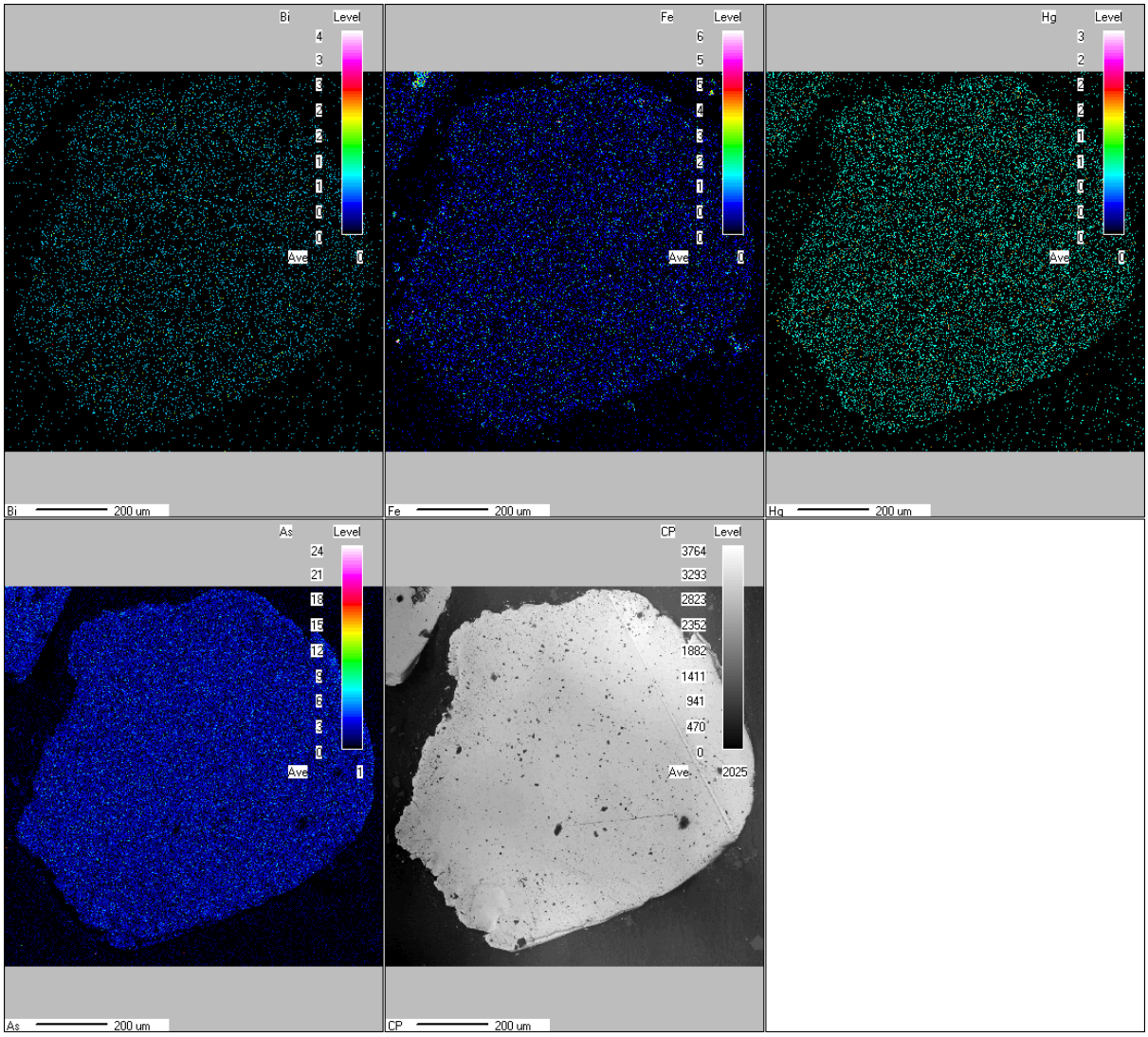

Grain ID: RC4-1

Accelerating Voltage: 15.0 kV

Probe Current: 20 nA

Sample Points: 300 X 300

Sampling Interval (µm): 0.20 X 0.20

Sample Size (µm): 60 X 60

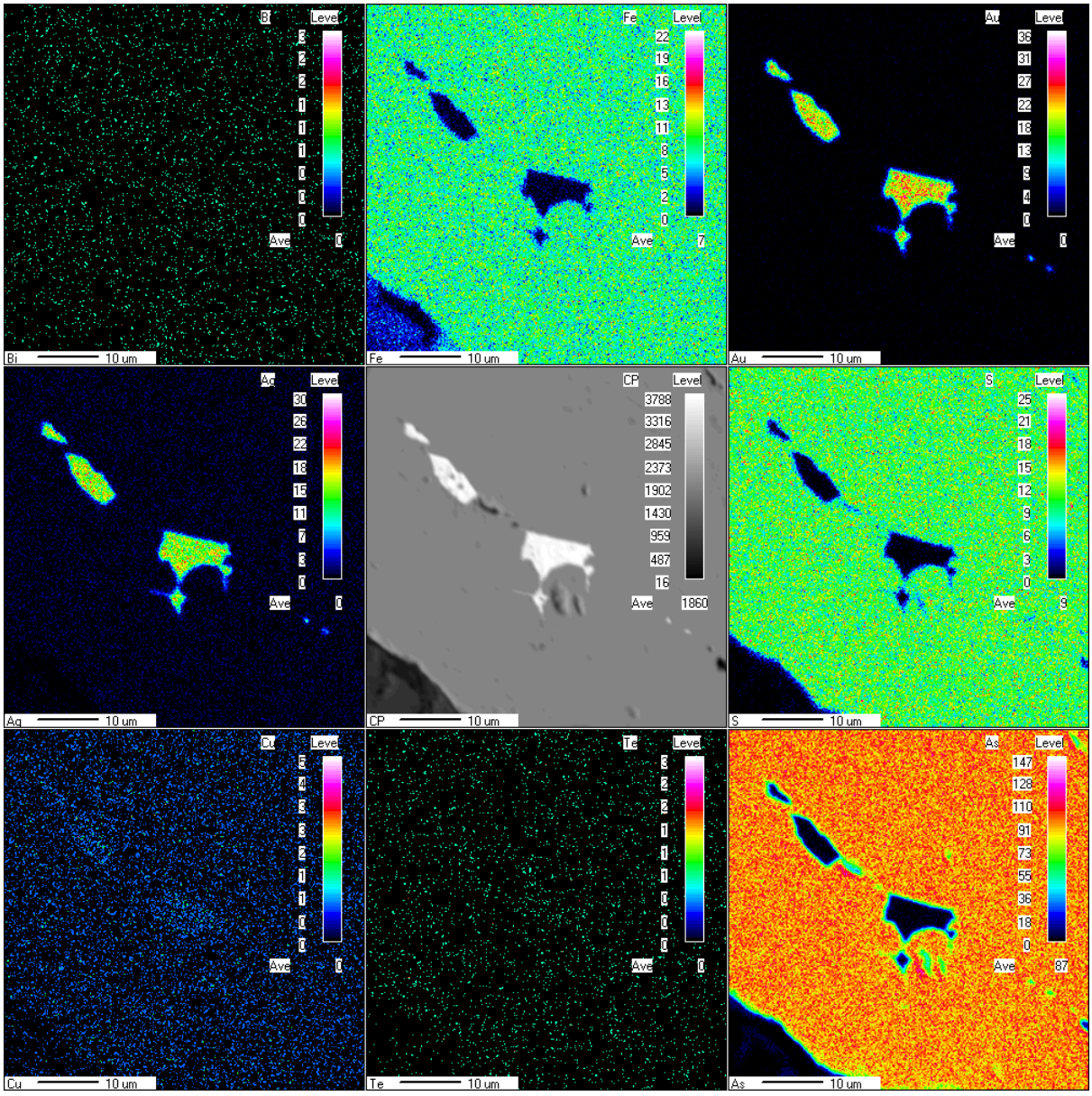

Grain ID: RC4-3

Accelerating Voltage: 15.0 kV

Probe Current: 20 nA

Sample Points: 500 X 250

Sampling Interval (µm): 0.20 X 0.20

Sample Size (µm): 100 X 50